

**THEORETICAL INVESTIGATION OF THE KINETICS AND
THERMODYNAMICS OF CONFORMATIONAL EQUILIBRIUM IN CROWDED
MEDIUM**

MUHAMMAD SAJID IQBAL
Bachelor of Science, Government College University Faisalabad, 2009
Master of Science, University of Eastern Finland, 2012

A Thesis
Submitted to the School of Graduate Studies
of the University of Lethbridge
in Partial Fulfillment of the
Requirements for the Degree

DOCTOR OF PHILOSOPHY

Department of Chemistry and Biochemistry
University of Lethbridge
LETHBRIDGE, ALBERTA, CANADA

© Muhammad Sajid Iqbal, 2017

THEORETICAL INVESTIGATION OF THE KINETICS AND THERMODYNAMICS
OF CONFORMATIONAL EQUILIBRIUM IN CROWDED MEDIUM

MUHAMMAD SAJID IQBAL

Date of Defence: June 06, 2017

Dr. Marc R. Roussel Supervisor	Professor	Ph.D.
Dr. H. J. Wieden Committee Member	Professor	Ph.D.
Dr. Kenneth Vos Committee Member	Associate Professor	Ph.D.
Dr. Athan Zovoilis Internal Examiner	Assistant Professor	Ph.D.
Dr. Ramon Grima External Examiner, The University of Edinburgh	Reader	Ph.D.
Dr. Michael Gerken Chair, Thesis Examination Committee	Professor	Ph.D.

Dedication

To my lovely parents,

Muhammad Iqbal and Zeenat Bibi

Abstract

Macromolecular crowding alters the thermodynamic activities and kinetics of biochemical processes through an excluded volume effect. A theoretical framework, comprised of the Monte Carlo, extended scaled particle theory, and the transition state theory models is employed to compute the thermodynamic activities of three systems in virtually crowded media filled with polyethylene glycol molecules chosen from appropriately constructed conformational ensembles. The theoretical framework covers all the key steps required to prepare the equilibrated crowded medium and subsequently calculate the thermodynamic activities and kinetics. The thermodynamic activity depends on the geometrical parameters of all fluid particles and the model extracts the geometrical parameters by generating a convex hull from atomic coordinates. Moreover, it considers the nonideal contributions of crowder aggregates. This model predicts low to moderate crowding effects consistently with experimental findings with an enhancement in the stability of folded conformations from -0.2 to $-2.0kT$ over open conformations due to crowding.

Acknowledgments

I would like to express my sincere gratitude to my advisor Prof. Marc R. Roussel for the continuous support to my Ph.D work. I really appreciate his guidance, patience, and great support. His guidance helped me in all the time of research and writing of this thesis. Your advice on both research as well as on my career have been priceless. Besides my advisor, I would like to thank the rest of my thesis committee Prof. Hans-Joachim Wieden and Prof. Ken Vos for their valuable guidance that has influenced the course of my project and is greatly appreciated.

My sincere thanks also goes to Dr. Marcio Duarte Albasini Mourao who provided me precious support in conducting simulations and stimulating discussion regarding different aspects of my research work. I would like to thank WestGrid and Compute Canada Calcul Canada as this research was enabled in part by support provided by WestGrid (www.westgrid.ca) and Compute Canada (www.computecanada.ca) and further for providing me valuable consultation support in setting up calculations to accomplish my goal. I also thank the scientific program developer communities, especially Amber, Sire, and PyRED developers, for their great support in performing simulations successfully. I also thank my fellow labmates, program and laboratory coordinators in the Chemistry & Biochemistry Department and friends: Catharine Roussel, Wayne Lippa, Susan Hill, Hossein Hosseini, Blessing Okeke, Dylan Girodat, Purshotam Sharma, Silky Sharma, R.J. Murphy, and Muhammad Akhtar for their stimulating discussions and encouragement.

A huge thank you to my family whose love and reassurance kept me going through the years. Finally, I would like to acknowledge the financial support provided by the University of Lethbridge.

Table of Contents

Dedication	iii
Abstract	iv
Acknowledgments	v
Table of Contents	vi
List of Tables	x
List of Figures	xi
List of Abbreviations	xiv
1 Introduction	1
1.1 Macromolecular crowding	1
1.2 Excluded volume effect	3
1.3 Crowding effects on the conformational equilibrium	7
1.3.1 Crowders: Polyethylene glycol	10
1.3.2 Telomerase RNA (2K96-1NA2)	12
1.3.3 Adenylate kinases (4AKE-1AKE)	13
1.3.4 The <i>lac</i> repressor (2PE5-2P9H)	14
1.4 Macromolecular crowding models	15
1.4.1 Theoretical model: The scaled particle theory	16
1.4.2 Computer simulation model: Monte Carlo simulations	20
1.4.3 The transition state theory	22
1.5 Objectives of the present study	24
2 Methods	26
2.1 Ensemble of PEG conformations	27
2.1.1 Forcefield parameters for PEG	28
2.1.2 Case 1. Whole molecule approach	30
2.1.3 Case 2. Fragment approach	30
2.1.4 MC sampling in MCCCSTowhee	33
2.1.5 MC sampling in Sire	35
2.1.6 MD sampling in Amber	38
2.2 Packing and equilibration	38
2.2.1 Minimization with Sire	40

2.2.2	Swapping equilibrium with Sire	41
2.2.3	MD Amber simulations	41
2.3	Fractional available volumes calculations	42
2.4	The scaled particle theory	46
2.5	The transition state theory	48
2.6	Summary	50
3	Construction of crowded medium	51
3.1	Forcefield parameters for PEG	53
3.1.1	PEG with methyl terminal group	55
3.1.2	Comparison of FF parameters with methyl, hydroxyethyl and propyl terminals	60
3.1.3	Effect of length of the central fragment	62
3.1.4	Effect of multiple PEG conformations	65
3.2	Ensemble of PEG conformations	69
3.2.1	MC sampling in MCCCSTowhee	70
3.2.2	MC sampling in Sire	76
3.2.3	MD sampling in AMBER	84
3.2.4	Conclusion - Ensemble of PEG conformations	88
3.3	Packing and equilibration	89
3.3.1	MC equilibration	92
3.3.2	MC swapping	93
3.3.3	MD Amber simulations	96
3.4	Summary	99
4	Conformational equilibrium in crowded media	100
4.1	Fractional available volume calculations	100
4.2	MC Simulations	101
4.2.1	Efficiency comparison of two MC algorithms	102
4.2.2	Effect of PEG aggregation	105
4.2.3	Statistical analysis	109
4.3	The scaled particle theory	110
4.3.1	Geometric parameters by the original and extended SPT models	111
4.3.2	Sensitivity of the SPT calculations	114
4.4	Comparison of SPT and MC simulations	123
4.4.1	Biological and experimental relevance of results	128
4.5	Kinetics study by the transition state theory	132
5	Conclusion	137
5.1	Summary	137
5.2	Recommended computational methods	138
5.2.1	Ensembles of crowder conformations	138
5.2.2	Packing and equilibration	139
5.2.3	Calculations of thermodynamic properties	140
5.2.4	Crowding effects on reaction kinetics	141

5.3	Future directions	142
5.3.1	Accuracy of the geometrical parameters and computational efficiency	142
5.3.2	Heterogeneity of crowded medium	143
5.3.3	Soft interactions contributions	144
5.3.4	Approximate better TS state structure	145
Bibliography		146
A Methods appendix		168
A.1	Forcefield parameters for PEG	168
A.1.1	System.config	168
A.1.2	Project.config	168
A.2	MCCCS Towhee input file	169
A.3	Sire sampling input file	182
A.3.1	Input file with all functions	182
A.3.2	Quenching sampling program	235
A.4	MD sampling in Amber	238
A.4.1	mini.in	238
A.4.2	md.in	238
A.5	Packing and Equilibration	239
A.5.1	Equilibration with Sire	241
A.5.2	Swapping equilibrium with Sire	243
A.5.3	MD Equilibration with Amber	245
A.6	Fractional available volumes calculations	248
A.6.1	Parallel-energy algorithm	248
A.6.2	Parallel-distance algorithm	251
A.7	The scaled particle theory	254
A.7.1	findcurvature.m	254
A.7.2	findactivity.m	259
A.7.3	The SPT main program	259
A.8	TST main program	267
B Construction of crowded medium appendix		269
B.1	PEG with a methyl terminal	269
B.1.1	FF libraries for ‘A’ fragment	269
B.1.2	FF libraries for ‘B’ fragment	270
B.1.3	FF libraries for ‘C’ fragment	271
B.1.4	FF parameters for PEG-M	271
B.1.5	Fitting statistics of a whole molecule approach	273
B.1.6	Fitting statistics of a fragment approach	278
B.1.7	Amber Leap script for PEG-M	284
B.2	PEG with a hydroxyethyl terminal, $n = 4$	287
B.2.1	FF libraries for ‘A’ fragment	287
B.2.2	FF libraries for ‘B’ fragment	289
B.2.3	FF libraries for ‘C’ fragment	290

B.2.4	FF parameters for PEG-H	292
B.2.5	Fitting statistics of a whole molecule approach	294
B.2.6	Fitting statistics of a fragment approach	304
B.2.7	Amber Leap script for PEG-H	314
B.3	PEG with hydroxyethyl terminal, multiple conformations	317
B.3.1	FF libraries for 'A' fragment	317
B.3.2	FF libraries for 'B' fragment	317
B.3.3	FF libraries for 'C' fragment	318
B.3.4	FF parameters for PEG-H(m)	319
B.3.5	Fitting statistics of a whole molecule approach	321
B.3.6	Fitting statistics of a fragment approach	426
B.3.7	Amber Leap script for PEG-H(m)	532
B.3.8	Multiple mini-PEG conformations	537
B.3.9	FF effect on the PEG folding	540
B.4	MCCCS Towhee plots	542
B.5	Sire plots	548
C	Conformational equilibrium in crowded media appendix	554
C.1	Extract clusters	554
C.2	Sensitivity coefficient calculations	557
C.2.1	Main program (Sensitivity coefficients) file	557
C.2.2	Sensitivity coefficients function	563
C.3	Fractional available volume plots	565
C.4	Nonideal chemical potential plots	572
C.5	Standard free energy change plots	578

List of Tables

1.1	Geometric parameters of different shapes	19
3.1	Predicted atomic charges of PEG with methyl by QM calculations	57
3.2	RRMS and Pearson correlation coefficient r^2 for three QM methods	59
3.3	Effect of length of the central fragment on the RRMS values	65
3.4	Validation of forcefield parameters	68
3.5	Types and ranges of MC moves	80
4.1	Comparison of geometrical parameters by the original and extended SPT models	111
4.2	Geometrical parameters R, S, V of one thousand conformations	115
4.3	Geometrical parameters R, S, V of six random conformations	120
4.4	Geometrical parameters of three structures of GAAA tetraloop receptor estimated by the extended SPT model	134

List of Figures

1.1	Macromolecular crowding in the cell	2
1.2	The fundamental concept of an excluded volume	3
1.3	Conformational equilibrium of telomerase RNA structures	13
1.4	Conformational equilibrium of adenylate kinase structures	14
1.5	Conformational equilibrium of the <i>lac</i> repressor structures	15
1.6	The basic concept of the Monte Carlo integration method	21
1.7	Illustration of the high energy transition state	23
2.1	The schematic diagram of the theoretical framework	27
2.2	Key steps to construct forcefield parameters	29
2.3	Fragmentation of PEG	31
2.4	Fragmentation of PEG with hydroxyethyl terminal	33
2.5	Key steps in the MC conformational sampling	36
2.6	Key steps in MD conformational sampling	39
2.7	Packing of PEG in the box	40
2.8	Measurement of steric clashes using the van der Waals radii	43
2.9	Workflow of MC method to estimate the fractional available volume	45
2.10	Construction of the convex hull	47
3.1	Major steps in the theoretical framework	52
3.2	Types of PEG structures differ in terminal groups	54
3.3	Key steps of a fragment approach	58
3.4	Total energy change for three PEGs in MD simulations	61
3.5	Radius of gyration change for three PEGs in MD simulations	61
3.6	Effect of the central fragment on the PEG folding	63
3.7	Effect of the central fragment on the MD energies	64
3.8	Effect of the central fragment on the MD radius of gyration	64
3.9	Formation of hydrogen bonds in PEG	66
3.10	Use of multiple conformations for forcefield development	67
3.11	Change in radius of gyration in MC sampling using MCCCSTowhee	72
3.12	Change in total energy in MC sampling using MCCCSTowhee	72
3.13	Snapshots of PEG initial structures used in MC simulations	75
3.14	Variation of radius of gyration and energy in MC simulations	75
3.15	Energy change of PEG in MC simulations with Sire	78
3.16	Radius of gyration change of PEG in MC simulations with Sire	78
3.17	Energy change in MC simulations using a temperature quenching method	81
3.18	Radius of gyration change in MC simulations using a temperature quenching method	81

3.19	Energy change with higher number of MC internal moves	82
3.20	Radius of gyration change with higher number of MC internal moves	82
3.21	Random PEG snapshots in the MC simulations	83
3.22	Random PEG snapshots in MD simulations	85
3.23	Effect of temperature in MD simulations	87
3.24	Size distribution of PEG in MC and MD simulations	89
3.25	Size distribution of PEG in MD simulations	91
3.26	Size distribution of PEG in MC simulations	91
3.27	Illustration of PEG packing in a cubic box	92
3.28	Energy change in MC equilibration simulations	94
3.29	Size distribution of PEG after MC equilibration simulations	94
3.30	Energy change in MC swapping simulations	95
3.31	Effect of MD equilibration on packing of PEG	96
3.32	Energy comparison of three equilibration methods	97
3.33	Efficiency comparison of three equilibration methods	98
4.1	Comparison of MC methods using distance and energy criteria	104
4.2	Effect of equilibration on size distribution and fractional available volumes	106
4.3	Effect of de-aggregation on fractional available volumes	107
4.4	Effect of MFF and HFF on clustering behaviour	107
4.5	Effect of MFF and HFF parameters on size distribution after equilibration	108
4.6	Effect of number of systems on the standard deviation	109
4.7	Geometrical parameters R , S , V of PEG1 and PEG2 using the extended SPT model	112
4.8	Comparisons of the fractional available volumes by original, extended SPT models and MC simulations	112
4.9	Effect of an increase of PEG2 geometrical parameters to the maximum values on nonideal chemical potential	115
4.10	Effect of an increase of PEG2 geometrical parameters on nonideal chemical potential	116
4.11	Sensitivity analysis of SPT calculations to the radius of curvature at 0.1 g cm^{-3}	117
4.12	Sensitivity analysis of SPT calculations to the surface area at 0.1 g cm^{-3}	117
4.13	Sensitivity analysis of SPT calculations to the volume at 0.1 g cm^{-3}	118
4.14	Sensitivity analysis of SPT calculations to the radius of curvature at 0.2 g cm^{-3}	118
4.15	Sensitivity analysis of SPT calculations to the surface area at 0.2 g cm^{-3}	119
4.16	Sensitivity analysis of SPT calculations to the volume at 0.2 g cm^{-3}	119
4.17	Effect of different conformations of PEG on the chemical potentials	121
4.18	The change in the chemical potential as a function of radius of curvature at 0.1 g cm^{-3} concentration	121
4.19	Variation of sensitivity coefficient with respect to radius of curvature with 0.1% increment	124
4.20	Variation of sensitivity coefficient with respect to surface area with 0.1% increment	124
4.21	Variation of sensitivity coefficient with respect to volume with 0.1% increment	125

4.22	Comparison of nonideal chemical potentials for 2K96	127
4.23	Standard free energy change of the 1NA2 \rightleftharpoons 2K96 reaction	130
4.24	Approximation of the TS of the GAAA tetraloop receptor	133
4.25	Comparison of theoretical and experimental folding rate constants	135
5.1	Methods to improve geometrical parameter calculations	141
B.1	Effect of the central fragment on radius of gyration in MD simulations using HFF parameters	540
B.2	Effect of the central fragment on radius of gyration in MD simulations using MFF parameters	541
B.3	Energy change in MC simulations at 300 K in MCCCC Towhee	542
B.4	Energy change in MC simulations at 600 K in MCCCC Towhee	543
B.5	Energy change in MC simulations at 1200 K in MCCCC Towhee	544
B.6	Radius of gyration change in MC simulations at 300 K in MCCCC Towhee	545
B.7	Radius of gyration change in MC simulations at 600 K in MCCCC Towhee	546
B.8	Radius of gyration change in MC simulations at 1200 K in MCCCC Towhee	547
B.9	Energy change in MC simulations at 1200 K in Sire	548
B.10	Radius of gyration change in MC simulations at 1200 K in Sire	549
B.11	Energy change in MC simulations in Sire using MFF parameters	550
B.12	Radius of gyration change in MC simulations in Sire using MFF parameters	551
B.13	Energy change in MC simulations in Sire using HFF parameters	552
B.14	Radius of gyration change in MC simulations in Sire using HFF parameters	553
C.1	Comparison of fractional available volumes for 1AKE	565
C.2	Comparison of fractional available volumes for 4AKE	566
C.3	Comparison of fractional available volumes for 4AKE	567
C.4	Comparison of fractional available volumes for 2P9H	568
C.5	Comparison of fractional available volumes for 2PE5	569
C.6	Comparison of fractional available volumes for 2K96	570
C.7	Comparison of fractional available volumes for 1NA2	571
C.8	Comparison of nonideal chemical potentials for 1AKE	572
C.9	Comparison of nonideal chemical potentials for 4AKE	573
C.10	Comparison of nonideal chemical potentials for 2P9H	574
C.11	Comparison of nonideal chemical potentials for 2PE5	575
C.12	Comparison of nonideal chemical potentials for 2K96	576
C.13	Comparison of nonideal chemical potentials for 1NA2	577
C.14	Standard free energy change of 4AKE \rightleftharpoons 1AKE reaction	578
C.15	Standard free energy change of 2PE5 \rightleftharpoons 2P9H reaction	579

List of Abbreviations

AdK	Adenylate kinase
BD	Brownian dynamics
BHS	Bonded hard-sphere
DFT	Density functional theory
ESP	Electrostatic potential
FF	Forcefield
FHS	Fused hard-sphere
FRET	Forster resonance energy transfer
FTIR	Fourier transform infrared spectroscopy
HF	Hartree Fock
HFF	Forcefield parameters for PEG with hydroxyethyl terminal
LJ	Lennard-Jones
MC	Monte Carlo
MD	Molecular dynamics
MEP	Molecular electrostatic potential
MFF	Forcefield parameter for PEG with methyl terminal
MP2	Møller-Plesset perturbation theory of second order
NI	Nonideal
PEG	Polyethylene glycol
PFF	Forcefield parameters for PEG with propyl terminal
PHF	Post-Hartree Fock
PVP	Polyvinylpyrrolidone
QM	Quantum mechanics
RESP	Restrained electrostatic potential
RRMS	Relative root mean square
SANS	Small-angle neutron scattering
SPT	Scaled particle theory
TER	Telomerase RNA
TERT	Telomerase reverse transcriptase
TS	Transition state
TST	Transition state theory

Chapter 1

Introduction

1.1 Macromolecular crowding

The kinetics and thermodynamics of biochemical reactions have traditionally been studied in experiments using dilute solutions of total concentrations less than about 1 g/l [1–6]. The total concentration of dilute solution includes the total amount of solute proteins, and buffer salts [7]. In contrast to experimental settings, the biochemical reactions occur naturally in highly concentrated and confined cellular environments in the presence of billions of proteins. The cellular environment contains a total concentration from 50 to 400 g/l of extensive, complex and cross-linked structures of proteins, nucleic acids, enzymes, polysaccharides and cytoskeleton fibers (Figure 1.1) [8–11].

The total concentration in the cell depends on the presence of a variety of macromolecules that are present at very high concentrations. In 1981, Minton [12, 13] named such a medium crowded rather than concentrated because no single species is present at high concentration. In the crowded medium, all these macromolecules are called background or crowder species [4, 5, 12, 14, 15]. All these macromolecules occupy a significant fraction of the total volume in the eukaryotic and prokaryotic cells [16] and alter the kinetics and thermodynamics of biochemical reactions significantly by increasing the total free energy of the reaction medium [4, 9, 14] through steric, electrostatic, and hydrophobic interactions [3, 7, 12].

Macromolecular crowding does not always increase the rate of reaction to the same extent [18–22]. The crowding alters the reaction rates based on the reaction mechanism

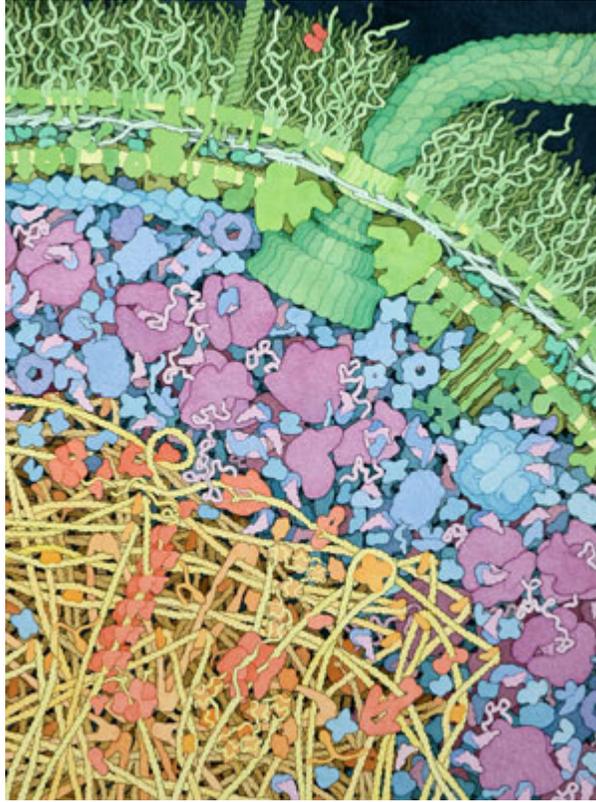


Figure 1.1: The cross section diagram of an *Escherichia coli* cell depicts different regions of the cell in different colors. A large flagellar motor passing through the cell wall is shown in green, the cytoplasmic proteins are blue, and the central nucleus region containing DNA and histones in yellow and orange colors. The cellular organization showed compact packing of different sized and shaped macromolecules at the total concentration [17]. (This illustration is provided by David S. Goodsell, the Scripps Research Institute, and is in the public domain. See <http://mgl.scripps.edu/people/goodsell/illustration/public>)

and type of molecules present in the medium. For example, crowding could reduce the rate constant of diffusion limited reactions by limiting the diffusion of reacting species through additional molecular obstacles [23], whereas the rate of an activation controlled reaction could increase by allowing more time for the formation of a transition complex and subsequently forming a final product [3, 20]. The majority of previous studies have shown that the crowding alters the reaction rate by the excluded volume effect [9, 12, 24, 25] and the magnitude of the excluded volume depends on the type, size and shape of molecules [3, 5, 26]. The excluded volume will be discussed in detail in the next section 1.2.

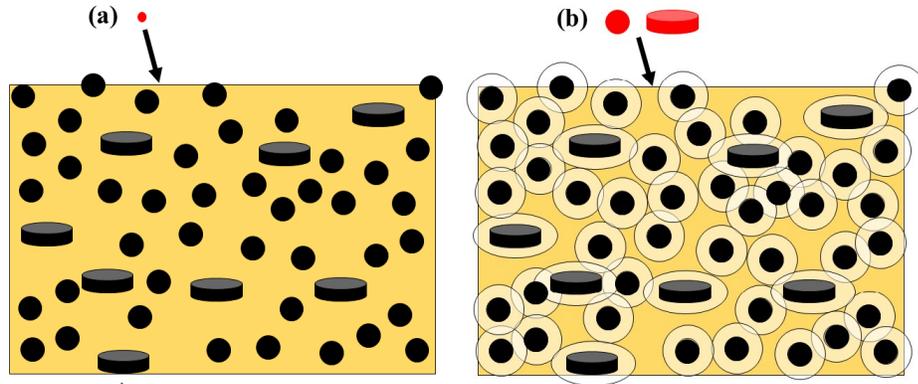


Figure 1.2: The concept of excluded volume is illustrated, using a rectangular shaped cell filled with sphere and disk shaped black molecules occupying approximately 30 percent of total space. Attempts to place three different sized and shaped red colored test molecules in the solution are made. The smallest spherically shaped molecule, in case (a), could be placed in the majority of the space in the yellow region, and more than sixty five percent of the total space is available for the test molecule. However, the percentage of free available volume varies for the other two particles shown in case (b). The sphere and disk shaped test molecules could occupy 10 to 15 percent and less than 5 percent of free space respectively. These amounts of available volume are rough estimations. The excluded volume for the red sphere is illustrated by the light color large circles around the solution particles.

1.2 Excluded volume effect

One can understand how macromolecular crowding affects the thermodynamics of a biochemical reaction through an excluded volume concept. The excluded volume is defined as free space that is excluded by the solution molecules to the solute particle, depending on the sizes and shapes of the solution and solute molecule. The extent of this virtually present free space depends on the sizes and shapes of the background molecules and the solute molecule [4, 9, 12, 27, 28]. The concept of the excluded volume can be understood from the illustration in Figure 1.2, which demonstrates the dependence of the magnitude of the excluded volume on the shapes and sizes of the background and solute molecules. The background molecules represent the solution molecules present in the rectangular outline whereas the solute molecules or test molecules represent the additional molecules that are tried to be placed in the solution. The excluded volume is fundamentally produced due to steric repulsion interactions among the fluid particles [3, 5, 7].

The example (Figure 1.2) explains the concept of excluded volume where the rectangu-

lar outline depicts the cell filled with spherical and disk shaped macromolecules occupying approximately 30 percent of the total volume. The percent of free available volume to the additional solute molecule is determined by its size and shape. If a very small test molecule (Figure 1.2 case a) relative to the background molecules is placed in the defined region, it can be placed almost anywhere in the yellow area that is not occupied by the background molecules. However, if a test molecule (Figure 1.2 case b) of the same or larger size (sphere, disk) relative to the background molecules is placed in the medium, there is very limited dark yellow space available to the new molecule. The free volume, the volume where additional test molecule can be placed, is reduced because the centre of a test molecule can only approach the centre of any background molecule to a certain distance, indicated by the black circular and elliptical lines around each spherical and disk background molecule, respectively. The circular or elliptical lines are formed by rotating the spherical test molecule around the background spherical and disk shaped molecules. However, the ellipse is not a true representation of the excluded volume for the disk shaped molecules in a three dimensional space. Due to steric repulsion, two molecules cannot occupy the same place at the same time. The additional volume occupied by the circular or elliptical shell is called excluded volume of the spherical shaped molecule and could not be occupied by any of the background or test molecule. The excluded volume depends on the sizes and shapes of solute and solvent molecules. The example illustrated that each molecular conformation has its own excluded volume. Thus, the excluded volume is defined as the volume which is present in the medium but physically inaccessible to an additional molecule of a particular size and shape [6, 29, 30].

The excluded volume alters the effective concentration of solute species in the crowded medium significantly. According to freshman chemistry, the reactivity of any solute species depends on the concentration or the number of molecules per unit volume, which is strictly true only for very dilute solutions. In the crowded medium where many different species are present at high total concentration, the solute molecules are no longer ideal and their

reactivity is defined by an effective concentration. Thus, the chemical potential (μ) [31] of the solute in dilute solution cannot represent the chemical potential of the same solute in a crowded nonideal (NI) solution truly. The chemical potential is a partial molar Gibbs free energy of a particular chemical specie in the solution at constant temperature, pressure and number of moles of other species in the mixture. The chemical potential can also be defined in more than one ways under different conditions as shown in equation 1.1. Therefore it is necessary to add NI contributions due to the excluded volume, electrostatic, hydrophobic and hydrophilic interactions to the chemical potential of an ideal solute that is present in the crowded medium to represent the real solution (Equation 1.2 [3]).

$$\mu_i = \left(\frac{\partial G}{\partial N_i} \right)_{T,p,N_j \neq i} = \left(\frac{\partial H}{\partial N_i} \right)_{S,p,N_j \neq i} = \left(\frac{\partial A}{\partial N_i} \right)_{V,T,N_j \neq i} = \left(\frac{\partial U}{\partial N_i} \right)_{S,V,N_j \neq i} \quad (1.1)$$

$$\mu_i = \mu_i^0 + kT \ln a_i \quad (1.2)$$

where:

$$a_i = \gamma_i c_i / c^\circ$$

$$\mu_i = \mu_i^{\text{ideal}} + \mu_i^{\text{NI}}$$

$$\mu_i^{\text{ideal}} = \mu_i^0 + kT \ln c_i / c^\circ$$

$$\mu_i^{\text{NI}} = kT \ln \gamma_i$$

where the ideal contribution (μ_i^{ideal}) is the free energy change in the absence of any type of solute-solute interactions whereas the NI contribution (μ_i^{NI}) is the free energy change due to the presence of solute-solute interactions. k is the Boltzmann constant, T is the temperature, γ_i is the activity coefficient, c_i is the solute concentration, c° is the standard

concentration, and a_i is the thermodynamic activity of solute i . Under ideal conditions the activity is approximately equal to concentration for each solute species.

The activity is described as an effective concentration of a particular species in a solution [32]. The excluded volume theory hypothesizes that the effect of crowders is to reduce the available volume, so that the contribution to the activity due strictly to the crowding effect can be computed by replacing the concentration by the number of solute particles per available volume. Crowding reduces the available volumes and causes significant NI effects [3, 13, 33, 34]. The reduction in the available volume due to excluded volume can increase the thermodynamic activity of the test particle by several orders of magnitude. Consequently, the activity coefficient is greater than unity and the molecule shows NI behaviour. In a simple way, the activity coefficient of solute i is expressed as a ratio of the total volume to the available volume in the crowded medium (Equation 1.3) [3, 7, 9, 14]. This expression for γ_i arises from the simplest theory of the effect of excluded volume on thermodynamic activities.

$$\gamma_i = \frac{V_{\text{total}}}{V_{\text{available}}} \quad (1.3)$$

where γ_i is the activity coefficient of solute i , V_{total} is the total volume of the compartment, and $V_{\text{available}}$ is the free volume available to the solute particle i in the solution.

The magnitude of the excluded volume is directly influenced by the number density, shapes, and sizes of the test and background species in *in vitro* experiments [35–37]. In living cells, especially in the eukaryotic cell, the amount of excluded volume depends on the concentration of bulk soluble species in each compartment and spaces confined by the cytoskeletal elements. Generally, these macromolecules occupy 5–40 percent of the total volume, in the range of 50–400 g/l concentration. Therefore, this is the most common concentration range used to study the consequences of crowding [8, 9, 11, 30, 38, 39].

The macromolecular crowding potentially affects the protein behaviour in the crowded milieu, such as conformational equilibrium [4, 19, 21, 24, 25, 28, 35, 38, 40–43], enzyme

activities [14, 44–47], protein binding events [19, 37, 48, 49], phase separation [50–52], pathological protein aggregation [53–56], and association reactions [10, 57–60]. Imagine a macromolecule with two different conformations, A and B, in a conformational equilibrium. There is an equilibrium between A and B in any medium which implies $\mu_A = \mu_B$. If this reaction is transferred from dilute solution to a solution with inflexible crowders, then the chemical potentials of both conformations increase, but the chemical potential of the least compact conformation increases more due to decrease in available volume. To restore equilibrium, the reaction will shift towards the more compact conformation until the condition $\mu_A = \mu_B$ is once again reached [13, 29, 53, 61]. Alternatively, the conformational equilibrium shift, from a dilute to a crowded solution, will initially cause the reaction to proceed in a direction that increases the available volume.

1.3 Crowding effects on the conformational equilibrium

Proteins form unique conformations to perform a variety of biological tasks [24, 62, 63]. These conformational changes occur due to genetically encoded information in proteins, protein-solvent interactions, ligand binding and release from active sites, phosphorylation, exposure to light, and macromolecular crowding [24, 47, 64–68]. A better understanding of conformational changes could unveil the reactivity mechanism of different states of a single protein in different biochemical reactions. Therefore, various experimental techniques such as Forster resonance energy transfer (FRET), neutron and X-ray scattering, NMR spectroscopy, X-ray crystallography, hydrogen-deuterium exchange, and mutation studies have been applied to investigate the mechanism of internal movements of proteins. Further, many computer simulations have been conducted to sample alternative conformations of probe proteins to understand the structure and function of each different conformation [24, 67–70].

For example, adenylate kinase (AdK) equilibrates between open and closed conformations. Explicit long time scale molecular dynamics (MD) and bias exchange metadynamics

simulations were conducted to investigate the intermediate conformational states and transition pathways in the presence and absence of ligands. The simulation results indicate no significant energy barrier is crossed to transit between open and closed conformations in the ligand-free AdK form, whereas a closed conformation is energetically favored in the ligand-bound AdK form by 8 kcal mol^{-1} and requires a high energy to pass the energy barrier in order to form an open conformation [44].

It is well recognized that small and large scale conformational changes play an essential role in triggering the catalytic activity of biological enzymes [67–69]. In these experimental and theoretical studies, the protein conformational changes have been examined under dilute conditions. However, proteins evolve and function in very heterogeneous and crowded medium, in which macromolecules occupy approximately 5 to 40 percent of the total volume [39, 71]. In this regard, the excluded volume theory explains the crowding effects on the conformational equilibria qualitatively [12, 19, 24, 25, 27, 72]. One of our goals is to explore whether it can be used quantitatively to estimate the macromolecular crowding effects on the conformational equilibrium between two conformations of a single macromolecule.

A vast majority of research on the macromolecular crowding has been dedicated to study its effects on protein folding, and on binding processes in experimental and theoretical studies [15, 25, 26, 29, 37, 42, 43, 51, 52, 55, 71, 73–79]. In *in vitro* experiments, the crowding effect is induced by using synthetic high molecular weight polymers such as polyethylene glycol (PEG) [51, 52, 58, 80], polyvinylpyrrolidone (PVP) [30, 63], Ficoll [58, 80], dextran [30, 58, 80], bovine serum albumin [80, 81], and ovalbumin [63]. These crowding agents have to comply with different criteria to generate the crowding effect in *in vitro* experiments. The crowding agents should have molecular mass in the range from 50 to 200 kDa, be globular shaped to keep the viscosity at a minimum level, neutral with no ability to develop any electrostatic, hydrodynamic or hydrophobic interactions with itself or with solute molecules, highly soluble, similar in size to the probe protein, and raise no difficulties in the spectroscopic testing [3, 10, 15, 29, 37, 82]. Experimental data showed

that low molecular weight crowding agents are not ideal to use due to formation of soft interaction among the crowder molecules whereas the high molecular weight crowding agents are found to be more effective in producing the excluded volume effects. However, none of the crowding agents is perfect [15, 26, 29, 37, 42, 43, 51, 52, 55, 73–79].

Recently, a few studies have been conducted to investigate the effect of macromolecular crowding on the conformational equilibrium. In this regards, a post-processing atomistic modelling approach [21, 37, 59] has been developed to study the conformational equilibria and the transition rates in crowded medium of seven different proteins pairs. In this model, a representative conformation of each protein is sampled by employing explicit MD simulations at room temperature and subsequently the change in the free energy is estimated by taking the difference of the chemical potential for each conformation in dilute and crowded medium. The spherical shaped crowders of 15 and 30 Å radius, occupying up to 35 percent of available space, were used to produce the excluded volume effect [19, 24, 25]. In another study, conformational equilibrium between pseudoknot and hairpin telomerase conformations was investigated by performing coarse grained Langevin dynamics simulations under crowded conditions. The simulated melting temperature curves for each conformations were found to be in agreement with experimental UV melting data [47]. The insertion algorithm based on the scaled particle theory has been applied to reproduce the simulation results in the presence of spherical shaped crowding agents.

Typically, the computer simulations and analytical scaled particle theory model approximates the shapes of solute and crowder molecules as hard spheres or cylinders and estimates the macromolecular crowding effect qualitatively. In this thesis, an attempt is made by using an extended scaled particle theory (SPT) model [83] and a Monte Carlo (MC) simulation model [84–86] to estimate the excluded volume effects on the conformational equilibria of three pair of macromolecules quantitatively through the transition state theory (TST) [87] in the presence of crowders. Conformational ensembles of polyethylene glycol (PEG) were used as a crowding agent in this investigation. The following section briefly describes the

appropriate criterion in light of experimental and theoretical studies to select PEG conformations that could be used as crowders and the details on three systems in conformational equilibrium. Later on, details on three methods, i.e. the SPT, MC and TST models, that will be used to estimate the crowding effects on the conformational equilibrium of three selected systems are discussed.

1.3.1 Crowders: Polyethylene glycol

Polyethylene glycol of molecular weight 8 kDa will be used as a crowding agent in this study because it is used in many experimental and theoretical studies of crowding due to its high solubility in water and in other solvents [55, 88, 89]. Experimental studies conducted in aqueous solutions of 8 kDa PEG revealed that PEG structures exist in diverse shapes such as pulled fibers [90, 91], coiled [90, 92–94], helical [89, 92–96], extended hairpin [93, 97] and compact globular conformations [55, 98] with a radius of gyration from 15 to 46 Å [55, 80, 90–92, 94–96, 98–102].

The radius of gyration is an important property with units of length that is used to characterize polymer size in the experiments and computer simulations [6, 103]. The radius of gyration is defined as the root mean square of the distance of all atoms from the centre of mass of the molecule. The radius of gyration is computed with equation 1.4 and has been used to track the structural changes in the conformational sampling simulations that are performed in different simulation programs [104–106]. The folding behaviour of PEG depends on various factors such as molecular weight of polymer, PEG concentration, type of solvent, impurities in water, temperature, and intra- and intermolecular hydrogen bonding [55, 89, 90, 92–96, 98–102].

$$R_g = \sqrt{\frac{1}{N} \sum_{i=1}^N (\vec{r}_i - \vec{r}_{CM})^2} \quad (1.4)$$

where R_g is radius of gyration, N is total number of atoms, \vec{r}_i is the position vector to each atom and \vec{r}_{CM} is the centre of mass of the molecule. Mathematically, \vec{r}_{CM} for the atoms of

a molecule with masses m_i and positions x_i can be represented by equation 1.5. The centre of mass moves as if the whole mass of the molecule is concentrated there.

$$\vec{r}_{CM} = \left(\frac{\sum m_i \sum x_i}{\sum m_i} \right) \quad (1.5)$$

Small-angle neutron scattering measurements revealed that different solvents played a crucial role toward the folding behavior of PEG [89, 93, 101]. PEG formed helices and coiled structures in H₂O and D₂O solvents respectively [89, 93]. Dynamic light scattering and small angle neutron scattering experiments demonstrated that PEG formed aggregates in water and formed conformations with radii of gyration in the range of 32 to 46 Å in water and deuterated water [107]. The water produced a hydration layer around the PEG and stabilized the helix structures through strong hydrogen bonding [89–92, 95, 96, 108]. It turned out that intra- and intermolecular hydrogen bonding present between terminal hydroxyl groups and ether oxygen atoms is responsible for PEG folding. Fourier transform infrared spectroscopy (FTIR) and X-ray spectroscopy measurements showed that PEG has a tendency to segregate from the aqueous solution containing a mixture of PEG and polypropyl glycol [89, 93, 101]. The segregated PEG stimulates the intermolecular hydrogen bonding between the PEG molecules. This mechanism induced the formation of PEG aggregates. Similarly, other studies demonstrated that PEG formed random coiled structures in purified water and methanol which inhibits aggregation [107, 109]. Moreover, quantum chemistry calculations indicated the presence of intra- and intermolecular hydrogen bonding in the global minimum PEG structures which produced compact conformations in computer simulations that agreed with experimental findings [101].

8 kDa PEG will be used as a crowding agent in this study. As seen above, the conformational analysis confirms that PEG has formed a variety of conformations that differ in sizes and shapes depending on the experimental conditions. It is therefore better to construct ensembles of PEG conformations of different shapes and sizes in order to model these diverse conformations of PEG crowders in the crowded medium than using a single PEG

conformation. To achieve this goal, computer simulations such as Monte Carlo and molecular dynamics simulation approaches were used to construct diverse PEG conformations and to prepare the crowded media by packing these conformations into simulation boxes. Previous experimental and theoretical studies showed that PEG formed conformations with radii of gyration in the range of 15 to 46 Å [55, 63, 90, 91, 107–112]. We sampled PEG conformations from a slightly wider range from 10 to 60 Å. The range is chosen arbitrarily by assuming it would capture enough diverse PEG conformations to mimic the full range of PEG aqueous solution structures. These simulation boxes would mimic the cellular crowded environments and would help us to investigate the macromolecular crowding effects on the conformational equilibrium of the three pairs of macromolecules presented in the following subsections.

1.3.2 Telomerase RNA (2K96-1NA2)

Telomerase is a ribonucleoprotein complex that plays an essential role in regulating the length of the telomere in the cells [113, 114]. The telomerase extends the 3' termini of linear chromosomes by adding successive units of telomere such as dTTAGGG in vertebrates [115, 116]. The shortening of telomeres is directly associated with short life time of cells and ultimately leading to death. The activity of telomerase is also essential for proliferation of cancer cells. Therefore, investigation on the telomerase activity mechanism is of tremendous interest due to its vital role in lengthening of telomeres, ageing, cancer, dyskeratosis congenita, and aplastic anemia diseases [117–119].

Two major components, namely telomerase reverse transcriptase (TERT) and telomerase RNA (TER) are required to assemble a functional ribonucleoprotein complex. The activity of the ribonucleoprotein complex is linked to the conformational changes of the TER component. Two conformations namely pseudoknot (2K96 [120]) and hairpin (1NA2 [119]) of TER component are found in equilibrium and work as a conformational switch [47]. The assembly and functionality of the ribonucleoprotein complex is associated with the forma-

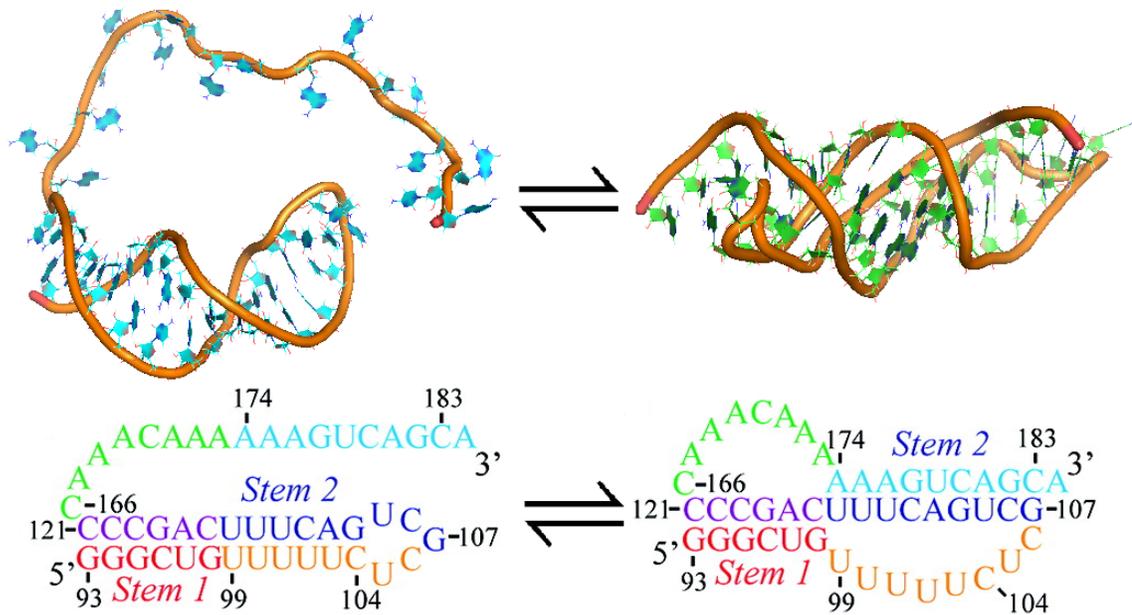


Figure 1.3: Tertiary structures and secondary structures of the telomerase RNA conformational switch. Human telomerase RNA equilibrates between hairpin (left) and pseudoknot (right) structures, acting as a conformational switch and the activity of the conformational switch is linked to the pseudoknot conformation.

tion of the pseudoknot conformation of the TER which is directly linked to the activity of telomerase. The basic secondary structure of the TER conformational switch consists of two stems, S1 and S2, and loops, L1 and L2 respectively [46, 113] (Figure 1.3). *In vitro* experiments and NMR findings showed evidence for the conformational equilibrium between RNA pseudoknot and RNA hairpin structures [120]. Other factors such as the mutations, temperature and crowding may affect the conformational changes of the switch [47].

1.3.3 Adenylate kinases (4AKE-1AKE)

Adenylate kinase (AdK) is one of the most important enzymes whose function is to regulate the concentration of adenine nucleotides and facilitate the interconversion reaction of ATP, ADP, and AMP [121–123]. Adenylate kinase is also sensitive to the cellular energy state changes due to fluctuations in the cellular AMP levels. The catalytic activity of adenylate kinase is linked to conformational changes where the enzyme switches from the open conformation (inactive conformation 4AKE [64]) to a rigid closed conformation

(active conformation 1AKE [122]) in the ligand bound form [124, 125] (Figure 1.4). Large conformational changes of an AdK occur by binding of ATP or AMP to the enzyme [126]. In the present studies, we will try to estimate the crowding effects on the free energy landscape of the conformational equilibrium. The ligand is relatively small sized as compared to crowders and both AdK conformations and therefore it is assumed that the crowding will not affect the thermodynamics of the ligand significantly. As a result, the nonideal contributions to the conformational equilibrium due to crowding on a small sized ligand would be negligible.

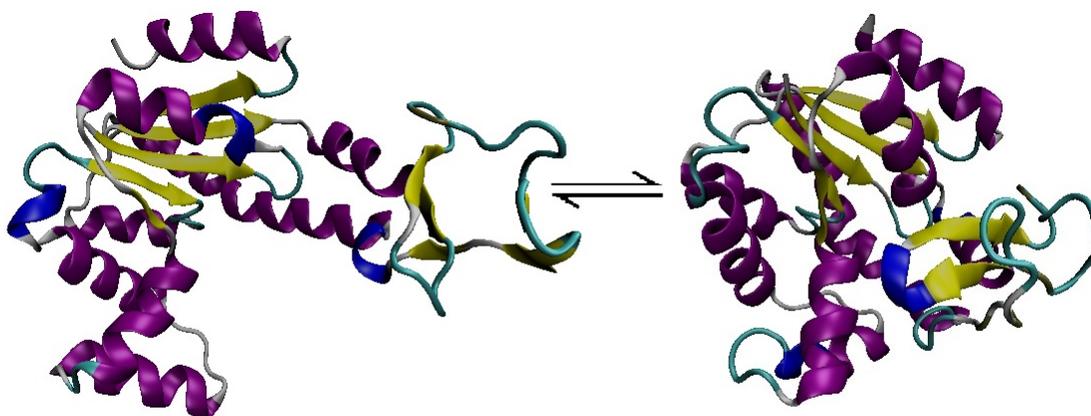


Figure 1.4: Conformational equilibrium between open (4AKE [64]) and closed (1AKE [64]) conformations of adenylate kinase enzyme.

1.3.4 The *lac* repressor (2PE5-2P9H)

Repressor proteins regulate the expression of particular genes by inhibiting their expression in the transcription process. The lactose (*lac*) repressor is one of the common examples of a repressor which limits the availability of proteins that are necessary to metabolise the sugar lactose [127–129]. In the absence of lactose, the *lac* repressor binds to the promoter region on the DNA in a closed conformation (2P9H [129]) (Figure 1.5). The *lac* repressor blocks the RNA polymerase's way on the DNA to transcribe the *lac* genes, and therefore limits the production of lactose metabolism proteins [130]. The conformational equilibrium of the *lac* repressor is driven by binding to allolactose [131]. These conformational changes

occur in the crowded medium and it is interesting to explore the effect of crowding on the energetic landscape changes.

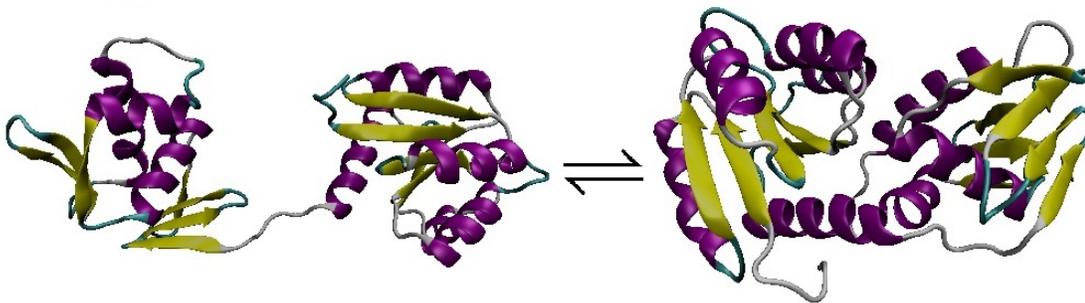


Figure 1.5: Conformational equilibrium between open (2PE5 [129]) and closed conformations (2P9H [129]) of the *lac* repressor. The activity of the repressor is linked to the formation of the closed conformation.

1.4 Macromolecular crowding models

Many experimental and computer simulation models have been developed to determine the excluded volume effects on various types of reactions occurring in crowded media [19, 24, 25, 38, 44, 45, 47, 53, 132]. In addition to experimental and computer simulations, other theoretical approaches such as Brownian dynamics (BD) simulations [133, 134], lattice-based models [134], the Smoluchowski theory [135] and the stochastic approaches [136, 137] to investigate the crowding effects by placing the hard sphere crowders in the three dimensional BD simulations which were found to be very expensive computationally. Further improvements were made to BD simulation models by incorporating crowder free method to enhance the computational efficiency of BD simulations and reproduce results quickly [134]. Typically, the protein and crowders are modeled as hard spheres of approximate sizes in these models and the stochastic nature of the biochemical reactions occurring in the cellular interiors is neglected. In this regard, robust analytical models based on the chemical master equation were developed to estimate the crowding effects on the intrinsic noise associated with the biochemical reactions [138].

The spherical representation of probe and crowder molecules is not a realistic repre-

sentation of the cellular interior which is filled with a variety of macromolecules [135]. Experimental investigations made by different techniques such as tandem affinity purification process, matrix-assisted laser desorption, and liquid chromatography tandem mass spectrometry were applied to determine the size distribution of different macromolecules in the cells [139, 140]. These investigations are helpful to explore the heterogeneity of the crowded medium incorporated by the presence of different types of macromolecules. It turns out that the reaction kinetics and thermodynamics could not follow the law of mass action and power-law approximation in the heterogeneous reaction medium [137, 141]. Further studies showed that the biochemical reactions such as enzymatic reactions follow a fractal-like kinetics in the crowded intracellular environments [141, 142].

The previous investigations were performed by using a variety of computer simulation models. In the present study, a statistical extended model of the scaled particle theory for convex shaped particles, Monte Carlo simulations and the transition state theory are employed to investigate the thermodynamics and kinetics of conformational equilibrium of three systems in crowded medium. In these models, the original shapes of molecules are used in computing the excluded volume by taking into account the atomic coordinate details.

1.4.1 Theoretical model: The scaled particle theory

To estimate the magnitude of the excluded volume effect based on the size and shape of molecules, a theoretical model of the scaled particle theory has been developed. This model estimates the amount of work required to place additional molecules in a fluid medium in the presence of other particles. The outcome relies on the virial coefficients and hard core repulsion interactions between the molecules. One of the earliest models of this type was developed by Laurent and Ogston where they examined the effect of high concentration of hyaluronic acid on protein partitioning [143–145]. Different variants of the scaled particle theory have been developed over the time, where the majority of them treated the fluid

particles as hard spheres, cylinders or fused spheres [146–157]. In 1971, Gibbons [83, 158] developed the most generalized model of the scaled particle theory, applicable to compute the thermodynamic properties of convex shaped particles of different sizes in a crowded medium. Subsequently, Minton and Zhou [29, 33, 37, 81] applied this model to compute the protein activity in a crowded solution by approximating the protein shapes as hard spheres and incorporating the additional attractive interactions. So far, the scaled particle theory model has been very helpful to develop theoretical insights on how the macromolecular crowding affects the protein conformational equilibrium, folding and association reactions based on the excluded volume effect.

Regarding the historical development of SPT models, the first statistical model of hard sphere particles was developed by Reiss *et al.* [159] and further extended to fluid mixtures by Helfand *et al.* [146]. Reiss *et al.* [159] developed an equation of state of rigid sphere fluid particles in 1959 by measuring the density of rigid spherical molecules as a function of distance from a rigid sphere solute particle of an arbitrary size. The accuracy of results depends on the accurate calculations of the virial coefficients and the equation of state computes the first three virial coefficients exactly and gives the next two coefficients within three and five percent error respectively. In the equation of state of a general gas (Equation 1.6) p is the pressure, v is the volume of each molecule, k is Boltzmann's constant, T is the absolute temperature, and the coefficients B , C , ... represent the second, third, ... virial coefficients. These coefficients are a function of temperature and indicate the deviation of a real gas from ideal behaviour. In other words, these coefficients calculate the interaction potential between the molecules which, for hard particles, depends on the shape, size and concentration of molecules in the given volume.

$$pv = kT(1 + Bv^{-1} + Cv^{-2} + \dots) \quad (1.6)$$

In 1964, Lebowitz *et al.* [160], derived a new scaled particle theory model in a simple manner to estimate the thermodynamic properties, i.e. partial molar volume change at constant

pressure in the mixtures of hard spheres. In the following year [148], this model was extended to one, two and three dimensional systems containing mixtures of hard spheres by integrating the exact solution of the radial distribution function [146, 159] obtained from the Percus-Yevick integral equation. Analytical results from the Percus-Yevick integral equation were tested against machine computations (molecular dynamics simulation results) and found in good agreement [160].

Later on, the SPT model was improved by including the solvation contributions [149, 153]. Additionally, numerous bonded hard-sphere (BHS) [161–165] and fused hard-sphere (FHS) models [166, 167] were developed and extended by Boulik [168–171] and Nezbeda [172]. The first FHS model approximated the shapes of linear homonuclear diatomic molecules as fused spheres. Later on, the FHS model was extended to diatomic dumbbell shaped heteronuclear molecules [170, 173], non-linear triatomic [172, 174], and four, six, or twelve hard fused spheres [166], and polyatomic fluids [173].

A new version of the scaled particle theory of arbitrarily shaped fluid particles has been introduced in 1969 by Gibbons [158] to capture the description of systems of arbitrary shaped particles more realistically. This new SPT model was an extension to the theory of Lebowitz *et al.* [148] and calculates the chemical potential and excluded volumes as a function of three geometrical parameters. In the following year, the model [83] was further extended to compute the thermodynamics of convex shaped particles of different sizes. Isihara and Hayashida [175, 176], Kihara [177], Labik *et al.* [174], Tjijto *et al.* [178] and Boublik [179] derived the shape dependent second virial coefficient for different convex shaped particles in terms of three geometrical parameters.

To understand the basic logic of the scaled particle theory model, let us consider a convex shaped particle of characteristic linear dimension R_j placed in a cube of finite dimensions in the presence of background molecules with a characteristic linear dimension R_i . The average radius of curvature, surface area and the volume of the characteristic convex shaped particles is expressed as R , S , and V , respectively. Alternatively, the geometrical

Table 1.1: Geometric parameters of different shapes [180]

Shape	Example	Dimensions	\mathbf{R} (curvature)	\mathbf{S} (area)	\mathbf{V} (volume)
Sphere	Ar	Radius r	r	$4\pi r^2$	$4\pi r^3/3$
Thin Rod	CO ₂	Length l	$l/4$	0	0
Circular disk	C ₆ H ₆	Radius r	$\pi r/4$	$2\pi r^2$	0
Rectangular parallelepiped	C ₂ H ₆	sides l_1, l_2, l_3	$(l_1 + l_2 + l_3)/4$	$2(l_1 l_2 + l_1 l_3 + l_2 l_3)$	$l_1 l_2 l_3$
Thin hexagon	C ₆ H ₆	side l	$3l/4$	$3l^2\sqrt{3}$	0
Regular tetrahedron	CH ₄	side l	$3(\tan^{-1}\sqrt{2}l)/2\pi$	$l^2\sqrt{3}$	$l^3\sqrt{2}/12$
Regular octahedron	SF ₆	side l	$(3/\pi)l \cot^{-1}\sqrt{2}$	$2l^2\sqrt{3}$	$(l^3\sqrt{2})/3$
Cylinder	C ₂ H ₆	Length l , Radius r	$(\pi r + l)/4$	$2\pi r(r + l)$	$\pi r^2 l$
Prolate spherocylinder	N ₂	Length l , Radius r	$(r + l)/4$	$2\pi r(2r + l)$	$\pi r^2(4r/3 + l)$
Oblate spherocylinder	C ₆ H ₆	Length l , Radius r	$(r + \pi l)/8$	$4\pi r^2 + \pi^2 r l + \pi l^2/2$	$\frac{\pi r(4r^2/3 + \pi l r/2 + l^2/2)}{\pi l r/2 + l^2/2}$

parameters can also be represented in terms of the characteristic shape parameters a , b and c . Then the average radius of curvature, surface area and the volume can be expressed as aR , bR^2 , cR^3 . For example, these coefficients a , b and c have values of 1, 4π and $4\pi/3$ for a sphere respectively. These coefficients give the radius of curvature, surface area and volume after multiplying with R , R^2 , and R^3 respectively. However, one can use values of R , S and V directly for a particle of known shape. The shape coefficients for six different shapes are presented by Gibbons [158] and the radius of curvature, surface area and volume for different shapes are provided in table 1.1. The NI part of the chemical potential of the j th type of particle depends on the total number density d , on the geometrical parameters R, S, V whose formulas are given below and on the fraction of occupied volume Y (Equation 1.7 [19]).

$$\frac{\mu_j^{\text{NI}}}{kT} = -\ln(1-Y) + \left(\frac{dS}{1-Y}\right)R_j + \left(\frac{dR_i}{(1-Y)} + \frac{(dS_i)^2}{8\pi(1-Y^2)}\right)S_j + \left(\frac{d}{1-Y} + \frac{d^2R_iS_i}{(1-Y)^2} + \frac{(dS_i)^3}{12\pi(1-Y)^3}\right)V_j \quad (1.7)$$

where:

$$d = \sum_{i=1}^n d_i$$

1.4.2 Computer simulation model: Monte Carlo simulations

Both molecular dynamics (MD) and Monte Carlo (MC) simulation methods are used to perform conformational sampling. The motion of molecules in MD simulation is defined in term of forces on the atoms, calculation of acceleration using Newton's second law and then building the trajectories by integrating the acceleration values over time [181]. The MD simulations could be performed in the Amber [105], CHARMM [106] and GRO-MACS [182] packages. Alternatively, the conformational sampling is performed using the MC algorithms [183]. The MC algorithms generate the new configurations of a molecule

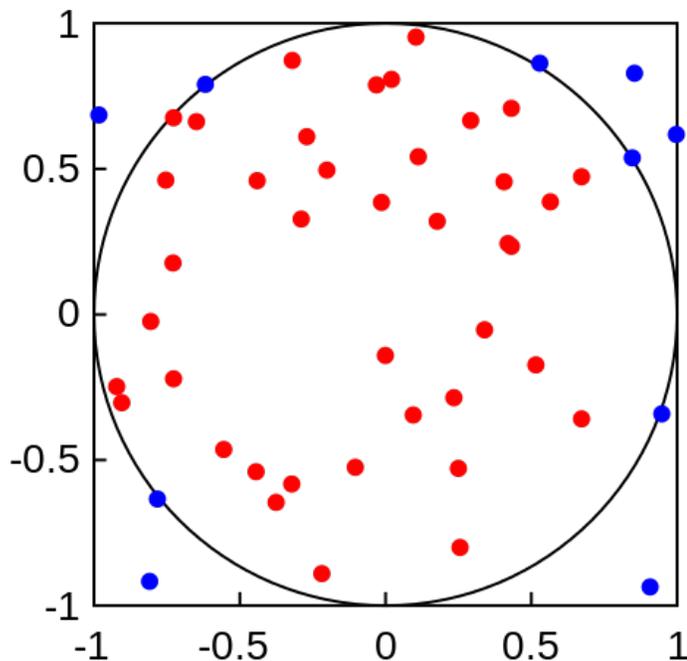


Figure 1.6: An illustration of Monte Carlo integration to estimate the value of π . The area of the circle is computed first by multiplying the area of the square with the ratio of points inside the circle to total number of points, and then the value of π is estimated by dividing the circle area by the square of the radius of the circle. (The figure is taken from <https://commons.wikimedia.org/wiki/File:MonteCarloIntegrationCircle.svg> and made available under the Creative Commons CC0 1.0 Universal Public Domain Dedication licence.)

of interest using stochastic methods. Due to the stochastic nature of MC algorithms, MC models generate a conformational ensemble equilibrated for a particular temperature. The MC algorithms are fast relative to MD methods due to no calculations of forces and accelerations to construct the trajectories. The working principle of MC simulations to perform conformational sampling is to select a random atom or group of atoms and move it randomly. In addition to these internal moves, the whole molecule could also be translated and rotated randomly. After performing each move, the new trial structure is evaluated using the Metropolis criterion based on initial and final energy values after performing an MC move [85, 86].

In addition to the standard MC conformational sampling algorithm, the MC integration technique is used for numerical integration using random numbers. A famous example of

MC integration is the determination of the value of π , where the accuracy of the estimated value is increased by increasing number of sample points (Figure 1.6) [184, 185]. The MC integration technique could also be applied to compute the fraction of available volume in a crowded medium. The working principle of the technique is inserting the protein of interest at random places and orientations in a crowded medium and determining the fractional available volume based on the fraction of successful insertions based on the lack of steric clashes.

1.4.3 The transition state theory

The transition state theory (TST) was originally developed by Henry Eyring [87] for gas phase reactions. The basic idea of TST is that the reactants are in equilibrium with the relatively high energy transition state (TS) (Figure 1.7). The high energy activated complex forms the products and the rate of such reaction is estimated using the kinetic theory. Moreover, TST is also used to investigate the various factors affecting rate constants, in particular thermodynamic quantities like activity coefficients, entropies, temperature, pressure and Gibbs free energies [186, 187]. Consider an open conformation A which is in equilibrium with the transition state TS. The TS forms a final compact conformation B. The reaction involving a conformational change proceeds in the forward direction (Equation 1.8) can be written in term of TST as follows (Equation 1.10):



$$\text{rate} = k_1[A] \quad (1.9)$$



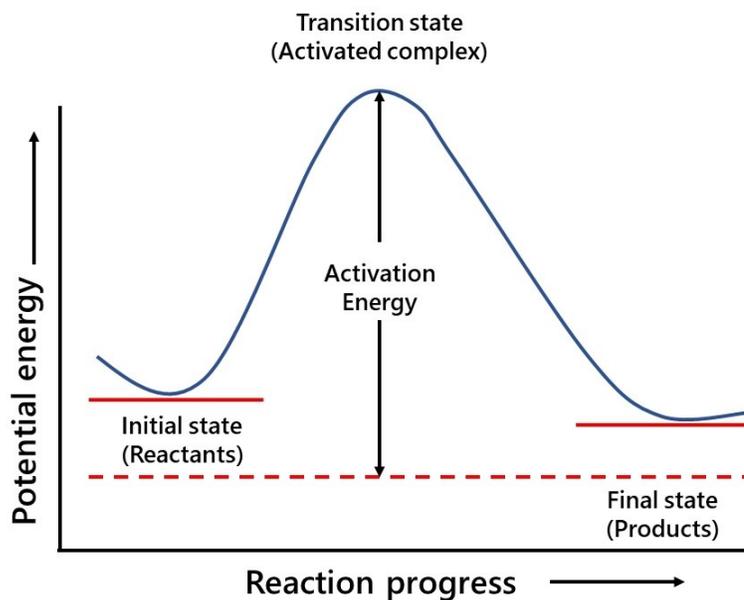


Figure 1.7: Illustration of the formation of high energy transition state of the reactants before converting into final products.

The rate of reaction depends on the concentration of the TS state, therefore

$$\text{rate} = k^\ddagger [TS]$$

The equilibrium constant K^\ddagger under crowded conditions is defined as

$$K^\ddagger = \frac{\gamma_{TS}[TS]}{\gamma_A[A]}$$

where γ_{TS} and γ_A are the activity coefficients of the transition state and the reactant A respectively. Rearranging the expression for the $[TS]$ value,

$$[TS] = \frac{K^\ddagger \gamma_A [A]}{\gamma_{TS}}$$

The rate of reaction using the TST model is therefore;

$$\text{rate} = k^\ddagger [TS] = k^\ddagger \left(\frac{K^\ddagger \gamma_A [A]}{\gamma_{TS}} \right)$$

Comparing the TST rate equation with the reaction rate from Equation 1.9, we observe

$$k_1 = k^\ddagger K^\ddagger \left(\frac{\gamma_A}{\gamma_{TS}} \right)$$

Alternatively, the final rate of reaction can be written as

$$k_1 = k_0 \left(\frac{\gamma_A}{\gamma_{TS}} \right) \quad (1.11)$$

where $k_0 = k^\ddagger K^\ddagger$ is the rate constant under dilute conditions.

Under ideal solution conditions the activity coefficients are taken as one in the TST expression (Equation 4.2). This approximation underestimates or overestimates the rate constant by ignoring the higher thermodynamic activities in crowded solutions. It depends on the ratio of activity coefficients of a reactant and the transition state. If, for example, the TS is less compact than A, then $\frac{\gamma_A}{\gamma_{TS}} < 1$, and the dilute-solution rate constant would overestimate the rate constant in the crowded solution. It is proposed that the accurate reaction rates could be achieved by incorporating the activity coefficient values which are computed by the scaled particle theory and MC simulations.

1.5 Objectives of the present study

Macromolecular crowding has a great impact on cellular processes such as the catalytic activities of proteins by favouring different conformations. A successfully developed kinetic theory including macromolecular crowding effects would be helpful to understand the behaviour of biochemical processes such as conformational equilibrium in detail. The objectives of the current study are classified into the following two key sections:

1. Preparation of crowded media by packing diverse and dynamic solution structures of 8 kDa PEG. This section will be composed of the selection of suitable computer simulation models (i.e. MC and MD simulations) to generate 8 kDa PEG conformations, packing and further equilibration of packed crowded media. This section will

also help to evaluate the aggregation behaviour of PEG after packing and equilibration process. The details regarding the selection of the suitable methods to pack and equilibrate the crowded medium and the corresponding results will be covered in the ‘Methods’ (Chapter 2) and ‘Construction of crowded medium’ (Chapter 3) respectively.

2. The development of appropriate models (i.e. SPT and MC models) to compute the thermodynamic activities of macromolecules of interest with minimum geometrical approximations and subsequently estimating the kinetics of conformational equilibrium via the transition state theory by incorporating the thermodynamic activities calculated in crowded solutions. This section will be composed of the extension of the SPT model and the development of the MC method to estimate the thermodynamic activities. The development of these models and the corresponding outcomes will be covered in ‘Methods’ (Chapter 2) and ‘Conformational equilibrium in crowded media’ (Chapter 4) respectively.

Chapter 2

Methods

The goal of this study is to investigate the crowding effects on conformational equilibrium by computing thermodynamic activities and fractional available volumes through analytical and computer simulation models. In this chapter, the detailed procedures used to determine the macromolecular crowding effects in each model are presented. In this context, two types of models are discussed, namely the scaled particle theory (SPT) [83, 146] and Monte Carlo (MC) simulations [188–190]. The SPT is a famous analytical model to compute the macromolecular crowding effect by calculating the excluded volume and chemical potential in the crowded medium using simple geometric approximations. The purpose of this chapter is to present the extended SPT and MC methods that will be used to estimate the crowding effects.

Figure 2.1 describes the overall setup applied in this work. The scheme includes all the key steps such as the conformational sampling of crowding agent molecules, packing and equilibration of simulation boxes and the calculation of fraction of available volumes and chemical activities. The process starts from the construction of conformational ensembles of crowders. In this regard, Monte Carlo and Molecular Dynamics sampling techniques are employed, which may require development of forcefield parameters for the crowder prior to performing the MD or MC sampling. Subsequently, the crowders are used to prepare the crowded environments. In the last step, MC and SPT calculations are performed to calculate the effect of crowding on the thermodynamics of conformational equilibrium.

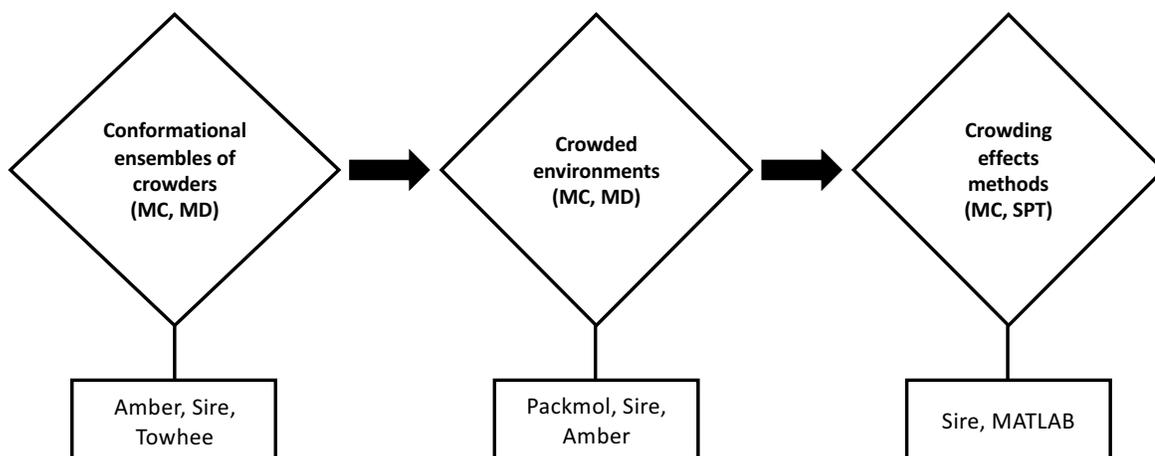


Figure 2.1: The schematic diagram represents the complete work-flow and techniques used in investigating the macromolecular crowding effects on the conformational equilibrium. The diamond shape represents the general step and the corresponding linked rectangle carries the appropriate computer programs to complete the task. Three major steps were performed in this investigation. The first step is the preparation of crowder molecules. This could be achieved through MD and MC conformational sampling with the Amber, Sire and MCCCSTowhee programs. The next step is the preparation of crowded environments, using these conformational ensembles of crowders. This step requires optimized packing and equilibration of the packed boxes. In the last step, the thermodynamics and kinetics of the conformational equilibrium is computed with the MC or SPT models under the crowded conditions.

2.1 Ensemble of PEG conformations

Polyethylene glycol (PEG) is commonly used in computer simulations and experiments to mimic the crowding *in vivo* [80, 98, 111, 191] but there is no representative crystal structure of high molecular weight PEG found in the protein data bank. A dimer of the PEG monomer ethylene oxide (<http://www.rcsb.org/pdb/ligand/ligandsummary.do?hetId=PEG>), is found in many different crystal structures as a ligand but this PEG fragment requires an additional 180 monomers to construct an 8 kDa PEG. Moreover, the crystal structures found in previous reports [55, 89, 93, 101, 109] are not directly relevant to the solution structures. To solve the problem of the missing PEG structure, the conformational sampling simulations are performed in two steps. In the first step, the structure of 8 kDa PEG is constructed and optimized. This single structure is not a representative of solution structures as a PEG solution contains random conformations of PEG [58, 92]. Therefore, conformational en-

sembles of PEG are generated by performing MC and MD simulations.

These computer simulations require forcefield parameters for the PEG if these parameters are not provided in the program of interest. These forcefield parameters are essential to perform simulations and helpful in evaluating the conformational changes by calculating the total energy of the structure. MCCCSTowhee [104], Sire [192, 193], and Amber [105, 194] packages were employed to construct the ensembles of PEG conformations. MCCCSTowhee provides general forcefield parameters that facilitates the construction of PEG, whereas Sire and Amber do not. The PEG forcefield parameters are critical to perform simulations in both programs. A number of publications on the development of the PEG forcefield parameters have been reported by different researchers over time [98, 132, 195–197]. However, PEG forcefield parameters did not come by default in Amber. The PyRED server [198] was used to construct the forcefield parameters for PEG which allows us to perform conformational sampling simulations. This section explains the details of forcefield parameters development and subsequently the details of MC and MD sampling methods that are employed to construct an initial PEG and its conformational ensembles.

2.1.1 Forcefield parameters for PEG

The automated tools for building forcefields reduce the probability of errors that arise when a forcefield is built manually. Many approaches such as the Mulliken [199], Lowdin population analysis [200], atoms in molecules theory [201], the AMI-BCC method [202, 203] and many other models [204–207] have been developed to derive the atomic charges and subsequent parameters with desired accuracy. However, none of the approaches has been proven to be the best in all respects [208]. To build the missing PEG forcefield parameters in Amber and Sire, the RESP (the restrained electrostatic potential) ESP (electrostatic potential) charge Derive (R.E.D.) toolkit was used [208, 209].

The RESP ESP charge Derive (R.E.D.) toolkit provides a straightforward way to generate the forcefield parameters for molecules that are not included in the standard Amber

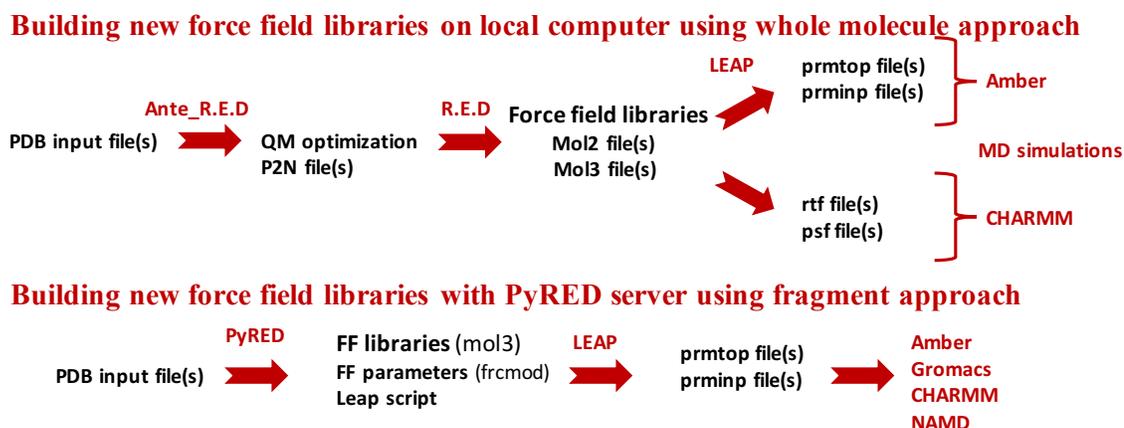


Figure 2.2: The schematic diagram represents the steps to carry out by R.E.D and PyRED server to construct the forcefield libraries of non-standard molecules.

forcefield with a two-step calculation [208, 210]. The first step is to compute the molecular electrostatic potential (MEP) surface around the optimized structure using a quantum mechanics (QM) program while the RESP and ESP charges are determined in the second step by fitting the charge values to reproduce the MEP surface. Geometry optimization and MEP surface calculations are performed using QM programs such as Gaussian09 [211], GAMESS [212, 213] or FIREFLY [214] while charge fitting to reproduce the MEP surface can be done using the RESP [209] or FITCHARGE [215] programs. The RESP, ESP charges and forcefield parameter of PEG can be generated using *antechamber* (Amber) or the R.E.D. program (<http://q4md-forcefieldtools.org/>). There are two ways to construct the PEG forcefield library files in the R.E.D program. The first option is to generate all the files on a local computer with Perl, a quantum mechanics optimization program such as Gaussian09, GAMESS, or FIREFLY, and *Ambertools14* (*xleap/tleap*). However the other way is simpler and all the jobs can be executed on the PyRED server [198]. The PyRED server offers two approaches, namely the “whole molecule approach” and the “fragment approach” to construct forcefield parameters. The required input and resultant output files description for both approaches is available at <http://q4md-forcefieldtools.org/>. The global procedure regarding development of forcefield parameters on R.E.D via a local machine and the PyRED server is illustrated in Figure 2.2.

2.1.2 Case 1. Whole molecule approach

Four key steps, formation of the optimized structure, determination of the MEP, calculation of atomic charges by reproducing the MEP, and generation of *top/crd* files are performed as follows:

1. The PEG structure was constructed in GaussView 5.0 and the geometry optimization was performed in the Gaussian09 QM program.
2. The first computation of the R.E.D program using a PDB file generates the three new files namely PDB, P2N and the script files necessary for QM optimization calculations in the local directory. The P2N file is important because it contains the detailed information of atom names and their connectivities, which are required in the charge fitting step and for creating the *top/crd* file.
3. The final step involves the generation of parameter files by executing the *leap* script in the presence of parameter files.

2.1.3 Case 2. Fragment approach

The forcefield parameters of the PEG polymer can also be developed easily through using a R.E.D.S Dev server at <http://q4md-forcefieldtools.org/>. A two-step fragment approach requires a PDB file, and two input files (*System.config* and *Project.config*) to construct parameters. (Input files are provided in Appendix A.1.1.) In the first step, the molecule is split into three fragments namely, A, B and C (Figure 2.3) by calculating the charges on the three groups. Before proceeding with the first step, the ‘A’ terminal has to be replaced with a methyl group because the program accepts only heavy atoms on a terminal site rather than a single hydrogen as fragments. If the hydrogen at the ‘A’ terminal is not replaced then the program produced only a single fragment rather than the three desired fragments. The second step is similar to the previous ‘whole molecule’ approach that constructs the forcefield parameters. These are the simplified key steps to implement the fragment approach for PEG:

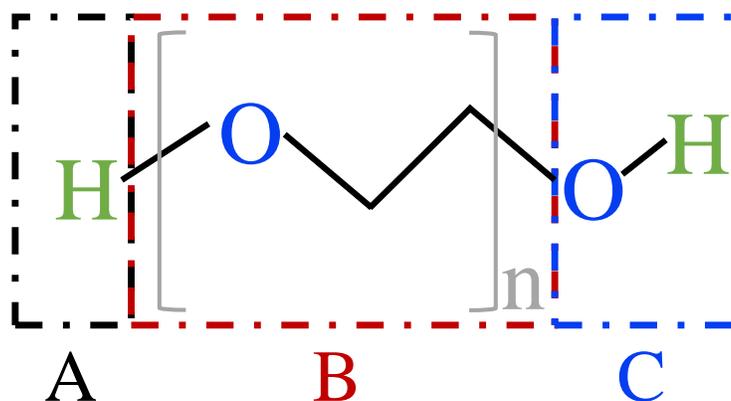


Figure 2.3: Definition of three PEG fragments as 'A', 'B' and 'C' where 'B' is the repeating monomer.

1. Generate the structure of a PEG molecule containing one monomer only ($n = 1$) using the GaussView 5.0 package, with unique atomic names.
2. PyRED requires *System.config* and *Project.config* configuration files to run jobs on the server. The *System.config* file contains details about the geometry optimization QM method, whereas the *Project.config* configuration file contains the information on charge constraints. The charge constraints are required to form desired fragments. The QM calculations were performed with Gaussian09 using Hartree Fock (HF)/6-31G (d) [216], density functional theory (DFT) B3LYP/6-31G (d) [217, 218], and Møller-Plesset perturbation theory of second order MP2/cc-pVTZ methods [219, 220].

Two charge constraints are applied to generate and compute charges on three fragments in a two-step process. In the first step, charges on the 'A' and 'C' terminals (methyl and hydroxyl groups respectively) are calculated by defining single INTRA-MCC2 charge constraint (Equation 2.1).

$$MOLECULE1 - INTRA - MCC1 = 0.0 \mid 1 \ 2 \ 3 \ 4 \ 12 \ 13 \mid Remove \quad (2.1)$$

where *MOLECULE1*, *INTRA*, *MCC1* represents the molecule name, intra-molecular charge constraint, and molecular charge constraint on two groups in a given molecule

respectively. The charge constraint is assigned a zero value which represents the overall charge of the molecule. In the next section, the atomic positions of the terminal groups ('A', and 'C' respectively) are defined and the *Remove* specifier cuts the structure.

After completing the job, charges on 'A' and 'C' terminals are calculated by taking the average of the sum of individual atomic charges of 'A' and 'C' terminal. Mathematically, it can be expressed by the following simple relation:

$$\text{Total charge} = |q_{\text{CH}_3}| + |q_{\text{OH}}| \quad (2.2)$$

$$\text{Fragment charge} = \frac{|\text{Total charge}|}{2} \quad (2.3)$$

Both terminal groups get equal and opposite charges. Thus, the methyl group has positive charge and hydroxyl has negative charge in the particular case considered here. In case of identical terminal groups, for example methyl on both sides, one terminal connected with subsequent atom of lower electronegativity will get positive charge and the other terminal attached to a subsequent atom of higher electronegativity will get negative. This charge definition is essential to build neutral fragments. For example, the charge values for the 'A' and 'C' terminals are found to be +0.230 and -0.230 respectively. The charge value for the central fragment is calculated by running a second PyRED job with two INTRA-MCC2 charge constraints on each terminal group.

$$\text{MOLECULE1} - \text{INTRA} - \text{MCC2} = 0.230 | 1 2 3 4 | \text{Remove} \quad (2.4)$$

$$\text{MOLECULE1} - \text{INTRA} - \text{MCC2} = -0.230 | 12 13 | \text{Remove} \quad (2.5)$$

3. Finally, forcefield parameter library files for any length of PEG molecule can be constructed by repeating the central fragment in the growing sequence of polymer in

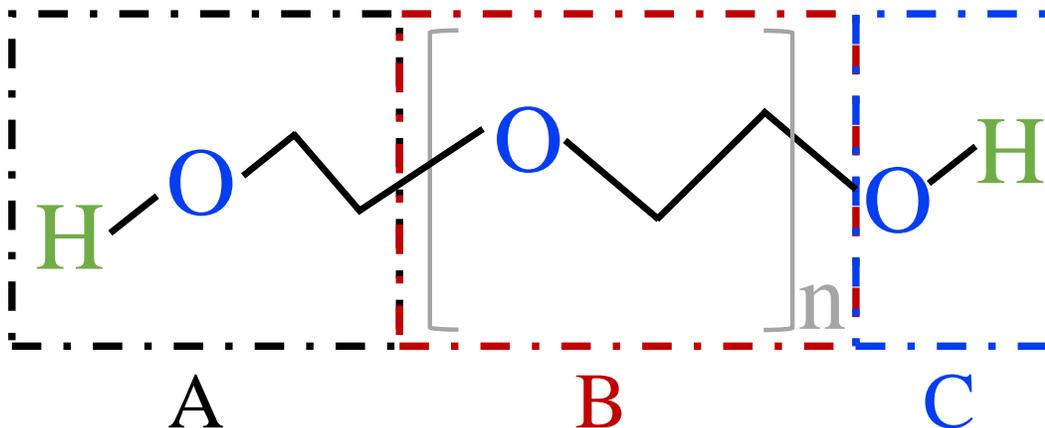


Figure 2.4: Three fragments namely, *A*, *B* and *C*, of a PEG molecule without methyl substitution.

xtleap/tleap script file.

$$PEG = [A - (B)_n - C] \quad (2.6)$$

where 'A', 'B', 'C', and 'n' represents methyl, central, and hydroxyl terminals and number of central monomers respectively.

The resultant PEG has one methyl terminal instead of the original hydrogen terminal. Winger et al. showed that the terminal methyl groups are responsible for compact structure formation during MD simulations [98]. Therefore, an attempt was made to construct the initial PEG structure with a hydrogen atom as the 'A' terminal by attaching a whole PEG residue on terminal 'A' (Figure 2.4). The forcefield parameters were built by applying the fragment approach as discussed in the present section. The results of these forcefields will be discussed in chapter 3.

2.1.4 MC sampling in MCCCSTowhee

MCCCSTowhee [104] was used to construct an initial optimized PEG structure at first, and subsequently conformational ensembles by conducting MC simulations. MCCCSTowhee was developed to perform vapour-liquid phase equilibrium simulations for flexible molecules using the Gibbs ensemble. It provides more than seventy built-in forcefields,

which facilitates the construction and optimization of large structures through MC conformational sampling. We experimented with MC simulations under different conditions such as using either NPT [221] or NVT [222–224] ensembles, different random number generators and different temperatures, pressures and box dimensions to maximize diversity of ensemble structures. The MC simulation protocol in MCCCS Towhee could be described in four steps:

1. Define the input parameters in MC protocol such as the type of ensemble, temperature, pressure and length of MC simulations.
2. Define the box dimensions, and the output frequency of the desired results such as how frequently the energy and structure coordinates are written to output files.
3. Select appropriate forcefield parameters and type of algorithm to perform MC moves on the structure.
4. Construct the desired structure by defining atomic names, charges and connectivities.

In the first simulation protocol to construct and optimize the PEG structure, NPT [221] ensemble MC simulations using the Amber96 [225] forcefield at 101 kPa pressure and 300, 600 and 1200 K temperatures were performed. The NPT ensemble was chosen because the calculations were found to be less expensive than NVT ensemble calculations. Since the aim is to enhance the conformational sampling at this point, therefore the MC simulations were performed at three temperatures, i.e. 300, 600 and 1200 K. The initial PEG molecule was built by joining 141 O–CH₂–CH₂ monomers in a 100 × 100 × 100 Å³ periodic box and optimized by performing 1.2 million Monte Carlo moves at 1200 K. Each MC move involves volume change to maintain a constant pressure, intra-molecular bond length and angle changes, and translation movement about the center of mass. The frequency at which each move is performed can be adjusted by defining the probability values between zero to one. The performance of any particular move can be suppressed by assigning the probability of zero. After equilibration with 1.2 million MC moves, an additional 180,000 MC

moves were performed to save the structure after every 60,000 moves for a total of three equilibrated structures to be used as starting points for the generation of conformational ensembles. These three PEG conformations differ significantly in radius of gyration from each other. To generate the PEG conformational ensembles in the second step, a total of nine 12-million-step-long MC simulations were performed at 300, 600, and 1200 K using three equilibrated structures obtained in the earlier equilibration step. The input file for MCCC'S Towhee is provided in Appendix A.2.

2.1.5 MC sampling in Sire

Sire is a free, open source molecular simulation framework that allows the users to write and develop new algorithms to conduct numerical and molecular simulations [193]. Sire is composed of a collection of independent libraries written in C++. These libraries are used as building blocks or modules that contain a set of attributes and operations to perform particular tasks. For example, 'Sire.Move' is a module that provides all necessary functions to perform all types of intra- and inter-molecular moves on the structure. By connecting these blocks via a Python interface, one can develop, perform and analyse MC simulations. Further, Sire is compatible with the Amber package and offers a complete implementation of the Amber [194, 226], OPLS, [227] and CHARMM [106] forcefields. There are three ways to accomplish MC sampling with Sire (Figure 2.5). Following are three key steps to construct a structure and conduct MC conformational sampling using Sire (all Sire inputs files are provided in Appendix A.3.2):

1. Load the Sire libraries.
 - The libraries contain all the necessary information such as atomic names, charges, and parameters to calculate energies.
2. Load the molecule from a Sire script, PDB file, or Amber topology and coordinate (*top/crd*) files.

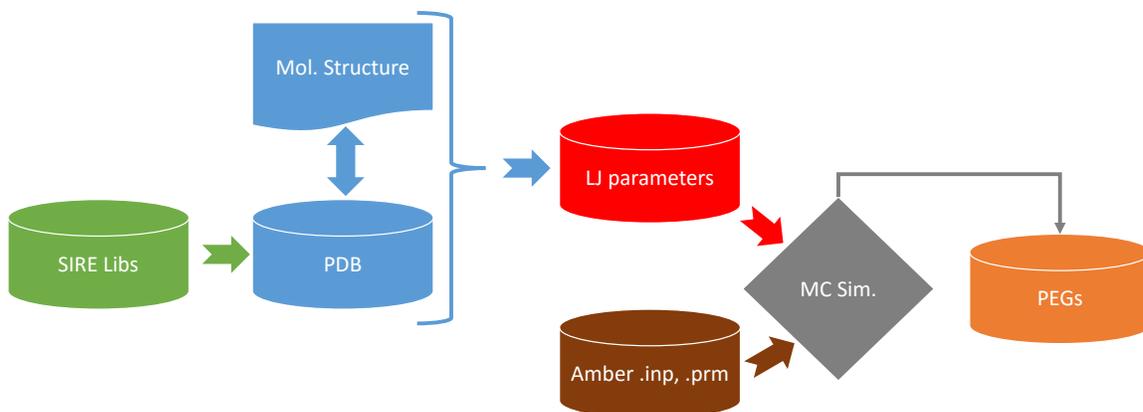


Figure 2.5: The schematic diagram represents the three key steps necessary to perform MC conformational sampling in Sire. In the first step, the Sire libraries are loaded, followed by loading the molecular structure in the form of PDB or Amber coordinate and topology files. The initial structure can also be constructed using a script. The script or PDB formats require Lennard-Jones (LJ) atomic charges and energy parameters, whereas Amber input *.prmtop* and *.inpcrd* files do not require any LJ forcefield parameters to initiate the MC simulations.

- In the Sire script, the new molecule can be constructed using the “Molecule()” constructor. This is the most complicated and tedious choice, requiring a lengthy script in order to populate the constructor with atomic names, connectivities, coordinates and Lennard-Jones (LJ) forcefield parameters. The advantage of this method is that Sire libraries provide all the necessary information regarding construction of the molecule and there is no need to build any forcefield parameter libraries as we do in the majority of simulations. The drawback of this choice is that the intra-molecular energies cannot be calculated in simulations with intra-molecular moves.
- The easiest and most efficient way to construct a molecule is with a structure builder program such as Gaussview [228], Chemdraw [229], or Avogadro [230]. Then the corresponding Amber topology *.top* and coordinate *.crd* files are generated using the *tleap* utility program.

3. Perform internal moves to conduct MC conformational sampling.

- Sire performs MC moves on the molecule with the help of a random number generator. The random numbers are used to pick the random bonds, angles and dihedral angles of a molecule and to perturb the selected bonds, angles and dihedrals by a randomly selected amount. After performing each move, the algorithm performs the canonical acceptance test to determine whether the given move is accepted or not. The energy difference is calculated by taking the difference of the energies before and after the move and then the canonical acceptance test uses the computed energy difference to calculate the values of x according to equation 2.7 [86]. Moves are accepted if they have a negative ΔE or if x is greater than a randomly generated number between 0 to 1.

$$x = \exp(-\Delta E/kT) \geq \text{random}(0,1) \quad (2.7)$$

where ΔE is the energy difference before and after performing an MC move, k is the Boltzmann constant, and T is the temperature in Kelvin. It is noted that x is a function of temperature, and that the number of accepted moves will increase as the temperature rises. Moreover, the number of accepted moves is also increased significantly if bonds and angles are perturbed by a small magnitude. This will take a long time to converge the system. The larger moves will help to explore the conformational space quickly, whereas small moves are useful to optimize the structure.

The equilibrated PEG structure in MCCCSTowhee and a linear PEG structure are used as starting points to generate PEG ensembles. The input Amber *.top* and *.crd* files are prepared using PEG parameters along with Amber96 forcefield parameters. In the MC simulation protocol, 2-million-move-long MC simulations were performed at 101 kPa and using temperature cycles alternating between 1200 and 300 K. The first 1000 internal moves were performed at 1200 K and then a structure is saved after performing an additional 1000

moves at 300 K. This temperature quenching approach was not only applied to enhance the sampling of the energy and conformational spaces but also to save the conformations at a physiological temperature. Each move perturbs the bond lengths and bond and dihedral angles randomly between -0.5 to $+0.5$ Å and -20 to $+20$ degrees respectively. The ranges of these moves were selected based on trial and error and these values produced reasonably diverse conformational ensembles in a reasonable amount of time.

2.1.6 MD sampling in Amber

Finally, MD simulations have been employed in Amber to construct the library of PEG conformations. In general, the Amber MD simulations are accomplished in two steps, namely minimization and MD simulations (Figure 2.6). The minimization is necessary to remove intermolecular steric clashes/overlapping while MD simulation samples the conformational space. In general, the Amber MD simulations are accomplished in two steps, namely minimization and MD simulations. The minimization is necessary to remove intermolecular steric clashes/overlapping while MD simulation samples the conformational space.

A library of PEG conformations was built by performing a two-step MD simulation on the PEG structure. The initial system containing a PEG molecule was minimized using the implicit solvent model (the standard pairwise generalized Born model [231]) with 5000 steepest descent and 2500 conjugate gradient minimization steps. The cut-off range for long-range non-bonded interactions was set to 10 Å. In the final step, 10 ns long MD simulations were run with a 1 fs time step. The temperature of the system was maintained at 300 K using the Langevin thermostat. All input files are provided in Appendix A.4.

2.2 Packing and equilibration

The next step is to pack and equilibrate the simulation boxes from 0.1 to 0.6 g cm⁻³ concentration. The Packmol package [232, 233] is used to pack the simulation boxes. Pack-

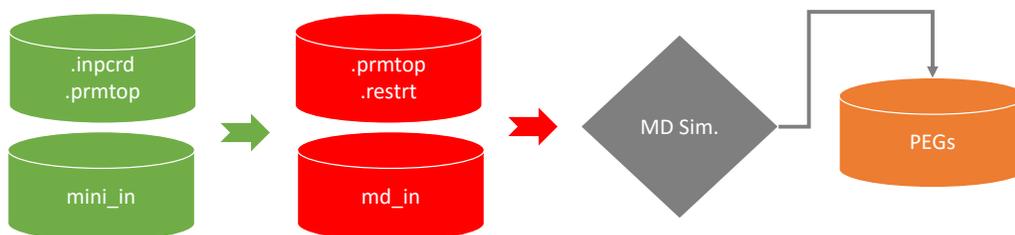


Figure 2.6: This schematic diagram represents the MD simulations performed with Amber. The process starts with PEG coordinate *crd* and topology *top* files. The ‘mini_in’ file contains the input parameters necessary for the minimization step. On completion of minimization, a new *.restrt* coordinate file is created. The resultant *.restrt* coordinate file and ‘MD_in’ file are used to conduct the MD simulations. The ‘MD_in’ file contains all necessary inputs such as length, step size and output files for MD simulations.

mol is a simple program that facilitates the construction of boxes with desired dimension, shape and concentration. Random conformations of PEG were chosen from the conformational libraries and packed in a cubic box of dimension $300 \times 300 \times 300 \text{ \AA}^3$. The details on the packing algorithm are described by Martinez [232, 233]. In the packing algorithm, tolerance is an important parameter to enhance the packing quality by keeping the minimum boundary-boundary distance between molecules without steric clashes. The default value of tolerance is 1 \AA and we used 3.0 to 5.0 \AA in packing of simulation boxes. The default tolerance can also be used to pack the systems. However it can produce systems with a tight packing at higher concentrations and result in very high total energies. A large tolerance facilitates the optimized packing without steric clashes but it takes a long time. Sometimes, it is hard to get a packing configuration satisfying the large tolerance criterion. In this situation, the program keeps the best packed configuration (input file available in Appendix A.5). Figure 2.7 illustrates a simulation box packed with PEG molecules.

The simulation boxes were packed using the PEG conformations prepared under dilute conditions. Therefore, in order to consider the effect of crowding on the distribution of PEG conformations, the six simulation boxes were further equilibrated using the three approaches as explained below.

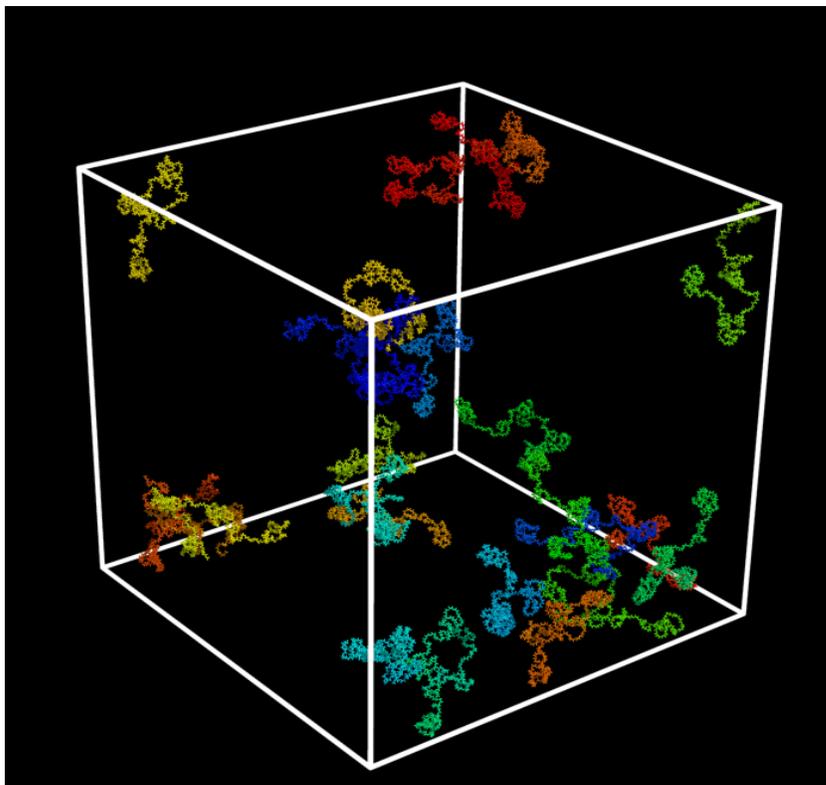


Figure 2.7: The packing of PEG at 0.1 g cm^{-3} concentration in a cubic box of $300 \times 300 \times 300 \text{ \AA}^3$ dimensions with Packmol using 3.0 \AA tolerance. The different colours are used for illustration purposes and represent the individual molecules.

2.2.1 Minimization with Sire

MC rigid body and internal moves were performed on the molecules in the simulation boxes (input file available in Appendix A.5.1). The rigid body moves are responsible for translating and rotating the molecule while internal moves fold/unfold the structure by moving randomly chosen bonds, angles and dihedral angles. The acceptance criterion for MC moves is the standard canonical MC acceptance test at 300 K temperature (Equation 2.7). The algorithm performs 1000 iterations in a series to minimize the system in which each iteration runs 10,000 in total MC rigid body and internal moves. The algorithm saves the restart file and prints out the ratio of the number of accepted to rejected moves after every 100 iterations. After completing the 1000 iterations, the algorithm runs an additional 2×10 iterations and populates these two windows with energy values. These energy values are used in a Student's t test [234, 235] to determine whether the system has equilibrated or not.

This test compares the energy values stored into two windows and checks the condition if the significance level $s < 0.1$ is satisfied to terminate the simulations, otherwise continue the loop for an additional 2×10 iterations until the condition is satisfied.

2.2.2 Swapping equilibrium with Sire

The algorithm swaps a randomly chosen molecule in the simulation box with a randomly selected molecule from the PEG library (input file available in Appendix A.5.2). Successful swaps were determined by the standard canonical MC acceptance criterion [86] at 300 K (Equation 2.7). If the molecule insertion is accepted, the algorithm keeps the configuration for the next step; otherwise, it returns the simulation box to its pre-swap configuration and starts the process over, selecting a new molecule for swapping. The algorithm places the molecule selected from the library randomly within the simulation box at a random orientation. It does not generate internal moves in any of the molecules, it is being assumed that the library contains a reasonable sampling of the conformational space. The swapping script performs 0.1 million iterations by default and saves the restart file at every 10,000 steps. The Student's t test with the same criterion as in method one is applied to stop the calculations. Equilibration by swapping is time consuming given that successful insertions may not occur after a certain number of successful insertions. Therefore, it is good to perform the Student's t test after completing 10 million iterations to allow the system to run for enough time to see if there are any successful insertions before employing the t test to terminate the simulations.

2.2.3 MD Amber simulations

MD simulations were performed under the same MD protocol as described for a single PEG molecule to equilibrate the simulation boxes (input file available in Appendix A.5.3). However, with this protocol, the pressure fluctuates and results in volume changes. It is important to keep the total volume fixed after equilibration. Therefore, the simulation boxes were equilibrated under periodic boundary conditions. In the first step, the simulation boxes

were minimized by performing 1000 and 500 steps of minimization and steepest descent minimization respectively using constant volume periodic boundary conditions with 10.0 Å cut-off range. In the second step of MD simulations, 20-40 ns long simulations were performed at a constant temperature of 300 K and constant pressure periodic boundary conditions with an average pressure of 1 atm. The MD simulation time increased monotonically with concentration of simulation box.

2.3 Fractional available volumes calculations

Fractional available volume in the packed simulation boxes was assessed by performing MC simulations in the Sire molecular simulation framework [16, 17]. Two different algorithms, termed parallel-energy (Appendix A.6.1) and parallel-distance (Appendix A.6.2), were developed. In both algorithms, a randomly oriented probe molecule (protein/RNA) is first placed at a random position inside the simulation box and the successful and failed trials are chosen based on the steric clashes. The fraction of available volume then can be calculated from the ratio (p') of successful insertions to total trials using the following equation.

$$p' = \frac{n_{\text{successful}}}{n_{\text{total}}} \quad (2.8)$$

The threshold energy criterion of 50,000 kcal/mol was set to determine whether there is a steric clash or not. The threshold energy criterion was found by trial and error. One way to predict the threshold energy criterion is to compare the energies of reference and test systems. The reference system contains all the molecules including background (PEGs) and probe molecule (RNA/protein). In contrast, the test system used to insert the probe molecule contains only the PEG background molecules at the same concentration of PEG as in the reference system. The two systems were prepared under the same packing conditions (tolerance and number of steps for packing) in the Packmol package. Reference system energies calculated using Sire ranged from -500 to 500 kcal/mol. The threshold energy at which a steric clash was recognized was set at 100 times the order of magnitude of

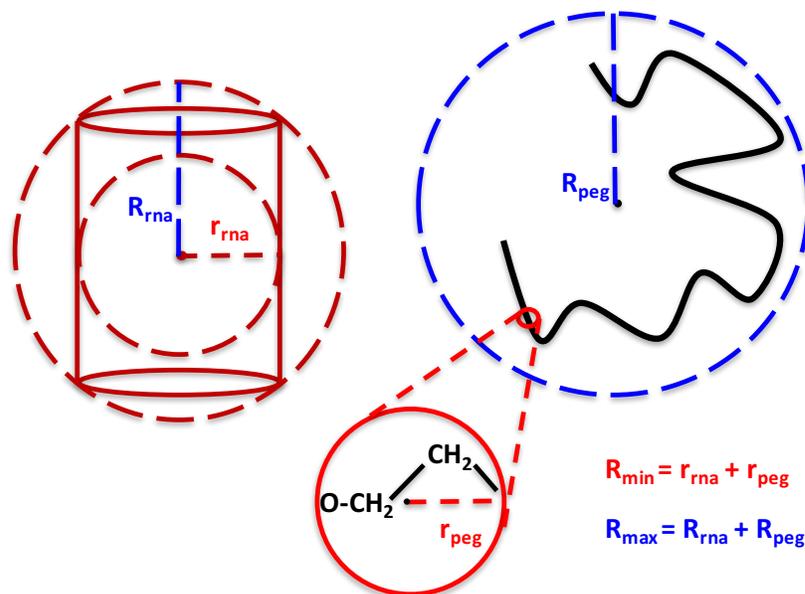


Figure 2.8: Estimation of cutoffs for atom-by-atom checking for steric clashes. The basic concept is described by providing an example where the probe RNA molecule and the PEG crowders are considered roughly cylindrical and spherical respectively. The relevant dimensions of the two molecules are added to generate the bounds R_{min} and R_{max} used as cutoffs in our calculations. The RNA studied here has a nearly cylindrical shape, so our estimates of r_{RNA} and R_{RNA} give a reasonable representation of the geometry of this molecule. On the other hand, PEG adopts a variety of conformations in solution. For r_{PEG} , we used the radius of a PEG monomer, yielding a very conservative estimate for R_{min} , thus avoiding false positives relative to a direct atom-by-atom test for clashes. For R_{PEG} , we used the radius of a bounding sphere for a typical PEG conformation, again yielding a conservative estimate of R_{max} , this time avoiding false negatives.

the reference system energies, i.e. 50,000 kcal/mol. The most accurate available volumes can be measured using the parallel distances algorithm. The steric clashes are determined on the basis of the distance between the atoms of probe and background molecules using the van der Waals radii. The minimum threshold distance was set using the sum of the van der Waals radii for each pair of atoms belonging respectively to the probe and a background molecule. The program calculates the distances between the geometric centroids of the probe molecule and all background molecules, and sorts them in ascending order. A simple test on the centroid-to-centroid distances was implemented in order to find the cases for which atom-by-atom checks for clashes were required, as illustrated in Figure 2.8. Molecules whose centroids were closer than R_{min} (10 Å for our example system

composed of PEG and RNA molecules) were immediately determined to clash, and thus the insertion trial to have failed, while molecules whose centroids were further than R_{max} (60 Å for our system) were determined to be non-clashing. Molecules whose centroids were between these two extremes were checked atom-by-atom for steric clashes.

The computational cost of both programs depends on the sizes of the molecules and on the concentrations. Energy calculations in Sire are very fast, so the energy threshold algorithm has a significant speed advantage over the distances measuring algorithm. The use of cutoffs to avoid calculating all pairwise atomic distances however greatly improved the speed of the parallel distance algorithm.

The flow chart summarises both algorithms for steric clash determination (Figure 2.9). Script files implementing these methods are provided in supplementary data. In the final step, the fraction of available volume is converted to the non-ideal chemical potential that facilitates the comparison of the scaled particle theory and computer simulation results. Mathematically, the fractional available volume in the crowded solution can be represented with equation 2.9 where p' represents the ratio of successful insertions to total trials as defined in equation 2.8.

$$\frac{\mu^{NI}}{kT} = \log \left(\frac{1}{p'} \right) \quad (2.9)$$

This expression is derived by considering a protein molecule (P) in equilibrium in dilute and crowded medium.



The free energy change for the reaction can be written as

$$\Delta G = kT \ln \left(\frac{\alpha_{crowded}}{\alpha_{ideal}} \right) \quad (2.11)$$

α is used to represent the activity of the solute instead of a which is a shape coefficient in

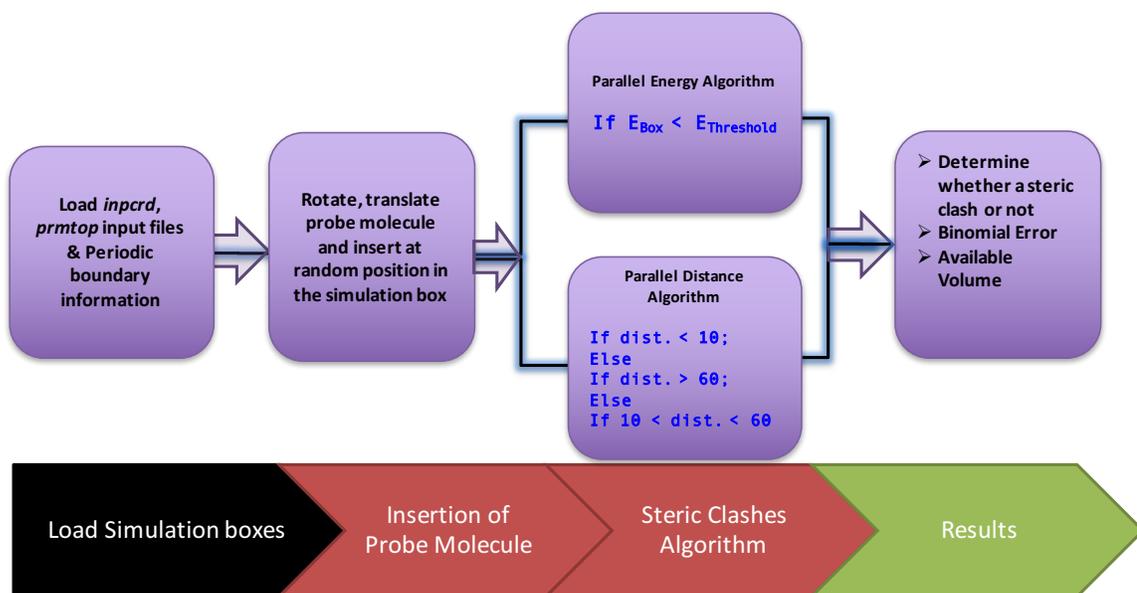


Figure 2.9: Workflow of Monte Carlo simulation algorithms to estimate the fractional available volume.

the scaled particle theory equation. The α_{crowded} is

$$\alpha_{\text{crowded}} = \gamma_{\text{crowded}} \left(\frac{C_{\text{crowded}}}{C^{\circ}} \right) \quad (2.12)$$

where C_{crowded} is the concentration under crowded conditions, and C° is the standard (reference) concentration. In the crowded solution, the occupied volume is an important quantity, so the concentration can be replaced by the volume and number of molecules.

$$\Delta G = kT \ln \left(\frac{n/V_{\text{available}}}{n/V_{\text{total}}} \right) \quad (2.13)$$

on simplifying equation 2.13,

$$\mu^{\text{NI}} = \Delta G = kT \ln \left(\frac{V_{\text{total}}}{V_{\text{available}}} \right) \quad (2.14)$$

which is equivalent to equation 2.9.

2.4 The scaled particle theory

Thermodynamic activity is a meaningful quantity in predicting the reaction rates and chemical equilibria [3]. The concentration dependent properties such as thermodynamic activities and nonideal contribution of excluded volume to the chemical potential of a given solute particle can be estimated using a statistical model of hard fluids [4, 12, 82]. This model is named the scaled particle theory and it estimates the concentration dependent properties as a function of shape and size of the particle. The shapes and sizes of given particles are characterized by three geometric parameters, namely; the volume (V), surface area (S) and radius of curvature (R).

An algorithm is presented here that is an extension to the SPT model [83] to estimate the thermodynamic activities of individual macromolecules of an arbitrary shape and size by convexification [236]. A convex shape encapsulates all the given points present in three dimensional space inside it and a line between any two points within the shape will be inside the shape entirely. The construction of the convex hull requires the identification of points on the boundary of the hull. This approximation could represent shapes and sizes more realistically than using a sphere of approximate radius encapsulating the whole molecule. The algorithm has been written in the MATLAB language [237] and is composed of two functions. The first function, *findcurvature.m* (Appendix A.7.1) computes the three geometric parameters while the *findactivity.m* function (Appendix A.7.2) determines the thermodynamic activities of macromolecules of interest at any given concentration. The global procedure for measuring the geometric parameters and predicting thermodynamics of conformational equilibrium involves the following key steps.

1. Extract the 3D coordinates via *pdb2mat.m* function. This file is available at <https://www.mathworks.com/matlabcentral/fileexchange/> with 'read and write PDB files using matlab' heading.
2. The 3D coordinates are fed to the convex-hull function [236] to generate the convex hull. This convexification method uses the Delaunay triangulation scheme to form

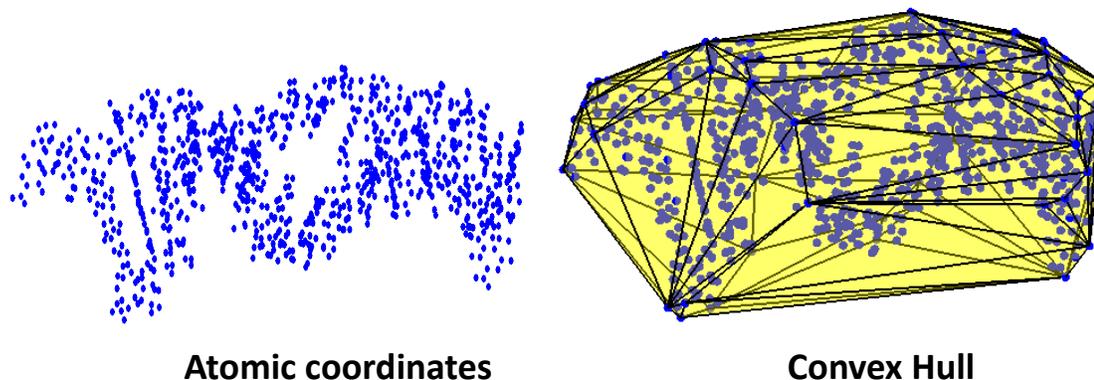


Figure 2.10: Construction of Delaunay triangles by joining the atomic coordinates that lie in the convex hull and to calculate the volume and surface areas.

the convex hull. Delaunay triangulation provides the set of points that are the vertices of the triangles forming a convex hull (Figure 2.10). These points are used in further calculations to estimate the geometric parameters of the molecule.

3. The convexification results in the formation of tetrahedra using the atomic coordinates. The sum of the volumes of all the tetrahedra gives the one possible measure of the volume of the molecule. This is an approximated volume which overestimates the volumes of non-linear molecule if the molecule is not overall convex. The volume of the molecule can also be estimated using different mathematical formulas such as the volume from the molecular weight, radius of curvature, and by rolling a virtual molecule on the surface of the macromolecule [238].
4. Summing the areas of the triangles present on the surface of the molecule gives a measure of the surface area of the molecule. The surface area can also be computed from solvent accessible surface area.
5. The mean radius of curvature R is computed by solving a least sum of squares sphere fit problem in terms of a least sum of squares plane fit problem using an inverse geometric transformation [239]. The algorithm was described by Coleman *et al.* [240]. In this algorithm a matrix M is constructed containing the atomic coordinates, $M = [p_1, p_2, p_3, \dots, p_{N-1}, p_N]$ where p is the vector of x, y, z coordinates of

each point. The convex-hull algorithm extracts the N boundary points on the convex hull and these boundary points are used to solve the least sum of squares plane fit problem through seven iterative steps.

- (a) The matrix M is split into two sets. Each point of matrix M is treated as an inversion point j_i with r , s , and t values in the first set, representing the x , y , and z coordinates of the inversion point, while the rest of the points $[x_i, y_i, z_i]$ in the second set are inverted with respect to inversion point j_i using the inverse geometric transformation formula. This geometric transformation results in a new set of point represented as $t_i = [t_{xi}, t_{yi}, t_{zi}]$, which represent the points on the plane.
- (b) Fit the least sum of squares plane to the set of t_i points. This step will give a point and a normal unit vector on the plane.
- (c) Find a point named 'a' on the plane closest to point j_i by solving the plane equation using the normal vector and point on the plane from the previous step.
- (d) Invert point 'a' by applying the same inversion formula with respect to t_a to generate j_i point.
- (e) Estimate the centre of the sphere by taking the average of points j_i and t_a points.
- (f) The radius of the first best-fit sphere is calculated by taking half of the distance between the j_i and t_a
- (g) The algorithm runs a loop over all j_i points of matrix M to find the best centre and mean radius of curvature of the fitted sphere through minimizing the mean square error.

2.5 The transition state theory

The TST model is applied to investigate the kinetics of conformational equilibrium in a crowded medium. TST computes the rate constant of a given biochemical reaction by in-

incorporating the activity coefficients of the transition state and reacting species as explained in section 1.4.3. Under dilute conditions, the activity coefficients of reacting and transition state species are unity and do not contribute to the rate constant. However, in crowded solution, the activity coefficients are no longer unity and cannot be ignored. Theoretically, the scaled particle theory computes the activity coefficients of a given molecule in the solution as a function of fractional occupied volume.

TST computes the rate constant for a conformational equilibrium reaction in a crowded medium using equation 1.1. According to the TST rate constant expression, the rate constant depends on the activity coefficients of the reactant and the transition state. The activity coefficient of existing structures is estimated with the SPT model. However, the structure of the transition state is generally unknown and the SPT model cannot estimate the activity coefficient of the transition state without knowing the corresponding geometrical parameters.

The exact structure of the transition state is hard to determine experimentally due to the transient lifetimes of the transition state. There have been developed transition state spectroscopic methods to characterize the transition state [241–244]. However these are non-routine experiments that cannot be carried out in most laboratories. A variety of theoretical and computation models have been developed to tackle this problem but each method comes with its own shortcomings [245]. For example, molecular mechanics predicts the transition state by locating the crossing point between two energy plots of breaking and new forming bonds. Moreover, structure optimization methods construct a path linking reactants and products. The reactant and product structures are used as endpoints in this process to predict the transition state of reactions [246].

To overcome the difficulty of the transition state structure, an average structure between two conformations is used as an initial guess transition state structure. Amber is used to generate the average structure by feeding the initial and final structures as inputs. Another quick way to construct intermediate structures between two conformations is through using

a morph server (<http://molmovdb.mbb.yale.edu/molmovdb/morph/>) [247]. This server constructs all intermediate structures between the given two conformations. The server moves the coordinates in a rigid body rotation fashion. The number of intermediate structures can vary from 8 to 32 frames. It is better to construct a larger number of intermediate frames because it involves smaller structural changes and minimizes the probability of any large chemical distortions. However, the morph server does not necessarily give structures according to the lowest energy path. The structure with the highest energy is selected as an approximated transition state structure by determining the single point energies for all the intermediate structures including initial and final structures. The program file implementing the transition state theory is available in Appendix A.8.

2.6 Summary

We presented two conformational sampling models based on MC and MD frameworks to achieve our first goal regarding the preparation of diverse PEG conformations and finally the preparation and equilibration of crowded media. Afterwards, an extended model of the scaled particle theory with a convexification algorithm and a Monte Carlo method was developed to compute the fractional available volumes and subsequently thermodynamic activities to incorporate the crowding effects on the conformational equilibrium.

Chapter 3

Construction of crowded medium

The aim of the current study was to investigate the macromolecular crowding effects on the conformational equilibrium in a more realistic crowded medium instead of a medium filled with hard spheres. Generally, a statistical model of scaled particle theory (SPT) [83, 158] is used to compute the crowding effects by incorporating the excluded volume effect. However, the SPT model is based on geometric approximations to the molecular shapes. For example, the SPT model treats the macromolecules as hard convex shapes which might either underestimate or overestimate the excluded volumes depending on the size and shape of the molecules, and subsequently predicts the inaccurate thermodynamic activities of molecules of interest [24, 25]. To overcome this difficulty, we introduced a new modified SPT model using a minimum of geometrical approximations. However this new model needs to be tested to see how accurately this extended model could capture the shapes and sizes of macromolecules to compute the crowding effects. To answer these questions, we developed a computer simulation model based on a Monte Carlo approach to test the outcomes of a new SPT model. The combination of these two models i.e. the SPT and computer simulations, offered a general systematic approach which could be used to model and investigate the crowding effects in any other biochemical reaction of interest.

The developed approach is grouped into two sections based on two key objectives. The first objective is to prepare crowded media, in which 5-40% of the total volume is occupied by crowder molecules and the second objective is to apply the SPT and computer simulations models to compute the crowding effects on a biochemical system of interest. We

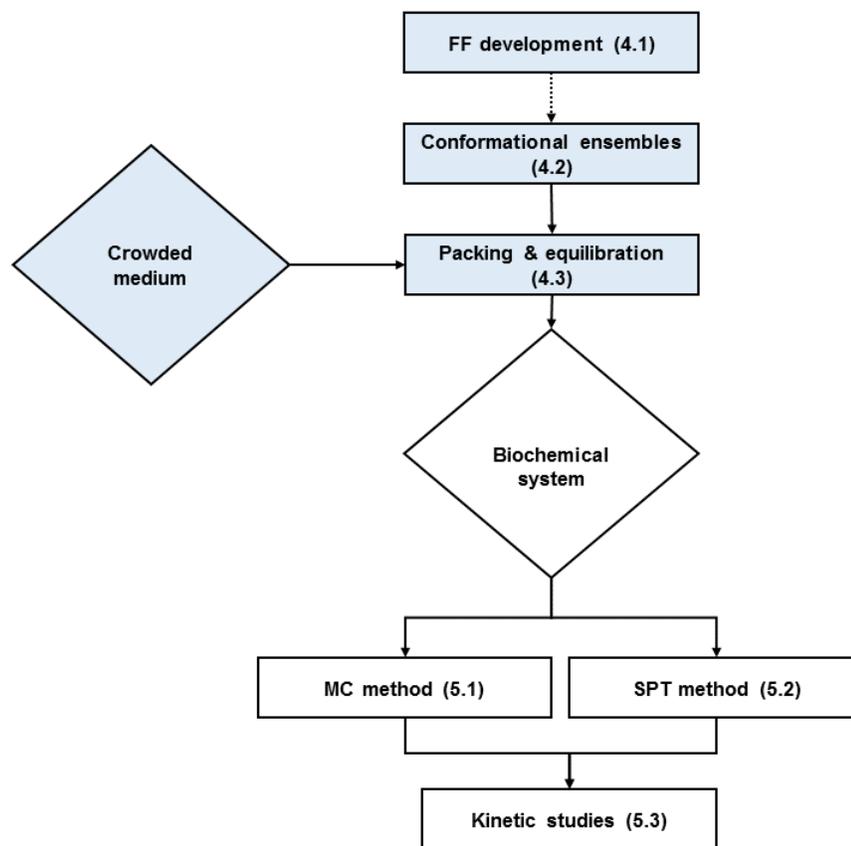


Figure 3.1: Classification of our approach used to determine the macromolecular crowding effects on the conformational equilibrium. This approach is classified into two sections, namely preparation of crowded media and the study of biochemical systems in crowded media via MC or SPT methods. The highlighted sections belong to the current chapter and the numbers indicate the corresponding results and discussion sections.

split our program recipe into two major sections for simplicity and convenience (Figure 3.1). The first section covers the preparation of crowded systems as highlighted with a blue colour in the figure, while the results that come after the execution of both computer simulation and SPT models will be discussed in the second section.

The first section is comprised of three key steps namely the development of forcefield parameters, construction of libraries of PEG structures, and finally packing and equilibration of crowded systems packed with dynamic solution structures of polyethylene glycol (PEG) of molecular weight 8 kDa (Figure 3.1). We selected PEG as a crowding agent in our model due to its extensive use in crowding studies. Due to the existence of diverse and dynamic PEG structures in solution, we need to develop diverse PEG confor-

mations to populate our crowded systems. PEG conformations of 15 to 40 Å of radius of gyration have been constructed in accordance with experimental studies conducted elsewhere [55, 63, 90, 91, 107–112]. To do so, we performed Molecular Dynamics (MD) or Monte Carlo (MC) conformational sampling simulations. To do that, we need a forcefield which is unavailable sometimes. In a nutshell, three key points of the present part are summarised here:

1. Developing the forcefield parameters for crowders if they are not provided by default with simulation package (section 3.1).
2. Constructing the libraries of crowder conformations by performing conformational sampling simulations (section 3.2).
3. Preparing the crowded systems by packing and equilibrating the crowded systems (section 3.3).

3.1 Forcefield parameters for PEG

Forcefield parameters play a critical role in the conformational sampling simulations by providing a means to calculate the total energy of the structure and thus to evaluate the acceptance/rejection of MC moves. The development of forcefield parameters for crowders may not be required if the forcefield parameters come with a simulation program. We used PEG of 8 kDa molecular weight as a crowding agent in the simulations because PEG of this molecular weight was commonly used in experiments and in computer simulations in crowding studies [15, 80, 82]. We used MCCCSTowhee, Sire and Amber to conduct conformational sampling of PEG. MCCCSTowhee provides forcefield parameters for all the atoms needed for PEG, whereas Sire and Amber do not. Amber provides the forcefield parameters for the majority of organic molecules [226] but not for PEG. Similarly, Sire does not come with PEG forcefield parameters and accepts forcefield parameters provided

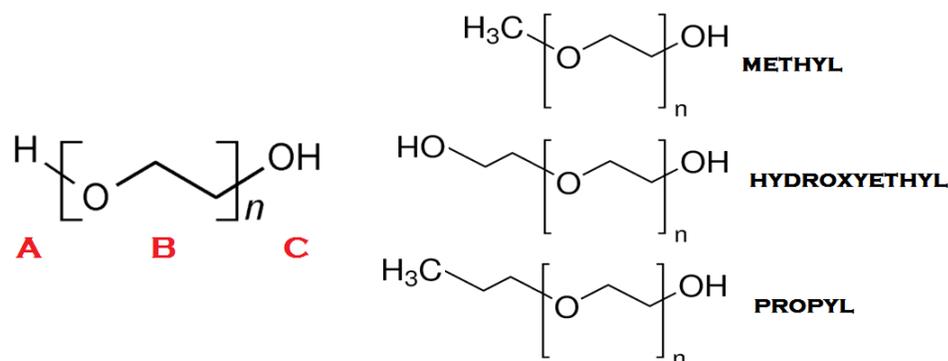


Figure 3.2: Three PEG structures used to develop the forcefield parameters for PEG in the PyRed program. The classification of structures is based on terminal ‘A’. Three PEG analogs were prepared by replacing hydrogen with methyl, hydroxyethyl and propyl groups respectively. The hydroxyethyl variant is an ordinary PEG, in which the last monomer moved into the group ‘A’.

by Amber. The availability of PEG forcefield parameters is critical to run simulations in both programs.

To accomplish the goal of constructing PEG forcefield parameters, the PyRED server was used. PyRED offers two methods for developing forcefield parameters, namely the whole molecule and fragment approaches. The whole molecule approach is only applicable to molecules made of less than 120 atoms, so it cannot be applied to 8 kDa PEG which has 1280 atoms, while the fragment approach is applicable to a polymer. Further, PyRED also provides the capability of generating average forcefield parameters by integrating multiple conformations of the given molecule.

The forcefield parameters of three types of PEGs were constructed as shown in Figure 3.2 through the fragment approach. The initial PEG structures were divided into three fragments namely, ‘A’, ‘B’ and ‘C’. All three structures differ in terminal ‘A’. The aim of choosing three types of PEG was to evaluate the effect of terminal groups on the resultant forcefield parameters and subsequently on the folding behaviour of PEG in the simulations. Previous studies demonstrated that the terminal groups have significant effect in PEG folding in simulation [98]. Moreover, the effects on the forcefield parameters of length of the central fragment by increasing the value of n , and the type of QM geometry optimization

methods are evaluated.

The results on the development of forcefield parameters are summarized into three major sections:

1. The development of forcefield parameters for PEG with a methyl using a single conformation of PEG that is optimized by different QM methods (subsection 3.1.1).
2. The comparison of forcefield parameters for PEGs with methyl, hydroxyethyl and propyl terminals groups, using a single conformation of PEG optimized by a single QM method (subsection 3.1.2).
3. The effect of increasing number of monomers in the central fragment with $n = 2, 3,$ and 4 on the forcefield parameters (subsection 3.1.3).
4. The effect of multiple conformations of PEG with hydroxyethyl terminal on the averaged PEG forcefield parameters. All these conformations were optimized by a single QM method (subsection 3.1.4).

3.1.1 PEG with methyl terminal group

The PyRED server constructs the forcefield parameters of a polymer in a two-step procedure. In the first step, PyRED optimized the structure and formed the Molecular Electrostatic Potential (MEP) surface using Quantum Mechanics (QM) calculations. Three QM methods, namely the *ab initio* method with the Hartree Fock (HF) approximation [216], Density Functional Theory (DFT) with the B3LYP approximation [218], and a post-Hartree Fock (PHF) Møller-Plesset perturbation theory [220] of second order (MP2) were selected to optimize the PEG structure. These three methods were selected to find out an appropriate method that could be used to construct the forcefield parameters accurately. In the second step, PyRED determined the atomic charges by reproducing the MEP surface through a charge fitting procedure.

The QM methods determine the wavefunction and energy of the system. HF determines the wavefunction of the system using a single Slater determinant approximation. A Slater determinant satisfies the anti-symmetry requirements of the wavefunction and thus the Pauli exclusion principle. It also represents the many electron wavefunction in terms of single electron wavefunctions and does not incorporate the electron correlation at all. As a result, HF overestimates the system energies. However, PHF methods improve on the HF results by incorporating electron correlation. On the other hand, DFT computes the system energy as a function of electron density without using the HF mean field approximation and considers the contribution of electron correlation. We used the polarized basis set 6-31G(d) with the HF and DFT methods to compute the wavefunction. The basis set choice involves a balance between wavefunction accuracy and computational cost. The small polarized basis set is a good choice for the small PEG molecule that is composed of simple elements such as hydrogen, carbon and oxygen and involves covalent bonding through hybridization. The polarized basis set would be a good choice as it considers atomic orbitals that become distorted in shape by other nuclei. The larger correlation-consistent polarized basis set ‘cc-pVTZ’ including Valence Triple Zeta and polarization on all atoms was also used with the MP2 method for comparison purposes.

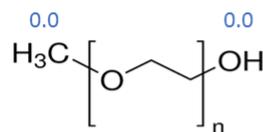
The comparison of all three QM methods was shown in terms of average Electrostatic Surface Potential (ESP) charges obtained by each method (Table 3.1). The HF sometimes gave a charge of opposite sign on a few atoms to the other two methods which turn out larger charge values on the PEG molecule. For example, DFT and MP2/cc-pVTZ calculated the sum of atomic charges of 0.0776 and 0.0974 respectively on the central fragment of PEG and these charges are smaller than 0.6139 estimated by the HF/6-31G(d) method. Consequently, the lower charge values result in lower total energies of 16.24 and 18.08 kcal/mol respectively as compared to 21.81 kcal/mol due to electron correlation treatment.

The fragment approach required two intra-molecular charge constraints in order to define three PEG fragments and to construct forcefield parameters of the PEG polymer prop-

Table 3.1: Predicted atomic charges of PEG with methyl by QM calculations

Atoms	HF/6-31G(d)	B3LYP/6-31G(d)	MP2/cc-pVTZ
1C	0.0203	-0.0134	-0.0586
2H	0.0896	0.0924	0.1066
3H	0.0399	0.0397	0.0476
4H	0.0399	0.0397	0.0476
5O	0.0399	-0.4047	-0.388
6C	0.284	0.2645	0.2467
7H	0.0179	0.0135	0.0268
8H	0.0179	0.0135	0.0268
9C	0.273	0.1888	0.1539
10H	-0.0094	0.001	0.0141
11H	-0.0094	0.001	0.0141
12O	-0.748	-0.6543	-0.6454
13H	0.455	0.4182	0.4077

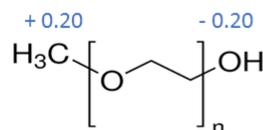
erly (Figure 3.3). The first intra-molecular charge constraint is applied with a total zero charge on PEG. This charge constraint helped to define and determine the atomic charges on methyl 'A' and hydroxyl 'C' terminal fragments. On completion of the PyRED job with the first charge constraint, the methyl and hydroxyl terminals had total charges of ± 0.47 , ± 0.20 and ± 0.19 with HF, DFT and MP levels of theory respectively. Both terminals should carry the same amount of charge but of opposite sign due to different electronegativities. These known charge values on both terminal fragments were used in the second intra-molecular charge constraint to construct the forcefield parameters of all three fragments. For example, in the second charge constraint, we used charge values of $+0.20$ and -0.20 on methyl and hydroxyl respectively obtained from DFT QM method calculations. The charge measurement on the central fragment is necessary step in dividing the PEG into three fragments and constructing the forcefield parameters. The charge measurements do not affect the overall charge on the PEG molecule and formed neutral PEG polymers after joining the three fragments. In a nutshell, the first charge constraint considers zero charges on the whole molecule and provide assistance in finding the charges on the defined terminal groups and the formation of fragments. The second charge constraint treats the ter-

Step 1. QM optimization

ATOM	CHARGE
1C	-0.0134
2H	0.0924
3H	0.0397
4H	0.0397
12O	-0.6453
13H	0.4182

Charge constraint-I 0.0 | 1 2 3 4 | 12 13 | Remove

Total Terminal Charges = (|CH₃|+|OH|)/2 = ± 0.20

Step 2. Fragmentation

Charge constraint-II + 0.20 | 1 2 3 4 | Remove

- 0.20 | 12 13 | Remove

Figure 3.3: Process of forcefield parameters development by using a fragment approach in the PyRED server. The fragment approach comprises two steps. The PEG structure is optimized with a QM method of choice and atomic charges are determined. In the second step, the three fragments are formed. This process requires two intra-molecular charge constraints to facilitate the fragmentation. A total charge of zero is assigned to terminal groups in the first charge constraint in step 1, whereas the average of the sum of atomic charges on the terminal groups of ± 0.20 is used in the second charge constraint. The first charge constraint facilitates the formation of fragments and is used to calculate the charges on the terminal groups. Therefore, an equal amount of the total terminal charge value of 0.20 is assigned to both terminal groups, but opposite in sign depending on the electronegativity of each terminal group. Completion of the PyRED job with a second set of charge constraints results in fragments and forcefield parameters of a PEG polymer.

minal groups as chemically equivalent groups with respective charges of +0.20 and -0.20 on methyl and hydroxyl terminals and built forcefield parameters and three fragments of the PEG by reproducing the molecular electrostatic surfaces.

The accuracy of the developed forcefield parameters is presented in terms of a relative root mean square (RRMS), a measure of the difference between two data sets, and Pearson correlation coefficient r^2 values. A small value of RRMS approaching zero and a value of r^2 close to one indicates the accuracy of the fitting step and the resultant developed forcefield parameters. In the fragment approach, the accuracy of the fitting procedure is

Table 3.2: RRMS and Pearson correlation coefficient r^2 for three QM methods

Charge Constraints	HF/6-31G(d)		B3LYP/6-31G(d)		MP2/cc-pVTZ	
	RRMS	r^2	RRMS	r^2	RRMS	r^2
No constraints	0.1549	0.9761	0.1595	0.9748	0.1984	0.9613
2 constraints	0.1688	0.9717	0.1692	0.9715	0.2079	0.9574
Difference	0.0139	0.0044	0.0097	0.0033	0.0095	0.0039

the comparison between charge fitting on the single molecule and charge fitting on the fragments of the molecule with charge constraints. A small difference of 0.0097 in the RRMS values between no and two charge constraints using the DFT method indicates the very weak effect of the charge constraints used. The same trend can also be seen in the r^2 values which are 0.97 and 0.97 without and with two charge constraints and indicates a good fit of the MEP. The biggest values of RRMS in Table 3.2 indicated that the electrostatic potential is least well fit to the MP2/cc-pVTZ results. We are not sure about the reason why the MP2/cc-pVTZ method is not producing a good fit. The MP2/cc-pVTZ method with a large basis set and including a correlation correction was used to get reasonably accurate results. It provided us a base to compare the results with what we have obtained from the cheaper DFT and HF methods. The DFT method is found to be more efficient in speed and to produce structures with minimum energies competitive with the MP2/cc-pVTZ outcomes. Based on this analysis, we choose to use DFT in all calculations regarding the development of the forcefield parameters of PEG.

PyRED offers 21 charge fitting models to reproduce the MEP surfaces. The charge models use atomic charges present in different forcefield parameters and computed using different QM levels of theory. For example, the RESP-O1 model uses the atomic charges from the OPLS forcefield parameters while ESP-A1 uses the type of charges from CHARMM FF parameterization. The RESP-A1 is the default charge fitting model and uses the atomic charges from HF/6-31G(d) model. Two charge fitting models, namely RESP-A1 and RESP-Y22 were tested using the B3LYP/6-31G(d) method to regenerate the MEP surface. The RESP-A1 model produced better results by smaller RRMS and larger r^2 values than RESP-

Y22.

3.1.2 Comparison of FF parameters with methyl, hydroxyethyl and propyl terminals

The forcefield parameters of PEG with hydroxyethyl (HFF) and propyl (PFF) terminals were also developed to incorporate the effect of the 'A' terminal group as compared to PEG with methyl terminal (MFF) (Figure 3.2) and subsequently the effect of resultant forcefield parameters on the folding behaviour of 8 kDa PEG in MD simulations. The B3LYP/6-31G(d) method was used to optimize these initial PEG structures in PyRED during the forcefield parameter development. The resultant forcefield parameters with each terminal were evaluated by performing MD simulations using an 8 kDa PEG.

The total energies of both PEGs with methyl and propyl terminals were converged after completing 5 ns of simulation time (Figure 3.4), while the energy of PEG with hydroxyethyl terminal started from an energy much closer to its final energy. The radius of gyration obtained using these three sets of forcefield parameters showed similar folding behaviour in which all the PEG structures collapsed to very compact conformations and the radius of gyration fluctuated over a very limited range of 1 to 3 Å in the stationary state around a mean value of 12 Å (Figure 3.5). However, PEG with MFF parameters took a long time to collapse to the same structure eventually as the other two. These results suggested the terminal groups did not have a significant effect on the folding behaviour of PEG in MD simulations that were performed in Amber.

It is noted that the starting structures of 8 kDa PEGs with methyl, hydroxyethyl, and propyl terminals differ in radius of gyration from the starting point of simulations. There are two ways to build an 8 kDa PEG structure after developing forcefield parameters. Firstly, we can construct a linear PEG structure by joining monomers in the central fragment and then use any set of forcefield parameters, i.e. MFF, HFF, or PFF to conduct the MD or MC simulations. The advantage of using this method would be the same PEG conformation used in the simulations. However, this method requires to change the terminal groups and

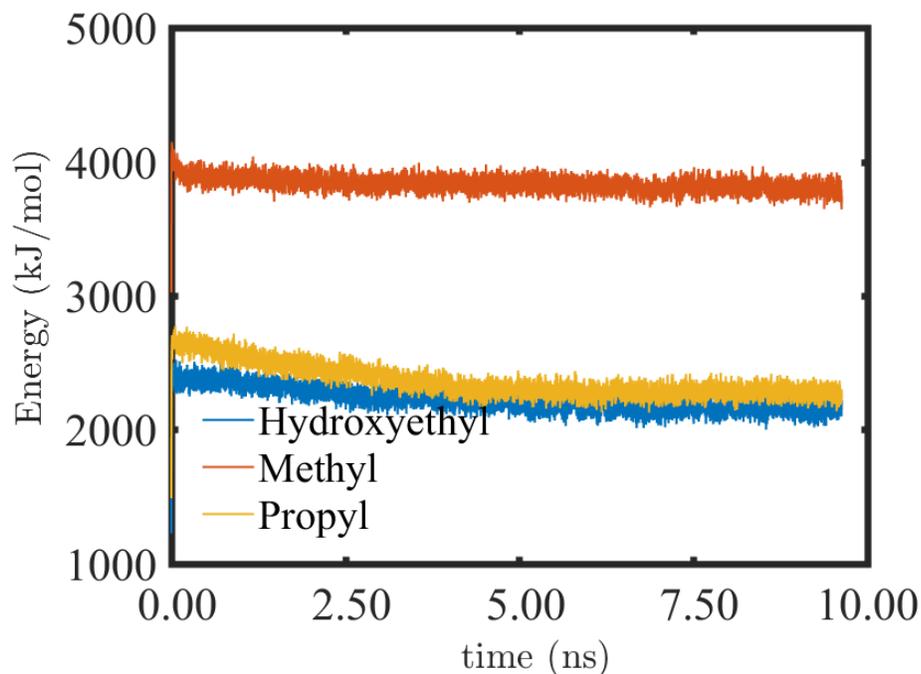


Figure 3.4: Total energy change for three PEG structures in 10 ns long MD simulations performed in Amber using an NPT ensemble at 300 K. All three simulations started using a linear 8 kDa PEG that differ in terminal groups. PEGs with methyl, hydroxyethyl and propyl terminals used the MFF, HFF and PFF forcefield parameters respectively.

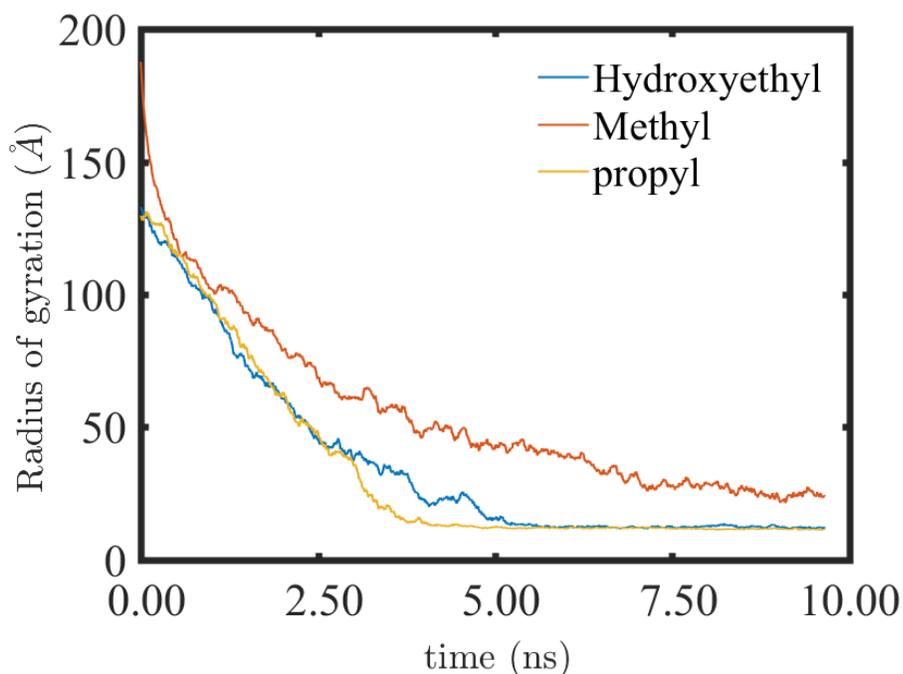


Figure 3.5: Radius of gyration change from start to stationary stage in the MD conformational sampling of three PEG structures with hydroxyethyl, methyl and propyl terminal groups. These 10 ns long simulations were performed at 300 K using an NPT ensemble and implicit solvation model.

rename the atomic names in the PDB file according to the forcefield parameters. The second method would be using the PEG fragments from each forcefield parameter set to construct the 8 kDa PEG structure. This method results in 8 kDa PEGs with different initial conformation depending on the shapes of the fragments. This does not require any additional editing in the PDB file. We used PEGs obtained from the second method and presented corresponding results. We also tested the first method and conducted the simulation with a constant PEG conformation by varying the FF parameters. It is worth noting here that since they all collapse to similar final structures if the simulations are performed for a long enough time, this shows that the results are insensitive to the starting structure. The results demonstrated that the initial conformation of PEG has no effect on the folding behaviour and total energies in MD and MC simulations. To illustrate how different types of conformations are formed in the second method, we construct four types of PEGs by joining ten monomers of different shapes and sizes (Figure 3.6). It showed that the shape of resultant PEG depends on the shapes of monomers of the central fragment.

3.1.3 Effect of length of the central fragment

The effect of the length of the central fragment on the resultant forcefield parameters was investigated by using PEGs with methyl and hydroxyethyl terminals. It was achieved by increasing the number of repeating monomer units ($n = 2, 3, 4$) within the central fragment. The B3LYP/6-31G(d) method was used to optimize all eight mini-PEG structures. The increase in length of the central fragment results in smaller RRMS values for PEGs with methyl terminals, whereas larger RRMS values are observed for PEGs with hydroxyethyl terminals (Table 3.3). These results showed that RRMS values are sensitive to the composition and structural orientation of the initial PEG structure.

Afterward, we applied each of the forcefield parameter sets to the same 8 kDa PEG in the MD conformational sampling and found that forcefield parameter sets obtained with an even number of monomers showed approximately a 500-1000 kJ/mol lower energy than

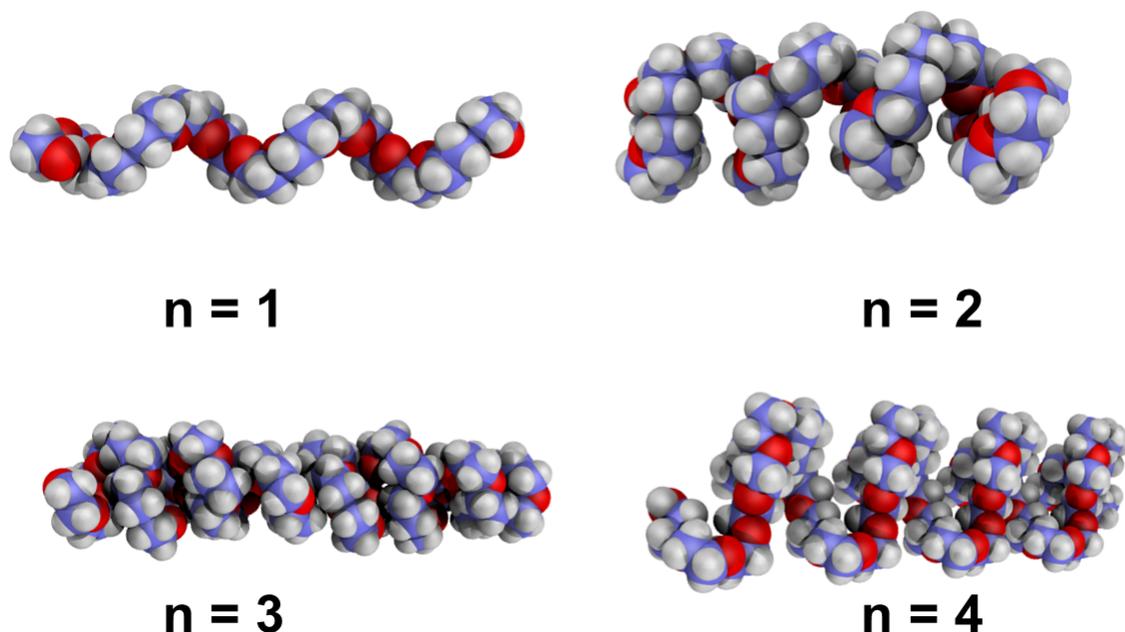


Figure 3.6: Formation of folded and coiled structures of PEG on polymerization of 10 monomers of the central fragment, where the $n = 1, 2, 3$ or 4 represents the number of monomers in the parental central fragment used in the force field parameter development. The folding trend increased as the length of the central fragment increased.

PEG with a methyl terminal using forcefield parameter sets obtained with an odd number of monomers (Figure 3.7). However, the energies of PEGs using sets of forcefield parameters of PEGs with hydroxyethyl terminals were comparable (Figure 3.8). The lower energies of PEGs utilizing forcefield parameters from a structure with an even number of monomers in the central fragment can be explained in terms of hydrogen bonding. PEG oligomers with an even number of monomers in the central fragment showed a larger number of hydrogen bonds. We assumed maximum of 2.5 to 2.6 Å [248] as a standard length of a hydrogen bond and under this criterion PEG with $n = 4$ showed four hydrogen bonds with approximate bond lengths of 2.2, 2.4, 2.5 and 2.6 Å (Figure 3.9 (right)) while PEG with $n = 3$ showed two hydrogen bonds of 2.0, and 1.8 Å (Figure 3.9 (left)). The results showed that the obvious structural differences seen in Figure 3.6 are indicative of the effects of the number of monomers in the central fragment on the types of structures that are favoured by the different forcefields.

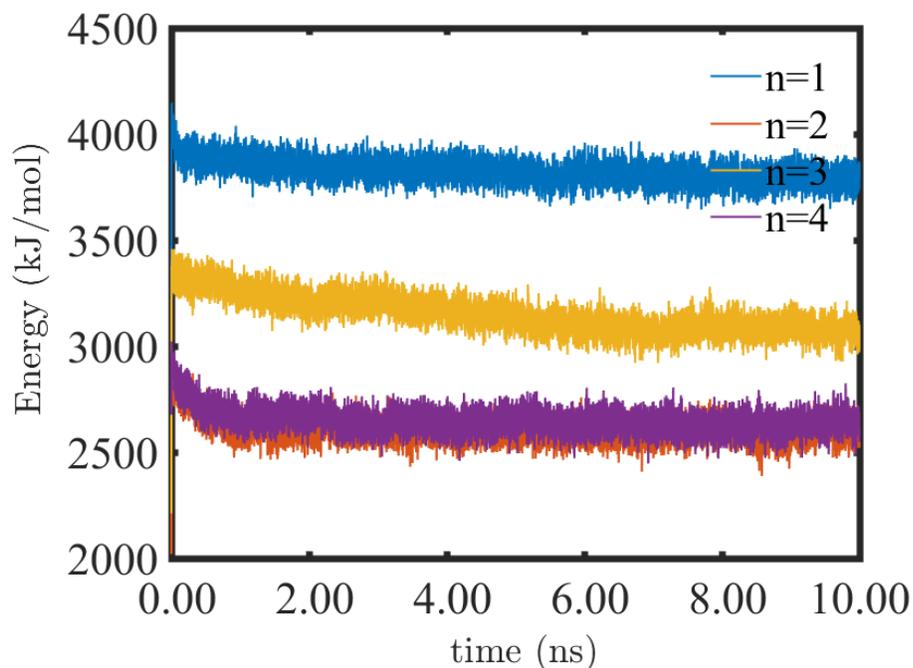


Figure 3.7: Effect of length of central fragments on the total energy of the 8 kDa PEG structure of methyl terminal in the 10 ns long MD conformational sampling simulations performed with an NPT ensemble in an implicit solvent at 300 K using MFF parameters.

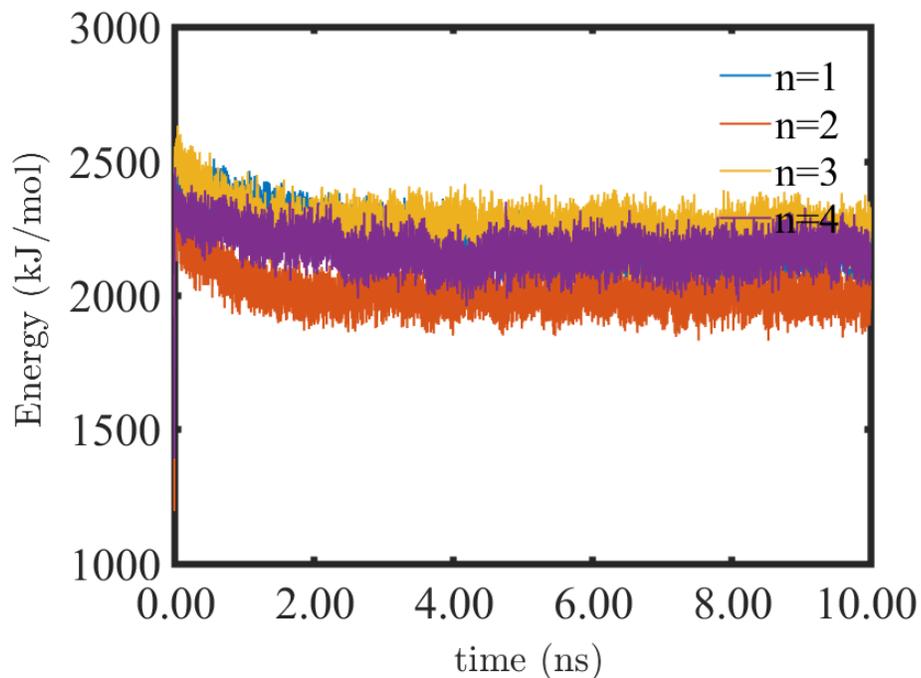


Figure 3.8: Effect of length of central fragments on the total energy of the 8 kDa PEG structure of hydroxyethyl terminal in the 10 ns long MD conformational sampling simulations performed with an NPT ensemble in an implicit solvent at 300 K using HFF parameters.

Table 3.3: Effect of length of the central fragment on the RRMS values for PEGs with methyl and hydroxyethyl terminals

PEG with methyl terminal				
Charge constraints	n1	n2	n3	n4
No constraints	0.15951	0.11475	0.11368	0.098698
Two constraints	0.28579	0.16252	0.14205	0.12250
PEG with hydroxyethyl terminal				
No constraints	0.16318	0.16784	0.19049	0.18355
Two constraints	0.16909	0.19313	0.18912	0.22304

These results demonstrated that the sets of forcefield parameters obtained with hydroxyethyl terminals are better than of PEGs with methyl terminals because it produced more stable structures of PEG with a small difference of energies for different length of central fragments (Figure 3.8). The calculations suggested that the initial conformation of PEG used in the step of developing forcefield parameters played a crucial role. Central fragments with $n=2$ and 4 monomers tend to form coiled structures through intra-molecular hydrogen bonding and subsequently result in lower total energies of 8 kDa PEGs in MD simulations. However, a central fragment composed of an odd number of monomers formed less coiled structures as compared to fragments with an even number of monomers. These results regarding total energy behaviour in MD simulations (Figures 3.7 & 3.8) suggested that the forcefield parameters that were developed with hydroxyethyl terminals are a good choice to conduct simulations to construct an ensemble of PEG conformations. The folding behaviour of 8 kDa PEG utilizing the MFF and HFF forcefield parameters varying in the length of the central fragment is provided in the Appendix B.3.9.

3.1.4 Effect of multiple PEG conformations

In the last step, average forcefield parameters of twenty three PEGs with hydroxyethyl terminals were developed. PyRED generates an average forcefield that minimizes the error in the PES over all the structures with RRMS value of 0.17307. These multiple conformations were collected in MC sampling conducted at 300 K using the initial structure of

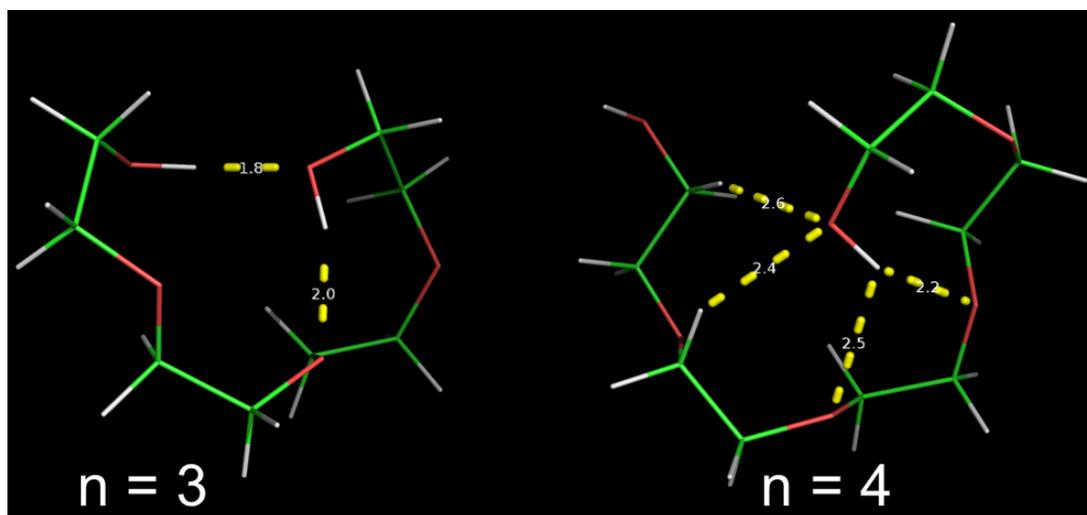


Figure 3.9: Number of hydrogen bonds in initial structures of PEGs with $n = 3$ and 4 used in the forcefield parameter development procedure. These structures were optimized using the B3LYP/6-31G(d) method in the GAUSSIAN program.

PEG with $n = 1$ and the corresponding set of forcefield parameters. These simulations were performed in Sire and a total of 5000 conformations were saved after every 250 internal moves (program code is available in the Appendix B.3.8). Twenty three conformations were picked with very different radii of gyration. All these conformations were optimized using the B3LYP/6-31G(d) method in the GAUSSIAN QM program. The resultant forcefield parameters such as bond lengths, angles, and dihedrals were found to be similar with the single PEG conformation except for a small variation in the atomic charges on each fragment. QM geometry optimization produced atomic charges on the terminal groups of ± 0.20 , which is equal to the atomic charges of ± 0.20 on fragments of PEG with a single conformation.

Sire required forcefield parameters to run MC conformational sampling simulations. These forcefield parameters were constructed at first using a single PEG with hydroxyethyl terminal, and then the simulations were performed by incorporating these parameters. These forcefield parameters were further evaluated by running the conformational sampling simulations of 8 kDa PEG and analysing the resultant total energies. The energy plots (Figure 3.10) showed that the total energy of the PEG decreased by 200 kJ/mol while

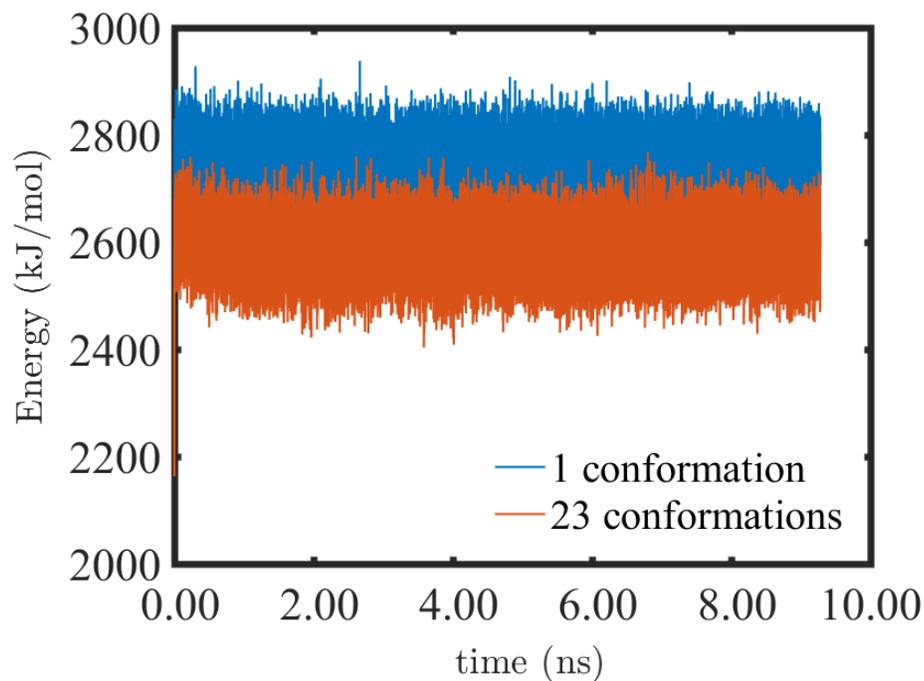


Figure 3.10: Effect of forcefield parameters using a single and multiple PEG conformations on the total energies of MD simulations conducted in Amber. These conformations were optimized with B3LYP/6-31G(d) QM method in the GAUSSIAN programs. 300 K MD simulations were performed using an NPT ensemble in an implicit solvation model with HFF parameters.

using the forcefield generated from multiple conformations. In conclusion, the forcefield parameters developed using multiple conformations and the forcefield parameters of mini-PEG with hydroxyethyl terminal and an even number of monomers in the central fragment result in the most suitable parameters based on the total energies analysis in MD and MC simulation. The complete sets of output forcefield parameter files for a PEG of $n = 1$ with a methyl terminal, PEG of $n = 4$ with a hydroxyethyl terminal and PEG of $n = 1$ with hydroxyethyl terminal with multiple conformations is provided in Appendices B.1, B.2, and B.3 respectively.

Table 3.4: Comparison of the partial atomic charges on the ether oxygen (-OE-) and carbon (-CH₂-) atoms between PyRED and three different GROMOS forcefield parameter sets, namely 53A6, 53A6v, 53A6o

Atom	methyl-PEG			MP2/ cc-pVTZ	PEG GROMOS		
	HF/ 6-31G(d)	B3LYP/6-31G(d)	B3LYP/ 6-31G(d)		53A6	53A6v	53A6o
-OE-	-0.48	-0.41	-0.40	-0.47	-0.32	-0.42	-0.57
-CH ₂ -	0.23	0.23	0.18	0.21	0.16	0.21	0.29

Concluding remarks - PEG forcefield parameters

The aim of the present section was to develop the appropriate forcefield parameters of PEG to employ in conformational sampling simulations. To achieve this goal, three sets of forcefield parameters of PEG were developed using three different terminal groups for a single and multiple PEG conformations by implementing the fragment approach. In particular, four different cases, namely PEG with methyl, hydroxyethyl, propyl terminals, and PEG with different lengths of central fragment, were studied. The results showed that the terminal groups did not affect the folding behaviour of 8 kDa PEG significantly as shown in the MD conformational sampling in Amber (Figure 3.5). In this regard, other studies showed the terminal methyl groups could be responsible for folding and formation of compact structures of PEG [98]. On the other hand, the length of the central fragment with an even number of monomers played a crucial role in lowering the total energy by 1500 kJ/mol as compared to the central fragment containing an odd number of monomers by incorporating a higher number of hydrogen bonds (Figures 3.7 & 3.9).

In the end, the accuracy of forcefield parameters was tested against the ether parameters present in the GROMOS forcefield. The atomic charges on the oxygen -OE- and methylene -CH₂-, generated by PyRED are in good agreement with the ether charges from the GROMOS forcefield parameters as shown in Table 3.4. The partial charges of -OE- and -CH₂- in methyl-PEG and hydrogen-PEG derived by three QM methods (i.e. HF, DFT, MP2) are in good agreement with the GROMOS parameters [197, 249–252]. However, the partial charges of carbon in the original hydrogen terminal PEG showed greater than 50 percent difference with GROMOS parameters. Based on this analysis, all the MC and

MD simulations were carried out using MFF and HFF sets of parameters. The rest of the parameters such as bond lengths, angles, dihedral angles, improper torsional potentials and van der Waals radii are in agreement with the Amber forcefield parameters [227].

In a nutshell, the development of forcefield parameters is the first step towards running the conformational sampling. An attempt was made to construct the missing forcefield parameters of PEG and the effect of different terminal groups, length of central fragments and multiple conformations of mini PEGs on the forcefield parameters was explored to determine if there is any major effect associated with these structural changes. These parameters were further compared with GROMOS parameters, however further experimental validation may be required. Our work on the forcefield parameter development is of an exploratory nature and the final results of crowding effects in the second step don't seem to depend all that strongly on the details of forcefield construction.

3.2 Ensemble of PEG conformations

The construction of the diverse conformational ensembles is the most vital component towards building the prerequisite crowded media. So far, we have discussed the general methodology to develop the unavailable forcefield parameters of any polymer and the effect of chain terminals on the folding properties. The objective of the current chapter is to prepare the crowded media where 0 to 40% of total volume is occupied by the crowder molecules of diverse conformations. We choose PEG as a crowding agent as it was commonly used as a crowding agent in many experimental and computer studies [80, 98, 111, 191]. Ensembles of PEG conformations are required in order to prepare these systems. Both Monte Carlo (MC) and Molecular Dynamics (MD) methods were carried out to achieve this goal. MC simulations were carried out in MCCCSTowhee [104] and Sire [193] whereas MD simulations were performed in Amber [105, 194]. These programs were chosen based on different capabilities they offer. For example, MCCCSTowhee runs the MC simulations through a very simple script file, and eliminates the need to develop

forcefield parameters because it provides a set of general forcefield parameters applicable to all elements in PEG. This forcefield is not tuned to PEG type structures and requires proper atomic charges to consider the Coulombic interactions reasonably. On the other hand, it does not provide much flexibility to design and perform simulations according to one's needs. Alternatively, Sire provides a much more flexible and easy approach to perform MC sampling simulations at the cost of requiring programming skills in Python. It accepts Amber [105, 194], CHARMM [106] and Gromacs [182] input files but requires that missing forcefield parameters for non-standard molecules be provided. Lastly, Amber is used to perform MD conformational sampling in addition to two MC simulations.

The conformational sampling simulations were employed using different temperatures, statistical ensembles, initial PEG conformations such as linear and folded, and implicit and explicit solvent models. These different parameters were used to enhance the diversity of the ensemble of PEG conformations to better sample the energetic and conformational space landscapes. The outcomes of these simulations were analysed and discussed by presenting total energy and radius of gyration changes while the efficiency of all methods were evaluated in terms of the distribution of PEG conformations.

3.2.1 MC sampling in MCCCSTowhee

A structure of a single PEG and corresponding conformational ensembles were built by performing MC simulations in MCCCSTowhee. The simulations were performed over two steps to achieve these goals.

1. Building the initial optimized 8 kDa PEG structure and constructing ensembles of PEG conformations at 300, 600 and 1200 K.
2. Investigating the effects of different simulation parameters such as the type of ensemble, temperature, initial PEG configurations, and random number generators to improve the conformational sampling.

First of all, 1.2 million-step-long MC simulations using the NPT (constant number of molecules, pressure and temperature) ensemble [221], at 101 kPa pressure, and 300 K temperature were performed to build and optimize the single PEG structure. The Amber forcefield parameters [225] were used to define the composition of PEG and to calculate the structure energies. Afterwards, three 6-million-step-long MC simulations at 101 kPa pressure and three different temperatures: 300, 600, and 1200 K were performed to build the library of PEG conformations using the optimized PEG structure, taken from the previous step. The higher 600 and 1200 K temperatures were chosen to enhance the diversity of ensembles of PEG conformations. In these simulations, the PEG conformations were saved to the library at every 30,000 MC steps up to 6 million total steps. The step size to save the resultant conformations was chosen arbitrarily.

The simulation results were analysed by interpreting the radius of gyration and energy behaviour of PEG. The radius of gyration is an important property that is used to characterize polymer size in the simulations [93]. The radius of gyration R_g is defined by Equation 1.4, where N is total number of atoms, \vec{r}_i is the position vector to each atom and \vec{r}_{CM} is the centre of mass of the molecule. R_g has been used to track the structural changes in the conformational sampling simulations that are performed in different simulation programs [104–106].

MC sampling simulations were performed at three temperatures in order to construct libraries containing diverse PEG conformations. MCCCSTowhee produced PEG conformations in three different ranges in three simulations performed at 300, 600 and 1200 K temperature (Figure 3.11). At 300 K, only small changes occur in the radius of gyration and energy as well. The 300 K data line showed minimal fluctuations in the radius of gyration due to the low number of accepted MC moves. The number of accepted moves at 300 K is quite insufficient for the structure to make significant jumps in the radius of gyration. The situation is slightly better at 600 K where the structure had a higher probability of accepted moves and therefore it helped the PEG to make a relatively larger jump of 2 Å in the begin-

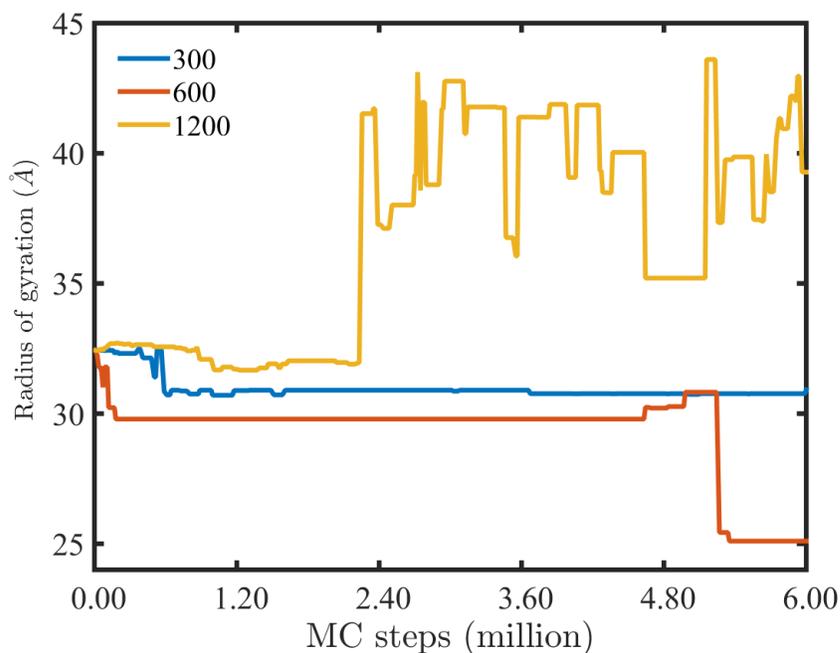


Figure 3.11: Change in gyration radii of the same initial PEG structure in the MC simulations conducted at 300, 600 and 1200 K. The radius of gyration fluctuates at higher amplitude at 1200 K as compared to 300 and 600 K. These simulations were performed using an NPT ensemble up to 6 million MC steps in MCCCSTowhee.

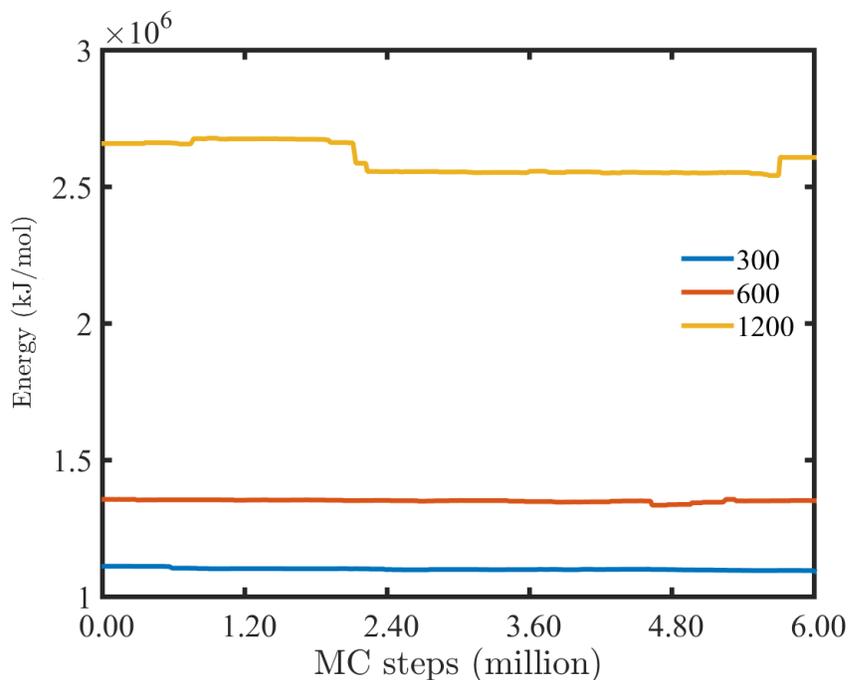


Figure 3.12: Total energy in the conformational sampling simulations conducted at 300, 600 and 1200 K using a same initial PEG structure in MCCCSTowhee. The energy fluctuates at higher magnitude at 1200 K as compared to 300 and 600 K.

ning. Moreover, the interesting behaviour started before 4.80 million steps where the radius of gyration started to edge upward, presumably as the structure explored some kind of low energy pathway out of the local minimum at 30 Å. The small change in the energy at the same point confirmed this behaviour (Figure 3.12) and finally made the structure to jump from 32 Å to 26 Å. In general, these sampling simulations generated conformations in a limited range of radii of gyration at 300 and 600 K. To observe larger structural fluctuations and consequently to build diverse PEG conformations, the simulations were performed at 1200 K. The 1200 K data showed that more diverse conformations were formed at 1200 K and they fell in a wide range from 31 to 44 Å with large fluctuations in energy as expected at higher temperature.

Overall, these results showed that the 300 K simulations did not do much. The 600 K simulations allowed more conformational sampling, eventually finding a very compact conformation and the 1200 K simulations showed large conformational changes. Similarly, the PEG conformation explored a limited range of the energy landscape in all three simulations conducted at 300, 600 and 1200 K (Figure 3.12). The 300 K energy was pretty flat without any significant upward changes. At 600 K, there were some upward changes in the region where the larger changes in the radius of gyration occurred and at 1200 K, we found a greater range of energy fluctuations, including one upward step in energy that was much larger than any seen at the lower temperatures.

Based on these results, it could be concluded that it is hard for MCCCSTowhee to construct diverse conformations for the large PEG structure at room temperature. Probably, the reason behind the inefficiency is the use of a very general forcefield, and therefore probably that is not very accurate for this kind of work. The other reason could be the limited control over defining the range of magnitude of internal moves, i.e. changes in angles and dihedral angles.

In the second section, different sets of simulation parameters were used to improve the conformational sampling. The simulation parameters includes changing the NPT ensem-

ble to NVT (constant number of molecules, volume and temperature), temperature from 1200 to 12,000K, three initial PEG configuration (Figure 3.13), random number generators ‘DX-1597-2-7’ [253] and ‘RANLUX’ [254] and doubling the length of simulations up to 12 million MC steps. The NPT ensemble was used previously because it is closer to the real experimental conditions and it ran the MC conformational sampling simulations faster than NVT or grand canonical ensembles in MCCCSTowhee. The NVT ensemble was tested only to see if it can produce diverse conformational ensembles. Three random PEG conformations were picked with very different radii of gyration from the previous MC simulations performed at 1200 K (Figure 3.11) and used to explore the effect of initial configuration on sampling behaviour. The DX-1597-2-7 and RANLUX pseudorandom number generators, with periods of 10^{14903} and 10^{171} respectively, were tested. In total, nine MC simulations were performed using three different initial PEG conformations at three different temperatures (300, 600, and 1200 K) and two different random number generators.

Of the nine simulations described above, only the results regarding total energy and radius of gyration change in a single simulation conducted at 300 K using the NPT ensemble and the ‘RANLUX’ random number generator are presented here. The results showed that the conformational sampling was improved while using the three initial conformations (Figure 3.14). The PEG explored more conformational space with relatively larger jumps from 41 to 29 Å (yellow line with ‘C’ PEG conformation) and 34 to 29 Å (blue line with ‘A’ PEG conformation) as compared to previous MC run performed at 300 K where the radius of gyration changed by 1 Å only (blue line in Figure 3.11). However, the large changes in the radius of gyration were diminished after 8.40 million steps and final conformations formed within a small range from 29 to 31 Å. The radii of gyration of final conformations fell in same range of 30-31 Å as found in the previous 300 K simulations (blue line in Figure 3.11). On the other hand, the energies showed consistent behaviour with small fluctuations after completing 1.20 million steps (Figure 3.14). The rest of the plots of energy and radius of gyration using different sets of parameters are provided in Appendix B.4. These results

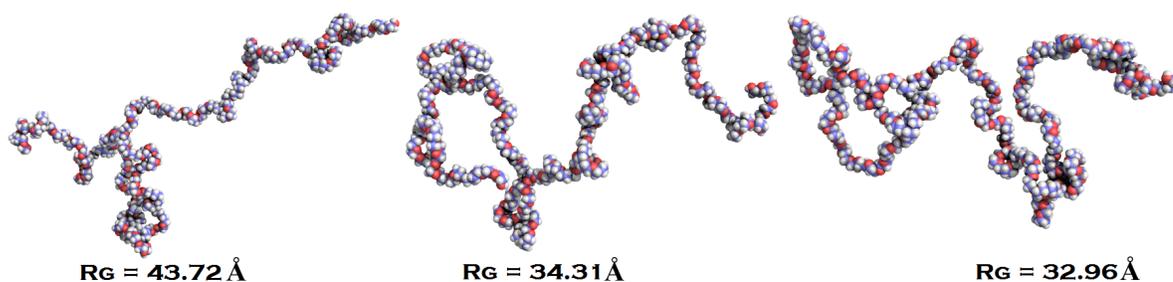


Figure 3.13: Snapshots of three PEG starting structures taken from 6 million steps long production run conducted in MCCCSTowhee using an NPT ensemble at 1200 K. These structures with very different radii of gyration, measured in Å, were picked to be used as an initial configurations in the PEG sampling simulations conducted at 300, 600 and 1200 K.

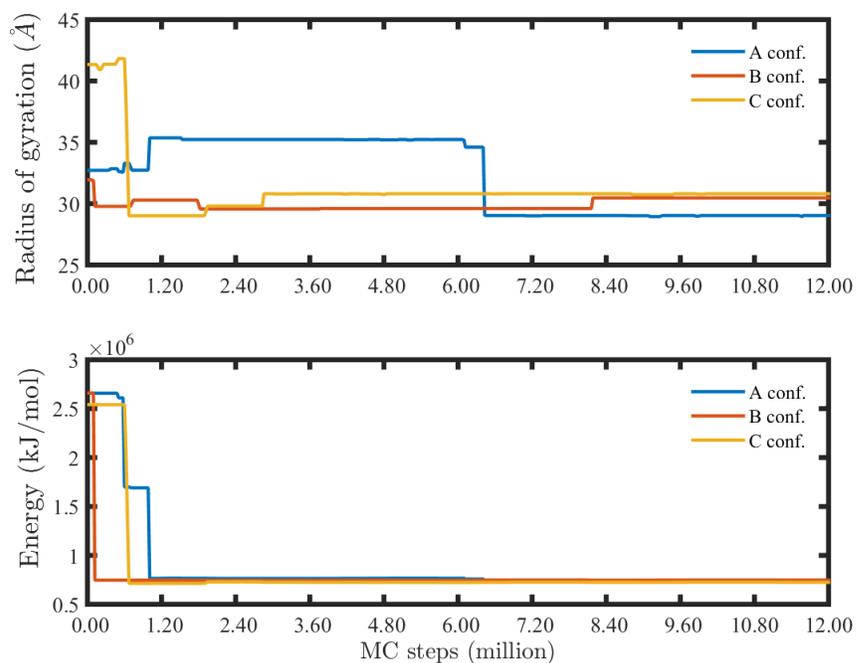


Figure 3.14: Radius of gyration and energy variations in MCCCSTowhee simulations at 300 K for three different starting conformations using the NPT ensemble and ‘RANLUX’ random number generator.

suggest that the change in the random number generators, and NPT to NVT ensemble does not bring any significant improvement in the conformational sampling. However, high temperatures help the PEG to explore the large conformational space and energy quickly by increasing the probability of accepting MC moves that increase energy (Figure 3.12).

Concluding remarks - MCCCSTowhee simulations

We tried MCCCSTowhee to run conformational sampling simulations because it provides general forcefield parameters to construct 8 kDa PEG and run simulations through a simple script. Mainly, this program is built to investigate the properties of reactions occurring in the gas phase utilizing small sized gas molecules. Probably, MCCCSTowhee was unable to do a great job regarding conformational sampling of large sized polymers due to the lack of a properly tuned forcefield. We have performed numerous simulations by varying temperature, pressure, ensembles and size of simulation box to generate the diverse conformations but the results were not promising. Added to this conclusion, the conformational sampling was improved at a high temperature of 1200 K only.

In a nutshell, MCCCSTowhee is good to build an initial optimized PEG structure quickly through MC simulations without worrying about developing the forcefield parameters and running high level quantum chemistry calculations for geometry optimization.

3.2.2 MC sampling in Sire

MCCCSTowhee produced a library of limited PEG conformations by performing MC simulations. An alternative conformational sampling was performed in Sire to build more diverse PEG conformational ensembles. To initialize the MC simulations in Sire, one can introduce the input structure file through a script, a PDB or Amber *top/crd* files. The most effective way is to use the Amber *top/crd* files because these files provide the necessary forcefield parameters to calculate the total structure energy during the simulation. Further, the total energy is also needed to validate any translational, rotational and vibrational move

that is performed on the structure during the simulations. However, the other input files lack this capability and result in distorted structures in the conformational sampling. In total, a set of three simulations were performed at two different temperatures, using two PEG molecules that differ in their terminal groups and starting linear and folded PEG conformation. These different parameters were used to enhance the diversity of PEG conformations in the library. It is noted that the first two sets of simulations used an original PEG with hydroxyethyl terminals whereas the last set of simulations were performed using PEG with methyl terminal (Figure 3.2). The following simulations were carried out:

1. Two individual MC conformational sampling runs conducted at 300 and 1200 K respectively, using an initial linear PEG structure.
2. One MC conformational sampling run started with an initial linear PEG structure at 1200 K with periodic quenching to 300 K.
3. Two MC simulations using linear PEG structures with methyl and hydroxyethyl terminals to inspect the terminal group effect.

First of all, two separate sampling simulations with one million MC moves were performed at 300 and 1200 K, using a linear PEG structure as a starting configuration. In these simulations, the resultant PEG conformations and the corresponding energies were saved after each one thousand MC moves. The results of simulations conducted at 300 K are presented here only, while the results of simulations performed at 1200 K are provided in Appendix B.5. In both simulations, the total energy increased precipitously in the beginning and then fluctuated about mean values of 1600 and 4800 kJ/mol, respectively, after reaching the equilibrium state (Figure 3.15). The collapse/folding of the initial linear PEG structure is entropy-driven and took the structure towards lower entropy at the expense an increase in the total energy. After reaching an equilibrium state, the energy stabilized and fluctuated about a mean of 1600 kJ/mol.

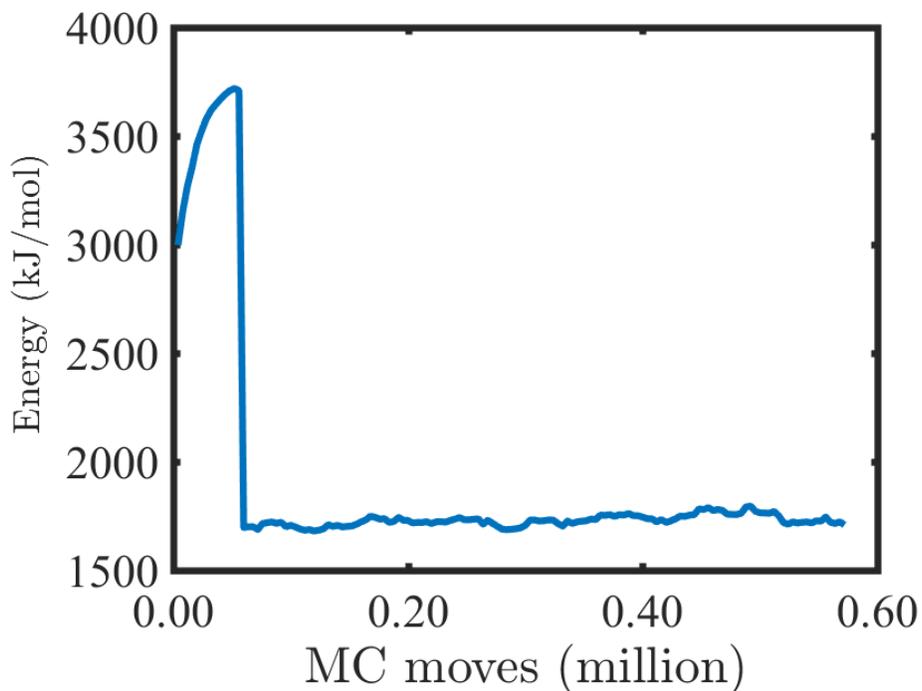


Figure 3.15: Energy fluctuations in the NPT ensemble MC conformational sampling simulations conducted at 300 K. These simulations were started with a linear PEG structure with a hydroxyethyl terminal and used HFF parameters.

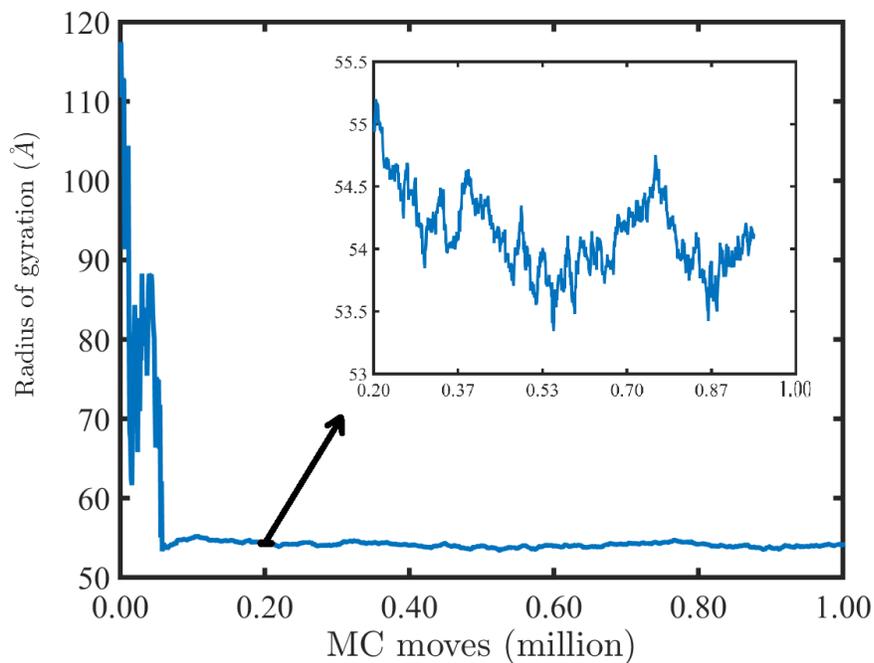


Figure 3.16: Change in the radius of gyration in MC conformational sampling conducted at 300 K, starting with a linear PEG structure. The structure reached an equilibrium state after completing less than 0.2 million steps. The inset diagram shows that large fluctuations that occurred in the beginning diminished in the equilibrium state.

The trend of radius of gyration indicates that the PEG molecule folds quickly in the beginning and remains in a semi-compact structure at the stationary state. There are quick and large fluctuations of a few tens of angstroms in the radius of gyration in the beginning of simulations and finally the structure acquired a stationary state at 54 Å after completing 0.12 million moves approximately (Figure 3.16) and remained in the equilibrated state until the end of simulations. The radius of gyration fluctuates over a small range in the stationary state with a standard deviation of 0.26 Å. These results suggest that PEG is not exploring the conformational space fully at 300 K. A similar trend is observed in sampling performed at 1200 K, in which the total energy and radius of gyration of an equilibrated structure fluctuates about mean values of energy of 4500 kJ/mol and of radius of gyration of 62 Å respectively with standard deviation of 0.16 Å in radius of gyration (Figures B.9 & B.10 in Appendix B.5).

In the second step of this section, a temperature quenching technique was applied to enhance the energetic and conformational sampling. The starting structure was simulated at 1200 K continuously from which a PEG structure was picked out periodically for quenching to 300 K. The quenched PEG structure was simulated further by performing an additional one thousand internal moves. The magnitude of each internal move, such as change in bond lengths, angles, dihedral angles and the number of moves at each step, were chosen using a trial-and-error method. The magnitude of each internal move used in the present simulations is tabulated in Table 3.5. We can change the number of moves and the magnitude of each move if necessary. For example, a larger number of internal moves could converge the structure quickly by changing the radius of gyration at greater rate in the beginning. However, the effect of increasing the number of internal moves diminished after reaching the stationary state. In these simulations, one thousand moves per step were optimal and produced one thousand conformations within four hours of processor time.

It was found that using the quenching approach, the energetic and conformational sampling space landscapes improved significantly in comparison to the simulations performed

Table 3.5: Type and magnitude of MC internal moves implemented in MC simulations in Sire.

Type of Move	Magnitude
Bond	-0.05, +0.05 Å
Angle	-15, +15 °
Dihedral	-15, +15 °

at single temperatures (Figures 3.17 & 3.18). For instance, the equilibrated structure fluctuated over a wide range of radius of gyration between 20 to 45 Å with standard deviation of 12 Å. The results showed the quenching approach enormously enhanced the conformational sampling in comparison to the single temperature simulations in MCCCSTowhee (Figure 3.11). The results showed that the folding rate of a linear PEG structure depends on the number of internal moves per step, the move ranges and the temperature. At higher temperatures, the stationary region includes larger sized open conformations as compared to the conformations at lower temperatures. The higher temperatures allow the execution of internal moves of larger magnitudes which resulted in more diverse and partially folded conformations.

To examine the effect of a larger number of internal moves on the folding rate, another simulation was run by performing 10,000 internal moves per step (Figures 3.19 & 3.20). The resultant energies and radii of gyration agreed with previous simulation results obtained after performing 1000 internal moves per step (Figures 3.17 & 3.18 respectively). The energies fluctuated over a slightly wider range from 4000–6500 kJ/mol as compared to previous energy range from 4200–5200 kJ/mol. However, radii of gyration in both simulations fluctuated in the same range from 20–45 Å. It is found that by increasing the number of internal moves per step vanished the higher energy peaks seen in Figure 3.17 and all the energies fluctuated about a mean value of 6000 kJ/mol (Figure 3.19). These results showed that a higher number of internal moves performed at 300 K results in more stable structures.

It is noted that the final energy fell in the range of 1200 to 1800 kJ/mol in the single temperature simulations conducted at 300 K (Figure 3.15) as compared to a quenching

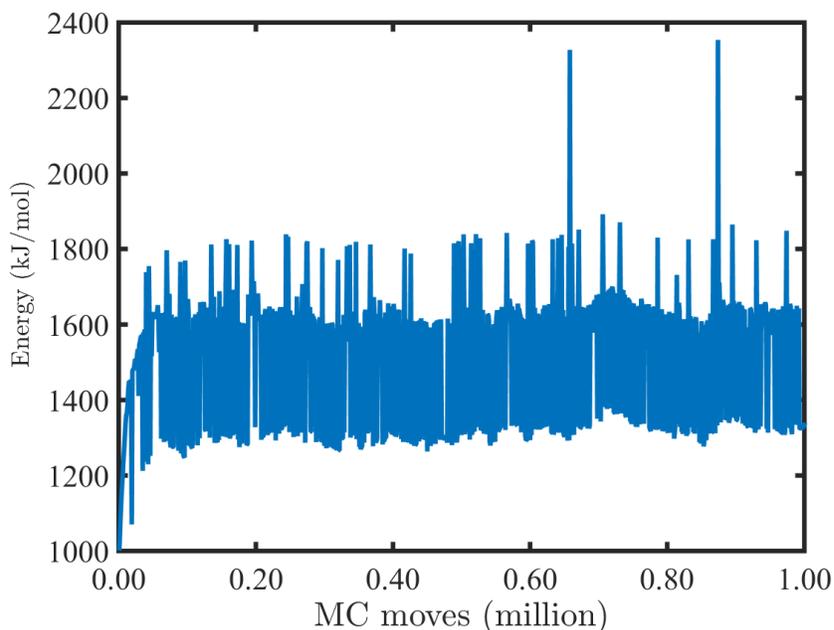


Figure 3.17: Energy change during MC conformational sampling at 300 K, using a temperature quenching approach between 300-1200 K. These simulations used a linear 8 kDa PEG with a hydroxyethyl terminal group and HFF parameters.

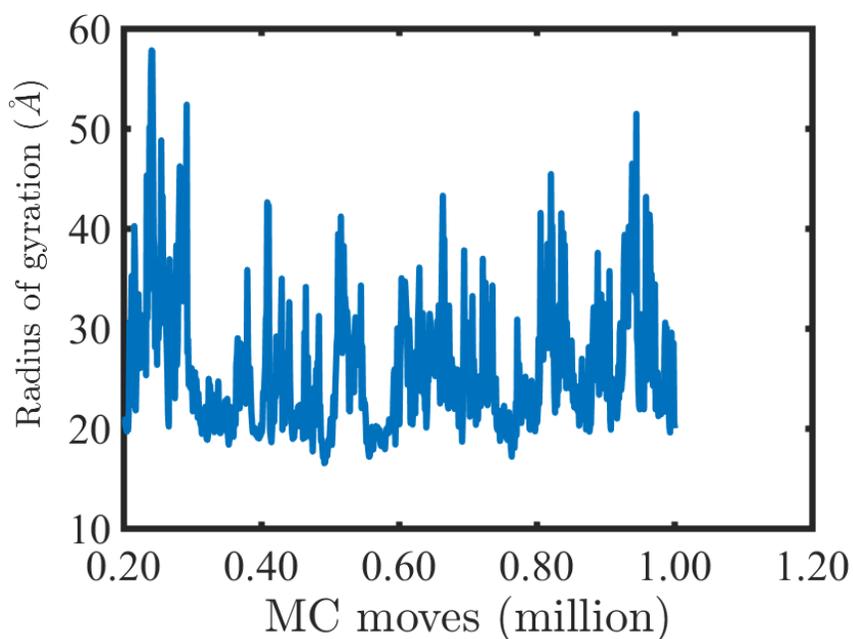


Figure 3.18: Change in the radius of gyration in MC conformational sampling at 300 K, performed with a temperature quenching method. The quenched PEG structures are optimized by performing an additional 1000 internal moves. These simulations started with a linear 8 kDa PEG with methyl terminal group and MFF parameters. Regardless of energy trends, a temperature quenching method is producing radii of gyration in a range that is consistent with the experimental data discussed in the concluding remarks on the Sire MC sampling.

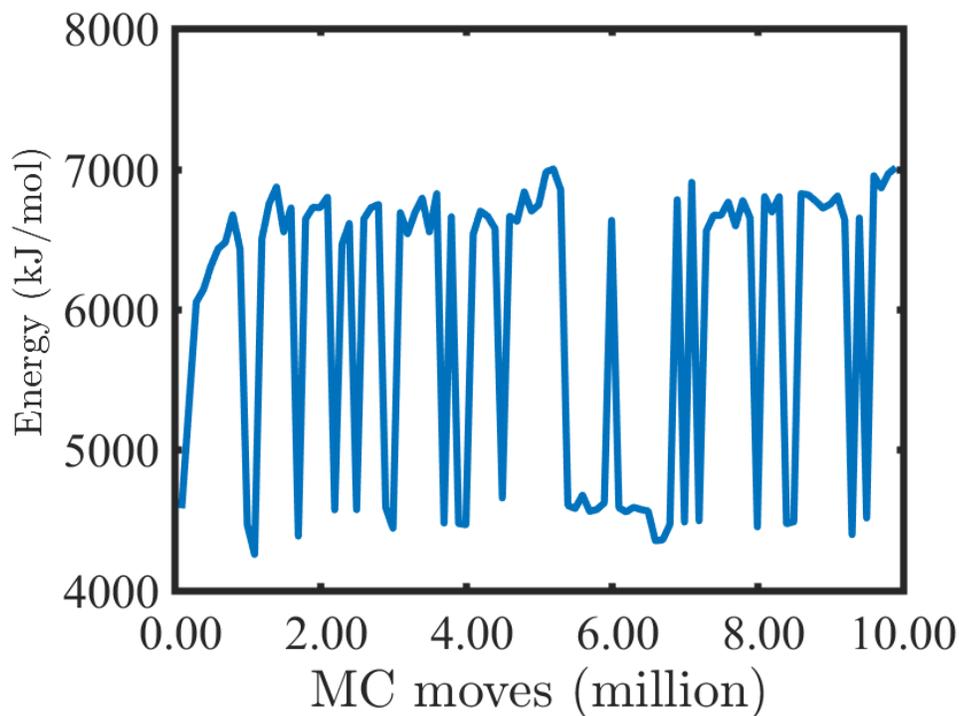


Figure 3.19: Energy change during MC conformational sampling at 300 K, using a temperature quenching approach between 300-1200 K with 10,000 MC moves. These simulations used a linear 8 kDa PEG with methyl terminal group and MFF parameters.

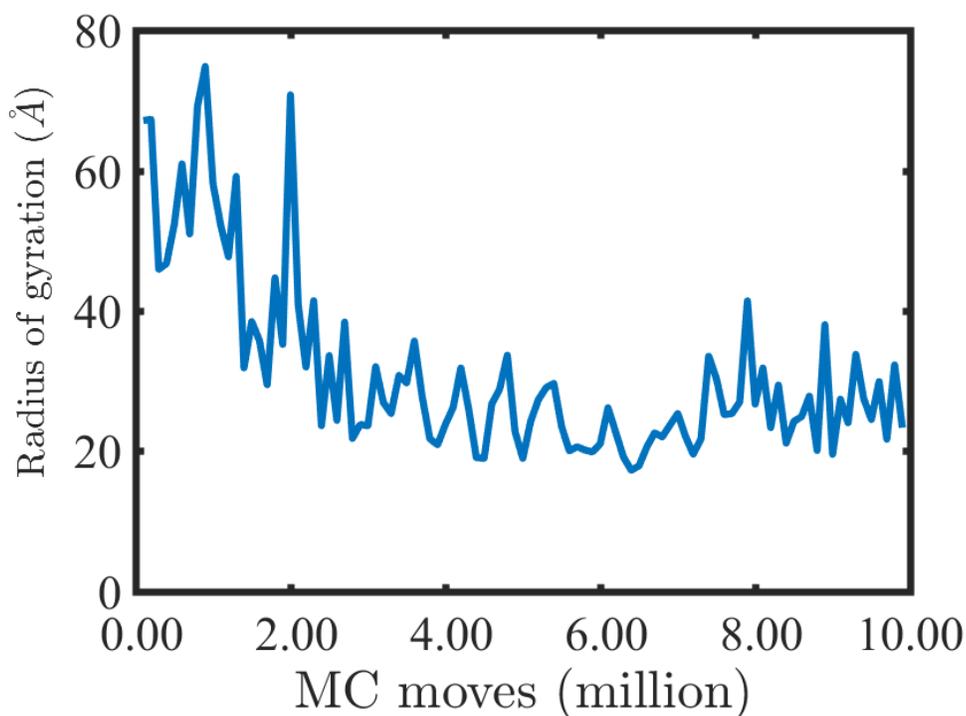


Figure 3.20: Change in the radius of gyration in MC conformational sampling, performed with a temperature quenching method using 10,000 MC moves. These simulations used a linear 8 kDa PEG with methyl terminal group and MFF parameters.

approach where the total energies of the resultant conformations simulated at 300 K fell in the range between 4500 to 7000 kJ/mol. The quenching approach resulted in higher total energies of the resultant structures, even after optimizing the structure at 300 K. To bring the structure energies down to the 1200-1800 kJ/mol range in the quenched simulations, a larger number of internal moves than 1000 were performed at 300 K. We performed an additional 10,000 and 0.5 millions internal moves per step in two individual simulations at 300 K but it was found that the higher number of moves were unable to bring the system energies to 1600-1800 kJ/mol range. However, it spread the energy spectrum over a broad range between 4200 to 6800 kJ/mol (Figures 3.19 and 3.20).

Three typical PEG conformations were chosen from the Sire simulations conducted at 300 K with a temperature quenching approach for illustration purposes (Figure 3.21). These pictures are taken at 0.05, 0.5 and 1.25 million MC moves and showed how the linear PEG folded over time.

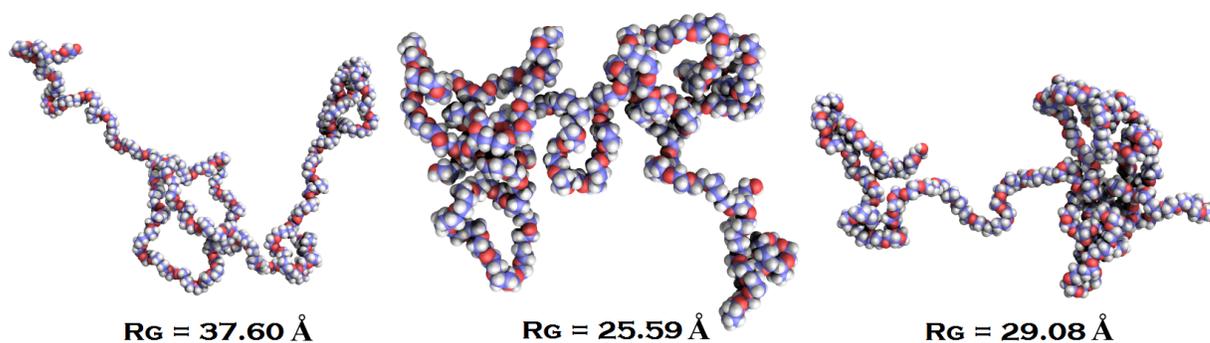


Figure 3.21: PEG snapshots taken at 0.05, 0.5 and 1.25 million MC moves (left to right) to illustrate the PEG conformational sampling. These conformations were picked from the simulation performed in Sire using a quenching approach and started with a linear PEG structure.

In the last step, two simulations using a PEG structure with methyl and hydroxyethyl terminals were performed to investigate the effect of terminal groups on folding behaviour. The results showed that both simulations produced similar energies and radii of gyration trends to the single temperature simulations (Figure 3.15 & 3.16) and the terminal groups did not play a significant role in changing folding behaviour. Since these simulations did

not make any difference in the results, the results are provided in Appendix B.5.

Concluding remarks - Sire MC sampling

Sire has done a great job in developing the library of diverse PEG conformations as compared to MCCCSTowhee (Figures 3.11 & 3.18 respectively). Sire generated the conformations in a wide range from 18 to 60 Å approximately whereas MCCCSTowhee produced conformations in a very limited range from 30 to 34 Å. It is worth noting that, regardless of large energy fluctuations (Figure 3.17), Sire is giving a spread of radii of gyration (Figure 3.18) that is consistent with the experimental spread. The theoretical and experimental investigations reported 15 [80, 255], 24.5 [63, 110, 112], 25 [90], 27 [55], 28.5 [55], 30 [111], 31 [90, 91], 36 [90], 40 [55], 43 [107], 46 [89, 107], and 40-60 [55] Å radii of gyration of an 8 kDa PEG. In addition, Sire provides a lot of control over simulation design and is also a good tool to optimize the structures locally.

3.2.3 MD sampling in AMBER

So far, two different programs, i.e. MCCCSTowhee and Sire, were used to conduct MC conformational sampling. In addition to MC simulations, conformational sampling simulations were also performed in Amber by using the MD simulation approach. MC simulations, a stochastic approach, are exploring the energy surface by probing the geometry of a given system by changing bond lengths, angles, and dihedral angles randomly [85, 86, 104] whereas MD simulations determine the particle trajectories from Newton's second law. MD simulations require an initial geometry and atomic velocities of the system. The atomic velocities are assigned from the Maxwell distribution and the system is run to achieve the equilibration. The progress of the process is monitored until the total kinetic energy becomes stable [256, 257]. We selected the Amber program [105, 194, 226] among the other MD programs [106, 182] due its vast use in studying biochemical reactions. Amber requires forcefield parameters for all the molecules involved in the simulations to

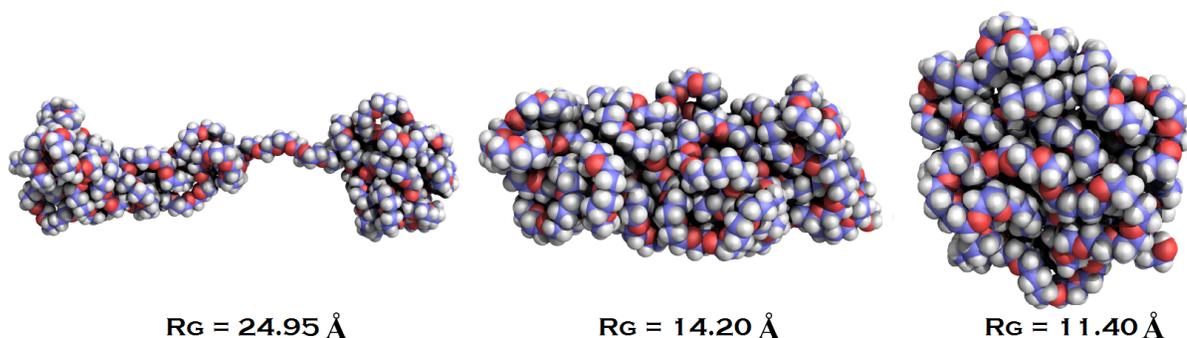


Figure 3.22: PEG snapshots taken at 2.5, 3.0, and 10 ns time steps (left to right) of MD simulations conducted at 300 K in Amber, using PEG of 8 kDa to illustrate the PEG folding.

calculate the total energy. Amber provides these necessary forcefield parameters for the majority of common molecules such as proteins, RNA, DNA, water and many other small organic molecules [226]. However, forcefield parameters for PEG are unavailable in Amber. Therefore, it is necessary to build PEG forcefield parameters before conducting MD conformational sampling. The missing PEG forcefield parameters for Amber MD simulations were generated on the PyRED server [208, 209]. The details on the development of forcefield parameters are covered in section 3.1.

In this section, three individual sets of MD simulations were performed to construct the libraries of PEG conformations. In these simulations, the effects of temperature, of chemical composition of PEG, and of implicit and explicit solvent models on the conformational sampling of PEG were studied. The sole purpose of testing these factors was to enhance the distribution of PEG conformations in the resultant libraries. Eventually, the following two sets of simulations were carried out:

1. MD conformational sampling at 300 K using a PEG with methyl, hydroxyethyl and propyl terminals in an implicit and explicit solvents.
2. Investigate the effect of high temperature by conducting simulations in an implicit solvent at 1200 K.

In the first case, three libraries of PEG conformations was constructed by running 10 ns

long 300 K MD simulations using an NPT ensemble, Langevin thermostat and the implicit solvent Born model [231]. These simulations started with three linear PEG structures. These structures were constructed by joining the three fragments generated during the forcefield parameter step (Figure 3.2). The results showed that PEGs with all three different terminals showed similar folding behaviour, in which the radius of gyration decreased to 12 Å approximately (Figure 3.5). The total energies of both PEGs with methyl and propyl terminals were converged after completing 5 ns of simulation time. However, the total energy of the PEG with hydroxyl terminal dipped over a period of about 5 ns. The only big difference is that it started from an energy much closer to its final energy. To illustrate the folding progress during the MD simulation three snapshots at 2.5, 3.0, and 10.0 ns time steps were taken (Figure 3.22). These snapshots showed that PEG folded to a compact conformation. The structures collapsed due to intra-molecular hydrogen bonding. Previous studies provided evidence of the presence of intra-molecular hydrogen bonding which lead to folded helical and coiled structures of PEG in water [89, 92, 95, 96, 101, 109].

In the second case, two additional 10 ns long MD simulations were performed using an NPT ensemble, Langevin thermostat and the explicit solvation (water) at 300 K to investigate the effect of terminal groups on folding behaviour of PEG. For this purpose, two PEG conformations with methyl and hydroxyethyl terminals were used. The results of these simulations demonstrated the same folding behaviour in which the PEG formed a very compact structure again after reaching the stationary state. Experimental and theoretical investigations showed contradictory results in which a few studies showed that PEG has a self aggregation property which not only leads to compact structures of individual PEG molecules in solution [101] but also forms PEG aggregates [101, 258], while others showed that PEG formed partially folded structures [109, 259]. Moreover, QM calculations also confirmed the presence of intra- and inter-molecular hydrogen bonding in PEG which could lead to such compact conformations [101]. These results demonstrated a folding pattern of coil formation similar to the previous experimental findings [89, 92, 93, 95, 101].

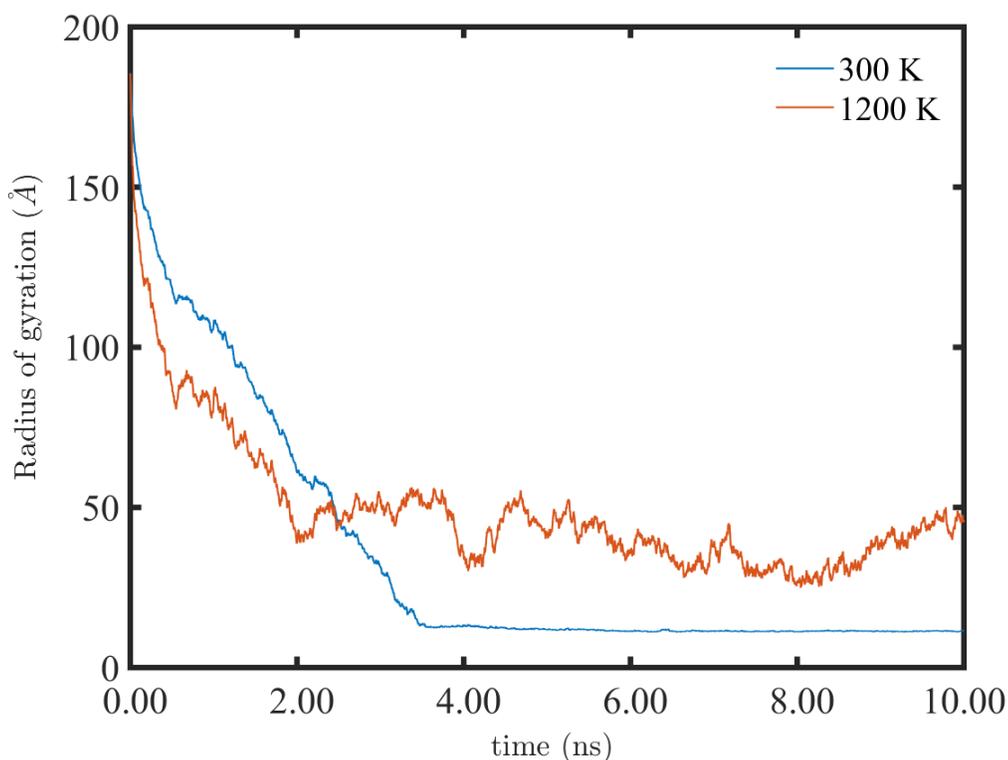


Figure 3.23: Radius of gyration change in the MD conformational sampling of PEG with methyl terminal group, conducted at 300 and 1200 K in Amber using NPT ensemble and implicit solvation model.

In the last step, another 10.0 ns long MD simulation was performed at 1200 K, using a PEG with a methyl terminal. The high temperature in these simulations (Figure 3.23) produced relatively open conformations and the radius of gyration was found fluctuating around a mean of 40 Å.

Concluding remarks - MD simulations

MD simulations in Amber provided an alternative method to MC simulations in Sire and could be used potentially to construct the ensemble of PEG conformations. MD conformational simulations were conducted on three types of linear PEG structures at 300 and 1200 K in implicit solvent. The folding behaviour of PEG was found to be insensitive to the terminal groups. Moreover, the explicit solvent model has no effect on the folding be-

haviour and eventually PEG with methyl, hydroxyethyl, and propyl terminals collapsed to a compact conformation.

3.2.4 Conclusion - Ensemble of PEG conformations

The objective of this section was to develop libraries of PEG conformations that can be used to mimic the crowding environment in computer simulations. In order to populate these libraries with conformations that are as diverse as possible, two approaches, i.e. MC and MD approaches, were chosen and performed under different temperature, PEG composition and explicit and implicit solvents. MC simulations were employed in MCCCOS Towhee and Sire while the MD simulations were performed in Amber. In the first category of MC methods, Sire was found to be more productive in terms of utilizing computer resources efficiently, flexibility in running desired types of simulations, and eventually yielding a diverse distribution of PEG conformations as compared to MCCCOS Towhee (Figures 3.18 & 3.11 respectively). MCCCOS Towhee sampled conformations over a limited energetic and conformational landscape and resulted in PEG conformations falling in a restricted range relative to Sire. Due to this fact, the resultant library of MCCCOS Towhee structures was not used for packing simulation boxes. Both MC and MD approaches produced diverse PEG conformations in Sire and Amber respectively. In contrast to MD simulations, MC sampling in Sire was quicker and formed partially folded conformations. It was found that the folding behaviour was insensitive to PEG terminal groups in Sire. However, PEGs with methyl and propyl terminals collapsed in all simulations irrespective of the presence of explicit or implicit solvent models in MD simulations. The diverse distribution is further shown by comparing the radius of gyration of sampled conformations taken from MC in Sire and MD simulations (Figure 3.24). The majority of conformations from MC prevailed in the central region in between 20 to 40 Å while MD simulations formed the majority of conformations from 10 to 20 Å with standard deviations of 7.35 and 5.80 Å

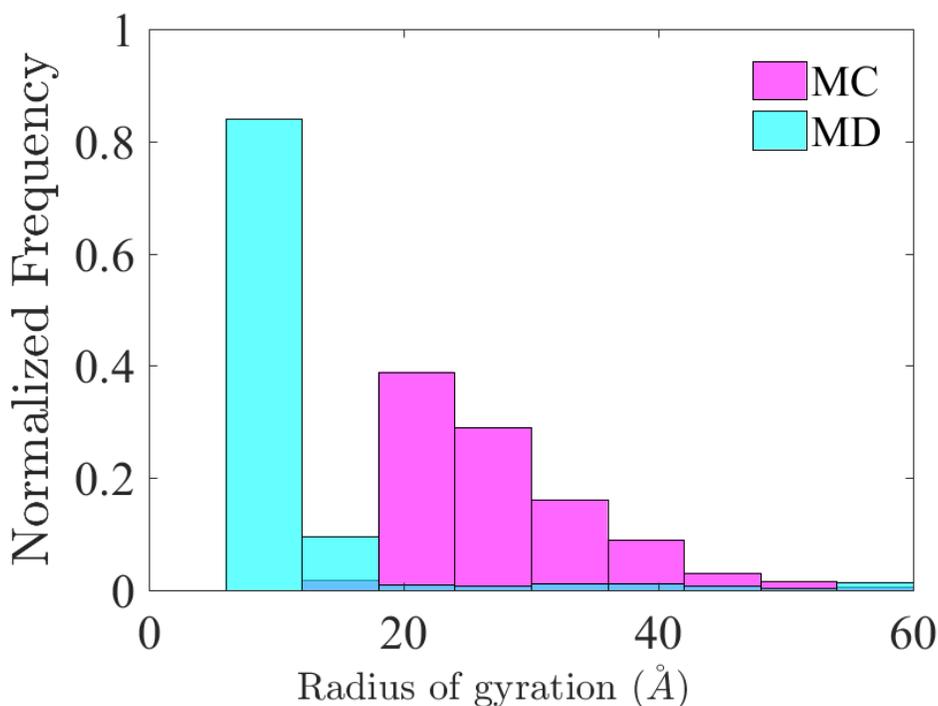


Figure 3.24: Distribution of PEG conformations from start to and end in MC Sire and MD Amber simulations performed at 300 K using linear structures of 8 kDa PEG with methyl terminal. PEG conformations of 20-60 radius of gyration were used for packing the crowded systems. The transparency of the bars results in a blue color where the two distributions overlap.

respectively. These results showed that MC sampling simulations produced conformations over a wide range and these values in good agreement with experimental radii of gyration of 24 to 36 Å [55, 63, 90, 91, 107–112].

In a nutshell, we have presented three approaches to develop libraries of PEG conformations. We have used these conformations from both methods to prepare the crowded systems.

3.3 Packing and equilibration

MC and MD conformational sampling was performed to build PEG conformational libraries. MD simulations produced diverse conformations with a slightly larger range of radius of gyration as compared to MC simulations in Sire (Figure 3.24). We performed a

variety of MC and MD simulations to achieve our goal of constructing libraries populated with representative diverse and dynamic solution structures of PEG falling in the range of 15 to 60 Å of radius of gyration. Four libraries were populated with PEG conformations from MC and MD simulations performed in Sire and Amber respectively. Two of the libraries contained equilibrated structures only taken from the stationary state region while the other two were populated from the beginning to the stationary state. The last two libraries contained more diverse conformations with radii of gyration from 10 to 125 Å (Figures 3.25 & 3.26).

These conformational ensembles of four libraries were used to prepare the simulation boxes at six different concentrations from 0.1 to 0.6 g cm⁻³. 25 to 150 PEG molecules of 8 kDa molecular weight were packed in boxes of dimensions 300 × 300 × 300 Å³. Fifteen copies of the simulation boxes at each concentration were prepared by packing randomly chosen PEG conformations from the library using Packmol [232]. Packmol performed 1,000 trials in total to pack and optimize each simulation box. Each trial tried to place the molecules at random points in space without steric clashes. Packmol saved the final packed configuration on satisfying the tolerance criterion. The tolerance criterion represents the minimum distance between the surface of two molecules. In the preparation of simulation boxes, the tolerance of 3 Å was set. The value of 3 Å was chosen using a trial-and-error method and it results in optimized packing with no steric clashes. A large value greater than 5 Å took a long time for packing the intermediate and high concentration boxes, i.e. 0.3 to 0.6 g cm⁻³, and required more than 1,000 trials to find an optimized configuration satisfying the tolerance criterion. The calculation cost depends on the concentration, type of conformations of the molecules, and the tolerance criterion. At the lowest concentration of 25 molecules of PEG, one trial of packing and optimization took approximately 5 seconds whereas 30 seconds were required at the maximum concentration. The lowest concentration systems were packed and optimized in less than 50 trials and the most concentrated systems completed 800 to 1,000 trials on average. The packed and optimized simulation boxes at

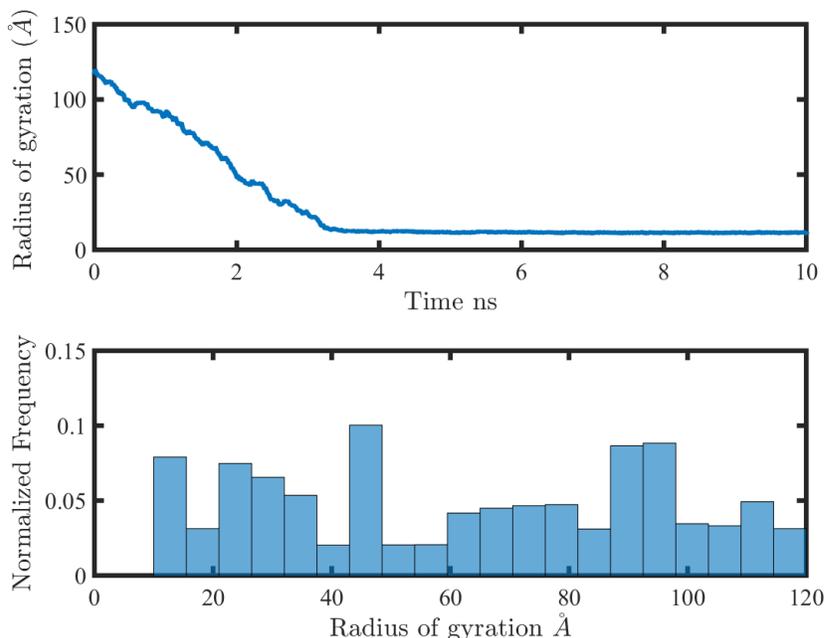


Figure 3.25: Radius of gyration change from start to stationary stage during MD sampling (top) while the distribution of PEG radii is illustrated in the histogram (bottom). The final structures were saved at 300 K up to 5 ns long MD simulations in Amber with a 1 fs time step and using an NPT ensemble, implicit solvation model and a linear PEG structure with a methyl terminal group, using a MFF parameters.

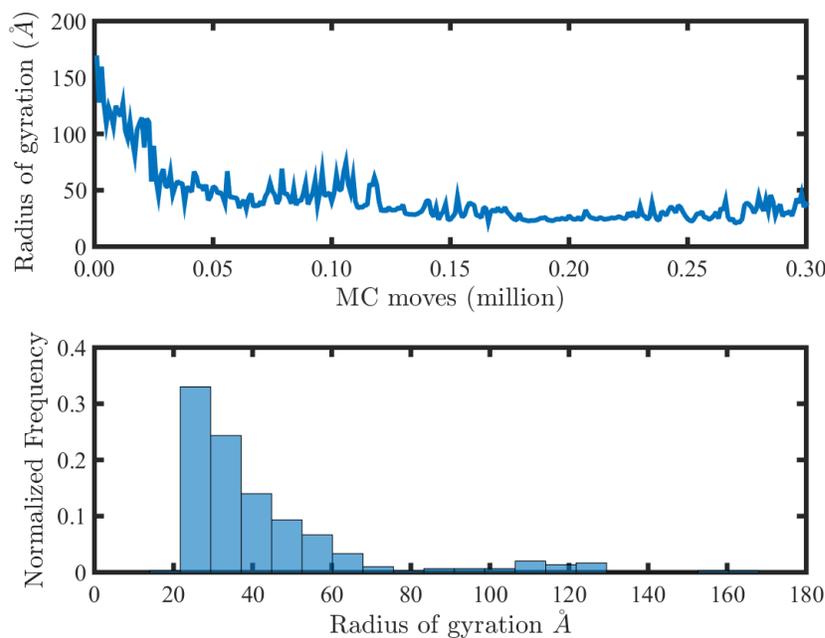


Figure 3.26: Radius of gyration change from start to stationary stage during MC sampling (top) while the distribution of PEG radii is illustrated in the histogram (bottom). The final structures were saved at 300 K up to 0.3 million moves of an MC simulation in Sire started with a linear PEG structure with a methyl terminal, using the MFF parameters.

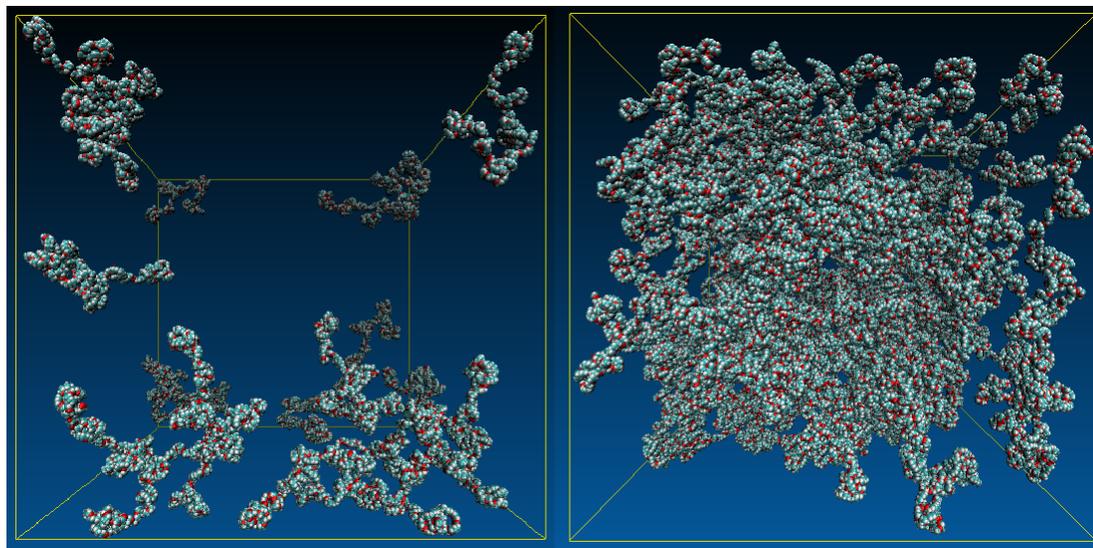


Figure 3.27: Sample packed simulation boxes at the lowest (left) and highest (right) concentration (0.1 and 0.6 g cm^{-3} respectively) by Packmol.

the lowest and highest concentrations in a $300 \times 300 \times 300 \text{ \AA}^3$ box present large spaces at low concentration whereas the box space is almost filled at the highest concentration (Figure 3.27).

It is noted that all of these conformational ensembles of PEG were prepared under dilute conditions. Therefore it was necessary to further equilibrate the simulation boxes to optimize the packing and observe the high concentration effects on the PEG conformations. We developed and applied three approaches, namely MC swapping, MC equilibration (in Sire) and MD simulations in Amber. The following two key points are discussed here to evaluate the efficiency of all three equilibration methods:

1. Equilibration of packed simulation boxes with two Monte Carlo methods (i.e. MC equilibration and MC swapping in Sire) and MD equilibration in Amber.
2. Efficiency of the three equilibration methods in terms of computational cost.

3.3.1 MC equilibration

MC equilibration is the first MC method developed to equilibrate the simulation boxes. 5,000 internal folding/unfolding and 5,000 rigid body translational/rotational moves were

performed in each step. Table 3.5 presents the sizes of various types of internal and rigid body moves, implemented in the MC equilibration algorithm. The computation cost depends on the size and concentration of the system. In a case study, the MC equilibration simulations were performed on the lowest concentration system of 0.1 g cm^{-3} , where each MC step took 3 minutes of real time on an eight core machine. The calculations run for 400 hours and it can be seen that the system requires more computation in order to reach the equilibrium state (Figure 3.28).

The large energy changes in Figure 3.28 are associated with major conformational changes while performing the internal moves on the PEG molecules. The working speed of the algorithm depends on the concentration directly. After performing 8,000 steps, it was found that PEG molecules folded towards more compact conformations in the presence of other PEG molecules (Figure 3.29). However, there is no evidence found that the PEG molecules formed any clusters or aggregates.

3.3.2 MC swapping

MC swapping is an alternative MC approach to the MC equilibration to equilibrate the given system. In this method, the algorithm swapped the PEG molecules between the simulation box and the conformational library. We assumed that the conformational library contains representative and equilibrated PEG solution structures. This was the aim of developing a library populated with diverse PEG conformations. The swapping algorithm performed 1 million steps in total before applying the convergence test. An MC step involves the selection of two random molecules, one in the simulation box and the other in the conformational ensemble library, rotation, translation and swapping the two molecules, and finally the energy calculations. The convergence test determines whether the system is equilibrated energetically or requires additional MC moves using the energy values. The convergence test uses a Student's t test [234, 235]. This test compared the energy values stored in two windows and checked the condition if the threshold value or significance

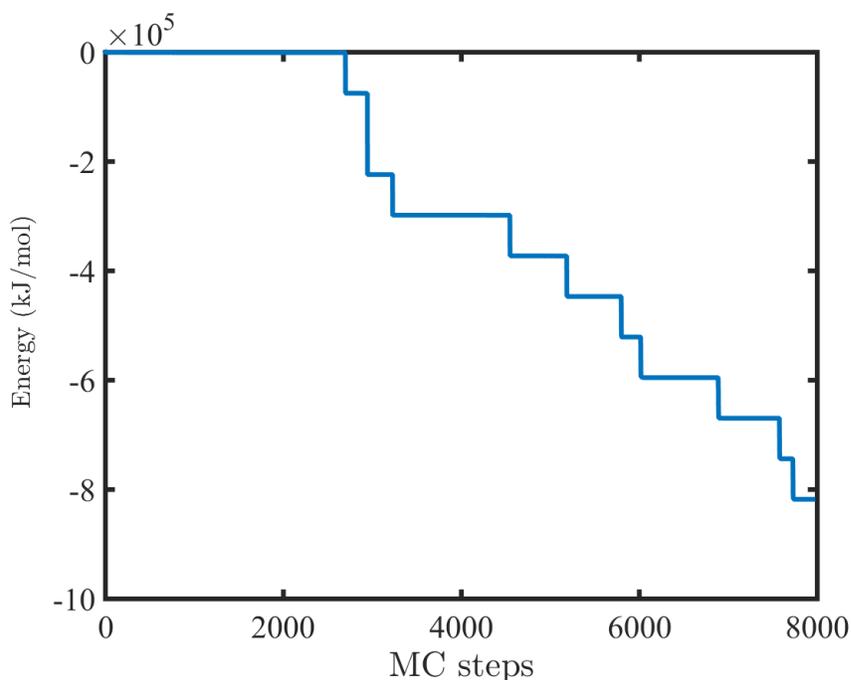


Figure 3.28: The energy change in a 400 hour MC equilibration, performing 5,000 internal and 5,000 rigid body moves in a single step, for a total of 8,000 steps. These MC simulations were performed using a least concentrated system with 0.1 g cm^{-3} concentration and used MFF parameters to compute the total energies.

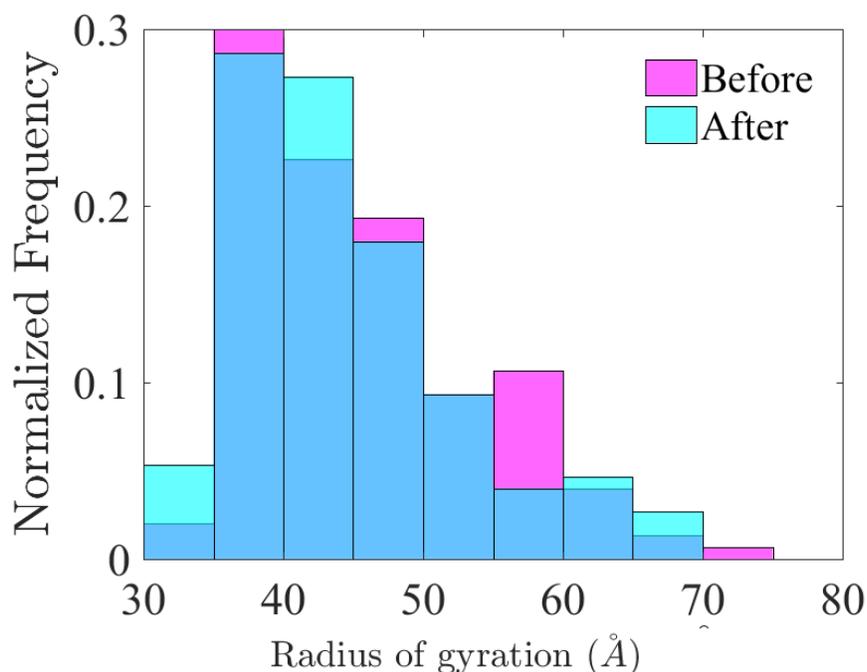


Figure 3.29: Distribution of PEG conformations before and after performing the MC equilibration algorithm at 300 K. These MC simulations were performed using a least concentrated system with 0.1 g cm^{-3} concentration. Larger sized conformations generally formed more compact conformation during the equilibration process. The transparency of the bars results in a blue color where the two distributions overlap.

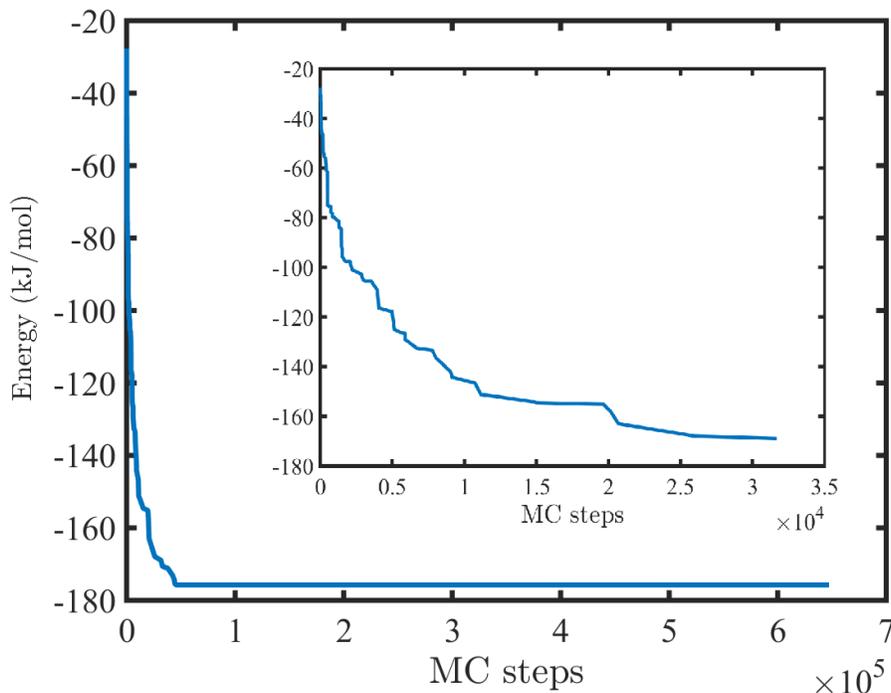


Figure 3.30: The energy change in a million step MC swapping simulation. The system reached the stationary state after completing less than 50 thousand steps. The inset demonstrated the rate of change of energy in the beginning of the simulation. These MC simulations were performed using a least concentrated system with 0.1 g cm^{-3} concentration and used MFF parameters to compute the total energies.

level of $s < 0.1$ is true to terminate the simulations, otherwise continue the loop for an additional 2×10 iterations until the condition is satisfied. The lowest concentration system reached an equilibrium state after completing 30 thousand steps (Figure 3.30). Each MC step takes a few seconds to complete.

The MC swapping method converged the system quickly as compared to the MC equilibration but at very high energy. This approach minimized the free energy by increasing the entropy while allowing the energy to increase. The computational cost also depends on the size and concentration of the system. This algorithm used a single core during the swapping process, excluding the energy calculation step where it used all the available cores.

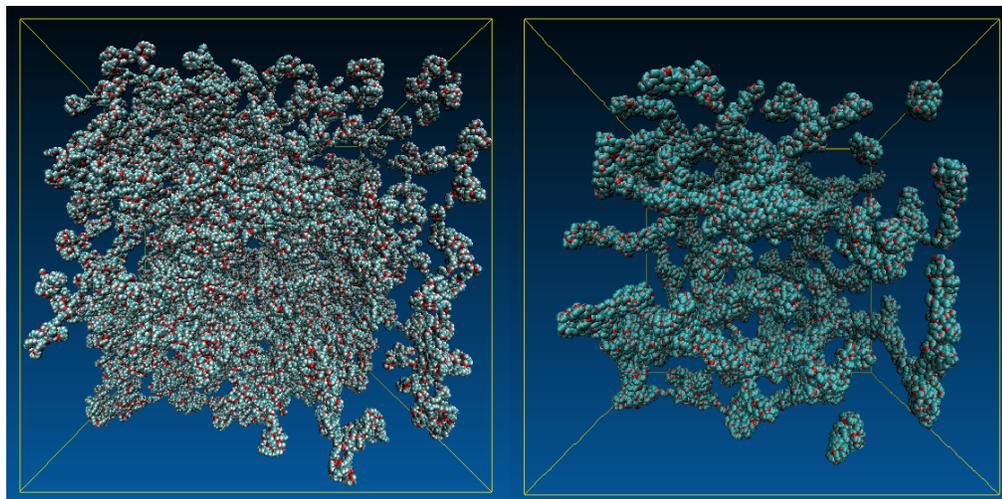


Figure 3.31: The presentation of the simulation box before and after the MD simulations and the formation of PEG aggregates after MD equilibration. These MD simulations were performed on the concentrated system with 0.6 g cm^{-3} concentration at 300 K, using an NPT ensemble in an implicit solvent and MFF parameters.

3.3.3 MD Amber simulations

MD simulation is the last method used to equilibrate the simulation boxes. The calculations were run on the WestGrid GPU machines using up to 4 nodes and 12 cores per node. It took approximately 60 hours to complete 20 ns long simulations for the lowest concentration (Figure 3.32). However, the computation time increased as a function of system concentration. The system is converged energetically after completing an 800 ps long MD simulation, where afterwards the energy fluctuates about a stable mean value of 10.5×10^4 kcal/mol. A comparison of energies of an equilibrated system with an MC and MD approach is provided in the concluding remarks of this section. The PEG formed clusters and aggregates in MD equilibration which is probably due to the forcefield parameters that are responsible for the formation of compact conformations and aggregates as shown in Figure 3.31.

Concluding remarks - Equilibration approaches

Three methods of equilibration namely MC equilibration, MC swapping and MD simulations are employed to equilibrate the packed simulation boxes. Among these methods, the

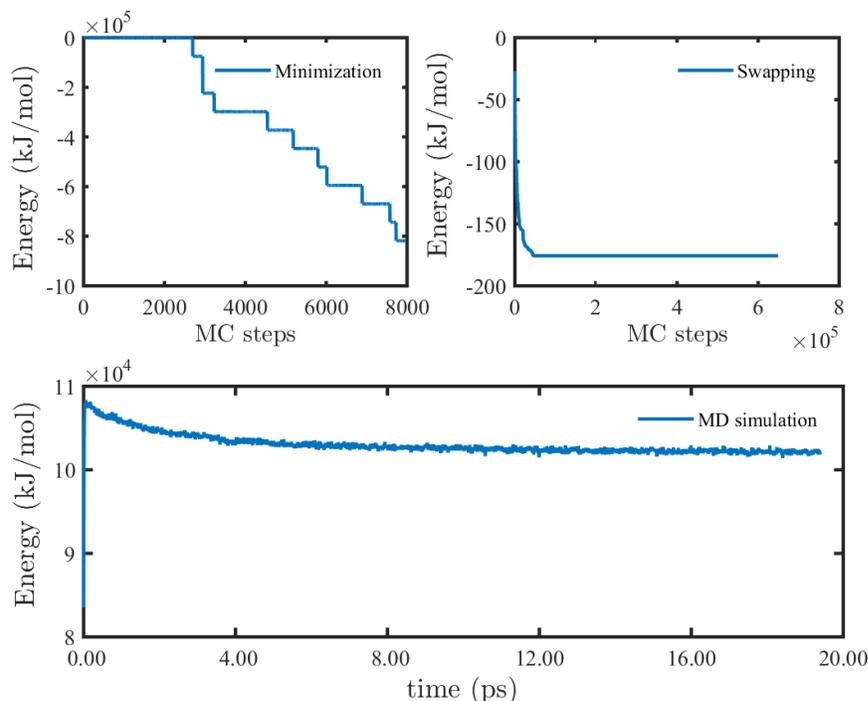


Figure 3.32: The energy change in the MD simulation in addition to MC equilibration and MC swapping. The system is converged after completing 20 ns of simulation time. MC equilibration and MC swapping methods were performed in Sire whereas the MD simulations were performed in Amber. The total energy change scale is different due to the different programs we used. However, all the simulations used the same input files.

MC swapping was found to be the least efficient in terms of using computer resources and taking the system to the lowest energy state. The MC equilibration approach is more efficient in terms of lowering the energy efficiently due to performing internal and rigid body moves. The MC swapping and minimization methods used multiple cores only in energy calculations which is why these approaches are time consuming. On the other hand, Amber MD simulation was the fastest approach using the Compute Canada WestGrid parallel-GPU machine. It equilibrated the simulation box of 0.1 g cm^{-3} in approximately 12 hours. However, the computation cost increases with the concentration and it took approximately 60–72 hours for the highest concentration systems.

Moreover, the MC simulation methods did not show any cluster formation during the equilibration process whereas the MD simulations resulted in the formation of aggregates of PEG molecules. The clustering behaviour depends on the number density of the molecules

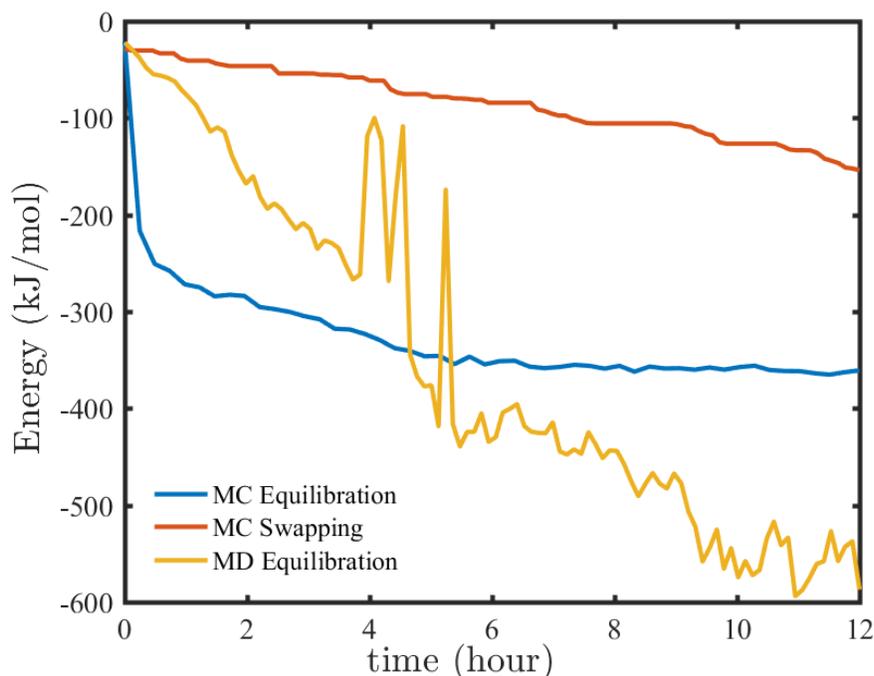


Figure 3.33: Comparison of real time for three methods along with energy decay. The simulations were run for 12 hours. MD simulations were more effective in terms of taking the system to the lowest energy in the given amount of time.

in the given system and a larger number of aggregates formed in the highest concentration of 0.6 g cm^{-3} . Previous studies showed that the PEG molecules form clusters in solution [95, 259–261]. Many causes of clustering such as intermolecular hydrogen bonding, impurities in solution, physical cross linking and chain end effects have been reported. The experimental findings of the small-angle neutron scattering (SANS) technique showed that the chain ends of the polymers are responsible for cluster formation [95, 259–261]. In our equilibration MD simulations, we tested the folding and aggregation behaviour of PEGs with methyl, propyl and hydroxyethyl terminal groups and found that PEG molecules showed spontaneous self-assembly behaviour regardless of terminal groups. This self-assembly behaviour leads to the emergence of individual compact structures and subsequently leads to aggregation [101].

The efficiencies of the three approaches were compared based on the real time elapsed using the same computer resources (Figure 3.33). The MD simulations took the system

to the lowest energy level in the given time of approximately 12 hours whereas the MC equilibration is the second best. Considering the real time efficiency, the MD simulations were used to equilibrate all the simulation boxes. Fifteen copies of simulation boxes at each concentration were saved for the calculation of the fraction available volumes and the statistical analysis.

3.4 Summary

The aim of the chapter was to prepare the crowded medium filled with diverse PEG conformations. In a nutshell, all the basic steps i.e. construction of forcefield parameters, construction of crowder conformations, packing and equilibration of crowded medium are covered that one needs to perform in order to achieve the goal. Regarding the first step of constructing the ensembles of PEG conformations, the MC simulations in Sire and MD simulations in Amber produced reasonably diverse PEG conformations that are consistent with experimental findings. MD simulations were found to be more efficient among two other MC equilibration methods to equilibrate the packed crowded medium in the final step. Moreover, MD equilibration result in further reduction in size of individual PEGs and also formation of PEG aggregates. Further, the efficiency of equilibration varies with system concentration.

Chapter 4

Conformational equilibrium in crowded media

This chapter presents the results of fractional available volumes and kinetics of conformational equilibrium obtained by executing the second part of the program recipe (Figure 4.1 (right)). In the previous chapter, we prepared six crowded systems filled with a variety of PEG conformations. Two methods, namely Monte Carlo (MC) simulations and the extended scaled particle theory (SPT) were used to compute the crowding effects on the conformational equilibrium of three pairs of macromolecules in these crowded systems. The MC and SPT models estimated the crowding effects by computing the fractional available volumes, and subsequently thermodynamic activities for all selected pairs of conformations in the crowded media. The results from both models are further compared with results obtained in other experimental and theoretical studies. Finally, the transition state theory model is applied to estimate the macromolecular crowding effects on the folding kinetics of the GAAA tetraloop receptor.

4.1 Fractional available volume calculations

An attempt was made to provide a quantitative description of the effect of macromolecular crowding on the conformational equilibrium of three systems by carrying out MC and SPT simulations. In this regard, various excluded volume theory models [143–157] including the SPT models [29, 33, 37, 81, 83, 158] have been developed to predict the macromolecular crowding effects on the various biochemical reactions. Generally these models

estimated the crowding effects on the equilibria and rates of biochemical reactions in a qualitative sense. However, the SPT formalism is successful in predicting the quantitative effects of crowding in certain cases [3, 12, 82, 262]. The SPT model predicts the crowding effects by estimating the magnitude of an excluded volume effect simply based on the sizes and shapes of molecules present in the medium. We are looking at the effects of crowding due to excluded volume rather than other effects contributed by the electrostatic potentials, enthalpic and entropic intermolecular interactions [37, 262].

It has been found that a mixture of crowders affects the activities more than a single type of crowder [21, 24, 49]. Also, these models present a static picture of the reaction media before and after placing the probe molecule but the cellular interiors are fluids and have characteristic properties of a mobile phase [8]. An addition of a probe molecule could possibly affect the packing of background molecules due to steric repulsion and could lead to a change in packing and size distribution of background molecules in the immediate vicinity of the probe. These factors are totally ignored which could potentially contribute to the thermodynamic activities of reacting species and thus predicting crowding effects quantitatively.

The present work is moving one step towards building a quantitative excluded volume theory model by introducing diverse conformations of PEG crowders to replace the ordinary spherical shaped fluid particles. Moreover multiple copies of crowded systems at each concentration were used to represent the dynamic size distribution of crowders in solution, as well as incorporating effects associated with crowder aggregation in the crowded media. In this regards, an MC simulation and extended SPT models were developed. The computational efficiency and outcomes of both methods is discussed in the following sections.

4.2 MC Simulations

MC simulation was our first method to compute the fractional available volumes for three given pairs of probe molecules in the equilibrated simulation boxes in addition to

the SPT model. This MC method calculated the fractional available volumes in a two-step procedure. At first, the algorithm inserted the probe molecule in the crowded medium at a random place with a random orientation and then it evaluated the success or failure of insertion in each trial by determining whether there were steric clashes. Regarding the success or failure of each insertion trial, two MC algorithms i.e. parallel-energy and parallel-distance algorithms were used to find the steric clashes. The name indicated the criterion used in these algorithms to evaluate the steric clashes. For example, the parallel-energy algorithm used the energy threshold to compare with the final energy after placing the probe molecule in the crowded medium to evaluate the success or failure of each insertion trial. We employed both algorithms to find the steric clashes and provided the comparison of resultant fractional available volumes. Moreover, the computational efficiency of both algorithms was also tested. A set of multiple copies of each crowded system with and without PEG aggregates was used to estimate the fractional available volumes for the probe molecules.

4.2.1 Efficiency comparison of two MC algorithms

Two MC methods namely parallel-energy and parallel-distance algorithms were developed to determine whether there is a steric clash or not on placing a molecule in the crowded medium at a random place and orientation. This information was used to determine the fractional available volumes in the crowded medium from the ratio of accepted to total number of trials. In these methods the steric clash is determined based on the atomic distances or energetic threshold criteria. The parallel-distance algorithm used the van der Waals atomic radii [60, 193] to determine the steric clashes whereas the parallel-energy algorithm used an energy threshold of 50,000 kcal/mol ($\sim 200,000$ kJ/mol). The energetic criterion was found by trial and error. It was observed that the system with a successful insertion has total energy less than 1000 kcal/mol (~ 4200 kJ/mol). However, in certain cases, it was found that the probe molecules are placed in a close vicinity of PEG molecules without steric clashes resulting in higher total energies of 5000–15,000 kcal/mol ($\sim 20,000$ – $62,000$ kJ/mol). The

ten times higher threshold energy of 50,000 kcal/mol was chosen to avoid false negatives, i.e. cases where there are not any steric clashes even though the energy is high, but it might be possible the simulations produced false positives with clashes that fall under the energy threshold.

In these two algorithms, computation cost depends on the concentration and type of calculations, i.e. total energies or van der Waals distance calculations. The parallel-energy algorithm was found to be faster than the parallel-distance algorithm. The parallel-energy algorithm estimated the total energy of the whole system at once using a built-in, highly optimized energy function. However, the parallel-distance algorithm performed distance measuring calculations between all atoms of probe and crowder molecules in each insertion trial through many loops. Since the 8 kDa PEG is fairly large, the algorithm spent a lot of time on this stage to determine a steric clash by measuring the atomic distances.

The computational cost of the parallel distance algorithm was reduced by defining additional criteria for determining the steric clashes. One additional criterion eliminated all the background molecules from the steric clash measurement whose centres are separated by more than 60 Å. This radius encapsulated the whole probe molecule and would differ with the size of the probe molecule. Similarly, the additional criterion reported a steric clash instantly if there is any background molecule found within a centre-to-centre distance of 10 Å of the probe molecule. The parallel-distance algorithm with these additional criteria reported a steric clash quickly and eliminates the extensive loop calculations. These threshold values were picked using trial and error considering the shapes and sizes of PEG molecules. Although the parallel-distance algorithm with additional criteria was found to be still expensive but it can give the correct fractional available volume given that it does not involve any approximations.

The parallel-distance algorithm with the additional criteria is computationally expensive but estimated the fractional available volumes more accurately than parallel-energy algorithm. A comparison of the fractional available volumes for the pseudoknot RNA (PDB

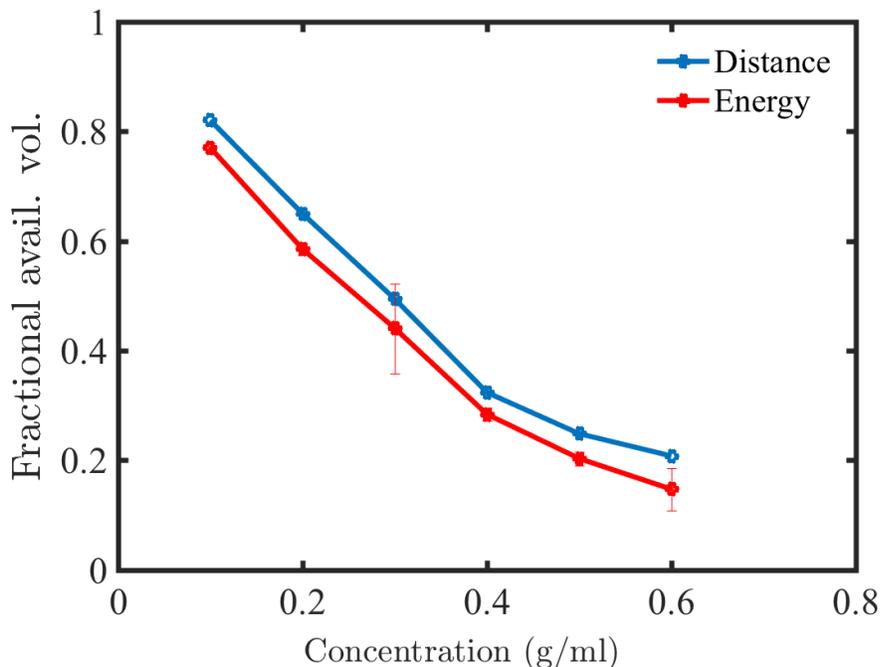


Figure 4.1: The comparison of the parallel distance and energy algorithms in measuring the fractional available volumes for the pseudoknot RNA conformation. The abscissa axis shows the fractional available volume and the ordinate is the concentration of PEG from 0.1 to 0.6 g cm⁻³ in the simulation box. Thirty copies of the simulation box at each concentration were used in the parallel-energy algorithm while a single copy was used in the parallel-distance algorithm with the additional criteria to speed up the calculation. The parallel-distance algorithm produced fractional available volumes approximately 5 percent higher than the parallel-energy algorithm.

ID: 2K96) is given in Figure 4.1, using both methods. The results showed a good agreement between both algorithms. The energy-based calculations showed a little less fractional available volumes than the parallel-distance method. The fractional available volumes were lower with the parallel-energy algorithm because these are average values over fifteen boxes while only a single copy was used in the parallel-distance algorithm. The reason to use a single copy of a simulation box was the computational time where the parallel-distance algorithm took an extreme amount of time. On average, the parallel-distance algorithm spends more real time on a single system of the minimum concentration than the parallel-energy algorithm that completes the same number of trials on all fifteen systems of the minimum concentration. The computational cost in both algorithms increased with con-

centration. The parallel-distances algorithm spent almost 80 hours to complete 12,000 insertion trials for the 0.1 g cm^{-3} system whereas the parallel-energy algorithm completed the same task in about half an hour using the same computer resources. Hereafter, the calculations of the fractional available volume in the simulation boxes were performed using the parallel-energy algorithm due to the lower computational cost.

4.2.2 Effect of PEG aggregation

The fraction of free volume for three pairs of macromolecules was estimated in the non-equilibrated simulation boxes. The simulation boxes were further equilibrated by MD simulations to observe the high concentration effects on the PEG folding and aggregation behaviour. The fraction of available volume was increased by 20 percent on equilibrating the simulation boxes (Figure 4.2). The significant increase in the fractional available volume was due to clustering and formation of very compact conformations of PEG molecules during the MD simulations. These MD simulations were performed using forcefield parameters of methyl-PEG and hydroxyethyl-PEG (Figure 4.4). We had seen in section 4.2.3 that PEG formed very compact structures during the MD simulations. The QM optimized structures confirmed the formation of intra- and inter-molecular hydrogen bonding which induced such folding and clustering behaviour.

Additional simulations were performed to investigate the effect of aggregation on the fractional available volumes by dissolving the aggregates. The PEG aggregates were dissolved by performing a two-step MC simulation. In the first step, rigid body MC simulations were performed using three systems of 0.1, 0.3, and 0.5 g cm^{-3} concentration. An extreme temperature of 298,000 K was set in the simulations to perform rotational and translational moves at large magnitude to dissolve the clusters quickly. These simulations were performed in Sire and the final configurations were saved after every 2500 MC moves. The values for each rotational and translational move were picked randomly between -50 to +50 degrees and -50 to +50 Å respectively. Finally, the resultant systems were further

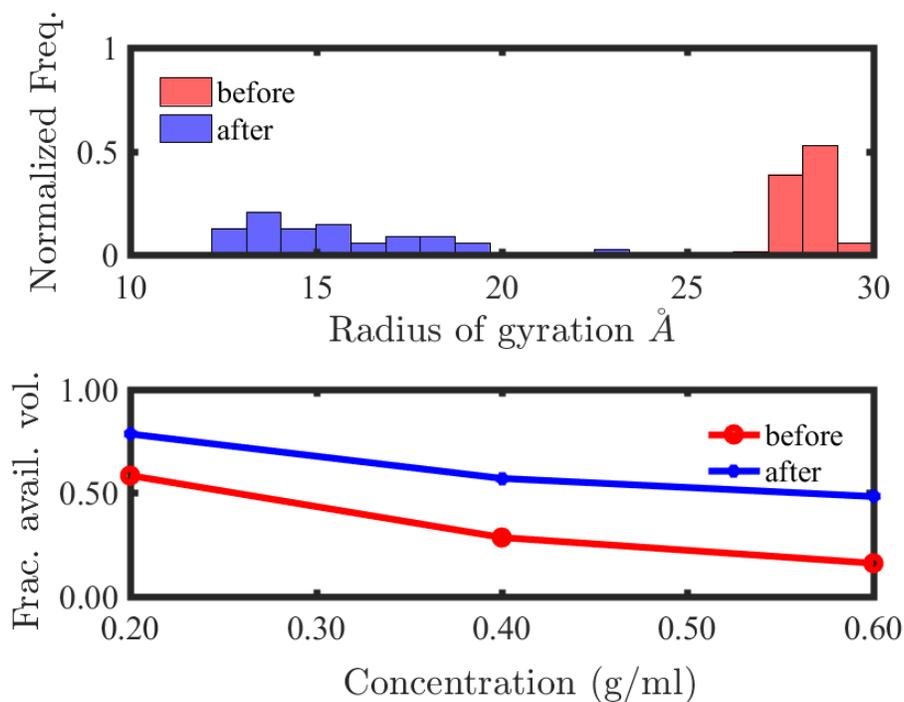


Figure 4.2: The size distribution of PEG conformations, in the system of 0.1 g cm^{-3} concentration, before and after the equilibration by performing the MD simulations (top). PEG formed more compact conformations in the range of 12 to 20 Å from 27 to 30 Å, after equilibrating the system. The bottom panel illustrated the significant increase in the fractional available volumes to the probe pseudoknot RNA (PDB:2K96) molecule in the equilibrated systems. The formation of compact PEG conformations along with PEG aggregates induced a significant increase in the fractional available volumes. Further, the clustering trend increases as a function of concentration and consequently the fraction available volume increased by a higher percentage at larger concentrations.

equilibrated by conducting MC simulations at 298 K to refine structures produced at an extreme temperature.

After removing the aggregates, the fractional available volume was estimated using the parallel-energy algorithm. The fraction of available volume decreased with the removal of PEG aggregates as illustrated in Figure 4.3. De-aggregation allows the molecules to disperse well in the given space and, consequently reduced the occurrence of large empty spaces. These results demonstrate that the packing of the background molecules including their sizes and shapes is also crucial in altering the fractional available volumes.

In another set of simulations, additional MD equilibration simulations were performed

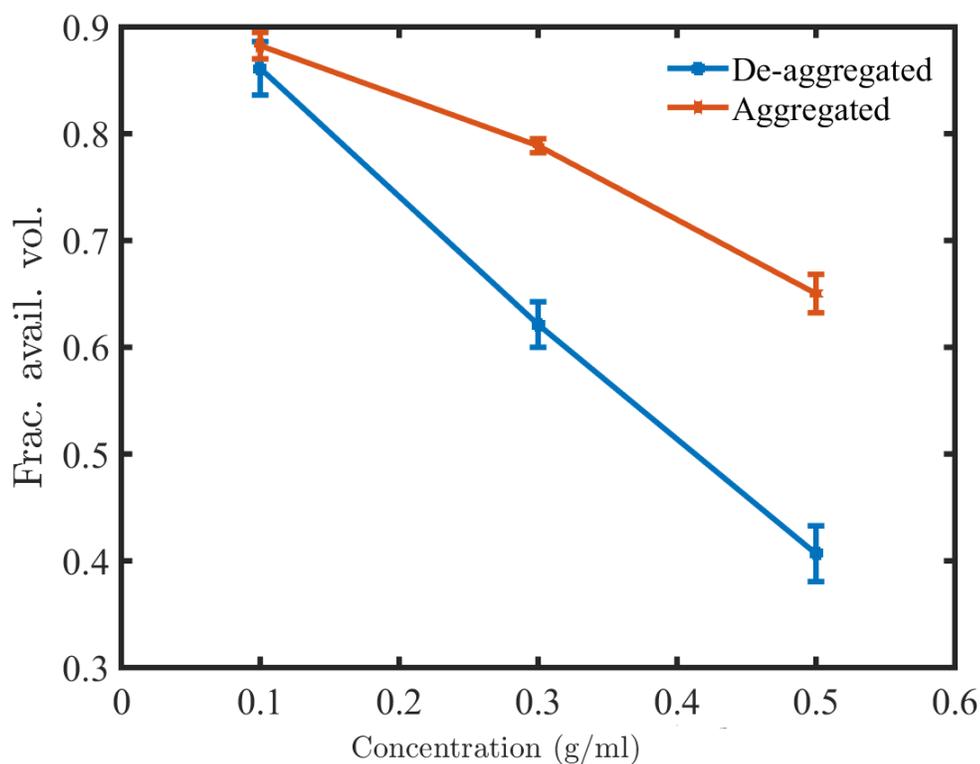


Figure 4.3: Effect of aggregation on the fractional available volume for the pseudoknot RNA (PDB:2K96) at three concentrations. The systems were equilibrated by performing MD simulations and the fractional available volumes were computed by implementing the MC method using the parallel-energy algorithm. In the second step, the aggregates were destroyed by performing MC simulations and then the fractional available volume was measured.

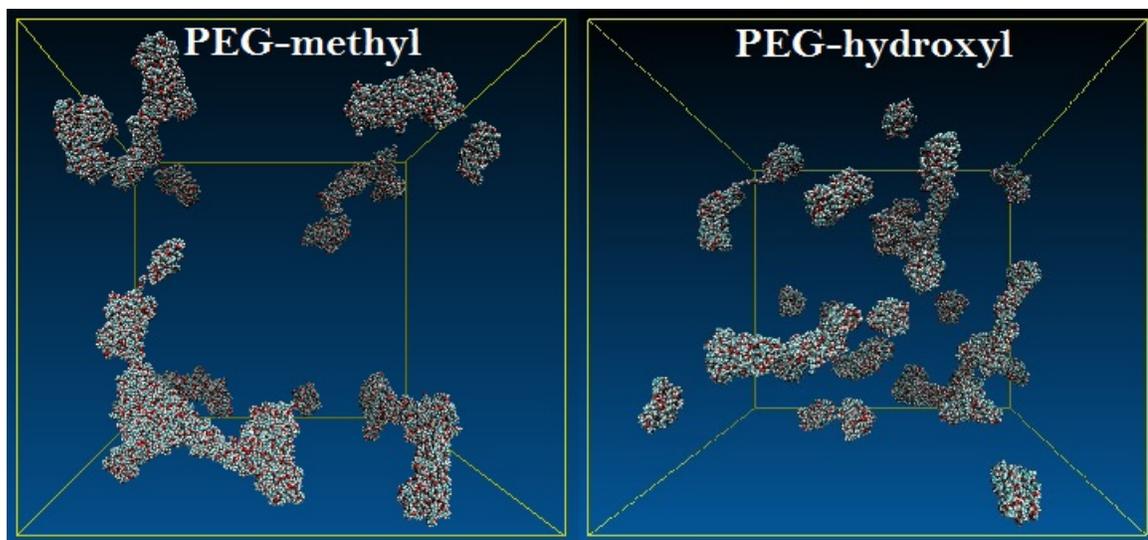


Figure 4.4: Effect of methyl and hydroxyl terminal groups on the folding of PEG and the formation of PEG aggregates in the MD equilibration simulations.

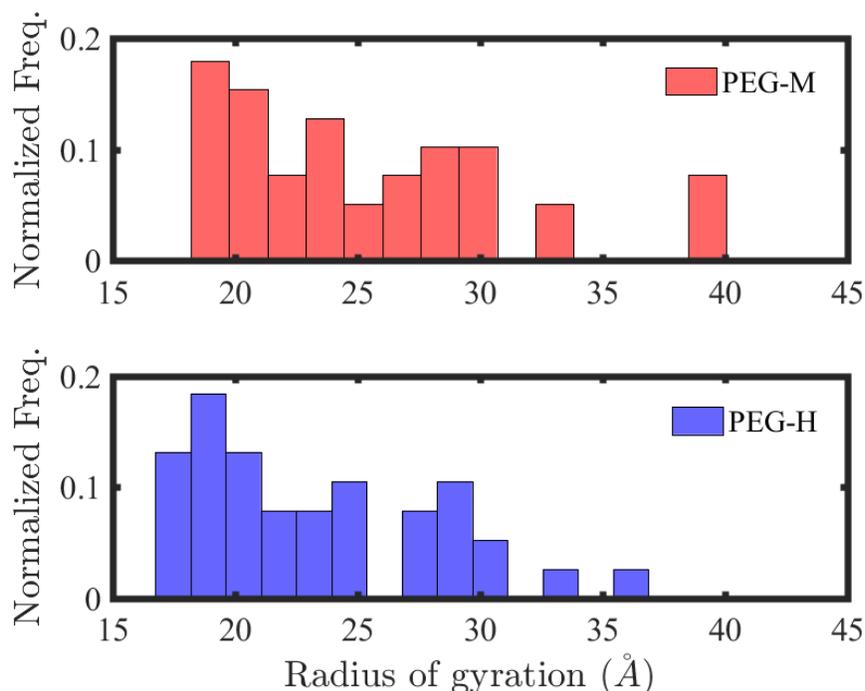


Figure 4.5: Size distribution of PEG aggregates after MD equilibration using forcefield parameters of PEG-methyl (PEG-M) and PEG-hydroxyl (PEG-H) terminals. PEG-H formed smaller sized clusters with a larger amount of individual molecules as compared to PEG-M.

to examine the effect of forcefield parameters on the aggregation behaviour of PEG molecules. It was found that the terminal groups did not play any significant role in affecting the folding behaviour of PEG in the MD sampling simulations and PEGs with methyl, hydroxyethyl and propyl terminals formed aggregates in the equilibration step. Here, additional MD equilibration simulations were performed on the three simulation boxes at 0.2 g cm^{-3} concentration that were packed with PEGs with hydroxyl terminals. To perform the MD equilibration simulations quickly and to observe any aggregation behaviour, an intermediate concentration of 0.2 g cm^{-3} was selected. The simulation results revealed that PEGs with hydroxyl terminals showed similar folding and aggregation behaviour to the PEG with methyl and propyl terminals. Moreover, these results showed that the presence of PEG molecules in the solution affects the folding and aggregation behaviour through intra- and inter-molecular hydrogen bonding interactions. The size of PEG aggregates was found to be similar in both cases (Figure 4.5) and the terminal groups also do not have a large effect

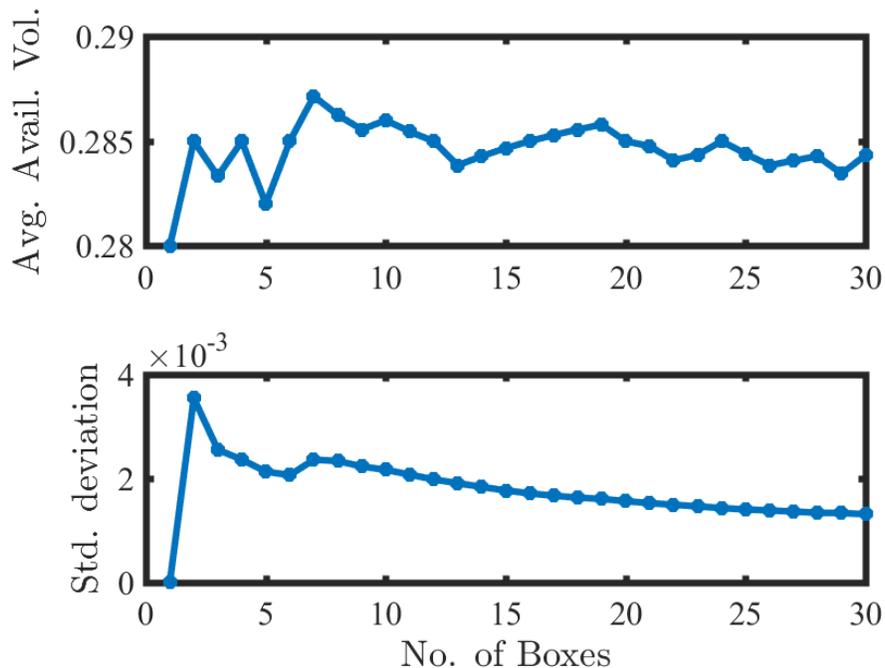


Figure 4.6: The estimated average fractional available volume and the standard deviation with respect to number of copies at 0.4 g cm^{-3} concentration. The fraction of available volumes was estimated using the MC simulation method with an energy threshold algorithm.

on the size distribution of PEG aggregates. However, the PEG-H forcefield formed a little bit smaller sized aggregates with a larger fraction of compact individual molecules as compared to the PEG-M. It is found that the PEG-H formed stronger intra-molecular hydrogen bonds as compared to PEG-M which leads to the formation of smaller sized individual molecules.

4.2.3 Statistical analysis

Thirty copies of simulation boxes at each concentration were used to compute the fraction of available volume. These copies of simulation boxes were prepared after equilibrating the packed simulation box using MD simulation. The idea of making thirty copies is to represent the diverse configurations at any given concentration. The change of fractional available volumes and corresponding standard deviation are shown in Figure 4.6 at 0.4 g cm^{-3} . The results indicate that thirty copies at each concentrations were sufficient to

converge the average of fractional available volume and standard deviation. The average fractional available volume and corresponding standard deviation stabilized after completing fifteen boxes approximately. Moreover, the size of the standard deviation obtained with fifteen boxes or more showed that sampling of this size range produced three significant figures in the fractional available volume which is really excellent and suggested that it might be reasonable to use fifteen copies to produce statistically accurate results.

The MC method was applied to estimate the fractional available volumes in the non-equilibrated and equilibrated crowded media. Similar calculations were performed using the extended SPT theory model and the results from both models are discussed in section 4.4.

4.3 The scaled particle theory

A scaled particle theory (SPT) model has been used to compute the nonideal (NI) chemical potential contribution due to the excluded volume effect of the solute particles in a crowded medium as a function of concentration [4, 7, 27–29, 83, 158, 263]. The NI chemical potential varies as a function of excluded volume which depends on the geometry and number density of molecules in the SPT framework. SPT as it currently exists requires three geometrical parameters namely, radius of curvature R , surface area S , and volume V , but there are certainly shapes, especially shapes of macromolecules, for which these parameters are not a complete description. Moreover, the SPT model currently applies to convex shapes only. Previous SPT models [12, 83, 146–148, 154, 156, 158] approximated the geometry of fluid particles as simple hard spheres or convex shapes. The calculations showed that the geometry played a very crucial role in changing the thermodynamics. Therefore, it is very important to calculate the geometrical parameters of macromolecules correctly in order to estimate the excluded volume effects effectively. One of the key objectives of this study was to build a more reliable model that could extract geometrical parameters of complex-shaped macromolecules effectively rather than using models with

Table 4.1: Comparison of predicted radius of curvature in the original and extended scaled particle theory models. The radius of curvature, measured in Å, is the half of the distance between the atoms present at the maximum distance in the original scaled particle theory while the extended scaled particle theory represents the radius of a least square fit sphere on the convex hull. All the molecules are represented by their respective PDB numbers except the PEG1 and PEG2 conformations. The PEG1 and PEG2 conformations are structures taken from the stationary regions in the MC and MD simulations respectively (Figure 4.7).

Molecule	Original SPT	Extended SPT
2K96 [120]	33.45	28.53
1NA2 [119]	37.52	32.73
1AKE [122]	25.96	22.78
4AKE [64]	30.89	25.41
2PE5 [129]	43.53	30.71
2P9H [129]	27.91	24.72
PEG1	45.78	36.16
PEG2	20.55	17.51
1HHO [264]	28.84	26.13
1FFK [265]	112.21	102.32

simplified geometrical approximation of simple hard spheres or convex shapes. To achieve this, a convexification approach was introduced to estimate the geometrical parameters of the macromolecules using the atomic coordinates. This section presents results from the original and the new extended SPT models.

4.3.1 Geometric parameters by the original and extended SPT models

The excluded volumes and subsequently NI chemical potentials are influenced by the shape, size, and number density of molecules present in the medium. To take into account the size and shape contribution, it is important to extract the geometrical parameters of all solution particles accurately. Two SPT models, i.e. the original and the extended SPT models, were used to measure the geometrical parameters. In the original SPT model, the radius of curvature represents half of the distance between two boundary points that can form a sphere encapsulating the whole molecule. These boundary points are located at maximum distance from each other. The surface area and the volume were calculated from

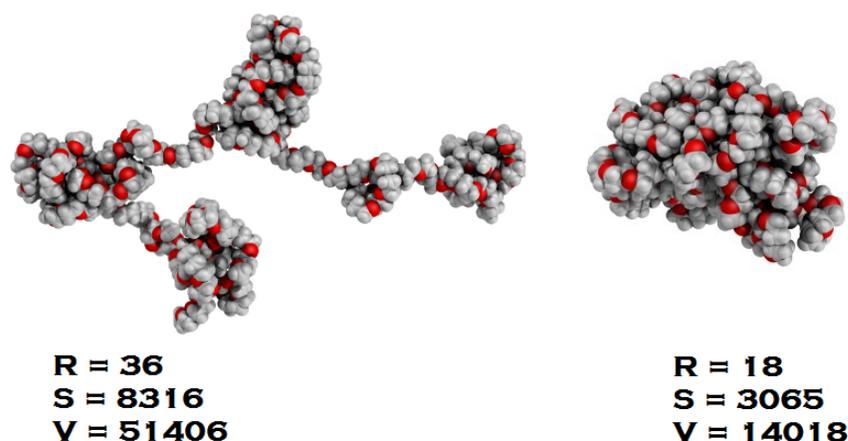


Figure 4.7: Geometrical parameters R , S , V of PEG1 (left) and PEG2 (right) measured in \AA , \AA^2 , and \AA^3 units respectively, using the extended SPT model. The red colour illustrated the oxygen atoms while grey colour represented the hydrogen and carbon atoms.

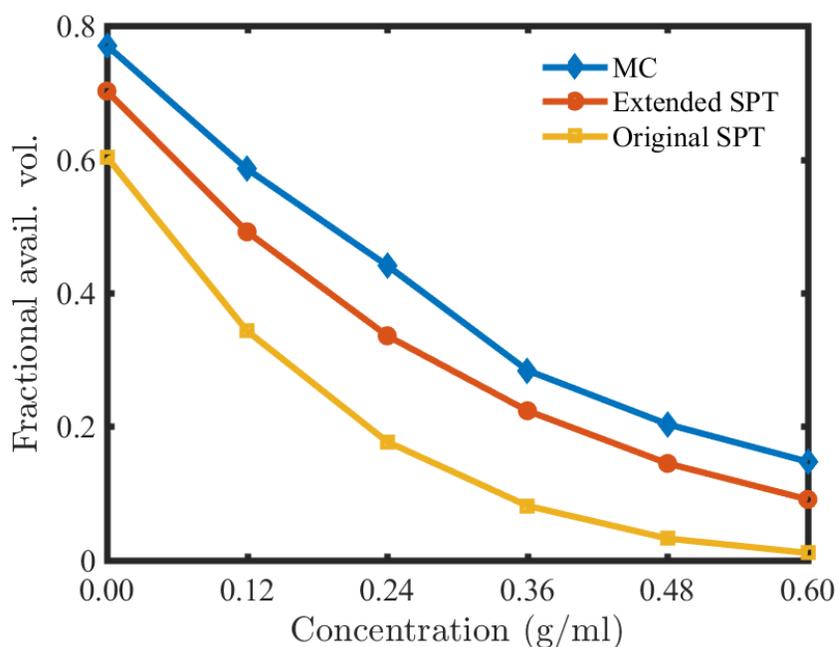


Figure 4.8: Fractional available volume for the pseudoknot RNA closed conformation (PDB:2K96) in the presence of PEG2 crowders. The original SPT model overestimated the sizes of crowders and probe molecules and thus predicted the sharp decrease in the fractional available volume and showed almost zero available volume at 0.6 g cm^{-3} concentration. On the other hand, the fraction of available volume decreased slowly in the extended SPT model relative to the original SPT model and produced results in better agreement with MC calculations.

the formulas for a sphere. On the other hand, an extended SPT model measured the radius of curvature by generating the least squares fitted sphere to a convex hull. The surface area and volume were measured by taking the sum of the areas of the triangles present on the surface of the convex hull and taking the sum of the volumes of all the tetrahedra in the convex hull respectively.

The radius of curvature for ten macromolecules is tabulated in Table 4.1 using the original and extended SPT approaches. All the structures were represented using a PDB identification number except PEG1 and PEG2. Both PEG1 and PEG2 structures were taken from the stationary state in the MC and MD simulations respectively (Figure 4.7). The original model predicted a larger radius of curvature than the extended model generally. Consequently, the surface areas and volumes showed larger values in the original model than in the extended model. The radius of curvature for spherical molecules is similar using either method of calculation as we can see in the cases of the 1AKE, 2P9H, PEG2, 1HHO, and 1FFK molecules. However, non-spherical and extended shapes showed a large discrepancy in radius of curvature as given for PEG1.

Both models worked fine for compact and globular shaped molecules. To illustrate the effect of shapes, fractional available volumes for the pseudoknot RNA (closed conformation PDB:2K96) were calculated in the presence of PEG2 using the original and extended SPT models (Figure 4.8). The very compact and spherical shapes of 2K96, and PEG2 conformations made them good candidates to use in both models to investigate the effect of geometrical parameters on the fractional available volume. As expected, lower fractional available volumes were predicted in the original SPT model due to larger geometrical parameters. The fractional available volume decreased quickly and eventually reached to zero after reaching the highest concentration of PEG using the original model.

4.3.2 Sensitivity of the SPT calculations

The SPT model estimates the NI contribution to the chemical potential due to crowding as a function of the geometrical parameters of probe and crowder molecules. A sensitivity analysis of the extended SPT model with respect to the geometrical parameters was performed by observing the changes in the chemical potentials by increasing the geometrical parameters of a single conformation of PEG, i.e. radius of curvature, surface area and volume, starting from the minimum to the mean value of each parameter at the different constant concentrations. The radius of curvature and surface area can be increased up to the maximum level, however the increment in the volume results in zero free space in the medium before reaching the maximum value of the volume. There was no available space left after reaching a concentration of 0.3 g cm^{-3} while increasing the volume to the maximum level (Figure 4.9). Therefore, the mean values were used for all calculations. The mean values of all three geometrical parameters are estimated by taking the average of geometrical parameters of one thousand conformations in the library. These minimum, average and maximum values are helpful to have a realistic range in which the geometrical parameters could be varied to assess the effect of changes in the geometrical parameters on the chemical potentials (Table 4.2). A series of calculations was performed using PEG2 crowders with the pseudoknot (2K96) probe molecule where the geometrical parameters are increased to average values. Both RNA pseudoknot conformation and crowders differ in size significantly from each other (Table 4.1). The results demonstrated that the radius of curvature and volume are likely to affect the chemical potential more than surface area by increasing the geometrical parameters by 50, 26 and 40% relative to the size of the PEG2 crowder (Figure 4.10).

The type of geometrical parameter affects the chemical potential to a different extent. For example, the chemical potential increased approximately linearly with respect to the radius of curvature with a slope of 0.12 \AA^{-1} (Figure 4.11), whereas the chemical potential also increased, but with significant curvature in the plots, as the volume and surface area

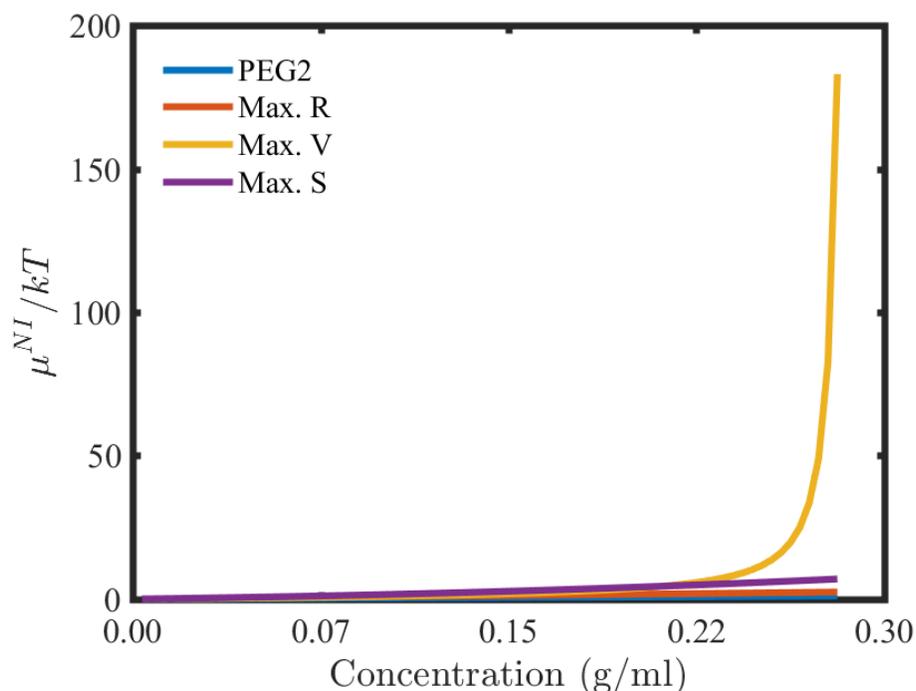


Figure 4.9: Effect of geometrical parameters of PEG2 on the chemical potential of the pseudoknot RNA (2K96) by increasing the R , S , and V of PEG2 crowders to the maximum magnitude of the original size of PEG2, using the extended SPT model.

Table 4.2: Geometrical parameters R , S , V of one thousand conformations of PEG measured in \AA , \AA^2 , and \AA^3 units respectively, using the extended SPT model.

Quantity	Radius	Surface area	Volume
Mean	31.41	7300	49507
Minimum	15.14	2704	11833
Maximum	59.59	30960	353070

increase (Figures 4.12 & 4.13). It was found that the chemical potentials tend to increase approximately linearly at first but then increased sharply in more concentrated solutions, e.g. at 0.2 g cm^{-3} (Figures 4.14, 4.15 & 4.16). Again, under higher concentration conditions at 0.2 g cm^{-3} , the volume was found to be most effective to influence the rate of change of the chemical potentials as compared to the radius of curvature and the surface area.

The dependence of the chemical potential on the crowder geometry for realistic crowder geometries drawn from six different PEG conformations in the library was also inves-

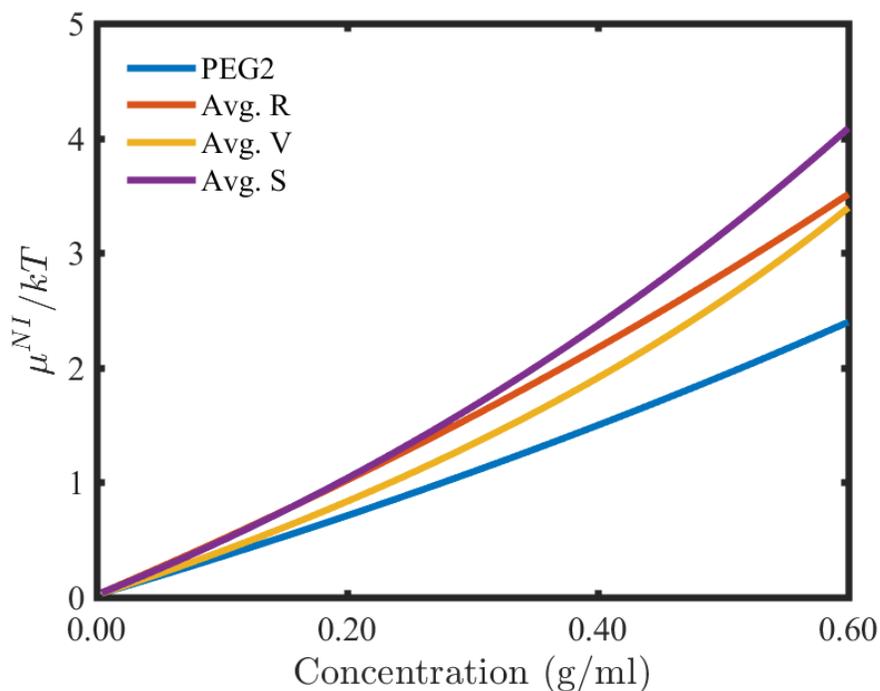


Figure 4.10: Effect of geometrical parameters of PEG2 on the chemical potential of the pseudoknot RNA (2K96) by increasing the R , S , and V of PEG2 crowders by 50, 26 and 40% of the original size of PEG2, using the extended SPT model.

tigated. A set of six random conformations were chosen from the stationary region of MD simulations and the corresponding geometrical parameters are tabulated in Table 4.3. The calculations showed that chemical potentials vary significantly at higher concentrations depending on the size and shape of the crowder (Figure 4.17). These conformations contribute differently to the chemical potential and therefore it can be concluded that use of a single conformation in the SPT model could be a poor choice to mimic the cellular medium which is populated with biomolecules of different sizes and shapes [3]. The importance of the construction of the PEG conformational ensembles can also be explained by analysing the change in the chemical potentials for different conformations with respect to the radius of curvature (Figure 4.18). The chemical potentials of conformations increase approximately directly with respect to the radius of curvature up to 20 \AA at 0.1 g cm^{-3} concentration of solution. The chemical potentials varied at small magnitudes for conformations with radius of curvature around 20 \AA , whereas the chemical potentials differ significantly for confor-

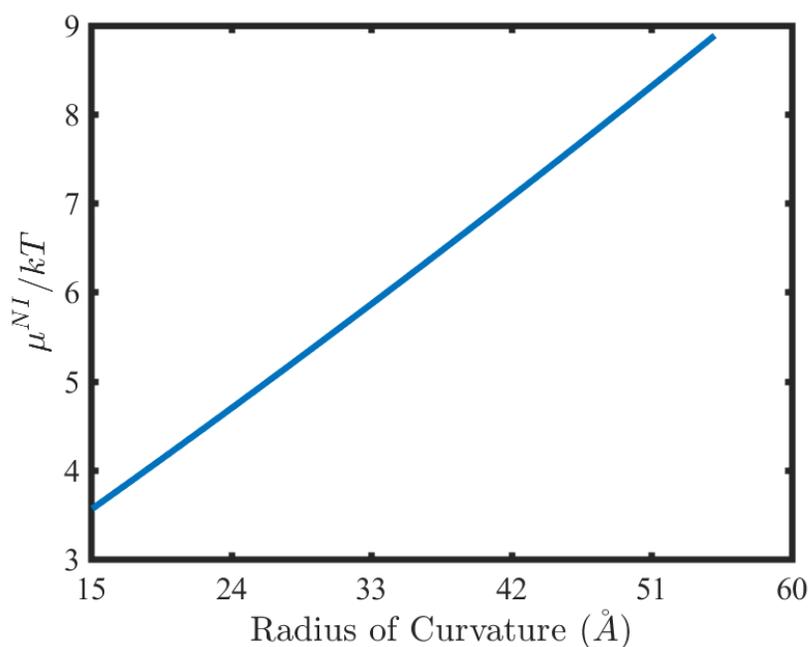


Figure 4.11: The nonideal contribution to the chemical potential of the pseudoknot RNA (2K96) due to increase in the radius of curvature of a single conformation of PEG at constant surface area (2904 \AA^2) and volume (12966 \AA^3) at constant concentration of 0.1 g cm^{-3} .

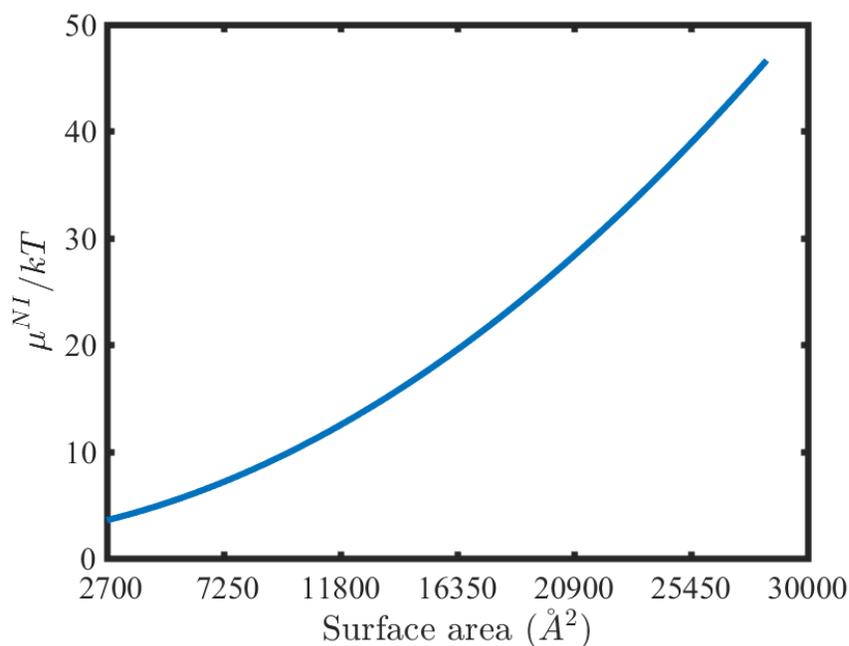


Figure 4.12: The nonideal contribution to the chemical potential of the pseudoknot RNA (2K96) due to increase in the surface area from of a single conformation of PEG at constant radius of curvature (16 \AA) and volume (12966 \AA^3) at constant concentration of 0.1 g cm^{-3} .

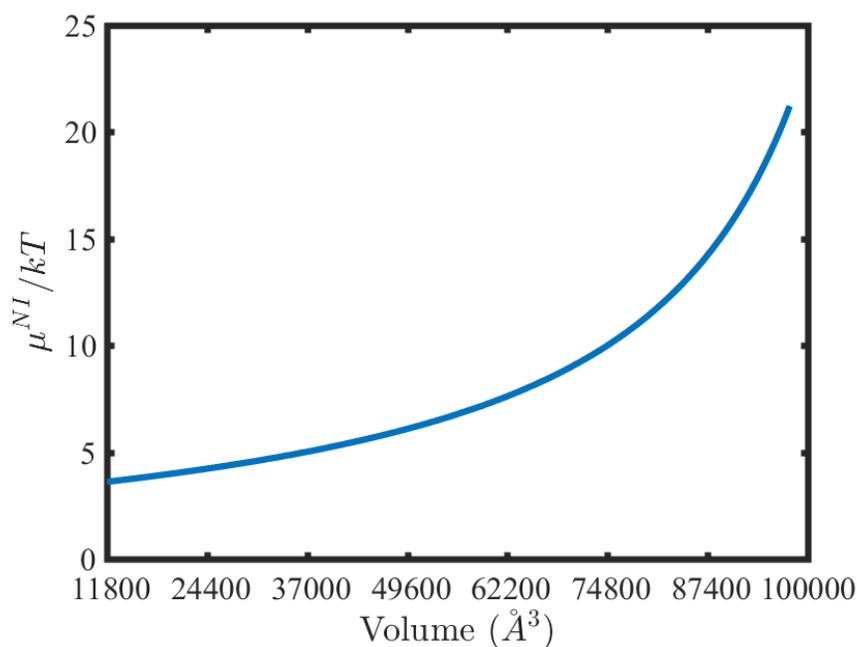


Figure 4.13: The nonideal contribution to the chemical potential of the pseudoknot RNA (2K96) due to increase in the volume of a single conformation of PEG at constant radius of curvature (16 \AA) and surface area (2904 \AA^2) at constant concentration of 0.1 g cm^{-3} .

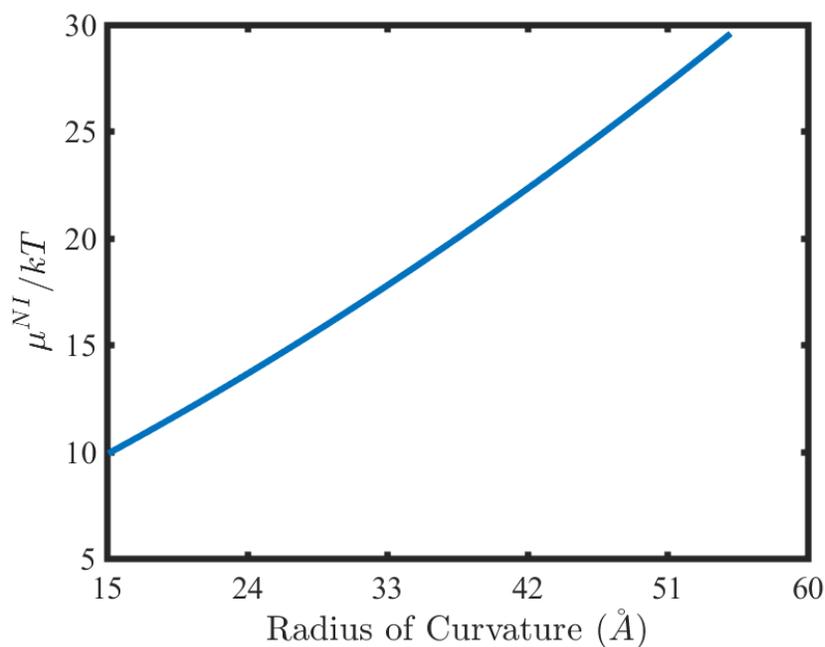


Figure 4.14: The nonideal contribution to the chemical potential of the pseudoknot RNA (2K96) due to increase in the radius of curvature of a single conformation of PEG at constant surface area (2904 \AA^2) and volume (12966 \AA^3) at constant concentration of 0.2 g cm^{-3} .

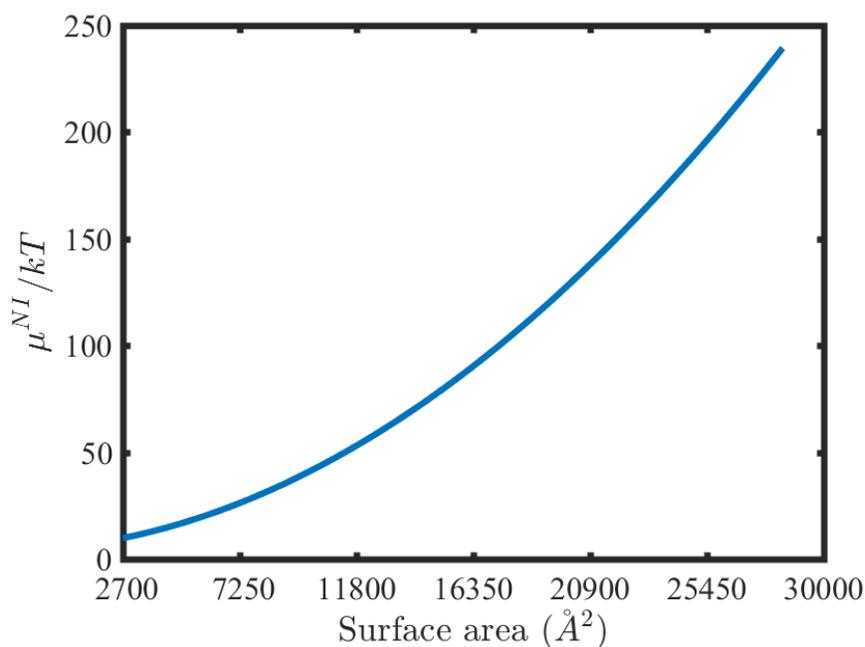


Figure 4.15: The nonideal contribution to the chemical potential of the pseudoknot RNA (2K96) due to increase in the surface area of a single conformation of PEG at constant radius of curvature (16 \AA) and volume (12966 \AA^3) at constant concentration of 0.2 g cm^{-3} .

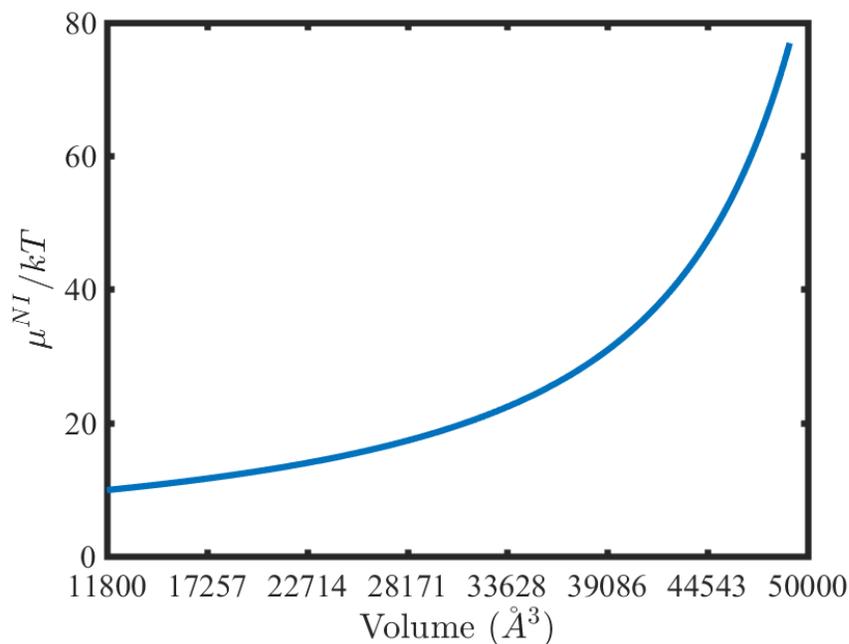


Figure 4.16: The nonideal contribution to the chemical potential of the pseudoknot RNA (2K96) due to increase in the volume from of a single conformation of PEG at constant radius of curvature (16 \AA) and surface area (2904 \AA^2) at constant concentration of 0.2 g cm^{-3} .

Table 4.3: Geometrical parameters R , S , V of six random equilibrated conformations of PEG measured in \AA , \AA^2 , and \AA^3 units respectively, using the extended SPT model.

Conformation	Radius	Surface area	Volume
PEG25	30.04	5679	28975
PEG75	29.65	4613	22649
PEG125	20.35	3458	15462
PEG281	16.32	2955	13166
PEG325	18.16	3054	13368
PEG450	17.51	3065	14018

mations with radius of curvature greater than 25 \AA .

This analysis showed that PEG conformations fall into two distinct regions based on their radius of curvature and the corresponding chemical potentials. Figure 4.18 points out an interesting feature that there are conformations in our library with similar radius of curvature that produce significantly different chemical potentials due to different surface areas and volumes. For instance, we chose all thirteen conformations with radius of curvature between 41–42 \AA and all produced different chemical potentials (μ^{NI}/kT from 2 to 10) due to different surface areas (from 4776 to 14241 \AA^2) and volumes (from 22780 to 119440 \AA^3). The volume is the most effective quantity to change the chemical potential in these calculations. These results strongly support that it would be appropriate to use an appropriately sampled conformational ensemble of crowders in SPT calculations to compute the nonideal contributions realistically. Further, it may be possible that the cells are populated with particles of similar radii but they could differ in the surface areas and volumes, or particles that have different shapes that differ in radius of curvature and surface area but have similar volumes. These variation in the geometrical parameters of different crowders produce additive effects and increase the chemical potentials significantly as compared to the medium filled with particle of the same sizes and shapes.

Finally, the sensitivity of the SPT model toward the geometrical parameters of a crowder was tested by computing the sensitivity coefficients [266]. The sensitivity coefficients determine the impact of a variable on the uncertainty of the output of a mathematical model. In

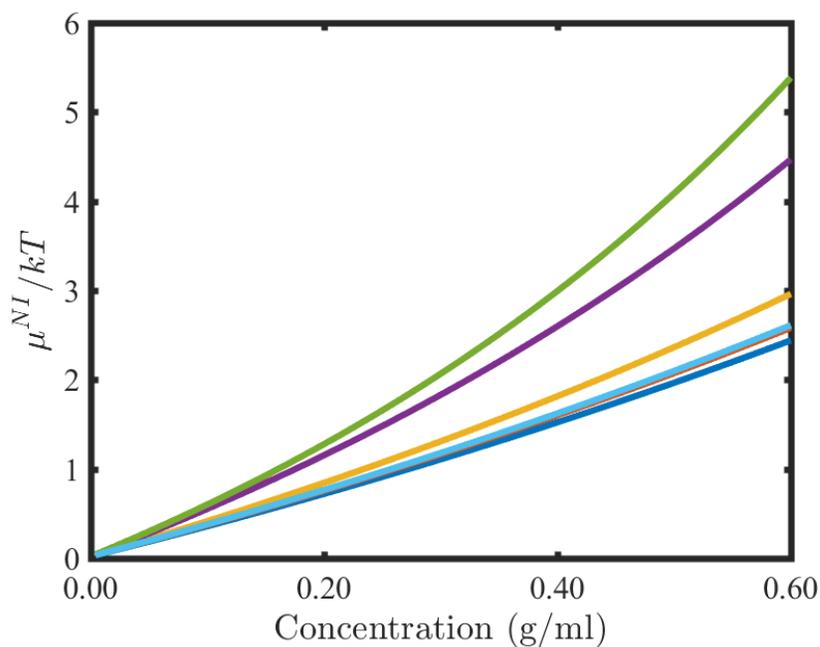


Figure 4.17: Comparisons of NI chemical potential contributions for the pseudoknot RNA (2K96) measured in the crowded boxes filled with 8 kDa PEGs of different conformations. All the six conformations were taken randomly from the stationary state of MD simulations.

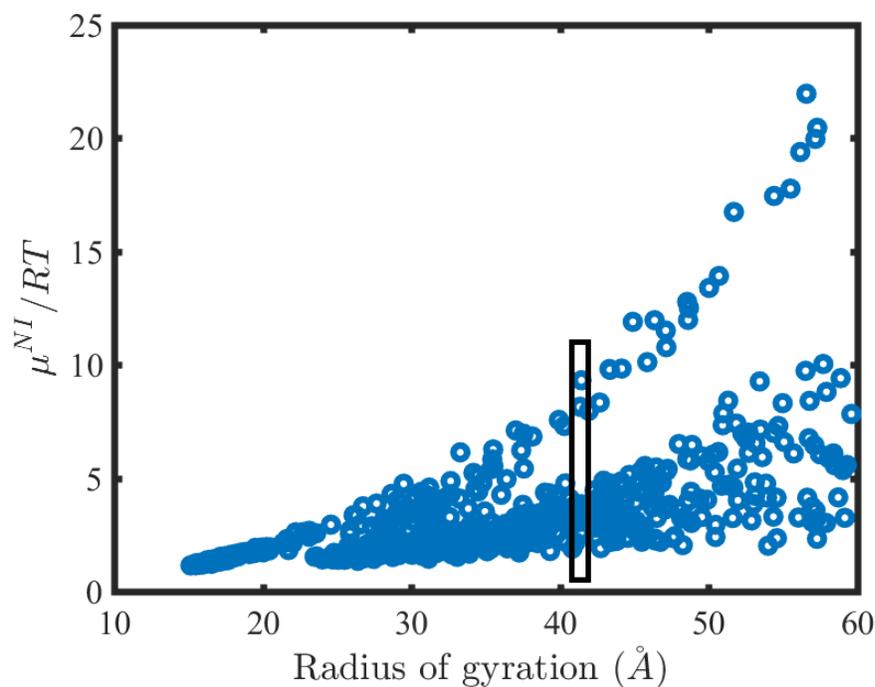


Figure 4.18: The nonideal chemical potential contributions of each conformation of PEG at a fixed concentration of 0.1 g cm^{-3} for one thousand PEG conformations. The inset rectangular shape is used to indicate the selected conformations that were used in the case study to evaluate the role of geometrical parameters in affecting the chemical potential of a protein molecule.

our case, the sensitivity coefficient is defined as a partial derivative of the fractional change in the available volume with respect to the fractional change in one of the three geometrical parameters, i.e. radius of curvature, surface area and volume. Mathematically, the sensitivity coefficient can be written in the form of equation 4.1 as a function of radius of curvature, surface area and volume. (All input files are provided in Appendix C.2.) Three sensitivity coefficients were measured by incorporating the small increments of 0.1, 1, 5, and 10% in the radius of curvature, surface area, and volume of the PEG crowder. The results regarding the change in the sensitivity coefficients with respect to radius of curvature, surface area and volume are shown in Figures 4.19– 4.21, and it was found that the sensitivity coefficient values are independent for small increments made in radius of curvature, surface area and volume of the crowder. Further, the sensitivity coefficients are found to be of the order of -1 for the most concentrated systems, which means that fractional available volume is approximately inversely proportional to radius of curvature. In these calculations, volume was found to be the least effective geometrical parameters to affect the sensitivity coefficients at the lowest magnitude of the order of -0.3 for the most concentrated systems. The sensitivity coefficients with respect to radius of curvature and surface area are consistently larger in magnitude than the sensitivity coefficient with respect to volume. It shows that a larger error in volume will not affect the results as badly as errors in the radius of curvature and surface area.

$$C_R^{\text{avail.vol.}} = \frac{\partial \ln(V_{\text{available}})}{\partial \ln(R)} \approx \frac{\ln(V_{\text{available},2}) - \ln(V_{\text{available},1})}{\ln(R_2) - \ln(R_1)} \quad (4.1)$$

$$C_S^{\text{avail.vol.}} = \frac{\partial \ln(V_{\text{available}})}{\partial \ln(S)} \approx \frac{\ln(V_{\text{available},2}) - \ln(V_{\text{available},1})}{\ln(S_2) - \ln(S_1)}$$

$$C_V^{\text{avail.vol.}} = \frac{\partial \ln(V_{\text{available}})}{\partial \ln(V)} \approx \frac{\ln(V_{\text{available},2}) - \ln(V_{\text{available},1})}{\ln(V_2) - \ln(V_1)}$$

This analysis indicates the dependence of the chemical potential on the geometrical parameters. Generally, the chemical potential was found to be more sensitive to the radius of curvature and surface area for smaller and compact shaped crowders but the chemical potential was found to be more influenced by the volume of the larger sized crowders. These calculations indicate that the chemical potential varies with the size and type of folding of crowders and it is crucial to estimate the geometrical parameters correctly in order to calculate the thermodynamic activity accurately.

The simple approximation of the original SPT overestimates the size of crowders as compared to the extended SPT model. Therefore, the fractional available volume decreased significantly as shown in Figure 4.8. Based on the results from the original and extended SPT models, we decided to use the extended SPT model to compute the fractional available volumes and NI chemical potentials at six different concentrations of crowded systems. These physical quantities are interchangeable and we presented our SPT results in terms of the chemical potentials for convenience in this chapter, while the corresponding plots on the fractional available volumes are available in Appendix C.3. This comparison between MC and SPT outcomes will allow us to benchmark the performance of our extended SPT model. Further, the biological significance of these calculations is discussed with reference to experimental results.

4.4 Comparison of SPT and MC simulations

So far, we have discussed the development of MC and SPT models to compute the fractional available volumes of the probe molecule in crowded systems. A single type of crowders of the same size and shape were used to compute the fractional available volumes in the original and extended models in the previous section. The cellular interior is filled with different types of macromolecules that differ in shapes and sizes which affect the chemical potentials of probe molecules at higher magnitude due to an additive effect [24, 25]. To mimic the cellular environment more closely, a mixture of crowders of differ-

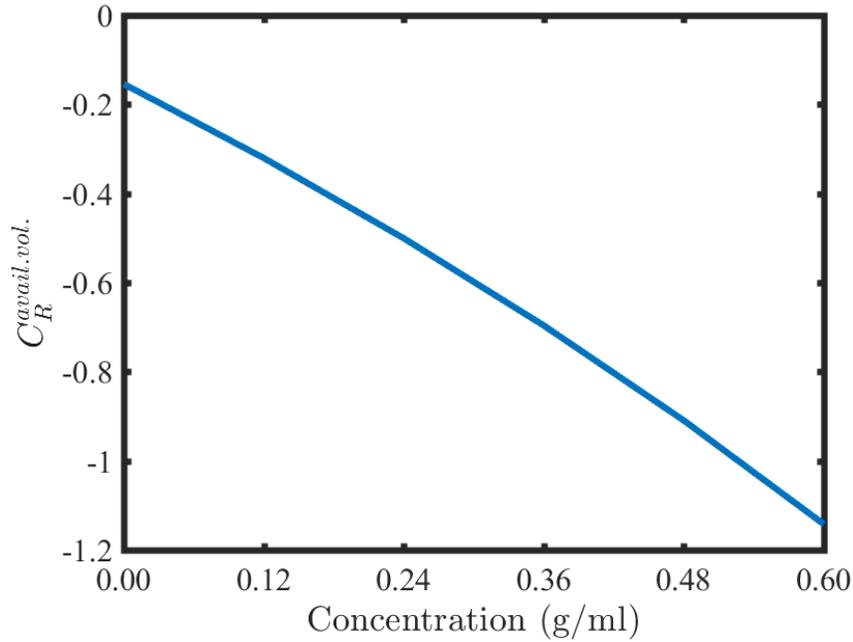


Figure 4.19: The sensitivity coefficient for the fractional available volume with respect to radius of curvature of PEG2 crowder. The radius of curvature was increased by 0.1% from the original radius of curvature at six different concentrations from 0.1 to 0.6 g cm^{-3} .

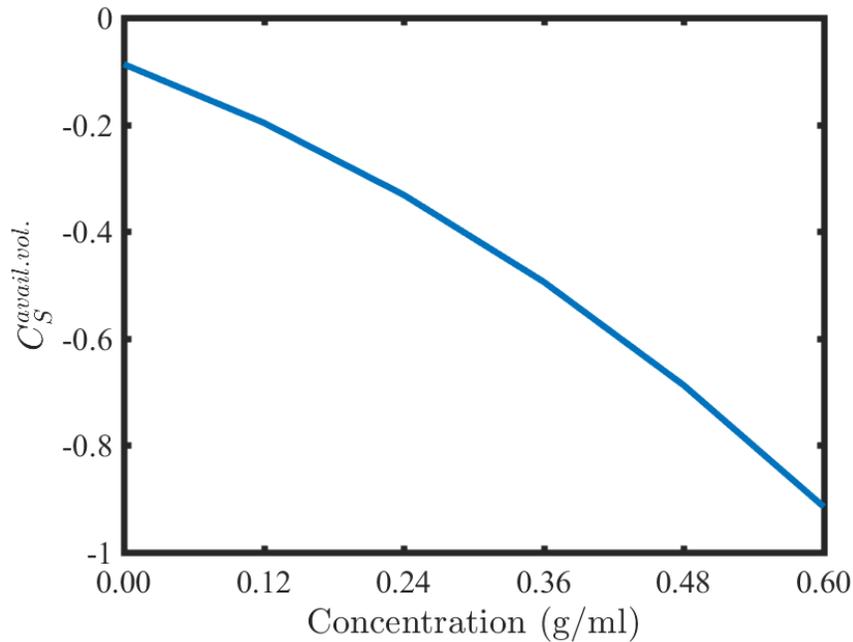


Figure 4.20: The sensitivity coefficient for the fractional available volume with respect to surface area of PEG2 crowder. The surface area was increased by 0.1% to the original surface area at six different concentrations from 0.1 to 0.6 g cm^{-3} .

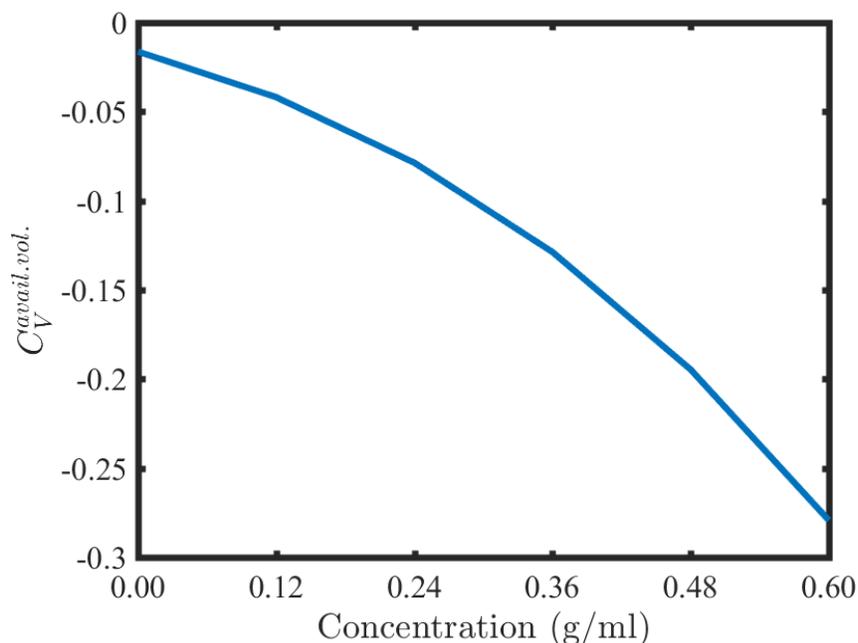


Figure 4.21: The sensitivity coefficient for the fractional available volume with respect to volume of PEG2 crowder. The volume was increased by 0.1% to the original radius of curvature at six different concentrations from 0.1 to 0.6 g cm^{-3} .

ent shapes and sizes has been used to pack the fifteen copies of simulation boxes at each concentration from 0.1 to 0.6 g cm^{-3} . These simulation boxes were further equilibrated using MD simulations. Finally, these equilibrated simulation boxes were used to determine the fractional available volumes for six probe molecules by using both the extended SPT and MC methods.

It was found that the aggregation of PEGs increased the fractional available volumes significantly while using the MC method (Figure 4.2). The SPT model computes the fractional available volumes based on the geometries of individual molecules without considering the effect of aggregates. To incorporate the effect of aggregation on the fractional available volume, an algorithm was developed that extracts the aggregates and saves them as a single ‘molecule’ in a PDB format. This algorithm requires a simulation box and the threshold distance between two molecules as input parameters. The threshold distance was used to evaluate whether the surrounding PEGs are a part of a certain cluster or not. The algorithm completes the cluster search in two iterative steps. At first, it picks a molecule randomly

and finds all the surrounding molecules that satisfy the threshold distance criterion and saves them in list 'A'. In the second step, it chooses each molecule from list 'A' and finds any additional surrounding PEGs within the threshold distance, excluding molecules that are already in List 'A'. This cycle continues until there are no more molecules associated with the particular cluster, and the cluster is saved as a single 'molecule'. The cluster extraction algorithm is provided in Appendix C.1. The geometric parameters of this molecule are extracted to be used in the extended SPT theory. A threshold of 20 Å was used to extract the PEG clusters. This threshold distance value was picked based on the average of the radius of gyration of all crowders (12 to 15 Å generally), present in the equilibrated boxes. The compact and tightly packed clusters were extracted from the boxes and were saved as a molecule by using this threshold radius of gyration. In this regard, the extended SPT theory is a better fit to the clusters that are at least roughly convex. Otherwise, the convex-hull algorithm overestimates the geometrical parameters of the molecules by encapsulating the large empty spaces inside the convex hull.

An extended SPT model was applied to compute the fractional available volumes and eventually chemical potentials for all six probe conformers with and without PEG aggregates in order to perform a comparison between MC and extended SPT model results (Figure 4.22). These results demonstrated that the MC simulations measured the least NI contribution of crowding towards the chemical potential of pseudoknot RNA (2K96) in the equilibrated systems (red line) as compared to non-equilibrated systems (blue line). The equilibration results in clusters, therefore it opens up lots of free space. The SPT model predicted higher values of chemical potential for pseudoknot RNA (2K96) while using the equilibrated crowded systems (dashed yellow line) as compared to the chemical potential using a single type of crowder (dashed green line). The higher chemical potential values with SPT in crowded systems filled with multiple conformations confirmed the additive contribution of multiple conformations over a single type of conformations. Note that the single crowder (PEG2) was selected from the stationary region in the MD simulations (Fig-

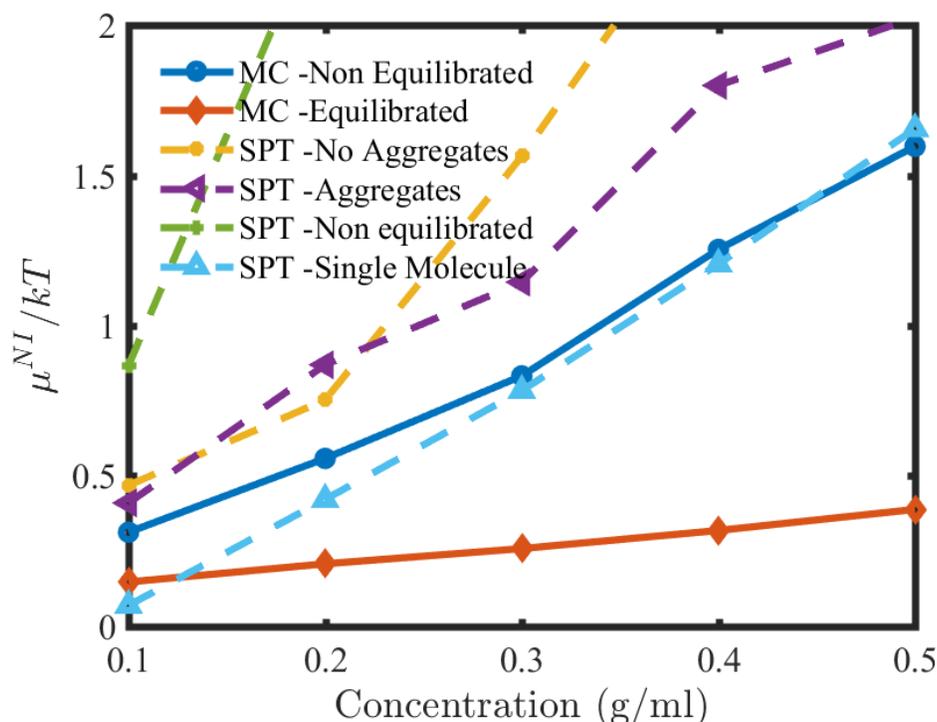


Figure 4.22: Comparisons of NI chemical potential contributions for pseudoknot RNA (2K96) measured in the crowded boxes filled with 8 kDa PEG by using the MC (solid lines) and extended SPT models (dashed lines). Only two types of crowded systems, i.e. non-equilibrated and equilibrated systems, were used to determine the chemical potentials using an MC method. The SPT approach used equilibrated systems only with and without aggregates, whereas ‘SPT Single Molecule’ represents the equilibrated single PEG conformation (PEG2) used to compute the chemical potential. The error bars of these simulations are small and not included for simplicity. For instance, the magnitude of error bars increased with concentration and the size of error bar was found to be less than 0.05 for a system of 0.1 g cm^{-3} concentration, whereas the size of error bar increased up to 0.01 for the concentrated systems i.e. 0.5 g cm^{-3} .

ure 4.7). The crowded systems were equilibrated with MD simulations resulting in compact and globular shaped crowders. To maintain consistency, the MD equilibrated PEG2 structure was chosen. A number of different MD equilibrated PEG conformations were also used to calculate the chemical potentials as compared to PEG2. It was found that most of the conformations produced different NI contributions to the chemical potentials of the pseudoknot RNA structure, which requires the use of multiple conformations to compute the average effect (Figure 4.17).

The SPT model reproduced the MC results while using a single equilibrated PEG struc-

ture where the chemical potential fit well at intermediate to higher concentrations but deviated at lower concentrations. However, this is not a fair comparison between MC results (solid blue line) and the extended SPT model (dashed green line) because both calculations used different crowded media. In this regard, MC used non-equilibrated crowded systems while the extended SPT used an equilibrated single PEG conformation. The extended SPT model predicted even larger chemical potential values in the non-equilibrated crowded systems. The results of rest of two systems are available in Appendix C.4.

4.4.1 Biological and experimental relevance of results

Conformational changes of macromolecules in the cellular interior are linked to different functions [24]. Here we have investigated how crowding affects the conformational equilibrium of three systems with the MC and SPT models. Figure 4.23 shows plots of the first system, ‘the telomerase RNA’, by presenting the NI contribution to the standard state free energy change ($\Delta G_{\text{NI}}/kT = (\mu_{2\text{K}96}^{\text{NI}} - \mu_{1\text{NA}2}^{\text{NI}})/kT$) of the conformational equilibrium as a function of concentration of PEG crowders. The change in energy values shows that the higher fractional available volumes are available for the compact shaped pseudoknot RNA conformation (2K96). Thus macromolecular crowding favours the formation of the pseudoknot conformation by shifting the conformational equilibrium ($1\text{NA}2 \rightleftharpoons 2\text{K}96$) towards the pseudoknot RNA conformation over the hairpin conformation (1NA2).

The MC method as compared to the extended SPT model predicted a fairly small change of the standard state free energy of about $-0.2kT$ and $-0.7kT$ relative to zero crowder concentration for the conformational equilibrium ($1\text{NA}2 \rightleftharpoons 2\text{K}96$) in the equilibrated and non-equilibrated crowded media respectively.

The MC method results showed the crowding exerts more modest effects on the conformational equilibria while the extended SPT predicted somewhat more significant crowding effects. The coarse-grained Langevin dynamics simulations [47] revealed that the pseudoknot conformation is in equilibrium with an extended hairpin conformation and that

crowding enhances the stability of the pseudoknot structure by $-0.5kT$ in the presence of spherical crowders of 12 \AA radius of gyration occupying 30% of the available volume relative to the hairpin structure. The extended SPT model also predicted the same amount of stabilization of about $-0.5kT$ at 30% occupancy using a single type of crowder (PEG2) (dashed yellow line), however the MC method estimated a slightly smaller stability of $-0.3kT$ roughly at 30% (solid blue line). The radius of curvature of 17.50 \AA , estimated with convex hull, of PEG2 is larger than 12 \AA but the volume (14018 \AA^3), estimated from the convex hull, is smaller than the value obtained using the sphere numerical formula with radius of 17.50 \AA (22449 \AA^3). However, our model, like the coarse-grained Langevin dynamics simulations [47], could not capture the heterogeneity of the cellular environment fully in which the local concentrations and the sizes of crowders can vary from point to point [267]. The local concentration variations may result in minimal to strong crowding effects on the biochemical reactions [47].

The sizes of probe and background molecules played an important role in determining the magnitude of the crowding effect. The conformational changes in the adenylate kinase and the *lac* repressor structures also experienced modest crowding effects similar to the telomerase RNA in general. The closed conformation of adenylate kinase experienced the least crowding effect as compared to the closed conformations of telomerase RNA and the *lac* repressor. The closed states of adenylate kinase and the *lac* repressor are relatively stabilized by -0.5 and $-2.0kT$ respectively. Our results (Appendix C.5) are in good agreement with other studies which suggest the crowding exerts moderate effects on the conformational changes of proteins [125, 268, 269]. The postprocessing approach, developed by Dong *et al.* [24], predicted the closed conformation of adenylate kinase (1AKE) is stabilized by an amount of approximately $-0.16kT$ at 35% occupied volume by the spherical crowders of 15 \AA radius. The extended SPT model estimated approximately $-0.2kT$ value in the presence of the PEG2 crowder at 35% which showed almost consistent results with the postprocessing approach outcomes.

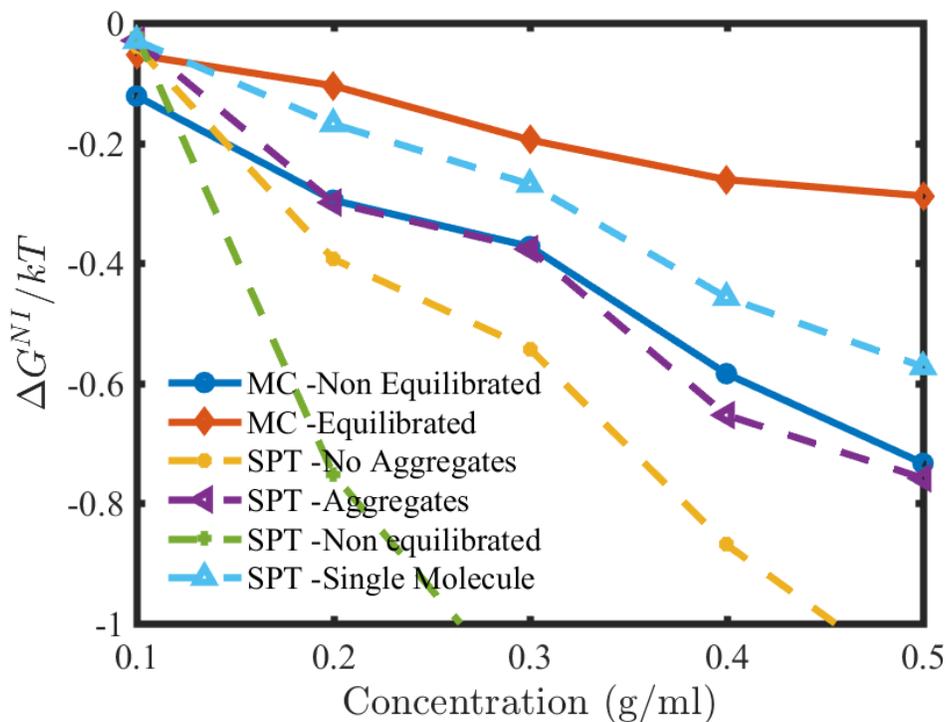


Figure 4.23: NI contribution to the standard state free energy change of conformational equilibrium between pseudoknot and hairpin conformers in the crowded medium (1NA2 \rightleftharpoons 2K96). Macromolecular crowding favors the formation of the compact conformation, i.e. pseudoknot conformation, of the telomerase RNA.

The SPT calculations were performed in different ways by using an equilibrated system (Figure 4.22) which differ in PEG aggregates (dashed yellow and violet lines). The results demonstrated the aggregation reduced the number density of crowding bodies while increasing their sizes. This caused a decrease in the chemical potential. Again, the SPT model predicted higher chemical potentials while using a mixture of conformations by incorporating additive effects. These results indicate that the SPT model including the contribution by PEG aggregates would be a good choice to compute the excluded volume effects on the biochemical reactions occurring in the presence of macromolecules of different sizes and shapes, whereas the extended SPT model with a single PEG conformation produced the best results against MC simulations. The extended SPT model with a single PEG conformation is a valid choice when the system is populated with compact shaped crowders of almost same geometrical parameters and the geometrical parameters did not differ sig-

nificantly from each other. For example, if a system is filled with different haemoglobin conformations, assuming all the conformations are of almost same geometrical parameters, the SPT with a single type of crowder could be applied and could produce reliable results. However, use of a single PEG conformation potentially neglects important features of the cellular interiors which are composed of different components. For example Cajal bodies, nuclear speckles and centrosomes in the nucleus, and ribosomes in the cytoplasm could be represented as clusters. The free energy change results (Figure 4.23) obtained from the extended SPT with aggregates predicted free energy changes for the conformational equilibrium reaction ($1NA2 \rightleftharpoons 2K96$) in good agreement with the MC outcomes. These results showed that the extended SPT with aggregates can be applied with confidence but sometime it may require additional trial and error calculations to determine the best SPT model that could reproduce the experimental or MC simulation results.

Concluding remarks - Fractional available volumes

To test the SPT results, the MC method was introduced to estimate the fractional available volumes by integrating one of the two approaches, i.e. the parallel-distance and parallel-energy approaches to determine the steric clashes. The MC parallel-distance algorithm produced more accurate results in comparison to the parallel-energy algorithm but it costs more time and computer resources. The computation cost of the MC parallel-distance algorithm was reduced further by introducing an additional criterion. The computation cost in both MC algorithms increased with concentration.

The extended scaled particle theory model and the MC simulations were performed to estimate the fractional available volumes and subsequently thermodynamic activities of probe molecules at six different concentrations. The aim of these simulations was to improve the SPT model by incorporating a better approximation to measure the geometrical parameters of crowders and probe molecules and to reproduce the MC results. The SPT model illustrated the effect of different shapes and sizes on the fractional available volumes

and chemical potentials. The convex-hull algorithm produced good results with globular shaped crowders but needs to be improved for partially folded and open conformations. The extended SPT model offers many advantages over the original scaled particle theory. The extended model tried to capture the exact shape by using atomic coordinates and subsequently measured the geometrical parameters through forming a convex hull. However, it has a drawback of overestimating the size of molecules of extended and partially folded states. The extended SPT model would be a better choice to estimate the crowding effects in the presence of compact convex shaped molecules over the original SPT model. The extended approach could possibly be used for a nonconvex shape by partitioning the given molecule into smaller convex shapes and the geometrical parameters can be obtained by integrating parameters for all components. This alternative method might work well for getting surface area and volume but might need care for getting the radius of curvature.

4.5 Kinetics study by the transition state theory

The transition state theory was used to study the kinetics of conformational equilibrium under crowding conditions. The successful implementation of the transition state theory in a unimolecular reaction requires the activity coefficients of the transition state and a single reactant measured in the crowded medium (Equation 4.2 [87]). Under dilute solution conditions, the activity coefficients of the reactants and the transition states are considered as unity. However, the activity coefficients of the reactant and the transition state are no longer unity in NI solutions. The final rate constant of a unimolecular reaction is derived in the introduction in section 1.4.3 and can be expressed as

$$k_1 = k_0 \left(\frac{\gamma_A}{\gamma_{TS}} \right) \quad (4.2)$$

where k_1 is the rate constant of the reaction, k_0 is the rate constant under dilute conditions, and γ is the activity coefficient of a reactant state A or of a TS state.

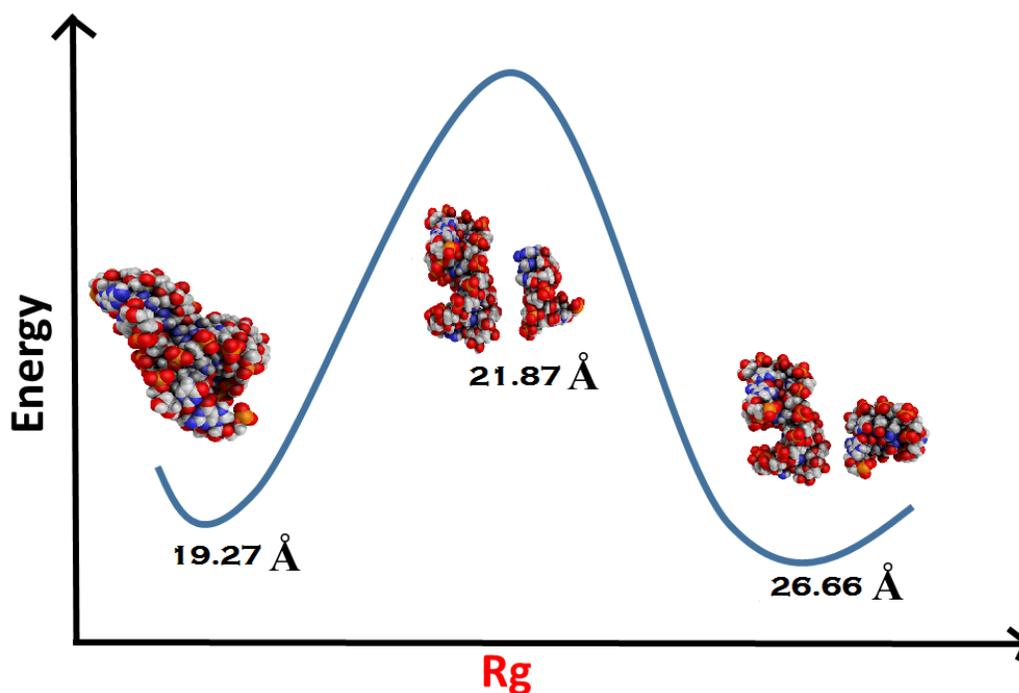


Figure 4.24: Approximation of the transition state between folded and unfolded states of the GAAA tetraloop receptor along with radius of curvature with the morphing approach.

The final rate constant k_1 is a function of the activity coefficients of a reactant and a transition state. These activity coefficients can be estimated by using the MC or extended SPT methods. Both methods can estimate the activity coefficients of the reactant and transition state by using the corresponding structures and the geometrical parameters. However, the structure of the transition state is unavailable and it posed a difficulty to determine the activity coefficient of the transition state in both methods. To overcome this difficulty the transition state structure was approximated by the morphing approach and the approximated structure was used to determine the activity coefficient of the transition state.

The morphing approach produced intermediate structures between two conformations, a reactant and a product. To locate the transition state, single point energy calculations were performed for initial, final and intermediate frames in Sire (Figure 4.24) and the frame with the highest energy was chosen as an approximation to the transition state. In this regard, the transition state of the GAAA tetraloop receptor was approximated between open and closed states. The folded/closed structure of GAAA tetraloop receptor was extracted from

Table 4.4: Geometrical parameters of three structures of GAAA tetraloop receptor estimated by the extended SPT model. The experimental column represents the values of the radii for the three states and PEG crowder approximated by Dupuis *et al.* [80] that were used in the original SPT model calculations. The convexification algorithm estimated the following geometrical parameters R , S , V for all structures in \AA , \AA^2 , and \AA^3 units respectively.

State	R	S	V	Experimental (R)
Folded	19.27	2,937	11,791	12.5
Unfolded	26.66	3,677	16,096	27
TS	21.87	3,417	15,307	16
Crowder	17.51	3,065	14,018	15

the crystal structure 1GID [270] by selecting the following nucleotides 147-156, 220-229, and 245-253, using the Pymol package [271]. These nucleotides represented the folded conformation of the GAAA tetraloop receptor. Similarly, Dupuis *et al.* [80] also extracted the folded structure of GAAA tetraloop receptor. The unfolded state or structure was constructed by editing the folded structure in GaussView 5.0 by following the secondary structure. Moreover, both components of the GAAA tetraloop receptor, i.e. GAAA tetraloop and receptor, moved apart until the radius of curvature by the extended SPT of the unfolded structure becomes almost equal to the approximated value of 27 \AA reported by Dupuis *et al.* [80]. Finally these two structures were used to approximate the transition state structure, and subsequently the geometric parameters (Table 4.4) and activity coefficients were estimated with the extended SPT model.

The experimental folding rate constant under dilute conditions (k_0) of GAAA tetraloop receptor was obtained from Dupuis *et al.* [80] where it was measured by using the FRET spectroscopic method and the final rate constant (k_1) was measured in the presence of 8 kDa PEG crowders. The measurement of the rate constant k_1 using the transition state theory expression showed a slightly lower rate constant in the presence of the PEG2 crowders by incorporating the activity coefficients for the unfolded and the transition states (Figure 4.25). Despite using the approximated structure of the transition state to predict the activity coefficient, a good estimate of k_1 was obtained. Even at the very highest PEG concentration

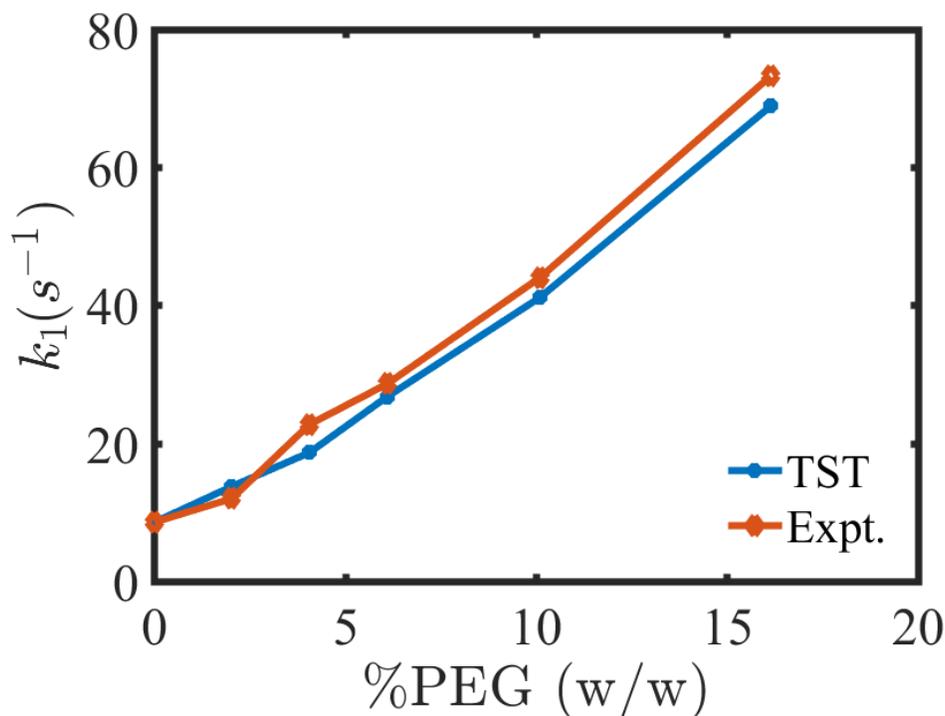


Figure 4.25: Change in the folding rate constant as a function of concentration of 8 kDa PEG. The extended SPT model predicted the slightly lower rate constant by incorporating the activity coefficients of the unfolded and the transition states in the transition state theory expression as compared to the experimental data. PEG2 molecules were used as crowders in these calculations as 15 Å radius of gyration of the PEG was assumed in the experimental measurements.

the estimated rate constant fell within about 5% of the correct rate constant.

Summary

The crowding effects on the conformational equilibrium of three systems have been investigated by carrying out the MC and SPT simulations. Macromolecular crowding exerts low to moderate effects on the conformational equilibrium and increases stability of folded states by -0.2 to $-2.0kT$ approximately. The magnitude of the crowding effect is directly influenced by the shapes and sizes of the probe and crowder molecules. Conformational equilibrium involving large conformational changes is expected to experience high crowding effects. The MC and SPT models utilized the real molecular structures to predict the crowding effects, however to get the quantitative effects of crowding these models need additional NI contribution terms such as electrostatic potentials, enthalpic and entropic in-

termolecular interactions. Further, the successful implementation of the transition state theory model along with the MC and extended SPT model might be capable of predicting the rate constants quantitatively for biochemical reactions occurring in crowded media.

Chapter 5

Conclusions and future directions

5.1 Summary

This research work was dedicated to the development of a new theoretical framework for computing the effects of macromolecular crowding on the activities of macromolecular solutes. This theoretical framework is then applied to study the macromolecular crowding effects on the conformational equilibrium of three systems. The theoretical framework is comprised of two major steps, i.e. the construction of crowded media at different concentrations followed by the study of a biochemical reaction of interest in the crowded media. The first step requires the availability of representative solution structures of the crowder to be used to pack and further to equilibrate the crowded medium. Ensembles of 8 kDa PEG conformations over a wide range of sizes (10–60 Å radius of gyration) were used as crowders. The first step will usually require conformational sampling simulations to generate the ensembles of crowder conformations as it would be unusual for structural libraries to contain solution structures of a large sized crowder. In our case, we constructed ensembles of PEG conformations using MC and MD simulations under different simulation conditions to get as diverse a set of conformations as possible. These conformations are used to pack the crowded systems and are further equilibrated to incorporate the PEG self-crowding effects. The second step comprised a set of methods to be used to estimate the crowding effects on the folding reaction or any other reaction of interest such as association reactions. These methods, i.e. the extended scaled particle theory and Monte Carlo simulations, are applied to estimate the activity coefficients in crowded systems. These can be used to determine the

effect of crowding on an equilibrium or, via TST, on the kinetics of a reaction, provided we can generate a guess for the transition state structure.

5.2 Recommended computational methods

The aim of developing the current program is to measure the crowding effects quantitatively. This could be one step towards achieving our goal by using the more realistic crowded medium with the extended scaled particle theory and MC methods. In the text that follows, the best procedures for calculating crowding effects based on the work in this thesis will be presented.

5.2.1 Ensembles of crowder conformations

Experimental studies can help to define a biochemical system that can be studied with our program. Our program required solution structures for all the species either of probe molecules or crowders. Different types of crowding agents have been used to mimic the crowding environments in *in vitro* experiments. The availability of the crowder structures may be limited due to lack of solution structures of crowders. For instance, 8 kDa PEG is one of the most commonly used crowders in experimental studies [80, 98, 111, 191], however we do not have detailed information on solution conformations of PEG to the best of my knowledge. Solution structures of PEG were constructed through performing conformational sampling simulations. In this regard, MC simulations in Sire and MD simulations in Amber are found to be equally effective and produced diverse conformational ensembles in a range of radii of gyration of 10 to 60 Å. The folding behaviour of PEG is found to be sensitive to the simulation methods, i.e. whether MC or MD simulations are used and a temperature parameter in these simulations. Therefore a combination of these two methods was used to produce diverse conformational ensembles of a PEG crowder. In this regard, the MD and MC simulations produced equilibrated compact (10–25 Å) and more extended conformations (18–60 Å) of PEG respectively. The recommendation on the selection of an

appropriate MC or MD simulation method is based on the required range of the solution structures of crowders and their folding sensitivity to each simulation method. For crowders insensitive to simulation methods, the MC simulation method would be a good choice for conformational sampling in producing diverse conformations. Moreover, the sensitivity of the crowders towards each method can be tested by conducting MC and MD simulations using an equilibrated structure.

5.2.2 Packing and equilibration

The second step involved the preparation of crowded media at different concentrations by packing the random PEG conformations generated in the previous step. Fifteen to thirty instances of crowded systems at each concentration from 0.1 to 0.6 g cm⁻³ were prepared. The packed crowded systems were further equilibrated by conducting MC equilibration, MC swapping and MD equilibration simulations to account for self crowding effects. The multiple instances at each concentration were useful to produce statistically converged results. In our calculations the standard deviation and the average of the fractional available volume were converged after including fifteen instances of crowded media. MD equilibration was found to be the most efficient technique among the other two and showed that PEG experienced large conformational changes in the crowded medium and formed PEG aggregates [89, 92, 93, 95, 101, 109, 258, 259].

The appropriate equilibration method can be selected based on the size of the system. This may also require trial and error calculations to find out the best method for the given system. In general, the MD equilibration method is a good choice for any sized systems filled with crowders of any molecular weight. A system with dimensions of 50 × 50 × 50 Å³ or greater and filled with crowders of molecular weight greater than 1 kDa can be classified as a larger sized system. The MC equilibration and swapping methods are almost equally effective to the MD equilibration in smaller sized systems of dimension less than 50 × 50 × 50 Å³ filled with crowders of molecular weight less than 0.5 kDa.

5.2.3 Calculations of thermodynamic properties

The third step is the application of the extended scaled particle theory or Monte Carlo method to determine the crowding effects on the biochemical reactions in terms of estimating the fractional available volumes and subsequently chemical potentials. The size and shape distribution of crowders and system molecules played a critical role in affecting the magnitude of the fractional available volume. The SPT model considered the nonideal contribution of individual molecules towards the chemical potentials by extracting the geometrical parameters from atomic coordinates and also taking into account the PEG aggregates contribution. The MC method measured the chemical potential by placing each conformation of the system over and over again in the equilibrated simulation boxes at a random position with a random orientation. The fraction of successful insertions to the total number of insertions gave the estimate of the activity coefficient for each probe molecule. In this regard, the MC method used parallel-energy and parallel-distance algorithms to measure the steric clashes and subsequently activity coefficients for each probe molecule.

The SPT model is very efficient and approximates the crowding effects quickly but depends on the extraction of the correct geometrical parameters of a system and crowder molecules. The MC method does not require extraction of geometrical parameters but uses the atomic coordinates and can estimate the chemical potential accurately. However, the MC method is computationally expensive. In this regard, a parallel-energy algorithm is found to be more efficient for larger systems used in this study as compared to a parallel-distance algorithm. Both algorithms are equally effective and efficient for small sized system as defined above. The SPT model would be a good choice for systems containing convex shaped molecules as it predicts the crowding effects quickly. However it overestimates the crowding effects for systems containing extended or open and non-convex structures due to the convex hull construction (Figure 5.1 (b)).

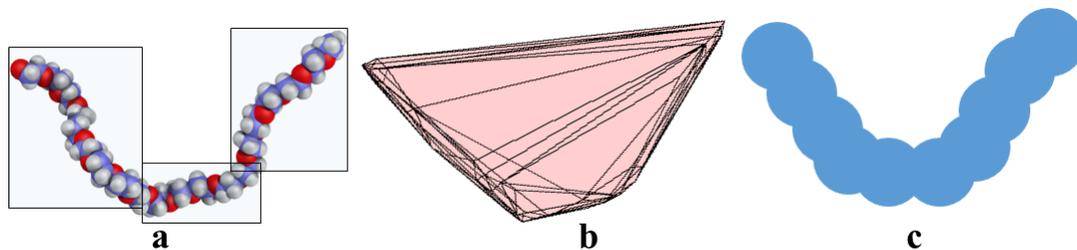


Figure 5.1: Illustration of a small fragment of a 8 kDa PEG to depict the concept of the construction of sub-units (a), convex hull (b) and a rolling method (c). The fragment represents a non-convex conformation where the convex hull algorithm overestimates the geometrical parameters by encapsulating the free space present in the cavity. These two methods could help to approximate more accurate geometrical parameters of a non-convex molecule.

5.2.4 Crowding effects on reaction kinetics

The transition state theory approximated the crowding effects on the folding kinetics. The transition state theory requires activity coefficients of the reactants and a transition state for any chemical reaction. These activity coefficients could be estimated by the extended SPT or MC models which requires the availability of the structures of the reactant(s) and transition state. In this regard, the morphing server provided an alternative solution to construct intermediate conformations between initial and final structures of the system to get an approximated transition state structure. The morphing server takes two input structures to start with and constructs the intermediate structures between these initial and final structures. Therefore, this can be applied to bimolecular association or dissociation reactions if the solution structure of a product in an association reaction or a structure of the reactant in a dissociation reaction is available. Alternatively, the dissociation reaction is the reverse of an association reaction and the approximated TS structure in the dissociation reaction can be used as a TS in the association reaction. It is important to prepare the input files properly and both input files should be equal in terms of number of atoms. For example, two reactants combined in bimolecular association reaction to form a single product. The reactant input file must contain both reactants so the reactant file will have an equal number of atomic coordinates to the product file. Both reactants can be placed at any arbitrarily large distance from each other in the first input file.

This TS model approximated crowding effects well in the unimolecular folding reaction of the GAAA tetraloop receptor (section 4.5). It might be concluded that this model can help one to estimate the crowding effects on the reaction kinetics using an approximated transition state structure with a reasonable accuracy. The MC method would be a good choice for reactions involving denatured and extended states of reactants and TS, while the SPT model is good for reactions containing compact globular shaped reactants and TS structures to approximate the activity coefficient. For example, for a unimolecular unfolding reaction forming an unfolded state from a compact globular folded state or for a bimolecular dissociation reaction occurring between two compact globular shaped proteins, SPT is good to apply to approximate the activity coefficients.

5.3 Future directions

The theoretical framework predicted low to moderate crowding effects on the conformational equilibrium correlated with many theoretical and experimental results [24, 47, 125, 268, 269]. The following future improvements can be made to the model to estimate the crowding effects quantitatively. Moreover, the possible steps that can be taken to improve the accuracy of the extraction of geometrical parameters in the extended SPT method and the computational efficiency of the MC method are described in the following section.

5.3.1 Accuracy of the geometrical parameters and computational efficiency

The convexification algorithm overestimates the geometrical parameters for non-convex shaped molecules. The accuracy of the geometrical parameters for non-convex shaped molecules can be improved by applying the convexification algorithm on compact shaped sub-units of the molecule. It will be challenging to define the criterion for defining the cut-off boundary points for each sub-unit. Figure 5.1 (a) depicts the idea of defining approximately convex shaped sub-units whose number will depend on the structure of the molecule. The sub-units can differ in size and contain different numbers of atoms. A

combination of three sub-units will represent a coiled cylinder and will give an estimate of geometrical parameters for this coiled cylinder shape. Eventually, this approach will approximate the activity coefficients in the SPT model. Alternatively, the rolling probe methods [238, 272–275] (Figure 5.1(c)) can be used to estimate the volume and the surface area of the molecule by rolling a virtual probe solvent convex shaped molecule of known radius. The virtual probe molecule can be a solvent molecule such as water of 1.5 Å radius [238]. The rolling probe method cannot estimate the radius of curvature but the convex hull algorithm can be used here. These methods may be computationally expensive but the efficiency can be improved by implementing the multiprocessing routines for larger and complexed shaped macromolecules.

In our program, the MC method with a parallel-distance algorithm to compute the fractional available volume is equally effective to the MC method with a parallel-energy algorithm for small sized systems filled with lower molecular weight crowders. Similarly, two equilibration methods i.e. MC equilibration and MC swapping are also equally effective to MD equilibration for small sized systems filled with lower molecular weight crowders. All of these three methods, i.e. MC method with a parallel-distance algorithm, MC equilibration and MC swapping were built in the Sire program. Sire is built in C/C++ and Python frameworks and we have implemented the Python multiprocessing routines to further improve the computational efficiency of an MC method with the parallel-distance algorithm. C/C++ is more powerful and its multiprocessing routines such as OpenMP [276] and MPI [277] would make the computation faster for larger sized systems to approximate the activity coefficients. This would require the rewriting of a single function in the parallel-distance algorithm that executes the iterative loops to find the steric clashes.

5.3.2 Heterogeneity of crowded medium

A heterogeneous and complex crowded medium similar to the cellular interior can mimic the cellular interior effectively [37, 262, 278]. For that we may need a set of crow-

ders that can resemble the contents of different types of cells. The heterogeneous crowded medium can be constructed by packing and equilibrating a mixture of routinely used crowders such as PEG, Ficoll, and dextran. This method will require to find the appropriate mixture of crowders of different sizes and shapes. Alternatively, solution structures of different macromolecules available in the protein data bank can be used to pack and equilibrate the crowded medium. This approach can provide a library of diverse molecules but it may require to choose macromolecules that can result in an appropriate medium without segregation of some components after packing and equilibration. Moreover, it is important to include the local concentration effects as the concentration varies from point to point inside the cells [47, 267] and these microenvironments can alter the thermodynamic activities of solutes substantially. The microenvironments within, e.g., the nucleus, like a Cajal body or nuclear speckle, may need an ensemble of microenvironments that differ somewhat in dimensions and/or composition. Conformational ensembles of microenvironments are required as the composition and dimensions of these microenvironments fluctuate with time due to flow of cell material such as proteins in between different cell compartments [8, 267, 278]. For example, nuclear speckles are dynamic structures that vary in size and shape and are found in the interchromatin regions of the nucleoplasm. The nuclear speckles are composed of a heterogeneous mixture of proteins and RNA-protein components. The transcriptional state of the cell controls the concentration of these proteins that keep changing continuously due to their exchange between speckles and other nuclear locations [279, 280].

5.3.3 Soft interactions contributions

It is worth incorporating the nonideal contributions due to attractive and repulsive electrostatic potentials, enthalpic and entropic intermolecular interactions to quantify the macromolecular crowding effect in the extended scaled particle and Monte Carlo methods. There are numerous ways to estimate the electrostatic contributions to the activity coefficients

such as the Debye-Hückel equations [281], semi-empirical models [281, 282], Poisson-Boltzmann [283–285], and thermodynamic models for solutions [282].

5.3.4 Approximate better TS state structure

The approximated transition state from the morphing server is not necessarily a close representative of a true transition state structure. Further development can be made in the theoretical framework to estimate a more realistic transition state structure. There are computational methods [241, 242, 244, 245, 286], as well as experimental transition state spectroscopic methods [243] available to determine the TS structures. However, these methods do not always work for all types of reactions involving complex macromolecules.

Alternatively, the transition state structure can be approximated by using experimental data fitting tools such as the least square error method [239]. The transition state theory equation (Equation 5.1) expresses the relationship between the final rate constant (k) of a unimolecular folding reaction, the ideal rate constant (k_0) and the activity coefficients of the reactant (γ_A) and TS (γ_{TS}) structures. This method requires experimental values of k under crowded conditions (ϕ) and k_0 for the reaction and the SPT method can approximate the activity coefficient of the reactant. Running a minimization tool as a function of the sum of squared error can predict the unknown geometric parameters (R_{TS} , A_{TS} , V_{TS}) of the transition state in the SPT equation. Mathematically this could be expressed by equation 5.2.

$$k = k_0 \gamma_A \left(\frac{1}{\gamma_{TS}} \right) = k_0 \gamma_A \left(\frac{1}{\gamma_{TS}(R_{TS}, S_{TS}, V_{TS})} \right) \quad (5.1)$$

$$\min \left\| \sum k(\phi) - k_0 \gamma_A \left(\frac{1}{\gamma_{TS}(\phi, k, k_0, R_{TS}, S_{TS}, V_{TS})} \right) \right\|^2 \quad (5.2)$$

Bibliography

- [1] T. C. Laurent. The interaction between polysaccharides and other macromolecules. 5. the solubility of proteins in the presence of dextran. *Biochemical Journal*, 89(2):253–257, 1963.
- [2] A. G. Ogston and P. Silpananta. The thermodynamics of interaction between sephadex and penetrating solutes. *Biochemical Journal*, 116(2):171–5, 1970.
- [3] R. John Ellis. Macromolecular crowding: obvious but underappreciated. *Trends in Biochemical Sciences*, 26(10):597–604, 2001.
- [4] A. P. Minton. Confinement as a determinant of macromolecular structure and reactivity. *Biophysical Journal*, 63(4):1090–1100.
- [5] Allen P Minton and Germán Rivas. Biochemical reactions in the crowded and confined physiological environment: physical chemistry meets synthetic biology. In *The Minimal Cell*, pages 73–89. Springer, 2011.
- [6] Huan-Xiang Zhou, Germn Rivas, and Allen P. Minton. Macromolecular crowding and confinement: biochemical, biophysical, and potential physiological consequences. *Annual Review of Biophysics*, 37:375–397, 2008.
- [7] Allen P. Minton. The influence of macromolecular crowding and macromolecular confinement on biochemical reactions in physiological media. *Journal of Biological Chemistry*, 276(14):10577–10580, 2001.
- [8] Alice B. Fulton. How crowded is the cytoplasm? *Cell*, 30(2):345–347.
- [9] Steven B. Zimmerman and Stefan O. Trach. Estimation of macromolecule concentrations and excluded volume effects for the cytoplasm of escherichia coli. *Journal of Molecular Biology*, 222(3):599–620, 1991.
- [10] B. van den Berg, R. J. Ellis, and C. M. Dobson. Effects of macromolecular crowding on protein folding and aggregation. *EMBO Journal*, 18(24):6927–33, 1999.
- [11] G. Rivas, F. Ferrone, and J. Herzfeld. Life in a crowded world. *EMBO Reports*, 5(1):23–7, 2004.
- [12] Allen P. Minton. Excluded volume as a determinant of macromolecular structure and reactivity. *Biopolymers*, 20(10):2093–2120, 1981.
- [13] Allen P. Minton. Macromolecular crowding. *Current Biology*, 16(8):R269–R271, 2006.

- [14] A. P. Minton and J. Wilf. Effect of macromolecular crowding upon the structure and function of an enzyme: glyceraldehyde-3-phosphate dehydrogenase. *Biochemistry*, 20(17):4821–4826, 1981.
- [15] Alexander Christiansen, Qian Wang, Margaret S. Cheung, and Pernilla Wittung-Stafshede. Effects of macromolecular crowding agents on protein folding in vitro and in silico. *Biophysical Reviews*, 5(2):137–145, 2013.
- [16] Michael Hoppert and Frank Mayer. Prokaryotes: Even without membrane-bounded compartments, prokaryotes display a high degree of subcellular organization. *American Scientist*, 87(6):518–525, 1999.
- [17] David S. Goodsell. Visual methods from atoms to cells. *Structure*, 13(3):347–354.
- [18] D. H. Atha and K. C. Ingham. Mechanism of precipitation of proteins by polyethylene glycols. analysis in terms of excluded volume. *Journal of Biological Chemistry*, 256, 1981.
- [19] Sanbo Qin and Huan-Xiang Zhou. Atomistic modeling of macromolecular crowding predicts modest increases in protein folding and binding stability. *Biophysical Journal*, 97(1):12–19.
- [20] J. Aden and P. Wittung-Stafshede. Folding of an unfolded protein by macromolecular crowding in vitro. *Biochemistry*, 53(14):2271–7, 2014.
- [21] S. Qin and H. X. Zhou. Atomistic modeling of macromolecular crowding predicts modest increases in protein folding and binding stability. *Biophysical Journal*, 97(1):12–9, 2009.
- [22] Douglas Tsao and Nikolay V. Dokholyan. Macromolecular crowding induces polypeptide compaction and decreases folding cooperativity. *Physical Chemistry Chemical Physics : PCCP*, 12(14):3491–3500, 2010.
- [23] Sean R McGuffee and Adrian H Elcock. Diffusion, crowding & protein stability in a dynamic molecular model of the bacterial cytoplasm. *PLoS Computational Biology*, 6(3):e1000694, 2010.
- [24] Hao Dong, Sanbo Qin, and Huan-Xiang Zhou. Effects of macromolecular crowding on protein conformational changes. *PLoS Computational Biology*, 6(7):e1000833, 2010.
- [25] S. Qin, J. Mittal, and H. X. Zhou. Folding free energy surfaces of three small proteins under crowding: validation of the postprocessing method by direct simulation. *Biophysical Journal*, 10(4):045001, 2013.
- [26] Adedayo A. Fodeke and Allen P. Minton. Quantitative characterization of polymerpolymer, proteinprotein, and polymerprotein interaction via tracer sedimentation equilibrium. *The Journal of Physical Chemistry B*, 114(33):10876–10880, 2010.

- [27] A. P. Minton. The effect of volume occupancy upon the thermodynamic activity of proteins - some biochemical consequences. *Molecular and Cellular Biochemistry*, 55(2):119–140, 1983.
- [28] A. P. Minton. Models for excluded volume interaction between an unfolded protein and rigid macromolecular cosolutes: macromolecular crowding and protein stability revisited. *Journal of Biophysics*, 88(2):971–85, 2005.
- [29] Allen P. Minton. Quantitative assessment of the relative contributions of steric repulsion and chemical interactions to macromolecular crowding. *Biopolymers*, 99(4):239–244, 2013.
- [30] N. A. Chebotareva, B. I. Kurganov, and N. B. Livanova. Biochemical effects of molecular crowding. *Biochemistry (Mosc)*, 69(11):1239–51, 2004.
- [31] Peter Atkins, Julio de Paula, and Julio de Paula Peter Atkins. Atkins’s physical chemistry. Technical report, 2010.
- [32] Alan D McNaught and Alan D McNaught. *Compendium of chemical terminology*, volume 1669. Blackwell Science Oxford, 1997.
- [33] Philip D. Ross and Allen P. Minton. Analysis of non-ideal behavior in concentrated hemoglobin solutions. *Journal of Molecular Biology*, 112(3):437–452, 1977.
- [34] Mahadevappa Kumbar. Excluded volume in macromolecules. *Journal of Macromolecular Science: Part A - Chemistry*, 5(8):1303–1310, 1971.
- [35] Jeetain Mittal and Robert B. Best. Dependence of protein folding stability and dynamics on the density and composition of macromolecular crowders. *Biophysical Journal*, 98(2):315–320.
- [36] Yael Phillip and Gideon Schreiber. Formation of protein complexes in crowded environments from in vitro to in vivo. *FEBS Letters*, 587(8):1046–1052, 2013.
- [37] H. X. Zhou. Influence of crowded cellular environments on protein folding, binding, and oligomerization: biological consequences and potentials of atomistic modeling. *FEBS Letters*, 587(8):1053–61, 2013.
- [38] S. S. Paul, P. Sil, R. Chakraborty, S. Haldar, and K. Chattopadhyay. Molecular crowding affects the conformational fluctuations, peroxidase activity, and folding landscape of yeast cytochrome c. *Biochemistry*, 55(16):2332–43, 2016.
- [39] MrcioA Mouro, JoeB Hakim, and Santiago Schnell. Connecting the dots: The effects of macromolecular crowding on cell physiology. *Biophysical Journal*, 107(12):2761–2766.
- [40] P. L. Privalov and S. J. Gill. Stability of protein structure and hydrophobic interaction. *Advance Protein Chemistry*, 39:191–234, 1988.

- [41] Laura A. Benton, Austin E. Smith, Gregory B. Young, and Gary J. Pielak. Unexpected effects of macromolecular crowding on protein stability. *Biochemistry*, 51(49):9773–9775, 2012.
- [42] Andrew C. Miklos, Mohona Sarkar, Yaqiang Wang, and Gary J. Pielak. Protein crowding tunes protein stability. *Journal of American Chemical Society*, 133(18):7116–7120, 2011.
- [43] L. Stagg, S. Q. Zhang, M. S. Cheung, and P. Wittung-Stafshede. Molecular crowding enhances native structure and stability of alpha/beta protein flavodoxin. *Proceedings National Academy Science U S A*, 104(48):18976–81, 2007.
- [44] D. Li, M. S. Liu, and B. Ji. Mapping the dynamics landscape of conformational transitions in enzyme: The adenylate kinase case. *Biophysical Journal*, 109(3):647–60, 2015.
- [45] Jie Ping, Pei Hao, Yi-Xue Li, and Jing-Fang Wang. Molecular dynamics studies on the conformational transitions of adenylate kinase: a computational evidence for the conformational selection mechanism. *BioMedical Research International*, 2013, 2013.
- [46] S. Cao and S. J. Chen. Biphasic folding kinetics of rna pseudoknots and telomerase rna activity. *Journal of Molecular Biology*, 367(3):909–24, 2007.
- [47] Natalia A. Denesyuk and D. Thirumalai. Crowding promotes the switch from hairpin to pseudoknot conformation in human telomerase rna. *Journal of American Chemical Society*, 133(31):11858–11861, 2011.
- [48] S. B. Zimmerman and S. O. Trach. Effects of macromolecular crowding on the association of e. coli ribosomal particles. *Nucleic Acids Research*, 16(14A):6309–6326, 1988.
- [49] Jyotica Batra, Ke Xu, Sanbo Qin, and Huan-Xiang Zhou. Effect of macromolecular crowding on protein binding stability: modest stabilization and significant biological consequences. *Biophysical Journal*, 97(3):906–911, 2009.
- [50] V. K. Shen, J. K. Cheung, J. R. Errington, and T. M. Truskett. Coarse-grained strategy for modeling protein stability in concentrated solutions. ii: phase behavior. *Biophysical Journal*, 90(6):1949–60, 2006.
- [51] J. Bloustone, T. Virmani, G. M. Thurston, and S. Fraden. Light scattering and phase behavior of lysozyme-poly(ethylene glycol) mixtures. *Physical Review Letters*, 96(8):087803, 2006.
- [52] G. Tubio, B. Nerli, and G. Pico. Relationship between the protein surface hydrophobicity and its partitioning behaviour in aqueous two-phase systems of polyethyleneglycol-dextran. *Journal of Chromatography B Analytical Technology Biomedical Life Sciences*, 799(2):293–301, 2004.

- [53] Allen P. Minton. Influence of macromolecular crowding upon the stability and state of association of proteins: Predictions and observations. *Journal of Pharmaceutical Sciences*, 94(8):1668–1675, 2005.
- [54] R. Engel, A. H. Westphal, D. H. Huberts, S. M. Nabuurs, S. Lindhoud, A. J. Visser, and C. P. van Mierlo. Macromolecular crowding compacts unfolded apoflavodoxin and causes severe aggregation of the off-pathway intermediate during apoflavodoxin folding. *Journal of Biological Chemistry*, 283(41):27383–94, 2008.
- [55] J. K. Armstrong, R. B. Wenby, H. J. Meiselman, and T. C. Fisher. The hydrodynamic radii of macromolecules and their effect on red blood cell aggregation. *Biophysical Journal*, 87(6):4259–4270, 2004.
- [56] Akira R. Kinjo and Shoji Takada. Effects of macromolecular crowding on protein folding and aggregation studied by density functional theory: Dynamics. *Physical Review E*, 66(5):051902, 2002.
- [57] Margaret S. Cheung, Dmitri Klimov, and D. Thirumalai. Molecular crowding enhances native state stability and refolding rates of globular proteins. *Proceedings of the National Academy of Sciences of the United States of America*, 102(13):4753–4758, 2005.
- [58] Noga Kozer, Yosef Yehuda Kuttner, Gilad Haran, and Gideon Schreiber. Protein-protein association in polymer solutions: From dilute to semidilute to concentrated. *Biophysical Journal*, 92(6):2139–2149.
- [59] S. Qin, L. Cai, and H. X. Zhou. A method for computing association rate constants of atomistically represented proteins under macromolecular crowding. *Biophysical Journal*, 9(6):066008, 2012.
- [60] Christopher J. Woods, Matusos Malaisree, Julien Michel, Ben Long, Simon McIntosh-Smith, and Adrian J. Mulholland. Rapid decomposition and visualisation of protein-ligand binding free energies by residue and by water. *Faraday Discussions*, 169(0):477–499, 2014.
- [61] G. B. Ralston. Effects of "crowding" in protein solutions. *Journal of Chemical Education*, 67(10):857, 1990.
- [62] R. M. Daniel, R. V. Dunn, J. L. Finney, and J. C. Smith. The role of dynamics in enzyme activity. *Annual Review of Biophysical Biomolecular Structure*, 32:69–92, 2003.
- [63] Irina M. Kuznetsova, Konstantin K. Turoverov, and Vladimir N. Uversky. What macromolecular crowding can do to a protein. *International Journal of Molecular Sciences*, 15(12):23090–23140, 2014.
- [64] C. W. Muller, G. J. Schlauderer, J. Reinstein, and G. E. Schulz. Adenylate kinase motions during catalysis: an energetic counterweight balancing substrate binding. *Structure*, 4(2):147–56, 1996.

- [65] S. J. Benkovic and S. Hammes-Schiffer. A perspective on enzyme catalysis. *Science*, 301(5637):1196–202, 2003.
- [66] P. K. Qasba, B. Ramakrishnan, and E. Boeggeman. Substrate-induced conformational changes in glycosyltransferases. *Trends in Biochemical Sciences*, 30(1):53–62, 2005.
- [67] P. K. Agarwal. Role of protein dynamics in reaction rate enhancement by enzymes. *Journal of American Chemical Society*, 127(43):15248–56, 2005.
- [68] O. A. Sytina, D. J. Heyes, C. N. Hunter, M. T. Alexandre, I. H. van Stokkum, R. van Grondelle, and M. L. Groot. Conformational changes in an ultrafast light-driven enzyme determine catalytic activity. *Nature*, 456(7224):1001–4, 2008.
- [69] E. Z. Eisenmesser, O. Millet, W. Labeikovsky, D. M. Korzhnev, M. Wolf-Watz, D. A. Bosco, J. J. Skalicky, L. E. Kay, and D. Kern. Intrinsic dynamics of an enzyme underlies catalysis. *Nature*, 438(7064):117–21, 2005.
- [70] Hamid Soleimaninejad, Moore Z. Chen, Xiaoding Lou, Trevor A. Smith, and Yuning Hong. Measuring macromolecular crowding in cells through fluorescence anisotropy imaging with an aie fluorogen. *Chemical Communications*, 53:2874–2877, 2017.
- [71] Shruti Mittal, Rimpay Kaur Chowhan, and Laishram Rajendrakumar Singh. Macromolecular crowding: Macromolecules friend or foe. *Biochimica et Biophysica Acta (BBA) - General Subjects*, 1850(9):1822–1831, 2015.
- [72] Allen P. Minton. Excluded volume as a determinant of protein structure and stability. *Biophysical Journal*, 32(1):77–79.
- [73] Donald J. Winzor and Peter R. Wills. Molecular crowding effects of linear polymers in protein solutions. *Biophysical Chemistry*, 119(2):186–195, 2006.
- [74] D. Homouz, H. Sanabria, M. N. Waxham, and M. S. Cheung. Modulation of calmodulin plasticity by the effect of macromolecular crowding. *Journal of Molecular Biology*, 391(5):933–43, 2009.
- [75] D. Homouz, L. Stagg, P. Wittung-Stafshede, and M. S. Cheung. Macromolecular crowding modulates folding mechanism of alpha/beta protein apoflavodoxin. *Biophysical Journal*, 96(2):671–80, 2009.
- [76] M. P. Bohrer, Gary D. Patterson, and P. J. Carroll. Hindered diffusion of dextran and ficoll in microporous membranes. *Macromolecules*, 17(6):1170–1173, 1984.
- [77] D. Venturoli and B. Rippe. Ficoll and dextran vs. globular proteins as probes for testing glomerular permselectivity: effects of molecular size, shape, charge, and deformability. *American Journal of Physiol Renal Physiol*, 288(4):F605–13, 2005.
- [78] Marc G. Davidson and William M. Deen. Hindered diffusion of water-soluble macromolecules in membranes. *Macromolecules*, 21(12):3474–3481, 1988.

- [79] Kirsti A. Granath. Solution properties of branched dextrans. *Journal of Colloid Science*, 13(4):308–328, 1958.
- [80] Nicholas F. Dupuis, Erik D. Holmstrom, and David J. Nesbitt. Molecular-crowding effects on single-molecule rna folding/unfolding thermodynamics and kinetics. *Proceedings of the National Academy of Sciences*, 111(23):8464–8469, 2014.
- [81] P. D. Ross and A. P. Minton. The effect of non-aggregating proteins upon the gelation of sickle cell hemoglobin: model calculations and data analysis. *Biochemical Biophysical Research Communications*, 88(4):1308–14, 1979.
- [82] Huan-Xiang Zhou. Effect of mixed macromolecular crowding agents on protein folding. *Proteins: Structure, Function, and Bioinformatics*, 72(4):1109–1113, 2008.
- [83] R. M. Gibbons. The scaled particle theory for mixtures of hard convex particles. *Molecular Physics*, 18(6):809–816, 1970.
- [84] Daan Frenkel and Berend Smit. *Chapter 3 - Monte Carlo Simulations*, pages 23–61. Academic Press, San Diego, 2002.
- [85] J. Hu, A. Ma, and A. R. Dinner. Monte carlo simulations of biomolecules: The mc module in charmm. *Journal of Computational Chemistry*, 27(2):203–16, 2006.
- [86] David J. Earl and Michael W. Deem. *Monte Carlo Simulations*, pages 25–36. Humana Press, Totowa, NJ, 2008.
- [87] Henry Eyring. The activated complex in chemical reactions. *The Journal of Chemical Physics*, 3(2):107–115, 1935.
- [88] Robyn A. Lindner and Gregory B. Ralston. Macromolecular crowding: effects on actin polymerisation. *Biophysical Chemistry*, 66(1):57 – 66, 1997.
- [89] Alexander I. Norman, Yiwei Fei, Derek L. Ho, and Sandra C. Greer. Folding and unfolding of polymer helices in solution. *Macromolecules*, 40(7):2559–2567, 2007.
- [90] Kenneth A. Rubinson and Susan Krueger. Poly(ethylene glycol)s 20008000 in water may be planar: A small-angle neutron scattering (sans) structure study. *Polymer*, 50(20):4852 – 4858, 2009.
- [91] Kenneth A. Rubinson and Curtis W. Meuse. Deep hydration: Poly(ethylene glycol) mw 20008000da probed by vibrational spectrometry and small-angle neutron scattering and assignment of g to individual water layers. *Polymer*, 54(2):709 – 723, 2013.
- [92] AlisterC French, AmberL Thompson, and BenjaminG Davis. High-purity discrete peg-oligomer crystals allow structural insight. *Angewandte Chemie International Edition*, 48(7):1248–1252, 2009.

- [93] Osmair Vital de Oliveira, Luciano Tavares Costa, and Edson Roberto Leite. Molecular modeling of a polymer nanocomposite model in water and chloroform solvents. *Computational and Theoretical Chemistry*, 1092:52 – 56, 2016.
- [94] Yasuhiro Takahashi and Hiroyuki Tadokoro. Structural studies of polyethers, $(-(\text{CH}_2)_m\text{-O})_n$. x. crystal structure of poly(ethylene oxide). *Macromolecules*, 6(5):672–675, 1973.
- [95] Aziz Azri, Philippe Giamarchi, Yves Grohens, Ren Olier, and Mireille Privat. Polyethylene glycol aggregates in water formed through hydrophobic helical structures. *Journal of Colloid and Interface Science*, 379(1):14–19, 2012.
- [96] R. Yang, X. R. Yang, D. F. Evans, W. A. Hendrickson, and J. Baker. Scanning tunneling microscopy images of poly(ethylene oxide) polymers: evidence for helical and superhelical structures. *The Journal of Physical Chemistry*, 94(15):6123–6125, 1990.
- [97] Jagannath Mondal, Eunsong Choi, and Arun Yethiraj. Atomistic simulations of poly(ethylene oxide) in water and an ionic liquid at room temperature. *Macromolecules*, 47(1):438–446, 2014.
- [98] Moritz Winger, Alex H. de Vries, and Wilfred F. van Gunsteren. Force-field dependence of the conformational properties of ω , ω -dimethoxypolyethylene glycol. *Molecular Physics*, 107(13):1313–1321, 2009.
- [99] Imre Bak, Tamas Grsz, Gbor Plinks, and Marie Claire Bellissent-Funel. Ethylene glycol dimers in the liquid phase: A study by x-ray and neutron diffraction. *The Journal of Chemical Physics*, 118(7):3215–3221, 2003.
- [100] H. Lee, S. Kim, J. Lee, S. Kim, and S. Lee. Reversible watermarking with localization for biometric images. pages 1590–1594, Dec 2008.
- [101] Hideyuki Shinzawa, Tadafumi Uchamaru, Junji Mizukado, and Sergei G. Kazarian. Non-equilibrium behavior of polyethylene glycol (peg)/polypropylene glycol (ppg) mixture studied by fourier transform infrared (ftir) spectroscopy. *Vibrational Spectroscopy*, 88:49 – 55, 2017.
- [102] Ian G. Elliott, Tonya L. Kuhl, and Roland Faller. Molecular simulation study of the structure of high density polymer brushes in good solvent. *Macromolecules*, 43(21):9131–9138, 2010.
- [103] H. Lee, R. M. Venable, A. D. Mackerell, and R. W. Pastor. Molecular dynamics studies of polyethylene oxide and polyethylene glycol: hydrodynamic radius and shape anisotropy. *Biophysical Journal*, 95, 2008.
- [104] Marcus G. Martin. Mccs towhee: a tool for monte carlo molecular simulation. *Molecular Simulation*, 39(14-15):1212–1222, 2013.

- [105] D. A. Case, 3rd Cheatham, T. E., T. Darden, H. Gohlke, R. Luo, Jr. Merz, K. M., A. Onufriev, C. Simmerling, B. Wang, and R. J. Woods. The amber biomolecular simulation programs. *Journal of Computational Chemistry*, 26(16):1668–88, 2005.
- [106] B. R. Brooks, 3rd Brooks, C. L., Jr. Mackerell, A. D., L. Nilsson, R. J. Petrella, B. Roux, Y. Won, G. Archontis, C. Bartels, S. Boresch, A. Caffisch, L. Caves, Q. Cui, A. R. Dinner, M. Feig, S. Fischer, J. Gao, M. Hodoscek, W. Im, K. Kuczera, T. Lazaridis, J. Ma, V. Ovchinnikov, E. Paci, R. W. Pastor, C. B. Post, J. Z. Pu, M. Schaefer, B. Tidor, R. M. Venable, H. L. Woodcock, X. Wu, W. Yang, D. M. York, and M. Karplus. Charmm: the biomolecular simulation program. *Journal of Computational Chemistry*, 30(10):1545–614, 2009.
- [107] K. L. Linegar, A. E. Adeniran, A. F. Kostko, and M. A. Anisimov. Hydrodynamic radius of polyethylene glycol in solution obtained by dynamic light scattering. *Colloid Journal*, 72(2):279–281, 2010.
- [108] Cemile zdemir Din, Gnay Kibarar, and Ali Gner. Solubility profiles of poly(ethylene glycol)/solvent systems. ii. comparison of thermodynamic parameters from viscosity measurements. *Journal of Applied Polymer Science*, 117(2):1100–1119, 2010.
- [109] K. Devanand and J. C. Selser. Polyethylene oxide does not necessarily aggregate in water. *Nature*, 343(6260):739–741, February 1990.
- [110] K. Devanand and J. Selser. Asymptotic behavior and long-range interactions in aqueous solutions of poly (ethylene oxide). *Macromolecules*, 24, 1991.
- [111] K. Ling, H. Jiang, and Q. Zhang. A colorimetric method for the molecular weight determination of polyethylene glycol using gold nanoparticles. *Nanoscale Research Letters*, 8(1):538, 2013.
- [112] Olesya V. Stepanenko, Olga V. Stepanenko, Irina M. Kuznetsova, Vladimir N. Uversky, and Konstantin K. Turoverov. Peculiarities of the super-folder gfp folding in a crowded milieu. *International Journal of Molecular Sciences*, 17(11), 2016.
- [113] J. D. Legassie and M. B. Jarstfer. The unmasking of telomerase. *Structure*, 14(11):1603–9, 2006.
- [114] J. D. Podlevsky and J. J. Chen. It all comes together at the ends: telomerase structure, function, and biogenesis. *Mutation Research*, 730(1-2):3–11, 2012.
- [115] C. A. Theimer, C. A. Blois, and J. Feigon. Structure of the human telomerase rna pseudoknot reveals conserved tertiary interactions essential for function. *Molecular Cell*, 17(5):671–82, 2005.
- [116] C. A. Theimer and J. Feigon. Structure and function of telomerase rna. *Current Opinion in Structural Biology*, 16(3):307–18, 2006.
- [117] Jiunn-Liang Chen and Carol W. Greider. Telomerase rna structure and function: implications for dyskeratosis congenita. *Trends in Biochemical Sciences*, 29(4):183–192, 2004.

- [118] C. A. Theimer, L. D. Finger, and J. Feigon. Ynmg tetraloop formation by a dyskeratosis congenita mutation in human telomerase rna. *Rna*, 9(12):1446–55, 2003.
- [119] Carla A. Theimer, L. David Finger, Lukas Trantirek, and Juli Feigon. Mutations linked to dyskeratosis congenita cause changes in the structural equilibrium in telomerase rna. *Proceedings of the National Academy of Sciences of the United States of America*, 100(2):449–454, 2003.
- [120] N. K. Kim, Q. Zhang, J. Zhou, C. A. Theimer, R. D. Peterson, and J. Feigon. Solution structure and dynamics of the wild-type pseudoknot of human telomerase rna. *Journal of Molecular Biology*, 384(5):1249–61, 2008.
- [121] Christoph W. Mller and Georg E. Schulz. Structure of the complex of adenylate kinase from escherichia coli with the inhibitor p1,p5-di(adenosine-5-)pentaphosphate. *Journal of Molecular Biology*, 202(4):909–912, 1988.
- [122] C. W. Muller and G. E. Schulz. Structure of the complex between adenylate kinase from escherichia coli and the inhibitor ap5a refined at 1.9 a resolution. a model for a catalytic transition state. *Journal of Molecular Biology*, 224(1):159–77, 1992.
- [123] Petras Dzeja and Andre Terzic. Adenylate kinase and amp signaling networks: Metabolic monitoring, signal communication and body energy sensing. *International Journal of Molecular Sciences*, 10(4):1729–1772, 2009.
- [124] S. J. Kerns, R. V. Agafonov, Y. J. Cho, F. Pontiggia, R. Otten, D. V. Pachov, S. Kutter, L. A. Phung, P. N. Murphy, V. Thai, T. Alber, M. F. Hagan, and D. Kern. The energy landscape of adenylate kinase during catalysis. *Nature Structure Molecular Biology*, 22(2):124–31, 2015.
- [125] Sanbo Qin and Huan-Xiang Zhou. Effects of macromolecular crowding on the conformational ensembles of disordered proteins. *The Journal of Physical Chemistry Letters*, 4(20):3429–3434, 2013.
- [126] Karunesh Arora and Charles L Brooks. Large-scale allosteric conformational transitions of adenylate kinase appear to involve a population-shift mechanism. *Proceedings of the National Academy of Sciences*, 104(47):18496–18501, 2007.
- [127] M. Lewis, G. Chang, N. C. Horton, M. A. Kercher, H. C. Pace, M. A. Schumacher, R. G. Brennan, and P. Lu. Crystal structure of the lactose operon repressor and its complexes with dna and inducer. *Science*, 271(5253):1247–54, 1996.
- [128] M. Lewis. The lac repressor. *Comptes Rendus Biologies*, 328(6):521–48, 2005.
- [129] Robert Daber, Steven Stayrook, Allison Rosenberg, and Mitchell Lewis. Structural analysis of lac repressor bound to allosteric effectors. *Journal of Molecular Biology*, 370(4):609–619, 2007.

- [130] M. Taraban, H. Zhan, A. E. Whitten, D. B. Langley, K. S. Matthews, L. Swint-Kruse, and J. Trehwella. Ligand-induced conformational changes and conformational dynamics in the solution structure of the lactose repressor protein. *Journal of Molecular Biology*, 376(2):466–81, 2008.
- [131] Robert Daber, Kim Sharp, and Mitchell Lewis. One is not enough. *Journal of Molecular Biology*, 392(5):1133–1144, 2009.
- [132] H. Lee, V. r. i. e. s. AHd, S. J. Marrink, and Pastor. A coarse-grained model for polyethylene oxide and polyethylene glycol: conformation and hydrodynamics. *journal of physical Chemistry B*, 113, 2009.
- [133] R Grima, SN Yaliraki, and M Barahona. Crowding-induced anisotropic transport modulates reaction kinetics in nanoscale porous media. *The Journal of Physical Chemistry B*, 114(16):5380–5385, 2010.
- [134] Stephen Smith and Ramon Grima. Fast simulation of brownian dynamics in a crowded environment. *The Journal of Chemical Physics*, 146(2):024105, 2017.
- [135] Jun Soo Kim and Arun Yethiraj. Effect of macromolecular crowding on reaction rates: A computational and theoretical study. *Biophysical Journal*, 96(4):1333–1340, 2009.
- [136] Ramon Grima and Santiago Schnell. Modelling reaction kinetics inside cells. *Essays in Biochemistry*, 45:41–56, 2008.
- [137] TE Turner, S Schnell, and K Burrage. Stochastic approaches for modelling in vivo reactions. *Computational Biology and Chemistry*, 28(3):165–178, 2004.
- [138] R Grima. Intrinsic biochemical noise in crowded intracellular conditions. *The Journal of Chemical Physics*, 132(18):185102, 2010.
- [139] Matthias Weiss, Markus Elsner, Fredrik Kartberg, and Tommy Nilsson. Anomalous subdiffusion is a measure for cytoplasmic crowding in living cells. *Biophysical Journal*, 87(5):3518–3524, 2004.
- [140] Nevan J Krogan, Gerard Cagney, Haiyuan Yu, Gouqing Zhong, Xinghua Guo, Alexandr Ignatchenko, Joyce Li, Shuye Pu, Nira Datta, Aaron P Tikuisis, et al. Global landscape of protein complexes in the yeast *saccharomyces cerevisiae*. *Nature*, 440(7084):637–643, 2006.
- [141] S Schnell and TE Turner. Reaction kinetics in intracellular environments with macromolecular crowding: simulations and rate laws. *Progress in Biophysics and Molecular Biology*, 85(2-3):235–260, 2004.
- [142] S Schnell and PK Maini. Enzyme kinetics at high enzyme concentration. *Bulletin of Mathematical Biology*, 62(3):483–499, 2000.
- [143] A. G. Ogston. The spaces in a uniform random suspension of fibres. *Transactions of the Faraday Society*, 54(0):1754–1757, 1958.

- [144] A. G. Ogston and C. F. Phelps. The partition of solutes between buffer solutions and solutions containing hyaluronic acid. *Biochemical Journal*, 78(4):827–833, 1961.
- [145] A. G. Ogston. On the interaction of solute molecules with porous networks. *The Journal of Physical Chemistry*, 74(3):668–669, 1970.
- [146] E. Helfand, H. Reiss, H. L. Frisch, and J. L. Lebowitz. Scaled particle theory of fluids. *Journal of Chemical Physics*, 33(5):1379–1385, 1960.
- [147] S. Labk and W. R. Smith. Scaled particle theory and the efficient calculation of the chemical potential of hard spheres in the nvt ensemble. *Molecular Simulation*, 12(1):23–31, 1994.
- [148] J. L. Lebowitz, E. Helfand, and E. Praestgaard. Scaled particle theory of fluid mixtures. *The Journal of Chemical Physics*, 43(3):774–779, 1965.
- [149] Robert A. Pierotti. A scaled particle theory of aqueous and nonaqueous solutions. *Chemical Reviews*, 76(6):717–726, 1976.
- [150] K. L. Savithramma and N. Madhusudana. Scaled particle theory of a system of spherocylinders: Extension of calculations to high pressures. *Molecular Crystals and Liquid Crystals*, 97(1):407–415, 1983.
- [151] K. L. Savithramma and N. V. Madhusudana. Scaled particle theory of a system of hard right circular cylinders. *Molecular Crystals and Liquid Crystals*, 74(1):243–259, 1981.
- [152] K. L. Savithramma and N. V. Madhusudana. Scaled particle theory of a system of right circular cylinders subjected to an attractive potential. *Molecular Crystals and Liquid Crystals*, 90(1-2):35–45, 1982.
- [153] K. E. Tang and V. A. Bloomfield. Excluded volume in solvation: sensitivity of scaled-particle theory to solvent size and density. *Biophysical Journal*, 79(5):2222–2234, 2000.
- [154] Erich Bergmann. Scaled particle theory for non-additive hard spheres. *Molecular Physics*, 32(1):237–256, 1976.
- [155] E. Bergmann and R. Tenne. Scaled particle theory of mixtures of hard spheres with negatively non-additive diameters. *Chemical Physics Letters*, 56(2):310–313, 1978.
- [156] Swaroop Chatterjee, Pablo G. Debenedetti, and Frank H. Stillinger. Scaled particle theory for hard sphere pairs. ii. numerical analysis. *The Journal of Chemical Physics*, 125(20):204505, 2006.
- [157] David S. Corti and Howard Reiss. Depletion force between a colloid particle and a wall: simple determination by means of scaled particle theory. *Molecular Physics*, 95(2):269–280, 1998.

- [158] R. M. Gibbons. The scaled particle theory for particles of arbitrary shape. *Molecular Physics*, 17(1):81–86, 1969.
- [159] H. Reiss, H. L. Frisch, and J. L. Lebowitz. Statistical mechanics of rigid spheres. *The Journal of Chemical Physics*, 31(2):369–380, 1959.
- [160] JL Lebowitz and JS Rowlinson. Thermodynamic properties of mixtures of hard spheres. *The Journal of Chemical Physics*, 41(1):133–138, 1964.
- [161] Michael D. Amos and George Jackson. Bhs theory and computer simulations of linear heteronuclear triatomic hard-sphere molecules. *Molecular Physics*, 74(1):191–210, 1991.
- [162] Amanda L. Archer and George Jackson. Theory and computer simulations of heteronuclear diatomic hard-sphere molecules (hard dumbbells). *Molecular Physics*, 73(4):881–896, 1991.
- [163] Horst L Vörtler, Jiří Kolafa, and Ivo Nezbeda. Computer simulation studies of hard body fluid mixtures ii. *Molecular Physics*, 68(3):547–561, 1989.
- [164] Ivo Nezbeda. Statistical thermodynamics of interaction-site molecules. *Molecular Physics*, 33(5):1287–1299, 1977.
- [165] Ivo Nezbeda and Stanislav Labik. Fluids of general hard triatomic molecules. *Molecular Physics*, 47(5):1087–1096, 1982.
- [166] Rolf Lustig. Surface and volume of three, four, six and twelve hard fused spheres. *Molecular Physics*, 55(2):305–317, 1985.
- [167] Rolf Lustig. Geometry of four hard fused spheres in an arbitrary spatial configuration. *Molecular Physics*, 59(2):195–207, 1986.
- [168] Tom Boublk. The equation of state of linear hard interaction site model fluids. *Molecular Physics*, 44(6):1369–1381, 1981.
- [169] Tom Boublk. Convex molecule perturbation theory for the gaussian overlap system. *Molecular Physics*, 65(1):209–217, 1988.
- [170] Tom Boublk. Equation of state of linear fused hard-sphere models. *Molecular Physics*, 68(1):191–198, 1989.
- [171] Tom Boublk. Equilibrium behaviour of quadrupolar kihara molecule fluids. *Molecular Physics*, 73(2):417–426, 1991.
- [172] Ivo Nezbeda, M. Rami Reddy, and William R. Smith. Computer simulation studies of molecular fluid mixtures. *Molecular Physics*, 55(2):447–462, 1985.
- [173] Jose Alejandre, Sergio E. Martinez-Casas, and Gustavo A. Chapela. On the calculation of the sphericity factor for fused hard sphere molecules. *Molecular Physics*, 65(5):1185–1193, 1988.

- [174] Stanislav Labik and Ivo Nezbeda. Fluid of general hard triatomic molecules. *Molecular Physics*, 48(1):97–109, 1983.
- [175] Akira Isihara and Tsuyoshi Hayashida. Theory of high polymer solutions. i. second virial coefficient for rigid ovaloids model. *Journal of the Physical Society of Japan*, 6(1):40–45, 1951.
- [176] Akira Isihara and Tsuyoshi Hayashida. Theory of high polymer solutions. ii. special forms of second osmotic coefficient. *Journal of the Physical Society of Japan*, 6(1):46–50, 1951.
- [177] T. Kihara. On isihara-hayashida theory of the 2nd virial coefficient for rigid convex molecules. *Journal of the Physical Society of Japan*, 8(5):686–687, 1953.
- [178] Broto Tjipto-Margo and Glenn T. Evans. A van der waals theory of nematic liquid crystals: a convex peg in a round hole potential. *Molecular Physics*, 74(1):85–101, 1991.
- [179] Tom Boubk. The second virial coefficient and an equation of state of two-dimensional fused hard-disc models. *Molecular Physics*, 57(2):287–293, 1986.
- [180] C.G. Gray, K.E. Gubbins, and C.G. Joslin. *Theory of Molecular Fluids 2: Applications. International Series of Monographs on Chemistry*. International series of monographs on chemistry. Oxford University Press, 2011.
- [181] Daan Frenkel and Berend Smit. *Chapter 7 - Free Energy Calculations*, pages 167–200. Academic Press, San Diego, 2002.
- [182] H. J. C. Berendsen, D. van der Spoel, and R. van Drunen. Gromacs: A message-passing parallel molecular dynamics implementation. *Computer Physics Communications*, 91(13):43–56, 1995.
- [183] Daan Frenkel and Berend Smit. *Chapter 8 - The Gibbs Ensemble*, pages 201–224. Academic Press, San Diego, 2002.
- [184] Russel E. Caflisch. Monte carlo and quasi-monte carlo methods. *Acta Numerica*, 7:1–49, 1998.
- [185] William H. Press and Glennys R. Farrar. Recursive stratified sampling for multidimensional monte carlo integration. *Computers in Physics*, 4(2):190–195, 1990.
- [186] J.I. Steinfeld, J.S. Francisco, and W.L. Hase. *Chemical Kinetics and Dynamics*. Prentice Hall, 1999.
- [187] K.J. Laidler. *Theories of chemical reaction rates*. McGraw-Hill, 1969.
- [188] Nicholas Metropolis, Arianna W. Rosenbluth, Marshall N. Rosenbluth, Augusta H. Teller, and Edward Teller. Equation of state calculations by fast computing machines. *The Journal of Chemical Physics*, 21(6):1087–1092, 1953.

- [189] M. P. Allen and D. J. Tildesley. *Computer simulation of liquids*. Clarendon Press, 1989.
- [190] D. Frenkel and B. Smit. *Understanding Molecular Simulation: From Algorithms to Applications*. Elsevier Science, 2001.
- [191] Stefan A. Oelmeier, Florian Dimer, and Jrgen Hubbuch. Molecular dynamics simulations on aqueous two-phase systems - single peg-molecules in solution. *BMC Biophysics*, 5(1):1–13, 2012.
- [192] Christopher J Woods, Frederick R Manby, and Adrian J Mulholland. An efficient method for the calculation of quantum mechanics/molecular mechanics free energies. *The Journal of Chemical Physics*, 128(1):01B605, 2008.
- [193] Christopher J. Woods, Matusos Malaisree, Supot Hannongbua, and Adrian J. Mulholland. A water-swap reaction coordinate for the calculation of absolute proteinligand binding free energies. *The Journal of Chemical Physics*, 134(5):054114, 2011.
- [194] Romelia Salomon-Ferrer, David A. Case, and Ross C. Walker. An overview of the amber biomolecular simulation package. *Wiley Interdisciplinary Reviews: Computational Molecular Science*, 3(2):198–210, 2013.
- [195] Grant D. Smith, Oleg Borodin, and Dmitry Bedrov. Quantum chemistry based force field for simulations of poly(propylene oxide) and its oligomers. *The Journal of Physical Chemistry A*, 102(50):10318–10323, 1998.
- [196] Siewert J. Marrink, H. Jelger Risselada, Serge Yefimov, D. Peter Tieleman, and Alex H. de Vries. The martini force field: coarse grained model for biomolecular simulations. *The Journal of Physical Chemistry B*, 111(27):7812–7824, 2007. PMID: 17569554.
- [197] Patrick F. J. Fuchs, Halvor S. Hansen, Philippe H. Hnenberger, and Bruno A. C. Horta. A gromos parameter set for vicinal diether functions: Properties of polyethyleneoxide and polyethyleneglycol. *Journal of Chemical Theory and Computation*, 8(10):3943–3963, 2012.
- [198] Enguerran Vanquelef, Sabrina Simon, Gaelle Marquant, Elodie Garcia, Geoffroy Klimerak, Jean Charles Delepine, Piotr Cieplak, and Franois-Yves Dupradeau. R.e.d. server: a web service for deriving resp and esp charges and building force field libraries for new molecules and molecular fragments. *Nucleic Acids Research*, 39(suppl 2):W511–W517, 2011.
- [199] Robert S Mulliken. Electronic population analysis on lcaomo molecular wave functions. i. *The Journal of Chemical Physics*, 23(10):1833–1840, 1955.
- [200] PerOlov Lwdin. On the nonorthogonality problem connected with the use of atomic wave functions in the theory of molecules and crystals. *The Journal of Chemical Physics*, 18(3):365–375, 1950.

- [201] AT Hagler, E Huler, and S Lifson. Energy functions for peptides and proteins. i. derivation of a consistent force field including the hydrogen bond from amide crystals. *Journal of American Chemical Society*, 96(17):5319–5327, 1974.
- [202] Araz Jakalian, Bruce L. Bush, David B. Jack, and Christopher I. Bayly. Fast, efficient generation of high-quality atomic charges. am1-bcc model: I. method. *Journal of Computational Chemistry*, 21(2):132–146, 2000.
- [203] A. Jakalian, D. B. Jack, and C. I. Bayly. Fast, efficient generation of high-quality atomic charges. am1-bcc model: II. parameterization and validation. *Journal of Computational Chemistry*, 23(16):1623–41, 2002.
- [204] R. F. W. Bader and T. T. Nguyen-Dang. *Quantum Theory of Atoms in Molecules Dalton Revisited*, volume Volume 14, pages 63–124. Academic Press, 1981.
- [205] S. R. Cox and D. E. Williams. Representation of the molecular electrostatic potential by a net atomic charge model. *Journal of Computational Chemistry*, 2(3):304–323, 1981.
- [206] U. Chandra Singh and Peter A. Kollman. An approach to computing electrostatic charges for molecules. *Journal of Computational Chemistry*, 5(2):129–145, 1984.
- [207] Donald E. Williams. Representation of the molecular electrostatic potential by atomic multipole and bond dipole models. *Journal of Computational Chemistry*, 9(7):745–763, 1988.
- [208] Francois-Yves Dupradeau, Adrien Pigache, Thomas Zaffran, Corentin Savineau, Rodolphe Lelong, Nicolas Grivel, Dimitri Lelong, Wilfried Rosanski, and Piotr Cieplak. The r.e.d. tools: advances in resp and esp charge derivation and force field library building. *Physical Chemistry Chemical Physics*, 12(28):7821–7839, 2010.
- [209] Christopher I. Bayly, Piotr Cieplak, Wendy Cornell, and Peter A. Kollman. A well-behaved electrostatic potential based method using charge restraints for deriving atomic charges: the resp model. *The Journal of Physical Chemistry*, 97(40):10269–10280, 1993.
- [210] Francois-Yves Dupradeau, Christine Czard, Rodolphe Lelong, Iodie Stanislawiak, Julien Płcher, Jean Charles Delepine, and Piotr Cieplak. R.e.dd.b.: A database for resp and esp atomic charges, and force field libraries. *Nucleic Acids Research*, 36(Database issue):D360–D367, 2008.
- [211] RevisionA Gaussian09. 02, mj frisch et al., gaussian. Inc., Wallingford CT, 2009.
- [212] Michael W. Schmidt, Kim K. Baldridge, Jerry A. Boatz, Steven T. Elbert, Mark S. Gordon, Jan H. Jensen, Shiro Koseki, Nikita Matsunaga, Kiet A. Nguyen, Shujun Su, Theresa L. Windus, Michel Dupuis, and John A. Montgomery. General atomic and molecular electronic structure system. *Journal of Computational Chemistry*, 14(11):1347–1363, 1993.

- [213] Mark S. Gordon and Michael W. Schmidt. *Chapter 41 - Advances in electronic structure theory: GAMESS a decade later A2 - Dykstra, Clifford E*, pages 1167–1189. Elsevier, Amsterdam, 2005.
- [214] A. A. Granovsky A. V. Nemukhin, B. L. Grigorenko. Molecular modeling by using the pc gamess program: From diatomic molecules to enzymes. *Moscow University Chemistry Bulletin.*, 45(2):75, 2004.
- [215] Victor M. Anisimov, Guillaume Lamoureux, Igor V. Vorobyov, Niu Huang, Benot Roux, and Alexander D. MacKerell. Determination of electrostatic parameters for a polarizable force field based on the classical drude oscillator. *Journal of Chemical Theory and Computation*, 1(1):153–168, 2005.
- [216] Charlotte Froese Fischer. General hartree-fock program. *Computer Physics Communications*, 43(3):355–365, 1987.
- [217] Axel D. Becke. Densityfunctional thermochemistry. iii. the role of exact exchange. *The Journal of Chemical Physics*, 98(7):5648–5652, 1993.
- [218] Stefan Grimme and Mirko Waletzke. A combination of kohnsham density functional theory and multi-reference configuration interaction methods. *The Journal of Chemical Physics*, 111(13):5645–5655, 1999.
- [219] Chr Miller and M. S. Plesset. Note on an approximation treatment for many-electron systems. *Physical Review*, 46(7):618–622, 1934.
- [220] Rodney J. Bartlett and George D. Purvis. Many-body perturbation theory, coupled-pair many-electron theory, and the importance of quadruple excitations for the correlation problem. *International Journal of Quantum Chemistry*, 14(5):561–581, 1978.
- [221] I. R. McDonald. Npt-ensemble monte carlo calculations for binary liquid mixtures. *Molecular Physics*, 23(1):41–58, 1972.
- [222] Athanassios Z. Panagiotopoulos. Direct determination of phase coexistence properties of fluids by monte carlo simulation in a new ensemble. *Molecular Physics*, 61(4):813–826, 1987.
- [223] A. Z. Panagiotopoulos, N. Quirke, M. Stapleton, and D. J. Tildesley. Phase equilibria by simulation in the gibbs ensemble. *Molecular Physics*, 63(4):527–545, 1988.
- [224] B. Smit, Ph De Smedt, and D. Frenkel. Computer simulations in the gibbs ensemble. *Molecular Physics*, 68(4):931–950, 1989.
- [225] Wendy D. Cornell, Piotr Cieplak, Christopher I. Bayly, Ian R. Gould, Kenneth M. Merz, David M. Ferguson, David C. Spellmeyer, Thomas Fox, James W. Caldwell, and Peter A. Kollman. A second generation force field for the simulation of proteins, nucleic acids, and organic molecules. *Journal of American Chemical Society*, 117(19):5179–5197, 1995.

- [226] J. Wang, R. M. Wolf, J. W. Caldwell, P. A. Kollman, and D. A. Case. Development and testing of a general amber force field. *Journal of Computational Chemistry*, 25(9):1157–74, 2004.
- [227] William L Jorgensen, David S Maxwell, and Julian Tirado-Rives. Development and testing of the opls all-atom force field on conformational energetics and properties of organic liquids. *Journal of American Chemical Society*, 118(45):11225–11236, 1996.
- [228] Roy Dennington, Todd Keith, John Millam, et al. Gaussview, version 5. *Semichem Inc., Shawnee Mission, KS*, 2009.
- [229] ChemDraw Ultra. 6.0 and chem3d ultra. *Cambridge Soft Corporation, Cambridge, USA*, 2001.
- [230] Marcus D Hanwell, Donald E Curtis, David C Lonie, Tim Vandermeersch, Eva Zurek, and Geoffrey R Hutchison. Avogadro: an advanced semantic chemical editor, visualization, and analysis platform. *Journal of Cheminformatics*, 4(1):17, 2012.
- [231] V. Tsui and D. A. Case. Theory and applications of the generalized born solvation model in macromolecular simulations. *Biopolymers*, 56(4):275–91, 2000.
- [232] L. Martinez, R. Andrade, E. G. Birgin, and J. M. Martinez. Packmol: a package for building initial configurations for molecular dynamics simulations. *Journal of Computational Chemistry*, 30(13):2157–64, 2009.
- [233] J. M. Martinez and L. Martinez. Packing optimization for automated generation of complex system’s initial configurations for molecular dynamics and docking. *Journal of Computational Chemistry*, 24(7):819–25, 2003.
- [234] Michael O’Mahony. *Sensory Evaluation of Food: Statistical Methods and Procedures*. CRC Press, 1986.
- [235] William T. Vetterling Brian P. Flannery William H. Press, Saul A. Teukolsky. *Numerical Recipes in C: The Art of Scientific Computing*. CAMBRIDGE UNIVERSITY PRESS, 1992.
- [236] C. Bradford Barber, David P. Dobkin, and Hannu Huhdanpaa. The quickhull algorithm for convex hulls. *ACM Transformation Mathematica Software*, 22(4):469–483, 1996.
- [237] MATLAB Users Guide. The mathworks. *Inc., Natick, MA*, 5:333, 1998.
- [238] Neil R. Voss and Mark Gerstein. 3v: cavity, channel and cleft volume calculator and extractor. *Nucleic Acids Research*, 38(Web Server issue):W555–W562, 2010.
- [239] Craig M Shakarji. Least-squares fitting algorithms of the nist algorithm testing system. *Journal of Research-National Institute of Standards and Technology*, 103:633–641, 1998.

- [240] R. G. Coleman, M. A. Burr, D. L. Souvaine, and A. C. Cheng. An intuitive approach to measuring protein surface curvature. *Proteins*, 61(4):1068–74, 2005.
- [241] Timothy J Lee, Julia E Rice, Gustavo E Scuseria, and Henry F Schaefer. Theoretical investigations of molecules composed only of fluorine, oxygen and nitrogen: determination of the equilibrium structures of foof,(no) 2 and fnnf and the transition state structure for fnnf cis-trans isomerization. *Theoretical Chemistry Accounts: Theory, Computation, and Modeling (Theoretica Chimica Acta)*, 75(2):81–98, 1989.
- [242] Hyung J Kim and James T Hynes. A theoretical model for sn1 ionic dissociation in solution. i: Activation free energetics and transition-state structure. *Journal of American Chemical Society*, 114(26):10508–10528, 1992.
- [243] Daniel M. Neumark. Transition-state spectroscopy via negative ion photodetachment. *Accounts of Chemical Research*, 26(2):33–40, 1993.
- [244] Takayuki Fueno. *Transition State: A Theoretical Approach*. CRC Press, 1999.
- [245] S. N. Chandrasekaran, J. Das, N. V. Dokholyan, and C. W. Carter. A modified path algorithm rapidly generates transition states comparable to those found by other well established algorithms. *Structural Dynamics*, 3(1), 2016.
- [246] David Young. *Computational chemistry: a practical guide for applying techniques to real world problems*. John Wiley & Sons, 2004.
- [247] W. G. Krebs and M. Gerstein. The morph server: a standardized system for analyzing and visualizing macromolecular motions in a database framework. *Nucleic Acids Research*, 28(8):1665–75, 2000.
- [248] Hiroshi Ishikita and Keisuke Saito. Proton transfer reactions and hydrogen-bond networks in protein environments. *Journal of The Royal Society Interface*, 11(91):20130518, 2014.
- [249] O. Borodin, D. Bedrov, and G. D. Smith. A molecular dynamics simulation study of polymer dynamics in aqueous poly(ethylene oxide) solutions. *Macromolecules*, 34, 2001.
- [250] Bruno A. C. Horta, Patrick F. J. Fuchs, Wilfred F. van Gunsteren, and Philippe H. Hünenberger. New interaction parameters for oxygen compounds in the gromos force field: Improved pure-liquid and solvation properties for alcohols, ethers, aldehydes, ketones, carboxylic acids, and esters. *Journal of Chemical Theory and Computation*, 7(4):1016–1031, 2011.
- [251] C. Oostenbrink, A. Villa, A. E. Mark, and W. F. van Gunsteren. A biomolecular force field based on the free enthalpy of hydration and solvation: the gromos force-field parameter sets 53a5 and 53a6. *Journal of Computational Chemistry*, 25(13):1656–76, 2004.

- [252] Lukas D. Schuler, Xavier Daura, and Wilfred F. van Gunsteren. An improved gromos96 force field for aliphatic hydrocarbons in the condensed phase. *Journal of Computational Chemistry*, 22(11):1205–1218, 2001.
- [253] Lih-Yuan Deng. Efficient and portable multiple recursive generators of large order. *ACM Trans. Modelling Computatioanl Simulation*, 15(1):1–13, 2005.
- [254] Martin Lscher. A portable high-quality random number generator for lattice field theory simulations. *Computer Physics Communications*, 79(1):100–110, 1994.
- [255] P. Thiyagarajan, D. J. Chaiko, and R. P. Hjelm. A neutron scattering study of poly(ethylene glycol) in electrolyte solutions. *Macromolecules*, 28(23):7730–7736, 1995.
- [256] Daan Frenkel and Berend Smit. *Chapter 4 - Molecular Dynamics Simulations*, pages 63–107. Academic Press, San Diego, 2002.
- [257] Thomas E Cheatham and Matthew A Young. Molecular dynamics simulation of nucleic acids: Successes, limitations, and promise*. *Biopolymers*, 56(4):232–256, 2000.
- [258] Mohammad Saleem Khan. Aggregate formation in poly (ethylene oxide) solutions. *Journal of Applied Polymer Science*, 102(3):2578–2583, 2006.
- [259] Boualem Hammouda, Derek L. Ho, and Steve Kline. Insight into clustering in poly(ethylene oxide) solutions. *Macromolecules*, 37(18):6932–6937, 2004.
- [260] Nawal Derkaoui, Sylvre Said, Yves Grohens, Ren Olier, and Mireille Privat. Peg400 novel phase description in water. *Journal of Colloid and Interface Science*, 305(2):330–338, 2007.
- [261] Yawen Li, Jinwei Wang, Jinwei Tang, Yupeng Liu, and Yedong He. Conductive performances of solid polymer electrolyte films based on pvb/liclo4 plasticized by peg200, peg400 and peg600. *Journal of Power Sources*, 187(2):305–311, 2009.
- [262] Germán Rivas and Allen P Minton. Macromolecular crowding in vitro, in vivo, and in between. *Trends in Biochemical Sciences*, 41(11):970–981, 2016.
- [263] S. B. Zimmerman and A. P. Minton. Macromolecular crowding: biochemical, biophysical, and physiological consequences. *Annual Revision Biophysical Biomolecular Structure*, 22:27–65, 1993.
- [264] Boaz Shaanan. Structure of human oxyhaemoglobin at 2· 1resolution. *Journal of Molecular Biology*, 171(1):31–59, 1983.
- [265] Nenad Ban, Poul Nissen, Jeffrey Hansen, Peter B Moore, and Thomas A Steitz. The complete atomic structure of the large ribosomal subunit at 2.4 Å resolution. *Science*, 289(5481):905–920, 2000.

- [266] Thanner M Perumal and Rudiyanto Gunawan. Impulse parametric sensitivity analysis. *IFAC Proceedings Volumes*, 44(1):9686–9690, 2011.
- [267] Harry Walter and Donald E. Brooks. Phase separation in cytoplasm, due to macromolecular crowding, is the basis for microcompartmentation. *FEBS Letters*, 361(2):135 – 139, 1995.
- [268] Tobias Vpel and George I. Makhatadze. Enzyme activity in the crowded milieu. *PLOS ONE*, 7(6):1–6, 06 2012.
- [269] Yael Phillip, Eilon Sherman, Gilad Haran, and Gideon Schreiber. Common crowding agents have only a small effect on protein-protein interactions. *Biophysical Journal*, 97(3):875 – 885, 2009.
- [270] Jamie H Cate, Anne R Gooding, Elaine Podell, Kaihong Zhou, et al. Crystal structure of a group i ribozyme domain: principles of rna packing. *Science*, 273(5282):1678, 1996.
- [271] Warren Lyford DeLano. Pymol. *DeLano Scientific, San Carlos, CA*, 700, 2002.
- [272] Byungkook Lee and Frederic M Richards. The interpretation of protein structures: estimation of static accessibility. *Journal of Molecular Biology*, 55(3):379IN3–400IN4, 1971.
- [273] Frederic M Richards. Areas, volumes, packing, and protein structure. *Annual Review of Biophysics and Bioengineering*, 6(1):151–176, 1977.
- [274] Michael L Connolly. Analytical molecular surface calculation. *Journal of Applied Crystallography*, 16(5):548–558, 1983.
- [275] Michel F Sanner, Arthur J Olson, and Jean-Claude Spohner. Reduced surface: an efficient way to compute molecular surfaces. *Biopolymers*, 38(3):305–320, 1996.
- [276] Leonardo Dagum and Ramesh Menon. Openmp: an industry standard api for shared-memory programming. *IEEE Computational Science and Engineering*, 5(1):46–55, 1998.
- [277] William Gropp, Ewing Lusk, Nathan Doss, and Anthony Skjellum. A high-performance, portable implementation of the mpi message passing interface standard. *Parallel Computing*, 22(6):789–828, 1996.
- [278] Jacqueline D Keighron and Christine D Keating. Towards a minimal cytoplasm. In *The Minimal Cell*, pages 3–30. Springer, 2011.
- [279] Angus I Lamond and David L Spector. Nuclear speckles: a model for nuclear organelles. *Nature Reviews Molecular Cell Biology*, 4(8):605–612, 2003.
- [280] David L Spector and Angus I Lamond. Nuclear speckles. *Cold Spring Harbor Perspectives in Biology*, 3(2):a000646, 2011.

- [281] Clive Marc Baumgarten. A program for calculation of activity coefficients at selected concentrations and temperatures. *Computers in Biology and Medicine*, 11(4):189–196, 1981.
- [282] John M Prausnitz, Rudiger N Lichtenthaler, and Edmundo Gomes de Azevedo. *Molecular thermodynamics of fluid-phase equilibria*. Pearson Education, 1998.
- [283] Masayuki Irida, Takuya Takahashi, Kuniaki Nagayama, and Fumio Hirata. Solvation free energies of non-polar and polar solutes reproduced by a combination of extended scaled particle theory and the poisson-boltzmann equation. *Molecular Physics*, 85(6):1227–1238, 1995.
- [284] Claudia Bertonati, Barry Honig, and Emil Alexov. Poisson-boltzmann calculations of nonspecific salt effects on protein-protein binding free energies. *Biophysical journal*, 92(6):1891–1899, 2007.
- [285] Shradha Mishra and Jeremy D Schmit. Electrostatic interactions in concentrated protein solutions. *arXiv preprint arXiv:1304.2481*, 2013.
- [286] Alan R. Fersht. Characterizing transition states in protein folding: an essential step in the puzzle. *Current Opinion in Structural Biology*, 5(1):79–84, 1995.

Appendix A

Methods appendix

A.1 Forcefield parameters for PEG

A.1.1 System.config

```
1  !!           System.config file
2
3  !! Method & Basis set used in geometry optimization
4  METHOD_OPTCALC = B3LYP
5  BASSET_OPTCALC = 6-31G(d)
6
7  !! Method & Basis set used for MEP computation
8  METHOD_MEPCALC = B3LYP
9  BASSET_MEPCALC = 6-31G(d)
10
11 !! Package used in QM calculations
12 QMSOFT          = GAUSSIAN09
13
14 !! Number of processor(s) used in parallel (in QM calculations)
15 NP              = 8
16
17 !! Maximal amount of memory available in MegaBytes (MB) for the QM jobs
18 MAXMEMVAL      = 12288
```

A.1.2 Project.config

```
1  !!           Project.config file
2
3  !! The title of molecule '$n': Methyl-PEG
4  MOLECULE1-TITLE = PEG
5
6  !! Request the use of an intra-molecular charge constraint for molecule
   '$n'
7
8  MOLECULE1-INTRA-MCC2 = + 0.0176 | 1 2 3 4 | R
9  MOLECULE1-INTRA-MCC2 = - 0.0176 | 13 14 | R
```

A.2 MCCCS Towhee input file

```
1 ## Input parameters ensembles, molecules, box dimensions ##
2 inputformat
3 'Towhee'
4 ensemble
5 'npt'
6 temperature
7 300.15d0
8 # ensemble external pressure in kPa
9 pressure
10 101.0d0
11 #types of molecules
12 nmolty
13 1
14 #number of molecules of each type
15 nmolectyp
16 1
17 numboxes
18 1
19 stepstyle
20 'cycles'
21 nstep
22 1
23 printfreq
24 1
25 #size of the blocks for computing block averages
26 blocksize
27 2
28 moviefreq
29 10
30 backupfreq
31 50
32 #information about the individual blocks of block averages and max.
    displacment updates.
33 runoutput
34 'full'
35 pdb_output_freq
36 25
37 #output files used with Tramonto
38 loutdft
39 F
40 #output file for lammps
41 loutlammps
42 .false.
```

```
43 #output files for DL_POLY
44 loutdlpoly
45 .false.
46 # output freq. for computing the pressure in each simulation box.
47 pressurefreq
48 10
49 #step freq. for updating max. translational and rotational displacement
    .
50 trmaxdispfreq
51 10
52 #step freq. for updating the max. volume displacement.
53 volmaxdispfreq
54 50
55 #chemical pot. in ensembles having no insertion/del. move.NPT,NVT.
56 chempotperstep
57 10
58 #Internal style consider the energies between atoms
59 potentialstyle
60 'internal'
61 #number of forcefields
62 fnumber
63 1
64 ff_filename
65 /usr/local/share/towhee/ForceFields/towhee_ff_Amber96
66 #setting for non-bonded potential types
67 classical_potential
68 'Lennard-Jones'
69 # specifies the manner in which the parameters for unlike atoms are
    determined.
70 classical_mixrule
71 'Lorentz-Berthelot'
72 #shift of nonbonded potential at cutoff
73 lshift
74 .false.
75 #Analytical tail correction
76 ltailc
77 .false.
78 #Hard inner cutoff to avoid the potential hitting infinity for
    repulsion system.0-1
79 rmin
80 1.0d0
81 #The distance beyond which nonbonded potentials are ignored
82 rcut
83 5.0d0
84 #The inner nonbonded cutoff-for noncolumbic and columbic have 5,10.
```

```
85 rcutin
86 4.0d0
87 #electrostatic potential none or computed by Coulomb's law
88 electrostatic_form
89 'none'
90 #T:start simulation by generating positions,box dimensions and max.
    displacement.
91 #F:use towhee_initial for input above parameters
92 linit
93 .false.
94 #initial boxes type
95 initboxtype
96 'dimensions'
97 #input for given molecule: with no input file i.e. coords,template..
    use full cbmc.
98 initstyle
99 'full cbmc'
100 #where to put molecule
101 initlattice
102 'simple cubic'
103 # initial number of each type of molecules place in box
104 initmol
105 1
106 #each number of molecules in each direction in each
107 inix iniy iniz
108 1 1 1
109 # initial box dimensions
110 hmatrix
111 100.0 0.0 0.0
112 0.0 100.0 0.0
113 0.0 0.0 100.0
114 ## types of moves to perform MC simulations ##
115 #pm* variable represents which move is going to perform. input values
    is 0-1
116 #selections of box and molecule for selected move by pm**pr and pm**mt
    respectively. usually input 0 or 1.
117 # Isotropic vol. move
118 pmvol
119 0.01d0
120         pmvlpr
121         1.0d0
122         rmvol
123         0.1d0
124         taval
125         0.5d0
```

```
126 pm1boxcbswap
127 0.20d0
128         pm1cbswmt
129         1.0d0
130 pmavb1
131 0.0d0
132         pmavb1in
133         0.5d0
134         pmavb1mt
135         1.0d0
136         pmavb1ct
137         1.0d0
138         avb1rad
139         0.05d0
140 pmavb2
141 0.0d0
142         pmavb2in
143         0.5d0
144         pmavb2mt
145         1.0d0
146         pmavb2ct
147         1.0d0
148         avb2rad
149         0.05d0
150 pmavb3
151 0.0d0
152         pmavb3mt
153         1.0d0
154         pmavb3ct
155         1.0d0
156         avb3rad
157         0.05d0
158 pmcb
159 0.60d0
160         pmcbmt
161         1.0d0
162         pmall
163         0.0d0
164 pmback
165 0.0d0
166         pmbkmt
167         1.0d0
168 pmpivot
169 0.0d0
170         pmpivmt
```

```
171          1.0d0
172 pmconrot
173 0.0d0
174          pmcrmt
175          1.0d0
176 pmcrback
177 0.0d0
178          pmcrbmt
179          1.0d0
180 pmplane
181 0.0d0
182          pmplanebox
183          1.0d0
184          planewidth
185          1.0d0
186 pmrow
187 0.0d0
188          pmrowbox
189          1.0d0
190          rowwidth
191          1.0d0
192 pmtraat
193 0.80d0
194          pmtamt
195          1.0d0
196          rmtraa
197          0.5d0
198          tatraa
199          0.5d0
200 pmtracm
201 0.90d0
202          pmtcmt
203          1.0d0
204          rmtrac
205          0.5d0
206          tatrac
207          0.5d0
208 pmrotate
209 1.0d0
210          pmromt
211          1.0d0
212          rmrot
213          0.05d0
214          tarot
215          0.5d0
```

```
216
217 ## cbmc_formulation optional parameter for bond length,bending angles,
    and dihedral selection. use the default options ##
218
219
220 #cbmc_formulation
221 #'Martin and Frischknecht 2006'
222 #cbmc_setting_style
223 #'Martin and Frischknecht'
224 ## Final section to construct the forcefield for the molecules in the
    system. 6 options are available for input_style
225 input_style
226 'basic connectivity map'
227 nunit
228 1277
229 nmaxcbmc
230 1277
231 lpdbnames
232 .false.
233 # see each force field for supporting atom name list
234 forcefield
235 'Amber96'
236 #writine a connectivity map based on structure here is H*OCH2CH2n*OH
    where n is 9.
237 charge_assignment
238 'none'
239 unit ntype
240 1 'HO'
241 vibration
242 1
243 2
244 improper torsion
245 0
246 unit ntype
247 2 'OH'
248 vibration
249 2
250 1 3
251 improper torsion
252 0
253 unit ntype
254 3 'CT'
255 vibration
256 4
257 2 4 5 6
```

```
258 improper torsion
259 0
260 unit ntype
261 4 'H1'
262 vibration
263 1
264 3
265 improper torsion
266 0
267 unit ntype
268 5 'H1'
269 vibration
270 1
271 3
272 improper torsion
273 0
274 unit ntype
275 6 'CT'
276 vibration
277 4
278 3 7 8 9
279 improper torsion
280 0
281 unit ntype
282 7 'H1'
283 vibration
284 1
285 6
286 improper torsion
287 0
288 unit ntype
289 8 'H1'
290 vibration
291 1
292 6
293 improper torsion
294 0
295 unit ntype
296 9 'OS'
297 vibration
298 2
299 6 10
300 improper torsion
301 0
302 unit ntype
```

```
303 10  'CT'  
304 vibration  
305 4  
306 9  11  12  13  
307 improper torsion  
308 0  
309 unit ntype  
310 11  'H1'  
311 vibration  
312 1  
313 10  
314 improper torsion  
315 0  
316 unit ntype  
317 12  'H1'  
318 vibration  
319 1  
320 10  
321 improper torsion  
322 0  
323 unit ntype  
324 13  'CT'  
325 vibration  
326 4  
327 10  14  15  16  
328 improper torsion  
329 0  
330 unit ntype  
331 14  'H1'  
332 vibration  
333 1  
334 13  
335 improper torsion  
336 0  
337 unit ntype  
338 15  'H1'  
339 vibration  
340 1  
341 13  
342 improper torsion  
343 0  
344 unit ntype  
345 16  'OS'  
346 vibration  
347 2
```

```
348 13 17
349 improper torsion
350 0
351 unit ntype
352 17 'CT'
353 vibration
354 4
355 16 18 19 20
356 improper torsion
357 0
358 unit ntype
359 18 'H1'
360 vibration
361 1
362 17
363 improper torsion
364 0
365 unit ntype
366 19 'H1'
367 vibration
368 1
369 17
370 improper torsion
371 0
372 unit ntype
373 20 'CT'
374 vibration
375 4
376 17 21 22 23
377 improper torsion
378 0
379 unit ntype
380 21 'H1'
381 vibration
382 1
383 20
384 improper torsion
385 0
386 unit ntype
387 22 'H1'
388 vibration
389 1
390 20
391 improper torsion
392 0
```

```
393 unit ntype
394 23  'OS'
395 vibration
396 2
397 20  24
398 improper torsion
399 0
400 unit ntype
401 24  'CT'
402 vibration
403 4
404 23  25  26  27
405 improper torsion
406 0
407 unit ntype
408 25  'H1'
409 vibration
410 1
411 24
412 improper torsion
413 0
414 unit ntype
415 26  'H1'
416 vibration
417 1
418 24
419 improper torsion
420 0
421 unit ntype
422 27  'CT'
423 vibration
424 4
425 24  28  29  30
426 improper torsion
427 0
428 unit ntype
429 28  'H1'
430 vibration
431 1
432 27
433 improper torsion
434 0
435 unit ntype
436 29  'H1'
437 vibration
```

```
438 1
439 27
440 improper torsion
441 0
442 unit ntype
443 30 'OS'
444 vibration
445 2
446 27 31
447 improper torsion
448 0
449 unit ntype
450 31 'CT'
451 vibration
452 4
453 30 32 33 34
454 improper torsion
455 0
456 unit ntype
457 32 'H1'
458 vibration
459 1
460 31
461 improper torsion
462 0
463 unit ntype
464 33 'H1'
465 vibration
466 1
467 31
468 improper torsion
469 0
470 unit ntype
471 34 'CT'
472 vibration
473 4
474 31 35 36 37
475 improper torsion
476 0
477 unit ntype
478 35 'H1'
479 vibration
480 1
481 34
482 improper torsion
```

```
483 0
484 unit ntype
485 36 'H1'
486 vibration
487 1
488 34
489 improper torsion
490 0
491 unit ntype
492 37 'OS'
493 vibration
494 2
495 34 38
496 improper torsion
497 0
498 .
499 .
500 .
501 unit ntype
502 1270 'CT'
503 vibration
504 4
505 1269 1271 1272 1273
506 improper torsion
507 0
508 unit ntype
509 1271 'H1'
510 vibration
511 1
512 1270
513 improper torsion
514 0
515 unit ntype
516 1272 'H1'
517 vibration
518 1
519 1270
520 improper torsion
521 0
522 unit ntype
523 1273 'CT'
524 vibration
525 4
526 1270 1274 1275 1276
527 improper torsion
```

```
528 0
529 unit ntype
530 1274 'H1'
531 vibration
532 1
533 1273
534 improper torsion
535 0
536 unit ntype
537 1275 'H1'
538 vibration
539 1
540 1273
541 improper torsion
542 0
543 unit ntype
544 1276 'OH'
545 vibration
546 2
547 1273 1277
548 improper torsion
549 0
550 unit ntype
551 1277 'HO'
552 vibration
553 1
554 1276
555 improper torsion
556 0
```

A.3 Sire sampling input file

A.3.1 Input file with all functions

```
1 #####
2 # MyFunctions.py file with all functions
3 #####
4
5 #####
6 # Import Libraries as listed in Sire sampling input file
7 #####
8
9 from Sire.Mol import *
10 from Sire.IO import *
11 from Sire.Vol import *
12 from Sire.FF import *
13 from Sire.MM import *
14 from Sire.CAS import *
15 from Sire.Maths import *
16 from Sire.Qt import *
17 from Sire.Units import *
18 from Sire.System import *
19 from Sire.Move import *
20 from Sire.Stream import *
21 from Sire.Cluster import *
22 import sys
23 from Sire.Vol import *
24 from Sire.Base import *
25 import operator
26 from numpy import *
27 from scipy import stats
28 from random import *
29 import time
30 import pyprind as prog_bar
31 import os.path
32 import re
33 from Sire.Tools import *
34 from Sire.Tools.AmberLoader import *
35 import math
36 from Sire.Tools import AmberLoader
37 import sys
38
39 #####
40 #         Define functions
41 #####
42
```

```
43 def switchTemp(temp1):
44     """
45     Function to quench temperature periodically
46     """
47     global temp
48     if temp1 == 300:
49         temp1 = 1200
50     else:
51         temp1 = 300
52     temp = temp1
53     return temp
54
55 def make_system(GiveMolec):
56     """
57     function to create system and determine energies.
58     """
59     bonds = GiveMolec.property("connectivity").getBonds()
60     angles = GiveMolec.property("connectivity").getAngles()
61     dihedrals = GiveMolec.property("connectivity").getDihedrals()
62     nbonds = len(bonds)
63     nangles = len(angles)
64     ndihedrals = len(dihedrals)
65     intraff = InternalFF("intraff")
66     intraclj = IntraCLJFF("intraclj")
67     intraff.add(GiveMolec)
68     intraclj.add(GiveMolec)
69     system = System()
70     system.add(intraff)
71     system.add(intraclj)
72     return system
73
74 def bondMove(temp, system):
75     """
76     function to perform bond length changing moves.
77     """
78     global naccept
79     global nreject
80
81     ## get the version of the Molecule, currently in the system
82     GiveMolec = system[ MolWithResID("F02") ]
83
84     ##calculate the energy before the move
85     old_energy = system.energy()
86
87     ## randomly choose a bond to move
```

```
88     bondid = bonds[ rangen.randint(0,nbonds-1) ]
89
90     ## randomly choose an amount to move the bond between -0.05 and
91         0.05 angstroms
92
93     delta = rangen.rand(-0.05, 0.05) * angstrom
94
95     ## change the bond
96     GiveMolec_new = GiveMolec.move().change(bondid, delta, map).commit
97         ()
98
99     ##update the system with the moved molecule
100    system.update(GiveMolec_new)
101
102    ## calculate the new energy after the move
103    new_energy = system.energy()
104
105    ## what is the difference in energy
106    delta_energy = new_energy - old_energy
107
108    ## calculate  $\exp(-dE / kT)$ 
109    x = math.exp(-delta_energy.value() / (k_boltz * temp) )
110
111    ##generate a random number between 0 and 1
112    random_number = rangen.rand(0,1)
113
114    ##Compare  $\exp(-dE/kT)$  against this random number
115    if x >= random_number:
116        naccept += 1
117    else:
118        nreject += 1
119        # move has been rejected, so we have to move the Moleculeback
120        to its old conformation
121        system.update(GiveMolec)
122
123    def angleMove(temp,system):
124        """
125        function to perform angle changing moves.
126        """
127
128    global naccept
129    global nreject
130
131    ## get the version of the Molecule currently in the system
132    GiveMolec = system[ MolWithResID("F02") ]
133
134
```

```
130     ##calculate the energy before the move
131     old_energy = system.energy()
132
133     ## randomly choose an angle to move
134     angleid = angles[ rangen.randint(0,nangles-1) ]
135
136     ## randomly choose an amount to move the angle between -15 and 15
137     degrees
138     delta = rangen.rand(-15, 15) * degrees
139
140     ## change the angle
141     GiveMolec_new = GiveMolec.move().change(angleid, delta, map).commit
142     ()
143
144     ##update the system with the moved molecule
145     system.update(GiveMolec_new)
146
147     ## calcualte the new energy after the move
148     new_energy = system.energy()
149
150     ## what is the difference in energy
151     delta_energy = new_energy - old_energy
152
153     ## calculate  $\exp(-dE / kT)$ 
154     x = math.exp(-delta_energy.value() / (k_boltz * temp) )
155
156     ##generate a random number between 0 and 1
157     random_number = rangen.rand(0,1)
158
159     ##Compare  $\exp(-dE/kT)$  against this random number
160     if x >= random_number:
161         naccept += 1
162     else:
163         nreject += 1
164         #move has been rejected, so we have to move the Molecule back
165         #to its old conformation
166         system.update(GiveMolec)
167
168 def dihedralMove(temp, system):
169     """
170     function to perform dihedral angles changing moves.
171     """
172
173     global naccept
174     global nreject
```

```
172
173     ## get the version of the Molecule currently in the system
174     GiveMolec = system[ MolWithResID("F02") ]
175
176     ##calculate the energy before the move
177     old_energy = system.energy()
178
179     ## randomly choose an dihedral to move
180     dihedralid = dihedrals[ rangen.randint(0,ndihedrals-1) ]
181
182     ## randomly choose an amount to move the dihedral between -15 and
183     15 degrees
184     delta = rangen.rand(-15, 15) * degrees
185
186     ## now randomly choose to move either the whole dihedral or just
187     rotate around the bond
188     if rangen.randBool():
189         GiveMolec_new = GiveMolec.move().change( BondID(dihedralid.atom1
190             (),dihedralid.atom2()),
191             delta, map).commit()
192     else:
193         GiveMolec_new = GiveMolec.move().change(dihedralid, delta, map)
194         .commit()
195
196     ##update the system with the moved molecule
197     system.update(GiveMolec_new)
198
199     ## calculate the new energy after the move
200     new_energy = system.energy()
201
202     ## what is the difference in energy
203     delta_energy = new_energy - old_energy
204
205     ## calculate  $\exp(-dE / kT)$ 
206     x = math.exp( -delta_energy.value() / (k_boltz * temp) )
207
208     ##generate a random number between 0 and 1
209     random_number = rangen.rand(0,1)
210
211     ## Compare  $\exp(-dE/kT)$  against this random number
212     if x >= random_number:
213         naccept += 1
214     else:
215         nreject += 1
```

```
212     # move has been rejected, so we have to move the Molecule back
213     to its old conformation
214     system.update(GiveMolec)
215 def quenched_conf(system,temp):
216     """
217     function to change temperature periodically.
218     """
219     print("***** 300 start *****")
220     print("Molecule energy Before moves at 300= %s" % system.energy())
221     for i in range(0,1):
222         move_type = rangen.randint(1,3)
223
224         if move_type == 1:
225             bondMove(temp,system)
226         elif move_type == 2:
227             angleMove(temp,system)
228         elif move_type == 3:
229             dihedralMove(temp,system)
230
231     print("Molecule energy After moves at 300= %s" % system.energy())
232     mol = system[MolIdx(0)].molecule()
233     radius = radgyr(mol)
234     print("radius of gyration after performing moves at 300 %s" %
235           radius)
236     PDB().write(system.molecules(), "outputHn300%003d.pdb" % i)
237     print("***** 300 end *****")
238     return
239 def condition_fn(initial_energy,final_energy):
240     """
241     Condition function for equilibration to give true or false output.
242     The output is used to reverse the system or keep the system to use
243     further minimization.
244     """
245     delta_energy = final_energy - initial_energy;
246     #print("delta energy %s"%delta_energy)
247     if delta_energy < 400:
248         delta_energy
249     else:
250         delta_energy = 400
251     #print("delta energy after condition %s" %delta_energy)
252     if final_energy <= initial_energy:
253         condition = "True" #print("insertion successful on first
254             criteria")
```

```
253     elif randgen.rand() > math.exp(delta_energy/(k_boltz*temperature.
254         to(kelvin))):
255         condition = "True" # print("insertion successful on second
256             condition")
257     else:
258         condition = "False" # print("insertion failed")
259     return condition
260
261 def energy_minimize_system_LJ_CL(box_mols,box_space):
262     """
263     Function to prepare the system containing the molecules, boxSpace
264     Input: Molecules box, boxSpace
265     """
266     # create simulation system to hold box of molecules
267     box_system = System("box")
268     # intermolecule coulomb and LJ energy
269     box_interff = InterFF("box_inter")
270     cljfunc = CLJShiftFunction()
271     cljfunc.setCoulombCutoff(15 * angstrom)
272     cljfunc.setLJCutoff(15 * angstrom)
273     cljfunc.setSpace(box_space)
274     box_interff.setCLJFunction(cljfunc)
275     box_interff.setUseParallelCalculation(True)
276     box_interff.add(box_mols)
277     # add all molecules and forcefields for box to system
278     box_system.add(box_mols)
279     box_system.add(box_interff)
280     # set the periodic box information for each box
281     box_system.setProperty("space", box_space)
282     # system energy (optional)
283     #box_system.energies()
284     box_system.add( SpaceWrapper(Vector(0), box_mols) )
285     return box_system
286
287 def createSystem(outputgroup, probeMolecules_mol, boxSpace):
288     """
289     create a system to hold all of the molecules and forcefields
290     Return the created system and the forcefield energy component
291     that you want to evaluate
292     """
293     system = System()
294     interff = InterFF("int1")
295     cljfunc = CLJShiftFunction()
296     #cljfunc.setCoulombCutoff(0 * angstrom)
```

```
296 #cljfunc.setLJCutoff(15 * angstrom)
297 cljfunc.setSpace(boxSpace)
298 interff.setCLJFunction(cljfunc)
299 #interff.setSwitchingFunction(cljfunc)
300 interff.setUseParallelCalculation(True)
301 system.setProperty("space", boxSpace)
302 outputgroup.add(probeMolecules_mol)
303 interff.add(outputgroup)
304 #interff.add(probeMolecules_mol)
305 system.add(interff)
306 system.add( SpaceWrapper(Vector(0), outputgroup) )
307 system.add(outputgroup)
308 return (system, interff.components().lj())
309
310 def loop_division2(nReplicates, system, residue):
311     """
312     function to determine steric clashes
313     """
314     throws = 0
315     count = 0
316     energyThreshold = 50000
317     for i in range(nReplicates):
318         throws += 1
319         random_translate = rangen.vectorOnSphere( max_translation.value
320             () )
321         random_rotate_axis = rangen.vectorOnSphere()
322         random_rotate_angle = rangen.rand(-max_rotation.value(),
323             max_rotation.value()) * degrees
324         random_Molecule = system[MolWithResID(residue)].molecule()
325         moved_Molecule = random_Molecule.move() \
326             .rotate( \
327                 Quaternion(random_rotate_angle, random_rotate_axis
328                     ), \
329                     random_Molecule.evaluate().center() ) \
330             .translate(random_translate).commit()
331         system.update(moved_Molecule)
332         output_energy = system.energy(lj_comp).value()
333         #print("energy of testing system=%s and default system =%r" %(
334             output_energy, energyThreshold))
335         # print("(took %s ms)" % (0.000001*ns))
336         #output_energy = if_function_energy(output_energy, tolerance)
337         montecarlotest = if_function(output_energy, energyThreshold)
338         count += montecarlotest
339         V_free = (count/throws)*output_vol
340         p = count/throws
```

```
338     std_binom = sqrt(throws*p*(1-p))
339     error_binom = (output_vol/throws)*std_binom
340     error_binom_fraction = error_binom/V_free
341     #if i % 100 == 0:
342         #print("STEPS %d: BINOMIAL ERROR T.VOLUME %s: ERROR F.VOLUME
           %s: ESTIMATED VOLUME %s:" % (i, error_binom,
           error_binom_fraction,p))
343     system.clearStatistics()
344     system.mustNowRecalculateFromScratch()
345     SystemExit(system)
346     ratio = count/nReplicates
347     return ratio
348
349 def log_file_writer(filename, steps, value1, value2):
350     """
351     function to write output log/text file containing available volume
           and corresponding
352     binomial error
353     Input:filename, steps(MC steps),value1(available volume), value2(
           binomial error)
354     """
355     string1 = ', Available volume = '
356     string2 = ', Binomial Error = '
357     # convert values to string
358     steps = str(steps)
359     value1 = str(value1)
360     value2 = str(value2)
361     #open log file and combine values and write in it
362     with open (filename, 'w') as f1:
363         f1.write(('Steps = '+steps) + (string1 + value1) + (string2 +
           value2) +'\n')
364     f1.close()
365     return
366 #
367 def log_file_writer2(filename, steps, value1, value2):
368     """
369     function to write output log/text file containing available volume
           and corresponding
370     binomial error
371     Input:filename, steps(MC steps),value1(available volume), value2(
           binomial error)
372     """
373     string1 = ', Available volume = '
374     string2 = ', molecules volume = '
375     # convert values to string
```

```

376     steps = str(steps)
377     value1 = str(value1)
378     value2 = str(value2)
379     #open log file and combine values and write in it
380     with open (filename, 'w') as f1:
381         f1.write(('Steps = '+steps) + (string1 + value1) + (string2 +
                 value2) +'\n')
382     f1.close()
383     return
384
385 def statistics_test(avg,output_vol,output):
386     """
387     function to determine the statistics of estimated volume.
388     the inputs are ...
389     (avg list of output volumes)steps*dsteps
390     (volume of box)
391     (number of steps)
392     output: print out t-statistics
393     """
394     p = sum(avg)/len(avg)
395     V_free = p*output_vol
396     std_binom = sqrt(output*p*(1-p))
397     error_binom = (output_vol/output)*std_binom
398     error_binom_fraction = error_binom/V_free
399     print ("STEPS %s: BINOMIAL ERROR T.VOLUME %s: ERROR F.VOLUME %s:
            ESTIMATED AVAILABLE VOLUME %s:" %(output, error_binom,
            error_binom_fraction*100,p))
400     return
401
402 def line_extract(myfile):
403     '''
404     utility function for a text file
405     '''
406     for line in myfile:
407         print ()
408     return line
409
410 def removeCommonElements(a, b):
411     '''
412     utility function for a text file
413     '''
414     for e in a[:]:
415         if e in b:
416             a.remove(e)
417             b.remove(e)

```

```
418     return a
419
420 def coordinates_check(total_cord):
421     '''
422     function to make sure, the box dimensions are greater than minimum
423     required value
424     '''
425     total_final1 = []
426     total_final2 = []
427     for i in total_cord[0:3]:
428         if i < -149.99:
429             total_final1.append(i)
430         else:
431             total_final1.append(-150.00)
432
433     for i in total_cord[-3:]:
434         if i > 149.99:
435             total_final2.append(i)
436         else:
437             total_final2.append(150.00)
438     total_final = total_final1+total_final2
439     return total_final
440
441 def radgyr(mol):
442     '''
443     function to determine the radius of gyration. the function take a
444     molecule as an input
445     '''
446     #step 1. determine centre of mass
447     cmass = mol.evaluate().centerOfMass()
448     #step 2. calculate the radius of gyration
449     vector_collection = []
450     for i in range(mol.nAtoms()):
451         atomicCenter = mol.atom(AtomIdx(i)).evaluate().centerOfMass()
452         difference = ((atomicCenter - cmass).magnitude())**2
453         vector_collection.append(difference)
454     summation = sum(vector_collection)
455     radgyr = sqrt(summation/len(vector_collection))
456     return radgyr
457
458 def collect_radgyr_box(sim_mols):
459     '''
460     function to determine and save the radius of gyration and volume in
461     a list. the function take box as an input
```

```

460     """
461     #step 1. collect molecules
462     sim_mols = collect_mc_molecs(sim_mols)
463     rad = []
464     vol = []
465     for molnum in sim_mols.molNums():
466         mol = sim_mols[molnum].molecule()
467         radgyrout = radgyr(mol)
468         volume = (4/3)*pi*(pow(radgyrout,3))
469         vol.append(volume)
470         rad.append(radgyrout)
471     return (rad,vol)
472
473 def list_of_energy_system(simSystem, probMolecule, boxSpace):
474     """
475     Function to generate the systems (molecule groups) to be executed
476         in a parallel fashion.
477     Inputs: Simulation boxes, probe molecule, Box dimensions
478     """
479     residue = probMolecule.residues(ResIdx(0)).residue().name().value()
480     system = System()
481     system.add(simSystem)
482     system.add(probMolecule)
483     system.setProperty("space", boxSpace)
484     random_translate = rangen.vectorOnSphere( max_translation.value() )
485     random_rotate_axis = rangen.vectorOnSphere()
486     random_rotate_angle = rangen.rand(-max_rotation.value(),
487                                     max_rotation.value()) * degrees
488     random_water = system[MolWithResID(residue)].molecule()
489     moved_water = random_water.move() \
490                 .rotate( \
491                     Quaternion(random_rotate_angle,random_rotate_axis), \
492                     random_water.evaluate().center() ) \
493                 .translate(random_translate).commit()
494     system.update(moved_water)
495     #PDB().write(system.molecules(),"parallel_random_translate.pdb")
496     new_sysm = collect_mc_molecs(system)
497     return new_sysm
498 def is_there_overlap_vwd(n):
499     """
500     Function to determine wether there is overlapping in the given
501         system or not by estimating parallel distances.
502     input : length of input system_list
503     """

```

```
503     count = 0
504     system_from_list = new_systems_list[n]
505     output_vwd = steric_closmol_clashes_vdw3(system_from_list,ResID)
506     count += output_vwd
507     return count
508
509 def multi_processing_files(input_system):
510
511     """
512     Function to run system_lists over multiprocessing using all
513     available cores.
514     Input: system_lists and box dimensions
515     """
516     import multiprocessing
517
518     if __name__=='__main__':
519         np = multiprocessing.cpu_count()
520         print ('You have {0:1d} CPUs'.format(np))
521         n = len(input_system)
522         part_count=[n/np for i in range(np)]
523         print(part_count)
524         pool = multiprocessing.Pool(processes=np)
525         count=pool.map(is_there_overlap_vwd, range(n))
526         accepted_moves = (sum(count))/n
527     return (accepted_moves, pool)
528
529 def steric_closmol_clashes_vdw3(boxMolecs,ResID):
530
531     """
532     Function to determine steric clashes using van der waal radii.
533     Input: simulation system containing probe molecule
534     """
535     boxMolecs.setName("boxMolecs")
536     p = PointRef(boxMolecs[MolWithResID(ResID)].molecule().evaluate().
537                 centerOfGeometry())
538     #p = PointRef(boxMolecs[number].molecule().evaluate().
539                 centerOfGeometry())
540     c = CloseMols(p,boxMolecs,boxMolecs.nMolecules())
541     g_random = c.closeMolecules()
542     #print(g_random)
543     g = sorted(g_random.items(), key=operator.itemgetter(1)) # sort
544         the dict by value which give tuple
545     #gg = extract_fn(g)
546     print(g)
547     gg = [(mol_num, distance) for mol_num, distance in g if 10 <
548           distance < 70]
```

```

543 print(gg)
544 t = [x[0] for x in gg] # extract sorted with respct to distance
      molnumbers from tuple
545 #print(t) # sorted molnumbers
546 t_dist = [x[1] for x in gg]
547 print(t_dist) # sorted distances
548 ## select the molecules with condition 10<dist<70
549 selected = boxMolec[MolWithResID(ResID)].molecule()
550 #selected = boxMolec[number].molecule()
551 closMol = boxMolec[t[1]].molecule()
552 if len(t) < 1:
553     return 1
554 else:
555     for i in range(1, len(t)):
556         simSystem_st = boxMolec[t[i]].molecule()
557         #print(simSystem_st)
558         for j in range(selected.nAtoms()):
559             icent = selected.atom(AtomIdx(j)).evaluate().center()
560             vdwprobMolecule = selected.atom(AtomIdx(j)).property(
                element)
561             vdwprobMoleculevalue = Element(vdwprobMolecule).
                vdwRadius().value()
562             #print(vdwprobMoleculevalue)
563             #print(vdwprobMolecule)
564             for k in range(simSystem_st.nAtoms()):
565                 dist = Vector.distance(icent, simSystem_st.atom(
                    AtomIdx(k)).evaluate().center())
566                 #print("distance of each background atom =%s" % dist)
567                 vdwsimSystem=simSystem_st.atom(AtomIdx(k)).property(
                    element)
568                 vdwsimSystemvalue= Element(vdwsimSystem).vdwRadius().
                    value()
569                 vdwsim= vdwprobMoleculevalue+vdwsimSystemvalue
570                 #print(vdwsim)
571                 if dist<vdwsim:
572                     return 0 #print ("there is a steric clash")
573 return 1 #print ("there is no steric clashes")
574
575 def gen_list(mol):
576     """
577     Function to generate the list of molecules. mol is amber inp/top
      file
578     """
579     mol_list = []
580     for i in mol.molNums():

```

```
581     j = mol[i].molecule()
582     mol_list.append(j)
583     return mol_list
584
585 def vectorize_distances(mol,mol_list):
586     """
587     function to collect distances between molecules
588     """
589     #dist_list1 = []
590     dist_list2 = []
591     #mol = mol_list[i]
592     #m1 = mol.evaluate().centerOfMass()
593     m2 = mol.evaluate().centerOfGeometry()
594     #del mol_list[i]
595     for i in range(0,len(mol_list)):
596         #dist1 = Vector.distance(m1,mol_list[i].evaluate().centerOfMass
597             ())
598         dist2 = Vector.distance(m2,mol_list[i].evaluate().
599             centerOfGeometry())
600         #dist_list1.append(dist1)
601         dist_list2.append(dist2)
602     return dist_list2
603
604 def list_joiner(parentList,newList):
605     """
606     Function to manipulate lists
607     """
608     totalList = [parentList,newList]
609     return totalList
610
611 def cluster_pdb(mol,remList,indx,set_no_mols):
612     """
613     Function to save a cluster as a pdb
614     """
615     mols = MoleculeGroup()
616     mols.add(mol)
617     for i in indx:
618         mols.add(remList[i])
619     mol_name = mols.nMolecules()
620     name = 'peg_'+str(mol_name)+'_'+str(set_no_mols)+'.pdb'
621     PDB().write(mols.molecules(),name)
622     return mols
623
624 def delete_cluster(mols,mol,remList,indx,set_no_mols):
625     """
```

```
624     function that deletes the cluster from the list and then give the
        new list of remaing molecules.
625     """
626     #print(mols.nMolecules())
627     #print(remList)
628     if int(mols.nMolecules()) > 1:
629         for i in indx:
630             del remList[i]
631     else :
632         remList
633         name = 'peg_1_'+str(set_no_mols)+'.pdb'
634         PDB().write(mol.molecule(),name)
635
636     return remList
637
638 def main_program(mol_list,clstr_tolrce):
639     """
640     Function to iterrate the whole program regarding cluster extraction
        . Not used in this script.
641     """
642     col = []
643     for i in range(0,1): #len(mol_list)
644         mol = mol_list[0]
645         remList = mol_list[0:i:]+mol_list[i+1::]
646         d1 = vectorize_distances(mol,remList)
647         #print(d1)
648         for i in d1:
649             if i < clstr_tolrce:
650                 k = d1.index(i)
651                 col.append(k)
652                 col.sort()
653                 col = col[::-1]
654                 #print(col)
655     return mol,remList,d1,col
656
657 def acc_molecules(presnt_mols,remList,indx,mol_grp,box):
658     """
659     Function to accumulate molecules in a cluster.
660     """
661     futr_mols = []
662     # step 1. remove the childern mols from the list and make it as a
        list of present mol for next iterration
663     if len(indx) > 0:
664         #print('phase 1 start')
665         for ind in indx:
```

```
666         ind.sort()
667         ind = ind[::-1]
668         for i in ind:
669             futr_mols.append(remList[i])
670             mol_grp.add(remList[i])
671             del remList[i]
672             #print(remList)
673             #print('phase 1 ends')
674 # step 2. if futr_mols > 0 then keep the mol_grp
675 if len(indx) == 0:
676     #print('phase 2 start')
677     set_no_mols = len(remList)
678     mol_name = mol_grp.nMolecules()
679     name = 'peg_'+box+str(mol_name)+'_'+str(set_no_mols)+'.pdb'
680     PDB().write(mol_grp.molecules(), name)
681     mol_grp.removeAll()
682     if len(remList) > 0:
683         mol = remList[0]
684         futr_mols.append(mol)
685         mol_grp.add(mol)
686         remList = remList[0:0:]+remList[0+1::]
687         #print('phase 2 ends')
688         #print(remList)
689     return futr_mols, remList, mol_grp
690
691 def cluster_search(mol, remList, clstr_tolrce):
692     """
693     Function that gives the list of molecules as an index that are part
694     of a cluster.
695     """
696     clust_list = []
697     clust_dist = []
698     clust_list2 = []
699     clust_dist2 = []
700     if len(mol) == 1:
701         #print('running step 1')
702         d1 = vectorize_distances(mol[0], remList)
703         clust_list.append(d1)
704         #print('step 1 done')
705         #print('running step 3')
706         #print(len(clust_list))
707         for i in clust_list[0]:
708             if i < clstr_tolrce:
709                 k = clust_list[0].index(i)
710                 clust_dist2.append(k)
```

```
710     clust_list2.append(clust_dist2)
711     #print(len(clust_list2))
712     #print('step 3 done')
713     else:
714         #print('running step 2')
715         for i in mol:
716             d1 = vectorize_distances(i,remList)
717             #print(d1)
718             #print(i)
719             clust_dist.append(d1)
720             clust_list.append(d1)
721         #print(clust_list)
722         #print('step 2 done')
723         #print('running step 4')
724         for i in clust_list:
725             #print('number of molects', len(clust_list))
726             for q in i:
727                 #print(q)
728                 if q < clstr_tolrce:
729                     l = i.index(q)
730                     #print(l)
731                     clust_dist2.append(l)
732                     #print(clust_dist2)
733                     clust_list2.append(clust_dist2)
734                     #print(clust_list2)
735             #print('step 4 done')
736         return clust_list2
737
738 def remove_lists(indx):
739     """
740     function to remove same lists from the indx
741     """
742     if len(indx) > 1:
743         indx2 = []
744         indx2.append(indx[0])
745         for i in indx:
746             if indx[0] != i:
747                 indx2.append(i)
748         print(indx2)
749     else:
750         indx2 = indx
751     return indx2
752
753 def average(list):
754     """
```

```
755     function to determine the average of the list:
756
757     """
758     average = float(sum(list))/float(len(list))
759     return average
760
761 def stanDev(values):
762     """
763     function to find the standard deviation:
764     """
765     length = len(values)
766     mean = average(values)
767     total_sum = 0
768     for i in range(length):
769         total_sum += (values[i]-mean)**2
770     std = sqrt(total_sum/length)
771     return std
772
773 def collect_values(inputfile):
774     """
775     function to collect fraction available volume from output log file.
776     example :
777     system_files = [f for f in os.listdir() if f.endswith('.log')]
778     with open ('volume_2k96_c2.log','w') as f1:
779     for file in system_files:
780         volume = collect_values(file)
781         f1.write(volume+'\n')
782     f1.close()
783
784     """
785     file = open(inputfile,'r')
786     for line in file:
787         volume = line.split(',')[1].split()[3]
788     return volume
789
790 def remove_charge_RNA_from_swap_sys(box1_mols):
791     """
792     function to remove charge, RNA, and exact number of water Molecules
793     from both boxes systems (s3 files)
794     input: control.s3 and waterbox.s3
795     """
796     box1_mols= collect_mc_molecs(box1_mols)
797     rna_residmolecule = box1_mols[ MolWithResID("RG5") ].molecule()
798     nwaters = rna_residmolecule.evaluate().mass().value()/18.01528
799     box1_mols.remove(rna_residmolecule)
```

```

799     charge_mass = 0
800     for molnum in box1_mols.molNums():
801         RNA_Charge = box1_mols[molnum].molecule()
802         if RNA_Charge.nAtoms() ==1:
803             box1_mols.remove(RNA_Charge)
804             charge_mass += RNA_Charge.evaluate().mass().value()/18.01528
805     print("charge ions mass in given system %s" % charge_mass)
806     nwaters = nwaters+charge_mass
807     return (box1_mols,nwaters)
808
809 def remove_nwaters_from_waterbox_sys(box2_mols,nwaters):
810     """
811     function to remove charge, RNA, and exact number of water Molecules
812     from both boxes systems (s3 files)
813     input: control.s3 and waterbox.s3
814     """
815     box2_mols= collect_mc_molecs(box2_mols)
816     nwaters = int(nwaters)
817     for i in range(nwaters):
818         nwater = box2_mols[MolIdx(i)].molecule()
819         box2_mols.remove(nwater)
820     return (box2_mols)
821
822 def add_swap_water_rna_sys(box1_mols,box2_mols,swapWATERS,swapRNA):
823     """
824     function to remove charge, RNA, and exact number of water Molecules
825     from both boxes systems (s3 files) and add swapWATER and
826     swapRNA to these systems (s3). before adding these groups the
827     systems are converted to groups using "collect_mc_molecule"
828     functions
829     input: control.s3 and waterbox.s3
830     *****
831
832     Function use to swap RNA and water molecules between two boxes.
833     where box1_mols is box containing RNA and background molecules
834     while box2_molecules is purely water box where RNA will be
835     placed and from there number of water molecules are moved to
836     box1_mols to keep density fix. It gives two boxes back as output
837     ...
838     Input: box1_mols, box2_mols
839     """
840     box1_mols.add(swapWATERS)
841     box2_mols.add(swapRNA)
842     return (box1_mols,box2_mols)
843

```

```
833 def charge_swap(box1_mols,box2_mols):
834     """
835     function to swap charges between two boxes
836     """
837     charge_mass = 0
838     for molnum in box1_mols.molNums():
839         RNA_Charge = box1_mols[molnum].molecule()
840         if RNA_Charge.nAtoms() ==1:
841             box1_mols.remove(RNA_Charge)
842             charge_mass += RNA_Charge.evaluate().mass().value()
843             box2_mols.add(RNA_Charge)
844     return (box1_mols,box2_mols,charge_mass)
845
846 def steric_closmol_clashes_vdw2(boxMolecs,ResID):
847     boxMolecs.setName("boxMolecs")
848     p = PointRef(boxMolecs[MolWithResID(ResID)].molecule().evaluate().
849                 centerOfGeometry())
850     #p = PointRef(boxMolecs[number].molecule().evaluate().
851                 centerOfGeometry())
852     c = CloseMols(p,boxMolecs,3)
853     g_random = c.closeMolecules()
854     #print(g_random)
855     g = sorted(g_random.items(), key=operator.itemgetter(1)) # sort
856     # the dict by value which give tuple
857     #print(g)
858     t = [x[0] for x in g] # extract sorted with respct to distance
859     # molnumbers from tuple
860     t_dist = [x[1] for x in g]
861     #print(t_dist[1])
862     selected = boxMolecs[MolWithResID(ResID)].molecule()
863     #selected = boxMolecs[number].molecule()
864     closMol = boxMolecs[t[1]].molecule()
865     if t_dist[1] > 70:
866         return 1
867     else:
868         if t_dist[1] < 10:
869             return 0
870         else:
871             for i in range(1,len(t)):
872                 peg50_st = boxMolecs[t[i]].molecule()
873                 #print(peg50_st)
874                 for j in range(selected.nAtoms()):
875                     icent = selected.atom(AtomIdx(j)).evaluate().center()
876                     vdwrna = selected.atom(AtomIdx(j)).property("element
877                             ")
```

```

873         vdwrnavalue = Element(vdwrna).vdwRadius().value()
874         #print(vdwrnavalue)
875         #print(vdwrna)
876         for k in range(peg50_st.nAtoms()):
877             dist = Vector.distance(icent, peg50_st.atom(
878                 AtomIdx(k)).evaluate().center())
879             #print("distance of each background atom =%s" %
880                 dist)
881             vdwpeg50=peg50_st.atom(AtomIdx(k)).property("
882                 element")
883             vdwpeg50value= Element(vdwpeg50).vdwRadius().
884                 value()
885             vdwsum= vdwrnavalue+vdwpeg50value
886             #print(vdwsum)
887             if dist<vdwsum:
888                 return 0 #print ("there is a steric clash")
889         return 1 #print ("there is no steric clashes")
890
891 def Minimization_criteria(dex50,box_space):
892     """
893     Function to determine wether there is need to run rigid body moves
894     to remove steric clashes in input system.
895     the system is then use for excluded volume measurment based on
896     energy calculations.
897     the input is system, if the energy of the control system is
898     greather than 1000, then it will run the 100000
899     moves to stabilies the system and then perform 800000 steps of
900     excluded volume. it will save the system after
901     mc for furhter use.
902     """
903     #if system_energy_control < 1000:
904     #print("No need to perform MC simulation for minimization")
905     #else:
906     systemdex50=energy_minimize_system_LJ_CL(dex50,box_space)
907     (systemdex50mc,wt_moves)=NVT_ensemble_moves(systemdex50)
908     print("Running Minimization Monte Carlo")
909     for i in range(1,21):
910         systemdex50mc = wt_moves.move(systemdex50mc, 500, True)
911         if i % 5 ==0:
912             print("System energy %s after running 5000 moves in 5th
913                 blocks"% systemdex50mc.energy())
914     Sire.Stream.save(systemdex50mc,"minimizedbox.s3")
915     dex50 = collect_mc_molecs(systemdex50mc)
916     return dex50
917
918

```

```
909 def list_of_energy_system(peg50, rna_mol, boxSpace):
910     """
911     Function to generate the systems (molecule groups) which are going
          to append to the list...
912     Inputs: background molecules, RNA molecule, Box space
913     ## New function where systems are appended to a list. and then call
          then to determine energy
914     """
915     randomvalues = createRandomValuesforRotationTranslation(boxSpace)
916     newMolec = rotateTranslateMolec(randomvalues,rna_mol)
917     new_sysm = makemolgroups(peg50,newMolec)
918     return new_sysm
919
920
921 def multi_processing_files_distances(input_system):
922
923     Function to run system_lists over multiprocessing using all
          available cores
924     Input: system_lists and box volume
925
926     # Multiprocessing code script
927
928     import multiprocessing
929
930     if __name__=='__main__':
931         np = multiprocessing.cpu_count()
932         print ('You have {0:1d} CPUs'.format(np))
933         n = len(new_systems_list)
934         part_count=[n/np for i in range(np)]
935         print(part_count)
936         pool = multiprocessing.Pool(processes=np)
937         count=pool.map(is_there_overlap_energy, range(n))
938         print ("Number of accepted moves ",(sum(count))/n)
939         pool.close()
940
941     import multiprocessing
942     if __name__=='__main__':
943         np = multiprocessing.cpu_count()
944         print ('You have {0:1d} CPUs'.format(np))
945         n = len(input_system)
946         part_count=[n/np for i in range(np)]
947         print(part_count)
948         pool = multiprocessing.Pool(processes=np)
949         countt=pool.map(is_there_overlap_vwd, range(n))
950         acceptedmoves = (sum(countt))/n
```

```

951     return (acceptedmoves,pool)
952
953 def multi_processing_files_energy(input_system,output_vol):
954
955     Function to run system_lists over multiprocessing using all
           available cores
956     Input: system_lists and box volume
957
958     import multiprocessing
959
960     if __name__=='__main__':
961         np = multiprocessing.cpu_count()
962         print ('You have {0:1d} CPUs'.format(np))
963         n = len(input_system)
964         part_count=[n/np for i in range(np)]
965         print(part_count)
966         pool = multiprocessing.Pool(processes=np)
967         count=pool.map(is_there_overlap_energy, range(n))
968         accepted_moves = (sum(count))/n
969         #pool.close()
970         #V_free = accepted_moves*output_vol
971         #p = accepted_moves
972         #std_binom = sqrt(n*p*(1-p))
973         #error_binom = (output_vol/n)*std_binom
974         #error_binom_fraction = error_binom/V_free
975         #print("SINGLE SYSTEM STEPS %d: BINOMIAL ERROR T.VOLUME %s:
           ERROR F.VOLUME %s: ESTIMATED VOLUME %s:" %(n, error_binom,
           error_binom_fraction,p))
976     return (accepted_moves, pool)
977
978 def multi_processing_files_dist(input_system):
979
980     Function to run system_lists over multiprocessing using all
           available cores
981     Input: system_lists and box volume
982
983     import multiprocessing
984
985     if __name__=='__main__':
986         np = multiprocessing.cpu_count()
987         print ('You have {0:1d} CPUs'.format(np))
988         n = len(input_system)
989         part_count=[n/np for i in range(np)]
990         print(part_count)
991         pool = multiprocessing.Pool(processes=np)

```

```

992     count=pool.map(is_there_overlap_energy, range(n))
993     accepted_moves = (sum(count))/n
994     #pool.close()
995     #V_free = accepted_moves*output_vol
996     #p = accepted_moves
997     #std_binom = sqrt(n*p*(1-p))
998     #error_binom = (output_vol/n)*std_binom
999     #error_binom_fraction = error_binom/V_free
1000     #print("SINGLE SYSTEM STEPS %d: BINOMIAL ERROR T.VOLUME %s:
        ERROR F.VOLUME %s: ESTIMATED VOLUME %s:" %(n, error_binom,
        error_binom_fraction,p))
1001     return (accepted_moves, pool)
1002
1003 def list_maker_for_multi(n,peg50, rna_mol, boxSpace):
1004     """
1005     Function to generates lists by appending systems from "
        list_of_energy_system(peg50, rna_mol, boxSpace)" function
1006     The function uses the "list_of_energy_system(peg50, rna_mol,
        boxSpace)" function...
1007     Inputs: number of systems in each list, background molecules, RNA
        molecule, Box space
1008     """
1009     new_systems_lists = []
1010     for i in range(n):
1011         new_systems = list_of_energy_system(peg50, rna_mol, boxSpace)
1012         new_systems_lists.append(new_systems)
1013     return new_systems_lists
1014
1015 def is_there_overlap_energy(n):
1016     """
1017     Function to determine whether there is overlapping in the given
        system or not by estimating energy.
1018     input : length of input system_list
1019     Note: the system_lists name should be (new_systems_list)
1020     """
1021     count = 0
1022     system_from_list = new_systems_list[n]
1023     output_energy = default_system_energy(system_from_list,boxSpace)
1024     montecarlotest = if_function(output_energy,
        percent_increase_tolerance)
1025     count += montecarlotest
1026     return count
1027
1028 def intrasclae_Na(na):
1029     """

```

```
1030 Interscale function to fix the interscale property of ions;
1031 this function is only for sodium, In order to work with other ions
1032 it needs to chage the atome name according to inpcrd and prmtop
1033 input files:
1034 Function Input= Molecule
1035 """
1036 sclpairs = CLJNBPairs(na)
1037 sclpairs.set( AtomName("Na+"), AtomName("Na+"), CLJScaleFactor(0,0)
1038             )
1038 na = na.edit().setProperty("intrascale", sclpairsna) \
1039             .commit()
1040 return na
1041
1042 def intrasclae_Cl(na):
1043     """
1044     Interscale function to fix the interscale property of ions;
1045     this function is only for sodium, In order to work with other ions
1046     it needs to chage the atome name according to inpcrd and prmtop
1047     input files:
1048     Function Input= Molecule
1049     """
1050     sclpairs = CLJNBPairs(na)
1051     sclpairs.set( AtomName("Cl-"), AtomName("Cl-"), CLJScaleFactor(0,0)
1052                 )
1052     na = na.edit().setProperty("intrascale", sclpairsna) \
1053             .commit()
1054     return na
1055
1056 def sodium_charge_group(rna):
1057     """
1058     Function to generate the new molecule group used to estimate
1059     the system intraCLJFF force field energetics. This function use
1060     the intrascale_Na function:
1061
1062     Function input: molecule group/direct molecule group from amber
1063     files and make sure the RNA/Protein ResID is similar to
1064     function
1065     """
1066     tt = MoleculeGroup()
1067     tt.add(rna[MolWithResID("RG5")].molecule())
1068     for molnum in rna.molNums():
1069         t = rna[molnum].molecule()
1070         if t.nAtoms() == 1:
1071             t = intrasclae_Na(t)
1072         tt.add(t)
```

```
1073     return tt
1074
1075 def chloride_charge_group(rna):
1076     """
1077     Function to generate the new molecule group used to estimate
1078     the system intraCLJFF force field energetics. This function use
1079     the intrascale_Na function:
1080
1081     Function input: molecule group/direct molecule group from amber
1082     files and make sure the RNA/Protein ResID is similar to
1083     function
1084     """
1085     tt = MoleculeGroup()
1086     tt.add(rna[MolWithResID("RG5")].molecule())
1087     for molnum in rna.molNums():
1088         t = rna[molnum].molecule()
1089         if t.nAtoms() == 1:
1090             t = intrasclae_Cl(t)
1091             tt.add(t)
1092     return tt
1093
1094 def createRandomValuesforRotationTranslation(boxSpace):
1095     """
1096     This function creates a random position, a random orientation
1097     vector and a random angle. It returns a list with these three
1098     components.
1099
1100     Function Input: boxspace
1101     """
1102     v=Vector(0,0,0) # Creates a vector for the random point generation
1103     #rand_seed = 140154
1104     gen=RanGenerator() # Creates a random generator object
1105     insertion_point=boxSpace.getRandomPoint(v,gen) # Creates a random
1106     point within the confinements of the box
1107     orientation_vector=gen.vectorOnSphere() # Creates a random
1108     orientation vector
1109     orientation_angle=gen.rand(-two_pi,two_pi)*radians # Creates a
1110     random orientation angle
1111     output=(insertion_point,orientation_vector,orientation_angle) #
1112     Creates the output list
1113     return output
1114
1115 def createRandomValuesforRotationTranslation2(boxSpace):
1116     """
1117     This function creates a random position, a random orientation
```

```
1114     vector and a random angle. It returns a list with these three
1115     components.
1116
1117     Function Input: boxspace
1118     """
1119     v=Vector(0,0,0) # Creates a vector for the random point generation
1120     #rand_seed = 140154
1121     gen=RanGenerator() # Creates a random generator object
1122     max_translation = 150 * angstrom
1123     max_rotation = 360 * degrees
1124     random_translate = gen.vectorOnSphere( max_translation.value() )
1125     random_rotate_axis = gen.vectorOnSphere()
1126     random_rotate_angle = gen.rand(-max_rotation.value(),
1127                                     max_rotation.value()) * degrees
1128     #insertion_point=boxSpace.getRandomPoint(v,gen) # Creates a random
1129     #point within the confinements of the box
1130     #orientation_vector=gen.vectorOnSphere() # Creates a random
1131     #orientation vector
1132     #orientation_angle=gen.rand(-two_pi,two_pi)*radians # Creates a
1133     #random orientation angle
1134     output=(random_translate,random_rotate_axis,random_rotate_angle) #
1135     #Creates the output list
1136     return output
1137
1138 def percise_swap_water_rna(box1_mols_pdb,box2_mols_pdb):
1139     """
1140     Function to remove and add water molecules more percisely the
1141     places where the RNA is removed and inserted.
1142     this function removes and adds water molecules simultaneously from
1143     both boxes while keeping the RNA as
1144     removed variable. when water molecules addition/removal done, then
1145     the rna molecule is added to to the waterbox.
1146     Inputs: boxgroup of rna+peg_removeRNA,waterbox_removewater,
1147            rna_tobeinserted,waterbox_tobetakentoinstert
1148
1149     this function also care about charges
1150     """
1151
1152     # UPLOAD SYSTEMS
1153     box1_mols_pdb= collect_mc_molecs(box1_mols_pdb)
1154     box2_mols_pdb= collect_mc_molecs(box1_mols_pdb)
1155     RNA_removed = box1_mols_pdb[MolWithResID("RG5")].molecule()
1156     box1_mols_pdb.remove(RNA_removed)
1157     RNA_removed = RNA_removed.edit().renumber().commit()
1158     nwaters = RNA_removed.evaluate().mass().value()
```

```
1151 charge_mass = 0
1152 charge_holder_group = MoleculeGroup()
1153 water_holder_group = MoleculeGroup()
1154 # COLLECT CHARGES
1155 for molnum in box1_mols_pdb.molNums():
1156     RNA_Charge = box1_mols_pdb[molnum].molecule()
1157     if RNA_Charge.nAtoms() == 1:
1158         box1_mols_pdb.remove(RNA_Charge)
1159         charge_holder_group.add(RNA_Charge)
1160         charge_mass += RNA_Charge.evaluate().mass().value()
1161 print("charge ions mass in given system %s" % charge_mass)
1162 nwaters = (nwaters+charge_mass)/18.01528
1163 nwaters = int(nwaters)
1164 print("number of water swap by rna =%s"%nwaters)
1165 # COLLECT WATERS
1166 for j in range(nwaters):
1167     RNA_removed_ref_point = PointRef(RNA_removed.atoms(AtomIdx(j)).
1168         evaluate().center())
1169     #print("center of %s atom =%s"%(j, RNA_removed_ref_point.point())
1170     )
1171     p = RNA_removed_ref_point.point()
1172     c = CloseMols(p, box2_mols_pdb, 10)
1173     g_random = c.closeMolecules()
1174     g = sorted(g_random.items(), key=operator.itemgetter(1))
1175     t = [x[0] for x in g]
1176     for i in range(0, len(t)):
1177         removal_water = box2_mols_pdb[t[i]].molecule()
1178         if removal_water.nAtoms() == 3:
1179             box2_mols_pdb.remove(removal_water)
1180             center_geometry =
1181                 createRandomValuesforRotationTranslationofSwapwaterMolecs
1182                 (p)
1183             removal_water = rotateTranslateMolec(center_geometry,
1184                 removal_water)
1185         water_holder_group.add(removal_water)
1186 print("number of water molecules swapped from waterbox =%s"%
1187     water_holder_group.nMolecules())
1188 # SWAPPING OF WATER AND RNA MOLECULES NOW
1189 print("swaping now ...")
1190 box2_mols_pdb.add(RNA_removed)
1191 for molnum in charge_holder_group.molNums():
1192     charge_mol = charge_holder_group[molnum].molecule().edit().
1193         renumber().commit()
1194     box2_mols_pdb.add(charge_mol)
1195 for molnum in water_holder_group.molNums():
```

```

1189     water_mol = water_holder_group[molnum].molecule().edit().
           renumber().commit()
1190     box1_mols_pdb.add(water_mol)
1191     print("done")
1192     output = (box1_mols_pdb, box2_mols_pdb)
1193     return output
1194
1195 def wswap_water(s1, s2):
1196     """
1197     Function to remove and add water molecules more percisely the
           places where the RNA is removed and inserted.
1198     this function removes and adds water molecules simultaneously from
           both boxes while keeping the RNA as
1199     removed variable. when water molecules addition/removal done, then
           the rna molecule is added to to the waterbox.
1200     Inputs: boxgroup of rna+peg_removeRNA, waterbox_removewater,
           rna_tobeinserted, waterbox_tobetakentoinstert
1201
1202     this function also care about charges
1203     """
1204     box1_mols_pdb= collect_mc_molecs(s1)
1205     box2_mols_pdb= collect_mc_molecs(s2)
1206     RNA_removed = box1_mols_pdb[MolWithResID("RG5")].molecule()
1207     box1_mols_pdb.remove(RNA_removed)
1208     RNA_removed = RNA_removed.edit().renumber().commit()
1209     nwaters = RNA_removed.evaluate().mass().value()
1210     charge_mass = 0
1211     charge_holder_group = MoleculeGroup()
1212     water_holder_group = MoleculeGroup()
1213     # COLLECT CHARGES
1214     for molnum in box1_mols_pdb.molNums():
1215         RNA_Charge = box1_mols_pdb[molnum].molecule()
1216         if RNA_Charge.nAtoms() ==1:
1217             box1_mols_pdb.remove(RNA_Charge)
1218             charge_holder_group.add(RNA_Charge)
1219             charge_mass += RNA_Charge.evaluate().mass().value()
1220     print("charge ions mass in given system %s" % charge_mass)
1221     nwaters = (nwaters+charge_mass)/18.01528
1222     nwaters = int(nwaters)
1223     print("number of water swap by rna =%s"%nwaters)
1224     # COLLECT WATERS
1225     for j in range(nwaters):
1226         RNA_removed_ref_point = PointRef(RNA_removed.atoms(AtomIdx(j)).
           evaluate().center())

```

```
1227     print("center of %s atom =%s"%(j, RNA_removed_ref_point.point()
1228         )
1229     p = RNA_removed_ref_point.point()
1230     c = CloseMols(p, box2_mols_pdb, 10)
1231     g_random = c.closeMolecules()
1232     g = sorted(g_random.items(), key=operator.itemgetter(1))
1233     t = [x[0] for x in g]
1234     for i in range(0, len(t)):
1235         removal_water = box2_mols_pdb[t[i]].molecule()
1236         if removal_water.nAtoms() == 3:
1237             box2_mols_pdb.remove(removal_water)
1238             center_geometry =
1239                 createRandomValuesforRotationTranslationofSwapwaterMolec
1240                 (p)
1241             removal_water = rotateTranslateMolec(center_geometry,
1242                 removal_water)
1243             water_holder_group.add(removal_water)
1244     print("number of water molecules swapped from waterbox =%s"%
1245         water_holder_group.nMolecules())
1246     # SWAPPING OF WATER AND RNA MOLECULES NOW
1247     print("swaping now ...")
1248     box2_mols_pdb.add(RNA_removed)
1249     for molnum in charge_holder_group.molNums():
1250         charge_mol = charge_holder_group[molnum].molecule().edit().
1251             renumber().commit()
1252         box2_mols_pdb.add(charge_mol)
1253     for molnum in water_holder_group.molNums():
1254         water_mol = water_holder_group[molnum].molecule().edit().
1255             renumber().commit()
1256         box1_mols_pdb.add(water_mol)
1257     print("done")
1258     output = (box1_mols_pdb, box2_mols_pdb)
1259     return output
1260
1261 def chemicalPotential_widom_insertion(systemi, insertionMolec, boxspace,
1262     nsteps):
1263     """
1264     Function to find the chemical potential by find the free energy
1265     change before and after adding the molecule
1266     to the given system.
1267     Input: systemi (system containing box of molecules), insertionMolec
1268         (insertion molecule), boxspace, nsteps (number of time water to
1269         be inserted)
1270     """
1271     import math
```

```
1261 # two lists to collect energy values as a testing case
1262 avg_delta_energies = 0
1263 avg_delta_accepted_energies = 0
1264 # throws is the number of configurations generated by placing
    additional water molecule in the box. this is used for taking
    average.
1265 throws = 0
1266 temperature = 298.15 * kelvin
1267 # 'collect_mc_molecs' is a function to generate a group which is
    use to add additional molecule. (we cant add additional molecule
    to systemi directly)
1268 outputgroup = collect_mc_molecs(systemi)
1269 insertionMolec = insertionMolec.edit().renumber().commit()
1270 # 'energy_minimize_system_LJ_CL' function makes a system to
    calculate energy. old_energy is the energy of the box without
    additional molecule
1271 old_system = energy_minimize_system_LJ_CL(outputgroup,boxspace)
1272 old_energy = old_system.energy().value()
1273 # 'createSystem_for_chemicalpotential' function adds the water to
    system and gives energy of total system
1274 (system,energy)=createSystem_for_chemicalpotential(outputgroup,
    insertionMolec, boxspace)
1275 # Running a loop over nsteps to generate nsteps configurations with
    different orientation and position of additional water in box.
1276 for i in range(nsteps):
1277     throws += 1
1278     # creat random angle and translation values for additional water
    molecule in box to generate configurations
1279     randomvalues = createRandomValuesforRotationTranslation(boxspace
    )
1280     newMolec = rotateTranslateMolec(randomvalues,insertionMolec)
1281     system.update(newMolec)
1282     new_energy = system.energy().value()
1283     ## what is the difference in energy
1284     delta_energy = (new_energy - old_energy)
1285     ## calculate  $RT \cdot \exp(-dE / RT)$  where k_boltz is value of gas
    constant; 1.9872041(18)103 kcalK1mol1
1286     x = -(k_boltz * temperature.value())*(math.exp(-delta_energy /
    (k_boltz * temperature.value()) ))
1287     avg_delta_energies += x/throws
1288     print("Energy before =%s and after adding water =%s; deltaE =%s
    and  $-RT \cdot \exp(-dE / RT) = %s$ "%(old_energy,new_energy,
    delta_energy,x))
1289     #other test
1290     selection_criterial = 1
```

```
1291     if x <= selection_criterial:
1292         avg_delta_accepted_energies += x/throws
1293     else:
1294         system.update(newMolec)
1295     mu = avg_delta_energies #-(k_boltz * temperature.value())*loglp(
1296         avg_delta_energies)
1297     mu2 = avg_delta_accepted_energies #-(k_boltz * temperature.value())
1298         *loglp(avg_delta_accepted_energies)
1299     print ("chemical potential of single water molecule for all
1300         configurations =%s and accepted configuratios =%s"%(mu,mu2) )
1301     output = (mu2,mu)
1302     return output
1303 """
1304 def chemicalPotential_widom_insertion(systemi,insertionMolec,boxspace,
1305     nsteps):
1306
1307     #Function to find the chemical potential by find the free energy
1308     #change before and after adding the molecule
1309     #to the given system.
1310     #Input: system, insertion molecule,number of steps for deltaE,
1311     #systemswapwaters(number of waters swap with RNA)
1312
1313     import math
1314     rangen = RanGenerator()
1315     avg_delta_energies = 0
1316     avg_delta_accepted_energies = 0
1317     throws = 0
1318     temperature = 298.15 * kelvin
1319     outputgroup = collect_mc_molecs(systemi)
1320     ingroup = MoleculeGroup()
1321     ingroup.add(insertionMolec)
1322     mol = ingroup.moleculeAt(0).molecule()
1323     insertionMolec = mol.edit().renumber().commit()
1324     old_system = energy_minimize_system_LJ_CL(outputgroup,boxspace)
1325     old_energy = old_system.energy().value()
1326     (system,energy)=createSystem_for_chemicalpotential(outputgroup,
1327         insertionMolec, boxspace)
1328     for i in range(nsteps):
1329         throws += 1
1330         randomvalues = createRandomValuesforRotationTranslation(boxspace
1331             )
1332         newMolec = rotateTranslateMolec(randomvalues,insertionMolec)
1333         system.update(newMolec)
1334         new_energy = system.energy().value()
1335         ## what is the difference in energy
```

```

1328     delta_energy = -(new_energy - old_energy)
1329     ## calculate exp( -dE / kT )
1330     x = math.exp( delta_energy / (k_boltz * temperature.value()) )
1331     avg_delta_energies += x/throws
1332     print("Energy before =%s and after adding water =%s; deltaE =%s
          and exp( -dE / kT ) = %s"%(old_energy,new_energy,
          delta_energy,x))
1333     #other test
1334     selection_criterial = 1
1335     selection_criteia2 = 0
1336     if x <= selection_criterial:
1337         avg_delta_accepted_energies += x/throws
1338     elif x > selection_criteia2:
1339         avg_delta_accepted_energies += x/throws
1340     else:
1341         system.update(newMolec)
1342     mu = avg_delta_energies #-(k_boltz * temperature.value())*loglp(
          avg_delta_energies)
1343     mu2 = avg_delta_accepted_energies #-(k_boltz * temperature.value())
          *loglp(avg_delta_accepted_energies)
1344     print("chemical potential of single water molecule for all
          configurations =%s and accepted configuratios =%s"%(mu,mu2))
1345     output = (mu2,mu)
1346     return output
1347     """
1348     def createRandomValuesforRotationTranslationofSwapwaterMolec(
          centerofgeometryofRNAatom):
1349         """
1350         This function creates a random orientation
1351         vector and a random angle values for water molecueles to be swaped
          with RNA.
1352         The function take the input of RNA atom (center of mass, or centre
          of geometry) and
1353         It returns a list with these three
1354         components.
1355
1356         Function Input: centre of mass or centre of geometry
1357         """
1358         v=Vector(0,0,0) # Creates a vector for the random point generation
1359         #rand_seed = 140154
1360         gen=RanGenerator() # Creates a random generator object
1361         insertion_point=centerofgeometryofRNAatom # Creates a random point
          within the confinements of the box
1362         orientation_vector=gen.vectorOnSphere() # Creates a random
          orientation vector

```

```
1363     orientation_angle=gen.rand(-two_pi,two_pi)*radians # Creates a
        random orientation angle
1364     output=(insertion_point,orientation_vector,orientation_angle) #
        Creates the output list
1365     return output
1366
1367 def rotateTranslateMolec(randomValues,molec):
1368     """
1369     This function uses a random position, a random orientation vector
1370     and a random angle in 'randomValues' to transform molecule 'molec'
1371     into a new molecule 'newMolec'.
1372
1373     Function Input: random values generated from
1374     createRandomValuesforRotationTranslation(boxSpace) function and the
1375     molecule required to rotate and translate.
1376
1377     """
1378     map=PropertyMap() # Creates a property Map object
1379     molCenter=molec.evaluate().center(map) # Obtains the center of the
        molecule using 'map'
1380     newMolec=Mover_Molecule_(molec) # Creates a new molecule 'newMolec'
        using a Mover constructor and the molecule 'molec' to be able
        to rotate and translate it
1381     newMolec=newMolec.rotate(Quaternion(randomValues[2],randomValues
        [1]),molCenter,map)# Rotates the molecule
1382     newMolec=newMolec.translate(randomValues[0]-molCenter,map) #
        Translates the molecule to a random position
1383     newMolec=newMolec.commit() # Commits the new molecule
1384     return newMolec
1385
1386 def makemolgroups(newMolec,peg):
1387     """
1388     Function use to make new molecule group by adding the RNA/protein
1389     background molecules. the output is a molecule group used for
        steric
1390     clash functions.
1391
1392     Function Input: rna molecule, crowders group
1393     """
1394     newmolgroup = MoleculeGroup()
1395     newmolgroup.add(newMolec)
1396     newmolgroup.add(peg)
1397     return newmolgroup
1398
1399 def steric_closmol_clashes(boxMolec):
```

```
1400 """
1401 function to estimate the parallel distances to determine whether
1402 there is any steric clash or not in the given molecule group.
1403
1404 Function Input: molecule group
1405 note: make sure the rna/protein ResID match in function and
1406       set the tolerance criteria if desired:
1407 """
1408 boxMolecules.setName("boxMolecules")
1409 p = PointRef(boxMolecules[MolWithResID("FUL")].molecule().evaluate().
1410              centerOfGeometry())
1410 c = CloseMols(p, boxMolecules, 5)
1411 g_random = c.closeMolecules()
1412 #print(g_random)
1413 g = sorted(g_random.items(), key=operator.itemgetter(1)) # sort
1414               the dict by value which give tuple
1414 #print(g)
1415 t = [x[0] for x in g] # extract sorted with respect to distance
1416               molnumbers from tuple
1416 selected = boxMolecules[MolWithResID("FUL")].molecule()
1417 closMol = boxMolecules[t[1]].molecule()
1418 for i in range(1, len(t)):
1419     peg_st = boxMolecules[t[i]].molecule()
1420     #print(peg_st) system.update(newMolec)
1421     for j in selected.atoms(AtomIdx()):
1422         icent = j.evaluate().center()
1423         for j in peg_st.atoms(AtomIdx()):
1424             dist = Vector.distance(icent, j.evaluate().center())
1425             if dist < 1.05:
1426                 return 0 #print ("there is a steric clash")
1427 return 1 #print ("there is no steric clashes")
1428
1429 def steric_closmol_clashes_vdw(boxMolecules):
1430     """
1431     function to estimate the parallel distances to determine whether
1432     there is any steric clash or not in the given molecule group using
1433     the vander waal radii as tolerance criteria.
1434     It estimate the sum vander waal radii of 2 elements and compare it
1435     with actual distance between them. if actual
1436     distance is LESS than vander waal radii then it will report steric
1437     clash.
1438     Function Input: molecule group
1439     note: make sure the rna/protein Rsystem.update(newMolec)esID match
1440           in function
1441 """
```

```

1438 """
1439 boxMolecs.setName("boxMolecs")
1440 p = PointRef(boxMolecs[MolWithResID("WAT")].molecule().evaluate().
    centerOfGeometry())
1441 #p = PointRef(boxMolecs[number].molecule().evaluate().
    centerOfGeometry())
1442 c = CloseMols(p,boxMolecs,2)
1443 g_random = c.closeMolecules()
1444 #print(g_random)
1445 g = sorted(g_random.items(), key=operator.itemgetter(1)) # sort
    the dict by value which give tuple
1446 #print(g)
1447 t = [x[0] for x in g] # extract sorted with respect to distance
    molnumbers from tuple
1448 selected = boxMolecs[MolWithResID("WAT")].molecule()
1449 #selected = boxMolecs[number].molecule()
1450 closMol = boxMolecs[t[1]].molecule()
1451 for i in range(1,len(t)):
1452     peg_st = boxMolecs[t[i]].molecule()
1453     #print(peg_st)
1454     for j in range(selected.nAtoms()):
1455         icient = selected.atom(AtomIdx(j)).evaluate().center()
1456         vdwrna = selected.atom(AtomIdx(j)).property("element")
1457         vdwrnavalue = Element(vdwrna).vdwRadius().value()
1458         #print(vdwrna)
1459         for k in range(peg_st.nAtoms()):
1460             dist = Vector.distance(icient, peg_st.atom(AtomIdx(k)).
                evaluate().center())
1461             #print("distance of each background atom =%s" % dist)
1462             vdwpeg=peg_st.atom(AtomIdx(k)).property("element")
1463             vdwpegvalue= Element(vdwpeg).vdwRadius().value()
1464             vdwsum= vdwrnavalue+vdwpegvalue
1465             #print(vdwsum)
1466             if dist<vdwsum:
1467                 return 0 #print ("there is a steric clash")
1468     return 1 #print ("there is no steric clashes")
1469 """
1470 """
1471 def default_system_energy3(outputgroup,boxSpace):
1472
1473     function to estimate the energy tsystem.update(newMolec)o determine
        wether
1474     there is any steric clash or not in the given molecule group.
1475
1476     Function Input: molecule group, boxspace

```

```
1477     note: set the tolerance criteria if desire:
1478
1479     system= System()
1480     int1 = InterCLJFF("int1")
1481     #int2 = InterCoulombFF("int2")
1482     #int3 = InterFF("int3")
1483     int1.add(outputgroup)
1484     #int2.add(outputgroup)
1485     #int3.add(outputgroup)
1486     system.add(outputgroup)
1487     system.add(int1)
1488     #system.add(int2)
1489     #system.add(int3)
1490     system.setProperty("space", boxSpace)
1491     system_energy = system.energy().value()
1492     print("energy of control system =%s" % system_energy)
1493     return system_energy
1494     """
1495
1496 def default_system_energy2(outputgroup,boxSpace):
1497     """
1498     function to estimate the energy to determine wether
1499     there is any steric clash or not in the given molecule group.
1500     Function Input: molecule group, boxspace
1501     note: set the tolerance criteria if desire:
1502     """
1503     #system= System()
1504     interff = InterFF("int1")
1505     cljfunc = CLJShiftFunction()
1506     cljfunc.setCoulombCutoff(0 * angstrom)
1507     cljfunc.setLJCutoff(5 * angstrom)
1508     cljfunc.setSpace(boxSpace)
1509     interff.setCLJFunction(cljfunc)
1510     #interff.setSwitchingFunction(cljfunc)
1511     interff.setUseParallelCalculation(True)
1512     interff.add(outputgroup)
1513     #system.add(outputgroup)
1514     #system.add(interff)
1515     #total_nrg = system.energy()
1516     #system.setProperty("space", boxSpace)
1517     #system_energy = (system.energy().value(), 3)
1518     #coul_nrg = int1.energy( int1.components().coulomb() )
1519     #print("coul energy = %s" % coul_nrg)
1520     #lj_nrg = system.energy( interff.components().lj() )
1521     lj_nrg = interff.energy( interff.components().lj() )
```

```
1522     #print("LJ energy = %s" % lj_nrg)
1523     #print("total energy of system =%s" % system_energy)
1524     #print("all energies = %s " % system.energies())
1525     return lj_nrg.value()
1526
1527 def add_newMolec_to_crowder(newMolec,peg):
1528     """ Add the molecule and crowders to generate the new molecule
1529         group
1530         used for further calculations:
1531         Function Input: rna molecule, crowder molecule group
1532     """
1533     outputgroup= peg.add(newMolec)
1534     return outputgroup
1535
1536 def steric_clash_energy(outputgroup,defaultenergy,boxSpace):
1537     """ Function similar to default_system_energy and used to
1538         determine the steric clashes via energy:
1539
1540         Function Input: moleculegroup containing everything,
1541                        default energy as tolerance criteria
1542                        boxspace
1543         note: BUGGY ! dont use until fixed!
1544     """
1545     systemc= System()
1546     int1 = InterCLJFF("int1")
1547     int2 = InterCoulombFF("int2")
1548     int3 = InterFF("int3")
1549     int1.add(outputgroup)
1550     int2.add(outputgroup)
1551     int3.add(outputgroup)
1552     systemc.setProperty("space", boxSpace)
1553     systemc.add(outputgroup)
1554     systemc.add(int1)
1555     systemc.add(int2)
1556     systemc.add(int3)
1557     #print(systemc.nMolecules())
1558     system_energy = systemc.energy().value()
1559     print("energy of testing system=%s and default system =%r" %(
1560         system_energy, defaultenergy))
1561     if system_energy > defaultenergy:
1562         return 0
1563     return 1
1564 def initial_configurations(newMolec,tolerance,boxspace):
```

```
1565     """
1566     Function to add the molecules to the new molecule group of defined
           space,
1567     the function take a single molecule as an input (backgroundmols)
           along with freshly defined
1568     molecule group(newemptygroup).tolerance distance between molecues
           while boxSpace is
1569     box dimensions
1570
1571     Function Input: crowdres molecules
1572                   tolerance, dist. between crowder molecs.
1573                   boxspace
1574     note: Not finished yet, Dont try!
1575     """
1576 #     randomvalues = createRandomValuesforRotationTranslation(boxSpace)
1577 #     newMolec = rotateTranslateMolec(randomvalues,mol)
1578     newgroup = MoleculeGroup()
1579     p = PointRef(newMolec.molecule().evaluate().centerOfGeometry())
1580     c = CloseMols(p,newgroup,5)
1581     g_random = c.closeMolecules()
1582     if len(g_random) == 0:
1583         newgroup.add(newMolec)
1584     else:
1585         g = sorted(g_random.items(), key=operator.itemgetter(1)) #
           sort the dict by value which give tuple
1586         #print(g)
1587         t = [x[0] for x in g]
1588         selected = newgroup[t[0]].molecule().evaluate().centerOfGeometry
           ()
1589         for i in range(1,len(t)):
1590             closemols = newgroup[t[i]].molecule().evaluate().
           centerOfGeometry()
1591             if (selected-closemols).length() > tolerance:
1592                 newgroup.add(newMolec)
1593     return newgroup
1594
1595 def if_function(system_energy,tolerance):
1596     """
1597     Function to determine wether the system has steric clash or not
           based on energies
1598     Input : system under study, default tolerance energy
1599     """
1600     if system_energy < tolerance:
1601         return 1
1602     return 0
```

```
1603
1604 def if_function_energy(system_energy, tolerance):
1605     """
1606     Function to determine wether the system has normal energy output or
           very small values
1607     Input : system energy under study
1608     """
1609     if system_energy < -tolerance:
1610         return abs(system_energy)
1611     return system_energy
1612
1613 def createSystem_for_chemicalpotential(outputgroup, biom_mol, boxSpace
):
1614     """
1615     create a system to hold all of the molecules and forcefields
1616     Return the created system and the forcefield energy component
1617     that you want to evaluate
1618
1619     """
1620     system = System()
1621     interff = InterFF("int1")
1622     cljfunc = CLJShiftFunction()
1623     cljfunc.setSpace(boxSpace)
1624     interff.setCLJFunction(cljfunc)
1625     #interff.setSwitchingFunction(cljfunc)
1626     interff.setUseParallelCalculation(True)
1627     system.setProperty("space", boxSpace)
1628     outputgroup.add(biom_mol)
1629     interff.add(outputgroup)
1630     system.add(interff)
1631     system.add( SpaceWrapper(Vector(0), outputgroup) )
1632     system.add(outputgroup)
1633     return (system,system.energy())
1634
1635 def createSystem(outputgroup, biom_mol, boxSpace):
1636     """
1637     create a system to hold all of the molecules and forcefields
1638     Return the created system and the forcefield energy component
1639     that you want to evaluate
1640
1641     """
1642     system = System()
1643     interff = InterFF("int1")
1644     cljfunc = CLJShiftFunction()
1645     #cljfunc.setCoulombCutoff(0 * angstrom)
```

```
1646 #cljfunc.setLJCutoff(15 * angstrom)
1647 cljfunc.setSpace(boxSpace)
1648 interff.setCLJFunction(cljfunc)
1649 #interff.setSwitchingFunction(cljfunc)
1650 interff.setUseParallelCalculation(True)
1651 system.setProperty("space", boxSpace)
1652 outputgroup.add(biom_mol)
1653 interff.add(outputgroup)
1654 #interff.add(biom_mol)
1655 system.add(interff)
1656 system.add( SpaceWrapper(Vector(0), outputgroup) )
1657 system.add(outputgroup)
1658 return (system, interff.components().lj())
1659
1660 def create_single_System(outputgroup,boxSpace):
1661     """
1662     create a system to hold all of the molecules and forcefields
1663     Return the created system and the forcefield energy component
1664     that you want to evaluate
1665
1666     """
1667     system = System()
1668     interff = InterFF("int1")
1669     cljfunc = CLJShiftFunction()
1670     cljfunc.setCoulombCutoff(10 * angstrom)
1671     cljfunc.setLJCutoff(10 * angstrom)
1672     cljfunc.setSpace(boxSpace)
1673     interff.setCLJFunction(cljfunc)
1674     #interff.setSwitchingFunction(cljfunc)
1675     interff.setUseParallelCalculation(True)
1676     system.setProperty("space", boxSpace)
1677     interff.add(outputgroup)
1678     system.add(interff)
1679     system.add( SpaceWrapper(Vector(0), outputgroup) )
1680     system.add(outputgroup)
1681     return (system, interff.components().lj())
1682
1683 def remove_water_to_balance_density(system_input,nwater):
1684     """
1685     function to remove the random extra water molecules from PDB file
1686     before making the top,cord files
1687     and running minimization...
1688     system, moleculegroup and number of nwater to remove.
1689     """
1689     system = collect_mc_molecs(system_input)
```

```

1690     rangen = RanGenerator()
1691     nwaters = system.nMolecules()
1692     for i in range(nwater):
1693         water_id = rangen.randint(0, nwaters-1)
1694         random_water = system[ MolIdx(water_id) ].molecule()
1695         if random_water.nAtoms() == 3:
1696             system.remove(random_water)
1697     system
1698     PDB().write(system.molecules(), "afterRemovingExWater.pdb")
1699     return system
1700
1701 def density_of_single_box(system, space):
1702     """
1703     Function to determine the total density of system
1704     Input : system or molecule group
1705     """
1706     box_volume = space.volume().value()
1707     grams = 1.6605402e-24 # convert the molecular mass in to grams
1708     cube_centimeter = 1.0e-24 # cubic angstrom to cubic centimeter --volume
1709     mass = 0
1710     massIdx = 0
1711     for molnum in system.molNums():
1712         mol = system[molnum].molecule()
1713         mass_mol = mol.evaluate().mass().value()
1714         mass += mass_mol
1715     """
1716     for i in range(system.nMolecules()):
1717         mol = system[MolIdx(i)].molecule()
1718         mass_mol = mol.evaluate().mass().value()
1719         massIdx += mass_mol
1720
1721     densityIdx = (massIdx*grams)/(box_volume*cube_centimeter)
1722     """
1723     density = (mass*grams)/(box_volume*cube_centimeter)
1724     print("density of given box is %s= g/cc "%density)
1725     return density
1726
1727 def box_density_printer(rna_mass, mass_singlepeg, peg_density, boxspace):
1728     """
1729     Function to estimate the density of box and number of background
1730     molecules
1731     to generate the initial configurations via PACKMOL package.
1732     Function also gives number of water molecules used to swap rna and
1733     fill the

```

```
1732 the second box of system to maintain overall density fix. density
      units g/cc
1733
1734 Function Input: rna single molecule/moleculgroup
1735                 peg single molecule/molecule group of peg only
1736                 required peg density in lg/cc overall concentration
1737                 [0.1,0.2,....0.9]
1738                 boxspace
1739
1740
1741 rna_mass = rna[MolIdx(0)].molecule().evaluate().mass().value()
1742 mass_singlepeg = peg[MolIdx(0)].molecule().evaluate().mass().value
      ()
1743 box_volume = boxspace.volume().value()
1744 peg_density= 0.2
1745
1746 note: the order of input files is critical!
1747       Desire density [1,2,3..]g/cc can be change in function
1748
1749 """
1750 #rna_mass = rna[MolIdx(0)].molecule().evaluate().mass().value()
1751 #mass_singlepeg = peg[MolIdx(0)].molecule().evaluate().mass().value
      ()
1752 box_volume = boxspace.volume().value()
1753 grams = 1.6605402e-24 # convert the molecular mass in to grams
1754 cube_centim = 1.0e-24 # cubic angstrom to cubic centimeter --volume
      conversion
1755 desired_density = 1 # desired overall density
1756 mass_peg = peg_density*(box_volume*cube_centim)/(grams)
1757 number_peg = mass_peg/mass_singlepeg
1758 print ("number of peg molecules %s at %s g/cc density" % (
      number_peg,peg_density))
1759 rna_density = (rna_mass*grams)/(box_volume*cube_centim)
1760 print ("density of rna molecule g/cc= ", rna_density)
1761 density_forwater = desired_density-(rna_density+peg_density)
1762 print ("density to be filled by water molecule g/cc= ",
      density_forwater)
1763 mass_water = density_forwater*(box_volume*cube_centim)/(grams)
1764 number_water = mass_water/18.01528 # mol.wegith of water = 18.01528
1765 print ("number of water molecules =%s" % number_water)
1766 mass_water_empty_box = desired_density*(box_volume*cube_centim)/(
      grams)
1767 number_warter_empty_box = mass_water_empty_box/18.01528
1768 print ("number of water molecules in empty box to make density 1 g/
      cc are =%s " % number_warter_empty_box)
```

```
1769     number_water_swap = rna_mass/18.01528
1770     print ("number of water molecules displace by RNA = %s" %
           number_water_swap)
1771     return
1772
1773 def box_density(rna_mass, mass_singlepeg, peg_density, box_volume):
1774     grams = 1.6605402e-24
1775     cube_centimeter = 1.0e-24
1776     desired_density = 1
1777     mass_peg = peg_density*(box_volume*cube_centimeter)/(grams)
1778     number_peg = mass_peg/mass_singlepeg
1779     #print("number of peg molecules %s at %s g/cc density" % (
           number_peg, peg_density))
1780     rna_density = (rna_mass*grams)/(box_volume*cube_centimeter)
1781     #print("density of rna molecule g/cc= ", rna_density)
1782     density_forwater = desired_density-(rna_density+peg_density)
1783     #print("density to be filled by water molecule g/cc= ",
           density_forwater)
1784     mass_water = density_forwater*(box_volume*cube_centimeter)/(grams)
1785     number_water = mass_water/18.01528
1786     #print("number of water molecules =%s" % number_water)
1787     mass_water_empty_box = desired_density*(box_volume*cube_centimeter)/(
           grams)
1788     number_water_empty_box = mass_water_empty_box/18.01528
1789     #print("number of water molecules in empty box to make density 1 g/
           cc are =%s " % number_water_empty_box)
1790     number_water_swap = rna_mass/18.01528
1791     #print("number of water molecules displace by RNA = %s" %
           number_water_swap)
1792     return (number_peg, number_water, number_water_empty_box)
1793
1794 def swap_nwaters_for_density(nwaters, box1_mols, box2_mols):
1795     """
1796     Function to swap water molecules between two boxes to maintain the
           density
1797     Input: nwaters, box1_mols, box2_mols
1798     """
1799     nwaters = int(nwaters)
1800     for i in range(nwaters):
1801         nwater = box2_mols[MolIdx(i)].molecule()
1802         box2_mols.remove(nwater)
1803         box1_mols.add(nwater)
1804     return (box1_mols, box2_mols)
1805
1806 def energy_minimize_system(box_mols, box_space):
```

```
1807     """
1808     Function to prepare the system containing the molecules, boxSpace
1809     Input: Molecules box, boxSpace
1810     """
1811     # create simulation system to hold box of molecules
1812     box_system = System("box")
1813     # intermolecule coulomb and LJ energy
1814     box_interff = InterCLJFF("box_inter")
1815     box_interff.add(box_mols)
1816     # intramolecular bond, angle and dihedral energy
1817     box_intraff = InternalFF("box_intra")
1818     box_intraff.add(box_mols)
1819     # intramolecular coulomb and LJ energy
1820     box_intraclj = IntraCLJFF("box_intraclj")
1821     box_intraclj.add(box_mols)
1822     # add all molecules and forcefields for box to system
1823     box_system.add(box_mols)
1824     box_system.add(box_interff)
1825     box_system.add(box_intraff)
1826     box_system.add(box_intraclj)
1827     # set the periodic box information for each box
1828     box_system.setProperty("space", box_space)
1829     # system energy (optional)
1830     box_system.energies()
1831     return box_system
1832
1833 def make_pdb(energy, system, energytol):
1834     energytol = - abs(energytol * 4)
1835     if energy < energytol:
1836         PDB().write(system.molecules(), "lower_energy.pdb")
1837     return
1838
1839 def default_system_energy(outputgroup, boxSpace):
1840     """
1841     function to estimate the energy to determine wether
1842     there is any steric clash or not in the given molecule group.
1843
1844     Function Input: molecule group, boxspace
1845     note: set the tolerance criteria if desire:
1846     """
1847     #system= System()
1848     interff = InterFF("int1")
1849     #cljfunc = CLJShiftFunction()
1850     cljfunc = CLJShiftFunction() # 10*angstrom
1851     #cljfunc.setCoulombCutoff(0 * angstrom)
```

```
1852 #cljfunc.setLJCutoff(5 * angstrom)
1853 cljfunc.setSpace(boxSpace)
1854 interff.setCLJFunction(cljfunc)
1855 #interff.setSwitchingFunction(cljfunc)
1856 interff.setUseParallelCalculation(True)
1857 interff.add(outputgroup)
1858 #system.add(outputgroup)
1859 #system.add(interff)
1860 #total_nrg = system.energy()
1861 #system.setProperty("space", boxSpace)
1862 #system_energy = (system.energy().value(), 3)
1863 #coul_nrg = int1.energy( int1.components().coulomb() )
1864 #print("coul energy = %s" % coul_nrg)
1865 #lj_nrg = system.energy( interff.components().lj() )
1866 lj_nrg = interff.energy( interff.components().lj() )
1867 #print("LJ energy = %s" % lj_nrg)
1868 #print("total energy of system =%s" % system_energy)
1869 #print("all energies = %s " % system.energies())
1870 return lj_nrg.value()
1871
1872 def swap_water_rna(box1_mols,box2_mols):
1873     """
1874     Function use to swap RNA and water molecules between two boxes.
        where box1_mols is box containing RNA and background molecules
        while box2_molecules is purely water box where RNA will be
        placed and from there number of water molecules are moved to
        box1_mols to keep density fix. It gives two boxes back as output
        ...
1875     Input: box1_mols, box2_mols
1876     """
1877     rna_residmolecule = box1_mols[ MolWithResID("RG5") ].molecule()
1878     nwaters = rna_residmolecule.evaluate().mass().value()/18.01528
1879     box1_mols.remove(rna_residmolecule)
1880     (box1_mols,box2_mols,charge_mass)=charge_swap(box1_mols,box2_mols)
1881     print("charge ions mass in given system %s" % charge_mass)
1882     nwaters = nwaters+charge_mass
1883     (box1_mols,box2_mols) = swap_nwaters_for_density(nwaters, box1_mols
        , box2_mols)
1884     box2_mols.add(rna_residmolecule)
1885     return (box1_mols,box2_mols)
1886
1887 def collect_mc_molecs(sim_mols):
1888     """
1889     Function to collect molecules in a new molecule group so to use in
        next MC steps of code
```

```
1890     """
1891     optimized_mols = MoleculeGroup()
1892     for molnum in sim_mols.molNums():
1893         mol = sim_mols[molnum].molecule()
1894         optimized_mols.add(mol)
1895     return optimized_mols
1896
1897 def NPT_ensemble_moves(system):
1898     """
1899     Function to define property of move(temp, pressure, volume)
1900     Input: system output from ("energy_minimize_system")function
1901     this function gives the system over which moves will be performed
1902         while wt_moves represent the collection of moves according to
1903         NPT ensemble.
1904     """
1905     ## create a Rigid Body move that will translate and rotate the
1906     ## molecules in system
1907     list_of_groups = system.groups()[-1]
1908     MGName = system.groupNames()[-1]
1909     system.add( SpaceWrapper(Vector(0), list_of_groups) )
1910     Rigid_move = RigidBodyMC(system[MGName])
1911     Rigid_move.setTemperature( 25*celsius )
1912     Rigid_move.setMaximumTranslation(0.50 * angstrom)
1913     Rigid_move.setMaximumRotation(0.50 * degrees)
1914     Rigid_move.setUseOptimisedMoves
1915     vol_mov = VolumeMove(system[MGName])
1916     vol_mov.setMaximumVolumeChange( 0.1 * system.nMolecules() *
1917         angstrom3 )
1918     vol_mov.setPressure( 1*atm )
1919     wt_moves = WeightedMoves()
1920     wt_moves.add( Rigid_move, system[MGName].nMolecules() )
1921     wt_moves.add( vol_mov, system[MGName].nMolecules() )
1922     system_out = wt_moves.move(system, 5, True)
1923     return (system,wt_moves)
1924
1925 def NPT_ensemble_moves_large_trans_rot(system):
1926     """
1927     Function to define property of move(temp, pressure, volume)
1928     Input: system output from ("energy_minimize_system")function
1929     this function gives the system over which moves will be performed
1930         while wt_moves represent the collection of moves according to
1931         NPT ensemble.
1932     """
1933     ## create a Rigid Body move that will translate and rotate the
1934     ## molecules in system
```

```
1928 list_of_groups = system.groups() [-1]
1929 MGName = system.groupNames() [-1]
1930 system.add( SpaceWrapper(Vector(0), list_of_groups) )
1931 Rigid_move = RigidBodyMC(system[MGName])
1932 Rigid_move.setTemperature( 25*celsius )
1933 Rigid_move.setMaximumTranslation(2.50 * angstrom)
1934 Rigid_move.setMaximumRotation(5.50 * degrees)
1935 Rigid_move.setUseOptimisedMoves
1936 vol_mov = VolumeMove(system[MGName])
1937 vol_mov.setMaximumVolumeChange( 0.1 * system.nMolecules() *
    angstrom3 )
1938 vol_mov.setPressure( 1*atm )
1939 wt_moves = WeightedMoves()
1940 wt_moves.add( Rigid_move, system[MGName].nMolecules() )
1941 wt_moves.add( vol_mov, system[MGName].nMolecules() )
1942 system_out = wt_moves.move(system, 5, True)
1943 return (system,wt_moves)
1944
1945 def NVT_ensemble_moves_large_trans_rot(system):
1946     """
1947     Function to define property of move(temp, pressure, volume)
1948     Input: system output from ("energy_minimize_system")function
1949     this function gives the system over which moves will be performed
    while wt_moves represent the collection of moves according to
    NPT ensemble.
1950     """
1951     ## create a Rigid Body move that will translate and rotate the
    molecules in system
1952     list_of_groups = system.groups() [-1]
1953     MGName = system.groupNames() [-1]
1954     system.add( SpaceWrapper(Vector(0), list_of_groups) )
1955     Rigid_move = RigidBodyMC(system[MGName])
1956     Rigid_move.setTemperature( 25*celsius )
1957     Rigid_move.setMaximumTranslation(5.50 * angstrom)
1958     Rigid_move.setMaximumRotation(15.0 * degrees)
1959     Rigid_move.setUseOptimisedMoves
1960     wt_moves = WeightedMoves()
1961     wt_moves.add( Rigid_move, system[MGName].nMolecules() )
1962     system_out = wt_moves.move(system, 5, True)
1963     return (system,wt_moves)
1964
1965 def NVT_ensemble_moves(system):
1966     """
1967     Function to define property of move(temp, pressure, volume)
1968     Input: system output from ("energy_minimize_system")function
```

```

1969     this function gives the system over which moves will be performed
        while wt_moves represent the collection of moves according to
        NPT ensemble.
1970     """
1971     ## create a Rigid Body move that will translate and rotate the
        molecules in system
1972     list_of_groups = system.groups() [-1]
1973     MGName = system.groupNames() [-1]
1974     system.add( SpaceWrapper(Vector(0), list_of_groups) )
1975     Rigid_move = RigidBodyMC(system[MGName])
1976     Rigid_move.setTemperature( 25*celsius )
1977     Rigid_move.setMaximumTranslation(2.50 * angstrom)
1978     Rigid_move.setMaximumRotation(10.50 * degrees)
1979     Rigid_move.setUseOptimisedMoves
1980     wt_moves = WeightedMoves()
1981     wt_moves.add( Rigid_move, system[MGName].nMolecules() )
1982     system_out = wt_moves.move(system, 5, True)
1983     return (system,wt_moves)
1984
1985 def simulation_moves(box_system_mc,box_wt_moves,steps,filename1,
        filename2,filename3):
1986     """
1987     Function to perform moves on a system to minimize the energy values
1988     Input: system_box containing all forcefield and molecules,
        weight_moves,steps,'file1.txt','file2.txt' names
1989     """
1990     first_energy = box_system_mc.energy().value()
1991     set_p_value = 0.1
1992     test_energy = [1,2,3,4,5,6,7,8,9,10,11,12,13,14,15,16,17,18,
        first_energy]
1993     calculated_p_value = float('inf')
1994     # energy_diff between moves while simulation
1995     x = 1
1996     with open (filename1, 'w') as f1:
1997         with open (filename2, 'w') as g1 :
1998             while calculated_p_value > set_p_value:
1999                 for i in range(x,x+20):
2000                     box_system_mc = box_wt_moves.move(box_system_mc, steps,
                        True)
2001                     #print("%d: %s" % (i, box2_system_mc.energy()))
2002                     energy = box_system_mc.energy().value()
2003                     test_energy.append(energy)
2004                     energy_difference= test_energy[-2]-test_energy[-1]
2005                     f1.write(str(energy_difference)+'\n')
2006                     g1.write(str(energy)+'\n')

```

```
2007         window1 = test_energy[-20:-10]
2008         window2 = test_energy[-10:]
2009         Individual_samples = stats.ttest_ind(window1, window2)
2010         calculated_p_value= Individual_samples[-1]
2011         x = x+1
2012         box_system_mc.update
2013         if i % 1 == 0:
2014             print ("The Individual t-statistic is %s and the p-
                    value is %s and energy of system is = %s" % (
                        Individual_samples[0],Individual_samples[1],energy)
                    )
2015                 #Sire.Stream.save(box_system_mc,filename3)
2016         E = min(test_energy[-20:])
2017         print ("Energy of system after Monte Carlo Minimization = %s:" % E)
2018         print ("Move information:")
2019         print(box_wt_moves)
2020         # collect the molecues in new molecule group for further MC
2021         box_mols_mc = collect_mc_molecs(box_system_mc)
2022         PDB().write(box_system_mc.molecules(), filename3)
2023         f1.close()
2024         gl.close()
2025         Sire.Stream.save(box_system_mc,filename3)
2026         return (E,box_mols_mc)
2027
2028 def simulation_moves_simple(box_system_mc,box_wt_moves,steps):
2029     """
2030     Function to perform moves on a system to minimize the energy values
2031     Input: system_box containing all forcefield and molecules,
           weight_moves,steps,'file1.txt','file2.txt' names
2032     """
2033     first_energy = box_system_mc.energy().value()
2034     box_system_mc = box_wt_moves.move(box_system_mc, steps, True)
2035     return (box_system_mc)
2036
2037 def pdbmaker(input_filename,output_filename,copy_numberoflines):
2038     """
2039     Function to create pdbs from pdb file containing all frames
2040     """
2041     file = open(input_filename,'r')
2042     lines = file.readlines()
2043     f1 = open(output_filename, 'w')
2044     for i in range(0,copy_numberoflines):
2045         f1.write(lines[i])
2046     f1.close()
2047     open('all.pdb', 'w').writelines(lines[copy_numberoflines:])
```

```
2048     return
2049
2050 def str_maker(filename):
2051     file = str(filename)
2052     return file
2053
2054 def pdbdist(input_filename, output_filename, set_1_start, set_1_end,
2055             set_2_start, set_2_end):
2056     #Function to find the distances between two sets atoms of each pdb
2057     #frame.
2058     """
2059     1- pdb file name
2060     2- output file name containing diameters
2061     3- start of first set of atoms
2062     4- end of first set of atoms
2063     5- start second
2064     6- end second
2065     Measure the distance between atoms of each set and write in output
2066     file
2067     """
2068     set1 = []
2069     set2 = []
2070     file = open(input_filename, 'r')
2071     lines = file.readlines()
2072     f1 = open(output_filename, 'w')
2073     for i in range(set_1_start, set_1_end):
2074         f1.write(lines[i])
2075     for j in range(set_2_start, set_2_end):
2076         f1.write(lines[j])
2077     f1.close()
2078     return
2079
2080 def radius_from_pdb(inputfilename, set1, set2):
2081     #set1 = 240
2082     #set2 =
2083     #molecule = PDB().read(inputfilename)
2084     molecule= inputfilename[MolIdx(0)].molecule()
2085     list1 = []
2086     list2 = []
2087     dist_list = []
2088
2089     for i in range(set1):
2090         l1 = molecule.atom(AtomIdx(i)).evaluate().center()
2091         #print(l1)
```

```
2090     list1.append(l1)
2091     #print("length of list1 %s" %list1)
2092     for j in range(set1,set2):
2093         l2 = molecule.atom(AtomIdx(j)).evaluate().center()
2094         #print(l2)
2095         list2.append(l2)
2096     #print("length of list2 %s" %list2)
2097     for k in range(len(list1)):
2098         atom1 = list1[k]
2099         for l in range(len(list2)):
2100             dist = Vector.distance(atom1,list2[l])
2101             #print(dist)
2102             dist_list.append(dist)
2103     #print(len(dist_list))
2104     dist = max(dist_list)
2105     return dist
2106
2107 def load_files_to_prepare_system_for_flexibility(inpcrd,prmtop,
2108 dimensions,save_sys_name):
2109     """
2110     function to load files (inpcrd, prmtop, dimensions of box files and
2111         assign flexibility)
2112     the input files added with route directories ....
2113     """
2114     # Load the molecules and the periodic box from the crd/top files
2115     (mols, space) = Amber().readCrdTop(inpcrd,prmtop)
2116     mols.setName("mols")
2117     cord_file = dimensions
2118     cord_file = open(cord_file,'r')
2119     line = line_extract(cord_file)
2120     total_cord = [float(b) for a in re.findall(r'{{(.*)}}', line) for
2121         b in a.split()]
2122     print("Original Box Dimensions %s" %total_cord)
2123     total_cord = coordinates_check(total_cord)
2124     maxcord = Vector(total_cord[0:3])
2125     mincord = Vector(total_cord[-3:])
2126     space = PeriodicBox(mincord, maxcord)
2127     print("assigning flexibility ... ")
2128     new_group = GenerateFlexibility_all_molecules(mols)
2129     print("flexibility assigned ... ")
2130     return (new_group,space)
2131
2132 def GenerateFlexibility_all_molecules(peg):
2133     """
```

```

2132     function to determine flexibility of all molecules in the box.
2133     """
2134     npeg = peg.nMolecules()
2135     new_group = MoleculeGroup("Mols")
2136     for i in range(npeg):
2137         print(i)
2138         random_peg = peg.moleculeAt(i).molecule()
2139         flexibility = AmberLoader.generateFlexibility(random_peg)
2140         random_peg = random_peg.edit() \
2141             .setProperty("flexibility", flexibility) \
2142             .commit()
2143         new_group.add(random_peg)
2144     return new_group

```

A.3.2 Quenching sampling program

```

1  """
2  Sire script to perform conformational sampling using a temperature
   quenching method.
3
4  Input Files: PEG.inpcrd, PEG.prmtop
5  output: pdb files save after every n steps
6
7  """
8  #####
9  #           Import Libraries
10 #####
11 From MyFunctions import *
12
13 #####
14 #           Main program
15 #####
16
17 # Get the structural details
18
19 map = { "weight function" : RelFromMass() }
20
21 # Load the molecule & extract structural details
22
23 (GiveMolec, space) = Amber().readCrdTop("peg.inpcrd", "peg.prmtop")
24 GiveMolec = GiveMolec[MolIdx(0)].molecule()
25 bonds = GiveMolec.property("connectivity").getBonds()
26 angles = GiveMolec.property("connectivity").getAngles()
27 dihedrals = GiveMolec.property("connectivity").getDihedrals()
28 nbonds = len(bonds)

```

```
29 nangles = len(angles)
30 ndihedrals = len(dihedrals)
31 nbonds = len(bonds)
32 nangles = len(angles)
33 ndihedrals = len(dihedrals)
34
35 # create a random number generator for the moves
36 rangen = RanGenerator()
37
38 # create a forcefield to calculate the intramolecular (bond, angle,
    dihedral) energy of the Molecule
39 intraff = InternalFF("intraff")
40
41 # create a forcefield to calculate the intramolecular (coulomb and LJ)
    energy of the Molecule
42 intraclj = IntraCLJFF("intraclj")
43 intrasoft = IntraSoftCLJFF("intrasoft")
44 intrabase = IntraCLJFFBase("intrabase")
45
46 # add the Molecule to both forcefields
47 intraff.add(GiveMolec)
48 intraclj.add(GiveMolec)
49
50 # create system to hold everything
51 system = System()
52 system.add(intraff)
53 system.add(intraclj)
54
55 # list two quenching temperatures
56 temp = 1200
57 temp2 = 300
58 naccept = 0
59 nreject = 0
60
61 # perform 200 blocks of 20 moves
62 for i in range(1,2000):
63     print("Molecule energy Initial = %s" % system.energy())
64     print("Performing block %s" % i)
65     print(" MC Temperature %s " %temp)
66
67     for j in range(0,10):
68         # randomly choose which move to run
69         move_type = rangen.randint(1,3)
70
71         if move_type == 1:
```

```
72         bondMove(temp,system)
73     elif move_type == 2:
74         angleMove(temp,system)
75     elif move_type == 3:
76         dihedralMove(temp,system)
77     print("Block complete: number of accepted moves = %s (acceptance
          ratio %s %%) " % \
78           (naccept, 100.0*naccept / (naccept+nreject)) )
79     print("Molecule energy Final = %s" % system.energy())
80     radius_list = []
81     #file2 = open('radiusoutput.log','w')
82     mol = system[MolIdx(0)].molecule()
83     radius = radgyr(mol)
84     print("radius of gyration %s" %radius)
85     #radius_list.append(radius)
86     PDB().write(system.molecules(), "peg%0d.pdb" % i)
87     system300 = system
88     PEG = system[MolIdx(0)].molecule()
89     if i % 1 ==0:
90         quenched_conf(system300, temp2)
91         system = make_system(PEG)
92     print("*****")
93     print("***** The End *****")
```

A.4 MD sampling in Amber

A.4.1 mini.in

```
1 initial minimization prior to MD GB model
2 &cntrl
3   imin = 1,
4   maxcyc = 500,
5   ncyc = 250,
6   ntb = 0,
7   igb = 1,
8   cut = 10
9 /
```

A.4.2 md.in

```
1 MD Generalized Born, 12 angstrom cut off
2 &cntrl
3   imin = 0, ntb = 0,
4   igb = 1, ntp = 100, ntwx = 100,
5   ntt = 3, gamma_ln = 1.0,
6   tempi = 300.0, temp0 = 300.0
7   nstlim = 10000000, dt = 0.001,
8   cut = 12.0
9 /
```

A.5 Packing and Equilibration

```
1 # Packmol input file
2 tolerance 3.0
3 discale 2.0
4 randominitialpoint
5 add_amber_ter
6 nseed 12345
7 nloop 1000
8 filetype pdb
9 output box101.pdb
10 structure peg725.pdb
11   number 1
12   inside box -150. -150. -150. 150. 150. 150.
13 end structure
14 structure peg328.pdb
15   number 1
16   inside box -150. -150. -150. 150. 150. 150.
17 end structure
18 structure peg576.pdb
19   number 1
20   inside box -150. -150. -150. 150. 150. 150.
21 end structure
22 structure peg770.pdb
23   number 1
24   inside box -150. -150. -150. 150. 150. 150.
25 end structure
26 structure peg768.pdb
27   number 1
28   inside box -150. -150. -150. 150. 150. 150.
29 end structure
30 structure peg701.pdb
31   number 1
32   inside box -150. -150. -150. 150. 150. 150.
33 end structure
34 structure peg366.pdb
35   number 1
36   inside box -150. -150. -150. 150. 150. 150.
37 end structure
38 structure peg506.pdb
39   number 1
40   inside box -150. -150. -150. 150. 150. 150.
41 end structure
42 structure peg709.pdb
43   number 1
```

```
44   inside box -150. -150. -150. 150. 150. 150.
45 end structure
46 structure peg540.pdb
47   number 1
48   inside box -150. -150. -150. 150. 150. 150.
49 end structure
50 structure peg816.pdb
51   number 1
52   inside box -150. -150. -150. 150. 150. 150.
53 end structure
54 structure peg37.pdb
55   number 1
56   inside box -150. -150. -150. 150. 150. 150.
57 end structure
58 structure peg396.pdb
59   number 1
60   inside box -150. -150. -150. 150. 150. 150.
61 end structure
62 structure peg24.pdb
63   number 1
64   inside box -150. -150. -150. 150. 150. 150.
65 end structure
66 structure peg513.pdb
67   number 1
68   inside box -150. -150. -150. 150. 150. 150.
69 end structure
70 structure peg677.pdb
71   number 1
72   inside box -150. -150. -150. 150. 150. 150.
73 end structure
74 structure peg306.pdb
75   number 1
76   inside box -150. -150. -150. 150. 150. 150.
77 end structure
78 structure peg724.pdb
79   number 1
80   inside box -150. -150. -150. 150. 150. 150.
81 end structure
82 structure peg318.pdb
83   number 1
84   inside box -150. -150. -150. 150. 150. 150.
85 end structure
86 structure peg192.pdb
87   number 1
88   inside box -150. -150. -150. 150. 150. 150.
```

```

89 end structure
90 structure peg783.pdb
91   number 1
92   inside box -150. -150. -150. 150. 150. 150.
93 end structure
94 structure peg109.pdb
95   number 1
96   inside box -150. -150. -150. 150. 150. 150.
97 end structure
98 structure peg827.pdb
99   number 1
100  inside box -150. -150. -150. 150. 150. 150.
101 end structure
102 structure peg679.pdb
103   number 1
104   inside box -150. -150. -150. 150. 150. 150.
105 end structure
106 structure peg644.pdb
107   number 1
108   inside box -150. -150. -150. 150. 150. 150.
109 end structure

```

A.5.1 Equilibration with Sire

```

1  """
2  MC Equilibration with sire
3  Input files: simulation systems, box dimensions
4  output: Equilibrated simulation system
5  """
6  #####
7  # Import Libraries as listed in Sire sampling input file
8  #####
9  from MyFunctions import *
10
11 #####
12 #           Main program
13 #####
14
15 # Load the systems to perform equilibration
16 inpcrd = "box1001.inpcrd"
17 prmtop = "box1001.prmtop"
18 dimensions = 'box1001.dat'
19 save_sys_name = "flex_system.s3"
20
21 # Determine number of systems needs to equilibrate

```

```
22 check = os.path.isfile("flex_system.s3")
23 check = str(check)
24 if check == 'True':
25     print ("Minimized or system with flexibility is available and load
           it")
26     new_groups = load("flex_system.s3")
27     new_group = collect_mc_molecs(new_groups)
28     (simSystem,ljcp)=create_single_System(new_group,new_groups.
           property('space'))
29 else:
30     print ("Making system with flexibility and defining rigid and
           internal moves...")
31     (new_group,space)=load_files_to_prepare_system_for_flexibility(
           inpcrd,prmtop,dimensions,save_sys_name)
32     (simSystem,ljcp)=create_single_System(new_group,space)
33
34     print ("system is done!")
35     ## Definition of parameters for simulations
36
37     # Initialize random generator
38     rangen = RanGenerator()
39     # Set the temperature
40     temperature = 298.15 * kelvin
41     # Specify the maximum amount to move thebonds, angles and dihedrals
42     max_delta_bond = 0.05 * angstrom
43     max_delta_angle = 3.5 * degrees
44     max_delta_dihedral = 10 * degrees
45     ##specify the maximum number of bonds, angles and dihedrals to move
           per move
46     max_num_move = 25
47     # set the maximum delta parameters
48     params = {}
49     params["bond flex"] = max_delta_bond
50     params["angle flex"] = max_delta_angle
51     params["dihedral flex"] = max_delta_dihedral
52     params["h dihedral flex"] = max_delta_dihedral
53     params["maxvar"] = max_num_move
54     Parameter.push(params)
55
56     # Perform Rigid body and internal MC moves
57     (system_mc,wt_moves)=NVT_ensemble_moves(simSystem)
58     MGName = system_mc.groupNames()[-1]
59     internalmove = InternalMove(system_mc[MGName])
60     Sire.Stream.save( system_mc, "flex_system.s3" )
61
```

```

62 # Save energy values
63 file = open('Energy_peg5.log','w')
64 print("Perform MC simulations")
65
66 # perform 5000 blocks of 2*5000 moves
67 for i in range(1,1001):
68     print("performing step %s"%i)
69     print("system_mc start energy %s"%system_mc.energy())
70     system_mc = simulation_moves_simple(system_mc,wt_moves,5000)
71     print("system energy after RIGID BODY mc % s " % system_mc.energy
72           ())
73     internalmove.move(system_mc, 5000)
74     print("Energy %s, nAccepted = %s, nRejected = %s" % \
75           (system_mc.energy(), internalmove.nAccepted(),
76             internalmove.nRejected() ) )
77     print("system final energy after internal Moves %s"%system_mc.
78           energy())
79     file.write(str(system_mc.energy())+'\n')
80     print("*****")
81     if i % 100 == 0:
82         #PDB().write(system_mc.molecules(), "peg_%000000d.pdb" % i)
83         Sire.Stream.save( system_mc, "rstpeg_%000000d.s3" % i )
84 file.close()

```

A.5.2 Swapping equilibrium with Sire

```

1  """
2  Script to equilibrate the PEG systems by inserting of a random peg from
3  PEG library. If the peg is placed then keep the configuration
4  otherwise reverse the configuration by placing the original peg in
5  the system.
6
7  3
8  Steps to perform equilibrium
9  1- load the initial configuration system of desired concentration and
10 determine energy E1
11 2- select random peg molecule and remove it from the system
12 3- pick the random molecule from the library and insert it and
13 determine E2
14 4- check if E2 < E1 -> accepted
15 5- if not, then reverse the system.
16 """
17 #####
18 # Import Libraries as listed in Sire sampling input file
19 #####
20 from MyFunctions import *

```

```
15
16 #####
17 #           Main program
18 #####
19
20 # time counter
21 start_time = time.clock()
22 t = QTime()
23 t.start()
24
25 # load simulation system and dimensions and estimate energy
26 (peg, boxSpace)= Amber().readCrdTop("box101.inpcrd", "box101.prmtop")
27 cord_file = 'box1001.dat'
28 cord_file = open(cord_file, 'r')
29 line = line_extract(cord_file)
30 total_cord = [float(b) for a in re.findall(r'{(.*?)}', line) for b
    in a.split()]
31 print("Original Box Dimensions %s" %total_cord)
32 total_cord = coordinates_check(total_cord)
33 maxcord = Vector(total_cord[0:3])
34 mincord = Vector(total_cord[-3:])
35 boxSpace = PeriodicBox(mincord, maxcord)
36 initial_energy = default_system_energy(peg,boxSpace)
37
38 # Place a molecule from a library to the simulation box
39 randgen = RanGenerator()
40 npeg = peg.nMolecules()
41 peg_id = randgen.randint(0,npeg-1)
42 random_peg = peg[MolIdx(peg_id)].molecule()
43 peg.remove(random_peg)
44 peg.update(peg)
45 after_remove_energy = default_system_energy(peg,boxSpace)
46 print("after removing peg %s"%peg.nMolecules())
47 peg.update(peg)
48
49 # select random molecule from the library
50 lib_peg_id = randgen.randint(1,887)
51 inpcrd = 'input_files/library/peg'+str(lib_peg_id)+'.inpcrd'
52 prmtop = 'input_files/library/peg'+str(lib_peg_id)+'.prmtop'
53 (new_peg, space)= Amber().readCrdTop(inpcrd,prmtop)
54 new_peg = new_peg[MolIdx(0)].molecule()
55 new_peg = new_peg.edit().renumber().commit()
56 molnum = new_peg.number()
57
```

```
58 # simulation temperature and internal moves performed on the molecule
    and add to system
59 temperature = 298.15 * kelvin
60 max_translation = 150 * angstrom
61 max_rotation = 360 * degrees
62 (system,lj_comp)=createSystem(peg, new_peg, boxSpace)
63 random_translate = randgen.vectorOnSphere( max_translation.value() )
64 random_rotate_axis = randgen.vectorOnSphere()
65 random_rotate_angle = randgen.rand(-max_rotation.value(),
66                                     max_rotation.value()) * degrees
67 random_water = system[molnum].molecule()
68 moved_water = random_water.move() \
69             .rotate( \
70                 Quaternion(random_rotate_angle,random_rotate_axis), \
71                 random_water.evaluate().center() ) \
72             .translate(random_translate).commit()
73 system.update(moved_water)
74 final_energy = system.energy(lj_comp).value()
75 print("intial peg system energy %s "%initial_energy)
76 print("after remove energy %s "%after_remove_energy)
77 print("system energy after adding %s "%final_energy)
78 #PDB().write(system.molecules(),"testing.pdb")
79 condition = condition_fn(initial_energy,final_energy)
80 print("result from condition %s"%condition)
81 if condition == "True":
82     new_system = collect_mc_molecs(system)
83     success_energy = default_system_energy(new_system,boxSpace)
84     print("successful insertion energy %s "% success_energy)
85 else:
86     new_system = collect_mc_molecs(system)
87     new_system.remove(random_water)
88     new_system.add(random_peg)
89     after_all_energy = default_system_energy(new_system,boxSpace)
90     print("reverse system energy %s " % after_all_energy)
91 print("*****")
```

A.5.3 MD Equilibration with Amber

A.5.3.1 Execution file

```
1 #!/bin/bash
2 #PBS -S /bin/bash
3 #PBS -l walltime=20:00:00
4 #PBS -l nodes=1:ppn=12
5 #PBS -l mem=22gb
```

```

6
7 cd $PBS_O_WORKDIR
8
9 echo "Current working directory is `pwd`"
10
11 INPUT=gbin2
12 OUTPUT=mdout.out
13 PARM=box106.prmtop
14 INPCRD=box106.inpcrd
15
16
17 #export AMBERHOME=/global/software/amber/amber11
18 #PATH=$PATH:$AMBERHOME/exe
19 export AMBERHOME=/global/software/amber/amber14p8_at14p21
20 . $AMBERHOME/amber.sh
21
22 echo "Node file: $PBS_NODEFILE :"
23 echo "-----"
24 cat $PBS_NODEFILE
25 echo "-----"
26 NUM_PROCS=`/bin/awk 'END {print NR}' $PBS_NODEFILE`
27 echo "Running on $NUM_PROCS processors."
28
29
30 echo "prog started at: `date`"
31 mpiexec -n $NUM_PROCS pmemd.MPI -O -i $INPUT -o $OUTPUT -p box106.
    prmtop -c box106.inpcrd -r box106_md.rst -x box106_md.mdcrd
32
33 echo "prog finished at: `date`"
34 -----

```

A.5.3.2 Parameter file

```

1 equilibration of crowded systems
2 &cntrl
3 imin = 0, irest = 0, ntx = 1,
4 ntb = 2, pres0 = 1.0, ntp = 1,
5 taup = 2.0,
6 cut = 10.0, ntr = 0,
7 ntc = 2, ntf = 2,
8 tempi = 300.0, temp0 = 300.0,
9 ntt = 3, gamma_ln = 1.0,
10 nstlim = 1200000, dt = 0.002,
11 ntpr = 100, ntwx = 100, ntwr = 100000
12 /

```


A.6 Fractional available volumes calculations

A.6.1 Parallel-energy algorithm

```

1  """
2  Parallel-energy algorithm to find the fractional available volume based
   on finding the system energies.
3
4  Input files: simulation systems, probe molecules, box dimensions
5  output: Txt file containing fractional available volume
6  """
7  #####
8  # Import Libraries as listed in Sire sampling input file
9  #####
10 from MyFunctions import *
11
12 #####
13 #           Main program
14 #####
15
16 # Name of of RNA/protein molecule to be inserted in a box
17 RNA = "2k96"
18 path2 = "../rna/"
19 inpcrd_prob = RNA+'.inpcrd'
20 inpcrd_prob = path2+inpcrd_prob
21 prmtop_prob = RNA+'.prmtop'
22 prmtop_prob = path2+prmtop_prob
23
24 # Box dimensions are uploaded automatically from vmd.dot files. These
   files should be in path1 directory.
25 nReplicates = 10001
26 dsteps =100
27 irange = int(nReplicates/dsteps)
28 prit =100
29
30 #Find total simulation systems to be used in Monte Carlo simulations
31 print("Loading the available files to be used in Monte Carlo
   Simulations")
32 path1 = "../peg1_samples/"
33 system_files1 = [for f in os.listdir(path1) if f.endswith('.inpcrd'
   )]
34 system_files2 = [for f in os.listdir(path1) if f.endswith('.prmtop'
   )]
35 system_files3 = [for f in os.listdir() if f.endswith('.log')]
36 print("Number of systems available are %d"% len(system_files1))
37 system_numbers = []

```

```
38 for f in system_files1:
39     system_numbers.append(f[4:6])
40 system_numbers2 = []
41 for f in system_files3:
42     system_numbers2.append(f[-6:-4:])
43 system_numbers = [elem for elem in system_numbers if elem not in
44     system_numbers2 ]
45 print("Number of systems to run MC %s" % len(system_numbers))
46 print()
47 print("Loading input molecule = %s" % RNA)
48 (probeMolecules, boxSpace1) = Amber().readCrdTop(inpcrd_prob,prmtop_prob
49     )
50 probeMolecules.setName("probeMolecules")
51 probeMolecules_mol = probeMolecules[MolIdx(0)].molecule()
52 number = probeMolecules_mol.number()
53 residue = probeMolecules_mol.residues(ResIdx(0)).residue().name().value
54     ()
55
56 print("+++++++START MC ++++++")
57 print()
58 # probeMolecules/PROTEIN INPUT
59 for i in system_numbers:
60     start_time = time.clock()
61     t = QTime()
62     t.start()
63     inpcrd = 'box1'+i+'.inpcrd'
64     inpcrd = path1+inpcrd
65     prmtop = 'box1'+i+'.prmtop'
66     prmtop = path1+prmtop
67     cord_file = 'box1'+i+'.dat'
68     cord_file = path1+cord_file
69     print("Running System %s" % i)
70     cord_file = open(cord_file,'r')
71     line = line_extract(cord_file)
72     total_cord = [float(b) for a in re.findall(r'{{.*?}}', line) for
73         b in a.split()]
74     print("Original Box Dimensions %s" %total_cord)
75
76 #total_cord = coordinates_check(total_cord)
77 mincord = Vector(total_cord[0:3])
78 maxcord = Vector(total_cord[-3:])
79 boxSpace = PeriodicBox(mincord, maxcord)
80 print(boxSpace)
81 (simSystem,boxSpace1) = Amber().readCrdTop(inpcrd,prmtop)
82 simSystem.setName("simSystem")
```

```
79
80 #residue = probeMolecules_mol.residues(ResIdx(0)).residue().name().
    value()
81 irange = int(nReplicates/dsteps)
82 count = 0
83 throws = 0
84 output_vol = boxSpace.volume().value()
85
86 # STERIC CLASHES AND SYSTEM ENERGIES CALCULATIONS
87 system_energy = default_system_energy(simSystem,boxSpace)
88 system_energy = abs(system_energy)
89 print("system energy ( crowders only ) from pdb = %s:"%
    system_energy)
90 system_energy_probeMolecules = default_system_energy(probeMolecules
    ,boxSpace)
91
92 # time counter
93 start_time = time.clock()
94 t = QTime()
95 t.start()
96
97 # Specify the temperature of the simulation
98 temperature = 298.15 * kelvin
99
100 # Specify the maximum amount by which to translate each Molecule
101 max_translation = 150 * angstrom
102
103 #Specify the maximum amount by which to rotate each Molecule
104 max_rotation = 360 * degrees
105 rangen = RanGenerator()
106
107 # create a system to hold the molecules and forcefields
108 (system,lj_comp) = createSystem(simSystem, probeMolecules_mol,
    boxSpace)
109 t2 = QElapsedTimer()
110 t2.start()
111 energy = system.energy(lj_comp)
112 ns = t2.nsecsElapsed()
113 print("Initial system energy = %s kcal mol-1 (took %s ms)" % \
114     (energy.value(),0.000001*ns))
115 loop_i = i
116 avg = []
117 for i in range(1,irange):
118     output = loop_division2((i * dsteps)-((i-1)*dsteps),system,
        residue)
```

```

119     avg.append(output)
120     t_steps = irange*dsteps-(dsteps)
121     if i % prit == 0:
122         statistics_test(avg,output_vol,i*dsteps)
123     p = sum(avg)/len(avg)
124     print("average of excluded volume %s" % p)
125     V_free = p*output_vol
126     std_binom = sqrt(t_steps*p*(1-p))
127     error_binom = (output_vol/t_steps)*std_binom
128     error_binom_fraction = error_binom/V_free
129     print("COMPLETE STEPS %s: BINOMIAL ERROR in Total Vol. %s: ERROR
          in Fraction vol. %s: Available VOLUME %s:" % (t_steps,
          error_binom,error_binom_fraction*100,p))
130     lloopi = str(loop_i)
131     filename = RNA +'box10'+lloopi+'.log'
132     filename2 = RNA +'radgy_box10'+lloopi+'.txt'
133     log_file_writer(filename,t_steps,p,error_binom_fraction*100)
134     v= boxSpace.volume().value()
135     print()
136     (rad_list,vol_list) = collect_radgyr_box(simSystem)
137     vol = sum(vol_list)
138     a = (v-4*vol)/v
139     log_file_writer2(filename2,t_steps,a,vol)
140     print("numerical estimate of available volume (radgyr) = % s" % a)
141     print("done system %s :)" % loop_i)
142     elapsed = (time.clock() - start_time)/3600
143     print("(wall time %d h for given system %s)" % (elapsed,loop_i))
144     print("*****")

```

A.6.2 Parallel-distance algorithm

```

1  """
2  Parallel-distance algorithm
3
4  Input Files: simulation box, probe molecule
5
6  output: Txt file containing fractional available volume
7  """
8  #####
9  # Import Libraries as listed in Sire sampling input file
10 #####
11 from MyFunctions import *
12
13 #####
14 #           Main program

```

```
15 #####
16
17 # time counter
18 start_time = time.clock()
19 t = QTime()
20 t.start()
21 # load simulation system
22 (simSystem,boxSpace)= Amber().readCrdTop("box1001.inpcrd","box1001.
    prmtop")
23 print("Number of Molecules in given system %s" % simSystem.nMolecules
    ())
24 simSystem.setName("peg")
25
26 # define system dimensions
27 mincoords = Vector( -150.0, -150.0, -150.0 )
28 maxcoords = Vector( 150.0, 150.0, 150.0)
29 boxSpace = PeriodicBox(mincoords, maxcoords)
30 output_vol = boxSpace.volume().value()
31
32 # load probe molecule
33 (probMolecule, boxSpace1)= Amber().readCrdTop("2k96.inpcrd","2k96.
    prmtop")
34 probMolecule.setName("probMolecule")
35 probMolecule = probMolecule[MolIdx(0)].molecule()
36 probMolecule=probMolecule.edit().renumber().commit()
37 number = probMolecule.number()
38 ResID = probMolecule.residues(ResIdx(0)).residue().name().value()
39
40 # Perform MC simulations to compute the steric clashes
41 print("Running Monte Carlo Simulations over lists of systems")
42 new_system_count_outputs = 0
43 output_of_lists_ratio = []
44 for k in range(1,3):
45     new_systems_list = list_maker_for_multi(4,simSystem, probMolecule,
        boxSpace)
46     n = (len(new_systems_list))
47     total = n*k
48     (accepted_moves,pool) = multi_processing_files(new_systems_list)
49     pool.close()
50     output_of_lists_ratio.append(accepted_moves)
51     new_system_count_outputs = sum(output_of_lists_ratio)/len(
        output_of_lists_ratio)
52     V_free = new_system_count_outputs*output_vol
53     p = new_system_count_outputs
54     std_binom = sqrt(n*p*(1-p))
```

A.6. FRACTIONAL AVAILABLE VOLUMES CALCULATIONS

```
55 error_binom = (output_vol/n)*std_binom
56 error_binom_fraction = error_binom/V_free
57 print ("TOTAL SYSTEM STEPS %d: BINOMIAL ERROR T.VOLUME %s: ERROR F.
        VOLUME %s: ESTIMATED VOLUME %s:" %(total, error_binom,
        error_binom_fraction,p))
58 # Compute the fractional available volumes from ratio of successful to
    total trials and standard deviations
59 new_system_count_outputs = sum(output_of_lists_ratio)/len(
    output_of_lists_ratio)
60 V_free = new_system_count_outputs*output_vol
61 p = new_system_count_outputs
62 std_binom = sqrt(n*p*(1-p))
63 error_binom = (output_vol/n)*std_binom
64 error_binom_fraction = error_binom/V_free
65 print ("FULL SYSTEM STEPS %d: BINOMIAL ERROR T.VOLUME %s: ERROR F.
        VOLUME %s: ESTIMATED VOLUME %s:" %(n,error_binom,
        error_binom_fraction,p))
66 print (new_system_count_outputs)
67 print ("(Done in %d ms)" % t.elapsed())
68 s = t.elapsed()/1000
69 hours, remainder = divmod(s, 3600)
70 minutes, seconds = divmod(remainder, 60)
71 print ('%s h:%s m:%s s' % (hours, minutes, seconds))
72 elapsed = (time.clock() - start_time)/3600
73 print ("(wall time %d h)" % elapsed)
```

A.7 The scaled particle theory

A.7.1 findcurvature.m

```

1 function [curvrad,Area,vi] = findcurvature_cav(x1,y1,z1);
2 %% Function to calculate the radius of curvature, volume and surface
   area of any arbitrarily shaped macromolecule
3 %inputs: x1,y1,z1 are coordinates of given macromolecules
4 %output: radius of curvature, surface area & volume
5
6 %% Step 1: Formation of convexhull to determine vertices k of
   convexhull and vol.
7
8
9     X = [x1;y1;z1]; % matrix of coordinates
10    %dt = DelaunayTri(x1,y1,z1)
11    dt = delaunayTriangulation(x1,y1,z1);
12    [K v] = convexHull(dt) ;
13    size (K);
14    kk = unique([K(:,1);K(:,2);K(:,3)]);
15    pt = dt.Points(kk,:);
16    size(pt);
17    pt11 = dt.Points(K(:,1));
18    pt21 = dt.Points(K(:,2));
19    pt31 = dt.Points(K(:,3));
20
21    figure
22    F = trisurf(K, dt.Points(:,1),dt.Points(:,2),dt.Points(:,3), '
       FaceColor', 'cyan');
23    vi = v*(10^-10)^3;
24    %K gives the vertices of each triangle which generate coordinates
       by dt.X(point,range) i.e.dt.X(4864,1:3)and for full list is
       get by pt1=dt.X9K(:,1),1:3) here :,1 means all rows of first
       column and 1:3 mean 1 to 3 column range.
25
26 %% Step 2: Area of a 3D triangle
27    %Computes area of the 3D triangle whose vertices are given by pt1,
       pt2 and pt3.
28
29    pt1 = dt.Points(K(:,1),1:3);
30    pt2 = dt.Points(K(:,2),1:3);
31    pt3 = dt.Points(K(:,3),1:3);
32
33    if nargin == 1
34    pt2 = pt1(2,:);
35    pt3 = pt1(3,:);

```

```

36     pt1 = pt1(1,:);
37     end
38
39 % compute individual vectors
40 v12 = bsxfun(@minus, pt2, pt1);
41 v13 = bsxfun(@minus, pt3, pt1);
42
43 % compute area from cross product
44 Area = (sum(vectorNorm3d(cross(v12, v13, 2)) / 2))*(10^-10)^2;
45
46 %% Step 3: Calculation of radius of curvature
47
48 % Reference: Coleman, R. G.; Burr, M. A.; Souvaine, D. L.; Cheng, A.
49 % C., An intuitive approach to measuring protein surface curvature
50 % . Proteins 2005, 61 (4), 1068-74.
51 %%
52 %% Step 3 has two major sections , (1,2) while second section has
53 % eight(a-h)steps.
54
55 %% Section 1: Define a set of points to find the least sum of squares
56 % sphere.
57 % set of all points from convex hull (P = K -> pt1,pt2,pt3)
58 % P = [pt11,pt21,pt31]; % Set of all convexhull points
59 %P = [pt1(:,1),pt2(:,2),pt3(:,3)]; % Previous set of points used
60 % for calculations
61 P = [pt(:,1),pt(:,2),pt(:,3)]; % points from unique set of K
62
63 %% Section 2 : For each point pi belongs to P where pi is one row
64 % vector from P.
65
66 s = size(P,1); %size of matrix
67 for i=1:s
68     pit = [P(i,:)] ; %set of pi = p,q,r points from P
69     %matrix
70     Px = [P(1:i-1,:);P(i+1:s,:)]; % corresponding Rest of points in
71     % P excluding p,q,r
72
73 %% Sec. 2 : (a) Let pi be the inversion point p,q,r and Px points be
74 % all other points in P .
75 % define the p,q,r points of pi row as Sp,Sq,Sr
76 % define the points xi, yi, zi of Px matrix as SPx, SPy, SPz
77
78 sPx = size(Px,1); % size of Px matrix
79 Sp = pit(1); %p point

```

```

72         Sq = pit(2) ; % q point
73         Sr = pit(3); %r point
74         for k = 1:sPx;
75             SPx = Px(k,1); % xi points
76             SPy = Px(k,2); % yi points
77             SPz = Px(k,3); % zi points
78
79 %% Sec. 2 : (b) Invert Px = xi,yi,zi points using the inversion defined
           in the methods to generate ti = Xi,Yi,Zi points %%
80     %Inversive transformation formula given as Xi, Yi, Zi. This will
           give a matix of ti points with respect to each pi point
81
82             K = 1;
83             Xi = K^2*(SPx-Sp)/((SPx-Sp)^2+(SPy-Sq)^2+(SPz-Sr)^2)+
                Sp;
84             Yi = K^2*(SPy-Sq)/((SPx-Sp)^2+(SPy-Sq)^2+(SPz-Sr)^2)+
                Sq;
85             Zi = K^2*(SPz-Sr)/((SPx-Sp)^2+(SPy-Sq)^2+(SPz-Sr)^2)+
                Sr;
86             ti(k,:) = [Xi Yi Zi];
87             tix = ti(:,1);
88             tiy = ti(:,2);
89             tiz = ti(:,3);
90         end
91 %% Sec. 2 : (c)Find the least sum of squares plane fit to the points ti
           .
92     % Fit the plane to the ti points by using affine_fit function to get
           normal vector n_plane and point (u) p_plane.
93
94             Cmtx = cov(ti);
95             [V, LAMBDA] = eig(Cmtx);
96             %the mean of the samples belongs to the plane
97             p_plane = mean(ti,1);
98             %The samples are reduced:
99             R = bsxfun(@minus,ti,p_plane);
100            %Computation of the principal directions if the samples
                cloud
101            [V,D] = eig(R'*R);
102            %Extract the output from the eigenvectors
103            n_plane = V(:,1);
104            nplanex = n_plane(1,1);
105            nplaney = n_plane(2,1);
106            nplanez = n_plane(3,1);
107            V = V(:,2:end);
108

```

```

109 %% Sec. 2 : (d) Find the point on the plane closest to pi . Call this
    point a .
110 % we have already normal vector(gives a,b,c) and point on plane(
    gives u -> x0,y0,z0) .
111 %Method 1:
112 %Equation of plane ax+by+cz = ax0 +by0+cz0=Kappa point
    on plane close to pi
113 %xi = pix+zeta*a
114 %yi = piy+zeta*b
115 %zi = piz+zeta*c
116 %to calculate zeta=
117 %a(pix+zeta*a)+b(piy+zeta*b)+c(piz+zeta*c)=kappa
118 %plugin the zeta value in xi,yi,zi equation to get
    the
119 %coodrinates of point on plane close to pi.
120 Kappa = n_plane(1,1)*p_plane(1,1)+n_plane(2,1)*
    p_plane(1,2)+n_plane(3,1)*p_plane(1,3);
121 %n_plane(1,1)*(pi(1,1)+zeta*n_plane(1,1))+n_plane
    (2,1)*(pi(1,2)+zeta*n_plane(2,1))+n_plane(3,1)*(
    piz+zeta*n_plane(3,1))
122 zeta =Kappa-((n_plane(1, 1)*pit(1, 1)+n_plane(2, 1)*
    pit(1, 2)+n_plane(3, 1)*pit(1, 3)*(n_plane(1, 1)
    ^2+n_plane(2, 1)^2+n_plane(3, 1)^2));
123 a1 = [pit(1,1)+zeta*n_plane(1, 1),pit(1,2)+zeta*
    n_plane(2,1),pit(1,3)+zeta*n_plane(3,1)] ;
124
125
126 %Method 2:
127
128
129 normal_row = [nplanex nplaney nplanez];
130 B = dot(normal_row,normal_row);
131 d = p_plane-pit;
132 % proj_nd = (n.d/n.n)*n = (C/B)*n
133 C = dot(normal_row,d);
134 proj_nd = (C/B)*normal_row;
135 a = proj_nd+pit;
136
137 %% Sec. 2 : (e) Transform a using the inversion defined in the methods
    to generate a-prime=tia .
138
139 %Define a as;
140 xia = a(1,1);
141 yia = a(1,2);
142 zia = a(1,3);

```

```

143     % inversive transformation of cls_a which is a points
144     Xia = K^2*(xia-Sp)/((xia-Sp)^2+(yia-Sq)^2+(zia-Sr)^2)
        +Sp;
145     Yia = K^2*(yia-Sq)/((xia-Sp)^2+(yia-Sq)^2+(zia-Sr)^2)
        +Sq;
146     Zia = K^2*(zia-Sr)/((xia-Sp)^2+(yia-Sq)^2+(zia-Sr)^2)
        +Sr;
147     tia = [Xia Yia Zia]; %vector of inversive a vector
148     tiax = tia(1,1);
149     tiay = tia(1,2);
150     tiaz = tia(1,3);
151 %% Sec. 2 : (f) Define the sphere center, ci , as the average of pi and
        tia .
152
153     ci=[(pit+tia)/2];
154 %% Sec. 2 : (g)Define the radius for the sphere given center ci
155     ri=norm(pit-tia)/2;
156
157 %% Sec. 2 : (h) If the least sum of squares is lower than the previous
        best fit, keep ci and the radius.
158     error1=0;
159     for k = 1:sPx
160
161         error1 = error1+(sqrt((Px(k,1)-ci(1,1))^2+(Px(k,2)-ci(1,2))^2+(Px(k,3)-ci(1,3))^2)-ri)^2;
162
163     end
164     error1;
165     if i==1
166         smallest_error = error1;
167         best_ci=ci;
168         best_ri=ri;
169     elseif error1<smallest_error;
170         smallest_error = error1;
171         best_ci=ci;
172         best_ri=ri;
173     end
174 %% Sec. 3 : Output the best found center and radius.
175     curvrad = best_ri*10^-10; %conversion from Angstrom to meters
176
177 end
178
179 end

```

A.7.2 findactivity.m

```

1 function [Y,mu] = findactivity(N,Vi,Rad,area,vcell)
2 % calculation of activity coefficients of given molecules under
   different concentration of crowders of different sizes and shapes
3 %Inputs Geometric parameters (Rs,Rc,As,Ac,vs,vc) are the radius, area,
   volume of under study and crowder molecule
4 %vcell volume of cell compartment containg reagents and crowder
   molecules. these are calculated by findcurvature.m function
5 %Ni(number of crowder molecules; values vary over a wide range,exmple,
   3000:6000 or 3000:100:6000)
6 %outputs :
7 %Y fraction volume occupancy,
8 %mu chemical potential
9
10 %% 2-calculation of chemical potential
11 % Vi,di,Ai,Bi,Ci,Yi individual molecule componenets,while d,A,B,C,Y are
   the sum of individual components to compute mu(chemical pot.)
12 %N1=1; Input N1 as part of N. It could be any number, not necessarily
   1. This could matter for really bulky solutes like ribosomes.
13
14         di = N/vcell;
15         Ai = Rad.*di;
16         Bi = area.*di;
17         Ci = Rad.^2.*di;
18         Yi = Vi.*di;
19         d = sum(di);
20         A = sum(Ai);
21         B = sum(Bi);
22         C = sum(Ci);
23         Y = sum(Yi);
24         mu= [(-log(1-Y)+B*Rad(1,1)/(1-Y)+4*pi*A*Rad(1,1)
               ^2/(1-Y)+B^2*Rad(1,1)^2/(2*(1-Y)^2)+(4*pi*(1/3))
               *(d/(1-Y)+B^2*C/(3*(1-Y)^3)+A*B/(1-Y)^2)*Rad
               (1,1)^3)];
25 end

```

A.7.3 The SPT main program

```

1 %% script to apply extended scaled particle theory to determine the
   chemical potential and standard devi. using all MD optimized and
   non-optimized simulation boxes
2 clc;
3 clear;
4

```

```

5 % conformational pair
6 probe1 = '1ake.pdb';
7 probe2 = '4ake.pdb';
8 %-----%
9 % Input coordinates of cell compartment containing all species to its
   determine volume 'vcell'.
10 side_length = 3.01*10^-8; % side of box in meters
11 cell_volume= side_length^3 ;%input('Enter volum of cell compartment');
12 %-----%
13 % extract coordinates of conformational pair molecules and subsequently
   calculate the geometrical parameters through convex-hull algorithm
14 cor = pdb2mat(probe1);
15 cor2 = pdb2mat(probe2);
16 x1 = (cor.X)';
17 y1 = (cor.Y)';
18 z1 = (cor.Z)';
19 [Rs1 As1 vs1] = findcurvature_cav2(x1,y1,z1);
20 x1 = (cor2.X)';
21 y1 = (cor2.Y)';
22 z1 = (cor2.Z)';
23 [Rs2 As2 vs2] = findcurvature_cav2(x1,y1,z1);
24
25 % dgk represents the number of copies of crowded media at each
   concentration
26 for dgk = 1:4
27 box =dgk;
28 num = num2str(box)
29 filename1 = strcat('box',num,probe1(1:4),'.txt')
30 filename2 = strcat('box',num,probe2(1:4),'.txt')
31 %-----%
32
33 %Rs2 = 2*Rs2;
34
35
36 % System 1-- PEG-25 -- 0.1 g/ml
37
38 dirs = sprintf('peg25/box');
39 for b = 1:box
40 list_of_file1 = generate_list(dirs,b) ;
41 [radius, area,vi] = crowderParameters2(list_of_file1,b,dirs);
42 range = length(list_of_file1);
43 [Ycp1 mucp1] = thermodynamics(radius, area,vi,Rs1, As1, vs1,cell_volume
   ,range);
44 fprintf('System %s thermodynamics is done \n',probe1)

```

```
45 [Ycp2 mucp2] = thermodynamics(radius, area,vi,Rs2, As2, vs2,cell_volume
    ,range);
46 fprintf('System %s thermodynamics is done \n',probe2)
47 Ycp1boxes(b) = Ycp1;
48 mucp1boxes(b)= mucp1;
49 Ycp2boxes(b) = Ycp2;
50 mucp2boxes(b)= mucp1;
51 end
52
53 % System 2-- PEG-50 -- 0.2 g/ml
54
55 dirs50 = sprintf('peg50/box');
56 for b = 1:box
57 list_of_file1 = generate_list(dirs50,b) ;
58 [radius50, area50,vi50] = crowderParameters2(list_of_file1,b,dirs50);
59 range50 = length(list_of_file1);
60 [Ycp1_50 mucp1_50] = thermodynamics(radius50, area50,vi50,Rs1, As1, vs1
    ,cell_volume,range50);
61 fprintf('System %s thermodynamics is done \n',probel)
62 [Ycp2_50 mucp2_50] = thermodynamics(radius50, area50,vi50,Rs2, As2, vs2
    ,cell_volume,range50);
63 fprintf('System %s thermodynamics is done \n',probe2)
64 Ycp1_50boxes(b) = Ycp1_50;
65 mucp1_50boxes(b)= mucp1_50;
66 Ycp2_50boxes(b) = Ycp2_50;
67 mucp2_50boxes(b)= mucp2_50;
68 end
69
70 % System 3-- PEG-75 -- 0.3 g/ml
71
72 dirs75 = sprintf('peg75/box');
73 for b = 1:box
74 list_of_file1 = generate_list(dirs75,b) ;
75 [radius75, area75,vi75] = crowderParameters2(list_of_file1,b,dirs75);
76 range75 = length(list_of_file1);
77 [Ycp1_75 mucp1_75] = thermodynamics(radius75, area75,vi75,Rs1, As1, vs1
    ,cell_volume,range75);
78 fprintf('System %s thermodynamics is done \n',probel)
79 [Ycp2_75 mucp2_75] = thermodynamics(radius75, area75,vi75,Rs2, As2, vs2
    ,cell_volume,range75);
80 fprintf('System %s thermodynamics is done \n',probe2)
81 Ycp1_75boxes(b) = Ycp1_75;
82 mucp1_75boxes(b)= mucp1_75;
83 Ycp2_75boxes(b) = Ycp2_75;
84 mucp2_75boxes(b)= mucp2_75;
```

```
85 end
86
87 % System 4-- PEG-100 -- 0.4 g/ml
88
89 dirs100 = sprintf('peg100/box');
90 for b = 1:box
91 list_of_file1 = generate_list(dirs100,b);
92 [radius100, areal100,vi100] = crowderParameters2(list_of_file1,b,dirs100
    );
93 range100 = length(list_of_file1);
94 [Ycp1_100 mucp1_100] = thermodynamics(radius100, areal100,vi100,Rs1, As1
    , vs1,cell_volume,range100);
95 fprintf('System %s thermodynamics is done \n',probe1)
96 [Ycp2_100 mucp2_100] = thermodynamics(radius100, areal100,vi100,Rs2, As2
    , vs2,cell_volume,range100);
97 fprintf('System %s thermodynamics is done \n',probe2)
98 Ycp1_100boxes(b) = Ycp1_100;
99 mucp1_100boxes(b)= mucp1_100;
100 Ycp2_100boxes(b) = Ycp2_100;
101 mucp2_100boxes(b)= mucp2_100;
102 end
103
104 % System 5-- PEG-125 -- 0.5 g/ml
105
106 dirs125 = sprintf('sample5/box');
107 for b = 1:box
108 list_of_file1 = generate_list(dirs125,b);
109 [radius125, areal125,vi125] = crowderParameters2(list_of_file1,b,dirs125
    );
110 range125 = length(list_of_file1);
111 [Ycp1_125 mucp1_125] = thermodynamics(radius125, areal125,vi125,Rs1, As1
    , vs1,cell_volume,range125);
112 fprintf('System %s thermodynamics is done \n',probe1)
113 [Ycp2_125 mucp2_125] = thermodynamics(radius125, areal125,vi125,Rs2, As2
    , vs2,cell_volume,range125);
114 fprintf('System %s thermodynamics is done \n',probe2)
115 Ycp1_125boxes(b) = Ycp1_125;
116 mucp1_125boxes(b)= mucp1_125;
117 Ycp2_125boxes(b) = Ycp2_125;
118 mucp2_125boxes(b)= mucp2_125;
119 end
120
121 % System 6-- PEG-150 -- 0.6 g/ml
122
123 dirs150 = sprintf('samples6/box');
```

```

124 for b = 1:box
125 list_of_file1 = generate_list(dirs150,b);
126 [radius150, area150,vi150] = crowderParameters2(list_of_file1,b,dirs150
    );
127 range150 = length(list_of_file1);
128 [Ycp1_150 mucp1_150] = thermodynamics(radius150, area150,vi150,Rs1, As1
    , vs1,cell_volume,range150);
129 fprintf('System %s thermodynamics is done \n',probe1)
130 [Ycp2_150 mucp2_150] = thermodynamics(radius150, area150,vi150,Rs2, As2
    , vs2,cell_volume,range150);
131 fprintf('System %s thermodynamics is done \n',probe2)
132
133 Ycp1_150boxes(b) = Ycp1_150;
134 mucp1_150boxes(b)= mucp1_150;
135 Ycp2_150boxes(b) = Ycp2_150;
136 mucp2_150boxes(b)= mucp2_150;
137 end
138 %-----
139
140 % collect chemical potentials and fraction of occupied volumes
141 %% Figure section
142 std_chem1 = [std(mucp1boxes) std(mucp1_50boxes) std(mucp1_75boxes)
    std(mucp1_100boxes) std(mucp1_125boxes) std(mucp1_150boxes)];
143 std_chem2 = [std(Ycp1boxes) std(Ycp1_50boxes) std(Ycp1_75boxes) std(
    Ycp1_100boxes) std(Ycp1_125boxes) std(Ycp1_150boxes)];
144 chem1_all = [mean(mucp1boxes) mean(mucp1_50boxes) mean(mucp1_75boxes
    ) mean(mucp1_100boxes) mean(mucp1_125boxes) mean(mucp1_150boxes)
    ];
145 exc1_all = [mean(Ycp1boxes) mean(Ycp1_50boxes) mean(Ycp1_75boxes)
    mean(Ycp1_100boxes) mean(Ycp1_125boxes) mean(Ycp1_150boxes)];
146 chem2_all = [mean(mucp2boxes) mean(mucp2_50boxes) mean(mucp2_75boxes
    ) mean(mucp2_100boxes) mean(mucp2_125boxes) mean(mucp2_150boxes)
    ];
147 exc2_all = [mean(Ycp2boxes) mean(Ycp2_50boxes) mean(Ycp2_75boxes)
    mean(Ycp2_100boxes) mean(Ycp2_125boxes) mean(Ycp2_150boxes)];
148
149 % write the files
150
151 writeFile(filename1,exc1_all',std_chem1',chem1_all')
152
153 writeFile(filename2,exc2_all',std_chem2',chem2_all')
154
155 end
156
157 peg = [0.1:0.1:0.6];

```

```

158
159 % chemical potential
160 h= figure;
161 plot(peg(~isnan(peg)),chem1_all(~isnan(peg)),'o-',peg(~isnan(peg)),
      chem2_all(~isnan(peg)),'ro-','LineWidth',3) ; % 'MarkerSize', 8
162 %hold on
163 %errorbar(peg(~isnan(peg)),vol_r(~isnan(peg)),p2k96std)
164 set(gca,'FontName','Times')
165 set(gca,'LineWidth',3);
166 set(gca,'FontSize',20);
167 xlabel('Concentration g/cc','interpreter','latex')
168 ylabel('\mu','interpreter','latex')
169 %title('Frac. avail. vol. in Single, Random and Random (after equi.)
      PEG conformations by MC simulations')
170 legend(probe1,probe2,'Location','southeast')
171 legend boxoff
172 set(gca,'LineWidth',3);
173 set(gca,'FontSize',22);
174 %axis ([0.1 0.6 0 0.9])
175 what = 'chem_pot';
176 directory = 'article1_thesis_plots/';
177 name = [ directory probe1(1:4) probe2(1:4) what];
178 print(h, '-dpng',name)
179
180
181
182 % excluded volumes
183 h= figure;
184 plot(peg(~isnan(peg)),excl_all(~isnan(peg)),'o-',peg(~isnan(peg)),
      exc2_all(~isnan(peg)),'ro-','LineWidth',3) ; % 'MarkerSize', 8
185 %hold on
186 %errorbar(peg(~isnan(peg)),vol_r(~isnan(peg)),p2k96std)
187 set(gca,'FontName','Times')
188 set(gca,'LineWidth',3);
189 set(gca,'FontSize',20);
190 xlabel('Concentration g/cc','interpreter','latex')
191 ylabel('\phi','interpreter','latex')
192 %title('Frac. avail. vol. in Single, Random and Random (after equi.)
      PEG conformations by MC simulations')
193 legend(probe1,probe2,'Location','southeast')
194 legend boxoff
195 set(gca,'LineWidth',3);
196 set(gca,'FontSize',22);
197 %axis ([0.1 0.6 0 0.9])
198 what = 'exc_vol';

```

```

199 directory = 'article1_thesis_plots/';
200 name = [ directory probe1(1:4) probe2(1:4) what];
201 print(h, '-dpng',name)
202
203
204 % total free energy change and stable conformation
205 con1 = [chem1_all-chem2_all];
206 con2 = [chem2_all-chem1_all];
207 h= figure;
208 plot(peg(~isnan(peg)),con1(~isnan(peg)),'o-','LineWidth',3) ; % '
    MarkerSize', 8
209 %hold on
210 %errorbar(peg(~isnan(peg)),vol_r(~isnan(peg)),p2k96std)
211 set(gca,'FontName','Times')
212 set(gca,'LineWidth',3);
213 set(gca,'FontSize',20);
214 xlabel('Concentration g/cc','interpreter','latex')
215 ylabel('ΔG','interpreter','latex')
216 %title('Frac. avail. vol. in Single, Random and Random (after equi.)
    PEG conformations by MC simulations')
217 legend(probe1,'Location','southeast')
218 legend boxoff
219 set(gca,'LineWidth',3);
220 set(gca,'FontSize',22);
221 %axis ([0.1 0.6 0 0.9])
222 what = 'Free_energy';
223 directory = 'article1_thesis_plots/';
224 name = [ directory probe1(1:4) what];
225 print(h, '-dpng',name)
226
227
228 h= figure;
229 plot(peg(~isnan(peg)),con2(~isnan(peg)),'ro-','LineWidth',3) ; % '
    MarkerSize', 8
230 %hold on
231 %errorbar(peg(~isnan(peg)),vol_r(~isnan(peg)),p2k96std)
232 set(gca,'FontName','Times')
233 set(gca,'LineWidth',3);
234 set(gca,'FontSize',20);
235 xlabel('Concentration g/cc','interpreter','latex')
236 ylabel('ΔG','interpreter','latex')
237 %title('Frac. avail. vol. in Single, Random and Random (after equi.)
    PEG conformations by MC simulations')
238 legend(probe2,'Location','southeast')
239 legend boxoff

```

```
240 set(gca, 'LineWidth', 3);
241 set(gca, 'FontSize', 22);
242 %axis ([0.1 0.6 0 0.9])
243 what = 'Free_energy';
244 directory = 'article1_thesis_plots/';
245 name = [ directory probe2(1:4) what];
246 print(h, '-dpng', name)
```

A.8 TST main program

```

1 %
  %%%%%%%%%%%%%%%%%%%%%%%%%%%%%%%%%%%%%%%%%%%%%%%%%%%%%%%%%%
2 %
3 %   Kinetics of conformational equilibrium
4 %
5 %
  %%%%%%%%%%%%%%%%%%%%%%%%%%%%%%%%%%%%%%%%%%%%%%%%%%%%%%%%%%
6
7 clc;
8 clear;
9
10 % load pdb structures of crowder, reactant, product and transition
    state
11 crowder = 'pegmd.pdb';
12 probe1 = 'unfold.pdb'
13 probe2 = 'fold.pdb';
14 tst_state = 'tsRNA.pdb';
15 %peg = 0.1:0.1:0.6;
16
17 % import rate experimental constant
18 kexdata = importdata('kexdata.txt');
19 concent_x = kexdata(:,2)';
20 k_ideal = kexdata(:,1)';
21
22 % call function to estimate the folding rate constant
23 [k_final1,k_final2] = tst_rate(k_ideal,probe1,probe2,crowder,tst_state)
    ;
24
25 % Comparison of experimental and theoretical folding rate constants
26 h= figure;
27 plot(concent_x,k_final1,'-*','LineWidth', 3);
28 hold on
29 plot(concent_x,k_ideal,'-d','LineWidth', 3);
30 set(gca,'FontName', 'Times')
31 set(gca, 'LineWidth', 3);
32 set(gca,'FontSize', 20);
33 xlabel('\%PEG (w/w)','interpreter','latex')
34 ylabel('$k_{1} s^{-1}$','interpreter','latex')
35 %ylabel('k','interpreter','latex')
36 %title('Frac. avail. vol. in Single, Random and Random (after equ.)
    PEG conformations by MC simulations')

```

```
37 legend('TST','Expt.','location','southeast')
38 legend boxoff
39 set(gca,'LineWidth',3);
40 set(gca,'FontSize',22);
41 filename = strcat('kinetics_plots/kinetics_',probel(1:4));
42 print(h,'-dpng','kinetics_plots/mu_nonEqui2KNA')
```

```
1 function [k_final1,k_final2] = tst_rate(k_ideal,probel,probe2,crowder
    ,tst_state)
2
3 % function to determine the final kinetic rate
4
5 % step 1. calculate the chemical potentials of conformational pair and
    its
6 % transition state.
7
8 [mu1, m] = spt_org_vs_ext_mu_calculations(probel, crowder);
9 [mu2, m] = spt_org_vs_ext_mu_calculations(probe2, crowder);
10 [mu3, m] = spt_org_vs_ext_mu_calculations(tst_state, crowder);
11 mu1 = mu1(8:8:50);
12 mu2 = mu2(8:8:50);
13 mu3 = mu3(8:8:50);
14 % step2. convert chemical potential to activity coefficients
15 gamma1 = exp(mu1)
16 gamma2 = exp(mu2)
17 gammatst = exp(mu3)
18
19 % step3. tst final rate calculations k = k_ideal(
    activity_coefficient_probel/activity_coefficient_tst_state)
20
21 k_final1 = k_ideal(1,1)*(gamma1./gammatst)
22 k_final2 = k_ideal(1,1)*(gamma2./gammatst)
23
24 end
```

Appendix B

Construction of crowded medium appendix

B.1 PEG with a methyl terminal

B.1.1 FF libraries for 'A' fragment

```
1 #
2 # Generated by PyRED version SEP-2015
3 #   http://q4md-forcefieldtools.org
4 #
5 @<TRIPOS>MOLECULE
6 F01
7   11   10   1   0   1
8 SMALL
9 USER_CHARGES
10 @<TRIPOS>ATOM
11   1 C1   -2.370830 -0.184098  0.000006 CT  1   F01 -0.4499 0.0000 ****
12   2 H11  -3.164666  0.567675  0.000013 H1  1   F01  0.1575 0.0000 ****
13   3 H12  -2.481280 -0.820832  0.892855 H1  1   F01  0.1575 0.0000 ****
14   4 H13  -2.481284 -0.820824 -0.892854 H1  1   F01  0.1575 0.0000 ****
15   5 O    -1.141292  0.507437  0.000007 OS  1   F01 -0.1875 0.0000 ****
16   6 C2   -0.025639 -0.360464 -0.000008 CT  1   F01  0.2409 0.0000 ****
17   7 H21  -0.027678 -1.012405 -0.889175 H1  1   F01  0.0469 0.0000 ****
18   8 H22  -0.027676 -1.012432  0.889144 H1  1   F01  0.0469 0.0000 ****
19   9 C3    1.229623  0.498292  0.000007 CT  1   F01 -0.5486 0.0000 ****
20  10 H31    1.221070  1.147076  0.889147 H1  1   F01  0.2007 0.0000 ****
21  11 H32    1.221067  1.147105 -0.889118 H1  1   F01  0.2007 0.0000 ****
22 @<TRIPOS>BOND
23   1     1     2  1
24   2     1     3  1
25   3     1     4  1
26   4     1     5  1
27   5     5     6  1
28   6     6     7  1
29   7     6     8  1
```

```

30      8      6      9  1
31      9      9     10  1
32     10      9     11  1
33 @<TRIPOS>SUBSTRUCTURE
34      1 F01          1 ****          0 **** ****
35 @<TRIPOS>HEADTAIL
36 0 0
37 C3 1
38 @<TRIPOS>RESIDUECONNECT
39 1 0 C3 0 0 0 0

```

B.1.2 FF libraries for 'B' fragment

```

1 #
2 # Generated by PyRED version SEP-2015
3 #   http://q4md-forcefieldtools.org
4 #
5 @<TRIPOS>MOLECULE
6 F02
7      7      6      1      0      1
8 SMALL
9 USER_CHARGES
10 @<TRIPOS>ATOM
11  1 O      -1.141292  0.507437  0.000007 OS 1  F02 -0.1875 0.0000 ****
12  2 C2     -0.025639 -0.360464 -0.000008 CT 1  F02  0.2409 0.0000 ****
13  3 H21    -0.027678 -1.012405 -0.889175 H1 1  F02  0.0469 0.0000 ****
14  4 H22    -0.027676 -1.012432  0.889144 H1 1  F02  0.0469 0.0000 ****
15  5 C3      1.229623  0.498292  0.000007 CT 1  F02 -0.5486 0.0000 ****
16  6 H31      1.221070  1.147076  0.889147 H1 1  F02  0.2007 0.0000 ****
17  7 H32      1.221067  1.147105 -0.889118 H1 1  F02  0.2007 0.0000 ****
18 @<TRIPOS>BOND
19  1      1      2  1
20  2      2      3  1
21  3      2      4  1
22  4      2      5  1
23  5      5      6  1
24  6      5      7  1
25 @<TRIPOS>SUBSTRUCTURE
26      1 F02          1 ****          0 **** ****
27 @<TRIPOS>HEADTAIL
28 0 1
29 C3 1
30 @<TRIPOS>RESIDUECONNECT
31 1 0 C3 0 0 0 0

```

B.1.3 FF libraries for 'C' fragment

```

1 # Generated by PyRED version SEP-2015
2 #   http://q4md-forcefieldtools.org
3 #
4 @<TRIPOS>MOLECULE
5 F00
6   9   8   1   0   1
7 SMALL
8 USER_CHARGES
9 @<TRIPOS>ATOM
10  1 O   -1.141292  0.507437  0.000007 OS  1  F00 -0.1875 0.0000 ****
11  2 C2  -0.025639 -0.360464 -0.000008 CT  1  F00  0.2409 0.0000 ****
12  3 H21 -0.027678 -1.012405 -0.889175 H1  1  F00  0.0469 0.0000 ****
13  4 H22 -0.027676 -1.012432  0.889144 H1  1  F00  0.0469 0.0000 ****
14  5 C3   1.229623  0.498292  0.000007 CT  1  F00 -0.5486 0.0000 ****
15  6 H31   1.221070  1.147076  0.889147 H1  1  F00  0.2007 0.0000 ****
16  7 H32   1.221067  1.147105 -0.889118 H1  1  F00  0.2007 0.0000 ****
17  8 O4    2.340493 -0.390181 -0.000010 OH  1  F00 -0.4160 0.0000 ****
18  9 H41   3.147923  0.144212 -0.000016 HO  1  F00  0.3934 0.0000 ****
19 @<TRIPOS>BOND
20  1   1   2  1
21  2   2   3  1
22  3   2   4  1
23  4   2   5  1
24  5   5   6  1
25  6   5   7  1
26  7   5   8  1
27  8   8   9  1
28 @<TRIPOS>SUBSTRUCTURE
29   1 F00          1 ****          0 **** ****
30 @<TRIPOS>HEADTAIL
31 0 1
32 0 0
33 @<TRIPOS>RESIDUECONNECT
34 1 0 0 0 0 0 0

```

B.1.4 FF parameters for PEG-M

```

1 FRCMOD file generated by PyRED version SEP-2015 - q4md-forcefieldtools
   .org
2 MASS      mass           pol           Source
3 CT        12.010         0.878        taken from parm10.dat
4 H1        1.008          0.135        taken from parm10.dat
5 HO        1.008          0.135        taken from parm10.dat

```

B.1. PEG WITH A METHYL TERMINAL

```

6 OH      16.000      0.465      taken from parm10.dat
7 OS      16.000      0.465      taken from parm10.dat
8
9 BOND    K(kcal.mol-1.ang-2) Dist0(ang) Source
10 CT-CT  310.0        1.526      taken from parm10.dat
11 CT-H1  340.0        1.090      taken from parm10.dat
12 CT-OH  320.0        1.410      taken from parm10.dat
13 CT-OS  320.0        1.410      taken from parm10.dat
14 HO-OH  555.0          0.960      adapted from parm10.dat 553.0
15
16 ANGLE   K(kcal.mol-1.rad-2) Theta0(deg) Source
17 CT-CT-H1  50.0        109.50     taken from parm10.dat
18 CT-CT-OH  50.0        109.50     taken from parm10.dat
19 CT-CT-OS  50.0        109.50     taken from parm10.dat
20 H1-CT-H1  35.0        109.50     taken from parm10.dat
21 H1-CT-OH  50.0        109.50     taken from parm10.dat
22 H1-CT-OS  50.0        109.50     taken from parm10.dat
23 CT-OH-HO  55.0        108.50     taken from parm10.dat
24 CT-OS-CT  60.0        109.50     taken from parm10.dat
25
26 DIHEDRAL Path V(kcal.mol-1.rad-1) Phase(deg.) Period Source
27 H1-CT-CT-H1 1 1.55555556e-01 0.0 3. adapted from parm10.
   dat i.e X-CT-CT-X 1.4/9
28 H1-CT-CT-OH 1 0.00000000e+00 0.0 -3. taken from parm10.
   dat
29 H1-CT-CT-OH 1 2.50000000e-01 0.0 1. taken from parm10.
   dat
30 H1-CT-CT-OS 1 0.00000000e+00 0.0 -3. taken from parm10.
   dat
31 H1-CT-CT-OS 1 2.50000000e-01 0.0 1. taken from parm10.
   dat
32 OH-CT-CT-OS 1 1.44000000e-01 0.0 -3. taken from parm10.
   dat
33 OH-CT-CT-OS 1 1.17500000e+00 0.0 2. taken from parm10.
   dat
34 CT-CT-OH-HO 1 1.60000000e-01 0.0 -3. taken from parm10.
   dat
35 CT-CT-OH-HO 1 2.50000000e-01 0.0 1. taken from parm10.
   dat
36 H1-CT-OH-HO 1 1.66666667e-01 0.0 3. adapted from parm10.
   dat i.e X-CT-OH-X 0.5/3
37 CT-CT-OS-CT 1 3.83000000e-01 0.0 -3. taken from parm10.
   dat
38 CT-CT-OS-CT 1 1.00000000e-01 180.0 2. taken from parm10.
   dat

```

```

39 H1-CT-OS-CT 1 3.83333333e-01 0.0 3. adapted from parm10.
    dat i.e X-CT-OS-X 1.15/3
40
41 IMPROPER          V(kcal.mol-1.rad-1) Phase(deg.) Period Source
42
43 NONBON          R*(ang) Eps(kcal.mol-1) Source
44 CT              1.9080 0.10940000 taken from parm10.dat
45 H1              1.3870 0.01570000 taken from parm10.dat
46 HO              0.0000 0.00000000 taken from parm10.dat
47 OH              1.7210 0.21040000 taken from parm10.dat
48 OS              1.6837 0.17000000 taken from parm10.dat

```

B.1.5 Fitting statistics of a whole molecule approach

```

1
2 -----
3   Restrained ESP Fit 2.4 q4md-forcefieldtools
4 -----
5   RESP-A1 - RESP input generated by PyRED version SEP-2015
6 -----
7
8
9   inopt      = 0   ioutopt   = 1
10  nmep       = 2   iqopt     = 2
11  ihfree     = 1   irstrnt   = 1
12  iunits     = 0   qwt       = 0.00100000
13
14  multiple-MEP run of 2 MEP
15
16  Reading input for MEP 1 weight: 1.000
17  PEG nconf=1 norient=1 nmep=1/2
18
19  Total charge (ich): 0
20  Number of centers: 13
21     1   6   0
22     2   1   0
23     3   1   2
24     4   1   2
25     5   8  -1
26     6   6   0
27     7   1   0
28     8   1   7
29     9   6   0
30    10   1   0
31    11   1  10

```

```

32    12    8   -1
33    13    1   -1
34
35 Reading input for MEP 2 weight: 1.000
36 PEG nconf=1 norient=2 nmep=2/2
37
38 Total charge (ich): 0
39 Number of centers: 13
40    14    6    0
41    15    1    0
42    16    1    2
43    17    1    2
44    18    8   -1
45    19    6    0
46    20    1    0
47    21    1    7
48    22    6    0
49    23    1    0
50    24    1   10
51    25    8   -1
52    26    1   -1
53     1    1    1    2    1    3    1    4
54 since IQOPT>1, 26 new q0 values
55 will be read in from file ESP.Q0 (unit 3)
56 -----
57 reading mult_esp constraint info
58 -----
59     1    1    2    1
60     1    2    2    2
61     1    6    2    6
62     1    7    2    7
63     1    9    2    9
64     1   10    2   10
65
66 -----
67     Atom  Ivary
68 -----
69     6    0
70     1    0
71     1    2
72     1    2
73     8   -1
74     6    0
75     1    0
76     1    7

```

```
77      6      0
78      1      0
79      1     10
80      8     -1
81      1     -1
82
83      6      1
84      1      2
85      1      2
86      1      2
87      8     -1
88      6      6
89      1      7
90      1      7
91      6      9
92      1     10
93      1     10
94      8     -1
95      1     -1
96
97 -----

98
99
100 Total number of atoms = 26
101 Weight factor on initial charge restraints= 0.001000
102
103
104 There are 3 charge constraints
105
106 Reading esp"s for MEP 1
107 total number of atoms = 13
108 total number of esp points = 699
109
110 Center      X              Y              Z
111      1      -0.1031513E+01 -0.2458118E+01  0.2078699E-04
112      2      -0.3087856E+01 -0.2257916E+01  0.9448630E-05
113      3      -0.4574554E+00 -0.3535972E+01  0.1687282E+01
114      4      -0.4574346E+00 -0.3536012E+01 -0.1687219E+01
115      5           0.0000000E+00  0.0000000E+00  0.0000000E+00
116      6           0.2671096E+01  0.0000000E+00  0.0000000E+00
117      7           0.3424533E+01 -0.9747906E+00 -0.1680261E+01
118      8           0.3424531E+01 -0.9747830E+00  0.1680274E+01
119      9           0.3546946E+01  0.2737385E+01  0.0000000E+00
120     10           0.2781372E+01  0.3695176E+01  0.1680210E+01
```

```

121  11      0.2781370E+01  0.3695170E+01 -0.1680223E+01
122  12      0.6234777E+01  0.2701150E+01 -0.3779452E-05
123  13      0.6819031E+01  0.4435102E+01 -0.3212534E-04
124
125  Reading esp"s for MEP 2
126  total number of atoms = 13
127  total number of esp points = 682
128
129  Center      X              Y              Z
130  1          0.6343621E+01  0.2777408E+01 -0.2078699E-04
131  2          0.6779594E+01  0.4796950E+01 -0.9448630E-05
132  3          0.7195270E+01  0.1902189E+01 -0.1687282E+01
133  4          0.7195302E+01  0.1902159E+01  0.1687219E+01
134  5          0.3688080E+01  0.2544046E+01  0.0000000E+00
135  6          0.2874090E+01  0.0000000E+00  0.0000000E+00
136  7          0.3572911E+01 -0.1014660E+01  0.1680261E+01
137  8          0.3572903E+01 -0.1014656E+01 -0.1680274E+01
138  9          0.0000000E+00  0.0000000E+00  0.0000000E+00
139  10         -0.6789332E+00  0.1021038E+01 -0.1680210E+01
140  11         -0.6789275E+00  0.1021038E+01  0.1680223E+01
141  12         -0.7845802E+00 -0.2571027E+01  0.3779452E-05
142  13         -0.2614103E+01 -0.2599086E+01  0.3212534E-04
143  Initial ssvpot = 0.200
144
145
146  Number of unique UNfrozen centers= 6
147
148  Non-linear optimization requested.
149  qchnge = 0.5760737946E-01
150  qchnge = 0.1258790760E-02
151  qchnge = 0.3838047843E-04
152  qchnge = 0.1523500291E-05
153  qchnge = 0.7222776353E-07
154
155  Convergence in 4 iterations
156
157  1  PEG nconf=1 norient=1 nmep=1/2
158  2  PEG nconf=1 norient=2 nmep=2/2
159
160  Point Charges Before & After Optimization
161
162  no. At.no.  q(init)      q(opt)      ivary  d(rstr)/dq
163  1  6      -0.448503    -0.449958    0      0.002169
164  2  1       0.183169     0.157519    0      0.000000
165  3  1       0.143968     0.157519    2      0.000000

```

166	4	1	0.143966	0.157519	2	0.000000
167	5	8	-0.187505	-0.187505	-1	0.004706
168	6	6	0.189513	0.240868	0	0.003834
169	7	1	0.072139	0.046930	0	0.000000
170	8	1	0.072139	0.046930	7	0.000000
171	9	6	-0.566528	-0.548535	0	0.001793
172	10	1	0.210122	0.200655	0	0.000000
173	11	1	0.210119	0.200655	10	0.000000
174	12	8	-0.415967	-0.415967	-1	0.002337
175	13	1	0.393367	0.393367	-1	0.000000
176						
177	14	6	-0.448503	-0.449958	1	0.002169
178	15	1	0.183169	0.157519	2	0.000000
179	16	1	0.143968	0.157519	2	0.000000
180	17	1	0.143966	0.157519	2	0.000000
181	18	8	-0.187505	-0.187505	-1	0.004706
182	19	6	0.189513	0.240868	6	0.003834
183	20	1	0.072139	0.046930	7	0.000000
184	21	1	0.072139	0.046930	7	0.000000
185	22	6	-0.566528	-0.548535	9	0.001793
186	23	1	0.210122	0.200655	10	0.000000
187	24	1	0.210119	0.200655	10	0.000000
188	25	8	-0.415967	-0.415967	-1	0.002337
189	26	1	0.393367	0.393367	-1	0.000000

190

191 Sum over the calculated charges: -0.000

192

193 Statistics of the fitting:

194	The initial sum of squares (ssvpot)	0.200
195	The residual sum of squares (chipot)	0.016
196	The std err of estimate (sqrt(chipot/N))	0.00344
197	ESP relative RMS (SQRT(chipot/ssvpot))	0.28579
198	The Pearson correlation coefficient (r2)	0.91986

199

200 Center of Mass (a.u.):

201	#MEP	X	Y	Z
202	1	2.33126	0.61925	0.00000
203	2	2.38786	0.51238	-0.00000

204

205 Dipole moments (Debye) computed:

206 -with respect to the origin of coordinates (ooc)

207 -with respect to the center of mass (com)

208	#MEP	D	Dx	Dy	Dz
209	1 ooc	0.40235	0.14725	0.37443	-0.00003
210	1 com	0.40235	0.14725	0.37443	-0.00003

```

211
212   2 ooc   0.40235  -0.40150  -0.02613  0.00003
213   2 com   0.40235  -0.40150  -0.02613  0.00003
214
215 Traceless Quadrupole moments (Buckingham) computed:
216 -with respect to the origin of coordinates (ooc)
217 -with respect to the center of mass (com)
218 #MEP      X      Y      Z
219   1 ooc X  -8.08665
220           Y   15.50912  15.92587
221           Z   -0.00035  -0.00026  -7.83922
222   1 com X  -8.56785
223           Y   13.97860  15.79837
224           Z   -0.00024  -0.00023  -7.23052
225
226   2 ooc X  19.63488
227           Y    3.88446 -13.43319
228           Z   -0.00019  -0.00014  -6.20170
229   2 com X  21.65003
230           Y    4.31011 -14.41950
231           Z   -0.00030  -0.00016  -7.23053
232
233 Traceless Quadrupole moments (Buckingham) in principal axes computed:
234 -with respect to the origin of coordinates (ooc)
235 -with respect to the center of mass (com)
236 #MEP      X      Y      Z
237   1 ooc X  23.53295
238           Y    0.00000  -7.83922
239           Z    0.00000  -0.00000 -15.69373
240   1 com X  22.15790
241           Y   -0.00000  -7.23052
242           Z   -0.00000   0.00000 -14.92738
243
244   2 ooc X  20.08506
245           Y    0.00000  -6.20170
246           Z   -0.00000   0.00000 -13.88336
247   2 com X  22.15791
248           Y    0.00000  -7.23053
249           Z   -0.00000   0.00000 -14.92739

```

B.1.6 Fitting statistics of a fragment approach

```

1
2 -----
3   Restrained ESP Fit 2.4 q4md-forcefieldtools

```

```
4 -----
5 RESP-A1 - RESP input generated by PyRED version SEP-2015
6 -----
7
8
9 inopt      =    0   ioutopt   =    1
10 nmep      =    2   iqopt    =    2
11 ihfree    =    1   irstrnt  =    1
12 iunits    =    0   qwt      = 0.00100000
13
14 multiple-MEP run of 2 MEP
15
16 Reading input for MEP 1 weight: 1.000
17 PEG nconf=1 norient=1 nmep=1/2
18
19 Total charge (ich): 0
20 Number of centers: 13
21   1   6   0
22   2   1   0
23   3   1   2
24   4   1   2
25   5   8  -1
26   6   6   0
27   7   1   0
28   8   1   7
29   9   6   0
30  10   1   0
31  11   1  10
32  12   8  -1
33  13   1  -1
34
35 Reading input for MEP 2 weight: 1.000
36 PEG nconf=1 norient=2 nmep=2/2
37
38 Total charge (ich): 0
39 Number of centers: 13
40  14   6   0
41  15   1   0
42  16   1   2
43  17   1   2
44  18   8  -1
45  19   6   0
46  20   1   0
47  21   1   7
48  22   6   0
```

```

49   23   1   0
50   24   1  10
51   25   8  -1
52   26   1  -1
53   since IQOPT>1, 26 new q0 values
54   will be read in from file ESP.Q0 (unit 3)
55   -----
56   reading mult_esp constraint info
57   -----
58     1   1   2   1
59     1   2   2   2
60     1   6   2   6
61     1   7   2   7
62     1   9   2   9
63     1  10   2  10
64
65   -----
66     Atom  Ivary
67   -----
68     6   0
69     1   0
70     1   2
71     1   2
72     8  -1
73     6   0
74     1   0
75     1   7
76     6   0
77     1   0
78     1  10
79     8  -1
80     1  -1
81
82     6   1
83     1   2
84     1   2
85     1   2
86     8  -1
87     6   6
88     1   7
89     1   7
90     6   9
91     1  10
92     1  10
93     8  -1

```

```
94      1  -1
95
96  -----

97
98
99  Total number of atoms = 26
100 Weight factor on initial charge restraints= 0.001000
101
102
103  There are 2 charge constraints
104
105  Reading esp"s for MEP 1
106  total number of atoms = 13
107  total number of esp points = 699
108
109  Center      X              Y              Z
110    1      -0.1031513E+01 -0.2458118E+01  0.2078699E-04
111    2      -0.3087856E+01 -0.2257916E+01  0.9448630E-05
112    3      -0.4574554E+00 -0.3535972E+01  0.1687282E+01
113    4      -0.4574346E+00 -0.3536012E+01 -0.1687219E+01
114    5          0.0000000E+00  0.0000000E+00  0.0000000E+00
115    6          0.2671096E+01  0.0000000E+00  0.0000000E+00
116    7          0.3424533E+01 -0.9747906E+00 -0.1680261E+01
117    8          0.3424531E+01 -0.9747830E+00  0.1680274E+01
118    9          0.3546946E+01  0.2737385E+01  0.0000000E+00
119   10          0.2781372E+01  0.3695176E+01  0.1680210E+01
120   11          0.2781370E+01  0.3695170E+01 -0.1680223E+01
121   12          0.6234777E+01  0.2701150E+01 -0.3779452E-05
122   13          0.6819031E+01  0.4435102E+01 -0.3212534E-04
123
124  Reading esp"s for MEP 2
125  total number of atoms = 13
126  total number of esp points = 682
127
128  Center      X              Y              Z
129    1          0.6343621E+01  0.2777408E+01 -0.2078699E-04
130    2          0.6779594E+01  0.4796950E+01 -0.9448630E-05
131    3          0.7195270E+01  0.1902189E+01 -0.1687282E+01
132    4          0.7195302E+01  0.1902159E+01  0.1687219E+01
133    5          0.3688080E+01  0.2544046E+01  0.0000000E+00
134    6          0.2874090E+01  0.0000000E+00  0.0000000E+00
135    7          0.3572911E+01 -0.1014660E+01  0.1680261E+01
136    8          0.3572903E+01 -0.1014656E+01 -0.1680274E+01
137    9          0.0000000E+00  0.0000000E+00  0.0000000E+00
```

```

138  10   -0.6789332E+00  0.1021038E+01 -0.1680210E+01
139  11   -0.6789275E+00  0.1021038E+01  0.1680223E+01
140  12   -0.7845802E+00 -0.2571027E+01  0.3779452E-05
141  13   -0.2614103E+01 -0.2599086E+01  0.3212534E-04
142  Initial ssvpot =  0.200
143
144
145  Number of unique UNfrozen centers= 6
146
147  Non-linear optimization requested.
148  qchnge =  0.4779949113E-01
149  qchnge =  0.2078834013E-02
150  qchnge =  0.3762550571E-03
151  qchnge =  0.8584675882E-04
152  qchnge =  0.2008878879E-04
153  qchnge =  0.4716565444E-05
154  qchnge =  0.1108009325E-05
155  qchnge =  0.2603213499E-06
156
157  Convergence in 7 iterations
158
159  1  PEG nconf=1 norient=1 nmep=1/2
160  2  PEG nconf=1 norient=2 nmep=2/2
161
162  Point Charges Before & After Optimization
163
164  no.  At.no.  q(init)  q(opt)  ivary  d(rstr)/dq
165  1  6  -0.016076  0.047733  0  0.009025
166  2  1  0.088113  0.041585  0  0.000000
167  3  1  0.040852  0.041585  2  0.000000
168  4  1  0.040851  0.041585  2  0.000000
169  5  8  -0.369797  -0.369797  -1  0.002610
170  6  6  0.163081  0.145121  0  0.005674
171  7  1  0.043831  0.036152  0  0.000000
172  8  1  0.043830  0.036152  7  0.000000
173  9  6  0.141422  0.165939  0  0.005162
174  10 1  0.020794  0.015819  0  0.000000
175  11 1  0.020792  0.015819  10 0.000000
176  12 8  -0.628092  -0.628092  -1  0.001572
177  13 1  0.410400  0.410400  -1  0.000000
178
179  14 6  -0.016076  0.047733  1  0.009025
180  15 1  0.088113  0.041585  2  0.000000
181  16 1  0.040852  0.041585  2  0.000000
182  17 1  0.040851  0.041585  2  0.000000

```

```

183  18  8  -0.369797  -0.369797  -1  0.002610
184  19  6  0.163081  0.145121  6  0.005674
185  20  1  0.043831  0.036152  7  0.000000
186  21  1  0.043830  0.036152  7  0.000000
187  22  6  0.141422  0.165939  9  0.005162
188  23  1  0.020794  0.015819  10 0.000000
189  24  1  0.020792  0.015819  10 0.000000
190  25  8  -0.628092  -0.628092  -1  0.001572
191  26  1  0.410400  0.410400  -1  0.000000
192
193 Sum over the calculated charges: -0.000
194
195     Statistics of the fitting:
196 The initial sum of squares (ssvpot)           0.200
197 The residual sum of squares (chipot)         0.005
198 The std err of estimate (sqrt(chipot/N))      0.00192
199 ESP relative RMS (SQRT(chipot/ssvpot))       0.15951
200 The Pearson correlation coefficient (r2)      0.97480
201
202 Center of Mass (a.u.):
203 #MEP  X      Y      Z
204  1  2.33126  0.61925  0.00000
205  2  2.38786  0.51238 -0.00000
206
207 Dipole moments (Debye) computed:
208 -with respect to the origin of coordinates (ooc)
209 -with respect to the center of mass (com)
210 #MEP  D      Dx      Dy      Dz
211  1 ooc  0.30717 -0.05429  0.30233 -0.00002
212  1 com  0.30717 -0.05429  0.30233 -0.00002
213
214  2 ooc  0.30717 -0.27141  0.14384  0.00002
215  2 com  0.30717 -0.27141  0.14384  0.00002
216
217 Traceless Quadrupole moments (Buckingham) computed:
218 -with respect to the origin of coordinates (ooc)
219 -with respect to the center of mass (com)
220 #MEP  X      Y      Z
221  1 ooc X -11.57828
222         Y  16.44103  18.38709
223         Z -0.00032 -0.00025 -6.80882
224  1 com X -11.11225
225         Y  15.37549  17.85687
226         Z -0.00026 -0.00024 -6.74461
227

```

```

228  2 ooc X  22.64213
229      Y   4.43607 -16.50541
230      Z  -0.00024 -0.00016 -6.13671
231  2 com X  24.09193
232      Y   4.11158 -17.34731
233      Z  -0.00030 -0.00017 -6.74461
234
235  Traceless Quadrupole moments (Buckingham) in principal axes computed:
236  -with respect to the origin of coordinates (ooc)
237  -with respect to the center of mass (com)
238  #MEP      X      Y      Z
239  1 ooc X  25.64825
240      Y  -0.00000 -6.80882
241      Z  -0.00000  0.00000 -18.83943
242  1 com X  24.49594
243      Y  -0.00000 -6.74461
244      Z  -0.00000  0.00000 -17.75133
245
246  2 ooc X  23.13851
247      Y   0.00000 -6.13671
248      Z  -0.00000  0.00000 -17.00180
249  2 com X  24.49594
250      Y   0.00000 -6.74461
251      Z  -0.00000  0.00000 -17.75133

```

B.1.7 Amber Leap script for PEG-M

```

1  #
2  # Generated by PyRED version SEP-2015
3  #   http://q4md-forcefieldtools.org
4  #
5  logfile q4md-forcefieldtools.log
6  source /home/sajid/amber14/dat/leap/cmd/oldff/leaprc.ff99SB
7  # Web site: http://ambermd.org/doc6/html/AMBER-sh-5.9.html#sh-5.9.8
8  alias q quit
9  alias e edit
10 alias c charge
11
12 # Web site: http://ambermd.org/doc6/html/AMBER-sh-5.9.html#sh-5.9.73
13 verbosity 2
14
15 # Web site: http://ambermd.org/doc6/html/AMBER-sh-5.9.html#sh-5.9.2
16 addAtomTypes {
17     { "CT" "C" "sp3" }
18     { "H1" "H" "sp3" }

```

```
19         { "HO" "H" "sp3" }
20         { "OH" "O" "sp3" }
21         { "OS" "O" "sp3" }
22     }
23
24 # To force the correspondance between residue names
25 # PDB file versus force field libraries:
26 # Web site: http://ambermd.org/doc6/html/AMBER-sh-5.9.html#sh-5.9.7
27 # addPdbResMap {
28 #     { 0 ALA NALA } { 1 ALA CALA }
29 #     { ADE DADE }
30 # }
31
32 # Web site: http://ambermd.org/doc6/html/AMBER-sh-5.9.html#sh-5.9.41
33 frcmod1 = loadAmberParams ./frcmod.known
34 frcmod2 = loadAmberParams ./frcmod.correspondence
35 frcmod3 = loadAmberParams ./frcmod.unknown
36
37 # Web site: http://q4md-forcefieldtools.org/Tutorial/leap-mol3.php
38 # Web site: http://q4md-forcefieldtools.org/Tutorial/leap-mol2.php
39 F00 = loadmol3 ../Mol_m1/Mol-ia1_m1-cl.mol2
40 F01 = loadmol3 ../Mol_m1/Mol-ia2_m1-cl.mol2
41 F02 = loadmol3 ../Mol_m1/Mol-ia3_m1-cl.mol2
42 U01 = loadmol3 ../Mol_m1/Mol-sm_m1-cl.mol2
43
44 # To match the residue names found in the PDB file
45 # Web site: http://ambermd.org/doc6/html/AMBER-sh-5.9.html#sh-5.9.19
46 # ZZZ = copy F00
47
48 # If a copy is done, define the molecule and residue
49 # Web site: http://ambermd.org/doc6/html/AMBER-sh-5.9.html#sh-5.9.63
50 # set ZZZ name "ZZZ"
51 # set ZZZ.1 name "ZZZ"
52
53 # Let's load the PDB file
54 # Web site: http://ambermd.org/doc6/html/AMBER-sh-5.9.html#sh-5.9.44
55 # VAR = loadPdb Your-PDB-file.ent
56
57 # Let's save the prmtop and prmcrd file with specific file extensions
58 # (to be automatically recognized by VMD http://www.ks.uiuc.edu/
59 #   Research/vmd/)
60 # saveAmberParm F00 F00.parm7 F00.rst7
61
62 # q
```


B.2 PEG with a hydroxyethyl terminal, $n = 4$ **B.2.1 FF libraries for 'A' fragment**

```
1 #
2 # Generated by PyRED version SEP-2015
3 #   http://q4md-forcefieldtools.org
4 #
5 @<TRIPOS>MOLECULE
6 F01
7   36   35   1   0   1
8 SMALL
9 USER_CHARGES
10 @<TRIPOS>ATOM
11   1 O      0.580060  0.596993  1.362506 OH  1   F01 -0.5648  0.0000  ****
12   2 H      0.956305 -0.258286  1.077795 HO  1   F01  0.3529  0.0000  ****
13   3 C1     1.618871  1.425664  1.857862 CT  1   F01  0.1140  0.0000  ****
14   4 H11    1.129961  2.292237  2.319691 H1  1   F01  0.0772  0.0000  ****
15   5 H12    2.200939  0.913356  2.638542 H1  1   F01  0.0772  0.0000  ****
16   6 C2     2.575896  1.915881  0.776888 CT  1   F01 -0.3406  0.0000  ****
17   7 H21    2.006000  2.374434 -0.043419 H1  1   F01  0.1496  0.0000  ****
18   8 H22    3.238036  2.685724  1.200975 H1  1   F01  0.1496  0.0000  ****
19   9 O2A    3.391276  0.846837  0.308560 OS  1   F01 -0.2183  0.0000  ****
20  10 C3     3.247128  0.471015 -1.046879 CT  1   F01  0.0320  0.0000  ****
21  11 H31    3.302948  1.346991 -1.714888 H1  1   F01  0.0630  0.0000  ****
22  12 H32    4.106735 -0.173556 -1.257141 H1  1   F01  0.0630  0.0000  ****
23  13 C4     1.966642 -0.299758 -1.357485 CT  1   F01  0.0458  0.0000  ****
24  14 H41    1.082105  0.340491 -1.237110 H1  1   F01  0.0320  0.0000  ****
25  15 H42    2.006303 -0.629912 -2.408737 H1  1   F01  0.0320  0.0000  ****
26  16 O4A    1.901618 -1.419033 -0.482965 OS  1   F01 -0.2479  0.0000  ****
27  17 C5     1.079023 -2.494176 -0.919166 CT  1   F01 -0.0149  0.0000  ****
28  18 H51    1.252522 -2.697451 -1.988036 H1  1   F01  0.0722  0.0000  ****
29  19 H52    1.406404 -3.365310 -0.342685 H1  1   F01  0.0722  0.0000  ****
30  20 C6     -0.407636 -2.277694 -0.681377 CT  1   F01  0.0291  0.0000  ****
31  21 H61    -0.769452 -1.367904 -1.174977 H1  1   F01  0.0565  0.0000  ****
32  22 H62    -0.962978 -3.128999 -1.112583 H1  1   F01  0.0565  0.0000  ****
33  23 O6A    -0.608171 -2.214190  0.722036 OS  1   F01 -0.2638  0.0000  ****
34  24 C7     -1.958554 -2.088639  1.141754 CT  1   F01  0.0414  0.0000  ****
35  25 H71    -2.606855 -2.776515  0.575989 H1  1   F01  0.0526  0.0000  ****
36  26 H72    -1.966234 -2.397915  2.193046 H1  1   F01  0.0526  0.0000  ****
37  27 C8     -2.515411 -0.675057  1.056055 CT  1   F01  0.0388  0.0000  ****
38  28 H81    -3.422234 -0.610989  1.683118 H1  1   F01  0.0579  0.0000  ****
39  29 H82    -1.765362  0.021519  1.450727 H1  1   F01  0.0579  0.0000  ****
40  30 O8A    -2.851627 -0.374587 -0.296695 OS  1   F01 -0.3569  0.0000  ****
41  31 C9     -3.230348  0.977760 -0.511287 CT  1   F01  0.1844  0.0000  ****
42  32 H91    -3.940873  0.987102 -1.345037 H1  1   F01  0.0646  0.0000  ****
```

B.2. PEG WITH A HYDROXYETHYL TERMINAL, $N = 4$

```

43  33 H92  -3.753836  1.379055  0.373108  H1  1  F01  0.0646  0.0000  ****
44  34 C1B  -2.028597  1.865663  -0.855680  CT  1  F01  -0.7797  0.0000  ****
45  35 H1   -1.248058  1.771187  -0.088120  H1  1  F01  0.3562  0.0000  ****
46  36 H1B  -1.597999  1.531544  -1.805348  H1  1  F01  0.3562  0.0000  ****
47  @<TRIPOS>BOND
48    1    1    2  1
49    2    1    3  1
50    3    3    4  1
51    4    3    5  1
52    5    3    6  1
53    6    6    7  1
54    7    6    8  1
55    8    6    9  1
56    9    9   10  1
57   10   10   11  1
58   11   10   12  1
59   12   10   13  1
60   13   13   14  1
61   14   13   15  1
62   15   13   16  1
63   16   16   17  1
64   17   17   18  1
65   18   17   19  1
66   19   17   20  1
67   20   20   21  1
68   21   20   22  1
69   22   20   23  1
70   23   23   24  1
71   24   24   25  1
72   25   24   26  1
73   26   24   27  1
74   27   27   28  1
75   28   27   29  1
76   29   27   30  1
77   30   30   31  1
78   31   31   32  1
79   32   31   33  1
80   33   31   34  1
81   34   34   35  1
82   35   34   36  1
83  @<TRIPOS>SUBSTRUCTURE
84    1 F01          1 ****          0 ****  ****
85  @<TRIPOS>HEADTAIL
86  0 0
87  C1B 1

```

```
88 @<TRIPOS>RESIDUECONNECT
89 1 0 C1B 0 0 0 0
```

B.2.2 FF libraries for 'B' fragment

```
1 #
2 # Generated by PyRED version SEP-2015
3 #   http://q4md-forcefieldtools.org
4 #
5 @<TRIPOS>MOLECULE
6 F02
7   28   27   1   0   1
8 SMALL
9 USER_CHARGES
10 @<TRIPOS>ATOM
11   1 O2A   3.391276  0.846837  0.308560 OS 1   F02 -0.2183  0.0000  ****
12   2 C3    3.247128  0.471015 -1.046879 CT 1   F02  0.0320  0.0000  ****
13   3 H31   3.302948  1.346991 -1.714888 H1 1   F02  0.0630  0.0000  ****
14   4 H32   4.106735 -0.173556 -1.257141 H1 1   F02  0.0630  0.0000  ****
15   5 C4    1.966642 -0.299758 -1.357485 CT 1   F02  0.0458  0.0000  ****
16   6 H41   1.082105  0.340491 -1.237110 H1 1   F02  0.0320  0.0000  ****
17   7 H42   2.006303 -0.629912 -2.408737 H1 1   F02  0.0320  0.0000  ****
18   8 O4A   1.901618 -1.419033 -0.482965 OS 1   F02 -0.2479  0.0000  ****
19   9 C5    1.079023 -2.494176 -0.919166 CT 1   F02 -0.0149  0.0000  ****
20  10 H51   1.252522 -2.697451 -1.988036 H1 1   F02  0.0722  0.0000  ****
21  11 H52   1.406404 -3.365310 -0.342685 H1 1   F02  0.0722  0.0000  ****
22  12 C6   -0.407636 -2.277694 -0.681377 CT 1   F02  0.0291  0.0000  ****
23  13 H61  -0.769452 -1.367904 -1.174977 H1 1   F02  0.0565  0.0000  ****
24  14 H62  -0.962978 -3.128999 -1.112583 H1 1   F02  0.0565  0.0000  ****
25  15 O6A  -0.608171 -2.214190  0.722036 OS 1   F02 -0.2638  0.0000  ****
26  16 C7   -1.958554 -2.088639  1.141754 CT 1   F02  0.0414  0.0000  ****
27  17 H71  -2.606855 -2.776515  0.575989 H1 1   F02  0.0526  0.0000  ****
28  18 H72  -1.966234 -2.397915  2.193046 H1 1   F02  0.0526  0.0000  ****
29  19 C8   -2.515411 -0.675057  1.056055 CT 1   F02  0.0388  0.0000  ****
30  20 H81  -3.422234 -0.610989  1.683118 H1 1   F02  0.0579  0.0000  ****
31  21 H82  -1.765362  0.021519  1.450727 H1 1   F02  0.0579  0.0000  ****
32  22 O8A  -2.851627 -0.374587 -0.296695 OS 1   F02 -0.3569  0.0000  ****
33  23 C9   -3.230348  0.977760 -0.511287 CT 1   F02  0.1844  0.0000  ****
34  24 H91  -3.940873  0.987102 -1.345037 H1 1   F02  0.0646  0.0000  ****
35  25 H92  -3.753836  1.379055  0.373108 H1 1   F02  0.0646  0.0000  ****
36  26 C1B  -2.028597  1.865663 -0.855680 CT 1   F02 -0.7797  0.0000  ****
37  27 H1   -1.248058  1.771187 -0.088120 H1 1   F02  0.3562  0.0000  ****
38  28 H1B  -1.597999  1.531544 -1.805348 H1 1   F02  0.3562  0.0000  ****
39 @<TRIPOS>BOND
40   1     1     2  1
```

```

41      2      2      3 1
42      3      2      4 1
43      4      2      5 1
44      5      5      6 1
45      6      5      7 1
46      7      5      8 1
47      8      8      9 1
48      9      9     10 1
49     10      9     11 1
50     11      9     12 1
51     12     12     13 1
52     13     12     14 1
53     14     12     15 1
54     15     15     16 1
55     16     16     17 1
56     17     16     18 1
57     18     16     19 1
58     19     19     20 1
59     20     19     21 1
60     21     19     22 1
61     22     22     23 1
62     23     23     24 1
63     24     23     25 1
64     25     23     26 1
65     26     26     27 1
66     27     26     28 1
67 @<TRIPOS>SUBSTRUCTURE
68      1 F02          1 *****          0 ***** *****
69 @<TRIPOS>HEADTAIL
70 O2A 1
71 C1B 1
72 @<TRIPOS>RESIDUECONNECT
73 1 O2A C1B 0 0 0 0

```

B.2.3 FF libraries for 'C' fragment

```

1 #
2 # Generated by PyRED version SEP-2015
3 #   http://q4md-forcefieldtools.org
4 #
5 @<TRIPOS>MOLECULE
6 F00
7   30   29   1   0   1
8 SMALL
9 USER_CHARGES

```

B.2. PEG WITH A HYDROXYETHYL TERMINAL, $N = 4$

```

10 @<TRIPOS>ATOM
11  1 O2A  3.391276  0.846837  0.308560 OS  1  F00 -0.2183  0.0000  ****
12  2 C3   3.247128  0.471015 -1.046879 CT  1  F00  0.0320  0.0000  ****
13  3 H31  3.302948  1.346991 -1.714888 H1  1  F00  0.0630  0.0000  ****
14  4 H32  4.106735 -0.173556 -1.257141 H1  1  F00  0.0630  0.0000  ****
15  5 C4   1.966642 -0.299758 -1.357485 CT  1  F00  0.0458  0.0000  ****
16  6 H41  1.082105  0.340491 -1.237110 H1  1  F00  0.0320  0.0000  ****
17  7 H42  2.006303 -0.629912 -2.408737 H1  1  F00  0.0320  0.0000  ****
18  8 O4A  1.901618 -1.419033 -0.482965 OS  1  F00 -0.2479  0.0000  ****
19  9 C5   1.079023 -2.494176 -0.919166 CT  1  F00 -0.0149  0.0000  ****
20 10 H51  1.252522 -2.697451 -1.988036 H1  1  F00  0.0722  0.0000  ****
21 11 H52  1.406404 -3.365310 -0.342685 H1  1  F00  0.0722  0.0000  ****
22 12 C6  -0.407636 -2.277694 -0.681377 CT  1  F00  0.0291  0.0000  ****
23 13 H61 -0.769452 -1.367904 -1.174977 H1  1  F00  0.0565  0.0000  ****
24 14 H62 -0.962978 -3.128999 -1.112583 H1  1  F00  0.0565  0.0000  ****
25 15 O6A -0.608171 -2.214190  0.722036 OS  1  F00 -0.2638  0.0000  ****
26 16 C7  -1.958554 -2.088639  1.141754 CT  1  F00  0.0414  0.0000  ****
27 17 H71 -2.606855 -2.776515  0.575989 H1  1  F00  0.0526  0.0000  ****
28 18 H72 -1.966234 -2.397915  2.193046 H1  1  F00  0.0526  0.0000  ****
29 19 C8  -2.515411 -0.675057  1.056055 CT  1  F00  0.0388  0.0000  ****
30 20 H81 -3.422234 -0.610989  1.683118 H1  1  F00  0.0579  0.0000  ****
31 21 H82 -1.765362  0.021519  1.450727 H1  1  F00  0.0579  0.0000  ****
32 22 O8A -2.851627 -0.374587 -0.296695 OS  1  F00 -0.3569  0.0000  ****
33 23 C9  -3.230348  0.977760 -0.511287 CT  1  F00  0.1844  0.0000  ****
34 24 H91 -3.940873  0.987102 -1.345037 H1  1  F00  0.0646  0.0000  ****
35 25 H92 -3.753836  1.379055  0.373108 H1  1  F00  0.0646  0.0000  ****
36 26 C1B -2.028597  1.865663 -0.855680 CT  1  F00 -0.7797  0.0000  ****
37 27 H1  -1.248058  1.771187 -0.088120 H1  1  F00  0.3562  0.0000  ****
38 28 H1B -1.597999  1.531544 -1.805348 H1  1  F00  0.3562  0.0000  ****
39 29 O1C -2.423158  3.220232 -1.059148 OH  1  F00 -0.4010  0.0000  ****
40 30 H1C -2.656440  3.589225 -0.193369 HO  1  F00  0.3859  0.0000  ****
41 @<TRIPOS>BOND
42  1  1  2  1
43  2  2  3  1
44  3  2  4  1
45  4  2  5  1
46  5  5  6  1
47  6  5  7  1
48  7  5  8  1
49  8  8  9  1
50  9  9 10  1
51 10  9 11  1
52 11  9 12  1
53 12 12 13  1
54 13 12 14  1

```

```

55  14  12  15  1
56  15  15  16  1
57  16  16  17  1
58  17  16  18  1
59  18  16  19  1
60  19  19  20  1
61  20  19  21  1
62  21  19  22  1
63  22  22  23  1
64  23  23  24  1
65  24  23  25  1
66  25  23  26  1
67  26  26  27  1
68  27  26  28  1
69  28  26  29  1
70  29  29  30  1
71 @<TRIPOS>SUBSTRUCTURE
72      1 F00          1 *****          0 ***** *****
73 @<TRIPOS>HEADTAIL
74 O2A 1
75 0 0
76 @<TRIPOS>RESIDUECONNECT
77 1 O2A 0 0 0 0 0

```

B.2.4 FF parameters for PEG-H

```

1  FRCMOD file generated by PyRED version SEP-2015 - q4md-forcefieldtools
   .org
2  MASS      mass          pol          Source
3  CT        12.010       0.878      taken from parm10.dat
4  H1         1.008       0.135      taken from parm10.dat
5  HO         1.008       0.135      taken from parm10.dat
6  OH         16.000      0.465      taken from parm10.dat
7  OS         16.000      0.465      taken from parm10.dat
8
9  BOND      K(kcal.mol-1.ang-2) Dist0(ang) Source
10 CT-CT     310.0         1.526      taken from parm10.dat
11 CT-H1     340.0         1.090      taken from parm10.dat
12 CT-OH     320.0         1.410      taken from parm10.dat
13 CT-OS     320.0         1.410      taken from parm10.dat
14 HO-OH     555.0         0.960      adapted from parm10.dat 553.0
15
16 ANGLE     K(kcal.mol-1.rad-2) Theta0(deg) Source
17 CT-CT-H1  50.0          109.50     taken from parm10.dat
18 CT-CT-OH  50.0          109.50     taken from parm10.dat

```

B.2. PEG WITH A HYDROXYETHYL TERMINAL, $N = 4$

19	CT-CT-OS	50.0	109.50	taken	from	parm10.dat
20	H1-CT-H1	35.0	109.50	taken	from	parm10.dat
21	H1-CT-OH	50.0	109.50	taken	from	parm10.dat
22	H1-CT-OS	50.0	109.50	taken	from	parm10.dat
23	CT-OH-HO	55.0	108.50	taken	from	parm10.dat
24	CT-OS-CT	60.0	109.50	taken	from	parm10.dat
25						
26	DIHEDRAL	Path V(kcal.mol-1.rad-1)	Phase(deg.)	Period	Source	
27	H1-CT-CT-H1	1 1.55555556e-01	0.0	3.	adapted	from parm10. dat i.e X-CT-CT-X 1.4/9
28	H1-CT-CT-OH	1 0.00000000e+00	0.0	-3.	taken	from parm10. dat
29	H1-CT-CT-OH	1 2.50000000e-01	0.0	1.	taken	from parm10. dat
30	H1-CT-CT-OS	1 0.00000000e+00	0.0	-3.	taken	from parm10. dat
31	H1-CT-CT-OS	1 2.50000000e-01	0.0	1.	taken	from parm10. dat
32	OH-CT-CT-OS	1 1.44000000e-01	0.0	-3.	taken	from parm10. dat
33	OH-CT-CT-OS	1 1.17500000e+00	0.0	2.	taken	from parm10. dat
34	OS-CT-CT-OS	1 1.44000000e-01	0.0	-3.	taken	from parm10. dat
35	OS-CT-CT-OS	1 1.17500000e+00	0.0	2.	taken	from parm10. dat
36	CT-CT-OH-HO	1 1.60000000e-01	0.0	-3.	taken	from parm10. dat
37	CT-CT-OH-HO	1 2.50000000e-01	0.0	1.	taken	from parm10. dat
38	H1-CT-OH-HO	1 1.66666667e-01	0.0	3.	adapted	from parm10. dat i.e X-CT-OH-X 0.5/3
39	CT-CT-OS-CT	1 3.83000000e-01	0.0	-3.	taken	from parm10. dat
40	CT-CT-OS-CT	1 1.00000000e-01	180.0	2.	taken	from parm10. dat
41	H1-CT-OS-CT	1 3.83333333e-01	0.0	3.	adapted	from parm10. dat i.e X-CT-OS-X 1.15/3
42						
43	IMPROPER	V(kcal.mol-1.rad-1)	Phase(deg.)	Period	Source	
44						
45	NONBON	R*(ang) Eps(kcal.mol-1)			Source	
46	CT	1.9080 0.10940000			taken	from parm10.dat
47	H1	1.3870 0.01570000			taken	from parm10.dat
48	HO	0.0000 0.00000000			taken	from parm10.dat

49	OH	1.7210	0.21040000	taken from parm10.dat
50	OS	1.6837	0.17000000	taken from parm10.dat

B.2.5 Fitting statistics of a whole molecule approach

```

1
2 -----
3   Restrained ESP Fit 2.4 q4md-forcefieldtools
4 -----
5   RESP-A1 - RESP input generated by PyRED version SEP-2015
6 -----
7
8
9   inopt      =    0   ioutopt   =    1
10  nmep       =    2   iqopt     =    2
11  ihfree     =    1   irstrnt  =    1
12  iunits     =    0   qwt      =  0.00100000
13
14  multiple-MEP run of 2 MEP
15
16  Reading input for MEP 1 weight: 1.000
17  PEG nconf=1 norient=1 nmep=1/2
18
19  Total charge (ich): 0
20  Number of centers: 38
21    1    8   -1
22    2    1   -1
23    3    6    0
24    4    1    0
25    5    1    4
26    6    6    0
27    7    1    0
28    8    1    7
29    9    8   -1
30   10    6    0
31   11    1    0
32   12    1   11
33   13    6    0
34   14    1    0
35   15    1   14
36   16    8   -1
37   17    6    0
38   18    1    0
39   19    1   18
40   20    6   17

```

```
41  21  1  18
42  22  1  18
43  23  8  -1
44  24  6  13
45  25  1  14
46  26  1  14
47  27  6  10
48  28  1  11
49  29  1  11
50  30  8  -1
51  31  6   6
52  32  1   7
53  33  1   7
54  34  6   3
55  35  1   4
56  36  1   4
57  37  8  -1
58  38  1  -1
59
60 Reading input for MEP 2 weight: 1.000
61 PEG nconf=1 norient=2 nmep=2/2
62
63 Total charge (ich): 0
64 Number of centers: 38
65  39  8  -1
66  40  1  -1
67  41  6   0
68  42  1   0
69  43  1   4
70  44  6   0
71  45  1   0
72  46  1   7
73  47  8  -1
74  48  6   0
75  49  1   0
76  50  1  11
77  51  6   0
78  52  1   0
79  53  1  14
80  54  8  -1
81  55  6   0
82  56  1   0
83  57  1  18
84  58  6  17
85  59  1  18
```

```
86    60    1   18
87    61    8   -1
88    62    6   13
89    63    1   14
90    64    1   14
91    65    6   10
92    66    1   11
93    67    1   11
94    68    8   -1
95    69    6    6
96    70    1    7
97    71    1    7
98    72    6    3
99    73    1    4
100   74    1    4
101   75    8   -1
102   76    1   -1
103   since IQOPT>1, 76 new q0 values
104   will be read in from file ESP.Q0 (unit 3)
105   -----
106   reading mult_esp constraint info
107   -----
108     1    3    2    3
109     1    4    2    4
110     1    6    2    6
111     1    7    2    7
112     1   10    2   10
113     1   11    2   11
114     1   13    2   13
115     1   14    2   14
116     1   17    2   17
117     1   18    2   18
118
119   -----
120     Atom  Ivary
121   -----
122     8   -1
123     1   -1
124     6    0
125     1    0
126     1    4
127     6    0
128     1    0
129     1    7
130     8   -1
```

131	6	0
132	1	0
133	1	11
134	6	0
135	1	0
136	1	14
137	8	-1
138	6	0
139	1	0
140	1	18
141	6	17
142	1	18
143	1	18
144	8	-1
145	6	13
146	1	14
147	1	14
148	6	10
149	1	11
150	1	11
151	8	-1
152	6	6
153	1	7
154	1	7
155	6	3
156	1	4
157	1	4
158	8	-1
159	1	-1
160		
161	8	-1
162	1	-1
163	6	3
164	1	4
165	1	4
166	6	6
167	1	7
168	1	7
169	8	-1
170	6	10
171	1	11
172	1	11
173	6	13
174	1	14
175	1	14

```
176 8 -1
177 6 17
178 1 18
179 1 18
180 6 17
181 1 18
182 1 18
183 8 -1
184 6 13
185 1 14
186 1 14
187 6 10
188 1 11
189 1 11
190 8 -1
191 6 6
192 1 7
193 1 7
194 6 3
195 1 4
196 1 4
197 8 -1
198 1 -1
199
200 -----
```

201

202

203 Total number of atoms = 76

204 Weight factor on initial charge restraints= 0.001000

205

206

207 There are 2 charge constraints

208

209 Reading esp"s for MEP 1

210 total number of atoms = 38

211 total number of esp points = 1343

212

213	Center	X	Y	Z
214	1	0.6921875E+01	0.0000000E+00	0.0000000E+00
215	2	0.5544932E+01	0.5228702E+00	-0.1112595E+01
216	3	0.9202531E+01	0.1152364E+01	-0.8079542E+00
217	4	0.1072558E+02	0.2609371E+00	0.2795339E+00
218	5	0.9562533E+01	0.7840227E+00	-0.2822476E+01
219	6	0.9277383E+01	0.3997800E+01	-0.3611852E+00

```
220 7 0.8802075E+01 0.4410003E+01 0.1618172E+01
221 8 0.1120370E+02 0.4696360E+01 -0.7156279E+00
222 9 0.7613559E+01 0.5264367E+01 -0.2054157E+01
223 10 0.5553478E+01 0.6584469E+01 -0.9804749E+00
224 11 0.6176675E+01 0.7837775E+01 0.5641002E+00
225 12 0.4813837E+01 0.7765209E+01 -0.2509881E+01
226 13 0.3430350E+01 0.4895583E+01 0.0000000E+00
227 14 0.4056095E+01 0.3789568E+01 0.1641580E+01
228 15 0.1852413E+01 0.6112052E+01 0.6096502E+00
229 16 0.2659389E+01 0.3276995E+01 -0.2001433E+01
230 17 0.1857468E+00 0.2249537E+01 -0.1779595E+01
231 18 -0.1154398E+01 0.3722932E+01 -0.1172917E+01
232 19 -0.3315184E+00 0.1637799E+01 -0.3686874E+01
233 20 0.0000000E+00 0.0000000E+00 0.0000000E+00
234 21 0.6444419E+00 0.4778852E+00 0.1910420E+01
235 22 -0.2000224E+01 -0.5758354E+00 0.1444752E+00
236 23 0.1471839E+01 -0.1979148E+01 -0.1052676E+01
237 24 0.1412512E+01 -0.4302171E+01 0.2879905E+00
238 25 -0.5345884E+00 -0.4774070E+01 0.8535023E+00
239 26 0.2058463E+01 -0.5732796E+01 -0.1062803E+01
240 27 0.3134847E+01 -0.4391665E+01 0.2589051E+01
241 28 0.3428997E+01 -0.6385129E+01 0.3132179E+01
242 29 0.4966289E+01 -0.3565571E+01 0.2077797E+01
243 30 0.1982725E+01 -0.3065992E+01 0.4632599E+01
244 31 0.3569103E+01 -0.2776484E+01 0.6779027E+01
245 32 0.2341747E+01 -0.2722364E+01 0.8445220E+01
246 33 0.4830066E+01 -0.4423860E+01 0.6986255E+01
247 34 0.5135153E+01 -0.3415831E+00 0.6656649E+01
248 35 0.6202132E+01 -0.2522557E+00 0.4877610E+01
249 36 0.3857658E+01 0.1285613E+01 0.6697336E+01
250 37 0.6728485E+01 -0.8666283E-01 0.8813608E+01
251 38 0.8069788E+01 -0.1325148E+01 0.8657421E+01
```

252

253 Reading esp"s for MEP 2

254 total number of atoms = 38

255 total number of esp points = 1345

256

```
257 Center X Y Z
258 1 0.6013108E+01 0.0000000E+00 0.0000000E+00
259 2 0.4787887E+01 0.8174350E+00 0.1112595E+01
260 3 0.6399177E+01 -0.2525923E+01 0.8079542E+00
261 4 0.8009296E+01 -0.3248305E+01 -0.2795339E+00
262 5 0.6908099E+01 -0.2605140E+01 0.2822476E+01
263 6 0.4126024E+01 -0.4239071E+01 0.3611852E+00
264 7 0.3514439E+01 -0.4091448E+01 -0.1618172E+01
```

```
265      8      0.4675813E+01 -0.6213011E+01  0.7156279E+00
266      9      0.2128742E+01 -0.3619902E+01  0.2054157E+01
267     10     -0.1422113E+00 -0.2709202E+01  0.9804749E+00
268     11     -0.8007317E+00 -0.3944316E+01 -0.5641002E+00
269     12     -0.1532987E+01 -0.2792624E+01  0.2509881E+01
270     13      0.0000000E+00  0.0000000E+00  0.0000000E+00
271     14      0.1263803E+01  0.1327589E+00 -0.1641580E+01
272     15     -0.1906626E+01  0.5783336E+00 -0.6096502E+00
273     16      0.8701149E+00  0.1567516E+01  0.2001433E+01
274     17      0.2702951E+00  0.4178031E+01  0.1779595E+01
275     18     -0.1707430E+01  0.4413583E+01  0.1172917E+01
276     19      0.4679925E+00  0.4954370E+01  0.3686874E+01
277     20      0.1993907E+01  0.5635456E+01  0.0000000E+00
278     21      0.1979032E+01  0.4833297E+01 -0.1910420E+01
279     22      0.1301290E+01  0.7598303E+01 -0.1444752E+00
280     23      0.4459859E+01  0.5586353E+01  0.1052676E+01
281     24      0.6316706E+01  0.6983522E+01 -0.2879905E+00
282     25      0.5570313E+01  0.8842767E+01 -0.8535023E+00
283     26      0.7856523E+01  0.7288316E+01  0.1062803E+01
284     27      0.7389643E+01  0.5633245E+01 -0.2589051E+01
285     28      0.9183424E+01  0.6551274E+01 -0.3132179E+01
286     29      0.7780508E+01  0.3662501E+01 -0.2077797E+01
287     30      0.5641361E+01  0.5801491E+01 -0.4632599E+01
288     31      0.6326793E+01  0.4341836E+01 -0.6779027E+01
289     32      0.5570064E+01  0.5309665E+01 -0.8445220E+01
290     33      0.8400187E+01  0.4271775E+01 -0.6986255E+01
291     34      0.5253744E+01  0.1653004E+01 -0.6656649E+01
292     35      0.5800561E+01  0.7324521E+00 -0.4877610E+01
293     36      0.3187180E+01  0.1748244E+01 -0.6697336E+01
294     37      0.5971372E+01  0.2077697E+00 -0.8813608E+01
295     38      0.7758518E+01 -0.1651261E+00 -0.8657421E+01
```

```
296 Initial ssvpot = 0.442
```

```
297
```

```
298
```

```
299 Number of unique UNfrozen centers= 10
```

```
300
```

```
301 Non-linear optimization requested.
```

```
302 qchnge = 0.2269581368E-01
```

```
303 qchnge = 0.1442777487E-02
```

```
304 qchnge = 0.1163225555E-03
```

```
305 qchnge = 0.9182987111E-05
```

```
306 qchnge = 0.7248932661E-06
```

```
307
```

```
308 Convergence in 4 iterations
```

```
309
```

```
310 1 PEG nconf=1 norient=1 nmep=1/2
311 2 PEG nconf=1 norient=2 nmep=2/2
312
313 Point Charges Before & After Optimization
314
315 no. At.no. q(init) q(opt) ivary d(rstr)/dq
316 1 8 -0.585064 -0.585064 -1 0.001685
317 2 1 0.386220 0.386220 -1 0.000000
318 3 6 0.128266 0.133478 0 0.005996
319 4 1 0.040840 0.050068 0 0.000000
320 5 1 0.041780 0.050068 4 0.000000
321 6 6 0.066218 0.050631 0 0.008921
322 7 1 0.048474 0.041777 0 0.000000
323 8 1 0.037129 0.041777 7 0.000000
324 9 8 -0.328538 -0.328538 -1 0.002912
325 10 6 -0.014615 0.019526 0 0.009815
326 11 1 0.064010 0.064468 0 0.000000
327 12 1 0.092006 0.064468 11 0.000000
328 13 6 0.071593 0.044207 0 0.009146
329 14 1 0.006493 0.053366 0 0.000000
330 15 1 0.055238 0.053366 14 0.000000
331 16 8 -0.284445 -0.284445 -1 0.003317
332 17 6 -0.000117 0.008855 0 0.009961
333 18 1 0.061387 0.067887 0 0.000000
334 19 1 0.084520 0.067887 18 0.000000
335 20 6 0.018437 0.008855 17 0.009961
336 21 1 0.051198 0.067887 18 0.000000
337 22 1 0.063521 0.067887 18 0.000000
338 23 8 -0.284445 -0.284445 -1 0.003317
339 24 6 -0.010209 0.044207 13 0.009146
340 25 1 0.073391 0.053366 14 0.000000
341 26 1 0.080815 0.053366 14 0.000000
342 27 6 0.006552 0.019526 10 0.009815
343 28 1 0.052308 0.064468 11 0.000000
344 29 1 0.096069 0.064468 11 0.000000
345 30 8 -0.328538 -0.328538 -1 0.002912
346 31 6 0.041494 0.050631 6 0.008921
347 32 1 0.079468 0.041777 7 0.000000
348 33 1 0.037826 0.041777 7 0.000000
349 34 6 -0.024871 0.133478 3 0.005996
350 35 1 0.137508 0.050068 4 0.000000
351 36 1 0.136925 0.050068 4 0.000000
352 37 8 -0.585064 -0.585064 -1 0.001685
353 38 1 0.386220 0.386220 -1 0.000000
354
```

B.2. PEG WITH A HYDROXYETHYL TERMINAL, $N = 4$

355	39	8	-0.585064	-0.585064	-1	0.001685
356	40	1	0.386220	0.386220	-1	0.000000
357	41	6	0.128266	0.133478	3	0.005996
358	42	1	0.040840	0.050068	4	0.000000
359	43	1	0.041780	0.050068	4	0.000000
360	44	6	0.066218	0.050631	6	0.008921
361	45	1	0.048474	0.041777	7	0.000000
362	46	1	0.037129	0.041777	7	0.000000
363	47	8	-0.328538	-0.328538	-1	0.002912
364	48	6	-0.014615	0.019526	10	0.009815
365	49	1	0.064010	0.064468	11	0.000000
366	50	1	0.092006	0.064468	11	0.000000
367	51	6	0.071593	0.044207	13	0.009146
368	52	1	0.006493	0.053366	14	0.000000
369	53	1	0.055238	0.053366	14	0.000000
370	54	8	-0.284445	-0.284445	-1	0.003317
371	55	6	-0.000117	0.008855	17	0.009961
372	56	1	0.061387	0.067887	18	0.000000
373	57	1	0.084520	0.067887	18	0.000000
374	58	6	0.018437	0.008855	17	0.009961
375	59	1	0.051198	0.067887	18	0.000000
376	60	1	0.063521	0.067887	18	0.000000
377	61	8	-0.284445	-0.284445	-1	0.003317
378	62	6	-0.010209	0.044207	13	0.009146
379	63	1	0.073391	0.053366	14	0.000000
380	64	1	0.080815	0.053366	14	0.000000
381	65	6	0.006552	0.019526	10	0.009815
382	66	1	0.052308	0.064468	11	0.000000
383	67	1	0.096069	0.064468	11	0.000000
384	68	8	-0.328538	-0.328538	-1	0.002912
385	69	6	0.041494	0.050631	6	0.008921
386	70	1	0.079468	0.041777	7	0.000000
387	71	1	0.037826	0.041777	7	0.000000
388	72	6	-0.024871	0.133478	3	0.005996
389	73	1	0.137508	0.050068	4	0.000000
390	74	1	0.136925	0.050068	4	0.000000
391	75	8	-0.585064	-0.585064	-1	0.001685
392	76	1	0.386220	0.386220	-1	0.000000

393

394 Sum over the calculated charges: -0.000

395

396 Statistics of the fitting:

397 The initial **sum** of squares (ssvpot) 0.442

398 The residual **sum** of squares (chipot) 0.015

399 The std err of estimate (sqrt(chipot/N)) 0.00235

```
400   ESP relative RMS (SQRT(chipot/ssvpot))           0.18355
401   The Pearson correlation coefficient (r2)         0.96784
402
403   Center of Mass (a.u.):
404   #MEP   X           Y           Z
405     1    4.30234    0.64250    1.33386
406     2    3.96897    1.75963   -1.33386
407
408   Dipole moments (Debye) computed:
409   -with respect to the origin of coordinates (ooc)
410   -with respect to the center of mass (com)
411   #MEP     D           Dx           Dy           Dz
412     1 ooc    0.70969    0.00509   -0.54961    0.44896
413     1 com    0.70969    0.00509   -0.54961    0.44896
414
415     2 ooc    0.70969    0.45043    0.31498   -0.44896
416     2 com    0.70969    0.45043    0.31498   -0.44896
417
418   Traceless Quadrupole moments (Buckingham) computed:
419   -with respect to the origin of coordinates (ooc)
420   -with respect to the center of mass (com)
421   #MEP     X           Y           Z
422     1 ooc X   24.68769
423             Y  -20.11401   19.26294
424             Z   16.51201  -4.80233  -43.95063
425     1 com X   24.90135
426             Y  -16.36531   20.66739
427             Z   13.43482  -4.09644  -45.56874
428
429     2 ooc X   40.13168
430             Y   -4.08858    6.64815
431             Z  -14.91870    6.63824  -46.77983
432     2 com X   37.56796
433             Y   -7.33151    8.00079
434             Z  -11.13609    8.55938  -45.56875
435
436   Traceless Quadrupole moments (Buckingham) in principal axes computed:
437   -with respect to the origin of coordinates (ooc)
438   -with respect to the center of mass (com)
439   #MEP     X           Y           Z
440     1 ooc X   45.04103
441             Y   -0.00000    2.67595
442             Z    0.00000    0.00000  -47.71698
443     1 com X   41.19415
444             Y    0.00000    6.86644
```

```
445      Z    0.00000   0.00000 -48.06059
446
447    2 ooc X 43.34445
448      Y   -0.00000   6.53850
449      Z   -0.00000   0.00000 -49.88296
450    2 com X 41.19417
451      Y   -0.00000   6.86643
452      Z    0.00000   0.00000 -48.06060
```

B.2.6 Fitting statistics of a fragment approach

```
1
2 -----
3   Restrained ESP Fit 2.4 q4md-forcefieldtools
4 -----
5   RESP-A1 - RESP input generated by PyRED version SEP-2015
6 -----
7
8
9   inopt      =    0   ioutopt   =    1
10  nmep       =    2   iqopt     =    2
11  ihfree     =    1   irstrnt   =    1
12  iunits     =    0   qwt       =  0.00100000
13
14  multiple-MEP run of 2 MEP
15
16  Reading input for MEP 1 weight: 1.000
17  PEG nconf=1 norient=1 nmep=1/2
18
19  Total charge (ich): 0
20  Number of centers: 38
21    1    8   -1
22    2    1  -1
23    3    6   0
24    4    1   0
25    5    1   4
26    6    6   0
27    7    1   0
28    8    1   7
29    9    8  -1
30   10    6   0
31   11    1   0
32   12    1  11
33   13    6   0
34   14    1   0
```

```
35 15 1 14
36 16 8 -1
37 17 6 0
38 18 1 0
39 19 1 18
40 20 6 0
41 21 1 0
42 22 1 21
43 23 8 -1
44 24 6 0
45 25 1 0
46 26 1 25
47 27 6 0
48 28 1 0
49 29 1 28
50 30 8 -1
51 31 6 0
52 32 1 0
53 33 1 32
54 34 6 0
55 35 1 0
56 36 1 35
57 37 8 -1
58 38 1 -1
59
60 Reading input for MEP 2 weight: 1.000
61 PEG nconf=1 norient=2 nmep=2/2
62
63 Total charge (ich): 0
64 Number of centers: 38
65 39 8 -1
66 40 1 -1
67 41 6 0
68 42 1 0
69 43 1 4
70 44 6 0
71 45 1 0
72 46 1 7
73 47 8 -1
74 48 6 0
75 49 1 0
76 50 1 11
77 51 6 0
78 52 1 0
79 53 1 14
```

```

80    54    8   -1
81    55    6    0
82    56    1    0
83    57    1   18
84    58    6    0
85    59    1    0
86    60    1   21
87    61    8   -1
88    62    6    0
89    63    1    0
90    64    1   25
91    65    6    0
92    66    1    0
93    67    1   28
94    68    8   -1
95    69    6    0
96    70    1    0
97    71    1   32
98    72    6    0
99    73    1    0
100   74    1   35
101   75    8   -1
102   76    1   -1
103    1    1    1    2    1    3    1    4    1    5    1    6    1    7    1    8
104   since IQOPT>1, 76 new q0 values
105   will be read in from file ESP.Q0 (unit 3)
106   -----
107   reading mult_esp constraint info
108   -----
109    1    3    2    3
110    1    4    2    4
111    1    6    2    6
112    1    7    2    7
113    1   10    2   10
114    1   11    2   11
115    1   13    2   13
116    1   14    2   14
117    1   17    2   17
118    1   18    2   18
119    1   20    2   20
120    1   21    2   21
121    1   24    2   24
122    1   25    2   25
123    1   27    2   27
124    1   28    2   28

```

125	1	31	2	31
126	1	32	2	32
127	1	34	2	34
128	1	35	2	35
129				
130	-----			
131	Atom	Ivary		
132	-----			
133	8	-1		
134	1	-1		
135	6	0		
136	1	0		
137	1	4		
138	6	0		
139	1	0		
140	1	7		
141	8	-1		
142	6	0		
143	1	0		
144	1	11		
145	6	0		
146	1	0		
147	1	14		
148	8	-1		
149	6	0		
150	1	0		
151	1	18		
152	6	0		
153	1	0		
154	1	21		
155	8	-1		
156	6	0		
157	1	0		
158	1	25		
159	6	0		
160	1	0		
161	1	28		
162	8	-1		
163	6	0		
164	1	0		
165	1	32		
166	6	0		
167	1	0		
168	1	35		
169	8	-1		

170	1	-1
171		
172	8	-1
173	1	-1
174	6	3
175	1	4
176	1	4
177	6	6
178	1	7
179	1	7
180	8	-1
181	6	10
182	1	11
183	1	11
184	6	13
185	1	14
186	1	14
187	8	-1
188	6	17
189	1	18
190	1	18
191	6	20
192	1	21
193	1	21
194	8	-1
195	6	24
196	1	25
197	1	25
198	6	27
199	1	28
200	1	28
201	8	-1
202	6	31
203	1	32
204	1	32
205	6	34
206	1	35
207	1	35
208	8	-1
209	1	-1

210
211

212
213

```
214 Total number of atoms = 76
215 Weight factor on initial charge restraints= 0.001000
216
217
218 There are 3 charge constraints
219
220 Reading esp"s for MEP 1
221 total number of atoms = 38
222 total number of esp points = 1343
223
224 Center      X          Y          Z
225 1      0.6921875E+01  0.0000000E+00  0.0000000E+00
226 2      0.5544932E+01  0.5228702E+00 -0.1112595E+01
227 3      0.9202531E+01  0.1152364E+01 -0.8079542E+00
228 4      0.1072558E+02  0.2609371E+00  0.2795339E+00
229 5      0.9562533E+01  0.7840227E+00 -0.2822476E+01
230 6      0.9277383E+01  0.3997800E+01 -0.3611852E+00
231 7      0.8802075E+01  0.4410003E+01  0.1618172E+01
232 8      0.1120370E+02  0.4696360E+01 -0.7156279E+00
233 9      0.7613559E+01  0.5264367E+01 -0.2054157E+01
234 10     0.5553478E+01  0.6584469E+01 -0.9804749E+00
235 11     0.6176675E+01  0.7837775E+01  0.5641002E+00
236 12     0.4813837E+01  0.7765209E+01 -0.2509881E+01
237 13     0.3430350E+01  0.4895583E+01  0.0000000E+00
238 14     0.4056095E+01  0.3789568E+01  0.1641580E+01
239 15     0.1852413E+01  0.6112052E+01  0.6096502E+00
240 16     0.2659389E+01  0.3276995E+01 -0.2001433E+01
241 17     0.1857468E+00  0.2249537E+01 -0.1779595E+01
242 18     -0.1154398E+01  0.3722932E+01 -0.1172917E+01
243 19     -0.3315184E+00  0.1637799E+01 -0.3686874E+01
244 20     0.0000000E+00  0.0000000E+00  0.0000000E+00
245 21     0.6444419E+00  0.4778852E+00  0.1910420E+01
246 22     -0.2000224E+01 -0.5758354E+00  0.1444752E+00
247 23     0.1471839E+01 -0.1979148E+01 -0.1052676E+01
248 24     0.1412512E+01 -0.4302171E+01  0.2879905E+00
249 25     -0.5345884E+00 -0.4774070E+01  0.8535023E+00
250 26     0.2058463E+01 -0.5732796E+01 -0.1062803E+01
251 27     0.3134847E+01 -0.4391665E+01  0.2589051E+01
252 28     0.3428997E+01 -0.6385129E+01  0.3132179E+01
253 29     0.4966289E+01 -0.3565571E+01  0.2077797E+01
254 30     0.1982725E+01 -0.3065992E+01  0.4632599E+01
255 31     0.3569103E+01 -0.2776484E+01  0.6779027E+01
256 32     0.2341747E+01 -0.2722364E+01  0.8445220E+01
257 33     0.4830066E+01 -0.4423860E+01  0.6986255E+01
258 34     0.5135153E+01 -0.3415831E+00  0.6656649E+01
```

```
259 35 0.6202132E+01 -0.2522557E+00 0.4877610E+01
260 36 0.3857658E+01 0.1285613E+01 0.6697336E+01
261 37 0.6728485E+01 -0.8666283E-01 0.8813608E+01
262 38 0.8069788E+01 -0.1325148E+01 0.8657421E+01
263
264 Reading esp"s for MEP 2
265 total number of atoms = 38
266 total number of esp points = 1345
267
268 Center X Y Z
269 1 0.6013108E+01 0.0000000E+00 0.0000000E+00
270 2 0.4787887E+01 0.8174350E+00 0.1112595E+01
271 3 0.6399177E+01 -0.2525923E+01 0.8079542E+00
272 4 0.8009296E+01 -0.3248305E+01 -0.2795339E+00
273 5 0.6908099E+01 -0.2605140E+01 0.2822476E+01
274 6 0.4126024E+01 -0.4239071E+01 0.3611852E+00
275 7 0.3514439E+01 -0.4091448E+01 -0.1618172E+01
276 8 0.4675813E+01 -0.6213011E+01 0.7156279E+00
277 9 0.2128742E+01 -0.3619902E+01 0.2054157E+01
278 10 -0.1422113E+00 -0.2709202E+01 0.9804749E+00
279 11 -0.8007317E+00 -0.3944316E+01 -0.5641002E+00
280 12 -0.1532987E+01 -0.2792624E+01 0.2509881E+01
281 13 0.0000000E+00 0.0000000E+00 0.0000000E+00
282 14 0.1263803E+01 0.1327589E+00 -0.1641580E+01
283 15 -0.1906626E+01 0.5783336E+00 -0.6096502E+00
284 16 0.8701149E+00 0.1567516E+01 0.2001433E+01
285 17 0.2702951E+00 0.4178031E+01 0.1779595E+01
286 18 -0.1707430E+01 0.4413583E+01 0.1172917E+01
287 19 0.4679925E+00 0.4954370E+01 0.3686874E+01
288 20 0.1993907E+01 0.5635456E+01 0.0000000E+00
289 21 0.1979032E+01 0.4833297E+01 -0.1910420E+01
290 22 0.1301290E+01 0.7598303E+01 -0.1444752E+00
291 23 0.4459859E+01 0.5586353E+01 0.1052676E+01
292 24 0.6316706E+01 0.6983522E+01 -0.2879905E+00
293 25 0.5570313E+01 0.8842767E+01 -0.8535023E+00
294 26 0.7856523E+01 0.7288316E+01 0.1062803E+01
295 27 0.7389643E+01 0.5633245E+01 -0.2589051E+01
296 28 0.9183424E+01 0.6551274E+01 -0.3132179E+01
297 29 0.7780508E+01 0.3662501E+01 -0.2077797E+01
298 30 0.5641361E+01 0.5801491E+01 -0.4632599E+01
299 31 0.6326793E+01 0.4341836E+01 -0.6779027E+01
300 32 0.5570064E+01 0.5309665E+01 -0.8445220E+01
301 33 0.8400187E+01 0.4271775E+01 -0.6986255E+01
302 34 0.5253744E+01 0.1653004E+01 -0.6656649E+01
303 35 0.5800561E+01 0.7324521E+00 -0.4877610E+01
```

```

304    36    0.3187180E+01  0.1748244E+01 -0.6697336E+01
305    37    0.5971372E+01  0.2077697E+00 -0.8813608E+01
306    38    0.7758518E+01 -0.1651261E+00 -0.8657421E+01
307 Initial ssvpot =  0.442
308
309
310 Number of unique UNfrozen centers= 20
311
312 Non-linear optimization requested.
313 qchnge =  0.2880537305E-01
314 qchnge =  0.3190330277E-02
315 qchnge =  0.4803236227E-03
316 qchnge =  0.1021344006E-03
317 qchnge =  0.2487031914E-04
318 qchnge =  0.6197372417E-05
319 qchnge =  0.1554030010E-05
320 qchnge =  0.3908564064E-06
321
322 Convergence in 7 iterations
323
324    1  PEG nconf=1 norient=1 nmep=1/2
325    2  PEG nconf=1 norient=2 nmep=2/2
326
327          Point Charges Before & After Optimization
328
329  no.  At.no.  q(init)    q(opt)    ivary  d(rstr)/dq
330    1    8    -0.564852  -0.564852  -1     0.001743
331    2    1     0.352783   0.352783  -1     0.000000
332    3    6     0.022844   0.113979   0     0.006595
333    4    1     0.086312   0.077240   0     0.000000
334    5    1     0.099246   0.077240   4     0.000000
335    6    6    -0.243550  -0.340580   0     0.002817
336    7    1     0.131838   0.149645   0     0.000000
337    8    1     0.130481   0.149645   7     0.000000
338    9    8    -0.218335  -0.218335  -1     0.004164
339   10    6    -0.033266   0.032006   0     0.009524
340   11    1     0.078702   0.062998   0     0.000000
341   12    1     0.072214   0.062998  11     0.000000
342   13    6     0.089346   0.045808   0     0.009092
343   14    1    -0.008153   0.031955   0     0.000000
344   15    1     0.047697   0.031955  14     0.000000
345   16    8    -0.247887  -0.247887  -1     0.003741
346   17    6    -0.019384  -0.014929   0     0.009890
347   18    1     0.063706   0.072222   0     0.000000
348   19    1     0.079755   0.072222  18     0.000000

```

B.2. PEG WITH A HYDROXYETHYL TERMINAL, $N = 4$

349	20	6	0.015047	0.029087	0	0.009602
350	21	1	0.069205	0.056516	0	0.000000
351	22	1	0.060809	0.056516	21	0.000000
352	23	8	-0.263812	-0.263812	-1	0.003544
353	24	6	-0.005199	0.041382	0	0.009240
354	25	1	0.070001	0.052584	0	0.000000
355	26	1	0.072293	0.052584	25	0.000000
356	27	6	0.028340	0.038840	0	0.009322
357	28	1	0.038177	0.057911	0	0.000000
358	29	1	0.110734	0.057911	28	0.000000
359	30	8	-0.356868	-0.356868	-1	0.002698
360	31	6	0.172652	0.184369	0	0.004767
361	32	1	0.104571	0.064579	0	0.000000
362	33	1	0.044342	0.064579	32	0.000000
363	34	6	-0.833795	-0.779558	0	0.001272
364	35	1	0.423482	0.356185	0	0.000000
365	36	1	0.345625	0.356185	35	0.000000
366	37	8	-0.400959	-0.400959	-1	0.002420
367	38	1	0.385859	0.385859	-1	0.000000
368						
369	39	8	-0.564852	-0.564852	-1	0.001743
370	40	1	0.352783	0.352783	-1	0.000000
371	41	6	0.022844	0.113979	3	0.006595
372	42	1	0.086312	0.077240	4	0.000000
373	43	1	0.099246	0.077240	4	0.000000
374	44	6	-0.243550	-0.340580	6	0.002817
375	45	1	0.131838	0.149645	7	0.000000
376	46	1	0.130481	0.149645	7	0.000000
377	47	8	-0.218335	-0.218335	-1	0.004164
378	48	6	-0.033266	0.032006	10	0.009524
379	49	1	0.078702	0.062998	11	0.000000
380	50	1	0.072214	0.062998	11	0.000000
381	51	6	0.089346	0.045808	13	0.009092
382	52	1	-0.008153	0.031955	14	0.000000
383	53	1	0.047697	0.031955	14	0.000000
384	54	8	-0.247887	-0.247887	-1	0.003741
385	55	6	-0.019384	-0.014929	17	0.009890
386	56	1	0.063706	0.072222	18	0.000000
387	57	1	0.079755	0.072222	18	0.000000
388	58	6	0.015047	0.029087	20	0.009602
389	59	1	0.069205	0.056516	21	0.000000
390	60	1	0.060809	0.056516	21	0.000000
391	61	8	-0.263812	-0.263812	-1	0.003544
392	62	6	-0.005199	0.041382	24	0.009240
393	63	1	0.070001	0.052584	25	0.000000

```

394  64  1    0.072293    0.052584    25    0.000000
395  65  6    0.028340    0.038840    27    0.009322
396  66  1    0.038177    0.057911    28    0.000000
397  67  1    0.110734    0.057911    28    0.000000
398  68  8   -0.356868   -0.356868   -1    0.002698
399  69  6    0.172652    0.184369    31    0.004767
400  70  1    0.104571    0.064579    32    0.000000
401  71  1    0.044342    0.064579    32    0.000000
402  72  6   -0.833795   -0.779558    34    0.001272
403  73  1    0.423482    0.356185    35    0.000000
404  74  1    0.345625    0.356185    35    0.000000
405  75  8   -0.400959   -0.400959   -1    0.002420
406  76  1    0.385859    0.385859   -1    0.000000
407
408 Sum over the calculated charges: -0.000
409
410     Statistics of the fitting:
411 The initial sum of squares (ssvpot)           0.442
412 The residual sum of squares (chipot)         0.022
413 The std err of estimate (sqrt(chipot/N))       0.00286
414 ESP relative RMS (SQRT(chipot/ssvpot))        0.22304
415 The Pearson correlation coefficient (r2)        0.95146
416
417 Center of Mass (a.u.):
418 #MEP   X           Y           Z
419   1    4.30234    0.64250    1.33386
420   2    3.96897    1.75963   -1.33386
421
422 Dipole moments (Debye) computed:
423 -with respect to the origin of coordinates (ooc)
424 -with respect to the center of mass (com)
425 #MEP      D      Dx      Dy      Dz
426   1 ooc    0.74627  -0.07127  -0.40243  0.62442
427   1 com    0.74627  -0.07127  -0.40243  0.62442
428
429   2 ooc    0.74627    0.28626    0.29169  -0.62442
430   2 com    0.74627    0.28626    0.29169  -0.62442
431
432 Traceless Quadrupole moments (Buckingham) computed:
433 -with respect to the origin of coordinates (ooc)
434 -with respect to the center of mass (com)
435 #MEP      X           Y           Z
436   1 ooc X   19.33560
437           Y  -18.04555  19.08803
438           Z   18.87377  -4.20002 -38.42363

```

```

439 1 com X 20.59248
440      Y -15.22423 20.19230
441      Z 14.75985 -3.98477 -40.78478
442
443 2 ooc X 35.70157
444      Y -2.50992 5.06592
445      Z -16.35508 7.34103 -40.76749
446 2 com X 34.72140
447      Y -5.14749 6.06340
448      Z -11.81455 9.70300 -40.78480
449
450 Traceless Quadrupole moments (Buckingham) in principal axes computed:
451 -with respect to the origin of coordinates (ooc)
452 -with respect to the center of mass (com)
453 #MEP      X      Y      Z
454 1 ooc X 40.75329
455      Y 0.00000 3.31249
456      Z 0.00000 0.00000 -44.06578
457 1 com X 37.91756
458      Y 0.00000 6.23629
459      Z 0.00000 0.00000 -44.15385
460
461 2 ooc X 39.50876
462      Y -0.00000 5.50625
463      Z -0.00000 0.00000 -45.01501
464 2 com X 37.91756
465      Y -0.00000 6.23631
466      Z 0.00000 0.00000 -44.15387

```

B.2.7 Amber Leap script for PEG-H

```

1 #
2 # Generated by PyRED version SEP-2015
3 #   http://q4md-forcefieldtools.org
4 #
5 logfile q4md-forcefieldtools.log
6 source /home/sajid/amber14/dat/leap/cmd/oldff/leaprc.ff99SB
7 # Web site: http://ambermd.org/doc6/html/AMBER-sh-5.9.html#sh-5.9.8
8 alias q quit
9 alias e edit
10 alias c charge
11
12 # Web site: http://ambermd.org/doc6/html/AMBER-sh-5.9.html#sh-5.9.73
13 verbosity 2
14

```

```
15 # Web site: http://ambermd.org/doc6/html/AMBER-sh-5.9.html#sh-5.9.2
16 addAtomTypes {
17     { "CT" "C" "sp3" }
18     { "H1" "H" "sp3" }
19     { "HO" "H" "sp3" }
20     { "OH" "O" "sp3" }
21     { "OS" "O" "sp3" }
22 }
23
24 # To force the correspondance between residue names
25 # PDB file versus force field libraries:
26 # Web site: http://ambermd.org/doc6/html/AMBER-sh-5.9.html#sh-5.9.7
27 # addPdbResMap {
28 #     { 0 ALA NALA } { 1 ALA CALA }
29 #     { ADE DADE }
30 # }
31
32 # Web site: http://ambermd.org/doc6/html/AMBER-sh-5.9.html#sh-5.9.41
33 frcmod1 = loadAmberParams ./frcmod.known
34 frcmod2 = loadAmberParams ./frcmod.correspondence
35 frcmod3 = loadAmberParams ./frcmod.unknown
36
37 # Web site: http://q4md-forcefieldtools.org/Tutorial/leap-mol3.php
38 # Web site: http://q4md-forcefieldtools.org/Tutorial/leap-mol2.php
39 F00 = loadmol3 ../Mol_m1/Mol-ia1_m1-cl.mol2
40 F01 = loadmol3 ../Mol_m1/Mol-ia2_m1-cl.mol2
41 F02 = loadmol3 ../Mol_m1/Mol-ia3_m1-cl.mol2
42 U01 = loadmol3 ../Mol_m1/Mol-sm_m1-cl.mol2
43
44 # To match the residue names found in the PDB file
45 # Web site: http://ambermd.org/doc6/html/AMBER-sh-5.9.html#sh-5.9.19
46 # ZZZ = copy F00
47
48 # If a copy is done, define the molecule and residue
49 # Web site: http://ambermd.org/doc6/html/AMBER-sh-5.9.html#sh-5.9.63
50 # set ZZZ name "ZZZ"
51 # set ZZZ.1 name "ZZZ"
52
53 # Let's load the PDB file
54 # Web site: http://ambermd.org/doc6/html/AMBER-sh-5.9.html#sh-5.9.44
55 # VAR = loadPdb Your-PDB-file.ent
56
57 # Let's save the prmtop and prmcrd file with specific file extensions
58 # (to be automatically recognized by VMD http://www.ks.uiuc.edu/
    Research/vmd/)
```

```
59 # Web site: http://ambermd.org/doc6/html/AMBER-sh-5.9.html#sh-5.9.54
60 # saveAmberParm F00 F00.parm7 F00.rst7
61
62 # q
63 PG8000 = sequence { F01 F02 F02 F02 F02 F02 F02 F02 F02 F02 F02 F02 F02 F02
      F02 F02 F02 F02 F02 F02 F02 F02 F02 F02 F02 F02 F02 F02 F02
      F02 F02 F02 F02 F02 F02 F02 F02 F02 F02 F02 F02 F02 F02 F02 F02
      F00 }
64 charge PG8000
65 saveoff PG8000 PG8000.off
66 savepdb PG8000 PG8000.pdb
67 saveamberparm PG8000 PG8000.prmtop PG8000.inpcrd
68 quit
```

B.3 PEG with hydroxyethyl terminal, multiple conformations**B.3.1 FF libraries for 'A' fragment**

```

1 #
2 # Generated by PyRED version SEP-2015
3 #   http://q4md-forcefieldtools.org
4 #
5 @<TRIPOS>MOLECULE
6 F00_0
7   9   8   1   0   1
8 SMALL
9 USER_CHARGES
10 @<TRIPOS>ATOM
11   1 O4   0.056039  0.238964 -0.333802 OS 1   F00 -0.1415  0.0000 ****
12   2 C5   0.862554 -0.062393  0.805661 CT 1   F00  0.0406  0.0000 ****
13   3 H51  0.362064 -0.773093  1.480781 H1 1   F00  0.0865  0.0000 ****
14   4 H52  1.072422  0.861795  1.364741 H1 1   F00  0.0865  0.0000 ****
15   5 C6   2.158639 -0.650715  0.268457 CT 1   F00 -0.4961  0.0000 ****
16   6 H61  1.937152 -1.598539 -0.249741 H1 1   F00  0.2120  0.0000 ****
17   7 H62  2.836539 -0.872771  1.099235 H1 1   F00  0.2120  0.0000 ****
18   8 O7   2.825121  0.263058 -0.582429 OH 1   F00 -0.3765  0.0000 ****
19   9 H71  2.154049  0.558849 -1.220066 HO 1   F00  0.3575  0.0000 ****
20 @<TRIPOS>BOND
21   1   1   2 1
22   2   2   3 1
23   3   2   4 1
24   4   2   5 1
25   5   5   6 1
26   6   5   7 1
27   7   5   8 1
28   8   8   9 1
29 @<TRIPOS>SUBSTRUCTURE
30   1 F00   1 ****   0 ***** *****
31 @<TRIPOS>HEADTAIL
32 O4 1
33 0 0
34 @<TRIPOS>RESIDUECONNECT
35 1 O4 0 0 0 0 0

```

B.3.2 FF libraries for 'B' fragment

```

1 #
2 # Generated by PyRED version SEP-2015
3 #   http://q4md-forcefieldtools.org
4 #

```

B.3. PEG WITH HYDROXYETHYL TERMINAL, MULTIPLE CONFORMATIONS

```
5 @<TRIPOS>MOLECULE
6 F00_1
7     9     8     1     0     1
8 SMALL
9 USER_CHARGES
10 @<TRIPOS>ATOM
11  1 O4      0.056042  0.239002 -0.333815 OS 1  F00 -0.1415 0.0000 ****
12  2 C5      0.862539 -0.062346  0.805655 CT 1  F00  0.0406 0.0000 ****
13  3 H51     0.362030 -0.773014  1.480797 H1 1  F00  0.0865 0.0000 ****
14  4 H52     1.072434  0.861848  1.364716 H1 1  F00  0.0865 0.0000 ****
15  5 C6      2.158613 -0.650718  0.268480 CT 1  F00 -0.4961 0.0000 ****
16  6 H61     1.937109 -1.598551 -0.249695 H1 1  F00  0.2120 0.0000 ****
17  7 H62     2.836498 -0.872765  1.099272 H1 1  F00  0.2120 0.0000 ****
18  8 O7      2.825130  0.263018 -0.582424 OH 1  F00 -0.3765 0.0000 ****
19  9 H71     2.154075  0.558808 -1.220079 HO 1  F00  0.3575 0.0000 ****
20 @<TRIPOS>BOND
21  1     1     2  1
22  2     2     3  1
23  3     2     4  1
24  4     2     5  1
25  5     5     6  1
26  6     5     7  1
27  7     5     8  1
28  8     8     9  1
29 @<TRIPOS>SUBSTRUCTURE
30      1 F00          1 ****          0 **** ****
31 @<TRIPOS>HEADTAIL
32 O4 1
33 0 0
34 @<TRIPOS>RESIDUECONNECT
35 1 O4 0 0 0 0 0
```

B.3.3 FF libraries for 'C' fragment

```
1 #
2 # Generated by PyRED version SEP-2015
3 #   http://q4md-forcefieldtools.org
4 #
5 @<TRIPOS>MOLECULE
6 F00
7     9     8     1     0     1
8 SMALL
9 USER_CHARGES
10 @<TRIPOS>ATOM
11  1 O4      0.120336  0.316293 -0.330261 OS 1  F00 -0.1415 0.0000 ****
```

B.3. PEG WITH HYDROXYETHYL TERMINAL, MULTIPLE CONFORMATIONS

```
12  2 C5    0.852468 -0.409806  0.648487 CT  1  F00  0.0406  0.0000  ****
13  3 H51    0.334290 -1.337227  0.937709 H1  1  F00  0.0865  0.0000  ****
14  4 H52    0.994444  0.207307  1.550713 H1  1  F00  0.0865  0.0000  ****
15  5 C6    2.201878 -0.728258  0.020348 CT  1  F00 -0.4961  0.0000  ****
16  6 H61    2.046413 -1.394144 -0.843957 H1  1  F00  0.2120  0.0000  ****
17  7 H62    2.834973 -1.253815  0.743166 H1  1  F00  0.2120  0.0000  ****
18  8 O7     2.884980  0.454842 -0.353210 OH  1  F00 -0.3765  0.0000  ****
19  9 H71    2.237247  0.967802 -0.865402 HO  1  F00  0.3575  0.0000  ****
20  @<TRIPOS>BOND
21    1      1      2  1
22    2      2      3  1
23    3      2      4  1
24    4      2      5  1
25    5      5      6  1
26    6      5      7  1
27    7      5      8  1
28    8      8      9  1
29  @<TRIPOS>SUBSTRUCTURE
30      1 F00          1 ****          0 **** ****
31  @<TRIPOS>HEADTAIL
32  O4  1
33  0  0
34  @<TRIPOS>RESIDUECONNECT
35  1 O4  0  0  0  0  0
```

B.3.4 FF parameters for PEG-H(m)

```
1  FRCMOD file generated by PyRED version SEP-2015 - q4md-forcefieldtools
   .org
2  MASS      mass              pol              Source
3  CT        12.010            0.878           taken from parm10.dat
4  H1        1.008             0.135           taken from parm10.dat
5  HO        1.008             0.135           taken from parm10.dat
6  OH        16.000            0.465           taken from parm10.dat
7  OS        16.000            0.465           taken from parm10.dat
8
9  BOND      K(kcal.mol-1.ang-2) Dist0(ang) Source
10 CT-CT     310.0              1.526           taken from parm10.dat
11 CT-H1     340.0              1.090           taken from parm10.dat
12 CT-OH     320.0              1.410           taken from parm10.dat
13 CT-OS     320.0              1.410           taken from parm10.dat
14 HO-OH     555.0              0.960           adapted from parm10.dat 553.0
15
16 ANGLE     K(kcal.mol-1.rad-2) Theta0(deg) Source
17 CT-CT-H1  50.0                    109.50          taken from parm10.dat
```

B.3. PEG WITH HYDROXYETHYL TERMINAL, MULTIPLE CONFORMATIONS

18	CT-CT-OH	50.0	109.50	taken	from	parm10.dat
19	CT-CT-OS	50.0	109.50	taken	from	parm10.dat
20	H1-CT-H1	35.0	109.50	taken	from	parm10.dat
21	H1-CT-OH	50.0	109.50	taken	from	parm10.dat
22	H1-CT-OS	50.0	109.50	taken	from	parm10.dat
23	CT-OH-HO	55.0	108.50	taken	from	parm10.dat
24	CT-OS-CT	60.0	109.50	taken	from	parm10.dat
25						
26	DIHEDRAL	Path	V(kcal.mol-1.rad-1)	Phase(deg.)	Period	Source
27	H1-CT-CT-H1	1	1.55555556e-01	0.0	3.	adapted from parm10. dat i.e X-CT-CT-X 1.4/9
28	H1-CT-CT-OH	1	0.00000000e+00	0.0	-3.	taken from parm10. dat
29	H1-CT-CT-OH	1	2.50000000e-01	0.0	1.	taken from parm10. dat
30	H1-CT-CT-OS	1	0.00000000e+00	0.0	-3.	taken from parm10. dat
31	H1-CT-CT-OS	1	2.50000000e-01	0.0	1.	taken from parm10. dat
32	OH-CT-CT-OS	1	1.44000000e-01	0.0	-3.	taken from parm10. dat
33	OH-CT-CT-OS	1	1.17500000e+00	0.0	2.	taken from parm10. dat
34	CT-CT-OH-HO	1	1.60000000e-01	0.0	-3.	taken from parm10. dat
35	CT-CT-OH-HO	1	2.50000000e-01	0.0	1.	taken from parm10. dat
36	H1-CT-OH-HO	1	1.66666667e-01	0.0	3.	adapted from parm10. dat i.e X-CT-OH-X 0.5/3
37	CT-CT-OS-CT	1	3.83000000e-01	0.0	-3.	taken from parm10. dat
38	CT-CT-OS-CT	1	1.00000000e-01	180.0	2.	taken from parm10. dat
39	H1-CT-OS-CT	1	3.83333333e-01	0.0	3.	adapted from parm10. dat i.e X-CT-OS-X 1.15/3
40						
41	IMPROPER		V(kcal.mol-1.rad-1)	Phase(deg.)	Period	Source
42						
43	NONBON	R* (ang)	Eps(kcal.mol-1)			Source
44	CT	1.9080	0.10940000			taken from parm10.dat
45	H1	1.3870	0.01570000			taken from parm10.dat
46	HO	0.0000	0.00000000			taken from parm10.dat
47	OH	1.7210	0.21040000			taken from parm10.dat
48	OS	1.6837	0.17000000			taken from parm10.dat

B.3.5 Fitting statistics of a whole molecule approach

```
1
2 -----
3   Restrained ESP Fit 2.4 q4md-forcefieldtools
4 -----
5   RESP-A1 - RESP input generated by PyRED version SEP-2015
6 -----
7
8
9   inopt      =    0   ioutopt   =    1
10  nmep       =   46   iqopt     =    2
11  ihfree     =    1   irstrnt   =    1
12  iunits     =    0   qwt       = 0.00100000
13
14  multiple-MEP run of 46 MEP
15
16  Reading input for MEP 1 weight: 1.000
17  PEG2 nconf=1 norient=1 nmep=1/46
18
19  Total charge (ich): 0
20  Number of centers: 17
21    1    8   -1
22    2    1  -1
23    3    6    0
24    4    1    0
25    5    1    4
26    6    6    0
27    7    1    0
28    8    1    7
29    9    8   -1
30   10    6    6
31   11    1    7
32   12    1    7
33   13    6    3
34   14    1    4
35   15    1    4
36   16    8   -1
37   17    1   -1
38
39  Reading input for MEP 2 weight: 1.000
40  PEG2 nconf=1 norient=2 nmep=2/46
41
42  Total charge (ich): 0
43  Number of centers: 17
```

B.3. PEG WITH HYDROXYETHYL TERMINAL, MULTIPLE CONFORMATIONS

```
44 18 8 -1
45 19 1 -1
46 20 6 0
47 21 1 0
48 22 1 4
49 23 6 0
50 24 1 0
51 25 1 7
52 26 8 -1
53 27 6 6
54 28 1 7
55 29 1 7
56 30 6 3
57 31 1 4
58 32 1 4
59 33 8 -1
60 34 1 -1
61
62 Reading input for MEP 3 weight: 1.000
63 PEG2 nconf=2 norient=1 nmep=3/46
64
65 Total charge (ich): 0
66 Number of centers: 17
67 35 8 -1
68 36 1 -1
69 37 6 0
70 38 1 0
71 39 1 4
72 40 6 0
73 41 1 0
74 42 1 7
75 43 8 -1
76 44 6 6
77 45 1 7
78 46 1 7
79 47 6 3
80 48 1 4
81 49 1 4
82 50 8 -1
83 51 1 -1
84
85 Reading input for MEP 4 weight: 1.000
86 PEG2 nconf=2 norient=2 nmep=4/46
87
88 Total charge (ich): 0
```

B.3. PEG WITH HYDROXYETHYL TERMINAL, MULTIPLE CONFORMATIONS

```
89  Number of centers: 17
90   52   8  -1
91   53   1  -1
92   54   6   0
93   55   1   0
94   56   1   4
95   57   6   0
96   58   1   0
97   59   1   7
98   60   8  -1
99   61   6   6
100  62   1   7
101  63   1   7
102  64   6   3
103  65   1   4
104  66   1   4
105  67   8  -1
106  68   1  -1
107
108  Reading input for MEP 5 weight: 1.000
109  PEG2 nconf=3 norient=1 nmep=5/46
110
111  Total charge (ich): 0
112  Number of centers: 17
113   69   8  -1
114   70   1  -1
115   71   6   0
116   72   1   0
117   73   1   4
118   74   6   0
119   75   1   0
120   76   1   7
121   77   8  -1
122   78   6   6
123   79   1   7
124   80   1   7
125   81   6   3
126   82   1   4
127   83   1   4
128   84   8  -1
129   85   1  -1
130
131  Reading input for MEP 6 weight: 1.000
132  PEG2 nconf=3 norient=2 nmep=6/46
133
```

B.3. PEG WITH HYDROXYETHYL TERMINAL, MULTIPLE CONFORMATIONS

```
134 Total charge (ich): 0
135 Number of centers: 17
136   86   8  -1
137   87   1  -1
138   88   6   0
139   89   1   0
140   90   1   4
141   91   6   0
142   92   1   0
143   93   1   7
144   94   8  -1
145   95   6   6
146   96   1   7
147   97   1   7
148   98   6   3
149   99   1   4
150  100   1   4
151  101   8  -1
152  102   1  -1
153
154 Reading input for MEP 7 weight: 1.000
155 PEG2 nconf=4 norient=1 nmep=7/46
156
157 Total charge (ich): 0
158 Number of centers: 17
159  103   8  -1
160  104   1  -1
161  105   6   0
162  106   1   0
163  107   1   4
164  108   6   0
165  109   1   0
166  110   1   7
167  111   8  -1
168  112   6   6
169  113   1   7
170  114   1   7
171  115   6   3
172  116   1   4
173  117   1   4
174  118   8  -1
175  119   1  -1
176
177 Reading input for MEP 8 weight: 1.000
178 PEG2 nconf=4 norient=2 nmep=8/46
```

B.3. PEG WITH HYDROXYETHYL TERMINAL, MULTIPLE CONFORMATIONS

```
179
180 Total charge (ich): 0
181 Number of centers: 17
182 120 8 -1
183 121 1 -1
184 122 6 0
185 123 1 0
186 124 1 4
187 125 6 0
188 126 1 0
189 127 1 7
190 128 8 -1
191 129 6 6
192 130 1 7
193 131 1 7
194 132 6 3
195 133 1 4
196 134 1 4
197 135 8 -1
198 136 1 -1
199
200 Reading input for MEP 9 weight: 1.000
201 PEG2 nconf=5 norient=1 nmep=9/46
202
203 Total charge (ich): 0
204 Number of centers: 17
205 137 8 -1
206 138 1 -1
207 139 6 0
208 140 1 0
209 141 1 4
210 142 6 0
211 143 1 0
212 144 1 7
213 145 8 -1
214 146 6 6
215 147 1 7
216 148 1 7
217 149 6 3
218 150 1 4
219 151 1 4
220 152 8 -1
221 153 1 -1
222
223 Reading input for MEP 10 weight: 1.000
```

B.3. PEG WITH HYDROXYETHYL TERMINAL, MULTIPLE CONFORMATIONS

```
224 PEG2 nconf=5 norient=2 nmep=10/46
225
226 Total charge (ich): 0
227 Number of centers: 17
228 154 8 -1
229 155 1 -1
230 156 6 0
231 157 1 0
232 158 1 4
233 159 6 0
234 160 1 0
235 161 1 7
236 162 8 -1
237 163 6 6
238 164 1 7
239 165 1 7
240 166 6 3
241 167 1 4
242 168 1 4
243 169 8 -1
244 170 1 -1
245
246 Reading input for MEP 11 weight: 1.000
247 PEG2 nconf=6 norient=1 nmep=11/46
248
249 Total charge (ich): 0
250 Number of centers: 17
251 171 8 -1
252 172 1 -1
253 173 6 0
254 174 1 0
255 175 1 4
256 176 6 0
257 177 1 0
258 178 1 7
259 179 8 -1
260 180 6 6
261 181 1 7
262 182 1 7
263 183 6 3
264 184 1 4
265 185 1 4
266 186 8 -1
267 187 1 -1
268
```

B.3. PEG WITH HYDROXYETHYL TERMINAL, MULTIPLE CONFORMATIONS

269 Reading **input for** MEP 12 weight: 1.000

270 PEG2 nconf=6 norient=2 nmep=12/46

271

272 Total charge (ich): 0

273 Number of centers: 17

274 188 8 -1

275 189 1 -1

276 190 6 0

277 191 1 0

278 192 1 4

279 193 6 0

280 194 1 0

281 195 1 7

282 196 8 -1

283 197 6 6

284 198 1 7

285 199 1 7

286 200 6 3

287 201 1 4

288 202 1 4

289 203 8 -1

290 204 1 -1

291

292 Reading **input for** MEP 13 weight: 1.000

293 PEG2 nconf=7 norient=1 nmep=13/46

294

295 Total charge (ich): 0

296 Number of centers: 17

297 205 8 -1

298 206 1 -1

299 207 6 0

300 208 1 0

301 209 1 4

302 210 6 0

303 211 1 0

304 212 1 7

305 213 8 -1

306 214 6 6

307 215 1 7

308 216 1 7

309 217 6 3

310 218 1 4

311 219 1 4

312 220 8 -1

313 221 1 -1

B.3. PEG WITH HYDROXYETHYL TERMINAL, MULTIPLE CONFORMATIONS

```
314
315 Reading input for MEP 14 weight: 1.000
316 PEG2 nconf=7 norient=2 nmep=14/46
317
318 Total charge (ich): 0
319 Number of centers: 17
320 222 8 -1
321 223 1 -1
322 224 6 0
323 225 1 0
324 226 1 4
325 227 6 0
326 228 1 0
327 229 1 7
328 230 8 -1
329 231 6 6
330 232 1 7
331 233 1 7
332 234 6 3
333 235 1 4
334 236 1 4
335 237 8 -1
336 238 1 -1
337
338 Reading input for MEP 15 weight: 1.000
339 PEG2 nconf=8 norient=1 nmep=15/46
340
341 Total charge (ich): 0
342 Number of centers: 17
343 239 8 -1
344 240 1 -1
345 241 6 0
346 242 1 0
347 243 1 4
348 244 6 0
349 245 1 0
350 246 1 7
351 247 8 -1
352 248 6 6
353 249 1 7
354 250 1 7
355 251 6 3
356 252 1 4
357 253 1 4
358 254 8 -1
```

B.3. PEG WITH HYDROXYETHYL TERMINAL, MULTIPLE CONFORMATIONS

```
359 255 1 -1
360
361 Reading input for MEP 16 weight: 1.000
362 PEG2 nconf=8 norient=2 nmep=16/46
363
364 Total charge (ich): 0
365 Number of centers: 17
366 256 8 -1
367 257 1 -1
368 258 6 0
369 259 1 0
370 260 1 4
371 261 6 0
372 262 1 0
373 263 1 7
374 264 8 -1
375 265 6 6
376 266 1 7
377 267 1 7
378 268 6 3
379 269 1 4
380 270 1 4
381 271 8 -1
382 272 1 -1
383
384 Reading input for MEP 17 weight: 1.000
385 PEG2 nconf=9 norient=1 nmep=17/46
386
387 Total charge (ich): 0
388 Number of centers: 17
389 273 8 -1
390 274 1 -1
391 275 6 0
392 276 1 0
393 277 1 4
394 278 6 0
395 279 1 0
396 280 1 7
397 281 8 -1
398 282 6 6
399 283 1 7
400 284 1 7
401 285 6 3
402 286 1 4
403 287 1 4
```

B.3. PEG WITH HYDROXYETHYL TERMINAL, MULTIPLE CONFORMATIONS

```
404 288 8 -1
405 289 1 -1
406
407 Reading input for MEP 18 weight: 1.000
408 PEG2 nconf=9 norient=2 nmep=18/46
409
410 Total charge (ich): 0
411 Number of centers: 17
412 290 8 -1
413 291 1 -1
414 292 6 0
415 293 1 0
416 294 1 4
417 295 6 0
418 296 1 0
419 297 1 7
420 298 8 -1
421 299 6 6
422 300 1 7
423 301 1 7
424 302 6 3
425 303 1 4
426 304 1 4
427 305 8 -1
428 306 1 -1
429
430 Reading input for MEP 19 weight: 1.000
431 PEG2 nconf=10 norient=1 nmep=19/46
432
433 Total charge (ich): 0
434 Number of centers: 17
435 307 8 -1
436 308 1 -1
437 309 6 0
438 310 1 0
439 311 1 4
440 312 6 0
441 313 1 0
442 314 1 7
443 315 8 -1
444 316 6 6
445 317 1 7
446 318 1 7
447 319 6 3
448 320 1 4
```

B.3. PEG WITH HYDROXYETHYL TERMINAL, MULTIPLE CONFORMATIONS

```
449 321 1 4
450 322 8 -1
451 323 1 -1
452
453 Reading input for MEP 20 weight: 1.000
454 PEG2 nconf=10 norient=2 nmep=20/46
455
456 Total charge (ich): 0
457 Number of centers: 17
458 324 8 -1
459 325 1 -1
460 326 6 0
461 327 1 0
462 328 1 4
463 329 6 0
464 330 1 0
465 331 1 7
466 332 8 -1
467 333 6 6
468 334 1 7
469 335 1 7
470 336 6 3
471 337 1 4
472 338 1 4
473 339 8 -1
474 340 1 -1
475
476 Reading input for MEP 21 weight: 1.000
477 PEG2 nconf=11 norient=1 nmep=21/46
478
479 Total charge (ich): 0
480 Number of centers: 17
481 341 8 -1
482 342 1 -1
483 343 6 0
484 344 1 0
485 345 1 4
486 346 6 0
487 347 1 0
488 348 1 7
489 349 8 -1
490 350 6 6
491 351 1 7
492 352 1 7
493 353 6 3
```

B.3. PEG WITH HYDROXYETHYL TERMINAL, MULTIPLE CONFORMATIONS

```
494 354 1 4
495 355 1 4
496 356 8 -1
497 357 1 -1
498
499 Reading input for MEP 22 weight: 1.000
500 PEG2 nconf=11 norient=2 nmep=22/46
501
502 Total charge (ich): 0
503 Number of centers: 17
504 358 8 -1
505 359 1 -1
506 360 6 0
507 361 1 0
508 362 1 4
509 363 6 0
510 364 1 0
511 365 1 7
512 366 8 -1
513 367 6 6
514 368 1 7
515 369 1 7
516 370 6 3
517 371 1 4
518 372 1 4
519 373 8 -1
520 374 1 -1
521
522 Reading input for MEP 23 weight: 1.000
523 PEG2 nconf=12 norient=1 nmep=23/46
524
525 Total charge (ich): 0
526 Number of centers: 17
527 375 8 -1
528 376 1 -1
529 377 6 0
530 378 1 0
531 379 1 4
532 380 6 0
533 381 1 0
534 382 1 7
535 383 8 -1
536 384 6 6
537 385 1 7
538 386 1 7
```

B.3. PEG WITH HYDROXYETHYL TERMINAL, MULTIPLE CONFORMATIONS

```
539 387 6 3
540 388 1 4
541 389 1 4
542 390 8 -1
543 391 1 -1
544
545 Reading input for MEP 24 weight: 1.000
546 PEG2 nconf=12 norient=2 nmep=24/46
547
548 Total charge (ich): 0
549 Number of centers: 17
550 392 8 -1
551 393 1 -1
552 394 6 0
553 395 1 0
554 396 1 4
555 397 6 0
556 398 1 0
557 399 1 7
558 400 8 -1
559 401 6 6
560 402 1 7
561 403 1 7
562 404 6 3
563 405 1 4
564 406 1 4
565 407 8 -1
566 408 1 -1
567
568 Reading input for MEP 25 weight: 1.000
569 PEG2 nconf=13 norient=1 nmep=25/46
570
571 Total charge (ich): 0
572 Number of centers: 17
573 409 8 -1
574 410 1 -1
575 411 6 0
576 412 1 0
577 413 1 4
578 414 6 0
579 415 1 0
580 416 1 7
581 417 8 -1
582 418 6 6
583 419 1 7
```

B.3. PEG WITH HYDROXYETHYL TERMINAL, MULTIPLE CONFORMATIONS

```
584 420 1 7
585 421 6 3
586 422 1 4
587 423 1 4
588 424 8 -1
589 425 1 -1
590
591 Reading input for MEP 26 weight: 1.000
592 PEG2 nconf=13 norient=2 nmep=26/46
593
594 Total charge (ich): 0
595 Number of centers: 17
596 426 8 -1
597 427 1 -1
598 428 6 0
599 429 1 0
600 430 1 4
601 431 6 0
602 432 1 0
603 433 1 7
604 434 8 -1
605 435 6 6
606 436 1 7
607 437 1 7
608 438 6 3
609 439 1 4
610 440 1 4
611 441 8 -1
612 442 1 -1
613
614 Reading input for MEP 27 weight: 1.000
615 PEG2 nconf=14 norient=1 nmep=27/46
616
617 Total charge (ich): 0
618 Number of centers: 17
619 443 8 -1
620 444 1 -1
621 445 6 0
622 446 1 0
623 447 1 4
624 448 6 0
625 449 1 0
626 450 1 7
627 451 8 -1
628 452 6 6
```

B.3. PEG WITH HYDROXYETHYL TERMINAL, MULTIPLE CONFORMATIONS

```
629 453 1 7
630 454 1 7
631 455 6 3
632 456 1 4
633 457 1 4
634 458 8 -1
635 459 1 -1
636
637 Reading input for MEP 28 weight: 1.000
638 PEG2 nconf=14 norient=2 nmep=28/46
639
640 Total charge (ich): 0
641 Number of centers: 17
642 460 8 -1
643 461 1 -1
644 462 6 0
645 463 1 0
646 464 1 4
647 465 6 0
648 466 1 0
649 467 1 7
650 468 8 -1
651 469 6 6
652 470 1 7
653 471 1 7
654 472 6 3
655 473 1 4
656 474 1 4
657 475 8 -1
658 476 1 -1
659
660 Reading input for MEP 29 weight: 1.000
661 PEG2 nconf=15 norient=1 nmep=29/46
662
663 Total charge (ich): 0
664 Number of centers: 17
665 477 8 -1
666 478 1 -1
667 479 6 0
668 480 1 0
669 481 1 4
670 482 6 0
671 483 1 0
672 484 1 7
673 485 8 -1
```

B.3. PEG WITH HYDROXYETHYL TERMINAL, MULTIPLE CONFORMATIONS

```
674 486 6 6
675 487 1 7
676 488 1 7
677 489 6 3
678 490 1 4
679 491 1 4
680 492 8 -1
681 493 1 -1
682
683 Reading input for MEP 30 weight: 1.000
684 PEG2 nconf=15 norient=2 nmep=30/46
685
686 Total charge (ich): 0
687 Number of centers: 17
688 494 8 -1
689 495 1 -1
690 496 6 0
691 497 1 0
692 498 1 4
693 499 6 0
694 500 1 0
695 501 1 7
696 502 8 -1
697 503 6 6
698 504 1 7
699 505 1 7
700 506 6 3
701 507 1 4
702 508 1 4
703 509 8 -1
704 510 1 -1
705
706 Reading input for MEP 31 weight: 1.000
707 PEG2 nconf=16 norient=1 nmep=31/46
708
709 Total charge (ich): 0
710 Number of centers: 17
711 511 8 -1
712 512 1 -1
713 513 6 0
714 514 1 0
715 515 1 4
716 516 6 0
717 517 1 0
718 518 1 7
```

B.3. PEG WITH HYDROXYETHYL TERMINAL, MULTIPLE CONFORMATIONS

```
719  519  8  -1
720  520  6   6
721  521  1   7
722  522  1   7
723  523  6   3
724  524  1   4
725  525  1   4
726  526  8  -1
727  527  1  -1
728
729  Reading input for MEP 32 weight: 1.000
730  PEG2 nconf=16 norient=2 nmep=32/46
731
732  Total charge (ich): 0
733  Number of centers: 17
734  528  8  -1
735  529  1  -1
736  530  6   0
737  531  1   0
738  532  1   4
739  533  6   0
740  534  1   0
741  535  1   7
742  536  8  -1
743  537  6   6
744  538  1   7
745  539  1   7
746  540  6   3
747  541  1   4
748  542  1   4
749  543  8  -1
750  544  1  -1
751
752  Reading input for MEP 33 weight: 1.000
753  PEG2 nconf=17 norient=1 nmep=33/46
754
755  Total charge (ich): 0
756  Number of centers: 17
757  545  8  -1
758  546  1  -1
759  547  6   0
760  548  1   0
761  549  1   4
762  550  6   0
763  551  1   0
```

B.3. PEG WITH HYDROXYETHYL TERMINAL, MULTIPLE CONFORMATIONS

```
764 552 1 7
765 553 8 -1
766 554 6 6
767 555 1 7
768 556 1 7
769 557 6 3
770 558 1 4
771 559 1 4
772 560 8 -1
773 561 1 -1
774
775 Reading input for MEP 34 weight: 1.000
776 PEG2 nconf=17 norient=2 nmep=34/46
777
778 Total charge (ich): 0
779 Number of centers: 17
780 562 8 -1
781 563 1 -1
782 564 6 0
783 565 1 0
784 566 1 4
785 567 6 0
786 568 1 0
787 569 1 7
788 570 8 -1
789 571 6 6
790 572 1 7
791 573 1 7
792 574 6 3
793 575 1 4
794 576 1 4
795 577 8 -1
796 578 1 -1
797
798 Reading input for MEP 35 weight: 1.000
799 PEG2 nconf=18 norient=1 nmep=35/46
800
801 Total charge (ich): 0
802 Number of centers: 17
803 579 8 -1
804 580 1 -1
805 581 6 0
806 582 1 0
807 583 1 4
808 584 6 0
```

B.3. PEG WITH HYDROXYETHYL TERMINAL, MULTIPLE CONFORMATIONS

```
809 585 1 0
810 586 1 7
811 587 8 -1
812 588 6 6
813 589 1 7
814 590 1 7
815 591 6 3
816 592 1 4
817 593 1 4
818 594 8 -1
819 595 1 -1
820
821 Reading input for MEP 36 weight: 1.000
822 PEG2 nconf=18 norient=2 nmep=36/46
823
824 Total charge (ich): 0
825 Number of centers: 17
826 596 8 -1
827 597 1 -1
828 598 6 0
829 599 1 0
830 600 1 4
831 601 6 0
832 602 1 0
833 603 1 7
834 604 8 -1
835 605 6 6
836 606 1 7
837 607 1 7
838 608 6 3
839 609 1 4
840 610 1 4
841 611 8 -1
842 612 1 -1
843
844 Reading input for MEP 37 weight: 1.000
845 PEG2 nconf=19 norient=1 nmep=37/46
846
847 Total charge (ich): 0
848 Number of centers: 17
849 613 8 -1
850 614 1 -1
851 615 6 0
852 616 1 0
853 617 1 4
```

B.3. PEG WITH HYDROXYETHYL TERMINAL, MULTIPLE CONFORMATIONS

```
854 618 6 0
855 619 1 0
856 620 1 7
857 621 8 -1
858 622 6 6
859 623 1 7
860 624 1 7
861 625 6 3
862 626 1 4
863 627 1 4
864 628 8 -1
865 629 1 -1
866
867 Reading input for MEP 38 weight: 1.000
868 PEG2 nconf=19 norient=2 nmep=38/46
869
870 Total charge (ich): 0
871 Number of centers: 17
872 630 8 -1
873 631 1 -1
874 632 6 0
875 633 1 0
876 634 1 4
877 635 6 0
878 636 1 0
879 637 1 7
880 638 8 -1
881 639 6 6
882 640 1 7
883 641 1 7
884 642 6 3
885 643 1 4
886 644 1 4
887 645 8 -1
888 646 1 -1
889
890 Reading input for MEP 39 weight: 1.000
891 PEG2 nconf=20 norient=1 nmep=39/46
892
893 Total charge (ich): 0
894 Number of centers: 17
895 647 8 -1
896 648 1 -1
897 649 6 0
898 650 1 0
```

B.3. PEG WITH HYDROXYETHYL TERMINAL, MULTIPLE CONFORMATIONS

```
899 651 1 4
900 652 6 0
901 653 1 0
902 654 1 7
903 655 8 -1
904 656 6 6
905 657 1 7
906 658 1 7
907 659 6 3
908 660 1 4
909 661 1 4
910 662 8 -1
911 663 1 -1
912
913 Reading input for MEP 40 weight: 1.000
914 PEG2 nconf=20 norient=2 nmep=40/46
915
916 Total charge (ich): 0
917 Number of centers: 17
918 664 8 -1
919 665 1 -1
920 666 6 0
921 667 1 0
922 668 1 4
923 669 6 0
924 670 1 0
925 671 1 7
926 672 8 -1
927 673 6 6
928 674 1 7
929 675 1 7
930 676 6 3
931 677 1 4
932 678 1 4
933 679 8 -1
934 680 1 -1
935
936 Reading input for MEP 41 weight: 1.000
937 PEG2 nconf=21 norient=1 nmep=41/46
938
939 Total charge (ich): 0
940 Number of centers: 17
941 681 8 -1
942 682 1 -1
943 683 6 0
```

B.3. PEG WITH HYDROXYETHYL TERMINAL, MULTIPLE CONFORMATIONS

```
944 684 1 0
945 685 1 4
946 686 6 0
947 687 1 0
948 688 1 7
949 689 8 -1
950 690 6 6
951 691 1 7
952 692 1 7
953 693 6 3
954 694 1 4
955 695 1 4
956 696 8 -1
957 697 1 -1
958
959 Reading input for MEP 42 weight: 1.000
960 PEG2 nconf=21 norient=2 nmep=42/46
961
962 Total charge (ich): 0
963 Number of centers: 17
964 698 8 -1
965 699 1 -1
966 700 6 0
967 701 1 0
968 702 1 4
969 703 6 0
970 704 1 0
971 705 1 7
972 706 8 -1
973 707 6 6
974 708 1 7
975 709 1 7
976 710 6 3
977 711 1 4
978 712 1 4
979 713 8 -1
980 714 1 -1
981
982 Reading input for MEP 43 weight: 1.000
983 PEG2 nconf=22 norient=1 nmep=43/46
984
985 Total charge (ich): 0
986 Number of centers: 17
987 715 8 -1
988 716 1 -1
```

B.3. PEG WITH HYDROXYETHYL TERMINAL, MULTIPLE CONFORMATIONS

```
989 717 6 0
990 718 1 0
991 719 1 4
992 720 6 0
993 721 1 0
994 722 1 7
995 723 8 -1
996 724 6 6
997 725 1 7
998 726 1 7
999 727 6 3
1000 728 1 4
1001 729 1 4
1002 730 8 -1
1003 731 1 -1
1004
1005 Reading input for MEP 44 weight: 1.000
1006 PEG2 nconf=22 norient=2 nmep=44/46
1007
1008 Total charge (ich): 0
1009 Number of centers: 17
1010 732 8 -1
1011 733 1 -1
1012 734 6 0
1013 735 1 0
1014 736 1 4
1015 737 6 0
1016 738 1 0
1017 739 1 7
1018 740 8 -1
1019 741 6 6
1020 742 1 7
1021 743 1 7
1022 744 6 3
1023 745 1 4
1024 746 1 4
1025 747 8 -1
1026 748 1 -1
1027
1028 Reading input for MEP 45 weight: 1.000
1029 PEG2 nconf=23 norient=1 nmep=45/46
1030
1031 Total charge (ich): 0
1032 Number of centers: 17
1033 749 8 -1
```

B.3. PEG WITH HYDROXYETHYL TERMINAL, MULTIPLE CONFORMATIONS

```
1034 750 1 -1
1035 751 6 0
1036 752 1 0
1037 753 1 4
1038 754 6 0
1039 755 1 0
1040 756 1 7
1041 757 8 -1
1042 758 6 6
1043 759 1 7
1044 760 1 7
1045 761 6 3
1046 762 1 4
1047 763 1 4
1048 764 8 -1
1049 765 1 -1
1050
1051 Reading input for MEP 46 weight: 1.000
1052 PEG2 nconf=23 norient=2 nmep=46/46
1053
1054 Total charge (ich): 0
1055 Number of centers: 17
1056 766 8 -1
1057 767 1 -1
1058 768 6 0
1059 769 1 0
1060 770 1 4
1061 771 6 0
1062 772 1 0
1063 773 1 7
1064 774 8 -1
1065 775 6 6
1066 776 1 7
1067 777 1 7
1068 778 6 3
1069 779 1 4
1070 780 1 4
1071 781 8 -1
1072 782 1 -1
1073 since IQOPT>1, 782 new q0 values
1074 will be read in from file ESP.Q0 (unit 3)
1075 -----
1076 reading mult_esp constraint info
1077 -----
1078 1 3 2 3 3 3 4 3 5 3 6 3 7 3 8 3
```

B.3. PEG WITH HYDROXYETHYL TERMINAL, MULTIPLE CONFORMATIONS

1079	9	3	10	3	11	3	12	3	13	3	14	3	15	3	16	3
1080	17	3	18	3	19	3	20	3	21	3	22	3	23	3	24	3
1081	25	3	26	3	27	3	28	3	29	3	30	3	31	3	32	3
1082	33	3	34	3	35	3	36	3	37	3	38	3	39	3	40	3
1083	41	3	42	3	43	3	44	3	45	3	46	3				
1084	1	4	2	4	3	4	4	4	5	4	6	4	7	4	8	4
1085	9	4	10	4	11	4	12	4	13	4	14	4	15	4	16	4
1086	17	4	18	4	19	4	20	4	21	4	22	4	23	4	24	4
1087	25	4	26	4	27	4	28	4	29	4	30	4	31	4	32	4
1088	33	4	34	4	35	4	36	4	37	4	38	4	39	4	40	4
1089	41	4	42	4	43	4	44	4	45	4	46	4				
1090	1	6	2	6	3	6	4	6	5	6	6	6	7	6	8	6
1091	9	6	10	6	11	6	12	6	13	6	14	6	15	6	16	6
1092	17	6	18	6	19	6	20	6	21	6	22	6	23	6	24	6
1093	25	6	26	6	27	6	28	6	29	6	30	6	31	6	32	6
1094	33	6	34	6	35	6	36	6	37	6	38	6	39	6	40	6
1095	41	6	42	6	43	6	44	6	45	6	46	6				
1096	1	7	2	7	3	7	4	7	5	7	6	7	7	7	8	7
1097	9	7	10	7	11	7	12	7	13	7	14	7	15	7	16	7
1098	17	7	18	7	19	7	20	7	21	7	22	7	23	7	24	7
1099	25	7	26	7	27	7	28	7	29	7	30	7	31	7	32	7
1100	33	7	34	7	35	7	36	7	37	7	38	7	39	7	40	7
1101	41	7	42	7	43	7	44	7	45	7	46	7				
1102																
1103	-----															
1104	Atom	Ivary														
1105	-----															
1106	8	-1														
1107	1	-1														
1108	6	0														
1109	1	0														
1110	1	4														
1111	6	0														
1112	1	0														
1113	1	7														
1114	8	-1														
1115	6	6														
1116	1	7														
1117	1	7														
1118	6	3														
1119	1	4														
1120	1	4														
1121	8	-1														
1122	1	-1														
1123																

B.3. PEG WITH HYDROXYETHYL TERMINAL, MULTIPLE CONFORMATIONS

1124	8	-1
1125	1	-1
1126	6	3
1127	1	4
1128	1	4
1129	6	6
1130	1	7
1131	1	7
1132	8	-1
1133	6	6
1134	1	7
1135	1	7
1136	6	3
1137	1	4
1138	1	4
1139	8	-1
1140	1	-1
1141		
1142	8	-1
1143	1	-1
1144	6	3
1145	1	4
1146	1	4
1147	6	6
1148	1	7
1149	1	7
1150	8	-1
1151	6	6
1152	1	7
1153	1	7
1154	6	3
1155	1	4
1156	1	4
1157	8	-1
1158	1	-1
1159		
1160	8	-1
1161	1	-1
1162	6	3
1163	1	4
1164	1	4
1165	6	6
1166	1	7
1167	1	7
1168	8	-1

B.3. PEG WITH HYDROXYETHYL TERMINAL, MULTIPLE CONFORMATIONS

1169	6	6
1170	1	7
1171	1	7
1172	6	3
1173	1	4
1174	1	4
1175	8	-1
1176	1	-1
1177		
1178	8	-1
1179	1	-1
1180	6	3
1181	1	4
1182	1	4
1183	6	6
1184	1	7
1185	1	7
1186	8	-1
1187	6	6
1188	1	7
1189	1	7
1190	6	3
1191	1	4
1192	1	4
1193	8	-1
1194	1	-1
1195		
1196	8	-1
1197	1	-1
1198	6	3
1199	1	4
1200	1	4
1201	6	6
1202	1	7
1203	1	7
1204	8	-1
1205	6	6
1206	1	7
1207	1	7
1208	6	3
1209	1	4
1210	1	4
1211	8	-1
1212	1	-1
1213		

B.3. PEG WITH HYDROXYETHYL TERMINAL, MULTIPLE CONFORMATIONS

1214	8	-1
1215	1	-1
1216	6	3
1217	1	4
1218	1	4
1219	6	6
1220	1	7
1221	1	7
1222	8	-1
1223	6	6
1224	1	7
1225	1	7
1226	6	3
1227	1	4
1228	1	4
1229	8	-1
1230	1	-1
1231		
1232	8	-1
1233	1	-1
1234	6	3
1235	1	4
1236	1	4
1237	6	6
1238	1	7
1239	1	7
1240	8	-1
1241	6	6
1242	1	7
1243	1	7
1244	6	3
1245	1	4
1246	1	4
1247	8	-1
1248	1	-1
1249		
1250	8	-1
1251	1	-1
1252	6	3
1253	1	4
1254	1	4
1255	6	6
1256	1	7
1257	1	7
1258	8	-1

B.3. PEG WITH HYDROXYETHYL TERMINAL, MULTIPLE CONFORMATIONS

1259	6	6
1260	1	7
1261	1	7
1262	6	3
1263	1	4
1264	1	4
1265	8	-1
1266	1	-1
1267		
1268	8	-1
1269	1	-1
1270	6	3
1271	1	4
1272	1	4
1273	6	6
1274	1	7
1275	1	7
1276	8	-1
1277	6	6
1278	1	7
1279	1	7
1280	6	3
1281	1	4
1282	1	4
1283	8	-1
1284	1	-1
1285		
1286	8	-1
1287	1	-1
1288	6	3
1289	1	4
1290	1	4
1291	6	6
1292	1	7
1293	1	7
1294	8	-1
1295	6	6
1296	1	7
1297	1	7
1298	6	3
1299	1	4
1300	1	4
1301	8	-1
1302	1	-1
1303		

B.3. PEG WITH HYDROXYETHYL TERMINAL, MULTIPLE CONFORMATIONS

1304	8	-1
1305	1	-1
1306	6	3
1307	1	4
1308	1	4
1309	6	6
1310	1	7
1311	1	7
1312	8	-1
1313	6	6
1314	1	7
1315	1	7
1316	6	3
1317	1	4
1318	1	4
1319	8	-1
1320	1	-1
1321		
1322	8	-1
1323	1	-1
1324	6	3
1325	1	4
1326	1	4
1327	6	6
1328	1	7
1329	1	7
1330	8	-1
1331	6	6
1332	1	7
1333	1	7
1334	6	3
1335	1	4
1336	1	4
1337	8	-1
1338	1	-1
1339		
1340	8	-1
1341	1	-1
1342	6	3
1343	1	4
1344	1	4
1345	6	6
1346	1	7
1347	1	7
1348	8	-1

B.3. PEG WITH HYDROXYETHYL TERMINAL, MULTIPLE CONFORMATIONS

1349	6	6
1350	1	7
1351	1	7
1352	6	3
1353	1	4
1354	1	4
1355	8	-1
1356	1	-1
1357		
1358	8	-1
1359	1	-1
1360	6	3
1361	1	4
1362	1	4
1363	6	6
1364	1	7
1365	1	7
1366	8	-1
1367	6	6
1368	1	7
1369	1	7
1370	6	3
1371	1	4
1372	1	4
1373	8	-1
1374	1	-1
1375		
1376	8	-1
1377	1	-1
1378	6	3
1379	1	4
1380	1	4
1381	6	6
1382	1	7
1383	1	7
1384	8	-1
1385	6	6
1386	1	7
1387	1	7
1388	6	3
1389	1	4
1390	1	4
1391	8	-1
1392	1	-1
1393		

B.3. PEG WITH HYDROXYETHYL TERMINAL, MULTIPLE CONFORMATIONS

1394	8	-1
1395	1	-1
1396	6	3
1397	1	4
1398	1	4
1399	6	6
1400	1	7
1401	1	7
1402	8	-1
1403	6	6
1404	1	7
1405	1	7
1406	6	3
1407	1	4
1408	1	4
1409	8	-1
1410	1	-1
1411		
1412	8	-1
1413	1	-1
1414	6	3
1415	1	4
1416	1	4
1417	6	6
1418	1	7
1419	1	7
1420	8	-1
1421	6	6
1422	1	7
1423	1	7
1424	6	3
1425	1	4
1426	1	4
1427	8	-1
1428	1	-1
1429		
1430	8	-1
1431	1	-1
1432	6	3
1433	1	4
1434	1	4
1435	6	6
1436	1	7
1437	1	7
1438	8	-1

B.3. PEG WITH HYDROXYETHYL TERMINAL, MULTIPLE CONFORMATIONS

1439	6	6
1440	1	7
1441	1	7
1442	6	3
1443	1	4
1444	1	4
1445	8	-1
1446	1	-1
1447		
1448	8	-1
1449	1	-1
1450	6	3
1451	1	4
1452	1	4
1453	6	6
1454	1	7
1455	1	7
1456	8	-1
1457	6	6
1458	1	7
1459	1	7
1460	6	3
1461	1	4
1462	1	4
1463	8	-1
1464	1	-1
1465		
1466	8	-1
1467	1	-1
1468	6	3
1469	1	4
1470	1	4
1471	6	6
1472	1	7
1473	1	7
1474	8	-1
1475	6	6
1476	1	7
1477	1	7
1478	6	3
1479	1	4
1480	1	4
1481	8	-1
1482	1	-1
1483		

B.3. PEG WITH HYDROXYETHYL TERMINAL, MULTIPLE CONFORMATIONS

1484	8	-1
1485	1	-1
1486	6	3
1487	1	4
1488	1	4
1489	6	6
1490	1	7
1491	1	7
1492	8	-1
1493	6	6
1494	1	7
1495	1	7
1496	6	3
1497	1	4
1498	1	4
1499	8	-1
1500	1	-1
1501		
1502	8	-1
1503	1	-1
1504	6	3
1505	1	4
1506	1	4
1507	6	6
1508	1	7
1509	1	7
1510	8	-1
1511	6	6
1512	1	7
1513	1	7
1514	6	3
1515	1	4
1516	1	4
1517	8	-1
1518	1	-1
1519		
1520	8	-1
1521	1	-1
1522	6	3
1523	1	4
1524	1	4
1525	6	6
1526	1	7
1527	1	7
1528	8	-1

B.3. PEG WITH HYDROXYETHYL TERMINAL, MULTIPLE CONFORMATIONS

1529	6	6
1530	1	7
1531	1	7
1532	6	3
1533	1	4
1534	1	4
1535	8	-1
1536	1	-1
1537		
1538	8	-1
1539	1	-1
1540	6	3
1541	1	4
1542	1	4
1543	6	6
1544	1	7
1545	1	7
1546	8	-1
1547	6	6
1548	1	7
1549	1	7
1550	6	3
1551	1	4
1552	1	4
1553	8	-1
1554	1	-1
1555		
1556	8	-1
1557	1	-1
1558	6	3
1559	1	4
1560	1	4
1561	6	6
1562	1	7
1563	1	7
1564	8	-1
1565	6	6
1566	1	7
1567	1	7
1568	6	3
1569	1	4
1570	1	4
1571	8	-1
1572	1	-1
1573		

B.3. PEG WITH HYDROXYETHYL TERMINAL, MULTIPLE CONFORMATIONS

1574	8	-1
1575	1	-1
1576	6	3
1577	1	4
1578	1	4
1579	6	6
1580	1	7
1581	1	7
1582	8	-1
1583	6	6
1584	1	7
1585	1	7
1586	6	3
1587	1	4
1588	1	4
1589	8	-1
1590	1	-1
1591		
1592	8	-1
1593	1	-1
1594	6	3
1595	1	4
1596	1	4
1597	6	6
1598	1	7
1599	1	7
1600	8	-1
1601	6	6
1602	1	7
1603	1	7
1604	6	3
1605	1	4
1606	1	4
1607	8	-1
1608	1	-1
1609		
1610	8	-1
1611	1	-1
1612	6	3
1613	1	4
1614	1	4
1615	6	6
1616	1	7
1617	1	7
1618	8	-1

B.3. PEG WITH HYDROXYETHYL TERMINAL, MULTIPLE CONFORMATIONS

1619	6	6
1620	1	7
1621	1	7
1622	6	3
1623	1	4
1624	1	4
1625	8	-1
1626	1	-1
1627		
1628	8	-1
1629	1	-1
1630	6	3
1631	1	4
1632	1	4
1633	6	6
1634	1	7
1635	1	7
1636	8	-1
1637	6	6
1638	1	7
1639	1	7
1640	6	3
1641	1	4
1642	1	4
1643	8	-1
1644	1	-1
1645		
1646	8	-1
1647	1	-1
1648	6	3
1649	1	4
1650	1	4
1651	6	6
1652	1	7
1653	1	7
1654	8	-1
1655	6	6
1656	1	7
1657	1	7
1658	6	3
1659	1	4
1660	1	4
1661	8	-1
1662	1	-1
1663		

B.3. PEG WITH HYDROXYETHYL TERMINAL, MULTIPLE CONFORMATIONS

1664	8	-1
1665	1	-1
1666	6	3
1667	1	4
1668	1	4
1669	6	6
1670	1	7
1671	1	7
1672	8	-1
1673	6	6
1674	1	7
1675	1	7
1676	6	3
1677	1	4
1678	1	4
1679	8	-1
1680	1	-1
1681		
1682	8	-1
1683	1	-1
1684	6	3
1685	1	4
1686	1	4
1687	6	6
1688	1	7
1689	1	7
1690	8	-1
1691	6	6
1692	1	7
1693	1	7
1694	6	3
1695	1	4
1696	1	4
1697	8	-1
1698	1	-1
1699		
1700	8	-1
1701	1	-1
1702	6	3
1703	1	4
1704	1	4
1705	6	6
1706	1	7
1707	1	7
1708	8	-1

B.3. PEG WITH HYDROXYETHYL TERMINAL, MULTIPLE CONFORMATIONS

1709	6	6
1710	1	7
1711	1	7
1712	6	3
1713	1	4
1714	1	4
1715	8	-1
1716	1	-1
1717		
1718	8	-1
1719	1	-1
1720	6	3
1721	1	4
1722	1	4
1723	6	6
1724	1	7
1725	1	7
1726	8	-1
1727	6	6
1728	1	7
1729	1	7
1730	6	3
1731	1	4
1732	1	4
1733	8	-1
1734	1	-1
1735		
1736	8	-1
1737	1	-1
1738	6	3
1739	1	4
1740	1	4
1741	6	6
1742	1	7
1743	1	7
1744	8	-1
1745	6	6
1746	1	7
1747	1	7
1748	6	3
1749	1	4
1750	1	4
1751	8	-1
1752	1	-1
1753		

B.3. PEG WITH HYDROXYETHYL TERMINAL, MULTIPLE CONFORMATIONS

1754	8	-1
1755	1	-1
1756	6	3
1757	1	4
1758	1	4
1759	6	6
1760	1	7
1761	1	7
1762	8	-1
1763	6	6
1764	1	7
1765	1	7
1766	6	3
1767	1	4
1768	1	4
1769	8	-1
1770	1	-1
1771		
1772	8	-1
1773	1	-1
1774	6	3
1775	1	4
1776	1	4
1777	6	6
1778	1	7
1779	1	7
1780	8	-1
1781	6	6
1782	1	7
1783	1	7
1784	6	3
1785	1	4
1786	1	4
1787	8	-1
1788	1	-1
1789		
1790	8	-1
1791	1	-1
1792	6	3
1793	1	4
1794	1	4
1795	6	6
1796	1	7
1797	1	7
1798	8	-1

B.3. PEG WITH HYDROXYETHYL TERMINAL, MULTIPLE CONFORMATIONS

1799	6	6
1800	1	7
1801	1	7
1802	6	3
1803	1	4
1804	1	4
1805	8	-1
1806	1	-1
1807		
1808	8	-1
1809	1	-1
1810	6	3
1811	1	4
1812	1	4
1813	6	6
1814	1	7
1815	1	7
1816	8	-1
1817	6	6
1818	1	7
1819	1	7
1820	6	3
1821	1	4
1822	1	4
1823	8	-1
1824	1	-1
1825		
1826	8	-1
1827	1	-1
1828	6	3
1829	1	4
1830	1	4
1831	6	6
1832	1	7
1833	1	7
1834	8	-1
1835	6	6
1836	1	7
1837	1	7
1838	6	3
1839	1	4
1840	1	4
1841	8	-1
1842	1	-1
1843		

B.3. PEG WITH HYDROXYETHYL TERMINAL, MULTIPLE CONFORMATIONS

1844	8	-1
1845	1	-1
1846	6	3
1847	1	4
1848	1	4
1849	6	6
1850	1	7
1851	1	7
1852	8	-1
1853	6	6
1854	1	7
1855	1	7
1856	6	3
1857	1	4
1858	1	4
1859	8	-1
1860	1	-1
1861		
1862	8	-1
1863	1	-1
1864	6	3
1865	1	4
1866	1	4
1867	6	6
1868	1	7
1869	1	7
1870	8	-1
1871	6	6
1872	1	7
1873	1	7
1874	6	3
1875	1	4
1876	1	4
1877	8	-1
1878	1	-1
1879		
1880	8	-1
1881	1	-1
1882	6	3
1883	1	4
1884	1	4
1885	6	6
1886	1	7
1887	1	7
1888	8	-1

B.3. PEG WITH HYDROXYETHYL TERMINAL, MULTIPLE CONFORMATIONS

1889	6	6
1890	1	7
1891	1	7
1892	6	3
1893	1	4
1894	1	4
1895	8	-1
1896	1	-1
1897		
1898	8	-1
1899	1	-1
1900	6	3
1901	1	4
1902	1	4
1903	6	6
1904	1	7
1905	1	7
1906	8	-1
1907	6	6
1908	1	7
1909	1	7
1910	6	3
1911	1	4
1912	1	4
1913	8	-1
1914	1	-1
1915		
1916	8	-1
1917	1	-1
1918	6	3
1919	1	4
1920	1	4
1921	6	6
1922	1	7
1923	1	7
1924	8	-1
1925	6	6
1926	1	7
1927	1	7
1928	6	3
1929	1	4
1930	1	4
1931	8	-1
1932	1	-1
1933		

B.3. PEG WITH HYDROXYETHYL TERMINAL, MULTIPLE CONFORMATIONS

```
1934 -----
1935
1936
1937 Total number of atoms = 782
1938 Weight factor on initial charge restraints= 0.001000
1939
1940
1941 There are 46 charge constraints
1942
1943 Reading esp"s for MEP 1
1944 total number of atoms = 17
1945 total number of esp points = 809
1946
1947 Center      X              Y              Z
1948 1      0.4978215E+01  0.2437140E+01 -0.4366318E+01
1949 2      0.4793776E+01  0.3312593E+01 -0.5963597E+01
1950 3      0.3655614E+01  0.3833419E+01 -0.2498507E+01
1951 4      0.1659618E+01  0.4112601E+01 -0.3022352E+01
1952 5      0.4485629E+01  0.5725104E+01 -0.2210686E+01
1953 6      0.3839901E+01  0.2415871E+01  0.0000000E+00
1954 7      0.3033619E+01  0.3609201E+01  0.1507497E+01
1955 8      0.5836249E+01  0.2080700E+01  0.4263770E+00
1956 9      0.2686593E+01  0.0000000E+00  0.0000000E+00
1957 10     0.0000000E+00  0.0000000E+00  0.0000000E+00
1958 11     -0.7670908E+00  0.5504753E+00 -0.1854086E+01
1959 12     -0.7163309E+00  0.1331210E+01  0.1433034E+01
1960 13     -0.8033584E+00 -0.2680877E+01  0.6642557E+00
1961 14     -0.1703059E+00 -0.3970396E+01 -0.8436512E+00
1962 15     -0.2867062E+01 -0.2790946E+01  0.7758157E+00
1963 16     0.1597215E+00 -0.3416785E+01  0.3050490E+01
1964 17     0.1951496E+01 -0.3017114E+01  0.2982980E+01
1965
1966 Reading esp"s for MEP 2
1967 total number of atoms = 17
1968 total number of esp points = 805
1969
1970 Center      X              Y              Z
1971 1      -0.5095967E+00 -0.1018099E+01  0.4366318E+01
1972 2      -0.1220183E+01 -0.4744951E+00  0.5963597E+01
1973 3      -0.1199859E+01  0.7770062E+00  0.2498507E+01
1974 4      -0.5919019E+00  0.2698551E+01  0.3022352E+01
1975 5      -0.3264575E+01  0.8429331E+00  0.2210686E+01
1976 6      0.0000000E+00  0.0000000E+00  0.0000000E+00
1977 7      -0.7295514E+00  0.1241726E+01 -0.1507497E+01
```

B.3. PEG WITH HYDROXYETHYL TERMINAL, MULTIPLE CONFORMATIONS

```
1978      8      -0.5575826E+00 -0.1945981E+01 -0.4263770E+00
1979      9       0.2677041E+01  0.0000000E+00  0.0000000E+00
1980     10       0.3834464E+01  0.2424490E+01  0.0000000E+00
1981     11       0.3668166E+01  0.3353897E+01  0.1854086E+01
1982     12       0.2941733E+01  0.3644440E+01 -0.1433034E+01
1983     13       0.6599893E+01  0.1994513E+01 -0.6642557E+00
1984     14       0.7490881E+01  0.8676790E+00  0.8436512E+00
1985     15       0.7588297E+01  0.3809465E+01 -0.7758157E+00
1986     16       0.6849098E+01  0.8083511E+00 -0.3050490E+01
1987     17       0.5716497E+01 -0.6364351E+00 -0.2982980E+01
```

1988

1989 Reading esp"s for MEP 3

1990 total number of atoms = 17

1991 total number of esp points = 803

1992

```
1993 Center      X              Y              Z
1994      1      0.5313660E+01  0.1803796E+01 -0.4290976E+01
1995      2      0.4633126E+01  0.1401969E+00 -0.3909044E+01
1996      3      0.4010528E+01  0.3496456E+01 -0.2678163E+01
1997      4      0.2098730E+01  0.3912011E+01 -0.3399611E+01
1998      5      0.5067053E+01  0.5277245E+01 -0.2670132E+01
1999      6      0.3854349E+01  0.2440630E+01  0.0000000E+00
2000      7      0.2834370E+01  0.3733664E+01  0.1270123E+01
2001      8      0.5765082E+01  0.2149541E+01  0.7380873E+00
2002      9      0.2698842E+01  0.0000000E+00  0.0000000E+00
2003     10      0.0000000E+00  0.0000000E+00  0.0000000E+00
2004     11     -0.7671758E+00  0.6775083E+00 -0.1810611E+01
2005     12     -0.6983785E+00  0.1238266E+01  0.1517429E+01
2006     13     -0.8077804E+00 -0.2714064E+01  0.4967315E+00
2007     14     -0.1680666E+00 -0.3915510E+01 -0.1081099E+01
2008     15     -0.2872338E+01 -0.2824749E+01  0.5817862E+00
2009     16      0.1282349E+00 -0.3593970E+01  0.2842611E+01
2010     17      0.1923705E+01 -0.3208479E+01  0.2827321E+01
```

2011

2012 Reading esp"s for MEP 4

2013 total number of atoms = 17

2014 total number of esp points = 813

2015

```
2016 Center      X              Y              Z
2017      1     -0.4887020E-01 -0.1591463E+01  0.4290976E+01
2018      2      0.1745933E+01 -0.1688255E+01  0.3909044E+01
2019      3     -0.1021108E+01  0.3106426E+00  0.2678163E+01
2020      4     -0.5786171E+00  0.2216384E+01  0.3399611E+01
2021      5     -0.3082720E+01  0.1177488E+00  0.2670132E+01
2022      6      0.0000000E+00  0.0000000E+00  0.0000000E+00
```

B.3. PEG WITH HYDROXYETHYL TERMINAL, MULTIPLE CONFORMATIONS

```
2023    7    -0.7322121E+00  0.1475181E+01 -0.1270123E+01
2024    8    -0.5545288E+00 -0.1851521E+01 -0.7380873E+00
2025    9     0.2700347E+01  0.0000000E+00  0.0000000E+00
2026   10     0.3855209E+01  0.2439271E+01  0.0000000E+00
2027   11     0.3571147E+01  0.3422573E+01  0.1810611E+01
2028   12     0.3034883E+01  0.3600347E+01 -0.1517429E+01
2029   13     0.6653895E+01  0.2007985E+01 -0.4967315E+00
2030   14     0.7466047E+01  0.9156856E+00  0.1081099E+01
2031   15     0.7637380E+01  0.3826612E+01 -0.5817862E+00
2032   16     0.7048642E+01  0.7854722E+00 -0.2842611E+01
2033   17     0.5931926E+01 -0.6723569E+00 -0.2827321E+01
```

2034

2035 Reading esp"s for MEP 5

2036 total number of atoms = 17

2037 total number of esp points = 803

2038

```
2039 Center    X            Y            Z
2040    1    0.5313484E+01  0.1803862E+01 -0.4291056E+01
2041    2    0.4632977E+01  0.1402592E+00 -0.3909108E+01
2042    3    0.4010431E+01  0.3496507E+01 -0.2678139E+01
2043    4    0.2098624E+01  0.3912114E+01 -0.3399521E+01
2044    5    0.5066992E+01  0.5277272E+01 -0.2670083E+01
2045    6    0.3854336E+01  0.2440615E+01  0.0000000E+00
2046    7    0.2834410E+01  0.3733636E+01  0.1270185E+01
2047    8    0.5765091E+01  0.2149509E+01  0.7380136E+00
2048    9    0.2698831E+01  0.0000000E+00  0.0000000E+00
2049   10    0.0000000E+00  0.0000000E+00  0.0000000E+00
2050   11   -0.7671891E+00  0.6776179E+00 -0.1810567E+01
2051   12   -0.6983917E+00  0.1238171E+01  0.1517501E+01
2052   13   -0.8077936E+00 -0.2714089E+01  0.4965690E+00
2053   14   -0.1680855E+00 -0.3915450E+01 -0.1081330E+01
2054   15   -0.2872351E+01 -0.2824762E+01  0.5816218E+00
2055   16    0.1282141E+00 -0.3594138E+01  0.2842405E+01
2056   17    0.1923688E+01 -0.3208660E+01  0.2827144E+01
```

2057

2058 Reading esp"s for MEP 6

2059 total number of atoms = 17

2060 total number of esp points = 813

2061

```
2062 Center    X            Y            Z
2063    1   -0.4887776E-01 -0.1591282E+01  0.4291056E+01
2064    2    0.1745920E+01 -0.1688102E+01  0.3909108E+01
2065    3   -0.1021130E+01  0.3107465E+00  0.2678139E+01
2066    4   -0.5786813E+00  0.2216520E+01  0.3399521E+01
2067    5   -0.3082738E+01  0.1178150E+00  0.2670083E+01
```

B.3. PEG WITH HYDROXYETHYL TERMINAL, MULTIPLE CONFORMATIONS

```
2068    6    0.0000000E+00  0.0000000E+00  0.0000000E+00
2069    7   -0.7322197E+00  0.1475128E+01 -0.1270185E+01
2070    8   -0.5545269E+00 -0.1851550E+01 -0.7380136E+00
2071    9    0.2700331E+01  0.0000000E+00  0.0000000E+00
2072   10    0.3855194E+01  0.2439258E+01  0.0000000E+00
2073   11    0.3571040E+01  0.3422621E+01  0.1810567E+01
2074   12    0.3034960E+01  0.3600306E+01 -0.1517501E+01
2075   13    0.6653909E+01  0.2007966E+01 -0.4965690E+00
2076   14    0.7465984E+01  0.9157083E+00  0.1081330E+01
2077   15    0.7637386E+01  0.3826597E+01 -0.5816218E+00
2078   16    0.7048784E+01  0.7854004E+00 -0.2842405E+01
2079   17    0.5932077E+01 -0.6724363E+00 -0.2827144E+01
```

2080

2081 Reading esp"s for MEP 7

2082 total number of atoms = 17

2083 total number of esp points = 803

2084

2085	Center	X	Y	Z
2086	1	0.5313641E+01	0.1803776E+01	-0.4290986E+01
2087	2	0.4633130E+01	0.1401799E+00	-0.3908998E+01
2088	3	0.4010535E+01	0.3496454E+01	-0.2678167E+01
2089	4	0.2098745E+01	0.3912030E+01	-0.3399617E+01
2090	5	0.5067081E+01	0.5277230E+01	-0.2670128E+01
2091	6	0.3854347E+01	0.2440628E+01	0.0000000E+00
2092	7	0.2834375E+01	0.3733668E+01	0.1270117E+01
2093	8	0.5765080E+01	0.2149539E+01	0.7380854E+00
2094	9	0.2698846E+01	0.0000000E+00	0.0000000E+00
2095	10	0.0000000E+00	0.0000000E+00	0.0000000E+00
2096	11	-0.7671758E+00	0.6775915E+00	-0.1810577E+01
2097	12	-0.6983747E+00	0.1238192E+01	0.1517488E+01
2098	13	-0.8077861E+00	-0.2714085E+01	0.4966068E+00
2099	14	-0.1680836E+00	-0.3915461E+01	-0.1081284E+01
2100	15	-0.2872344E+01	-0.2824759E+01	0.5816633E+00
2101	16	0.1282406E+00	-0.3594108E+01	0.2842437E+01
2102	17	0.1923701E+01	-0.3208579E+01	0.2827181E+01

2103

2104 Reading esp"s for MEP 8

2105 total number of atoms = 17

2106 total number of esp points = 813

2107

2108	Center	X	Y	Z
2109	1	-0.4884375E-01	-0.1591457E+01	0.4290986E+01
2110	2	0.1745948E+01	-0.1688264E+01	0.3908998E+01
2111	3	-0.1021113E+01	0.3106313E+00	0.2678167E+01
2112	4	-0.5786454E+00	0.2216378E+01	0.3399617E+01

B.3. PEG WITH HYDROXYETHYL TERMINAL, MULTIPLE CONFORMATIONS

```
2113    5    -0.3082723E+01  0.1177110E+00  0.2670128E+01
2114    6     0.0000000E+00  0.0000000E+00  0.0000000E+00
2115    7    -0.7322235E+00  0.1475175E+01 -0.1270117E+01
2116    8    -0.5545288E+00 -0.1851521E+01 -0.7380854E+00
2117    9     0.2700341E+01  0.0000000E+00  0.0000000E+00
2118   10     0.3855202E+01  0.2439275E+01  0.0000000E+00
2119   11     0.3571061E+01  0.3422613E+01  0.1810577E+01
2120   12     0.3034938E+01  0.3600317E+01 -0.1517488E+01
2121   13     0.6653910E+01  0.2007989E+01 -0.4966068E+00
2122   14     0.7466007E+01  0.9157329E+00  0.1081284E+01
2123   15     0.7637382E+01  0.3826623E+01 -0.5816633E+00
2124   16     0.7048759E+01  0.7854193E+00 -0.2842437E+01
2125   17     0.5932016E+01 -0.6723872E+00 -0.2827181E+01
```

2126

2127 Reading esp"s for MEP 9

2128 total number of atoms = 17

2129 total number of esp points = 803

2130

```
2131 Center    X            Y            Z
2132    1    0.5313681E+01  0.1803785E+01 -0.4290971E+01
2133    2    0.4633147E+01  0.1401874E+00 -0.3909038E+01
2134    3    0.4010543E+01  0.3496449E+01 -0.2678163E+01
2135    4    0.2098749E+01  0.3912003E+01 -0.3399619E+01
2136    5    0.5067068E+01  0.5277236E+01 -0.2670126E+01
2137    6    0.3854346E+01  0.2440628E+01  0.0000000E+00
2138    7    0.2834362E+01  0.3733668E+01  0.1270111E+01
2139    8    0.5765072E+01  0.2149541E+01  0.7381024E+00
2140    9    0.2698841E+01  0.0000000E+00  0.0000000E+00
2141   10    0.0000000E+00  0.0000000E+00  0.0000000E+00
2142   11   -0.7671796E+00  0.6774857E+00 -0.1810616E+01
2143   12   -0.6983860E+00  0.1238279E+01  0.1517414E+01
2144   13   -0.8077861E+00 -0.2714059E+01  0.4967598E+00
2145   14   -0.1680703E+00 -0.3915526E+01 -0.1081055E+01
2146   15   -0.2872344E+01 -0.2824734E+01  0.5818126E+00
2147   16    0.1282274E+00 -0.3593938E+01  0.2842651E+01
2148   17    0.1923699E+01 -0.3208452E+01  0.2827359E+01
```

2149

2150 Reading esp"s for MEP 10

2151 total number of atoms = 17

2152 total number of esp points = 813

2153

```
2154 Center    X            Y            Z
2155    1   -0.4887209E-01 -0.1591489E+01  0.4290971E+01
2156    2    0.1745931E+01 -0.1688281E+01  0.3909038E+01
2157    3   -0.1021111E+01  0.3106218E+00  0.2678163E+01
```

B.3. PEG WITH HYDROXYETHYL TERMINAL, MULTIPLE CONFORMATIONS

```
2158 4 -0.5786209E+00 0.2216361E+01 0.3399619E+01
2159 5 -0.3082723E+01 0.1177299E+00 0.2670126E+01
2160 6 0.0000000E+00 0.0000000E+00 0.0000000E+00
2161 7 -0.7322159E+00 0.1475188E+01 -0.1270111E+01
2162 8 -0.5545269E+00 -0.1851514E+01 -0.7381024E+00
2163 9 0.2700345E+01 0.0000000E+00 0.0000000E+00
2164 10 0.3855205E+01 0.2439268E+01 0.0000000E+00
2165 11 0.3571165E+01 0.3422566E+01 0.1810616E+01
2166 12 0.3034870E+01 0.3600357E+01 -0.1517414E+01
2167 13 0.6653890E+01 0.2007989E+01 -0.4967598E+00
2168 14 0.7466062E+01 0.9156800E+00 0.1081055E+01
2169 15 0.7637367E+01 0.3826621E+01 -0.5818126E+00
2170 16 0.7048614E+01 0.7854911E+00 -0.2842651E+01
2171 17 0.5931903E+01 -0.6723418E+00 -0.2827359E+01
```

2172

2173 Reading esp"s for MEP 11

2174 total number of atoms = 17

2175 total number of esp points = 810

2176

```
2177 Center X Y Z
2178 1 0.5213693E+01 0.1800017E+01 -0.4306839E+01
2179 2 0.4580599E+01 0.1385831E+00 -0.3838846E+01
2180 3 0.3953456E+01 0.3511400E+01 -0.2677564E+01
2181 4 0.2038020E+01 0.3948235E+01 -0.3378240E+01
2182 5 0.5028559E+01 0.5281616E+01 -0.2681015E+01
2183 6 0.3816995E+01 0.2445183E+01 0.0000000E+00
2184 7 0.2799860E+01 0.3732642E+01 0.1279161E+01
2185 8 0.5733349E+01 0.2165333E+01 0.7283306E+00
2186 9 0.2684290E+01 0.0000000E+00 0.0000000E+00
2187 10 0.0000000E+00 0.0000000E+00 0.0000000E+00
2188 11 -0.7626745E+00 0.6819190E+00 -0.1813307E+01
2189 12 -0.7198722E+00 0.1240242E+01 0.1506990E+01
2190 13 -0.9314081E+00 -0.2670854E+01 0.4558983E+00
2191 14 0.3880930E-01 -0.3951037E+01 -0.8665717E+00
2192 15 -0.2969837E+01 -0.2732765E+01 0.2377086E-01
2193 16 -0.4466235E+00 -0.3322922E+01 0.3011643E+01
2194 17 -0.7822010E+00 -0.5110904E+01 0.3213243E+01
```

2195

2196 Reading esp"s for MEP 12

2197 total number of atoms = 17

2198 total number of esp points = 817

2199

```
2200 Center X Y Z
2201 1 -0.1668628E-02 -0.1538507E+01 0.4306839E+01
2202 2 0.1771975E+01 -0.1662405E+01 0.3838846E+01
```

B.3. PEG WITH HYDROXYETHYL TERMINAL, MULTIPLE CONFORMATIONS

```
2203  3  -0.1024814E+01  0.3243431E+00  0.2677564E+01
2204  4  -0.6160677E+00  0.2245970E+01  0.3378240E+01
2205  5  -0.3082956E+01  0.9290271E-01  0.2681015E+01
2206  6   0.0000000E+00  0.0000000E+00  0.0000000E+00
2207  7  -0.7406687E+00  0.1464078E+01 -0.1279161E+01
2208  8  -0.5515751E+00 -0.1856474E+01 -0.7283306E+00
2209  9   0.2694798E+01  0.0000000E+00  0.0000000E+00
2210 10   0.3823088E+01  0.2435647E+01  0.0000000E+00
2211 11   0.3524910E+01  0.3414308E+01  0.1813307E+01
2212 12   0.3000312E+01  0.3610149E+01 -0.1506990E+01
2213 13   0.6638040E+01  0.2158139E+01 -0.4558983E+00
2214 14   0.7391831E+01  0.7396917E+00  0.8665717E+00
2215 15   0.7551031E+01  0.3981726E+01 -0.2377086E-01
2216 16   0.7025941E+01  0.1444176E+01 -0.3011643E+01
2217 17   0.8789356E+01  0.9971253E+00 -0.3213243E+01
```

2218

2219 Reading esp"s for MEP 13

2220 total number of atoms = 17

2221 total number of esp points = 814

2222

```
2223 Center  X          Y          Z
2224  1  0.5368704E+01  0.1752536E+01 -0.4247125E+01
2225  2  0.4708965E+01  0.9276665E-01 -0.3813066E+01
2226  3  0.4033437E+01  0.3471111E+01 -0.2687899E+01
2227  4  0.2137439E+01  0.3874297E+01 -0.3457539E+01
2228  5  0.5088244E+01  0.5253185E+01 -0.2683530E+01
2229  6  0.3819728E+01  0.2448437E+01  0.0000000E+00
2230  7  0.2763919E+01  0.3751828E+01  0.1229864E+01
2231  8  0.5714745E+01  0.2180613E+01  0.7864227E+00
2232  9  0.2683721E+01  0.0000000E+00  0.0000000E+00
2233 10  0.0000000E+00  0.0000000E+00  0.0000000E+00
2234 11 -0.7664313E+00  0.8737224E+00 -0.1731220E+01
2235 12 -0.7338392E+00  0.1077582E+01  0.1620357E+01
2236 13 -0.8845675E+00 -0.2741533E+01  0.1807693E+00
2237 14 -0.2055965E+00 -0.3567750E+01  0.1949046E+01
2238 15 -0.6428848E-01 -0.3843788E+01 -0.1380626E+01
2239 16 -0.3562708E+01 -0.2909146E+01  0.2415467E+00
2240 17 -0.4191777E+01 -0.2471939E+01 -0.1422947E+01
```

2241

2242 Reading esp"s for MEP 14

2243 total number of atoms = 17

2244 total number of esp points = 825

2245

```
2246 Center  X          Y          Z
2247  1 -0.2066604E-01 -0.1697993E+01  0.4247125E+01
```

B.3. PEG WITH HYDROXYETHYL TERMINAL, MULTIPLE CONFORMATIONS

```
2248 2 0.1762610E+01 -0.1798091E+01 0.3813066E+01
2249 3 -0.1017631E+01 0.2365616E+00 0.2687899E+01
2250 4 -0.5853842E+00 0.2126148E+01 0.3457539E+01
2251 5 -0.3078126E+01 0.2976318E-01 0.2683530E+01
2252 6 0.0000000E+00 0.0000000E+00 0.0000000E+00
2253 7 -0.7379607E+00 0.1506312E+01 -0.1229864E+01
2254 8 -0.5546232E+00 -0.1831723E+01 -0.7864227E+00
2255 9 0.2699141E+01 0.0000000E+00 0.0000000E+00
2256 10 0.3828659E+01 0.2434449E+01 0.0000000E+00
2257 11 0.3358663E+01 0.3497422E+01 0.1731220E+01
2258 12 0.3160023E+01 0.3553658E+01 -0.1620357E+01
2259 13 0.6687846E+01 0.2083005E+01 -0.1807693E+00
2260 14 0.7151558E+01 0.1119362E+01 -0.1949046E+01
2261 15 0.7342483E+01 0.8750017E+00 0.1380626E+01
2262 16 0.7967060E+01 0.4441848E+01 -0.2415467E+00
2263 17 0.7835223E+01 0.5196499E+01 0.1422947E+01
```

2264

2265 Reading esp"s for MEP 15

2266 total number of atoms = 17

2267 total number of esp points = 811

2268

```
2269 Center X Y Z
2270 1 0.5391275E+01 0.1760108E+01 -0.4235290E+01
2271 2 0.4713606E+01 0.1008585E+00 -0.3828165E+01
2272 3 0.4032129E+01 0.3472045E+01 -0.2688642E+01
2273 4 0.2138898E+01 0.3859136E+01 -0.3471468E+01
2274 5 0.5075598E+01 0.5260799E+01 -0.2681068E+01
2275 6 0.3809039E+01 0.2452828E+01 0.0000000E+00
2276 7 0.2741359E+01 0.3754474E+01 0.1221797E+01
2277 8 0.5701825E+01 0.2196976E+01 0.7962266E+00
2278 9 0.2685199E+01 0.0000000E+00 0.0000000E+00
2279 10 0.0000000E+00 0.0000000E+00 0.0000000E+00
2280 11 -0.7820915E+00 0.9058250E+00 -0.1699030E+01
2281 12 -0.7293265E+00 0.1023655E+01 0.1657121E+01
2282 13 -0.8630889E+00 -0.2740318E+01 0.9894416E-01
2283 14 -0.9331467E-01 -0.3634077E+01 0.1811703E+01
2284 15 -0.9511936E-01 -0.3757404E+01 -0.1546053E+01
2285 16 -0.3548703E+01 -0.2707424E+01 0.9553510E-01
2286 17 -0.4134275E+01 -0.4439316E+01 0.1729988E+00
```

2287

2288 Reading esp"s for MEP 16

2289 total number of atoms = 17

2290 total number of esp points = 824

2291

```
2292 Center X Y Z
```

B.3. PEG WITH HYDROXYETHYL TERMINAL, MULTIPLE CONFORMATIONS

```
2293 1 -0.2930020E-01 -0.1726985E+01 0.4235290E+01
2294 2 0.1761429E+01 -0.1802047E+01 0.3828165E+01
2295 3 -0.1019513E+01 0.2217291E+00 0.2688642E+01
2296 4 -0.5828180E+00 0.2104138E+01 0.3471468E+01
2297 5 -0.3080348E+01 0.1818105E-01 0.2681068E+01
2298 6 0.0000000E+00 0.0000000E+00 0.0000000E+00
2299 7 -0.7386164E+00 0.1512833E+01 -0.1221797E+01
2300 8 -0.5558232E+00 -0.1827337E+01 -0.7962266E+00
2301 9 0.2698034E+01 0.0000000E+00 0.0000000E+00
2302 10 0.3816527E+01 0.2441161E+01 0.0000000E+00
2303 11 0.3318797E+01 0.3529487E+01 0.1699030E+01
2304 12 0.3189697E+01 0.3530600E+01 -0.1657121E+01
2305 13 0.6667309E+01 0.2084356E+01 -0.9894416E-01
2306 14 0.7159199E+01 0.1012256E+01 -0.1811703E+01
2307 15 0.7272068E+01 0.9625244E+00 0.1546053E+01
2308 16 0.7756070E+01 0.4539596E+01 -0.9553510E-01
2309 17 0.9574478E+01 0.4350546E+01 -0.1729988E+00
```

2310

2311 Reading esp"s for MEP 17

2312 total number of atoms = 17

2313 total number of esp points = 811

2314

```
2315 Center X Y Z
2316 1 0.5391248E+01 0.1760140E+01 -0.4235301E+01
2317 2 0.4713564E+01 0.1008944E+00 -0.3828186E+01
2318 3 0.4032101E+01 0.3472069E+01 -0.2688638E+01
2319 4 0.2138871E+01 0.3859166E+01 -0.3471457E+01
2320 5 0.5075570E+01 0.5260825E+01 -0.2681062E+01
2321 6 0.3809032E+01 0.2452840E+01 0.0000000E+00
2322 7 0.2741348E+01 0.3754466E+01 0.1221810E+01
2323 8 0.5701819E+01 0.2196988E+01 0.7962096E+00
2324 9 0.2685199E+01 0.0000000E+00 0.0000000E+00
2325 10 0.0000000E+00 0.0000000E+00 0.0000000E+00
2326 11 -0.7820971E+00 0.9057759E+00 -0.1699054E+01
2327 12 -0.7293265E+00 0.1023706E+01 0.1657093E+01
2328 13 -0.8630851E+00 -0.2740316E+01 0.9900841E-01
2329 14 -0.9334302E-01 -0.3634034E+01 0.1811797E+01
2330 15 -0.9508534E-01 -0.3757433E+01 -0.1545956E+01
2331 16 -0.3548703E+01 -0.2707442E+01 0.9555400E-01
2332 17 -0.4134254E+01 -0.4439331E+01 0.1731991E+00
```

2333

2334 Reading esp"s for MEP 18

2335 total number of atoms = 17

2336 total number of esp points = 824

2337

B.3. PEG WITH HYDROXYETHYL TERMINAL, MULTIPLE CONFORMATIONS

2338	Center	X	Y	Z
2339	1	-0.2930398E-01	-0.1726956E+01	0.4235301E+01
2340	2	0.1761429E+01	-0.1801999E+01	0.3828186E+01
2341	3	-0.1019517E+01	0.2217499E+00	0.2688638E+01
2342	4	-0.5828350E+00	0.2104161E+01	0.3471457E+01
2343	5	-0.3080352E+01	0.1819428E-01	0.2681062E+01
2344	6	0.0000000E+00	0.0000000E+00	0.0000000E+00
2345	7	-0.7386032E+00	0.1512826E+01	-0.1221810E+01
2346	8	-0.5558157E+00	-0.1827341E+01	-0.7962096E+00
2347	9	0.2698041E+01	0.0000000E+00	0.0000000E+00
2348	10	0.3816525E+01	0.2441165E+01	0.0000000E+00
2349	11	0.3318837E+01	0.3529473E+01	0.1699054E+01
2350	12	0.3189644E+01	0.3530622E+01	-0.1657093E+01
2351	13	0.6667303E+01	0.2084372E+01	-0.9900841E-01
2352	14	0.7159174E+01	0.1012317E+01	-0.1811797E+01
2353	15	0.7272083E+01	0.9625017E+00	0.1545956E+01
2354	16	0.7756076E+01	0.4539609E+01	-0.9555400E-01
2355	17	0.9574473E+01	0.4350550E+01	-0.1731991E+00

2356

2357 Reading esp"s for MEP 19

2358 total number of atoms = 17

2359 total number of esp points = 814

2360

2361	Center	X	Y	Z
2362	1	0.5435935E+01	0.1755421E+01	-0.4221058E+01
2363	2	0.4749316E+01	0.9443528E-01	-0.3837622E+01
2364	3	0.4055717E+01	0.3462615E+01	-0.2689348E+01
2365	4	0.2167132E+01	0.3840159E+01	-0.3488351E+01
2366	5	0.5091305E+01	0.5255876E+01	-0.2677383E+01
2367	6	0.3814975E+01	0.2450627E+01	0.0000000E+00
2368	7	0.2743876E+01	0.3758162E+01	0.1213070E+01
2369	8	0.5702573E+01	0.2192243E+01	0.8074308E+00
2370	9	0.2683207E+01	0.0000000E+00	0.0000000E+00
2371	10	0.0000000E+00	0.0000000E+00	0.0000000E+00
2372	11	-0.7863490E+00	0.9644897E+00	-0.1664416E+01
2373	12	-0.7133716E+00	0.9908608E+00	0.1692529E+01
2374	13	-0.8857032E+00	-0.2746981E+01	0.1661447E-01
2375	14	-0.4428384E-01	-0.3737398E+01	0.1639075E+01
2376	15	-0.2306335E+00	-0.3695480E+01	-0.1699648E+01
2377	16	-0.3564569E+01	-0.2917342E+01	-0.3140725E-02
2378	17	-0.4173494E+01	-0.2375879E+01	0.1637933E+01

2379

2380 Reading esp"s for MEP 20

2381 total number of atoms = 17

2382 total number of esp points = 821

B.3. PEG WITH HYDROXYETHYL TERMINAL, MULTIPLE CONFORMATIONS

```
2383
2384 Center      X          Y          Z
2385   1    -0.4847903E-01 -0.1763086E+01  0.4221058E+01
2386   2     0.1747345E+01 -0.1836143E+01  0.3837622E+01
2387   3    -0.1019681E+01  0.2057401E+00  0.2689348E+01
2388   4    -0.5706009E+00  0.2078604E+01  0.3488351E+01
2389   5    -0.3081905E+01  0.1744028E-01  0.2677383E+01
2390   6     0.0000000E+00  0.0000000E+00  0.0000000E+00
2391   7    -0.7379739E+00  0.1520623E+01 -0.1213070E+01
2392   8    -0.5568456E+00 -0.1822010E+01 -0.8074308E+00
2393   9     0.2699347E+01  0.0000000E+00  0.0000000E+00
2394  10     0.3824346E+01  0.2435976E+01  0.0000000E+00
2395  11     0.3278421E+01  0.3554255E+01  0.1664416E+01
2396  12     0.3223882E+01  0.3499058E+01 -0.1692529E+01
2397  13     0.6689573E+01  0.2088331E+01 -0.1661447E-01
2398  14     0.7235946E+01  0.9091831E+00 -0.1639075E+01
2399  15     0.7276023E+01  0.1095937E+01  0.1699648E+01
2400  16     0.7967416E+01  0.4448937E+01  0.3140725E-02
2401  17     0.7731149E+01  0.5228777E+01 -0.1637933E+01
```

2402

2403 Reading esp"s for MEP 21

2404 total number of atoms = 17

2405 total number of esp points = 756

2406

```
2407 Center      X          Y          Z
2408   1     0.4363459E+01  0.2381799E+01 -0.4597811E+01
2409   2     0.3217119E+01  0.9348871E+00 -0.4665097E+01
2410   3     0.3596697E+01  0.3826106E+01 -0.2497702E+01
2411   4     0.1627139E+01  0.4494158E+01 -0.2703790E+01
2412   5     0.4787770E+01  0.5521375E+01 -0.2437121E+01
2413   6     0.3897915E+01  0.2398873E+01  0.0000000E+00
2414   7     0.3238015E+01  0.3576208E+01  0.1588919E+01
2415   8     0.5896913E+01  0.1964329E+01  0.2996765E+00
2416   9     0.2676963E+01  0.0000000E+00  0.0000000E+00
2417  10     0.0000000E+00  0.0000000E+00  0.0000000E+00
2418  11    -0.7703071E+00  0.1927447E+01 -0.1283275E+00
2419  12    -0.6936579E+00 -0.8221234E+00  0.1782293E+01
2420  13    -0.9503734E+00 -0.1595479E+01 -0.2204277E+01
2421  14    -0.3012212E+01 -0.1834395E+01 -0.2074919E+01
2422  15    -0.7977856E-01 -0.3466751E+01 -0.2105680E+01
2423  16    -0.2407738E+00 -0.6022840E+00 -0.4613777E+01
2424  17    -0.1236741E+01  0.9027788E+00 -0.4937739E+01
```

2425

2426 Reading esp"s for MEP 22

2427 total number of atoms = 17

B.3. PEG WITH HYDROXYETHYL TERMINAL, MULTIPLE CONFORMATIONS

2428 total number of esp points = 762

2429

2430	Center	X	Y	Z
2431	1	-0.1959514E+00	-0.4226410E+00	0.4597811E+01
2432	2	0.1613524E+01	-0.5732862E-01	0.4665097E+01
2433	3	-0.1135328E+01	0.9158349E+00	0.2497702E+01
2434	4	-0.8373168E+00	0.2974145E+01	0.2703790E+01
2435	5	-0.3186430E+01	0.6233110E+00	0.2437121E+01
2436	6	0.0000000E+00	0.0000000E+00	0.0000000E+00
2437	7	-0.7499208E+00	0.1122142E+01	-0.1588919E+01
2438	8	-0.5194687E+00	-0.1978630E+01	-0.2996765E+00
2439	9	0.2691712E+01	0.0000000E+00	0.0000000E+00
2440	10	0.3905975E+01	0.2385728E+01	0.0000000E+00
2441	11	0.2537628E+01	0.3946515E+01	0.1283275E+00
2442	12	0.4953299E+01	0.2631009E+01	-0.1782293E+01
2443	13	0.5758963E+01	0.2509004E+01	0.2204277E+01
2444	14	0.6907128E+01	0.4238160E+01	0.2074919E+01
2445	15	0.7031755E+01	0.8843218E+00	0.2105680E+01
2446	16	0.4551949E+01	0.2327114E+01	0.4613777E+01
2447	17	0.3662393E+01	0.3897416E+01	0.4937739E+01

2448

2449 Reading esp"s for MEP 23

2450 total number of atoms = 17

2451 total number of esp points = 756

2452

2453	Center	X	Y	Z
2454	1	0.4363392E+01	0.2381892E+01	-0.4597811E+01
2455	2	0.3217122E+01	0.9349211E+00	-0.4665070E+01
2456	3	0.3596632E+01	0.3826155E+01	-0.2497658E+01
2457	4	0.1627067E+01	0.4494184E+01	-0.2703710E+01
2458	5	0.4787689E+01	0.5521430E+01	-0.2437068E+01
2459	6	0.3897909E+01	0.2398881E+01	0.0000000E+00
2460	7	0.3238064E+01	0.3576172E+01	0.1588974E+01
2461	8	0.5896922E+01	0.1964336E+01	0.2996047E+00
2462	9	0.2676967E+01	0.0000000E+00	0.0000000E+00
2463	10	0.0000000E+00	0.0000000E+00	0.0000000E+00
2464	11	-0.7703147E+00	0.1927441E+01	-0.1283389E+00
2465	12	-0.6936598E+00	-0.8221177E+00	0.1782295E+01
2466	13	-0.9503715E+00	-0.1595496E+01	-0.2204273E+01
2467	14	-0.3012216E+01	-0.1834395E+01	-0.2074930E+01
2468	15	-0.7978990E-01	-0.3466770E+01	-0.2105654E+01
2469	16	-0.2407416E+00	-0.6023256E+00	-0.4613777E+01
2470	17	-0.1236682E+01	0.9027504E+00	-0.4937750E+01

2471

2472 Reading esp"s for MEP 24

B.3. PEG WITH HYDROXYETHYL TERMINAL, MULTIPLE CONFORMATIONS

```
2473 total number of atoms = 17
2474 total number of esp points = 762
2475
2476 Center      X              Y              Z
2477   1      -0.1959986E+00 -0.4225484E+00  0.4597811E+01
2478   2       0.1613495E+01 -0.5731728E-01  0.4665070E+01
2479   3      -0.1135342E+01  0.9159029E+00  0.2497658E+01
2480   4      -0.8373149E+00  0.2974210E+01  0.2703710E+01
2481   5      -0.3186441E+01  0.6233885E+00  0.2437068E+01
2482   6       0.0000000E+00  0.0000000E+00  0.0000000E+00
2483   7      -0.7499113E+00  0.1122072E+01 -0.1588974E+01
2484   8      -0.5194687E+00 -0.1978643E+01 -0.2996047E+00
2485   9       0.2691716E+01  0.0000000E+00  0.0000000E+00
2486  10       0.3905969E+01  0.2385736E+01  0.0000000E+00
2487  11       0.2537626E+01  0.3946521E+01  0.1283389E+00
2488  12       0.4953287E+01  0.2631024E+01 -0.1782295E+01
2489  13       0.5758970E+01  0.2509010E+01  0.2204273E+01
2490  14       0.6907119E+01  0.4238181E+01  0.2074930E+01
2491  15       0.7031778E+01  0.8843426E+00  0.2105654E+01
2492  16       0.4551966E+01  0.2327077E+01  0.4613777E+01
2493  17       0.3662382E+01  0.3897359E+01  0.4937750E+01
2494
2495 Reading esp"s for MEP 25
2496 total number of atoms = 17
2497 total number of esp points = 756
2498
2499 Center      X              Y              Z
2500   1       0.4363421E+01  0.2381892E+01 -0.4597813E+01
2501   2       0.3217121E+01  0.9349457E+00 -0.4665104E+01
2502   3       0.3596647E+01  0.3826153E+01 -0.2497658E+01
2503   4       0.1627075E+01  0.4494161E+01 -0.2703714E+01
2504   5       0.4787689E+01  0.5521435E+01 -0.2437072E+01
2505   6       0.3897919E+01  0.2398879E+01  0.0000000E+00
2506   7       0.3238064E+01  0.3576174E+01  0.1588965E+01
2507   8       0.5896928E+01  0.1964334E+01  0.2996161E+00
2508   9       0.2676965E+01  0.0000000E+00  0.0000000E+00
2509  10       0.0000000E+00  0.0000000E+00  0.0000000E+00
2510  11      -0.7703147E+00  0.1927445E+01 -0.1282973E+00
2511  12      -0.6936579E+00 -0.8221517E+00  0.1782280E+01
2512  13      -0.9503772E+00 -0.1595460E+01 -0.2204299E+01
2513  14      -0.3012216E+01 -0.1834368E+01 -0.2074951E+01
2514  15      -0.7977856E-01 -0.3466729E+01 -0.2105712E+01
2515  16      -0.2407719E+00 -0.6022443E+00 -0.4613794E+01
2516  17      -0.1236695E+01  0.9028525E+00 -0.4937722E+01
2517
```

B.3. PEG WITH HYDROXYETHYL TERMINAL, MULTIPLE CONFORMATIONS

```
2518 Reading esp"s for MEP 26
2519 total number of atoms = 17
2520 total number of esp points = 762
2521
2522 Center      X              Y              Z
2523 1      -0.1960118E+00 -0.4225635E+00 0.4597813E+01
2524 2       0.1613476E+01 -0.5730216E-01 0.4665104E+01
2525 3      -0.1135340E+01 0.9159029E+00 0.2497658E+01
2526 4      -0.8372847E+00 0.2974206E+01 0.2703714E+01
2527 5      -0.3186441E+01 0.6234112E+00 0.2437072E+01
2528 6       0.0000000E+00 0.0000000E+00 0.0000000E+00
2529 7      -0.7499056E+00 0.1122083E+01 -0.1588965E+01
2530 8      -0.5194743E+00 -0.1978638E+01 -0.2996161E+00
2531 9       0.2691718E+01 0.0000000E+00 0.0000000E+00
2532 10     0.3905981E+01 0.2385730E+01 0.0000000E+00
2533 11     0.2537639E+01 0.3946523E+01 0.1282973E+00
2534 12     0.4953329E+01 0.2630997E+01 -0.1782280E+01
2535 13     0.5758953E+01 0.2509018E+01 0.2204299E+01
2536 14     0.6907113E+01 0.4238175E+01 0.2074951E+01
2537 15     0.7031742E+01 0.8843351E+00 0.2105712E+01
2538 16     0.4551917E+01 0.2327133E+01 0.4613794E+01
2539 17     0.3662314E+01 0.3897414E+01 0.4937722E+01
2540
2541 Reading esp"s for MEP 27
2542 total number of atoms = 17
2543 total number of esp points = 756
2544
2545 Center      X              Y              Z
2546 1       0.4363402E+01 0.2381860E+01 -0.4597811E+01
2547 2       0.3217151E+01 0.9348701E+00 -0.4665046E+01
2548 3       0.3596630E+01 0.3826136E+01 -0.2497675E+01
2549 4       0.1627058E+01 0.4494143E+01 -0.2703729E+01
2550 5       0.4787672E+01 0.5521420E+01 -0.2437104E+01
2551 6       0.3897909E+01 0.2398882E+01 0.0000000E+00
2552 7       0.3238044E+01 0.3576180E+01 0.1588957E+01
2553 8       0.5896918E+01 0.1964346E+01 0.2996217E+00
2554 9       0.2676965E+01 0.0000000E+00 0.0000000E+00
2555 10     0.0000000E+00 0.0000000E+00 0.0000000E+00
2556 11     -0.7703147E+00 0.1927441E+01 -0.1283880E+00
2557 12     -0.6936636E+00 -0.8220743E+00 0.1782314E+01
2558 13     -0.9503602E+00 -0.1595543E+01 -0.2204241E+01
2559 14     -0.3012206E+01 -0.1834433E+01 -0.2074912E+01
2560 15     -0.7978423E-01 -0.3466820E+01 -0.2105584E+01
2561 16     -0.2407076E+00 -0.6024182E+00 -0.4613760E+01
2562 17     -0.1236665E+01 0.9026371E+00 -0.4937782E+01
```

B.3. PEG WITH HYDROXYETHYL TERMINAL, MULTIPLE CONFORMATIONS

2563

2564 Reading esp"s for MEP 28

2565 total number of atoms = 17

2566 total number of esp points = 762

2567

2568	Center	X	Y	Z
2569	1	-0.1959721E+00	-0.4225730E+00	0.4597811E+01
2570	2	0.1613527E+01	-0.5736830E-01	0.4665046E+01
2571	3	-0.1135323E+01	0.9158935E+00	0.2497675E+01
2572	4	-0.8372715E+00	0.2974196E+01	0.2703729E+01
2573	5	-0.3186422E+01	0.6233960E+00	0.2437104E+01
2574	6	0.0000000E+00	0.0000000E+00	0.0000000E+00
2575	7	-0.7499075E+00	0.1122091E+01	-0.1588957E+01
2576	8	-0.5194724E+00	-0.1978638E+01	-0.2996217E+00
2577	9	0.2691718E+01	0.0000000E+00	0.0000000E+00
2578	10	0.3905971E+01	0.2385736E+01	0.0000000E+00
2579	11	0.2537628E+01	0.3946519E+01	0.1283880E+00
2580	12	0.4953252E+01	0.2631048E+01	-0.1782314E+01
2581	13	0.5759010E+01	0.2508978E+01	0.2204241E+01
2582	14	0.6907149E+01	0.4238153E+01	0.2074912E+01
2583	15	0.7031820E+01	0.8843143E+00	0.2105584E+01
2584	16	0.4552034E+01	0.2327003E+01	0.4613760E+01
2585	17	0.3662474E+01	0.3897292E+01	0.4937782E+01

2586

2587 Reading esp"s for MEP 29

2588 total number of atoms = 17

2589 total number of esp points = 840

2590

2591	Center	X	Y	Z
2592	1	0.7218638E+01	0.7890230E+00	0.2501100E+01
2593	2	0.6168396E+01	-0.7174137E+00	0.2497503E+01
2594	3	0.6598109E+01	0.2089525E+01	0.2451636E+00
2595	4	0.7300837E+01	0.1079326E+01	-0.1434884E+01
2596	5	0.7539066E+01	0.3930908E+01	0.3254429E+00
2597	6	0.3756970E+01	0.2453446E+01	0.0000000E+00
2598	7	0.3284125E+01	0.3474250E+01	-0.1755125E+01
2599	8	0.3039316E+01	0.3559607E+01	0.1612254E+01
2600	9	0.2668463E+01	0.0000000E+00	0.0000000E+00
2601	10	0.0000000E+00	0.0000000E+00	0.0000000E+00
2602	11	-0.7233852E+00	0.9762684E+00	-0.1700736E+01
2603	12	-0.7403002E+00	0.1032308E+01	0.1655750E+01
2604	13	-0.9643612E+00	-0.2709848E+01	0.6500657E-01
2605	14	-0.3030523E+01	-0.2658631E+01	0.3410029E+00
2606	15	-0.1391462E+00	-0.3685653E+01	0.1691305E+01
2607	16	-0.2802123E+00	-0.4162908E+01	-0.2077294E+01

B.3. PEG WITH HYDROXYETHYL TERMINAL, MULTIPLE CONFORMATIONS

2608 17 -0.9913937E+00 -0.3350934E+01 -0.3558923E+01
2609

2610 Reading esp"s for MEP 30

2611 total number of atoms = 17

2612 total number of esp points = 835

2613

Center	X	Y	Z	
2615	1	0.1175561E+00	-0.3839222E+01	-0.2501100E+01
2616	2	0.1920472E+01	-0.3490146E+01	-0.2497503E+01
2617	3	-0.8195496E+00	-0.2744604E+01	-0.2451636E+00
2618	4	-0.1811378E+00	-0.3796630E+01	0.1434884E+01
2619	5	-0.2884313E+01	-0.2857950E+01	-0.3254429E+00
2620	6	0.0000000E+00	0.0000000E+00	0.0000000E+00
2621	7	-0.7413319E+00	0.8461947E+00	0.1755125E+01
2622	8	-0.7200763E+00	0.1104586E+01	-0.1612254E+01
2623	9	0.2684072E+01	0.0000000E+00	0.0000000E+00
2624	10	0.3766249E+01	0.2439179E+01	0.0000000E+00
2625	11	0.3167228E+01	0.3496328E+01	0.1700736E+01
2626	12	0.3122863E+01	0.3534513E+01	-0.1655750E+01
2627	13	0.6634346E+01	0.2221721E+01	-0.6500657E-01
2628	14	0.7425446E+01	0.4131120E+01	-0.3410029E+00
2629	15	0.7191645E+01	0.1071681E+01	-0.1691305E+01
2630	16	0.7685100E+01	0.1007078E+01	0.2077294E+01
2631	17	0.7231309E+01	0.1986442E+01	0.3558923E+01

2632

2633 Reading esp"s for MEP 31

2634 total number of atoms = 17

2635 total number of esp points = 838

2636

Center	X	Y	Z	
2638	1	0.7181499E+01	0.8565334E+00	0.2647765E+01
2639	2	0.6101241E+01	-0.6273493E+00	0.2689758E+01
2640	3	0.6625364E+01	0.2083272E+01	0.3343360E+00
2641	4	0.7370646E+01	0.1017729E+01	-0.1293684E+01
2642	5	0.7572716E+01	0.3922223E+01	0.3781512E+00
2643	6	0.3795462E+01	0.2452014E+01	0.0000000E+00
2644	7	0.3369897E+01	0.3448561E+01	-0.1778557E+01
2645	8	0.3036931E+01	0.3572468E+01	0.1580225E+01
2646	9	0.2689777E+01	0.0000000E+00	0.0000000E+00
2647	10	0.0000000E+00	0.0000000E+00	0.0000000E+00
2648	11	-0.7095959E+00	0.1152153E+01	-0.1580164E+01
2649	12	-0.7335255E+00	0.7975022E+00	0.1778595E+01
2650	13	-0.8271387E+00	-0.2731310E+01	-0.3344947E+00
2651	14	-0.2892961E+01	-0.2838986E+01	-0.3783099E+00
2652	15	-0.1621366E+00	-0.3848816E+01	0.1293455E+01

B.3. PEG WITH HYDROXYETHYL TERMINAL, MULTIPLE CONFORMATIONS

2653 16 0.6254804E-01 -0.3742425E+01 -0.2647986E+01
2654 17 0.1859322E+01 -0.3367611E+01 -0.2689964E+01

2655

2656 Reading esp"s for MEP 32

2657 total number of atoms = 17

2658 total number of esp points = 838

2659

Center	X	Y	Z
2661 1	0.6255182E-01	-0.3742578E+01	-0.2647765E+01
2662 2	0.1859326E+01	-0.3367788E+01	-0.2689758E+01
2663 3	-0.8271387E+00	-0.2731329E+01	-0.3343360E+00
2664 4	-0.1621461E+00	-0.3848741E+01	0.1293684E+01
2665 5	-0.2892959E+01	-0.2839003E+01	-0.3781512E+00
2666 6	0.0000000E+00	0.0000000E+00	0.0000000E+00
2667 7	-0.7335198E+00	0.7975967E+00	0.1778557E+01
2668 8	-0.7096016E+00	0.1152064E+01	-0.1580225E+01
2669 9	0.2689779E+01	0.0000000E+00	0.0000000E+00
2670 10	0.3795464E+01	0.2452014E+01	0.0000000E+00
2671 11	0.3036848E+01	0.3572499E+01	0.1580164E+01
2672 12	0.3369986E+01	0.3448527E+01	-0.1778595E+01
2673 13	0.6625347E+01	0.2083279E+01	0.3344947E+00
2674 14	0.7572701E+01	0.3922230E+01	0.3783099E+00
2675 15	0.7370710E+01	0.1017689E+01	-0.1293455E+01
2676 16	0.7181361E+01	0.8565996E+00	0.2647986E+01
2677 17	0.6101082E+01	-0.6272719E+00	0.2689964E+01

2678

2679 Reading esp"s for MEP 33

2680 total number of atoms = 17

2681 total number of esp points = 827

2682

Center	X	Y	Z
2683 1	0.7407913E+01	0.9460138E+00	0.2367834E+01
2684 2	0.6446606E+01	-0.6127153E+00	0.2462479E+01
2685 3	0.6620644E+01	0.2155376E+01	0.1110573E+00
2686 4	0.7258851E+01	0.1113553E+01	-0.1575387E+01
2687 5	0.7519755E+01	0.4018693E+01	0.8754156E-01
2688 6	0.3766579E+01	0.2462880E+01	0.0000000E+00
2689 7	0.3208311E+01	0.3497630E+01	-0.1720185E+01
2690 8	0.3100995E+01	0.3536429E+01	0.1653865E+01
2691 9	0.2688481E+01	0.0000000E+00	0.0000000E+00
2692 10	0.0000000E+00	0.0000000E+00	0.0000000E+00
2693 11	-0.7240598E+00	0.9262794E+00	-0.1720223E+01
2694 12	-0.7165765E+00	0.1040288E+01	0.1653816E+01
2695 13	-0.8628205E+00	-0.2737845E+01	0.1111726E+00
2696 14	-0.1643022E+00	-0.3740363E+01	-0.1575190E+01

B.3. PEG WITH HYDROXYETHYL TERMINAL, MULTIPLE CONFORMATIONS

2698 15 -0.2930305E+01 -0.2814297E+01 0.8760581E-01
2699 16 -0.7073244E-01 -0.3943894E+01 0.2368048E+01
2700 17 0.1742700E+01 -0.3688518E+01 0.2462625E+01

2701

2702 Reading esp"s for MEP 34

2703 total number of atoms = 17

2704 total number of esp points = 827

2705

2706	Center	X	Y	Z
2707	1	-0.7061528E-01	-0.3944009E+01	-0.2367834E+01
2708	2	0.1742787E+01	-0.3688431E+01	-0.2462479E+01
2709	3	-0.8627884E+00	-0.2737854E+01	-0.1110573E+00
2710	4	-0.1643192E+00	-0.3740274E+01	0.1575387E+01
2711	5	-0.2930275E+01	-0.2814314E+01	-0.8754156E-01
2712	6	0.0000000E+00	0.0000000E+00	0.0000000E+00
2713	7	-0.7240447E+00	0.9263531E+00	0.1720185E+01
2714	8	-0.7165520E+00	0.1040222E+01	-0.1653865E+01
2715	9	0.2688508E+01	0.0000000E+00	0.0000000E+00
2716	10	0.3766594E+01	0.2462857E+01	0.0000000E+00
2717	11	0.3208400E+01	0.3497592E+01	0.1720223E+01
2718	12	0.3100959E+01	0.3536454E+01	-0.1653816E+01
2719	13	0.6620664E+01	0.2155387E+01	-0.1111726E+00
2720	14	0.7258942E+01	0.1113478E+01	0.1575190E+01
2721	15	0.7519768E+01	0.4018705E+01	-0.8760581E-01
2722	16	0.7407870E+01	0.9461423E+00	-0.2368048E+01
2723	17	0.6446736E+01	-0.6126945E+00	-0.2462625E+01

2724

2725 Reading esp"s for MEP 35

2726 total number of atoms = 17

2727 total number of esp points = 762

2728

2729	Center	X	Y	Z
2730	1	0.3191796E+01	0.3130546E+01	0.4488982E+01
2731	2	0.2383649E+01	0.1476269E+01	0.4645417E+01
2732	3	0.5069003E+01	0.2912782E+01	0.2599176E+01
2733	4	0.6446298E+01	0.1419007E+01	0.3056868E+01
2734	5	0.6094313E+01	0.4714042E+01	0.2543828E+01
2735	6	0.3943388E+01	0.2378299E+01	0.0000000E+00
2736	7	0.5445293E+01	0.2291565E+01	-0.1431082E+01
2737	8	0.2636510E+01	0.3903361E+01	-0.5275189E+00
2738	9	0.2674527E+01	0.0000000E+00	0.0000000E+00
2739	10	0.0000000E+00	0.0000000E+00	0.0000000E+00
2740	11	-0.6995237E+00	-0.7193110E+00	-0.1826080E+01
2741	12	-0.7514854E+00	0.1924032E+01	0.2387215E+00
2742	13	-0.9977678E+00	-0.1704393E+01	0.2098444E+01

B.3. PEG WITH HYDROXYETHYL TERMINAL, MULTIPLE CONFORMATIONS

```
2743 14 -0.2995783E-01 -0.3527943E+01 0.2012902E+01
2744 15 -0.3030414E+01 -0.2039774E+01 0.1813092E+01
2745 16 -0.5295182E+00 -0.7491233E+00 0.4582914E+01
2746 17 -0.1594451E+01 0.7247364E+00 0.4831232E+01
```

2747

2748 Reading esp"s for MEP 36

2749 total number of atoms = 17

2750 total number of esp points = 772

2751

2752	Center	X	Y	Z
2753	1	-0.3099113E+00	0.1017213E+01	-0.4488982E+01
2754	2	0.1530039E+01	0.9515375E+00	-0.4645417E+01
2755	3	-0.1001409E+01	-0.7415247E+00	-0.2599176E+01
2756	4	-0.3317849E+00	-0.2659835E+01	-0.3056868E+01
2757	5	-0.3073265E+01	-0.7982637E+00	-0.2543828E+01
2758	6	0.0000000E+00	0.0000000E+00	0.0000000E+00
2759	7	-0.6304428E+00	-0.1365935E+01	0.1431082E+01
2760	8	-0.7303753E+00	0.1870910E+01	0.5275189E+00
2761	9	0.2695611E+01	0.0000000E+00	0.0000000E+00
2762	10	0.3954548E+01	0.2359697E+01	0.0000000E+00
2763	11	0.4918460E+01	0.2638288E+01	0.1826080E+01
2764	12	0.2610736E+01	0.3928391E+01	-0.2387215E+00
2765	13	0.5927974E+01	0.2437731E+01	-0.2098444E+01
2766	14	0.7081302E+01	0.7254753E+00	-0.2012902E+01
2767	15	0.7180670E+01	0.4073238E+01	-0.1813092E+01
2768	16	0.4864740E+01	0.2474260E+01	-0.4582914E+01
2769	17	0.4065653E+01	0.4107601E+01	-0.4831232E+01

2770

2771 Reading esp"s for MEP 37

2772 total number of atoms = 17

2773 total number of esp points = 827

2774

2775	Center	X	Y	Z
2776	1	0.7407902E+01	0.9461253E+00	0.2367976E+01
2777	2	0.6446730E+01	-0.6126888E+00	0.2462598E+01
2778	3	0.6620655E+01	0.2155363E+01	0.1111197E+00
2779	4	0.7258885E+01	0.1113447E+01	-0.1575259E+01
2780	5	0.7519762E+01	0.4018678E+01	0.8752455E-01
2781	6	0.3766585E+01	0.2462853E+01	0.0000000E+00
2782	7	0.3208373E+01	0.3497599E+01	-0.1720212E+01
2783	8	0.3100976E+01	0.3536439E+01	0.1653835E+01
2784	9	0.2688485E+01	0.0000000E+00	0.0000000E+00
2785	10	0.0000000E+00	0.0000000E+00	0.0000000E+00
2786	11	-0.7240561E+00	0.9262889E+00	-0.1720220E+01
2787	12	-0.7165746E+00	0.1040279E+01	0.1653820E+01

B.3. PEG WITH HYDROXYETHYL TERMINAL, MULTIPLE CONFORMATIONS

```
2788 13 -0.8628092E+00 -0.2737848E+01 0.1111461E+00
2789 14 -0.1642739E+00 -0.3740344E+01 -0.1575227E+01
2790 15 -0.2930292E+01 -0.2814307E+01 0.8756234E-01
2791 16 -0.7073055E-01 -0.3943913E+01 0.2368012E+01
2792 17 0.1742700E+01 -0.3688530E+01 0.2462610E+01
```

2793

2794 Reading esp"s for MEP 38

2795 total number of atoms = 17

2796 total number of esp points = 827

2797

2798	Center	X	Y	Z
2799	1	-0.7075323E-01	-0.3943938E+01	-0.2367976E+01
2800	2	0.1742673E+01	-0.3688528E+01	-0.2462598E+01
2801	3	-0.8628149E+00	-0.2737848E+01	-0.1111197E+00
2802	4	-0.1642777E+00	-0.3740331E+01	0.1575259E+01
2803	5	-0.2930298E+01	-0.2814297E+01	-0.8752455E-01
2804	6	0.0000000E+00	0.0000000E+00	0.0000000E+00
2805	7	-0.7240580E+00	0.9263040E+00	0.1720212E+01
2806	8	-0.7165709E+00	0.1040262E+01	-0.1653835E+01
2807	9	0.2688485E+01	0.0000000E+00	0.0000000E+00
2808	10	0.3766585E+01	0.2462855E+01	0.0000000E+00
2809	11	0.3208384E+01	0.3497592E+01	0.1720220E+01
2810	12	0.3100961E+01	0.3536448E+01	-0.1653820E+01
2811	13	0.6620651E+01	0.2155359E+01	-0.1111461E+00
2812	14	0.7258895E+01	0.1113440E+01	0.1575227E+01
2813	15	0.7519768E+01	0.4018667E+01	-0.8756234E-01
2814	16	0.7407870E+01	0.9461140E+00	-0.2368012E+01
2815	17	0.6446721E+01	-0.6127134E+00	-0.2462610E+01

2816

2817 Reading esp"s for MEP 39

2818 total number of atoms = 17

2819 total number of esp points = 827

2820

2821	Center	X	Y	Z
2822	1	0.7407887E+01	0.9460649E+00	0.2367942E+01
2823	2	0.6446642E+01	-0.6127040E+00	0.2462574E+01
2824	3	0.6620655E+01	0.2155357E+01	0.1111083E+00
2825	4	0.7258876E+01	0.1113470E+01	-0.1575293E+01
2826	5	0.7519777E+01	0.4018665E+01	0.8754911E-01
2827	6	0.3766587E+01	0.2462861E+01	0.0000000E+00
2828	7	0.3208358E+01	0.3497607E+01	-0.1720204E+01
2829	8	0.3100986E+01	0.3536437E+01	0.1653841E+01
2830	9	0.2688489E+01	0.0000000E+00	0.0000000E+00
2831	10	0.0000000E+00	0.0000000E+00	0.0000000E+00
2832	11	-0.7240561E+00	0.9263361E+00	-0.1720197E+01

B.3. PEG WITH HYDROXYETHYL TERMINAL, MULTIPLE CONFORMATIONS

```
2833 12 -0.7165652E+00 0.1040243E+01 0.1653847E+01
2834 13 -0.8628149E+00 -0.2737848E+01 0.1110611E+00
2835 14 -0.1643230E+00 -0.3740282E+01 -0.1575368E+01
2836 15 -0.2930300E+01 -0.2814299E+01 0.8751132E-01
2837 16 -0.7070032E-01 -0.3944019E+01 0.2367857E+01
2838 17 0.1742722E+01 -0.3688592E+01 0.2462468E+01
```

2839

2840 Reading esp"s for MEP 40

2841 total number of atoms = 17

2842 total number of esp points = 827

2843

2844	Center	X	Y	Z
2845	1	-0.7067953E-01	-0.3943949E+01	-0.2367942E+01
2846	2	0.1742735E+01	-0.3688450E+01	-0.2462574E+01
2847	3	-0.8627979E+00	-0.2737854E+01	-0.1111083E+00
2848	4	-0.1642795E+00	-0.3740314E+01	0.1575293E+01
2849	5	-0.2930281E+01	-0.2814322E+01	-0.8754911E-01
2850	6	0.0000000E+00	0.0000000E+00	0.0000000E+00
2851	7	-0.7240523E+00	0.9263191E+00	0.1720204E+01
2852	8	-0.7165671E+00	0.1040251E+01	-0.1653841E+01
2853	9	0.2688490E+01	0.0000000E+00	0.0000000E+00
2854	10	0.3766589E+01	0.2462859E+01	0.0000000E+00
2855	11	0.3208345E+01	0.3497615E+01	0.1720197E+01
2856	12	0.3100995E+01	0.3536429E+01	-0.1653847E+01
2857	13	0.6620659E+01	0.2155372E+01	-0.1110611E+00
2858	14	0.7258865E+01	0.1113519E+01	0.1575368E+01
2859	15	0.7519766E+01	0.4018688E+01	-0.8751132E-01
2860	16	0.7407960E+01	0.9460535E+00	-0.2367857E+01
2861	17	0.6446777E+01	-0.6127512E+00	-0.2462468E+01

2862

2863 Reading esp"s for MEP 41

2864 total number of atoms = 17

2865 total number of esp points = 827

2866

2867	Center	X	Y	Z
2868	1	0.7407830E+01	0.9461234E+00	0.2368086E+01
2869	2	0.6446621E+01	-0.6126700E+00	0.2462700E+01
2870	3	0.6620655E+01	0.2155370E+01	0.1112141E+00
2871	4	0.7258942E+01	0.1113464E+01	-0.1575149E+01
2872	5	0.7519756E+01	0.4018688E+01	0.8765683E-01
2873	6	0.3766589E+01	0.2462855E+01	0.0000000E+00
2874	7	0.3208433E+01	0.3497575E+01	-0.1720244E+01
2875	8	0.3100917E+01	0.3536465E+01	0.1653794E+01
2876	9	0.2688490E+01	0.0000000E+00	0.0000000E+00
2877	10	0.0000000E+00	0.0000000E+00	0.0000000E+00

B.3. PEG WITH HYDROXYETHYL TERMINAL, MULTIPLE CONFORMATIONS

```
2878 11 -0.7240523E+00 0.9261982E+00 -0.1720269E+01
2879 12 -0.7165652E+00 0.1040379E+01 0.1653763E+01
2880 13 -0.8628168E+00 -0.2737837E+01 0.1112992E+00
2881 14 -0.1643136E+00 -0.3740427E+01 -0.1575030E+01
2882 15 -0.2930302E+01 -0.2814282E+01 0.8774376E-01
2883 16 -0.7071544E-01 -0.3943788E+01 0.2368214E+01
2884 17 0.1742696E+01 -0.3688278E+01 0.2462840E+01
```

2885

2886 Reading esp"s for MEP 42

2887 total number of atoms = 17

2888 total number of esp points = 827

2889

2890	Center	X	Y	Z
2891	1	-0.7071733E-01	-0.3943871E+01	-0.2368086E+01
2892	2	0.1742705E+01	-0.3688414E+01	-0.2462700E+01
2893	3	-0.8628187E+00	-0.2737845E+01	-0.1112141E+00
2894	4	-0.1643098E+00	-0.3740372E+01	0.1575149E+01
2895	5	-0.2930302E+01	-0.2814288E+01	-0.8765683E-01
2896	6	0.0000000E+00	0.0000000E+00	0.0000000E+00
2897	7	-0.7240580E+00	0.9262416E+00	0.1720244E+01
2898	8	-0.7165709E+00	0.1040328E+01	-0.1653794E+01
2899	9	0.2688485E+01	0.0000000E+00	0.0000000E+00
2900	10	0.3766587E+01	0.2462859E+01	0.0000000E+00
2901	11	0.3208467E+01	0.3497558E+01	0.1720269E+01
2902	12	0.3100868E+01	0.3536484E+01	-0.1653763E+01
2903	13	0.6620646E+01	0.2155376E+01	-0.1112992E+00
2904	14	0.7258991E+01	0.1113451E+01	0.1575030E+01
2905	15	0.7519749E+01	0.4018693E+01	-0.8774376E-01
2906	16	0.7407752E+01	0.9461575E+00	-0.2368214E+01
2907	17	0.6446496E+01	-0.6126019E+00	-0.2462840E+01

2908

2909 Reading esp"s for MEP 43

2910 total number of atoms = 17

2911 total number of esp points = 827

2912

2913	Center	X	Y	Z
2914	1	0.7407856E+01	0.9461045E+00	0.2368019E+01
2915	2	0.6446649E+01	-0.6126870E+00	0.2462625E+01
2916	3	0.6620647E+01	0.2155376E+01	0.1111631E+00
2917	4	0.7258921E+01	0.1113491E+01	-0.1575217E+01
2918	5	0.7519747E+01	0.4018693E+01	0.8761714E-01
2919	6	0.3766583E+01	0.2462857E+01	0.0000000E+00
2920	7	0.3208390E+01	0.3497592E+01	-0.1720223E+01
2921	8	0.3100944E+01	0.3536448E+01	0.1653816E+01
2922	9	0.2688487E+01	0.0000000E+00	0.0000000E+00

B.3. PEG WITH HYDROXYETHYL TERMINAL, MULTIPLE CONFORMATIONS

```
2923 10 0.0000000E+00 0.0000000E+00 0.0000000E+00
2924 11 -0.7240561E+00 0.9262832E+00 -0.1720221E+01
2925 12 -0.7165671E+00 0.1040281E+01 0.1653822E+01
2926 13 -0.8628016E+00 -0.2737854E+01 0.1111423E+00
2927 14 -0.1643192E+00 -0.3740321E+01 -0.1575270E+01
2928 15 -0.2930289E+01 -0.2814308E+01 0.8761526E-01
2929 16 -0.7065686E-01 -0.3943949E+01 0.2367957E+01
2930 17 0.1742764E+01 -0.3688505E+01 0.2462544E+01
```

2931

2932 Reading esp"s for MEP 44

2933 total number of atoms = 17

2934 total number of esp points = 827

2935

2936	Center	X	Y	Z
2937	1	-0.7070599E-01	-0.3943909E+01	-0.2368019E+01
2938	2	0.1742715E+01	-0.3688452E+01	-0.2462625E+01
2939	3	-0.8628149E+00	-0.2737843E+01	-0.1111631E+00
2940	4	-0.1643211E+00	-0.3740350E+01	0.1575217E+01
2941	5	-0.2930300E+01	-0.2814288E+01	-0.8761714E-01
2942	6	0.0000000E+00	0.0000000E+00	0.0000000E+00
2943	7	-0.7240580E+00	0.9262794E+00	0.1720223E+01
2944	8	-0.7165671E+00	0.1040290E+01	-0.1653816E+01
2945	9	0.2688487E+01	0.0000000E+00	0.0000000E+00
2946	10	0.3766581E+01	0.2462859E+01	0.0000000E+00
2947	11	0.3208386E+01	0.3497594E+01	0.1720221E+01
2948	12	0.3100951E+01	0.3536446E+01	-0.1653822E+01
2949	13	0.6620653E+01	0.2155359E+01	-0.1111423E+00
2950	14	0.7258893E+01	0.1113502E+01	0.1575270E+01
2951	15	0.7519762E+01	0.4018674E+01	-0.8761526E-01
2952	16	0.7407873E+01	0.9460441E+00	-0.2367957E+01
2953	17	0.6446677E+01	-0.6127550E+00	-0.2462544E+01

2954

2955 Reading esp"s for MEP 45

2956 total number of atoms = 17

2957 total number of esp points = 827

2958

2959	Center	X	Y	Z
2960	1	0.7407887E+01	0.9460460E+00	0.2367942E+01
2961	2	0.6446657E+01	-0.6127304E+00	0.2462551E+01
2962	3	0.6620653E+01	0.2155359E+01	0.1111216E+00
2963	4	0.7258893E+01	0.1113496E+01	-0.1575287E+01
2964	5	0.7519762E+01	0.4018672E+01	0.8758502E-01
2965	6	0.3766585E+01	0.2462855E+01	0.0000000E+00
2966	7	0.3208373E+01	0.3497599E+01	-0.1720212E+01
2967	8	0.3100969E+01	0.3536441E+01	0.1653831E+01

B.3. PEG WITH HYDROXYETHYL TERMINAL, MULTIPLE CONFORMATIONS

```
2968 9 0.2688483E+01 0.0000000E+00 0.0000000E+00
2969 10 0.0000000E+00 0.0000000E+00 0.0000000E+00
2970 11 -0.7240580E+00 0.9262757E+00 -0.1720225E+01
2971 12 -0.7165728E+00 0.1040294E+01 0.1653814E+01
2972 13 -0.8628187E+00 -0.2737846E+01 0.1111631E+00
2973 14 -0.1643173E+00 -0.3740344E+01 -0.1575221E+01
2974 15 -0.2930304E+01 -0.2814290E+01 0.8760770E-01
2975 16 -0.7071355E-01 -0.3943915E+01 0.2368012E+01
2976 17 0.1742711E+01 -0.3688481E+01 0.2462621E+01
```

2977

2978 Reading esp"s for MEP 46

2979 total number of atoms = 17

2980 total number of esp points = 827

2981

2982	Center	X	Y	Z
2983	1	-0.7067764E-01	-0.3943956E+01	-0.2367942E+01
2984	2	0.1742739E+01	-0.3688479E+01	-0.2462551E+01
2985	3	-0.8628130E+00	-0.2737848E+01	-0.1111216E+00
2986	4	-0.1643268E+00	-0.3740318E+01	0.1575287E+01
2987	5	-0.2930296E+01	-0.2814299E+01	-0.8758502E-01
2988	6	0.0000000E+00	0.0000000E+00	0.0000000E+00
2989	7	-0.7240561E+00	0.9263021E+00	0.1720212E+01
2990	8	-0.7165690E+00	0.1040270E+01	-0.1653831E+01
2991	9	0.2688487E+01	0.0000000E+00	0.0000000E+00
2992	10	0.3766587E+01	0.2462852E+01	0.0000000E+00
2993	11	0.3208401E+01	0.3497586E+01	0.1720225E+01
2994	12	0.3100951E+01	0.3536450E+01	-0.1653814E+01
2995	13	0.6620657E+01	0.2155361E+01	-0.1111631E+00
2996	14	0.7258916E+01	0.1113474E+01	0.1575221E+01
2997	15	0.7519760E+01	0.4018678E+01	-0.8760770E-01
2998	16	0.7407866E+01	0.9460913E+00	-0.2368012E+01
2999	17	0.6446672E+01	-0.6127096E+00	-0.2462621E+01

3000 Initial ssvpot = 9.136

3001

3002

3003 Number of unique UNfrozen centers= 4

3004

3005 Non-linear optimization requested.

3006 qchnge = 0.8642012652E-02

3007 qchnge = 0.2080586726E-03

3008 qchnge = 0.9660723586E-05

3009 qchnge = 0.4841979518E-06

3010

3011 Convergence in 3 iterations

3012

B.3. PEG WITH HYDROXYETHYL TERMINAL, MULTIPLE CONFORMATIONS

3013	1	PEG2	nconf=1	noorient=1	nmep=1/46
3014	2	PEG2	nconf=1	noorient=2	nmep=2/46
3015	3	PEG2	nconf=2	noorient=1	nmep=3/46
3016	4	PEG2	nconf=2	noorient=2	nmep=4/46
3017	5	PEG2	nconf=3	noorient=1	nmep=5/46
3018	6	PEG2	nconf=3	noorient=2	nmep=6/46
3019	7	PEG2	nconf=4	noorient=1	nmep=7/46
3020	8	PEG2	nconf=4	noorient=2	nmep=8/46
3021	9	PEG2	nconf=5	noorient=1	nmep=9/46
3022	10	PEG2	nconf=5	noorient=2	nmep=10/46
3023	11	PEG2	nconf=6	noorient=1	nmep=11/46
3024	12	PEG2	nconf=6	noorient=2	nmep=12/46
3025	13	PEG2	nconf=7	noorient=1	nmep=13/46
3026	14	PEG2	nconf=7	noorient=2	nmep=14/46
3027	15	PEG2	nconf=8	noorient=1	nmep=15/46
3028	16	PEG2	nconf=8	noorient=2	nmep=16/46
3029	17	PEG2	nconf=9	noorient=1	nmep=17/46
3030	18	PEG2	nconf=9	noorient=2	nmep=18/46
3031	19	PEG2	nconf=10	noorient=1	nmep=19/46
3032	20	PEG2	nconf=10	noorient=2	nmep=20/46
3033	21	PEG2	nconf=11	noorient=1	nmep=21/46
3034	22	PEG2	nconf=11	noorient=2	nmep=22/46
3035	23	PEG2	nconf=12	noorient=1	nmep=23/46
3036	24	PEG2	nconf=12	noorient=2	nmep=24/46
3037	25	PEG2	nconf=13	noorient=1	nmep=25/46
3038	26	PEG2	nconf=13	noorient=2	nmep=26/46
3039	27	PEG2	nconf=14	noorient=1	nmep=27/46
3040	28	PEG2	nconf=14	noorient=2	nmep=28/46
3041	29	PEG2	nconf=15	noorient=1	nmep=29/46
3042	30	PEG2	nconf=15	noorient=2	nmep=30/46
3043	31	PEG2	nconf=16	noorient=1	nmep=31/46
3044	32	PEG2	nconf=16	noorient=2	nmep=32/46
3045	33	PEG2	nconf=17	noorient=1	nmep=33/46
3046	34	PEG2	nconf=17	noorient=2	nmep=34/46
3047	35	PEG2	nconf=18	noorient=1	nmep=35/46
3048	36	PEG2	nconf=18	noorient=2	nmep=36/46
3049	37	PEG2	nconf=19	noorient=1	nmep=37/46
3050	38	PEG2	nconf=19	noorient=2	nmep=38/46
3051	39	PEG2	nconf=20	noorient=1	nmep=39/46
3052	40	PEG2	nconf=20	noorient=2	nmep=40/46
3053	41	PEG2	nconf=21	noorient=1	nmep=41/46
3054	42	PEG2	nconf=21	noorient=2	nmep=42/46
3055	43	PEG2	nconf=22	noorient=1	nmep=43/46
3056	44	PEG2	nconf=22	noorient=2	nmep=44/46
3057	45	PEG2	nconf=23	noorient=1	nmep=45/46

B.3. PEG WITH HYDROXYETHYL TERMINAL, MULTIPLE CONFORMATIONS

3058 46 PEG2 nconf=23 norient=2 nmep=46/46

3059

3060 Point Charges Before & After Optimization

3061

3062	no.	At.no.	q(init)	q(opt)	ivary	d(rstr)/dq
3063	1	8	-0.540571	-0.540571	-1	0.001819
3064	2	1	0.359859	0.359859	-1	0.000000
3065	3	6	0.090819	0.139118	0	0.005836
3066	4	1	0.035601	0.036348	0	0.000000
3067	5	1	0.068479	0.036348	4	0.000000
3068	6	6	0.011388	-0.010513	0	0.009945
3069	7	1	0.043297	0.061234	0	0.000000
3070	8	1	0.069417	0.061234	7	0.000000
3071	9	8	-0.286114	-0.286114	-1	0.003299
3072	10	6	0.000727	-0.010513	6	0.009945
3073	11	1	0.047995	0.061234	7	0.000000
3074	12	1	0.063336	0.061234	7	0.000000
3075	13	6	0.132235	0.139118	3	0.005836
3076	14	1	0.029096	0.036348	4	0.000000
3077	15	1	0.055147	0.036348	4	0.000000
3078	16	8	-0.540571	-0.540571	-1	0.001819
3079	17	1	0.359859	0.359859	-1	0.000000
3080						
3081	18	8	-0.540571	-0.540571	-1	0.001819
3082	19	1	0.359859	0.359859	-1	0.000000
3083	20	6	0.090819	0.139118	3	0.005836
3084	21	1	0.035601	0.036348	4	0.000000
3085	22	1	0.068479	0.036348	4	0.000000
3086	23	6	0.011388	-0.010513	6	0.009945
3087	24	1	0.043297	0.061234	7	0.000000
3088	25	1	0.069417	0.061234	7	0.000000
3089	26	8	-0.286114	-0.286114	-1	0.003299
3090	27	6	0.000727	-0.010513	6	0.009945
3091	28	1	0.047995	0.061234	7	0.000000
3092	29	1	0.063336	0.061234	7	0.000000
3093	30	6	0.132235	0.139118	3	0.005836
3094	31	1	0.029096	0.036348	4	0.000000
3095	32	1	0.055147	0.036348	4	0.000000
3096	33	8	-0.540571	-0.540571	-1	0.001819
3097	34	1	0.359859	0.359859	-1	0.000000
3098						
3099	35	8	-0.540571	-0.540571	-1	0.001819
3100	36	1	0.359859	0.359859	-1	0.000000
3101	37	6	0.090819	0.139118	3	0.005836
3102	38	1	0.035601	0.036348	4	0.000000

B.3. PEG WITH HYDROXYETHYL TERMINAL, MULTIPLE CONFORMATIONS

3103	39	1	0.068479	0.036348	4	0.000000
3104	40	6	0.011388	-0.010513	6	0.009945
3105	41	1	0.043297	0.061234	7	0.000000
3106	42	1	0.069417	0.061234	7	0.000000
3107	43	8	-0.286114	-0.286114	-1	0.003299
3108	44	6	0.000727	-0.010513	6	0.009945
3109	45	1	0.047995	0.061234	7	0.000000
3110	46	1	0.063336	0.061234	7	0.000000
3111	47	6	0.132235	0.139118	3	0.005836
3112	48	1	0.029096	0.036348	4	0.000000
3113	49	1	0.055147	0.036348	4	0.000000
3114	50	8	-0.540571	-0.540571	-1	0.001819
3115	51	1	0.359859	0.359859	-1	0.000000
3116						
3117	52	8	-0.540571	-0.540571	-1	0.001819
3118	53	1	0.359859	0.359859	-1	0.000000
3119	54	6	0.090819	0.139118	3	0.005836
3120	55	1	0.035601	0.036348	4	0.000000
3121	56	1	0.068479	0.036348	4	0.000000
3122	57	6	0.011388	-0.010513	6	0.009945
3123	58	1	0.043297	0.061234	7	0.000000
3124	59	1	0.069417	0.061234	7	0.000000
3125	60	8	-0.286114	-0.286114	-1	0.003299
3126	61	6	0.000727	-0.010513	6	0.009945
3127	62	1	0.047995	0.061234	7	0.000000
3128	63	1	0.063336	0.061234	7	0.000000
3129	64	6	0.132235	0.139118	3	0.005836
3130	65	1	0.029096	0.036348	4	0.000000
3131	66	1	0.055147	0.036348	4	0.000000
3132	67	8	-0.540571	-0.540571	-1	0.001819
3133	68	1	0.359859	0.359859	-1	0.000000
3134						
3135	69	8	-0.540571	-0.540571	-1	0.001819
3136	70	1	0.359859	0.359859	-1	0.000000
3137	71	6	0.090819	0.139118	3	0.005836
3138	72	1	0.035601	0.036348	4	0.000000
3139	73	1	0.068479	0.036348	4	0.000000
3140	74	6	0.011388	-0.010513	6	0.009945
3141	75	1	0.043297	0.061234	7	0.000000
3142	76	1	0.069417	0.061234	7	0.000000
3143	77	8	-0.286114	-0.286114	-1	0.003299
3144	78	6	0.000727	-0.010513	6	0.009945
3145	79	1	0.047995	0.061234	7	0.000000
3146	80	1	0.063336	0.061234	7	0.000000
3147	81	6	0.132235	0.139118	3	0.005836

B.3. PEG WITH HYDROXYETHYL TERMINAL, MULTIPLE CONFORMATIONS

3148	82	1	0.029096	0.036348	4	0.000000
3149	83	1	0.055147	0.036348	4	0.000000
3150	84	8	-0.540571	-0.540571	-1	0.001819
3151	85	1	0.359859	0.359859	-1	0.000000
3152						
3153	86	8	-0.540571	-0.540571	-1	0.001819
3154	87	1	0.359859	0.359859	-1	0.000000
3155	88	6	0.090819	0.139118	3	0.005836
3156	89	1	0.035601	0.036348	4	0.000000
3157	90	1	0.068479	0.036348	4	0.000000
3158	91	6	0.011388	-0.010513	6	0.009945
3159	92	1	0.043297	0.061234	7	0.000000
3160	93	1	0.069417	0.061234	7	0.000000
3161	94	8	-0.286114	-0.286114	-1	0.003299
3162	95	6	0.000727	-0.010513	6	0.009945
3163	96	1	0.047995	0.061234	7	0.000000
3164	97	1	0.063336	0.061234	7	0.000000
3165	98	6	0.132235	0.139118	3	0.005836
3166	99	1	0.029096	0.036348	4	0.000000
3167	100	1	0.055147	0.036348	4	0.000000
3168	101	8	-0.540571	-0.540571	-1	0.001819
3169	102	1	0.359859	0.359859	-1	0.000000
3170						
3171	103	8	-0.540571	-0.540571	-1	0.001819
3172	104	1	0.359859	0.359859	-1	0.000000
3173	105	6	0.090819	0.139118	3	0.005836
3174	106	1	0.035601	0.036348	4	0.000000
3175	107	1	0.068479	0.036348	4	0.000000
3176	108	6	0.011388	-0.010513	6	0.009945
3177	109	1	0.043297	0.061234	7	0.000000
3178	110	1	0.069417	0.061234	7	0.000000
3179	111	8	-0.286114	-0.286114	-1	0.003299
3180	112	6	0.000727	-0.010513	6	0.009945
3181	113	1	0.047995	0.061234	7	0.000000
3182	114	1	0.063336	0.061234	7	0.000000
3183	115	6	0.132235	0.139118	3	0.005836
3184	116	1	0.029096	0.036348	4	0.000000
3185	117	1	0.055147	0.036348	4	0.000000
3186	118	8	-0.540571	-0.540571	-1	0.001819
3187	119	1	0.359859	0.359859	-1	0.000000
3188						
3189	120	8	-0.540571	-0.540571	-1	0.001819
3190	121	1	0.359859	0.359859	-1	0.000000
3191	122	6	0.090819	0.139118	3	0.005836
3192	123	1	0.035601	0.036348	4	0.000000

B.3. PEG WITH HYDROXYETHYL TERMINAL, MULTIPLE CONFORMATIONS

3193	124	1	0.068479	0.036348	4	0.000000
3194	125	6	0.011388	-0.010513	6	0.009945
3195	126	1	0.043297	0.061234	7	0.000000
3196	127	1	0.069417	0.061234	7	0.000000
3197	128	8	-0.286114	-0.286114	-1	0.003299
3198	129	6	0.000727	-0.010513	6	0.009945
3199	130	1	0.047995	0.061234	7	0.000000
3200	131	1	0.063336	0.061234	7	0.000000
3201	132	6	0.132235	0.139118	3	0.005836
3202	133	1	0.029096	0.036348	4	0.000000
3203	134	1	0.055147	0.036348	4	0.000000
3204	135	8	-0.540571	-0.540571	-1	0.001819
3205	136	1	0.359859	0.359859	-1	0.000000
3206						
3207	137	8	-0.540571	-0.540571	-1	0.001819
3208	138	1	0.359859	0.359859	-1	0.000000
3209	139	6	0.090819	0.139118	3	0.005836
3210	140	1	0.035601	0.036348	4	0.000000
3211	141	1	0.068479	0.036348	4	0.000000
3212	142	6	0.011388	-0.010513	6	0.009945
3213	143	1	0.043297	0.061234	7	0.000000
3214	144	1	0.069417	0.061234	7	0.000000
3215	145	8	-0.286114	-0.286114	-1	0.003299
3216	146	6	0.000727	-0.010513	6	0.009945
3217	147	1	0.047995	0.061234	7	0.000000
3218	148	1	0.063336	0.061234	7	0.000000
3219	149	6	0.132235	0.139118	3	0.005836
3220	150	1	0.029096	0.036348	4	0.000000
3221	151	1	0.055147	0.036348	4	0.000000
3222	152	8	-0.540571	-0.540571	-1	0.001819
3223	153	1	0.359859	0.359859	-1	0.000000
3224						
3225	154	8	-0.540571	-0.540571	-1	0.001819
3226	155	1	0.359859	0.359859	-1	0.000000
3227	156	6	0.090819	0.139118	3	0.005836
3228	157	1	0.035601	0.036348	4	0.000000
3229	158	1	0.068479	0.036348	4	0.000000
3230	159	6	0.011388	-0.010513	6	0.009945
3231	160	1	0.043297	0.061234	7	0.000000
3232	161	1	0.069417	0.061234	7	0.000000
3233	162	8	-0.286114	-0.286114	-1	0.003299
3234	163	6	0.000727	-0.010513	6	0.009945
3235	164	1	0.047995	0.061234	7	0.000000
3236	165	1	0.063336	0.061234	7	0.000000
3237	166	6	0.132235	0.139118	3	0.005836

B.3. PEG WITH HYDROXYETHYL TERMINAL, MULTIPLE CONFORMATIONS

3238	167	1	0.029096	0.036348	4	0.000000
3239	168	1	0.055147	0.036348	4	0.000000
3240	169	8	-0.540571	-0.540571	-1	0.001819
3241	170	1	0.359859	0.359859	-1	0.000000
3242						
3243	171	8	-0.540571	-0.540571	-1	0.001819
3244	172	1	0.359859	0.359859	-1	0.000000
3245	173	6	0.090819	0.139118	3	0.005836
3246	174	1	0.035601	0.036348	4	0.000000
3247	175	1	0.068479	0.036348	4	0.000000
3248	176	6	0.011388	-0.010513	6	0.009945
3249	177	1	0.043297	0.061234	7	0.000000
3250	178	1	0.069417	0.061234	7	0.000000
3251	179	8	-0.286114	-0.286114	-1	0.003299
3252	180	6	0.000727	-0.010513	6	0.009945
3253	181	1	0.047995	0.061234	7	0.000000
3254	182	1	0.063336	0.061234	7	0.000000
3255	183	6	0.132235	0.139118	3	0.005836
3256	184	1	0.029096	0.036348	4	0.000000
3257	185	1	0.055147	0.036348	4	0.000000
3258	186	8	-0.540571	-0.540571	-1	0.001819
3259	187	1	0.359859	0.359859	-1	0.000000
3260						
3261	188	8	-0.540571	-0.540571	-1	0.001819
3262	189	1	0.359859	0.359859	-1	0.000000
3263	190	6	0.090819	0.139118	3	0.005836
3264	191	1	0.035601	0.036348	4	0.000000
3265	192	1	0.068479	0.036348	4	0.000000
3266	193	6	0.011388	-0.010513	6	0.009945
3267	194	1	0.043297	0.061234	7	0.000000
3268	195	1	0.069417	0.061234	7	0.000000
3269	196	8	-0.286114	-0.286114	-1	0.003299
3270	197	6	0.000727	-0.010513	6	0.009945
3271	198	1	0.047995	0.061234	7	0.000000
3272	199	1	0.063336	0.061234	7	0.000000
3273	200	6	0.132235	0.139118	3	0.005836
3274	201	1	0.029096	0.036348	4	0.000000
3275	202	1	0.055147	0.036348	4	0.000000
3276	203	8	-0.540571	-0.540571	-1	0.001819
3277	204	1	0.359859	0.359859	-1	0.000000
3278						
3279	205	8	-0.540571	-0.540571	-1	0.001819
3280	206	1	0.359859	0.359859	-1	0.000000
3281	207	6	0.090819	0.139118	3	0.005836
3282	208	1	0.035601	0.036348	4	0.000000

B.3. PEG WITH HYDROXYETHYL TERMINAL, MULTIPLE CONFORMATIONS

3283	209	1	0.068479	0.036348	4	0.000000
3284	210	6	0.011388	-0.010513	6	0.009945
3285	211	1	0.043297	0.061234	7	0.000000
3286	212	1	0.069417	0.061234	7	0.000000
3287	213	8	-0.286114	-0.286114	-1	0.003299
3288	214	6	0.000727	-0.010513	6	0.009945
3289	215	1	0.047995	0.061234	7	0.000000
3290	216	1	0.063336	0.061234	7	0.000000
3291	217	6	0.132235	0.139118	3	0.005836
3292	218	1	0.029096	0.036348	4	0.000000
3293	219	1	0.055147	0.036348	4	0.000000
3294	220	8	-0.540571	-0.540571	-1	0.001819
3295	221	1	0.359859	0.359859	-1	0.000000
3296						
3297	222	8	-0.540571	-0.540571	-1	0.001819
3298	223	1	0.359859	0.359859	-1	0.000000
3299	224	6	0.090819	0.139118	3	0.005836
3300	225	1	0.035601	0.036348	4	0.000000
3301	226	1	0.068479	0.036348	4	0.000000
3302	227	6	0.011388	-0.010513	6	0.009945
3303	228	1	0.043297	0.061234	7	0.000000
3304	229	1	0.069417	0.061234	7	0.000000
3305	230	8	-0.286114	-0.286114	-1	0.003299
3306	231	6	0.000727	-0.010513	6	0.009945
3307	232	1	0.047995	0.061234	7	0.000000
3308	233	1	0.063336	0.061234	7	0.000000
3309	234	6	0.132235	0.139118	3	0.005836
3310	235	1	0.029096	0.036348	4	0.000000
3311	236	1	0.055147	0.036348	4	0.000000
3312	237	8	-0.540571	-0.540571	-1	0.001819
3313	238	1	0.359859	0.359859	-1	0.000000
3314						
3315	239	8	-0.540571	-0.540571	-1	0.001819
3316	240	1	0.359859	0.359859	-1	0.000000
3317	241	6	0.090819	0.139118	3	0.005836
3318	242	1	0.035601	0.036348	4	0.000000
3319	243	1	0.068479	0.036348	4	0.000000
3320	244	6	0.011388	-0.010513	6	0.009945
3321	245	1	0.043297	0.061234	7	0.000000
3322	246	1	0.069417	0.061234	7	0.000000
3323	247	8	-0.286114	-0.286114	-1	0.003299
3324	248	6	0.000727	-0.010513	6	0.009945
3325	249	1	0.047995	0.061234	7	0.000000
3326	250	1	0.063336	0.061234	7	0.000000
3327	251	6	0.132235	0.139118	3	0.005836

B.3. PEG WITH HYDROXYETHYL TERMINAL, MULTIPLE CONFORMATIONS

3328	252	1	0.029096	0.036348	4	0.000000
3329	253	1	0.055147	0.036348	4	0.000000
3330	254	8	-0.540571	-0.540571	-1	0.001819
3331	255	1	0.359859	0.359859	-1	0.000000
3332						
3333	256	8	-0.540571	-0.540571	-1	0.001819
3334	257	1	0.359859	0.359859	-1	0.000000
3335	258	6	0.090819	0.139118	3	0.005836
3336	259	1	0.035601	0.036348	4	0.000000
3337	260	1	0.068479	0.036348	4	0.000000
3338	261	6	0.011388	-0.010513	6	0.009945
3339	262	1	0.043297	0.061234	7	0.000000
3340	263	1	0.069417	0.061234	7	0.000000
3341	264	8	-0.286114	-0.286114	-1	0.003299
3342	265	6	0.000727	-0.010513	6	0.009945
3343	266	1	0.047995	0.061234	7	0.000000
3344	267	1	0.063336	0.061234	7	0.000000
3345	268	6	0.132235	0.139118	3	0.005836
3346	269	1	0.029096	0.036348	4	0.000000
3347	270	1	0.055147	0.036348	4	0.000000
3348	271	8	-0.540571	-0.540571	-1	0.001819
3349	272	1	0.359859	0.359859	-1	0.000000
3350						
3351	273	8	-0.540571	-0.540571	-1	0.001819
3352	274	1	0.359859	0.359859	-1	0.000000
3353	275	6	0.090819	0.139118	3	0.005836
3354	276	1	0.035601	0.036348	4	0.000000
3355	277	1	0.068479	0.036348	4	0.000000
3356	278	6	0.011388	-0.010513	6	0.009945
3357	279	1	0.043297	0.061234	7	0.000000
3358	280	1	0.069417	0.061234	7	0.000000
3359	281	8	-0.286114	-0.286114	-1	0.003299
3360	282	6	0.000727	-0.010513	6	0.009945
3361	283	1	0.047995	0.061234	7	0.000000
3362	284	1	0.063336	0.061234	7	0.000000
3363	285	6	0.132235	0.139118	3	0.005836
3364	286	1	0.029096	0.036348	4	0.000000
3365	287	1	0.055147	0.036348	4	0.000000
3366	288	8	-0.540571	-0.540571	-1	0.001819
3367	289	1	0.359859	0.359859	-1	0.000000
3368						
3369	290	8	-0.540571	-0.540571	-1	0.001819
3370	291	1	0.359859	0.359859	-1	0.000000
3371	292	6	0.090819	0.139118	3	0.005836
3372	293	1	0.035601	0.036348	4	0.000000

B.3. PEG WITH HYDROXYETHYL TERMINAL, MULTIPLE CONFORMATIONS

3373	294	1	0.068479	0.036348	4	0.000000
3374	295	6	0.011388	-0.010513	6	0.009945
3375	296	1	0.043297	0.061234	7	0.000000
3376	297	1	0.069417	0.061234	7	0.000000
3377	298	8	-0.286114	-0.286114	-1	0.003299
3378	299	6	0.000727	-0.010513	6	0.009945
3379	300	1	0.047995	0.061234	7	0.000000
3380	301	1	0.063336	0.061234	7	0.000000
3381	302	6	0.132235	0.139118	3	0.005836
3382	303	1	0.029096	0.036348	4	0.000000
3383	304	1	0.055147	0.036348	4	0.000000
3384	305	8	-0.540571	-0.540571	-1	0.001819
3385	306	1	0.359859	0.359859	-1	0.000000
3386						
3387	307	8	-0.540571	-0.540571	-1	0.001819
3388	308	1	0.359859	0.359859	-1	0.000000
3389	309	6	0.090819	0.139118	3	0.005836
3390	310	1	0.035601	0.036348	4	0.000000
3391	311	1	0.068479	0.036348	4	0.000000
3392	312	6	0.011388	-0.010513	6	0.009945
3393	313	1	0.043297	0.061234	7	0.000000
3394	314	1	0.069417	0.061234	7	0.000000
3395	315	8	-0.286114	-0.286114	-1	0.003299
3396	316	6	0.000727	-0.010513	6	0.009945
3397	317	1	0.047995	0.061234	7	0.000000
3398	318	1	0.063336	0.061234	7	0.000000
3399	319	6	0.132235	0.139118	3	0.005836
3400	320	1	0.029096	0.036348	4	0.000000
3401	321	1	0.055147	0.036348	4	0.000000
3402	322	8	-0.540571	-0.540571	-1	0.001819
3403	323	1	0.359859	0.359859	-1	0.000000
3404						
3405	324	8	-0.540571	-0.540571	-1	0.001819
3406	325	1	0.359859	0.359859	-1	0.000000
3407	326	6	0.090819	0.139118	3	0.005836
3408	327	1	0.035601	0.036348	4	0.000000
3409	328	1	0.068479	0.036348	4	0.000000
3410	329	6	0.011388	-0.010513	6	0.009945
3411	330	1	0.043297	0.061234	7	0.000000
3412	331	1	0.069417	0.061234	7	0.000000
3413	332	8	-0.286114	-0.286114	-1	0.003299
3414	333	6	0.000727	-0.010513	6	0.009945
3415	334	1	0.047995	0.061234	7	0.000000
3416	335	1	0.063336	0.061234	7	0.000000
3417	336	6	0.132235	0.139118	3	0.005836

B.3. PEG WITH HYDROXYETHYL TERMINAL, MULTIPLE CONFORMATIONS

3418	337	1	0.029096	0.036348	4	0.000000
3419	338	1	0.055147	0.036348	4	0.000000
3420	339	8	-0.540571	-0.540571	-1	0.001819
3421	340	1	0.359859	0.359859	-1	0.000000
3422						
3423	341	8	-0.540571	-0.540571	-1	0.001819
3424	342	1	0.359859	0.359859	-1	0.000000
3425	343	6	0.090819	0.139118	3	0.005836
3426	344	1	0.035601	0.036348	4	0.000000
3427	345	1	0.068479	0.036348	4	0.000000
3428	346	6	0.011388	-0.010513	6	0.009945
3429	347	1	0.043297	0.061234	7	0.000000
3430	348	1	0.069417	0.061234	7	0.000000
3431	349	8	-0.286114	-0.286114	-1	0.003299
3432	350	6	0.000727	-0.010513	6	0.009945
3433	351	1	0.047995	0.061234	7	0.000000
3434	352	1	0.063336	0.061234	7	0.000000
3435	353	6	0.132235	0.139118	3	0.005836
3436	354	1	0.029096	0.036348	4	0.000000
3437	355	1	0.055147	0.036348	4	0.000000
3438	356	8	-0.540571	-0.540571	-1	0.001819
3439	357	1	0.359859	0.359859	-1	0.000000
3440						
3441	358	8	-0.540571	-0.540571	-1	0.001819
3442	359	1	0.359859	0.359859	-1	0.000000
3443	360	6	0.090819	0.139118	3	0.005836
3444	361	1	0.035601	0.036348	4	0.000000
3445	362	1	0.068479	0.036348	4	0.000000
3446	363	6	0.011388	-0.010513	6	0.009945
3447	364	1	0.043297	0.061234	7	0.000000
3448	365	1	0.069417	0.061234	7	0.000000
3449	366	8	-0.286114	-0.286114	-1	0.003299
3450	367	6	0.000727	-0.010513	6	0.009945
3451	368	1	0.047995	0.061234	7	0.000000
3452	369	1	0.063336	0.061234	7	0.000000
3453	370	6	0.132235	0.139118	3	0.005836
3454	371	1	0.029096	0.036348	4	0.000000
3455	372	1	0.055147	0.036348	4	0.000000
3456	373	8	-0.540571	-0.540571	-1	0.001819
3457	374	1	0.359859	0.359859	-1	0.000000
3458						
3459	375	8	-0.540571	-0.540571	-1	0.001819
3460	376	1	0.359859	0.359859	-1	0.000000
3461	377	6	0.090819	0.139118	3	0.005836
3462	378	1	0.035601	0.036348	4	0.000000

B.3. PEG WITH HYDROXYETHYL TERMINAL, MULTIPLE CONFORMATIONS

3463	379	1	0.068479	0.036348	4	0.000000
3464	380	6	0.011388	-0.010513	6	0.009945
3465	381	1	0.043297	0.061234	7	0.000000
3466	382	1	0.069417	0.061234	7	0.000000
3467	383	8	-0.286114	-0.286114	-1	0.003299
3468	384	6	0.000727	-0.010513	6	0.009945
3469	385	1	0.047995	0.061234	7	0.000000
3470	386	1	0.063336	0.061234	7	0.000000
3471	387	6	0.132235	0.139118	3	0.005836
3472	388	1	0.029096	0.036348	4	0.000000
3473	389	1	0.055147	0.036348	4	0.000000
3474	390	8	-0.540571	-0.540571	-1	0.001819
3475	391	1	0.359859	0.359859	-1	0.000000
3476						
3477	392	8	-0.540571	-0.540571	-1	0.001819
3478	393	1	0.359859	0.359859	-1	0.000000
3479	394	6	0.090819	0.139118	3	0.005836
3480	395	1	0.035601	0.036348	4	0.000000
3481	396	1	0.068479	0.036348	4	0.000000
3482	397	6	0.011388	-0.010513	6	0.009945
3483	398	1	0.043297	0.061234	7	0.000000
3484	399	1	0.069417	0.061234	7	0.000000
3485	400	8	-0.286114	-0.286114	-1	0.003299
3486	401	6	0.000727	-0.010513	6	0.009945
3487	402	1	0.047995	0.061234	7	0.000000
3488	403	1	0.063336	0.061234	7	0.000000
3489	404	6	0.132235	0.139118	3	0.005836
3490	405	1	0.029096	0.036348	4	0.000000
3491	406	1	0.055147	0.036348	4	0.000000
3492	407	8	-0.540571	-0.540571	-1	0.001819
3493	408	1	0.359859	0.359859	-1	0.000000
3494						
3495	409	8	-0.540571	-0.540571	-1	0.001819
3496	410	1	0.359859	0.359859	-1	0.000000
3497	411	6	0.090819	0.139118	3	0.005836
3498	412	1	0.035601	0.036348	4	0.000000
3499	413	1	0.068479	0.036348	4	0.000000
3500	414	6	0.011388	-0.010513	6	0.009945
3501	415	1	0.043297	0.061234	7	0.000000
3502	416	1	0.069417	0.061234	7	0.000000
3503	417	8	-0.286114	-0.286114	-1	0.003299
3504	418	6	0.000727	-0.010513	6	0.009945
3505	419	1	0.047995	0.061234	7	0.000000
3506	420	1	0.063336	0.061234	7	0.000000
3507	421	6	0.132235	0.139118	3	0.005836

B.3. PEG WITH HYDROXYETHYL TERMINAL, MULTIPLE CONFORMATIONS

3508	422	1	0.029096	0.036348	4	0.000000
3509	423	1	0.055147	0.036348	4	0.000000
3510	424	8	-0.540571	-0.540571	-1	0.001819
3511	425	1	0.359859	0.359859	-1	0.000000
3512						
3513	426	8	-0.540571	-0.540571	-1	0.001819
3514	427	1	0.359859	0.359859	-1	0.000000
3515	428	6	0.090819	0.139118	3	0.005836
3516	429	1	0.035601	0.036348	4	0.000000
3517	430	1	0.068479	0.036348	4	0.000000
3518	431	6	0.011388	-0.010513	6	0.009945
3519	432	1	0.043297	0.061234	7	0.000000
3520	433	1	0.069417	0.061234	7	0.000000
3521	434	8	-0.286114	-0.286114	-1	0.003299
3522	435	6	0.000727	-0.010513	6	0.009945
3523	436	1	0.047995	0.061234	7	0.000000
3524	437	1	0.063336	0.061234	7	0.000000
3525	438	6	0.132235	0.139118	3	0.005836
3526	439	1	0.029096	0.036348	4	0.000000
3527	440	1	0.055147	0.036348	4	0.000000
3528	441	8	-0.540571	-0.540571	-1	0.001819
3529	442	1	0.359859	0.359859	-1	0.000000
3530						
3531	443	8	-0.540571	-0.540571	-1	0.001819
3532	444	1	0.359859	0.359859	-1	0.000000
3533	445	6	0.090819	0.139118	3	0.005836
3534	446	1	0.035601	0.036348	4	0.000000
3535	447	1	0.068479	0.036348	4	0.000000
3536	448	6	0.011388	-0.010513	6	0.009945
3537	449	1	0.043297	0.061234	7	0.000000
3538	450	1	0.069417	0.061234	7	0.000000
3539	451	8	-0.286114	-0.286114	-1	0.003299
3540	452	6	0.000727	-0.010513	6	0.009945
3541	453	1	0.047995	0.061234	7	0.000000
3542	454	1	0.063336	0.061234	7	0.000000
3543	455	6	0.132235	0.139118	3	0.005836
3544	456	1	0.029096	0.036348	4	0.000000
3545	457	1	0.055147	0.036348	4	0.000000
3546	458	8	-0.540571	-0.540571	-1	0.001819
3547	459	1	0.359859	0.359859	-1	0.000000
3548						
3549	460	8	-0.540571	-0.540571	-1	0.001819
3550	461	1	0.359859	0.359859	-1	0.000000
3551	462	6	0.090819	0.139118	3	0.005836
3552	463	1	0.035601	0.036348	4	0.000000

B.3. PEG WITH HYDROXYETHYL TERMINAL, MULTIPLE CONFORMATIONS

3553	464	1	0.068479	0.036348	4	0.000000
3554	465	6	0.011388	-0.010513	6	0.009945
3555	466	1	0.043297	0.061234	7	0.000000
3556	467	1	0.069417	0.061234	7	0.000000
3557	468	8	-0.286114	-0.286114	-1	0.003299
3558	469	6	0.000727	-0.010513	6	0.009945
3559	470	1	0.047995	0.061234	7	0.000000
3560	471	1	0.063336	0.061234	7	0.000000
3561	472	6	0.132235	0.139118	3	0.005836
3562	473	1	0.029096	0.036348	4	0.000000
3563	474	1	0.055147	0.036348	4	0.000000
3564	475	8	-0.540571	-0.540571	-1	0.001819
3565	476	1	0.359859	0.359859	-1	0.000000
3566						
3567	477	8	-0.540571	-0.540571	-1	0.001819
3568	478	1	0.359859	0.359859	-1	0.000000
3569	479	6	0.090819	0.139118	3	0.005836
3570	480	1	0.035601	0.036348	4	0.000000
3571	481	1	0.068479	0.036348	4	0.000000
3572	482	6	0.011388	-0.010513	6	0.009945
3573	483	1	0.043297	0.061234	7	0.000000
3574	484	1	0.069417	0.061234	7	0.000000
3575	485	8	-0.286114	-0.286114	-1	0.003299
3576	486	6	0.000727	-0.010513	6	0.009945
3577	487	1	0.047995	0.061234	7	0.000000
3578	488	1	0.063336	0.061234	7	0.000000
3579	489	6	0.132235	0.139118	3	0.005836
3580	490	1	0.029096	0.036348	4	0.000000
3581	491	1	0.055147	0.036348	4	0.000000
3582	492	8	-0.540571	-0.540571	-1	0.001819
3583	493	1	0.359859	0.359859	-1	0.000000
3584						
3585	494	8	-0.540571	-0.540571	-1	0.001819
3586	495	1	0.359859	0.359859	-1	0.000000
3587	496	6	0.090819	0.139118	3	0.005836
3588	497	1	0.035601	0.036348	4	0.000000
3589	498	1	0.068479	0.036348	4	0.000000
3590	499	6	0.011388	-0.010513	6	0.009945
3591	500	1	0.043297	0.061234	7	0.000000
3592	501	1	0.069417	0.061234	7	0.000000
3593	502	8	-0.286114	-0.286114	-1	0.003299
3594	503	6	0.000727	-0.010513	6	0.009945
3595	504	1	0.047995	0.061234	7	0.000000
3596	505	1	0.063336	0.061234	7	0.000000
3597	506	6	0.132235	0.139118	3	0.005836

B.3. PEG WITH HYDROXYETHYL TERMINAL, MULTIPLE CONFORMATIONS

3598	507	1	0.029096	0.036348	4	0.000000
3599	508	1	0.055147	0.036348	4	0.000000
3600	509	8	-0.540571	-0.540571	-1	0.001819
3601	510	1	0.359859	0.359859	-1	0.000000
3602						
3603	511	8	-0.540571	-0.540571	-1	0.001819
3604	512	1	0.359859	0.359859	-1	0.000000
3605	513	6	0.090819	0.139118	3	0.005836
3606	514	1	0.035601	0.036348	4	0.000000
3607	515	1	0.068479	0.036348	4	0.000000
3608	516	6	0.011388	-0.010513	6	0.009945
3609	517	1	0.043297	0.061234	7	0.000000
3610	518	1	0.069417	0.061234	7	0.000000
3611	519	8	-0.286114	-0.286114	-1	0.003299
3612	520	6	0.000727	-0.010513	6	0.009945
3613	521	1	0.047995	0.061234	7	0.000000
3614	522	1	0.063336	0.061234	7	0.000000
3615	523	6	0.132235	0.139118	3	0.005836
3616	524	1	0.029096	0.036348	4	0.000000
3617	525	1	0.055147	0.036348	4	0.000000
3618	526	8	-0.540571	-0.540571	-1	0.001819
3619	527	1	0.359859	0.359859	-1	0.000000
3620						
3621	528	8	-0.540571	-0.540571	-1	0.001819
3622	529	1	0.359859	0.359859	-1	0.000000
3623	530	6	0.090819	0.139118	3	0.005836
3624	531	1	0.035601	0.036348	4	0.000000
3625	532	1	0.068479	0.036348	4	0.000000
3626	533	6	0.011388	-0.010513	6	0.009945
3627	534	1	0.043297	0.061234	7	0.000000
3628	535	1	0.069417	0.061234	7	0.000000
3629	536	8	-0.286114	-0.286114	-1	0.003299
3630	537	6	0.000727	-0.010513	6	0.009945
3631	538	1	0.047995	0.061234	7	0.000000
3632	539	1	0.063336	0.061234	7	0.000000
3633	540	6	0.132235	0.139118	3	0.005836
3634	541	1	0.029096	0.036348	4	0.000000
3635	542	1	0.055147	0.036348	4	0.000000
3636	543	8	-0.540571	-0.540571	-1	0.001819
3637	544	1	0.359859	0.359859	-1	0.000000
3638						
3639	545	8	-0.540571	-0.540571	-1	0.001819
3640	546	1	0.359859	0.359859	-1	0.000000
3641	547	6	0.090819	0.139118	3	0.005836
3642	548	1	0.035601	0.036348	4	0.000000

B.3. PEG WITH HYDROXYETHYL TERMINAL, MULTIPLE CONFORMATIONS

3643	549	1	0.068479	0.036348	4	0.000000
3644	550	6	0.011388	-0.010513	6	0.009945
3645	551	1	0.043297	0.061234	7	0.000000
3646	552	1	0.069417	0.061234	7	0.000000
3647	553	8	-0.286114	-0.286114	-1	0.003299
3648	554	6	0.000727	-0.010513	6	0.009945
3649	555	1	0.047995	0.061234	7	0.000000
3650	556	1	0.063336	0.061234	7	0.000000
3651	557	6	0.132235	0.139118	3	0.005836
3652	558	1	0.029096	0.036348	4	0.000000
3653	559	1	0.055147	0.036348	4	0.000000
3654	560	8	-0.540571	-0.540571	-1	0.001819
3655	561	1	0.359859	0.359859	-1	0.000000
3656						
3657	562	8	-0.540571	-0.540571	-1	0.001819
3658	563	1	0.359859	0.359859	-1	0.000000
3659	564	6	0.090819	0.139118	3	0.005836
3660	565	1	0.035601	0.036348	4	0.000000
3661	566	1	0.068479	0.036348	4	0.000000
3662	567	6	0.011388	-0.010513	6	0.009945
3663	568	1	0.043297	0.061234	7	0.000000
3664	569	1	0.069417	0.061234	7	0.000000
3665	570	8	-0.286114	-0.286114	-1	0.003299
3666	571	6	0.000727	-0.010513	6	0.009945
3667	572	1	0.047995	0.061234	7	0.000000
3668	573	1	0.063336	0.061234	7	0.000000
3669	574	6	0.132235	0.139118	3	0.005836
3670	575	1	0.029096	0.036348	4	0.000000
3671	576	1	0.055147	0.036348	4	0.000000
3672	577	8	-0.540571	-0.540571	-1	0.001819
3673	578	1	0.359859	0.359859	-1	0.000000
3674						
3675	579	8	-0.540571	-0.540571	-1	0.001819
3676	580	1	0.359859	0.359859	-1	0.000000
3677	581	6	0.090819	0.139118	3	0.005836
3678	582	1	0.035601	0.036348	4	0.000000
3679	583	1	0.068479	0.036348	4	0.000000
3680	584	6	0.011388	-0.010513	6	0.009945
3681	585	1	0.043297	0.061234	7	0.000000
3682	586	1	0.069417	0.061234	7	0.000000
3683	587	8	-0.286114	-0.286114	-1	0.003299
3684	588	6	0.000727	-0.010513	6	0.009945
3685	589	1	0.047995	0.061234	7	0.000000
3686	590	1	0.063336	0.061234	7	0.000000
3687	591	6	0.132235	0.139118	3	0.005836

B.3. PEG WITH HYDROXYETHYL TERMINAL, MULTIPLE CONFORMATIONS

3688	592	1	0.029096	0.036348	4	0.000000
3689	593	1	0.055147	0.036348	4	0.000000
3690	594	8	-0.540571	-0.540571	-1	0.001819
3691	595	1	0.359859	0.359859	-1	0.000000
3692						
3693	596	8	-0.540571	-0.540571	-1	0.001819
3694	597	1	0.359859	0.359859	-1	0.000000
3695	598	6	0.090819	0.139118	3	0.005836
3696	599	1	0.035601	0.036348	4	0.000000
3697	600	1	0.068479	0.036348	4	0.000000
3698	601	6	0.011388	-0.010513	6	0.009945
3699	602	1	0.043297	0.061234	7	0.000000
3700	603	1	0.069417	0.061234	7	0.000000
3701	604	8	-0.286114	-0.286114	-1	0.003299
3702	605	6	0.000727	-0.010513	6	0.009945
3703	606	1	0.047995	0.061234	7	0.000000
3704	607	1	0.063336	0.061234	7	0.000000
3705	608	6	0.132235	0.139118	3	0.005836
3706	609	1	0.029096	0.036348	4	0.000000
3707	610	1	0.055147	0.036348	4	0.000000
3708	611	8	-0.540571	-0.540571	-1	0.001819
3709	612	1	0.359859	0.359859	-1	0.000000
3710						
3711	613	8	-0.540571	-0.540571	-1	0.001819
3712	614	1	0.359859	0.359859	-1	0.000000
3713	615	6	0.090819	0.139118	3	0.005836
3714	616	1	0.035601	0.036348	4	0.000000
3715	617	1	0.068479	0.036348	4	0.000000
3716	618	6	0.011388	-0.010513	6	0.009945
3717	619	1	0.043297	0.061234	7	0.000000
3718	620	1	0.069417	0.061234	7	0.000000
3719	621	8	-0.286114	-0.286114	-1	0.003299
3720	622	6	0.000727	-0.010513	6	0.009945
3721	623	1	0.047995	0.061234	7	0.000000
3722	624	1	0.063336	0.061234	7	0.000000
3723	625	6	0.132235	0.139118	3	0.005836
3724	626	1	0.029096	0.036348	4	0.000000
3725	627	1	0.055147	0.036348	4	0.000000
3726	628	8	-0.540571	-0.540571	-1	0.001819
3727	629	1	0.359859	0.359859	-1	0.000000
3728						
3729	630	8	-0.540571	-0.540571	-1	0.001819
3730	631	1	0.359859	0.359859	-1	0.000000
3731	632	6	0.090819	0.139118	3	0.005836
3732	633	1	0.035601	0.036348	4	0.000000

B.3. PEG WITH HYDROXYETHYL TERMINAL, MULTIPLE CONFORMATIONS

3733	634	1	0.068479	0.036348	4	0.000000
3734	635	6	0.011388	-0.010513	6	0.009945
3735	636	1	0.043297	0.061234	7	0.000000
3736	637	1	0.069417	0.061234	7	0.000000
3737	638	8	-0.286114	-0.286114	-1	0.003299
3738	639	6	0.000727	-0.010513	6	0.009945
3739	640	1	0.047995	0.061234	7	0.000000
3740	641	1	0.063336	0.061234	7	0.000000
3741	642	6	0.132235	0.139118	3	0.005836
3742	643	1	0.029096	0.036348	4	0.000000
3743	644	1	0.055147	0.036348	4	0.000000
3744	645	8	-0.540571	-0.540571	-1	0.001819
3745	646	1	0.359859	0.359859	-1	0.000000
3746						
3747	647	8	-0.540571	-0.540571	-1	0.001819
3748	648	1	0.359859	0.359859	-1	0.000000
3749	649	6	0.090819	0.139118	3	0.005836
3750	650	1	0.035601	0.036348	4	0.000000
3751	651	1	0.068479	0.036348	4	0.000000
3752	652	6	0.011388	-0.010513	6	0.009945
3753	653	1	0.043297	0.061234	7	0.000000
3754	654	1	0.069417	0.061234	7	0.000000
3755	655	8	-0.286114	-0.286114	-1	0.003299
3756	656	6	0.000727	-0.010513	6	0.009945
3757	657	1	0.047995	0.061234	7	0.000000
3758	658	1	0.063336	0.061234	7	0.000000
3759	659	6	0.132235	0.139118	3	0.005836
3760	660	1	0.029096	0.036348	4	0.000000
3761	661	1	0.055147	0.036348	4	0.000000
3762	662	8	-0.540571	-0.540571	-1	0.001819
3763	663	1	0.359859	0.359859	-1	0.000000
3764						
3765	664	8	-0.540571	-0.540571	-1	0.001819
3766	665	1	0.359859	0.359859	-1	0.000000
3767	666	6	0.090819	0.139118	3	0.005836
3768	667	1	0.035601	0.036348	4	0.000000
3769	668	1	0.068479	0.036348	4	0.000000
3770	669	6	0.011388	-0.010513	6	0.009945
3771	670	1	0.043297	0.061234	7	0.000000
3772	671	1	0.069417	0.061234	7	0.000000
3773	672	8	-0.286114	-0.286114	-1	0.003299
3774	673	6	0.000727	-0.010513	6	0.009945
3775	674	1	0.047995	0.061234	7	0.000000
3776	675	1	0.063336	0.061234	7	0.000000
3777	676	6	0.132235	0.139118	3	0.005836

B.3. PEG WITH HYDROXYETHYL TERMINAL, MULTIPLE CONFORMATIONS

3778	677	1	0.029096	0.036348	4	0.000000
3779	678	1	0.055147	0.036348	4	0.000000
3780	679	8	-0.540571	-0.540571	-1	0.001819
3781	680	1	0.359859	0.359859	-1	0.000000
3782						
3783	681	8	-0.540571	-0.540571	-1	0.001819
3784	682	1	0.359859	0.359859	-1	0.000000
3785	683	6	0.090819	0.139118	3	0.005836
3786	684	1	0.035601	0.036348	4	0.000000
3787	685	1	0.068479	0.036348	4	0.000000
3788	686	6	0.011388	-0.010513	6	0.009945
3789	687	1	0.043297	0.061234	7	0.000000
3790	688	1	0.069417	0.061234	7	0.000000
3791	689	8	-0.286114	-0.286114	-1	0.003299
3792	690	6	0.000727	-0.010513	6	0.009945
3793	691	1	0.047995	0.061234	7	0.000000
3794	692	1	0.063336	0.061234	7	0.000000
3795	693	6	0.132235	0.139118	3	0.005836
3796	694	1	0.029096	0.036348	4	0.000000
3797	695	1	0.055147	0.036348	4	0.000000
3798	696	8	-0.540571	-0.540571	-1	0.001819
3799	697	1	0.359859	0.359859	-1	0.000000
3800						
3801	698	8	-0.540571	-0.540571	-1	0.001819
3802	699	1	0.359859	0.359859	-1	0.000000
3803	700	6	0.090819	0.139118	3	0.005836
3804	701	1	0.035601	0.036348	4	0.000000
3805	702	1	0.068479	0.036348	4	0.000000
3806	703	6	0.011388	-0.010513	6	0.009945
3807	704	1	0.043297	0.061234	7	0.000000
3808	705	1	0.069417	0.061234	7	0.000000
3809	706	8	-0.286114	-0.286114	-1	0.003299
3810	707	6	0.000727	-0.010513	6	0.009945
3811	708	1	0.047995	0.061234	7	0.000000
3812	709	1	0.063336	0.061234	7	0.000000
3813	710	6	0.132235	0.139118	3	0.005836
3814	711	1	0.029096	0.036348	4	0.000000
3815	712	1	0.055147	0.036348	4	0.000000
3816	713	8	-0.540571	-0.540571	-1	0.001819
3817	714	1	0.359859	0.359859	-1	0.000000
3818						
3819	715	8	-0.540571	-0.540571	-1	0.001819
3820	716	1	0.359859	0.359859	-1	0.000000
3821	717	6	0.090819	0.139118	3	0.005836
3822	718	1	0.035601	0.036348	4	0.000000

B.3. PEG WITH HYDROXYETHYL TERMINAL, MULTIPLE CONFORMATIONS

3823	719	1	0.068479	0.036348	4	0.000000
3824	720	6	0.011388	-0.010513	6	0.009945
3825	721	1	0.043297	0.061234	7	0.000000
3826	722	1	0.069417	0.061234	7	0.000000
3827	723	8	-0.286114	-0.286114	-1	0.003299
3828	724	6	0.000727	-0.010513	6	0.009945
3829	725	1	0.047995	0.061234	7	0.000000
3830	726	1	0.063336	0.061234	7	0.000000
3831	727	6	0.132235	0.139118	3	0.005836
3832	728	1	0.029096	0.036348	4	0.000000
3833	729	1	0.055147	0.036348	4	0.000000
3834	730	8	-0.540571	-0.540571	-1	0.001819
3835	731	1	0.359859	0.359859	-1	0.000000
3836						
3837	732	8	-0.540571	-0.540571	-1	0.001819
3838	733	1	0.359859	0.359859	-1	0.000000
3839	734	6	0.090819	0.139118	3	0.005836
3840	735	1	0.035601	0.036348	4	0.000000
3841	736	1	0.068479	0.036348	4	0.000000
3842	737	6	0.011388	-0.010513	6	0.009945
3843	738	1	0.043297	0.061234	7	0.000000
3844	739	1	0.069417	0.061234	7	0.000000
3845	740	8	-0.286114	-0.286114	-1	0.003299
3846	741	6	0.000727	-0.010513	6	0.009945
3847	742	1	0.047995	0.061234	7	0.000000
3848	743	1	0.063336	0.061234	7	0.000000
3849	744	6	0.132235	0.139118	3	0.005836
3850	745	1	0.029096	0.036348	4	0.000000
3851	746	1	0.055147	0.036348	4	0.000000
3852	747	8	-0.540571	-0.540571	-1	0.001819
3853	748	1	0.359859	0.359859	-1	0.000000
3854						
3855	749	8	-0.540571	-0.540571	-1	0.001819
3856	750	1	0.359859	0.359859	-1	0.000000
3857	751	6	0.090819	0.139118	3	0.005836
3858	752	1	0.035601	0.036348	4	0.000000
3859	753	1	0.068479	0.036348	4	0.000000
3860	754	6	0.011388	-0.010513	6	0.009945
3861	755	1	0.043297	0.061234	7	0.000000
3862	756	1	0.069417	0.061234	7	0.000000
3863	757	8	-0.286114	-0.286114	-1	0.003299
3864	758	6	0.000727	-0.010513	6	0.009945
3865	759	1	0.047995	0.061234	7	0.000000
3866	760	1	0.063336	0.061234	7	0.000000
3867	761	6	0.132235	0.139118	3	0.005836

B.3. PEG WITH HYDROXYETHYL TERMINAL, MULTIPLE CONFORMATIONS

3868	762	1	0.029096	0.036348	4	0.000000
3869	763	1	0.055147	0.036348	4	0.000000
3870	764	8	-0.540571	-0.540571	-1	0.001819
3871	765	1	0.359859	0.359859	-1	0.000000
3872						
3873	766	8	-0.540571	-0.540571	-1	0.001819
3874	767	1	0.359859	0.359859	-1	0.000000
3875	768	6	0.090819	0.139118	3	0.005836
3876	769	1	0.035601	0.036348	4	0.000000
3877	770	1	0.068479	0.036348	4	0.000000
3878	771	6	0.011388	-0.010513	6	0.009945
3879	772	1	0.043297	0.061234	7	0.000000
3880	773	1	0.069417	0.061234	7	0.000000
3881	774	8	-0.286114	-0.286114	-1	0.003299
3882	775	6	0.000727	-0.010513	6	0.009945
3883	776	1	0.047995	0.061234	7	0.000000
3884	777	1	0.063336	0.061234	7	0.000000
3885	778	6	0.132235	0.139118	3	0.005836
3886	779	1	0.029096	0.036348	4	0.000000
3887	780	1	0.055147	0.036348	4	0.000000
3888	781	8	-0.540571	-0.540571	-1	0.001819
3889	782	1	0.359859	0.359859	-1	0.000000

3890

3891 Sum over the calculated charges: -0.000

3892

3893 Statistics of the fitting:

3894 The initial **sum** of squares (ssvpot) 9.136

3895 The residual **sum** of squares (chipot) 0.319

3896 The std err of estimate (sqrt(chipot/N)) 0.00293

3897 ESP relative RMS (SQRT(chipot/ssvpot)) 0.18693

3898 The Pearson correlation coefficient (r2) 0.96548

3899

3900 Center of Mass (a.u.):

3901	#MEP	X	Y	Z
3902	1	2.10084	0.36011	-0.47027
3903	2	2.60441	0.68375	0.47027
3904	3	2.19529	0.16307	-0.52164
3905	4	2.76843	0.52490	0.52164
3906	5	2.19524	0.16306	-0.52170
3907	6	2.76845	0.52493	0.52170
3908	7	2.19529	0.16305	-0.52168
3909	8	2.76845	0.52489	0.52168
3910	9	2.19529	0.16308	-0.52163
3911	10	2.76842	0.52490	0.52163
3912	11	2.03978	0.19351	-0.50206

B.3. PEG WITH HYDROXYETHYL TERMINAL, MULTIPLE CONFORMATIONS

```
3913 12 2.79012 0.66614 0.50206
3914 13 1.60287 0.25389 -0.97223
3915 14 2.92374 1.08732 0.97223
3916 15 1.61049 0.26767 -0.98910
3917 16 2.90235 1.08853 0.98910
3918 17 1.61048 0.26767 -0.98909
3919 18 2.90235 1.08854 0.98909
3920 19 1.61502 0.25239 -0.99994
3921 20 2.91807 1.07559 0.99994
3922 21 1.88907 0.91761 -2.06707
3923 22 2.23132 1.11840 2.06707
3924 23 1.88906 0.91762 -2.06706
3925 24 2.23131 1.11842 2.06706
3926 25 1.88906 0.91764 -2.06707
3927 26 2.23130 1.11843 2.06707
3928 27 1.88906 0.91760 -2.06706
3929 28 2.23134 1.11840 2.06706
3930 29 2.71741 -0.26663 0.09590
3931 30 2.90794 -0.15287 -0.09590
3932 31 2.81917 -0.20027 -0.00006
3933 32 2.81915 -0.20028 0.00006
3934 33 2.82451 -0.20803 0.75642
3935 34 2.82453 -0.20803 -0.75642
3936 35 1.87223 0.86154 2.04528
3937 36 2.31314 1.11340 -2.04528
3938 37 2.82451 -0.20802 0.75644
3939 38 2.82450 -0.20803 -0.75644
3940 39 2.82451 -0.20805 0.75640
3941 40 2.82453 -0.20804 -0.75640
3942 41 2.82450 -0.20800 0.75653
3943 42 2.82449 -0.20801 -0.75653
3944 43 2.82452 -0.20803 0.75645
3945 44 2.82451 -0.20803 -0.75645
3946 45 2.82451 -0.20804 0.75644
3947 46 2.82451 -0.20804 -0.75644
3948
3949 Dipole moments (Debye) computed:
3950 -with respect to the origin of coordinates (ooc)
3951 -with respect to the center of mass (com)
3952 #MEP      D      Dx      Dy      Dz
3953 1 ooc    3.90866  -0.50085  3.42197  -1.82124
3954 1 com    3.90866  -0.50085  3.42197  -1.82124
3955
3956 2 ooc    3.90866  -2.87235  1.92622  1.82124
3957 2 com    3.90866  -2.87235  1.92622  1.82124
```

B.3. PEG WITH HYDROXYETHYL TERMINAL, MULTIPLE CONFORMATIONS

3958					
3959	3 ooc	1.60120	-0.92151	1.30476	-0.11071
3960	3 com	1.60120	-0.92151	1.30476	-0.11071
3961					
3962	4 ooc	1.60120	-0.78495	1.39120	0.11071
3963	4 com	1.60120	-0.78495	1.39120	0.11071
3964					
3965	5 ooc	1.60119	-0.92144	1.30481	-0.11060
3966	5 com	1.60119	-0.92144	1.30481	-0.11060
3967					
3968	6 ooc	1.60119	-0.78502	1.39116	0.11060
3969	6 com	1.60119	-0.78502	1.39116	0.11060
3970					
3971	7 ooc	1.60127	-0.92149	1.30487	-0.11061
3972	7 com	1.60127	-0.92149	1.30487	-0.11061
3973					
3974	8 ooc	1.60127	-0.78505	1.39123	0.11061
3975	8 com	1.60127	-0.78505	1.39123	0.11061
3976					
3977	9 ooc	1.60119	-0.92151	1.30475	-0.11072
3978	9 com	1.60119	-0.92151	1.30475	-0.11072
3979					
3980	10 ooc	1.60119	-0.78493	1.39120	0.11072
3981	10 com	1.60119	-0.78493	1.39120	0.11072
3982					
3983	11 ooc	2.69491	-2.58171	-0.77134	0.04888
3984	11 com	2.69491	-2.58171	-0.77134	0.04888
3985					
3986	12 ooc	2.69491	1.78506	2.01835	-0.04888
3987	12 com	2.69491	1.78506	2.01835	-0.04888
3988					
3989	13 ooc	1.61957	-1.21993	0.99114	-0.39040
3990	13 com	1.61957	-1.21993	0.99114	-0.39040
3991					
3992	14 ooc	1.61957	-0.38564	1.52377	0.39040
3993	14 com	1.61957	-0.38564	1.52377	0.39040
3994					
3995	15 ooc	2.01573	-1.20776	-1.08718	1.19269
3996	15 com	2.01573	-1.20776	-1.08718	1.19269
3997					
3998	16 ooc	2.01573	1.49146	0.64515	-1.19269
3999	16 com	2.01573	1.49146	0.64515	-1.19269
4000					
4001	17 ooc	2.01583	-1.20776	-1.08717	1.19288
4002	17 com	2.01583	-1.20776	-1.08717	1.19288

B.3. PEG WITH HYDROXYETHYL TERMINAL, MULTIPLE CONFORMATIONS

4003						
4004	18	ooc	2.01583	1.49144	0.64515	-1.19288
4005	18	com	2.01583	1.49144	0.64515	-1.19288
4006						
4007	19	ooc	3.07315	-1.25050	1.08139	2.59058
4008	19	com	3.07315	-1.25050	1.08139	2.59058
4009						
4010	20	ooc	3.07315	-0.45744	1.58868	-2.59058
4011	20	com	3.07315	-0.45744	1.58868	-2.59058
4012						
4013	21	ooc	4.20502	-3.46745	1.43040	1.90079
4014	21	com	4.20502	-3.46745	1.43040	1.90079
4015						
4016	22	ooc	4.20502	0.29804	3.73903	-1.90079
4017	22	com	4.20502	0.29804	3.73903	-1.90079
4018						
4019	23	ooc	4.20496	-3.46737	1.43035	1.90083
4020	23	com	4.20496	-3.46737	1.43035	1.90083
4021						
4022	24	ooc	4.20496	0.29804	3.73895	-1.90083
4023	24	com	4.20496	0.29804	3.73895	-1.90083
4024						
4025	25	ooc	4.20497	-3.46738	1.43036	1.90083
4026	25	com	4.20497	-3.46738	1.43036	1.90083
4027						
4028	26	ooc	4.20497	0.29805	3.73896	-1.90083
4029	26	com	4.20497	0.29805	3.73896	-1.90083
4030						
4031	27	ooc	4.20496	-3.46739	1.43034	1.90080
4032	27	com	4.20496	-3.46739	1.43034	1.90080
4033						
4034	28	ooc	4.20496	0.29805	3.73896	-1.90080
4035	28	com	4.20496	0.29805	3.73896	-1.90080
4036						
4037	29	ooc	3.82911	-3.01243	1.91372	-1.38746
4038	29	com	3.82911	-3.01243	1.91372	-1.38746
4039						
4040	30	ooc	3.82911	-0.52762	3.52968	1.38746
4041	30	com	3.82911	-0.52762	3.52968	1.38746
4042						
4043	31	ooc	1.48959	-0.80834	1.25118	0.00004
4044	31	com	1.48959	-0.80834	1.25118	0.00004
4045						
4046	32	ooc	1.48959	-0.80830	1.25121	-0.00004
4047	32	com	1.48959	-0.80830	1.25121	-0.00004

B.3. PEG WITH HYDROXYETHYL TERMINAL, MULTIPLE CONFORMATIONS

4048					
4049	33	ooc	2.63084	-0.77332	1.18254 -2.21922
4050	33	com	2.63084	-0.77332	1.18254 -2.21922
4051					
4052	34	ooc	2.63084	-0.77319	1.18262 2.21922
4053	34	com	2.63084	-0.77319	1.18262 2.21922
4054					
4055	35	ooc	2.46612	-1.63900	0.30879 -1.81662
4056	35	com	2.46612	-1.63900	0.30879 -1.81662
4057					
4058	36	ooc	2.46612	0.49906	1.59141 1.81662
4059	36	com	2.46612	0.49906	1.59141 1.81662
4060					
4061	37	ooc	2.63078	-0.77317	1.18240 -2.21926
4062	37	com	2.63078	-0.77317	1.18240 -2.21926
4063					
4064	38	ooc	2.63078	-0.77313	1.18243 2.21926
4065	38	com	2.63078	-0.77313	1.18243 2.21926
4066					
4067	39	ooc	2.63082	-0.77326	1.18257 -2.21919
4068	39	com	2.63082	-0.77326	1.18257 -2.21919
4069					
4070	40	ooc	2.63082	-0.77324	1.18258 2.21919
4071	40	com	2.63082	-0.77324	1.18258 2.21919
4072					
4073	41	ooc	2.63083	-0.77320	1.18249 -2.21927
4074	41	com	2.63083	-0.77320	1.18249 -2.21927
4075					
4076	42	ooc	2.63083	-0.77319	1.18250 2.21927
4077	42	com	2.63083	-0.77319	1.18250 2.21927
4078					
4079	43	ooc	2.63084	-0.77323	1.18252 -2.21926
4080	43	com	2.63084	-0.77323	1.18252 -2.21926
4081					
4082	44	ooc	2.63084	-0.77321	1.18253 2.21926
4083	44	com	2.63084	-0.77321	1.18253 2.21926
4084					
4085	45	ooc	2.63083	-0.77324	1.18253 -2.21923
4086	45	com	2.63083	-0.77324	1.18253 -2.21923
4087					
4088	46	ooc	2.63083	-0.77321	1.18254 2.21923
4089	46	com	2.63083	-0.77321	1.18254 2.21923
4090					
4091	Traceless Quadrupole moments (Buckingham) computed:				
4092	-with respect to the origin of coordinates (ooc)				

B.3. PEG WITH HYDROXYETHYL TERMINAL, MULTIPLE CONFORMATIONS

4093 -with respect to the center of mass (com)
4094 #MEP X Y Z
4095 1 ooc X -10.17280
4096 Y 9.32337 8.91971
4097 Z 7.21166 -3.90688 1.25309
4098 1 com X -5.73492
4099 Y -1.80307 6.10414
4100 Z 12.91184 -0.31095 -0.36922
4101
4102 2 ooc X -15.63020
4103 Y -0.89035 7.66311
4104 Z 10.66763 15.20111 7.96709
4105 2 com X 2.50479
4106 Y -5.73662 -2.13556
4107 Z 5.28199 11.78614 -0.36922
4108
4109 3 ooc X -2.53130
4110 Y -7.47020 11.38053
4111 Z 23.05689 17.27343 -8.84923
4112 3 com X 2.03710
4113 Y -11.77886 8.85023
4114 Z 22.67962 18.38259 -10.88732
4115
4116 4 ooc X -6.94212
4117 Y -4.64006 16.18017
4118 Z 26.15598 13.87655 -9.23805
4119 4 com X -1.50837
4120 Y -10.10026 12.39569
4121 Z 26.31942 12.63221 -10.88732
4122
4123 5 ooc X -2.52989
4124 Y -7.47054 11.37918
4125 Z 23.05662 17.27389 -8.84929
4126 5 com X 2.03800
4127 Y -11.77931 8.84906
4128 Z 22.67891 18.38318 -10.88706
4129
4130 6 ooc X -6.94366
4131 Y -4.63979 16.18137
4132 Z 26.15560 13.87563 -9.23771
4133 6 com X -1.50953
4134 Y -10.09974 12.39660
4135 Z 26.31968 12.63128 -10.88707
4136
4137 7 ooc X -2.53068

B.3. PEG WITH HYDROXYETHYL TERMINAL, MULTIPLE CONFORMATIONS

4138		Y	-7.47011	11.37952	
4139		Z	23.05677	17.27339	-8.84884
4140	7	com X	2.03755		
4141		Y	-11.77918	8.84926	
4142		Z	22.67909	18.38270	-10.88681
4143					
4144	8	ooc X	-6.94364		
4145		Y	-4.63967	16.18096	
4146		Z	26.15523	13.87611	-9.23732
4147	8	com X	-1.50928		
4148		Y	-10.09997	12.39609	
4149		Z	26.31927	12.63174	-10.88681
4150					
4151	9	ooc X	-2.53144		
4152		Y	-7.47016	11.38081	
4153		Z	23.05701	17.27336	-8.84937
4154	9	com X	2.03697		
4155		Y	-11.77876	8.85051	
4156		Z	22.67978	18.38248	-10.88748
4157					
4158	10	ooc X	-6.94171		
4159		Y	-4.64019	16.17996	
4160		Z	26.15602	13.87672	-9.23825
4161	10	com X	-1.50808		
4162		Y	-10.10037	12.39557	
4163		Z	26.31940	12.63240	-10.88748
4164					
4165	11	ooc X	-13.86098		
4166		Y	3.35645	30.58090	
4167		Z	15.53735	6.34346	-16.71993
4168	11	com X	-2.89807		
4169		Y	6.64732	25.29744	
4170		Z	13.32134	5.71365	-22.39938
4171					
4172	12	ooc X	34.53180		
4173		Y	4.37262	-5.38635	
4174		Z	11.99000	11.24280	-29.14545
4175	12	com X	25.38644		
4176		Y	-6.45520	-2.98708	
4177		Z	10.78376	9.68580	-22.39937
4178					
4179	13	ooc X	-13.02510		
4180		Y	-8.06725	14.33749	
4181		Z	26.87810	14.19440	-1.31239
4182	13	com X	-8.21810		

B.3. PEG WITH HYDROXYETHYL TERMINAL, MULTIPLE CONFORMATIONS

4183		Y	-10.09760	12.13706	
4184		Z	25.98863	15.88152	-3.91897
4185					
4186	14	ooc X	-3.72068		
4187		Y	-7.88463	7.39642	
4188		Z	26.56131	19.91630	-3.67575
4189	14	com X	0.82115		
4190		Y	-14.29157	3.09782	
4191		Z	25.34445	16.89056	-3.91897
4192					
4193	15	ooc X	-20.31001		
4194		Y	4.98306	30.25000	
4195		Z	16.06261	7.21350	-9.93998
4196	15	com X	-17.74934		
4197		Y	8.27589	27.55883	
4198		Z	11.11679	4.99956	-9.80949
4199					
4200	16	ooc X	35.63349		
4201		Y	-6.20351	-18.00234	
4202		Z	6.02229	6.97591	-17.63115
4203	16	com X	25.96551		
4204		Y	-11.75343	-16.15601	
4205		Z	9.17578	8.02395	-9.80950
4206					
4207	17	ooc X	-20.31029		
4208		Y	4.98281	30.25002	
4209		Z	16.06157	7.21226	-9.93974
4210	17	com X	-17.74982		
4211		Y	8.27559	27.55870	
4212		Z	11.11530	4.99828	-9.80888
4213					
4214	18	ooc X	35.63320		
4215		Y	-6.20361	-18.00233	
4216		Z	6.01955	6.97476	-17.63087
4217	18	com X	25.96516		
4218		Y	-11.75356	-16.15627	
4219		Z	9.17396	8.02315	-9.80889
4220					
4221	19	ooc X	-14.17167		
4222		Y	-9.02599	13.58768	
4223		Z	6.42660	2.28809	0.58400
4224	19	com X	-12.34952		
4225		Y	-11.29749	8.13093	
4226		Z	-2.20045	2.96673	4.21860
4227					

B.3. PEG WITH HYDROXYETHYL TERMINAL, MULTIPLE CONFORMATIONS

4228	20 ooc X	-5.96236		
4229	Y	-8.54270	7.62267	
4230	Z	-10.95630	-5.14314	-1.66032
4231	20 com X	-4.06997		
4232	Y	-15.12121	-0.14862	
4233	Z	1.77078	-3.24159	4.21859
4234				
4235	21 ooc X	-5.66039		
4236	Y	-0.76221	16.94400	
4237	Z	24.55729	0.62901	-11.28361
4238	21 com X	5.43538		
4239	Y	-0.00075	3.07491	
4240	Z	7.47837	2.55397	-8.51029
4241				
4242	22 ooc X	4.70019		
4243	Y	14.72767	17.25635	
4244	Z	-0.08683	14.40123	-21.95654
4245	22 com X	3.55997		
4246	Y	0.95377	4.95031	
4247	Z	5.66827	5.50630	-8.51028
4248				
4249	23 ooc X	-5.65948		
4250	Y	-0.76250	16.94337	
4251	Z	24.55690	0.62961	-11.28390
4252	23 com X	5.43581		
4253	Y	-0.00089	3.07446	
4254	Z	7.47818	2.55429	-8.51027
4255				
4256	24 ooc X	4.69990		
4257	Y	14.72762	17.25675	
4258	Z	-0.08677	14.40051	-21.95665
4259	24 com X	3.55958		
4260	Y	0.95404	4.95069	
4261	Z	5.66846	5.50602	-8.51027
4262				
4263	25 ooc X	-5.65984		
4264	Y	-0.76273	16.94388	
4265	Z	24.55680	0.62952	-11.28404
4266	25 com X	5.43549		
4267	Y	-0.00107	3.07484	
4268	Z	7.47799	2.55419	-8.51032
4269				
4270	26 ooc X	4.70001		
4271	Y	14.72723	17.25680	
4272	Z	-0.08688	14.40039	-21.95681

B.3. PEG WITH HYDROXYETHYL TERMINAL, MULTIPLE CONFORMATIONS

4273	26	com	X	3.55967			
4274			Y	0.95365	4.95065		
4275			Z	5.66832	5.50587	-8.51032	
4276							
4277	27	ooc	X	-5.65953			
4278			Y	-0.76228	16.94301		
4279			Z	24.55712	0.62950	-11.28349	
4280	27	com	X	5.43590			
4281			Y	-0.00080	3.07420		
4282			Z	7.47841	2.55427	-8.51011	
4283							
4284	28	ooc	X	4.69986			
4285			Y	14.72802	17.25646		
4286			Z	-0.08663	14.40084	-21.95632	
4287	28	com	X	3.55947			
4288			Y	0.95424	4.95064		
4289			Z	5.66853	5.50622	-8.51011	
4290							
4291	29	ooc	X	-13.62223			
4292			Y	4.13358	0.96711		
4293			Z	-13.86029	-9.42668	12.65511	
4294	29	com	X	3.02434			
4295			Y	-5.39726	-6.75737		
4296			Z	-7.41617	-10.30531	3.73304	
4297							
4298	30	ooc	X	-11.68585			
4299			Y	16.42673	6.03958		
4300			Z	-5.94194	-3.47380	5.64627	
4301	30	com	X	-9.15012			
4302			Y	0.00411	5.41710		
4303			Z	-12.42741	-2.59970	3.73303	
4304							
4305	31	ooc	X	-8.77148			
4306			Y	-6.97707	9.24399		
4307			Z	-24.33867	-15.72368	-0.47252	
4308	31	com	X	-4.21301			
4309			Y	-12.83376	7.36254		
4310			Z	-24.33892	-15.72356	-3.14954	
4311							
4312	32	ooc	X	-8.77008			
4313			Y	-6.97747	9.24271		
4314			Z	-24.33888	-15.72386	-0.47263	
4315	32	com	X	-4.21191			
4316			Y	-12.83425	7.36145		
4317			Z	-24.33863	-15.72399	-3.14954	

B.3. PEG WITH HYDROXYETHYL TERMINAL, MULTIPLE CONFORMATIONS

4318					
4319	33 ooc X	-10.95985			
4320	Y	-9.97125	8.79373		
4321	Z	-9.91576	0.68055	2.16612	
4322	33 com X	-8.37345			
4323	Y	-15.52914	5.22613		
4324	Z	0.96383	-1.47241	3.14731	
4325					
4326	34 ooc X	-10.95564			
4327	Y	-9.97239	8.78986		
4328	Z	9.91720	-0.67967	2.16578	
4329	34 com X	-8.36994			
4330	Y	-15.53065	5.22263		
4331	Z	-0.96234	1.47338	3.14730	
4332					
4333	35 ooc X	16.20878			
4334	Y	1.48682	-1.58369		
4335	Z	-12.49419	-5.95001	-14.62509	
4336	35 com X	19.05329			
4337	Y	2.81072	-9.32674		
4338	Z	-1.77307	-4.46800	-9.72654	
4339					
4340	36 ooc X	3.79665			
4341	Y	20.07759	16.89155		
4342	Z	0.27389	-1.41747	-20.68820	
4343	36 com X	-0.70392			
4344	Y	13.35152	10.43046		
4345	Z	-4.77666	0.53880	-9.72655	
4346					
4347	37 ooc X	-10.95751			
4348	Y	-9.97307	8.79234		
4349	Z	-9.91619	0.67965	2.16517	
4350	37 com X	-8.37203			
4351	Y	-15.53031	5.22502		
4352	Z	0.96345	-1.47318	3.14701	
4353					
4354	38 ooc X	-10.95689			
4355	Y	-9.97312	8.79184		
4356	Z	9.91638	-0.67953	2.16506	
4357	38 com X	-8.37167			
4358	Y	-15.53047	5.22466		
4359	Z	-0.96319	1.47335	3.14701	
4360					
4361	39 ooc X	-10.95818			
4362	Y	-9.97213	8.79178		

B.3. PEG WITH HYDROXYETHYL TERMINAL, MULTIPLE CONFORMATIONS

4363		Z	-9.91653	0.67994	2.16640
4364	39	com X	-8.37206		
4365		Y	-15.53018	5.22447	
4366		Z	0.96289	-1.47307	3.14759
4367					
4368	40	ooc X	-10.95806		
4369		Y	-9.97210	8.79170	
4370		Z	9.91614	-0.68019	2.16636
4371	40	com X	-8.37200		
4372		Y	-15.53021	5.22440	
4373		Z	-0.96332	1.47279	3.14760
4374					
4375	41	ooc X	-10.95680		
4376		Y	-9.97172	8.79222	
4377		Z	-9.91614	0.67999	2.16458
4378	41	com X	-8.37134		
4379		Y	-15.52931	5.22460	
4380		Z	0.96364	-1.47301	3.14674
4381					
4382	42	ooc X	-10.95655		
4383		Y	-9.97179	8.79197	
4384		Z	9.91676	-0.67959	2.16458
4385	42	com X	-8.37114		
4386		Y	-15.52939	5.22439	
4387		Z	-0.96296	1.47345	3.14676
4388					
4389	43	ooc X	-10.95706		
4390		Y	-9.97210	8.79183	
4391		Z	-9.91678	0.67990	2.16523
4392	43	com X	-8.37125		
4393		Y	-15.52988	5.22438	
4394		Z	0.96294	-1.47309	3.14687
4395					
4396	44	ooc X	-10.95735		
4397		Y	-9.97189	8.79218	
4398		Z	9.91636	-0.68017	2.16517
4399	44	com X	-8.37169		
4400		Y	-15.52971	5.22481	
4401		Z	-0.96332	1.47285	3.14687
4402					
4403	45	ooc X	-10.95803		
4404		Y	-9.97181	8.79246	
4405		Z	-9.91627	0.68013	2.16557
4406	45	com X	-8.37216		
4407		Y	-15.52964	5.22505	

B.3. PEG WITH HYDROXYETHYL TERMINAL, MULTIPLE CONFORMATIONS

```
4408          Z    0.96333  -1.47287   3.14711
4409
4410    46 ooc X -10.95693
4411          Y   -9.97216   8.79142
4412          Z    9.91662  -0.67991   2.16551
4413    46 com X  -8.37119
4414          Y  -15.53006   5.22408
4415          Z   -0.96296   1.47311   3.14711
4416
4417 Traceless Quadrupole moments (Buckingham) in principal axes computed:
4418 -with respect to the origin of coordinates (ooc)
4419 -with respect to the center of mass (com)
4420 #MEP          X          Y          Z
4421    1 ooc X   12.80610
4422          Y    0.00000   4.71039
4423          Z    0.00000  -0.00000  -17.51649
4424    1 com X   10.56694
4425          Y   -0.00000   5.73747
4426          Z    0.00000   0.00000  -16.30441
4427
4428    2 ooc X   24.29523
4429          Y   -0.00000  -2.86205
4430          Z   -0.00000   0.00000  -21.43318
4431    2 com X   10.56695
4432          Y   -0.00000   5.73747
4433          Z    0.00000   0.00000  -16.30443
4434
4435    3 ooc X   23.28277
4436          Y    0.00000  12.57320
4437          Z   -0.00000   0.00000  -35.85598
4438    3 com X   20.57720
4439          Y    0.00000  17.53163
4440          Z   -0.00000   0.00000  -38.10883
4441
4442    4 ooc X   24.88040
4443          Y    0.00000  12.69174
4444          Z    0.00000   0.00000  -37.57214
4445    4 com X   20.57720
4446          Y    0.00000  17.53163
4447          Z    0.00000   0.00000  -38.10883
4448
4449    5 ooc X   23.28240
4450          Y    0.00000  12.57345
4451          Z   -0.00000  -0.00000  -35.85585
4452    5 com X   20.57689
```

B.3. PEG WITH HYDROXYETHYL TERMINAL, MULTIPLE CONFORMATIONS

4453		Y	0.00000	17.53177	
4454		Z	0.00000	0.00000	-38.10865
4455					
4456	6	ooc X	24.88014		
4457		Y	0.00000	12.69164	
4458		Z	0.00000	0.00000	-37.57179
4459	6	com X	20.57689		
4460		Y	0.00000	17.53177	
4461		Z	0.00000	0.00000	-38.10866
4462					
4463	7	ooc X	23.28249		
4464		Y	0.00000	12.57303	
4465		Z	-0.00000	0.00000	-35.85553
4466	7	com X	20.57676		
4467		Y	0.00000	17.53163	
4468		Z	-0.00000	0.00000	-38.10839
4469					
4470	8	ooc X	24.88037		
4471		Y	0.00000	12.69101	
4472		Z	0.00000	0.00000	-37.57138
4473	8	com X	20.57676		
4474		Y	0.00000	17.53164	
4475		Z	0.00000	0.00000	-38.10840
4476					
4477	9	ooc X	23.28284		
4478		Y	0.00000	12.57326	
4479		Z	-0.00000	-0.00000	-35.85611
4480	9	com X	20.57727		
4481		Y	0.00000	17.53165	
4482		Z	0.00000	0.00000	-38.10892
4483					
4484	10	ooc X	24.88037		
4485		Y	0.00000	12.69185	
4486		Z	0.00000	0.00000	-37.57222
4487	10	com X	20.57727		
4488		Y	-0.00000	17.53165	
4489		Z	0.00000	0.00000	-38.10892
4490					
4491	11	ooc X	32.10917		
4492		Y	0.00000	-1.11797	
4493		Z	-0.00000	0.00000	-30.99120
4494	11	com X	28.33442		
4495		Y	0.00000	0.90618	
4496		Z	0.00000	0.00000	-29.24060
4497					

B.3. PEG WITH HYDROXYETHYL TERMINAL, MULTIPLE CONFORMATIONS

4498	12 ooc X	37.67503		
4499	Y	0.00000	-2.70736	
4500	Z	-0.00000	0.00000	-34.96768
4501	12 com X	28.33441		
4502	Y	-0.00000	0.90619	
4503	Z	0.00000	0.00000	-29.24061
4504				
4505	13 ooc X	25.34940		
4506	Y	-0.00000	13.69800	
4507	Z	0.00000	-0.00000	-39.04740
4508	13 com X	23.96405		
4509	Y	-0.00000	14.73855	
4510	Z	-0.00000	-0.00000	-38.70259
4511				
4512	14 ooc X	28.03776		
4513	Y	-0.00000	10.79590	
4514	Z	0.00000	-0.00000	-38.83367
4515	14 com X	23.96405		
4516	Y	-0.00000	14.73855	
4517	Z	0.00000	0.00000	-38.70260
4518				
4519	15 ooc X	32.73059		
4520	Y	0.00000	-0.72606	
4521	Z	0.00000	-0.00000	-32.00453
4522	15 com X	30.26097		
4523	Y	-0.00000	-4.37635	
4524	Z	0.00000	0.00000	-25.88462
4525				
4526	16 ooc X	36.84618		
4527	Y	-0.00000	-10.83837	
4528	Z	0.00000	-0.00000	-26.00780
4529	16 com X	30.26098		
4530	Y	-0.00000	-4.37635	
4531	Z	0.00000	0.00000	-25.88463
4532				
4533	17 ooc X	32.72994		
4534	Y	0.00000	-0.72633	
4535	Z	0.00000	0.00000	-32.00362
4536	17 com X	30.26018		
4537	Y	-0.00000	-4.37670	
4538	Z	0.00000	0.00000	-25.88348
4539				
4540	18 ooc X	36.84541		
4541	Y	-0.00000	-10.83937	
4542	Z	-0.00000	-0.00000	-26.00604

B.3. PEG WITH HYDROXYETHYL TERMINAL, MULTIPLE CONFORMATIONS

4543	18	com	X	30.26017			
4544			Y	-0.00000	-4.37672		
4545			Z	0.00000	0.00000	-25.88345	
4546							
4547	19	ooc	X	16.27378			
4548			Y	0.00000	2.92110		
4549			Z	0.00000	0.00000	-19.19488	
4550	19	com	X	14.41490			
4551			Y	0.00000	2.97314		
4552			Z	-0.00000	0.00000	-17.38804	
4553							
4554	20	ooc	X	11.74666			
4555			Y	-0.00000	6.94026		
4556			Z	-0.00000	0.00000	-18.68692	
4557	20	com	X	14.41490			
4558			Y	-0.00000	2.97313		
4559			Z	-0.00000	-0.00000	-17.38803	
4560							
4561	21	ooc	X	16.99314			
4562			Y	-0.00000	16.21560		
4563			Z	-0.00000	0.00000	-33.20874	
4564	21	com	X	8.87453			
4565			Y	0.00000	3.24990		
4566			Z	-0.00000	0.00000	-12.12443	
4567							
4568	22	ooc	X	29.85417			
4569			Y	0.00000	-2.40370		
4570			Z	-0.00000	0.00000	-27.45047	
4571	22	com	X	8.87452			
4572			Y	0.00000	3.24990		
4573			Z	-0.00000	0.00000	-12.12442	
4574							
4575	23	ooc	X	16.99250			
4576			Y	-0.00000	16.21564		
4577			Z	-0.00000	-0.00000	-33.20814	
4578	23	com	X	8.87472			
4579			Y	0.00000	3.24961		
4580			Z	0.00000	0.00000	-12.12433	
4581							
4582	24	ooc	X	29.85406			
4583			Y	-0.00000	-2.40403		
4584			Z	-0.00000	0.00000	-27.45003	
4585	24	com	X	8.87473			
4586			Y	0.00000	3.24961		
4587			Z	-0.00000	0.00000	-12.12433	

B.3. PEG WITH HYDROXYETHYL TERMINAL, MULTIPLE CONFORMATIONS

4588				
4589	25 ooc X	16.99306		
4590	Y	-0.00000	16.21521	
4591	Z	-0.00000	0.00000	-33.20828
4592	25 com X	8.87426		
4593	Y	0.00000	3.25002	
4594	Z	0.00000	0.00000	-12.12428
4595				
4596	26 ooc X	29.85372		
4597	Y	-0.00000	-2.40365	
4598	Z	-0.00000	0.00000	-27.45007
4599	26 com X	8.87426		
4600	Y	0.00000	3.25002	
4601	Z	-0.00000	-0.00000	-12.12429
4602				
4603	27 ooc X	16.99213		
4604	Y	-0.00000	16.21602	
4605	Z	-0.00000	0.00000	-33.20814
4606	27 com X	8.87502		
4607	Y	0.00000	3.24932	
4608	Z	-0.00000	0.00000	-12.12434
4609				
4610	28 ooc X	29.85436		
4611	Y	-0.00000	-2.40435	
4612	Z	-0.00000	-0.00000	-27.45001
4613	28 com X	8.87501		
4614	Y	0.00000	3.24931	
4615	Z	-0.00000	0.00000	-12.12433
4616				
4617	29 ooc X	23.34807		
4618	Y	-0.00000	-3.76624	
4619	Z	0.00000	0.00000	-19.58183
4620	29 com X	12.04248		
4621	Y	-0.00000	4.74610	
4622	Z	0.00000	-0.00000	-16.78858
4623				
4624	30 ooc X	18.68799		
4625	Y	0.00000	3.21541	
4626	Z	-0.00000	-0.00000	-21.90340
4627	30 com X	12.04248		
4628	Y	-0.00000	4.74610	
4629	Z	-0.00000	-0.00000	-16.78858
4630				
4631	31 ooc X	25.03159		
4632	Y	0.00000	9.83719	

B.3. PEG WITH HYDROXYETHYL TERMINAL, MULTIPLE CONFORMATIONS

4633		Z	-0.00000	-0.00000	-34.86878
4634	31	com X	21.52450		
4635		Y	-0.00000	15.65325	
4636		Z	-0.00000	-0.00000	-37.17775
4637					
4638	32	ooc X	25.03147		
4639		Y	-0.00000	9.83729	
4640		Z	-0.00000	-0.00000	-34.86876
4641	32	com X	21.52449		
4642		Y	-0.00000	15.65325	
4643		Z	0.00000	-0.00000	-37.17774
4644					
4645	33	ooc X	14.90611		
4646		Y	0.00000	4.06378	
4647		Z	-0.00000	0.00000	-18.96988
4648	33	com X	15.62712		
4649		Y	0.00000	2.89916	
4650		Z	-0.00000	-0.00000	-18.52627
4651					
4652	34	ooc X	14.90530		
4653		Y	0.00000	4.06362	
4654		Z	-0.00000	-0.00000	-18.96892
4655	34	com X	15.62710		
4656		Y	0.00000	2.89915	
4657		Z	-0.00000	0.00000	-18.52625
4658					
4659	35	ooc X	21.15575		
4660		Y	0.00000	-0.69826	
4661		Z	0.00000	-0.00000	-20.45749
4662	35	com X	19.49834		
4663		Y	0.00000	-5.48552	
4664		Z	0.00000	0.00000	-14.01282
4665					
4666	36	ooc X	31.48097		
4667		Y	-0.00000	-10.66350	
4668		Z	0.00000	-0.00000	-20.81747
4669	36	com X	19.49834		
4670		Y	0.00000	-5.48552	
4671		Z	0.00000	-0.00000	-14.01282
4672					
4673	37	ooc X	14.90648		
4674		Y	0.00000	4.06338	
4675		Z	-0.00000	0.00000	-18.96987
4676	37	com X	15.62794		
4677		Y	0.00000	2.89875	

B.3. PEG WITH HYDROXYETHYL TERMINAL, MULTIPLE CONFORMATIONS

4678		Z	-0.00000	-0.00000	-18.52669
4679					
4680	38	ooc X	14.90631		
4681		Y	0.00000	4.06334	
4682		Z	0.00000	-0.00000	-18.96965
4683	38	com X	15.62794		
4684		Y	-0.00000	2.89875	
4685		Z	-0.00000	0.00000	-18.52669
4686					
4687	39	ooc X	14.90581		
4688		Y	0.00000	4.06409	
4689		Z	-0.00000	0.00000	-18.96989
4690	39	com X	15.62733		
4691		Y	-0.00000	2.89942	
4692		Z	0.00000	-0.00000	-18.52676
4693					
4694	40	ooc X	14.90578		
4695		Y	0.00000	4.06370	
4696		Z	0.00000	-0.00000	-18.96948
4697	40	com X	15.62733		
4698		Y	0.00000	2.89943	
4699		Z	0.00000	0.00000	-18.52676
4700					
4701	41	ooc X	14.90568		
4702		Y	0.00000	4.06294	
4703		Z	-0.00000	0.00000	-18.96862
4704	41	com X	15.62693		
4705		Y	0.00000	2.89848	
4706		Z	-0.00000	-0.00000	-18.52541
4707					
4708	42	ooc X	14.90560		
4709		Y	0.00000	4.06341	
4710		Z	0.00000	-0.00000	-18.96901
4711	42	com X	15.62692		
4712		Y	0.00000	2.89849	
4713		Z	-0.00000	0.00000	-18.52541
4714					
4715	43	ooc X	14.90593		
4716		Y	0.00000	4.06347	
4717		Z	-0.00000	0.00000	-18.96940
4718	43	com X	15.62724		
4719		Y	-0.00000	2.89870	
4720		Z	0.00000	-0.00000	-18.52594
4721					
4722	44	ooc X	14.90594		

B.3. PEG WITH HYDROXYETHYL TERMINAL, MULTIPLE CONFORMATIONS

```
4723      Y   0.00000   4.06319
4724      Z   0.00000  -0.00000 -18.96913
4725  44 com X 15.62726
4726      Y   0.00000   2.89870
4727      Z   0.00000   0.00000 -18.52596
4728
4729  45 ooc X 14.90593
4730      Y   0.00000   4.06353
4731      Z  -0.00000   0.00000 -18.96946
4732  45 com X 15.62723
4733      Y  -0.00000   2.89892
4734      Z  -0.00000  -0.00000 -18.52616
4735
4736  46 ooc X 14.90574
4737      Y   0.00000   4.06348
4738      Z  -0.00000  -0.00000 -18.96922
4739  46 com X 15.62723
4740      Y   0.00000   2.89893
4741      Z  -0.00000   0.00000 -18.52616
```

B.3.6 Fitting statistics of a fragment approach

```
1
2 -----
3   Restrained ESP Fit 2.4 q4md-forcefieldtools
4 -----
5   RESP-A1 - RESP input generated by PyRED version SEP-2015
6 -----
7
8
9   inopt      =    0   ioutopt   =    1
10  nmep       =   46   iqopt     =    2
11  ihfree     =    1   irstrnt   =    1
12  iunits     =    0   qwt       = 0.00100000
13
14  multiple-MEP run of 46 MEP
15
16  Reading input for MEP 1 weight: 1.000
17  PEG2 nconf=1 norient=1 nmep=1/46
18
19  Total charge (ich): 0
20  Number of centers: 17
21    1    8   -1
22    2    1   -1
23    3    6    0
```

B.3. PEG WITH HYDROXYETHYL TERMINAL, MULTIPLE CONFORMATIONS

```
24    4    1    0
25    5    1    4
26    6    6    0
27    7    1    0
28    8    1    7
29    9    8   -1
30   10    6    0
31   11    1    0
32   12    1   11
33   13    6    0
34   14    1    0
35   15    1   14
36   16    8   -1
37   17    1   -1
38
39 Reading input for MEP 2 weight: 1.000
40 PEG2 nconf=1 norient=2 nmep=2/46
41
42 Total charge (ich): 0
43 Number of centers: 17
44   18    8   -1
45   19    1   -1
46   20    6    0
47   21    1    0
48   22    1    4
49   23    6    0
50   24    1    0
51   25    1    7
52   26    8   -1
53   27    6    0
54   28    1    0
55   29    1   11
56   30    6    0
57   31    1    0
58   32    1   14
59   33    8   -1
60   34    1   -1
61
62 Reading input for MEP 3 weight: 1.000
63 PEG2 nconf=2 norient=1 nmep=3/46
64
65 Total charge (ich): 0
66 Number of centers: 17
67   35    8   -1
68   36    1   -1
```

B.3. PEG WITH HYDROXYETHYL TERMINAL, MULTIPLE CONFORMATIONS

```
69    37    6    0
70    38    1    0
71    39    1    4
72    40    6    0
73    41    1    0
74    42    1    7
75    43    8   -1
76    44    6    0
77    45    1    0
78    46    1   11
79    47    6    0
80    48    1    0
81    49    1   14
82    50    8   -1
83    51    1   -1
84
85    Reading input for MEP 4 weight: 1.000
86    PEG2 nconf=2 norient=2 nmep=4/46
87
88    Total charge (ich): 0
89    Number of centers: 17
90     52    8   -1
91     53    1   -1
92     54    6    0
93     55    1    0
94     56    1    4
95     57    6    0
96     58    1    0
97     59    1    7
98     60    8   -1
99     61    6    0
100    62    1    0
101    63    1   11
102    64    6    0
103    65    1    0
104    66    1   14
105    67    8   -1
106    68    1   -1
107
108    Reading input for MEP 5 weight: 1.000
109    PEG2 nconf=3 norient=1 nmep=5/46
110
111    Total charge (ich): 0
112    Number of centers: 17
113     69    8   -1
```

B.3. PEG WITH HYDROXYETHYL TERMINAL, MULTIPLE CONFORMATIONS

```
114    70    1   -1
115    71    6    0
116    72    1    0
117    73    1    4
118    74    6    0
119    75    1    0
120    76    1    7
121    77    8   -1
122    78    6    0
123    79    1    0
124    80    1   11
125    81    6    0
126    82    1    0
127    83    1   14
128    84    8   -1
129    85    1   -1
130
131 Reading input for MEP 6 weight: 1.000
132 PEG2 nconf=3 norient=2 nmep=6/46
133
134 Total charge (ich): 0
135 Number of centers: 17
136    86    8   -1
137    87    1   -1
138    88    6    0
139    89    1    0
140    90    1    4
141    91    6    0
142    92    1    0
143    93    1    7
144    94    8   -1
145    95    6    0
146    96    1    0
147    97    1   11
148    98    6    0
149    99    1    0
150   100    1   14
151   101    8   -1
152   102    1   -1
153
154 Reading input for MEP 7 weight: 1.000
155 PEG2 nconf=4 norient=1 nmep=7/46
156
157 Total charge (ich): 0
158 Number of centers: 17
```

B.3. PEG WITH HYDROXYETHYL TERMINAL, MULTIPLE CONFORMATIONS

```
159 103 8 -1
160 104 1 -1
161 105 6 0
162 106 1 0
163 107 1 4
164 108 6 0
165 109 1 0
166 110 1 7
167 111 8 -1
168 112 6 0
169 113 1 0
170 114 1 11
171 115 6 0
172 116 1 0
173 117 1 14
174 118 8 -1
175 119 1 -1
176
177 Reading input for MEP 8 weight: 1.000
178 PEG2 nconf=4 norient=2 nmep=8/46
179
180 Total charge (ich): 0
181 Number of centers: 17
182 120 8 -1
183 121 1 -1
184 122 6 0
185 123 1 0
186 124 1 4
187 125 6 0
188 126 1 0
189 127 1 7
190 128 8 -1
191 129 6 0
192 130 1 0
193 131 1 11
194 132 6 0
195 133 1 0
196 134 1 14
197 135 8 -1
198 136 1 -1
199
200 Reading input for MEP 9 weight: 1.000
201 PEG2 nconf=5 norient=1 nmep=9/46
202
203 Total charge (ich): 0
```

B.3. PEG WITH HYDROXYETHYL TERMINAL, MULTIPLE CONFORMATIONS

```
204 Number of centers: 17
205 137 8 -1
206 138 1 -1
207 139 6 0
208 140 1 0
209 141 1 4
210 142 6 0
211 143 1 0
212 144 1 7
213 145 8 -1
214 146 6 0
215 147 1 0
216 148 1 11
217 149 6 0
218 150 1 0
219 151 1 14
220 152 8 -1
221 153 1 -1
222
223 Reading input for MEP 10 weight: 1.000
224 PEG2 nconf=5 norient=2 nmep=10/46
225
226 Total charge (ich): 0
227 Number of centers: 17
228 154 8 -1
229 155 1 -1
230 156 6 0
231 157 1 0
232 158 1 4
233 159 6 0
234 160 1 0
235 161 1 7
236 162 8 -1
237 163 6 0
238 164 1 0
239 165 1 11
240 166 6 0
241 167 1 0
242 168 1 14
243 169 8 -1
244 170 1 -1
245
246 Reading input for MEP 11 weight: 1.000
247 PEG2 nconf=6 norient=1 nmep=11/46
248
```

B.3. PEG WITH HYDROXYETHYL TERMINAL, MULTIPLE CONFORMATIONS

```
249 Total charge (ich): 0
250 Number of centers: 17
251 171 8 -1
252 172 1 -1
253 173 6 0
254 174 1 0
255 175 1 4
256 176 6 0
257 177 1 0
258 178 1 7
259 179 8 -1
260 180 6 0
261 181 1 0
262 182 1 11
263 183 6 0
264 184 1 0
265 185 1 14
266 186 8 -1
267 187 1 -1
268
269 Reading input for MEP 12 weight: 1.000
270 PEG2 nconf=6 norient=2 nmep=12/46
271
272 Total charge (ich): 0
273 Number of centers: 17
274 188 8 -1
275 189 1 -1
276 190 6 0
277 191 1 0
278 192 1 4
279 193 6 0
280 194 1 0
281 195 1 7
282 196 8 -1
283 197 6 0
284 198 1 0
285 199 1 11
286 200 6 0
287 201 1 0
288 202 1 14
289 203 8 -1
290 204 1 -1
291
292 Reading input for MEP 13 weight: 1.000
293 PEG2 nconf=7 norient=1 nmep=13/46
```

B.3. PEG WITH HYDROXYETHYL TERMINAL, MULTIPLE CONFORMATIONS

```
294
295 Total charge (ich): 0
296 Number of centers: 17
297 205 8 -1
298 206 1 -1
299 207 6 0
300 208 1 0
301 209 1 4
302 210 6 0
303 211 1 0
304 212 1 7
305 213 8 -1
306 214 6 0
307 215 1 0
308 216 1 11
309 217 6 0
310 218 1 0
311 219 1 14
312 220 8 -1
313 221 1 -1
314
315 Reading input for MEP 14 weight: 1.000
316 PEG2 nconf=7 norient=2 nmep=14/46
317
318 Total charge (ich): 0
319 Number of centers: 17
320 222 8 -1
321 223 1 -1
322 224 6 0
323 225 1 0
324 226 1 4
325 227 6 0
326 228 1 0
327 229 1 7
328 230 8 -1
329 231 6 0
330 232 1 0
331 233 1 11
332 234 6 0
333 235 1 0
334 236 1 14
335 237 8 -1
336 238 1 -1
337
338 Reading input for MEP 15 weight: 1.000
```

B.3. PEG WITH HYDROXYETHYL TERMINAL, MULTIPLE CONFORMATIONS

```
339 PEG2 nconf=8 norient=1 nmep=15/46
340
341 Total charge (ich): 0
342 Number of centers: 17
343 239 8 -1
344 240 1 -1
345 241 6 0
346 242 1 0
347 243 1 4
348 244 6 0
349 245 1 0
350 246 1 7
351 247 8 -1
352 248 6 0
353 249 1 0
354 250 1 11
355 251 6 0
356 252 1 0
357 253 1 14
358 254 8 -1
359 255 1 -1
360
361 Reading input for MEP 16 weight: 1.000
362 PEG2 nconf=8 norient=2 nmep=16/46
363
364 Total charge (ich): 0
365 Number of centers: 17
366 256 8 -1
367 257 1 -1
368 258 6 0
369 259 1 0
370 260 1 4
371 261 6 0
372 262 1 0
373 263 1 7
374 264 8 -1
375 265 6 0
376 266 1 0
377 267 1 11
378 268 6 0
379 269 1 0
380 270 1 14
381 271 8 -1
382 272 1 -1
383
```

B.3. PEG WITH HYDROXYETHYL TERMINAL, MULTIPLE CONFORMATIONS

384 Reading **input for** MEP 17 weight: 1.000

385 PEG2 nconf=9 norient=1 nmep=17/46

386

387 Total charge (ich): 0

388 Number of centers: 17

389 273 8 -1

390 274 1 -1

391 275 6 0

392 276 1 0

393 277 1 4

394 278 6 0

395 279 1 0

396 280 1 7

397 281 8 -1

398 282 6 0

399 283 1 0

400 284 1 11

401 285 6 0

402 286 1 0

403 287 1 14

404 288 8 -1

405 289 1 -1

406

407 Reading **input for** MEP 18 weight: 1.000

408 PEG2 nconf=9 norient=2 nmep=18/46

409

410 Total charge (ich): 0

411 Number of centers: 17

412 290 8 -1

413 291 1 -1

414 292 6 0

415 293 1 0

416 294 1 4

417 295 6 0

418 296 1 0

419 297 1 7

420 298 8 -1

421 299 6 0

422 300 1 0

423 301 1 11

424 302 6 0

425 303 1 0

426 304 1 14

427 305 8 -1

428 306 1 -1

B.3. PEG WITH HYDROXYETHYL TERMINAL, MULTIPLE CONFORMATIONS

```
429
430 Reading input for MEP 19 weight: 1.000
431 PEG2 nconf=10 norient=1 nmep=19/46
432
433 Total charge (ich): 0
434 Number of centers: 17
435   307   8  -1
436   308   1  -1
437   309   6   0
438   310   1   0
439   311   1   4
440   312   6   0
441   313   1   0
442   314   1   7
443   315   8  -1
444   316   6   0
445   317   1   0
446   318   1  11
447   319   6   0
448   320   1   0
449   321   1  14
450   322   8  -1
451   323   1  -1
452
453 Reading input for MEP 20 weight: 1.000
454 PEG2 nconf=10 norient=2 nmep=20/46
455
456 Total charge (ich): 0
457 Number of centers: 17
458   324   8  -1
459   325   1  -1
460   326   6   0
461   327   1   0
462   328   1   4
463   329   6   0
464   330   1   0
465   331   1   7
466   332   8  -1
467   333   6   0
468   334   1   0
469   335   1  11
470   336   6   0
471   337   1   0
472   338   1  14
473   339   8  -1
```

B.3. PEG WITH HYDROXYETHYL TERMINAL, MULTIPLE CONFORMATIONS

```
474 340 1 -1
475
476 Reading input for MEP 21 weight: 1.000
477 PEG2 nconf=11 norient=1 nmep=21/46
478
479 Total charge (ich): 0
480 Number of centers: 17
481 341 8 -1
482 342 1 -1
483 343 6 0
484 344 1 0
485 345 1 4
486 346 6 0
487 347 1 0
488 348 1 7
489 349 8 -1
490 350 6 0
491 351 1 0
492 352 1 11
493 353 6 0
494 354 1 0
495 355 1 14
496 356 8 -1
497 357 1 -1
498
499 Reading input for MEP 22 weight: 1.000
500 PEG2 nconf=11 norient=2 nmep=22/46
501
502 Total charge (ich): 0
503 Number of centers: 17
504 358 8 -1
505 359 1 -1
506 360 6 0
507 361 1 0
508 362 1 4
509 363 6 0
510 364 1 0
511 365 1 7
512 366 8 -1
513 367 6 0
514 368 1 0
515 369 1 11
516 370 6 0
517 371 1 0
518 372 1 14
```

B.3. PEG WITH HYDROXYETHYL TERMINAL, MULTIPLE CONFORMATIONS

```
519  373  8  -1
520  374  1  -1
521
522  Reading input for MEP 23 weight: 1.000
523  PEG2 nconf=12 norient=1 nmep=23/46
524
525  Total charge (ich): 0
526  Number of centers: 17
527  375  8  -1
528  376  1  -1
529  377  6  0
530  378  1  0
531  379  1  4
532  380  6  0
533  381  1  0
534  382  1  7
535  383  8  -1
536  384  6  0
537  385  1  0
538  386  1  11
539  387  6  0
540  388  1  0
541  389  1  14
542  390  8  -1
543  391  1  -1
544
545  Reading input for MEP 24 weight: 1.000
546  PEG2 nconf=12 norient=2 nmep=24/46
547
548  Total charge (ich): 0
549  Number of centers: 17
550  392  8  -1
551  393  1  -1
552  394  6  0
553  395  1  0
554  396  1  4
555  397  6  0
556  398  1  0
557  399  1  7
558  400  8  -1
559  401  6  0
560  402  1  0
561  403  1  11
562  404  6  0
563  405  1  0
```

B.3. PEG WITH HYDROXYETHYL TERMINAL, MULTIPLE CONFORMATIONS

```
564 406 1 14
565 407 8 -1
566 408 1 -1
567
568 Reading input for MEP 25 weight: 1.000
569 PEG2 nconf=13 norient=1 nmep=25/46
570
571 Total charge (ich): 0
572 Number of centers: 17
573 409 8 -1
574 410 1 -1
575 411 6 0
576 412 1 0
577 413 1 4
578 414 6 0
579 415 1 0
580 416 1 7
581 417 8 -1
582 418 6 0
583 419 1 0
584 420 1 11
585 421 6 0
586 422 1 0
587 423 1 14
588 424 8 -1
589 425 1 -1
590
591 Reading input for MEP 26 weight: 1.000
592 PEG2 nconf=13 norient=2 nmep=26/46
593
594 Total charge (ich): 0
595 Number of centers: 17
596 426 8 -1
597 427 1 -1
598 428 6 0
599 429 1 0
600 430 1 4
601 431 6 0
602 432 1 0
603 433 1 7
604 434 8 -1
605 435 6 0
606 436 1 0
607 437 1 11
608 438 6 0
```

B.3. PEG WITH HYDROXYETHYL TERMINAL, MULTIPLE CONFORMATIONS

```
609 439 1 0
610 440 1 14
611 441 8 -1
612 442 1 -1
613
614 Reading input for MEP 27 weight: 1.000
615 PEG2 nconf=14 norient=1 nmep=27/46
616
617 Total charge (ich): 0
618 Number of centers: 17
619 443 8 -1
620 444 1 -1
621 445 6 0
622 446 1 0
623 447 1 4
624 448 6 0
625 449 1 0
626 450 1 7
627 451 8 -1
628 452 6 0
629 453 1 0
630 454 1 11
631 455 6 0
632 456 1 0
633 457 1 14
634 458 8 -1
635 459 1 -1
636
637 Reading input for MEP 28 weight: 1.000
638 PEG2 nconf=14 norient=2 nmep=28/46
639
640 Total charge (ich): 0
641 Number of centers: 17
642 460 8 -1
643 461 1 -1
644 462 6 0
645 463 1 0
646 464 1 4
647 465 6 0
648 466 1 0
649 467 1 7
650 468 8 -1
651 469 6 0
652 470 1 0
653 471 1 11
```

B.3. PEG WITH HYDROXYETHYL TERMINAL, MULTIPLE CONFORMATIONS

```
654 472 6 0
655 473 1 0
656 474 1 14
657 475 8 -1
658 476 1 -1
659
660 Reading input for MEP 29 weight: 1.000
661 PEG2 nconf=15 norient=1 nmep=29/46
662
663 Total charge (ich): 0
664 Number of centers: 17
665 477 8 -1
666 478 1 -1
667 479 6 0
668 480 1 0
669 481 1 4
670 482 6 0
671 483 1 0
672 484 1 7
673 485 8 -1
674 486 6 0
675 487 1 0
676 488 1 11
677 489 6 0
678 490 1 0
679 491 1 14
680 492 8 -1
681 493 1 -1
682
683 Reading input for MEP 30 weight: 1.000
684 PEG2 nconf=15 norient=2 nmep=30/46
685
686 Total charge (ich): 0
687 Number of centers: 17
688 494 8 -1
689 495 1 -1
690 496 6 0
691 497 1 0
692 498 1 4
693 499 6 0
694 500 1 0
695 501 1 7
696 502 8 -1
697 503 6 0
698 504 1 0
```

B.3. PEG WITH HYDROXYETHYL TERMINAL, MULTIPLE CONFORMATIONS

```
699  505  1  11
700  506  6  0
701  507  1  0
702  508  1  14
703  509  8  -1
704  510  1  -1
705
706  Reading input for MEP 31 weight: 1.000
707  PEG2 nconf=16 norient=1 nmep=31/46
708
709  Total charge (ich): 0
710  Number of centers: 17
711  511  8  -1
712  512  1  -1
713  513  6  0
714  514  1  0
715  515  1  4
716  516  6  0
717  517  1  0
718  518  1  7
719  519  8  -1
720  520  6  0
721  521  1  0
722  522  1  11
723  523  6  0
724  524  1  0
725  525  1  14
726  526  8  -1
727  527  1  -1
728
729  Reading input for MEP 32 weight: 1.000
730  PEG2 nconf=16 norient=2 nmep=32/46
731
732  Total charge (ich): 0
733  Number of centers: 17
734  528  8  -1
735  529  1  -1
736  530  6  0
737  531  1  0
738  532  1  4
739  533  6  0
740  534  1  0
741  535  1  7
742  536  8  -1
743  537  6  0
```

B.3. PEG WITH HYDROXYETHYL TERMINAL, MULTIPLE CONFORMATIONS

```
744 538 1 0
745 539 1 11
746 540 6 0
747 541 1 0
748 542 1 14
749 543 8 -1
750 544 1 -1
751
752 Reading input for MEP 33 weight: 1.000
753 PEG2 nconf=17 norient=1 nmep=33/46
754
755 Total charge (ich): 0
756 Number of centers: 17
757 545 8 -1
758 546 1 -1
759 547 6 0
760 548 1 0
761 549 1 4
762 550 6 0
763 551 1 0
764 552 1 7
765 553 8 -1
766 554 6 0
767 555 1 0
768 556 1 11
769 557 6 0
770 558 1 0
771 559 1 14
772 560 8 -1
773 561 1 -1
774
775 Reading input for MEP 34 weight: 1.000
776 PEG2 nconf=17 norient=2 nmep=34/46
777
778 Total charge (ich): 0
779 Number of centers: 17
780 562 8 -1
781 563 1 -1
782 564 6 0
783 565 1 0
784 566 1 4
785 567 6 0
786 568 1 0
787 569 1 7
788 570 8 -1
```

B.3. PEG WITH HYDROXYETHYL TERMINAL, MULTIPLE CONFORMATIONS

```
789 571 6 0
790 572 1 0
791 573 1 11
792 574 6 0
793 575 1 0
794 576 1 14
795 577 8 -1
796 578 1 -1
797
798 Reading input for MEP 35 weight: 1.000
799 PEG2 nconf=18 norient=1 nmep=35/46
800
801 Total charge (ich): 0
802 Number of centers: 17
803 579 8 -1
804 580 1 -1
805 581 6 0
806 582 1 0
807 583 1 4
808 584 6 0
809 585 1 0
810 586 1 7
811 587 8 -1
812 588 6 0
813 589 1 0
814 590 1 11
815 591 6 0
816 592 1 0
817 593 1 14
818 594 8 -1
819 595 1 -1
820
821 Reading input for MEP 36 weight: 1.000
822 PEG2 nconf=18 norient=2 nmep=36/46
823
824 Total charge (ich): 0
825 Number of centers: 17
826 596 8 -1
827 597 1 -1
828 598 6 0
829 599 1 0
830 600 1 4
831 601 6 0
832 602 1 0
833 603 1 7
```

B.3. PEG WITH HYDROXYETHYL TERMINAL, MULTIPLE CONFORMATIONS

```
834 604 8 -1
835 605 6 0
836 606 1 0
837 607 1 11
838 608 6 0
839 609 1 0
840 610 1 14
841 611 8 -1
842 612 1 -1
843
844 Reading input for MEP 37 weight: 1.000
845 PEG2 nconf=19 norient=1 nmep=37/46
846
847 Total charge (ich): 0
848 Number of centers: 17
849 613 8 -1
850 614 1 -1
851 615 6 0
852 616 1 0
853 617 1 4
854 618 6 0
855 619 1 0
856 620 1 7
857 621 8 -1
858 622 6 0
859 623 1 0
860 624 1 11
861 625 6 0
862 626 1 0
863 627 1 14
864 628 8 -1
865 629 1 -1
866
867 Reading input for MEP 38 weight: 1.000
868 PEG2 nconf=19 norient=2 nmep=38/46
869
870 Total charge (ich): 0
871 Number of centers: 17
872 630 8 -1
873 631 1 -1
874 632 6 0
875 633 1 0
876 634 1 4
877 635 6 0
878 636 1 0
```

B.3. PEG WITH HYDROXYETHYL TERMINAL, MULTIPLE CONFORMATIONS

```
879 637 1 7
880 638 8 -1
881 639 6 0
882 640 1 0
883 641 1 11
884 642 6 0
885 643 1 0
886 644 1 14
887 645 8 -1
888 646 1 -1
889
890 Reading input for MEP 39 weight: 1.000
891 PEG2 nconf=20 norient=1 nmep=39/46
892
893 Total charge (ich): 0
894 Number of centers: 17
895 647 8 -1
896 648 1 -1
897 649 6 0
898 650 1 0
899 651 1 4
900 652 6 0
901 653 1 0
902 654 1 7
903 655 8 -1
904 656 6 0
905 657 1 0
906 658 1 11
907 659 6 0
908 660 1 0
909 661 1 14
910 662 8 -1
911 663 1 -1
912
913 Reading input for MEP 40 weight: 1.000
914 PEG2 nconf=20 norient=2 nmep=40/46
915
916 Total charge (ich): 0
917 Number of centers: 17
918 664 8 -1
919 665 1 -1
920 666 6 0
921 667 1 0
922 668 1 4
923 669 6 0
```

B.3. PEG WITH HYDROXYETHYL TERMINAL, MULTIPLE CONFORMATIONS

```
924 670 1 0
925 671 1 7
926 672 8 -1
927 673 6 0
928 674 1 0
929 675 1 11
930 676 6 0
931 677 1 0
932 678 1 14
933 679 8 -1
934 680 1 -1
935
936 Reading input for MEP 41 weight: 1.000
937 PEG2 nconf=21 norient=1 nmep=41/46
938
939 Total charge (ich): 0
940 Number of centers: 17
941 681 8 -1
942 682 1 -1
943 683 6 0
944 684 1 0
945 685 1 4
946 686 6 0
947 687 1 0
948 688 1 7
949 689 8 -1
950 690 6 0
951 691 1 0
952 692 1 11
953 693 6 0
954 694 1 0
955 695 1 14
956 696 8 -1
957 697 1 -1
958
959 Reading input for MEP 42 weight: 1.000
960 PEG2 nconf=21 norient=2 nmep=42/46
961
962 Total charge (ich): 0
963 Number of centers: 17
964 698 8 -1
965 699 1 -1
966 700 6 0
967 701 1 0
968 702 1 4
```

B.3. PEG WITH HYDROXYETHYL TERMINAL, MULTIPLE CONFORMATIONS

```
969 703 6 0
970 704 1 0
971 705 1 7
972 706 8 -1
973 707 6 0
974 708 1 0
975 709 1 11
976 710 6 0
977 711 1 0
978 712 1 14
979 713 8 -1
980 714 1 -1
981
982 Reading input for MEP 43 weight: 1.000
983 PEG2 nconf=22 norient=1 nmep=43/46
984
985 Total charge (ich): 0
986 Number of centers: 17
987 715 8 -1
988 716 1 -1
989 717 6 0
990 718 1 0
991 719 1 4
992 720 6 0
993 721 1 0
994 722 1 7
995 723 8 -1
996 724 6 0
997 725 1 0
998 726 1 11
999 727 6 0
1000 728 1 0
1001 729 1 14
1002 730 8 -1
1003 731 1 -1
1004
1005 Reading input for MEP 44 weight: 1.000
1006 PEG2 nconf=22 norient=2 nmep=44/46
1007
1008 Total charge (ich): 0
1009 Number of centers: 17
1010 732 8 -1
1011 733 1 -1
1012 734 6 0
1013 735 1 0
```

B.3. PEG WITH HYDROXYETHYL TERMINAL, MULTIPLE CONFORMATIONS

```
1014 736 1 4
1015 737 6 0
1016 738 1 0
1017 739 1 7
1018 740 8 -1
1019 741 6 0
1020 742 1 0
1021 743 1 11
1022 744 6 0
1023 745 1 0
1024 746 1 14
1025 747 8 -1
1026 748 1 -1
1027
1028 Reading input for MEP 45 weight: 1.000
1029 PEG2 nconf=23 norient=1 nmep=45/46
1030
1031 Total charge (ich): 0
1032 Number of centers: 17
1033 749 8 -1
1034 750 1 -1
1035 751 6 0
1036 752 1 0
1037 753 1 4
1038 754 6 0
1039 755 1 0
1040 756 1 7
1041 757 8 -1
1042 758 6 0
1043 759 1 0
1044 760 1 11
1045 761 6 0
1046 762 1 0
1047 763 1 14
1048 764 8 -1
1049 765 1 -1
1050
1051 Reading input for MEP 46 weight: 1.000
1052 PEG2 nconf=23 norient=2 nmep=46/46
1053
1054 Total charge (ich): 0
1055 Number of centers: 17
1056 766 8 -1
1057 767 1 -1
1058 768 6 0
```

B.3. PEG WITH HYDROXYETHYL TERMINAL, MULTIPLE CONFORMATIONS

```

1059 769 1 0
1060 770 1 4
1061 771 6 0
1062 772 1 0
1063 773 1 7
1064 774 8 -1
1065 775 6 0
1066 776 1 0
1067 777 1 11
1068 778 6 0
1069 779 1 0
1070 780 1 14
1071 781 8 -1
1072 782 1 -1
1073 1 1 1 2 1 3 1 4 1 5 1 6 1 7 1 8
1074 since IQOPT>1, 782 new q0 values
1075 will be read in from file ESP.Q0 (unit 3)
1076 -----
1077 reading mult_esp constraint info
1078 -----
1079 1 3 2 3 3 3 4 3 5 3 6 3 7 3 8 3
1080 9 3 10 3 11 3 12 3 13 3 14 3 15 3 16 3
1081 17 3 18 3 19 3 20 3 21 3 22 3 23 3 24 3
1082 25 3 26 3 27 3 28 3 29 3 30 3 31 3 32 3
1083 33 3 34 3 35 3 36 3 37 3 38 3 39 3 40 3
1084 41 3 42 3 43 3 44 3 45 3 46 3
1085 1 4 2 4 3 4 4 4 5 4 6 4 7 4 8 4
1086 9 4 10 4 11 4 12 4 13 4 14 4 15 4 16 4
1087 17 4 18 4 19 4 20 4 21 4 22 4 23 4 24 4
1088 25 4 26 4 27 4 28 4 29 4 30 4 31 4 32 4
1089 33 4 34 4 35 4 36 4 37 4 38 4 39 4 40 4
1090 41 4 42 4 43 4 44 4 45 4 46 4
1091 1 6 2 6 3 6 4 6 5 6 6 6 7 6 8 6
1092 9 6 10 6 11 6 12 6 13 6 14 6 15 6 16 6
1093 17 6 18 6 19 6 20 6 21 6 22 6 23 6 24 6
1094 25 6 26 6 27 6 28 6 29 6 30 6 31 6 32 6
1095 33 6 34 6 35 6 36 6 37 6 38 6 39 6 40 6
1096 41 6 42 6 43 6 44 6 45 6 46 6
1097 1 7 2 7 3 7 4 7 5 7 6 7 7 7 8 7
1098 9 7 10 7 11 7 12 7 13 7 14 7 15 7 16 7
1099 17 7 18 7 19 7 20 7 21 7 22 7 23 7 24 7
1100 25 7 26 7 27 7 28 7 29 7 30 7 31 7 32 7
1101 33 7 34 7 35 7 36 7 37 7 38 7 39 7 40 7
1102 41 7 42 7 43 7 44 7 45 7 46 7
1103 1 10 2 10 3 10 4 10 5 10 6 10 7 10 8 10

```

B.3. PEG WITH HYDROXYETHYL TERMINAL, MULTIPLE CONFORMATIONS

1104	9	10	10	10	11	10	12	10	13	10	14	10	15	10	16	10
1105	17	10	18	10	19	10	20	10	21	10	22	10	23	10	24	10
1106	25	10	26	10	27	10	28	10	29	10	30	10	31	10	32	10
1107	33	10	34	10	35	10	36	10	37	10	38	10	39	10	40	10
1108	41	10	42	10	43	10	44	10	45	10	46	10				
1109	1	11	2	11	3	11	4	11	5	11	6	11	7	11	8	11
1110	9	11	10	11	11	11	12	11	13	11	14	11	15	11	16	11
1111	17	11	18	11	19	11	20	11	21	11	22	11	23	11	24	11
1112	25	11	26	11	27	11	28	11	29	11	30	11	31	11	32	11
1113	33	11	34	11	35	11	36	11	37	11	38	11	39	11	40	11
1114	41	11	42	11	43	11	44	11	45	11	46	11				
1115	1	13	2	13	3	13	4	13	5	13	6	13	7	13	8	13
1116	9	13	10	13	11	13	12	13	13	13	14	13	15	13	16	13
1117	17	13	18	13	19	13	20	13	21	13	22	13	23	13	24	13
1118	25	13	26	13	27	13	28	13	29	13	30	13	31	13	32	13
1119	33	13	34	13	35	13	36	13	37	13	38	13	39	13	40	13
1120	41	13	42	13	43	13	44	13	45	13	46	13				
1121	1	14	2	14	3	14	4	14	5	14	6	14	7	14	8	14
1122	9	14	10	14	11	14	12	14	13	14	14	14	15	14	16	14
1123	17	14	18	14	19	14	20	14	21	14	22	14	23	14	24	14
1124	25	14	26	14	27	14	28	14	29	14	30	14	31	14	32	14
1125	33	14	34	14	35	14	36	14	37	14	38	14	39	14	40	14
1126	41	14	42	14	43	14	44	14	45	14	46	14				
1127																
1128	-----															
1129	Atom	Ivary														
1130	-----															
1131	8	-1														
1132	1	-1														
1133	6	0														
1134	1	0														
1135	1	4														
1136	6	0														
1137	1	0														
1138	1	7														
1139	8	-1														
1140	6	0														
1141	1	0														
1142	1	11														
1143	6	0														
1144	1	0														
1145	1	14														
1146	8	-1														
1147	1	-1														
1148																

B.3. PEG WITH HYDROXYETHYL TERMINAL, MULTIPLE CONFORMATIONS

1149	8	-1
1150	1	-1
1151	6	3
1152	1	4
1153	1	4
1154	6	6
1155	1	7
1156	1	7
1157	8	-1
1158	6	10
1159	1	11
1160	1	11
1161	6	13
1162	1	14
1163	1	14
1164	8	-1
1165	1	-1
1166		
1167	8	-1
1168	1	-1
1169	6	3
1170	1	4
1171	1	4
1172	6	6
1173	1	7
1174	1	7
1175	8	-1
1176	6	10
1177	1	11
1178	1	11
1179	6	13
1180	1	14
1181	1	14
1182	8	-1
1183	1	-1
1184		
1185	8	-1
1186	1	-1
1187	6	3
1188	1	4
1189	1	4
1190	6	6
1191	1	7
1192	1	7
1193	8	-1

B.3. PEG WITH HYDROXYETHYL TERMINAL, MULTIPLE CONFORMATIONS

1194	6	10
1195	1	11
1196	1	11
1197	6	13
1198	1	14
1199	1	14
1200	8	-1
1201	1	-1
1202		
1203	8	-1
1204	1	-1
1205	6	3
1206	1	4
1207	1	4
1208	6	6
1209	1	7
1210	1	7
1211	8	-1
1212	6	10
1213	1	11
1214	1	11
1215	6	13
1216	1	14
1217	1	14
1218	8	-1
1219	1	-1
1220		
1221	8	-1
1222	1	-1
1223	6	3
1224	1	4
1225	1	4
1226	6	6
1227	1	7
1228	1	7
1229	8	-1
1230	6	10
1231	1	11
1232	1	11
1233	6	13
1234	1	14
1235	1	14
1236	8	-1
1237	1	-1
1238		

B.3. PEG WITH HYDROXYETHYL TERMINAL, MULTIPLE CONFORMATIONS

1239	8	-1
1240	1	-1
1241	6	3
1242	1	4
1243	1	4
1244	6	6
1245	1	7
1246	1	7
1247	8	-1
1248	6	10
1249	1	11
1250	1	11
1251	6	13
1252	1	14
1253	1	14
1254	8	-1
1255	1	-1
1256		
1257	8	-1
1258	1	-1
1259	6	3
1260	1	4
1261	1	4
1262	6	6
1263	1	7
1264	1	7
1265	8	-1
1266	6	10
1267	1	11
1268	1	11
1269	6	13
1270	1	14
1271	1	14
1272	8	-1
1273	1	-1
1274		
1275	8	-1
1276	1	-1
1277	6	3
1278	1	4
1279	1	4
1280	6	6
1281	1	7
1282	1	7
1283	8	-1

B.3. PEG WITH HYDROXYETHYL TERMINAL, MULTIPLE CONFORMATIONS

1284	6	10
1285	1	11
1286	1	11
1287	6	13
1288	1	14
1289	1	14
1290	8	-1
1291	1	-1
1292		
1293	8	-1
1294	1	-1
1295	6	3
1296	1	4
1297	1	4
1298	6	6
1299	1	7
1300	1	7
1301	8	-1
1302	6	10
1303	1	11
1304	1	11
1305	6	13
1306	1	14
1307	1	14
1308	8	-1
1309	1	-1
1310		
1311	8	-1
1312	1	-1
1313	6	3
1314	1	4
1315	1	4
1316	6	6
1317	1	7
1318	1	7
1319	8	-1
1320	6	10
1321	1	11
1322	1	11
1323	6	13
1324	1	14
1325	1	14
1326	8	-1
1327	1	-1
1328		

B.3. PEG WITH HYDROXYETHYL TERMINAL, MULTIPLE CONFORMATIONS

1329	8	-1
1330	1	-1
1331	6	3
1332	1	4
1333	1	4
1334	6	6
1335	1	7
1336	1	7
1337	8	-1
1338	6	10
1339	1	11
1340	1	11
1341	6	13
1342	1	14
1343	1	14
1344	8	-1
1345	1	-1
1346		
1347	8	-1
1348	1	-1
1349	6	3
1350	1	4
1351	1	4
1352	6	6
1353	1	7
1354	1	7
1355	8	-1
1356	6	10
1357	1	11
1358	1	11
1359	6	13
1360	1	14
1361	1	14
1362	8	-1
1363	1	-1
1364		
1365	8	-1
1366	1	-1
1367	6	3
1368	1	4
1369	1	4
1370	6	6
1371	1	7
1372	1	7
1373	8	-1

B.3. PEG WITH HYDROXYETHYL TERMINAL, MULTIPLE CONFORMATIONS

1374	6	10
1375	1	11
1376	1	11
1377	6	13
1378	1	14
1379	1	14
1380	8	-1
1381	1	-1
1382		
1383	8	-1
1384	1	-1
1385	6	3
1386	1	4
1387	1	4
1388	6	6
1389	1	7
1390	1	7
1391	8	-1
1392	6	10
1393	1	11
1394	1	11
1395	6	13
1396	1	14
1397	1	14
1398	8	-1
1399	1	-1
1400		
1401	8	-1
1402	1	-1
1403	6	3
1404	1	4
1405	1	4
1406	6	6
1407	1	7
1408	1	7
1409	8	-1
1410	6	10
1411	1	11
1412	1	11
1413	6	13
1414	1	14
1415	1	14
1416	8	-1
1417	1	-1
1418		

B.3. PEG WITH HYDROXYETHYL TERMINAL, MULTIPLE CONFORMATIONS

1419	8	-1
1420	1	-1
1421	6	3
1422	1	4
1423	1	4
1424	6	6
1425	1	7
1426	1	7
1427	8	-1
1428	6	10
1429	1	11
1430	1	11
1431	6	13
1432	1	14
1433	1	14
1434	8	-1
1435	1	-1
1436		
1437	8	-1
1438	1	-1
1439	6	3
1440	1	4
1441	1	4
1442	6	6
1443	1	7
1444	1	7
1445	8	-1
1446	6	10
1447	1	11
1448	1	11
1449	6	13
1450	1	14
1451	1	14
1452	8	-1
1453	1	-1
1454		
1455	8	-1
1456	1	-1
1457	6	3
1458	1	4
1459	1	4
1460	6	6
1461	1	7
1462	1	7
1463	8	-1

B.3. PEG WITH HYDROXYETHYL TERMINAL, MULTIPLE CONFORMATIONS

1464	6	10
1465	1	11
1466	1	11
1467	6	13
1468	1	14
1469	1	14
1470	8	-1
1471	1	-1
1472		
1473	8	-1
1474	1	-1
1475	6	3
1476	1	4
1477	1	4
1478	6	6
1479	1	7
1480	1	7
1481	8	-1
1482	6	10
1483	1	11
1484	1	11
1485	6	13
1486	1	14
1487	1	14
1488	8	-1
1489	1	-1
1490		
1491	8	-1
1492	1	-1
1493	6	3
1494	1	4
1495	1	4
1496	6	6
1497	1	7
1498	1	7
1499	8	-1
1500	6	10
1501	1	11
1502	1	11
1503	6	13
1504	1	14
1505	1	14
1506	8	-1
1507	1	-1
1508		

B.3. PEG WITH HYDROXYETHYL TERMINAL, MULTIPLE CONFORMATIONS

1509	8	-1
1510	1	-1
1511	6	3
1512	1	4
1513	1	4
1514	6	6
1515	1	7
1516	1	7
1517	8	-1
1518	6	10
1519	1	11
1520	1	11
1521	6	13
1522	1	14
1523	1	14
1524	8	-1
1525	1	-1
1526		
1527	8	-1
1528	1	-1
1529	6	3
1530	1	4
1531	1	4
1532	6	6
1533	1	7
1534	1	7
1535	8	-1
1536	6	10
1537	1	11
1538	1	11
1539	6	13
1540	1	14
1541	1	14
1542	8	-1
1543	1	-1
1544		
1545	8	-1
1546	1	-1
1547	6	3
1548	1	4
1549	1	4
1550	6	6
1551	1	7
1552	1	7
1553	8	-1

B.3. PEG WITH HYDROXYETHYL TERMINAL, MULTIPLE CONFORMATIONS

1554	6	10
1555	1	11
1556	1	11
1557	6	13
1558	1	14
1559	1	14
1560	8	-1
1561	1	-1
1562		
1563	8	-1
1564	1	-1
1565	6	3
1566	1	4
1567	1	4
1568	6	6
1569	1	7
1570	1	7
1571	8	-1
1572	6	10
1573	1	11
1574	1	11
1575	6	13
1576	1	14
1577	1	14
1578	8	-1
1579	1	-1
1580		
1581	8	-1
1582	1	-1
1583	6	3
1584	1	4
1585	1	4
1586	6	6
1587	1	7
1588	1	7
1589	8	-1
1590	6	10
1591	1	11
1592	1	11
1593	6	13
1594	1	14
1595	1	14
1596	8	-1
1597	1	-1
1598		

B.3. PEG WITH HYDROXYETHYL TERMINAL, MULTIPLE CONFORMATIONS

1599	8	-1
1600	1	-1
1601	6	3
1602	1	4
1603	1	4
1604	6	6
1605	1	7
1606	1	7
1607	8	-1
1608	6	10
1609	1	11
1610	1	11
1611	6	13
1612	1	14
1613	1	14
1614	8	-1
1615	1	-1
1616		
1617	8	-1
1618	1	-1
1619	6	3
1620	1	4
1621	1	4
1622	6	6
1623	1	7
1624	1	7
1625	8	-1
1626	6	10
1627	1	11
1628	1	11
1629	6	13
1630	1	14
1631	1	14
1632	8	-1
1633	1	-1
1634		
1635	8	-1
1636	1	-1
1637	6	3
1638	1	4
1639	1	4
1640	6	6
1641	1	7
1642	1	7
1643	8	-1

B.3. PEG WITH HYDROXYETHYL TERMINAL, MULTIPLE CONFORMATIONS

1644	6	10
1645	1	11
1646	1	11
1647	6	13
1648	1	14
1649	1	14
1650	8	-1
1651	1	-1
1652		
1653	8	-1
1654	1	-1
1655	6	3
1656	1	4
1657	1	4
1658	6	6
1659	1	7
1660	1	7
1661	8	-1
1662	6	10
1663	1	11
1664	1	11
1665	6	13
1666	1	14
1667	1	14
1668	8	-1
1669	1	-1
1670		
1671	8	-1
1672	1	-1
1673	6	3
1674	1	4
1675	1	4
1676	6	6
1677	1	7
1678	1	7
1679	8	-1
1680	6	10
1681	1	11
1682	1	11
1683	6	13
1684	1	14
1685	1	14
1686	8	-1
1687	1	-1
1688		

B.3. PEG WITH HYDROXYETHYL TERMINAL, MULTIPLE CONFORMATIONS

1689	8	-1
1690	1	-1
1691	6	3
1692	1	4
1693	1	4
1694	6	6
1695	1	7
1696	1	7
1697	8	-1
1698	6	10
1699	1	11
1700	1	11
1701	6	13
1702	1	14
1703	1	14
1704	8	-1
1705	1	-1
1706		
1707	8	-1
1708	1	-1
1709	6	3
1710	1	4
1711	1	4
1712	6	6
1713	1	7
1714	1	7
1715	8	-1
1716	6	10
1717	1	11
1718	1	11
1719	6	13
1720	1	14
1721	1	14
1722	8	-1
1723	1	-1
1724		
1725	8	-1
1726	1	-1
1727	6	3
1728	1	4
1729	1	4
1730	6	6
1731	1	7
1732	1	7
1733	8	-1

B.3. PEG WITH HYDROXYETHYL TERMINAL, MULTIPLE CONFORMATIONS

1734	6	10
1735	1	11
1736	1	11
1737	6	13
1738	1	14
1739	1	14
1740	8	-1
1741	1	-1
1742		
1743	8	-1
1744	1	-1
1745	6	3
1746	1	4
1747	1	4
1748	6	6
1749	1	7
1750	1	7
1751	8	-1
1752	6	10
1753	1	11
1754	1	11
1755	6	13
1756	1	14
1757	1	14
1758	8	-1
1759	1	-1
1760		
1761	8	-1
1762	1	-1
1763	6	3
1764	1	4
1765	1	4
1766	6	6
1767	1	7
1768	1	7
1769	8	-1
1770	6	10
1771	1	11
1772	1	11
1773	6	13
1774	1	14
1775	1	14
1776	8	-1
1777	1	-1
1778		

B.3. PEG WITH HYDROXYETHYL TERMINAL, MULTIPLE CONFORMATIONS

1779	8	-1
1780	1	-1
1781	6	3
1782	1	4
1783	1	4
1784	6	6
1785	1	7
1786	1	7
1787	8	-1
1788	6	10
1789	1	11
1790	1	11
1791	6	13
1792	1	14
1793	1	14
1794	8	-1
1795	1	-1
1796		
1797	8	-1
1798	1	-1
1799	6	3
1800	1	4
1801	1	4
1802	6	6
1803	1	7
1804	1	7
1805	8	-1
1806	6	10
1807	1	11
1808	1	11
1809	6	13
1810	1	14
1811	1	14
1812	8	-1
1813	1	-1
1814		
1815	8	-1
1816	1	-1
1817	6	3
1818	1	4
1819	1	4
1820	6	6
1821	1	7
1822	1	7
1823	8	-1

B.3. PEG WITH HYDROXYETHYL TERMINAL, MULTIPLE CONFORMATIONS

1824	6	10
1825	1	11
1826	1	11
1827	6	13
1828	1	14
1829	1	14
1830	8	-1
1831	1	-1
1832		
1833	8	-1
1834	1	-1
1835	6	3
1836	1	4
1837	1	4
1838	6	6
1839	1	7
1840	1	7
1841	8	-1
1842	6	10
1843	1	11
1844	1	11
1845	6	13
1846	1	14
1847	1	14
1848	8	-1
1849	1	-1
1850		
1851	8	-1
1852	1	-1
1853	6	3
1854	1	4
1855	1	4
1856	6	6
1857	1	7
1858	1	7
1859	8	-1
1860	6	10
1861	1	11
1862	1	11
1863	6	13
1864	1	14
1865	1	14
1866	8	-1
1867	1	-1
1868		

B.3. PEG WITH HYDROXYETHYL TERMINAL, MULTIPLE CONFORMATIONS

1869	8	-1
1870	1	-1
1871	6	3
1872	1	4
1873	1	4
1874	6	6
1875	1	7
1876	1	7
1877	8	-1
1878	6	10
1879	1	11
1880	1	11
1881	6	13
1882	1	14
1883	1	14
1884	8	-1
1885	1	-1
1886		
1887	8	-1
1888	1	-1
1889	6	3
1890	1	4
1891	1	4
1892	6	6
1893	1	7
1894	1	7
1895	8	-1
1896	6	10
1897	1	11
1898	1	11
1899	6	13
1900	1	14
1901	1	14
1902	8	-1
1903	1	-1
1904		
1905	8	-1
1906	1	-1
1907	6	3
1908	1	4
1909	1	4
1910	6	6
1911	1	7
1912	1	7
1913	8	-1

B.3. PEG WITH HYDROXYETHYL TERMINAL, MULTIPLE CONFORMATIONS

1914	6	10
1915	1	11
1916	1	11
1917	6	13
1918	1	14
1919	1	14
1920	8	-1
1921	1	-1
1922		
1923	8	-1
1924	1	-1
1925	6	3
1926	1	4
1927	1	4
1928	6	6
1929	1	7
1930	1	7
1931	8	-1
1932	6	10
1933	1	11
1934	1	11
1935	6	13
1936	1	14
1937	1	14
1938	8	-1
1939	1	-1
1940		
1941	8	-1
1942	1	-1
1943	6	3
1944	1	4
1945	1	4
1946	6	6
1947	1	7
1948	1	7
1949	8	-1
1950	6	10
1951	1	11
1952	1	11
1953	6	13
1954	1	14
1955	1	14
1956	8	-1
1957	1	-1
1958		

B.3. PEG WITH HYDROXYETHYL TERMINAL, MULTIPLE CONFORMATIONS

1959 -----

1960

1961

1962 Total number of atoms = 782

1963 Weight factor on initial charge restraints= 0.001000

1964

1965

1966 There are 47 charge constraints

1967

1968 Reading esp"s for MEP 1

1969 total number of atoms = 17

1970 total number of esp points = 809

1971

1972	Center	X	Y	Z
1973	1	0.4978215E+01	0.2437140E+01	-0.4366318E+01
1974	2	0.4793776E+01	0.3312593E+01	-0.5963597E+01
1975	3	0.3655614E+01	0.3833419E+01	-0.2498507E+01
1976	4	0.1659618E+01	0.4112601E+01	-0.3022352E+01
1977	5	0.4485629E+01	0.5725104E+01	-0.2210686E+01
1978	6	0.3839901E+01	0.2415871E+01	0.0000000E+00
1979	7	0.3033619E+01	0.3609201E+01	0.1507497E+01
1980	8	0.5836249E+01	0.2080700E+01	0.4263770E+00
1981	9	0.2686593E+01	0.0000000E+00	0.0000000E+00
1982	10	0.0000000E+00	0.0000000E+00	0.0000000E+00
1983	11	-0.7670908E+00	0.5504753E+00	-0.1854086E+01
1984	12	-0.7163309E+00	0.1331210E+01	0.1433034E+01
1985	13	-0.8033584E+00	-0.2680877E+01	0.6642557E+00
1986	14	-0.1703059E+00	-0.3970396E+01	-0.8436512E+00
1987	15	-0.2867062E+01	-0.2790946E+01	0.7758157E+00
1988	16	0.1597215E+00	-0.3416785E+01	0.3050490E+01
1989	17	0.1951496E+01	-0.3017114E+01	0.2982980E+01

1990

1991 Reading esp"s for MEP 2

1992 total number of atoms = 17

1993 total number of esp points = 805

1994

1995	Center	X	Y	Z
1996	1	-0.5095967E+00	-0.1018099E+01	0.4366318E+01
1997	2	-0.1220183E+01	-0.4744951E+00	0.5963597E+01
1998	3	-0.1199859E+01	0.7770062E+00	0.2498507E+01
1999	4	-0.5919019E+00	0.2698551E+01	0.3022352E+01
2000	5	-0.3264575E+01	0.8429331E+00	0.2210686E+01
2001	6	0.0000000E+00	0.0000000E+00	0.0000000E+00
2002	7	-0.7295514E+00	0.1241726E+01	-0.1507497E+01

B.3. PEG WITH HYDROXYETHYL TERMINAL, MULTIPLE CONFORMATIONS

```
2003      8      -0.5575826E+00 -0.1945981E+01 -0.4263770E+00
2004      9       0.2677041E+01  0.0000000E+00  0.0000000E+00
2005     10       0.3834464E+01  0.2424490E+01  0.0000000E+00
2006     11       0.3668166E+01  0.3353897E+01  0.1854086E+01
2007     12       0.2941733E+01  0.3644440E+01 -0.1433034E+01
2008     13       0.6599893E+01  0.1994513E+01 -0.6642557E+00
2009     14       0.7490881E+01  0.8676790E+00  0.8436512E+00
2010     15       0.7588297E+01  0.3809465E+01 -0.7758157E+00
2011     16       0.6849098E+01  0.8083511E+00 -0.3050490E+01
2012     17       0.5716497E+01 -0.6364351E+00 -0.2982980E+01
```

2013

2014 Reading esp"s for MEP 3

2015 total number of atoms = 17

2016 total number of esp points = 803

2017

```
2018 Center      X              Y              Z
2019      1      0.5313660E+01  0.1803796E+01 -0.4290976E+01
2020      2      0.4633126E+01  0.1401969E+00 -0.3909044E+01
2021      3      0.4010528E+01  0.3496456E+01 -0.2678163E+01
2022      4      0.2098730E+01  0.3912011E+01 -0.3399611E+01
2023      5      0.5067053E+01  0.5277245E+01 -0.2670132E+01
2024      6      0.3854349E+01  0.2440630E+01  0.0000000E+00
2025      7      0.2834370E+01  0.3733664E+01  0.1270123E+01
2026      8      0.5765082E+01  0.2149541E+01  0.7380873E+00
2027      9      0.2698842E+01  0.0000000E+00  0.0000000E+00
2028     10      0.0000000E+00  0.0000000E+00  0.0000000E+00
2029     11     -0.7671758E+00  0.6775083E+00 -0.1810611E+01
2030     12     -0.6983785E+00  0.1238266E+01  0.1517429E+01
2031     13     -0.8077804E+00 -0.2714064E+01  0.4967315E+00
2032     14     -0.1680666E+00 -0.3915510E+01 -0.1081099E+01
2033     15     -0.2872338E+01 -0.2824749E+01  0.5817862E+00
2034     16      0.1282349E+00 -0.3593970E+01  0.2842611E+01
2035     17      0.1923705E+01 -0.3208479E+01  0.2827321E+01
```

2036

2037 Reading esp"s for MEP 4

2038 total number of atoms = 17

2039 total number of esp points = 813

2040

```
2041 Center      X              Y              Z
2042      1     -0.4887020E-01 -0.1591463E+01  0.4290976E+01
2043      2      0.1745933E+01 -0.1688255E+01  0.3909044E+01
2044      3     -0.1021108E+01  0.3106426E+00  0.2678163E+01
2045      4     -0.5786171E+00  0.2216384E+01  0.3399611E+01
2046      5     -0.3082720E+01  0.1177488E+00  0.2670132E+01
2047      6      0.0000000E+00  0.0000000E+00  0.0000000E+00
```

B.3. PEG WITH HYDROXYETHYL TERMINAL, MULTIPLE CONFORMATIONS

```
2048 7 -0.7322121E+00 0.1475181E+01 -0.1270123E+01
2049 8 -0.5545288E+00 -0.1851521E+01 -0.7380873E+00
2050 9 0.2700347E+01 0.0000000E+00 0.0000000E+00
2051 10 0.3855209E+01 0.2439271E+01 0.0000000E+00
2052 11 0.3571147E+01 0.3422573E+01 0.1810611E+01
2053 12 0.3034883E+01 0.3600347E+01 -0.1517429E+01
2054 13 0.6653895E+01 0.2007985E+01 -0.4967315E+00
2055 14 0.7466047E+01 0.9156856E+00 0.1081099E+01
2056 15 0.7637380E+01 0.3826612E+01 -0.5817862E+00
2057 16 0.7048642E+01 0.7854722E+00 -0.2842611E+01
2058 17 0.5931926E+01 -0.6723569E+00 -0.2827321E+01
```

2059

2060 Reading esp"s for MEP 5

2061 total number of atoms = 17

2062 total number of esp points = 803

2063

Center	X	Y	Z
2065 1	0.5313484E+01	0.1803862E+01	-0.4291056E+01
2066 2	0.4632977E+01	0.1402592E+00	-0.3909108E+01
2067 3	0.4010431E+01	0.3496507E+01	-0.2678139E+01
2068 4	0.2098624E+01	0.3912114E+01	-0.3399521E+01
2069 5	0.5066992E+01	0.5277272E+01	-0.2670083E+01
2070 6	0.3854336E+01	0.2440615E+01	0.0000000E+00
2071 7	0.2834410E+01	0.3733636E+01	0.1270185E+01
2072 8	0.5765091E+01	0.2149509E+01	0.7380136E+00
2073 9	0.2698831E+01	0.0000000E+00	0.0000000E+00
2074 10	0.0000000E+00	0.0000000E+00	0.0000000E+00
2075 11	-0.7671891E+00	0.6776179E+00	-0.1810567E+01
2076 12	-0.6983917E+00	0.1238171E+01	0.1517501E+01
2077 13	-0.8077936E+00	-0.2714089E+01	0.4965690E+00
2078 14	-0.1680855E+00	-0.3915450E+01	-0.1081330E+01
2079 15	-0.2872351E+01	-0.2824762E+01	0.5816218E+00
2080 16	0.1282141E+00	-0.3594138E+01	0.2842405E+01
2081 17	0.1923688E+01	-0.3208660E+01	0.2827144E+01

2082

2083 Reading esp"s for MEP 6

2084 total number of atoms = 17

2085 total number of esp points = 813

2086

Center	X	Y	Z
2088 1	-0.4887776E-01	-0.1591282E+01	0.4291056E+01
2089 2	0.1745920E+01	-0.1688102E+01	0.3909108E+01
2090 3	-0.1021130E+01	0.3107465E+00	0.2678139E+01
2091 4	-0.5786813E+00	0.2216520E+01	0.3399521E+01
2092 5	-0.3082738E+01	0.1178150E+00	0.2670083E+01

B.3. PEG WITH HYDROXYETHYL TERMINAL, MULTIPLE CONFORMATIONS

```
2093 6 0.0000000E+00 0.0000000E+00 0.0000000E+00
2094 7 -0.7322197E+00 0.1475128E+01 -0.1270185E+01
2095 8 -0.5545269E+00 -0.1851550E+01 -0.7380136E+00
2096 9 0.2700331E+01 0.0000000E+00 0.0000000E+00
2097 10 0.3855194E+01 0.2439258E+01 0.0000000E+00
2098 11 0.3571040E+01 0.3422621E+01 0.1810567E+01
2099 12 0.3034960E+01 0.3600306E+01 -0.1517501E+01
2100 13 0.6653909E+01 0.2007966E+01 -0.4965690E+00
2101 14 0.7465984E+01 0.9157083E+00 0.1081330E+01
2102 15 0.7637386E+01 0.3826597E+01 -0.5816218E+00
2103 16 0.7048784E+01 0.7854004E+00 -0.2842405E+01
2104 17 0.5932077E+01 -0.6724363E+00 -0.2827144E+01
```

2105

2106 Reading esp"s for MEP 7

2107 total number of atoms = 17

2108 total number of esp points = 803

2109

```
2110 Center X Y Z
2111 1 0.5313641E+01 0.1803776E+01 -0.4290986E+01
2112 2 0.4633130E+01 0.1401799E+00 -0.3908998E+01
2113 3 0.4010535E+01 0.3496454E+01 -0.2678167E+01
2114 4 0.2098745E+01 0.3912030E+01 -0.3399617E+01
2115 5 0.5067081E+01 0.5277230E+01 -0.2670128E+01
2116 6 0.3854347E+01 0.2440628E+01 0.0000000E+00
2117 7 0.2834375E+01 0.3733668E+01 0.1270117E+01
2118 8 0.5765080E+01 0.2149539E+01 0.7380854E+00
2119 9 0.2698846E+01 0.0000000E+00 0.0000000E+00
2120 10 0.0000000E+00 0.0000000E+00 0.0000000E+00
2121 11 -0.7671758E+00 0.6775915E+00 -0.1810577E+01
2122 12 -0.6983747E+00 0.1238192E+01 0.1517488E+01
2123 13 -0.8077861E+00 -0.2714085E+01 0.4966068E+00
2124 14 -0.1680836E+00 -0.3915461E+01 -0.1081284E+01
2125 15 -0.2872344E+01 -0.2824759E+01 0.5816633E+00
2126 16 0.1282406E+00 -0.3594108E+01 0.2842437E+01
2127 17 0.1923701E+01 -0.3208579E+01 0.2827181E+01
```

2128

2129 Reading esp"s for MEP 8

2130 total number of atoms = 17

2131 total number of esp points = 813

2132

```
2133 Center X Y Z
2134 1 -0.4884375E-01 -0.1591457E+01 0.4290986E+01
2135 2 0.1745948E+01 -0.1688264E+01 0.3908998E+01
2136 3 -0.1021113E+01 0.3106313E+00 0.2678167E+01
2137 4 -0.5786454E+00 0.2216378E+01 0.3399617E+01
```

B.3. PEG WITH HYDROXYETHYL TERMINAL, MULTIPLE CONFORMATIONS

```
2138 5 -0.3082723E+01 0.1177110E+00 0.2670128E+01
2139 6 0.0000000E+00 0.0000000E+00 0.0000000E+00
2140 7 -0.7322235E+00 0.1475175E+01 -0.1270117E+01
2141 8 -0.5545288E+00 -0.1851521E+01 -0.7380854E+00
2142 9 0.2700341E+01 0.0000000E+00 0.0000000E+00
2143 10 0.3855202E+01 0.2439275E+01 0.0000000E+00
2144 11 0.3571061E+01 0.3422613E+01 0.1810577E+01
2145 12 0.3034938E+01 0.3600317E+01 -0.1517488E+01
2146 13 0.6653910E+01 0.2007989E+01 -0.4966068E+00
2147 14 0.7466007E+01 0.9157329E+00 0.1081284E+01
2148 15 0.7637382E+01 0.3826623E+01 -0.5816633E+00
2149 16 0.7048759E+01 0.7854193E+00 -0.2842437E+01
2150 17 0.5932016E+01 -0.6723872E+00 -0.2827181E+01
```

2151

2152 Reading esp"s for MEP 9

2153 total number of atoms = 17

2154 total number of esp points = 803

2155

```
2156 Center X Y Z
2157 1 0.5313681E+01 0.1803785E+01 -0.4290971E+01
2158 2 0.4633147E+01 0.1401874E+00 -0.3909038E+01
2159 3 0.4010543E+01 0.3496449E+01 -0.2678163E+01
2160 4 0.2098749E+01 0.3912003E+01 -0.3399619E+01
2161 5 0.5067068E+01 0.5277236E+01 -0.2670126E+01
2162 6 0.3854346E+01 0.2440628E+01 0.0000000E+00
2163 7 0.2834362E+01 0.3733668E+01 0.1270111E+01
2164 8 0.5765072E+01 0.2149541E+01 0.7381024E+00
2165 9 0.2698841E+01 0.0000000E+00 0.0000000E+00
2166 10 0.0000000E+00 0.0000000E+00 0.0000000E+00
2167 11 -0.7671796E+00 0.6774857E+00 -0.1810616E+01
2168 12 -0.6983860E+00 0.1238279E+01 0.1517414E+01
2169 13 -0.8077861E+00 -0.2714059E+01 0.4967598E+00
2170 14 -0.1680703E+00 -0.3915526E+01 -0.1081055E+01
2171 15 -0.2872344E+01 -0.2824734E+01 0.5818126E+00
2172 16 0.1282274E+00 -0.3593938E+01 0.2842651E+01
2173 17 0.1923699E+01 -0.3208452E+01 0.2827359E+01
```

2174

2175 Reading esp"s for MEP 10

2176 total number of atoms = 17

2177 total number of esp points = 813

2178

```
2179 Center X Y Z
2180 1 -0.4887209E-01 -0.1591489E+01 0.4290971E+01
2181 2 0.1745931E+01 -0.1688281E+01 0.3909038E+01
2182 3 -0.1021111E+01 0.3106218E+00 0.2678163E+01
```

B.3. PEG WITH HYDROXYETHYL TERMINAL, MULTIPLE CONFORMATIONS

```
2183 4 -0.5786209E+00 0.2216361E+01 0.3399619E+01
2184 5 -0.3082723E+01 0.1177299E+00 0.2670126E+01
2185 6 0.0000000E+00 0.0000000E+00 0.0000000E+00
2186 7 -0.7322159E+00 0.1475188E+01 -0.1270111E+01
2187 8 -0.5545269E+00 -0.1851514E+01 -0.7381024E+00
2188 9 0.2700345E+01 0.0000000E+00 0.0000000E+00
2189 10 0.3855205E+01 0.2439268E+01 0.0000000E+00
2190 11 0.3571165E+01 0.3422566E+01 0.1810616E+01
2191 12 0.3034870E+01 0.3600357E+01 -0.1517414E+01
2192 13 0.6653890E+01 0.2007989E+01 -0.4967598E+00
2193 14 0.7466062E+01 0.9156800E+00 0.1081055E+01
2194 15 0.7637367E+01 0.3826621E+01 -0.5818126E+00
2195 16 0.7048614E+01 0.7854911E+00 -0.2842651E+01
2196 17 0.5931903E+01 -0.6723418E+00 -0.2827359E+01
```

2197

2198 Reading esp"s for MEP 11

2199 total number of atoms = 17

2200 total number of esp points = 810

2201

```
2202 Center X Y Z
2203 1 0.5213693E+01 0.1800017E+01 -0.4306839E+01
2204 2 0.4580599E+01 0.1385831E+00 -0.3838846E+01
2205 3 0.3953456E+01 0.3511400E+01 -0.2677564E+01
2206 4 0.2038020E+01 0.3948235E+01 -0.3378240E+01
2207 5 0.5028559E+01 0.5281616E+01 -0.2681015E+01
2208 6 0.3816995E+01 0.2445183E+01 0.0000000E+00
2209 7 0.2799860E+01 0.3732642E+01 0.1279161E+01
2210 8 0.5733349E+01 0.2165333E+01 0.7283306E+00
2211 9 0.2684290E+01 0.0000000E+00 0.0000000E+00
2212 10 0.0000000E+00 0.0000000E+00 0.0000000E+00
2213 11 -0.7626745E+00 0.6819190E+00 -0.1813307E+01
2214 12 -0.7198722E+00 0.1240242E+01 0.1506990E+01
2215 13 -0.9314081E+00 -0.2670854E+01 0.4558983E+00
2216 14 0.3880930E-01 -0.3951037E+01 -0.8665717E+00
2217 15 -0.2969837E+01 -0.2732765E+01 0.2377086E-01
2218 16 -0.4466235E+00 -0.3322922E+01 0.3011643E+01
2219 17 -0.7822010E+00 -0.5110904E+01 0.3213243E+01
```

2220

2221 Reading esp"s for MEP 12

2222 total number of atoms = 17

2223 total number of esp points = 817

2224

```
2225 Center X Y Z
2226 1 -0.1668628E-02 -0.1538507E+01 0.4306839E+01
2227 2 0.1771975E+01 -0.1662405E+01 0.3838846E+01
```

B.3. PEG WITH HYDROXYETHYL TERMINAL, MULTIPLE CONFORMATIONS

```
2228 3 -0.1024814E+01 0.3243431E+00 0.2677564E+01
2229 4 -0.6160677E+00 0.2245970E+01 0.3378240E+01
2230 5 -0.3082956E+01 0.9290271E-01 0.2681015E+01
2231 6 0.0000000E+00 0.0000000E+00 0.0000000E+00
2232 7 -0.7406687E+00 0.1464078E+01 -0.1279161E+01
2233 8 -0.5515751E+00 -0.1856474E+01 -0.7283306E+00
2234 9 0.2694798E+01 0.0000000E+00 0.0000000E+00
2235 10 0.3823088E+01 0.2435647E+01 0.0000000E+00
2236 11 0.3524910E+01 0.3414308E+01 0.1813307E+01
2237 12 0.3000312E+01 0.3610149E+01 -0.1506990E+01
2238 13 0.6638040E+01 0.2158139E+01 -0.4558983E+00
2239 14 0.7391831E+01 0.7396917E+00 0.8665717E+00
2240 15 0.7551031E+01 0.3981726E+01 -0.2377086E-01
2241 16 0.7025941E+01 0.1444176E+01 -0.3011643E+01
2242 17 0.8789356E+01 0.9971253E+00 -0.3213243E+01
```

2243

2244 Reading esp"s for MEP 13

2245 total number of atoms = 17

2246 total number of esp points = 814

2247

```
2248 Center X Y Z
2249 1 0.5368704E+01 0.1752536E+01 -0.4247125E+01
2250 2 0.4708965E+01 0.9276665E-01 -0.3813066E+01
2251 3 0.4033437E+01 0.3471111E+01 -0.2687899E+01
2252 4 0.2137439E+01 0.3874297E+01 -0.3457539E+01
2253 5 0.5088244E+01 0.5253185E+01 -0.2683530E+01
2254 6 0.3819728E+01 0.2448437E+01 0.0000000E+00
2255 7 0.2763919E+01 0.3751828E+01 0.1229864E+01
2256 8 0.5714745E+01 0.2180613E+01 0.7864227E+00
2257 9 0.2683721E+01 0.0000000E+00 0.0000000E+00
2258 10 0.0000000E+00 0.0000000E+00 0.0000000E+00
2259 11 -0.7664313E+00 0.8737224E+00 -0.1731220E+01
2260 12 -0.7338392E+00 0.1077582E+01 0.1620357E+01
2261 13 -0.8845675E+00 -0.2741533E+01 0.1807693E+00
2262 14 -0.2055965E+00 -0.3567750E+01 0.1949046E+01
2263 15 -0.6428848E-01 -0.3843788E+01 -0.1380626E+01
2264 16 -0.3562708E+01 -0.2909146E+01 0.2415467E+00
2265 17 -0.4191777E+01 -0.2471939E+01 -0.1422947E+01
```

2266

2267 Reading esp"s for MEP 14

2268 total number of atoms = 17

2269 total number of esp points = 825

2270

```
2271 Center X Y Z
2272 1 -0.2066604E-01 -0.1697993E+01 0.4247125E+01
```

B.3. PEG WITH HYDROXYETHYL TERMINAL, MULTIPLE CONFORMATIONS

```
2273 2 0.1762610E+01 -0.1798091E+01 0.3813066E+01
2274 3 -0.1017631E+01 0.2365616E+00 0.2687899E+01
2275 4 -0.5853842E+00 0.2126148E+01 0.3457539E+01
2276 5 -0.3078126E+01 0.2976318E-01 0.2683530E+01
2277 6 0.0000000E+00 0.0000000E+00 0.0000000E+00
2278 7 -0.7379607E+00 0.1506312E+01 -0.1229864E+01
2279 8 -0.5546232E+00 -0.1831723E+01 -0.7864227E+00
2280 9 0.2699141E+01 0.0000000E+00 0.0000000E+00
2281 10 0.3828659E+01 0.2434449E+01 0.0000000E+00
2282 11 0.3358663E+01 0.3497422E+01 0.1731220E+01
2283 12 0.3160023E+01 0.3553658E+01 -0.1620357E+01
2284 13 0.6687846E+01 0.2083005E+01 -0.1807693E+00
2285 14 0.7151558E+01 0.1119362E+01 -0.1949046E+01
2286 15 0.7342483E+01 0.8750017E+00 0.1380626E+01
2287 16 0.7967060E+01 0.4441848E+01 -0.2415467E+00
2288 17 0.7835223E+01 0.5196499E+01 0.1422947E+01
```

2289

2290 Reading esp"s for MEP 15

2291 total number of atoms = 17

2292 total number of esp points = 811

2293

```
2294 Center X Y Z
2295 1 0.5391275E+01 0.1760108E+01 -0.4235290E+01
2296 2 0.4713606E+01 0.1008585E+00 -0.3828165E+01
2297 3 0.4032129E+01 0.3472045E+01 -0.2688642E+01
2298 4 0.2138898E+01 0.3859136E+01 -0.3471468E+01
2299 5 0.5075598E+01 0.5260799E+01 -0.2681068E+01
2300 6 0.3809039E+01 0.2452828E+01 0.0000000E+00
2301 7 0.2741359E+01 0.3754474E+01 0.1221797E+01
2302 8 0.5701825E+01 0.2196976E+01 0.7962266E+00
2303 9 0.2685199E+01 0.0000000E+00 0.0000000E+00
2304 10 0.0000000E+00 0.0000000E+00 0.0000000E+00
2305 11 -0.7820915E+00 0.9058250E+00 -0.1699030E+01
2306 12 -0.7293265E+00 0.1023655E+01 0.1657121E+01
2307 13 -0.8630889E+00 -0.2740318E+01 0.9894416E-01
2308 14 -0.9331467E-01 -0.3634077E+01 0.1811703E+01
2309 15 -0.9511936E-01 -0.3757404E+01 -0.1546053E+01
2310 16 -0.3548703E+01 -0.2707424E+01 0.9553510E-01
2311 17 -0.4134275E+01 -0.4439316E+01 0.1729988E+00
```

2312

2313 Reading esp"s for MEP 16

2314 total number of atoms = 17

2315 total number of esp points = 824

2316

```
2317 Center X Y Z
```

B.3. PEG WITH HYDROXYETHYL TERMINAL, MULTIPLE CONFORMATIONS

```
2318 1 -0.2930020E-01 -0.1726985E+01 0.4235290E+01
2319 2 0.1761429E+01 -0.1802047E+01 0.3828165E+01
2320 3 -0.1019513E+01 0.2217291E+00 0.2688642E+01
2321 4 -0.5828180E+00 0.2104138E+01 0.3471468E+01
2322 5 -0.3080348E+01 0.1818105E-01 0.2681068E+01
2323 6 0.0000000E+00 0.0000000E+00 0.0000000E+00
2324 7 -0.7386164E+00 0.1512833E+01 -0.1221797E+01
2325 8 -0.5558232E+00 -0.1827337E+01 -0.7962266E+00
2326 9 0.2698034E+01 0.0000000E+00 0.0000000E+00
2327 10 0.3816527E+01 0.2441161E+01 0.0000000E+00
2328 11 0.3318797E+01 0.3529487E+01 0.1699030E+01
2329 12 0.3189697E+01 0.3530600E+01 -0.1657121E+01
2330 13 0.6667309E+01 0.2084356E+01 -0.9894416E-01
2331 14 0.7159199E+01 0.1012256E+01 -0.1811703E+01
2332 15 0.7272068E+01 0.9625244E+00 0.1546053E+01
2333 16 0.7756070E+01 0.4539596E+01 -0.9553510E-01
2334 17 0.9574478E+01 0.4350546E+01 -0.1729988E+00
```

2335

2336 Reading esp"s for MEP 17

2337 total number of atoms = 17

2338 total number of esp points = 811

2339

```
2340 Center X Y Z
2341 1 0.5391248E+01 0.1760140E+01 -0.4235301E+01
2342 2 0.4713564E+01 0.1008944E+00 -0.3828186E+01
2343 3 0.4032101E+01 0.3472069E+01 -0.2688638E+01
2344 4 0.2138871E+01 0.3859166E+01 -0.3471457E+01
2345 5 0.5075570E+01 0.5260825E+01 -0.2681062E+01
2346 6 0.3809032E+01 0.2452840E+01 0.0000000E+00
2347 7 0.2741348E+01 0.3754466E+01 0.1221810E+01
2348 8 0.5701819E+01 0.2196988E+01 0.7962096E+00
2349 9 0.2685199E+01 0.0000000E+00 0.0000000E+00
2350 10 0.0000000E+00 0.0000000E+00 0.0000000E+00
2351 11 -0.7820971E+00 0.9057759E+00 -0.1699054E+01
2352 12 -0.7293265E+00 0.1023706E+01 0.1657093E+01
2353 13 -0.8630851E+00 -0.2740316E+01 0.9900841E-01
2354 14 -0.9334302E-01 -0.3634034E+01 0.1811797E+01
2355 15 -0.9508534E-01 -0.3757433E+01 -0.1545956E+01
2356 16 -0.3548703E+01 -0.2707442E+01 0.9555400E-01
2357 17 -0.4134254E+01 -0.4439331E+01 0.1731991E+00
```

2358

2359 Reading esp"s for MEP 18

2360 total number of atoms = 17

2361 total number of esp points = 824

2362

B.3. PEG WITH HYDROXYETHYL TERMINAL, MULTIPLE CONFORMATIONS

Center	X	Y	Z	
2363				
2364	1	-0.2930398E-01	-0.1726956E+01	0.4235301E+01
2365	2	0.1761429E+01	-0.1801999E+01	0.3828186E+01
2366	3	-0.1019517E+01	0.2217499E+00	0.2688638E+01
2367	4	-0.5828350E+00	0.2104161E+01	0.3471457E+01
2368	5	-0.3080352E+01	0.1819428E-01	0.2681062E+01
2369	6	0.0000000E+00	0.0000000E+00	0.0000000E+00
2370	7	-0.7386032E+00	0.1512826E+01	-0.1221810E+01
2371	8	-0.5558157E+00	-0.1827341E+01	-0.7962096E+00
2372	9	0.2698041E+01	0.0000000E+00	0.0000000E+00
2373	10	0.3816525E+01	0.2441165E+01	0.0000000E+00
2374	11	0.3318837E+01	0.3529473E+01	0.1699054E+01
2375	12	0.3189644E+01	0.3530622E+01	-0.1657093E+01
2376	13	0.6667303E+01	0.2084372E+01	-0.9900841E-01
2377	14	0.7159174E+01	0.1012317E+01	-0.1811797E+01
2378	15	0.7272083E+01	0.9625017E+00	0.1545956E+01
2379	16	0.7756076E+01	0.4539609E+01	-0.9555400E-01
2380	17	0.9574473E+01	0.4350550E+01	-0.1731991E+00

2381

2382 Reading esp"s for MEP 19

2383 total number of atoms = 17

2384 total number of esp points = 814

2385

Center	X	Y	Z	
2386				
2387	1	0.5435935E+01	0.1755421E+01	-0.4221058E+01
2388	2	0.4749316E+01	0.9443528E-01	-0.3837622E+01
2389	3	0.4055717E+01	0.3462615E+01	-0.2689348E+01
2390	4	0.2167132E+01	0.3840159E+01	-0.3488351E+01
2391	5	0.5091305E+01	0.5255876E+01	-0.2677383E+01
2392	6	0.3814975E+01	0.2450627E+01	0.0000000E+00
2393	7	0.2743876E+01	0.3758162E+01	0.1213070E+01
2394	8	0.5702573E+01	0.2192243E+01	0.8074308E+00
2395	9	0.2683207E+01	0.0000000E+00	0.0000000E+00
2396	10	0.0000000E+00	0.0000000E+00	0.0000000E+00
2397	11	-0.7863490E+00	0.9644897E+00	-0.1664416E+01
2398	12	-0.7133716E+00	0.9908608E+00	0.1692529E+01
2399	13	-0.8857032E+00	-0.2746981E+01	0.1661447E-01
2400	14	-0.4428384E-01	-0.3737398E+01	0.1639075E+01
2401	15	-0.2306335E+00	-0.3695480E+01	-0.1699648E+01
2402	16	-0.3564569E+01	-0.2917342E+01	-0.3140725E-02
2403	17	-0.4173494E+01	-0.2375879E+01	0.1637933E+01

2404

2405 Reading esp"s for MEP 20

2406 total number of atoms = 17

2407 total number of esp points = 821

B.3. PEG WITH HYDROXYETHYL TERMINAL, MULTIPLE CONFORMATIONS

```
2408
2409 Center      X          Y          Z
2410   1    -0.4847903E-01 -0.1763086E+01  0.4221058E+01
2411   2     0.1747345E+01 -0.1836143E+01  0.3837622E+01
2412   3    -0.1019681E+01  0.2057401E+00  0.2689348E+01
2413   4    -0.5706009E+00  0.2078604E+01  0.3488351E+01
2414   5    -0.3081905E+01  0.1744028E-01  0.2677383E+01
2415   6     0.0000000E+00  0.0000000E+00  0.0000000E+00
2416   7    -0.7379739E+00  0.1520623E+01 -0.1213070E+01
2417   8    -0.5568456E+00 -0.1822010E+01 -0.8074308E+00
2418   9     0.2699347E+01  0.0000000E+00  0.0000000E+00
2419  10     0.3824346E+01  0.2435976E+01  0.0000000E+00
2420  11     0.3278421E+01  0.3554255E+01  0.1664416E+01
2421  12     0.3223882E+01  0.3499058E+01 -0.1692529E+01
2422  13     0.6689573E+01  0.2088331E+01 -0.1661447E-01
2423  14     0.7235946E+01  0.9091831E+00 -0.1639075E+01
2424  15     0.7276023E+01  0.1095937E+01  0.1699648E+01
2425  16     0.7967416E+01  0.4448937E+01  0.3140725E-02
2426  17     0.7731149E+01  0.5228777E+01 -0.1637933E+01
```

2427

2428 Reading esp"s for MEP 21

2429 total number of atoms = 17

2430 total number of esp points = 756

2431

```
2432 Center      X          Y          Z
2433   1     0.4363459E+01  0.2381799E+01 -0.4597811E+01
2434   2     0.3217119E+01  0.9348871E+00 -0.4665097E+01
2435   3     0.3596697E+01  0.3826106E+01 -0.2497702E+01
2436   4     0.1627139E+01  0.4494158E+01 -0.2703790E+01
2437   5     0.4787770E+01  0.5521375E+01 -0.2437121E+01
2438   6     0.3897915E+01  0.2398873E+01  0.0000000E+00
2439   7     0.3238015E+01  0.3576208E+01  0.1588919E+01
2440   8     0.5896913E+01  0.1964329E+01  0.2996765E+00
2441   9     0.2676963E+01  0.0000000E+00  0.0000000E+00
2442  10     0.0000000E+00  0.0000000E+00  0.0000000E+00
2443  11    -0.7703071E+00  0.1927447E+01 -0.1283275E+00
2444  12    -0.6936579E+00 -0.8221234E+00  0.1782293E+01
2445  13    -0.9503734E+00 -0.1595479E+01 -0.2204277E+01
2446  14    -0.3012212E+01 -0.1834395E+01 -0.2074919E+01
2447  15    -0.7977856E-01 -0.3466751E+01 -0.2105680E+01
2448  16    -0.2407738E+00 -0.6022840E+00 -0.4613777E+01
2449  17    -0.1236741E+01  0.9027788E+00 -0.4937739E+01
```

2450

2451 Reading esp"s for MEP 22

2452 total number of atoms = 17

B.3. PEG WITH HYDROXYETHYL TERMINAL, MULTIPLE CONFORMATIONS

2453 total number of esp points = 762

2454

2455	Center	X	Y	Z
2456	1	-0.1959514E+00	-0.4226410E+00	0.4597811E+01
2457	2	0.1613524E+01	-0.5732862E-01	0.4665097E+01
2458	3	-0.1135328E+01	0.9158349E+00	0.2497702E+01
2459	4	-0.8373168E+00	0.2974145E+01	0.2703790E+01
2460	5	-0.3186430E+01	0.6233110E+00	0.2437121E+01
2461	6	0.0000000E+00	0.0000000E+00	0.0000000E+00
2462	7	-0.7499208E+00	0.1122142E+01	-0.1588919E+01
2463	8	-0.5194687E+00	-0.1978630E+01	-0.2996765E+00
2464	9	0.2691712E+01	0.0000000E+00	0.0000000E+00
2465	10	0.3905975E+01	0.2385728E+01	0.0000000E+00
2466	11	0.2537628E+01	0.3946515E+01	0.1283275E+00
2467	12	0.4953299E+01	0.2631009E+01	-0.1782293E+01
2468	13	0.5758963E+01	0.2509004E+01	0.2204277E+01
2469	14	0.6907128E+01	0.4238160E+01	0.2074919E+01
2470	15	0.7031755E+01	0.8843218E+00	0.2105680E+01
2471	16	0.4551949E+01	0.2327114E+01	0.4613777E+01
2472	17	0.3662393E+01	0.3897416E+01	0.4937739E+01

2473

2474 Reading esp"s for MEP 23

2475 total number of atoms = 17

2476 total number of esp points = 756

2477

2478	Center	X	Y	Z
2479	1	0.4363392E+01	0.2381892E+01	-0.4597811E+01
2480	2	0.3217122E+01	0.9349211E+00	-0.4665070E+01
2481	3	0.3596632E+01	0.3826155E+01	-0.2497658E+01
2482	4	0.1627067E+01	0.4494184E+01	-0.2703710E+01
2483	5	0.4787689E+01	0.5521430E+01	-0.2437068E+01
2484	6	0.3897909E+01	0.2398881E+01	0.0000000E+00
2485	7	0.3238064E+01	0.3576172E+01	0.1588974E+01
2486	8	0.5896922E+01	0.1964336E+01	0.2996047E+00
2487	9	0.2676967E+01	0.0000000E+00	0.0000000E+00
2488	10	0.0000000E+00	0.0000000E+00	0.0000000E+00
2489	11	-0.7703147E+00	0.1927441E+01	-0.1283389E+00
2490	12	-0.6936598E+00	-0.8221177E+00	0.1782295E+01
2491	13	-0.9503715E+00	-0.1595496E+01	-0.2204273E+01
2492	14	-0.3012216E+01	-0.1834395E+01	-0.2074930E+01
2493	15	-0.7978990E-01	-0.3466770E+01	-0.2105654E+01
2494	16	-0.2407416E+00	-0.6023256E+00	-0.4613777E+01
2495	17	-0.1236682E+01	0.9027504E+00	-0.4937750E+01

2496

2497 Reading esp"s for MEP 24

B.3. PEG WITH HYDROXYETHYL TERMINAL, MULTIPLE CONFORMATIONS

```
2498 total number of atoms = 17
2499 total number of esp points = 762
2500
2501 Center      X              Y              Z
2502   1      -0.1959986E+00 -0.4225484E+00  0.4597811E+01
2503   2       0.1613495E+01 -0.5731728E-01  0.4665070E+01
2504   3      -0.1135342E+01  0.9159029E+00  0.2497658E+01
2505   4      -0.8373149E+00  0.2974210E+01  0.2703710E+01
2506   5      -0.3186441E+01  0.6233885E+00  0.2437068E+01
2507   6       0.0000000E+00  0.0000000E+00  0.0000000E+00
2508   7      -0.7499113E+00  0.1122072E+01 -0.1588974E+01
2509   8      -0.5194687E+00 -0.1978643E+01 -0.2996047E+00
2510   9       0.2691716E+01  0.0000000E+00  0.0000000E+00
2511  10       0.3905969E+01  0.2385736E+01  0.0000000E+00
2512  11       0.2537626E+01  0.3946521E+01  0.1283389E+00
2513  12       0.4953287E+01  0.2631024E+01 -0.1782295E+01
2514  13       0.5758970E+01  0.2509010E+01  0.2204273E+01
2515  14       0.6907119E+01  0.4238181E+01  0.2074930E+01
2516  15       0.7031778E+01  0.8843426E+00  0.2105654E+01
2517  16       0.4551966E+01  0.2327077E+01  0.4613777E+01
2518  17       0.3662382E+01  0.3897359E+01  0.4937750E+01
2519
2520 Reading esp"s for MEP 25
2521 total number of atoms = 17
2522 total number of esp points = 756
2523
2524 Center      X              Y              Z
2525   1      0.4363421E+01  0.2381892E+01 -0.4597813E+01
2526   2      0.3217121E+01  0.9349457E+00 -0.4665104E+01
2527   3      0.3596647E+01  0.3826153E+01 -0.2497658E+01
2528   4      0.1627075E+01  0.4494161E+01 -0.2703714E+01
2529   5      0.4787689E+01  0.5521435E+01 -0.2437072E+01
2530   6      0.3897919E+01  0.2398879E+01  0.0000000E+00
2531   7      0.3238064E+01  0.3576174E+01  0.1588965E+01
2532   8      0.5896928E+01  0.1964334E+01  0.2996161E+00
2533   9      0.2676965E+01  0.0000000E+00  0.0000000E+00
2534  10      0.0000000E+00  0.0000000E+00  0.0000000E+00
2535  11     -0.7703147E+00  0.1927445E+01 -0.1282973E+00
2536  12     -0.6936579E+00 -0.8221517E+00  0.1782280E+01
2537  13     -0.9503772E+00 -0.1595460E+01 -0.2204299E+01
2538  14     -0.3012216E+01 -0.1834368E+01 -0.2074951E+01
2539  15     -0.7977856E-01 -0.3466729E+01 -0.2105712E+01
2540  16     -0.2407719E+00 -0.6022443E+00 -0.4613794E+01
2541  17     -0.1236695E+01  0.9028525E+00 -0.4937722E+01
2542
```

B.3. PEG WITH HYDROXYETHYL TERMINAL, MULTIPLE CONFORMATIONS

```
2543 Reading esp"s for MEP 26
2544 total number of atoms = 17
2545 total number of esp points = 762
2546
2547 Center X Y Z
2548 1 -0.1960118E+00 -0.4225635E+00 0.4597813E+01
2549 2 0.1613476E+01 -0.5730216E-01 0.4665104E+01
2550 3 -0.1135340E+01 0.9159029E+00 0.2497658E+01
2551 4 -0.8372847E+00 0.2974206E+01 0.2703714E+01
2552 5 -0.3186441E+01 0.6234112E+00 0.2437072E+01
2553 6 0.0000000E+00 0.0000000E+00 0.0000000E+00
2554 7 -0.7499056E+00 0.1122083E+01 -0.1588965E+01
2555 8 -0.5194743E+00 -0.1978638E+01 -0.2996161E+00
2556 9 0.2691718E+01 0.0000000E+00 0.0000000E+00
2557 10 0.3905981E+01 0.2385730E+01 0.0000000E+00
2558 11 0.2537639E+01 0.3946523E+01 0.1282973E+00
2559 12 0.4953329E+01 0.2630997E+01 -0.1782280E+01
2560 13 0.5758953E+01 0.2509018E+01 0.2204299E+01
2561 14 0.6907113E+01 0.4238175E+01 0.2074951E+01
2562 15 0.7031742E+01 0.8843351E+00 0.2105712E+01
2563 16 0.4551917E+01 0.2327133E+01 0.4613794E+01
2564 17 0.3662314E+01 0.3897414E+01 0.4937722E+01
2565
2566 Reading esp"s for MEP 27
2567 total number of atoms = 17
2568 total number of esp points = 756
2569
2570 Center X Y Z
2571 1 0.4363402E+01 0.2381860E+01 -0.4597811E+01
2572 2 0.3217151E+01 0.9348701E+00 -0.4665046E+01
2573 3 0.3596630E+01 0.3826136E+01 -0.2497675E+01
2574 4 0.1627058E+01 0.4494143E+01 -0.2703729E+01
2575 5 0.4787672E+01 0.5521420E+01 -0.2437104E+01
2576 6 0.3897909E+01 0.2398882E+01 0.0000000E+00
2577 7 0.3238044E+01 0.3576180E+01 0.1588957E+01
2578 8 0.5896918E+01 0.1964346E+01 0.2996217E+00
2579 9 0.2676965E+01 0.0000000E+00 0.0000000E+00
2580 10 0.0000000E+00 0.0000000E+00 0.0000000E+00
2581 11 -0.7703147E+00 0.1927441E+01 -0.1283880E+00
2582 12 -0.6936636E+00 -0.8220743E+00 0.1782314E+01
2583 13 -0.9503602E+00 -0.1595543E+01 -0.2204241E+01
2584 14 -0.3012206E+01 -0.1834433E+01 -0.2074912E+01
2585 15 -0.7978423E-01 -0.3466820E+01 -0.2105584E+01
2586 16 -0.2407076E+00 -0.6024182E+00 -0.4613760E+01
2587 17 -0.1236665E+01 0.9026371E+00 -0.4937782E+01
```

B.3. PEG WITH HYDROXYETHYL TERMINAL, MULTIPLE CONFORMATIONS

2588

2589 Reading esp"s for MEP 28

2590 total number of atoms = 17

2591 total number of esp points = 762

2592

2593	Center	X	Y	Z
2594	1	-0.1959721E+00	-0.4225730E+00	0.4597811E+01
2595	2	0.1613527E+01	-0.5736830E-01	0.4665046E+01
2596	3	-0.1135323E+01	0.9158935E+00	0.2497675E+01
2597	4	-0.8372715E+00	0.2974196E+01	0.2703729E+01
2598	5	-0.3186422E+01	0.6233960E+00	0.2437104E+01
2599	6	0.0000000E+00	0.0000000E+00	0.0000000E+00
2600	7	-0.7499075E+00	0.1122091E+01	-0.1588957E+01
2601	8	-0.5194724E+00	-0.1978638E+01	-0.2996217E+00
2602	9	0.2691718E+01	0.0000000E+00	0.0000000E+00
2603	10	0.3905971E+01	0.2385736E+01	0.0000000E+00
2604	11	0.2537628E+01	0.3946519E+01	0.1283880E+00
2605	12	0.4953252E+01	0.2631048E+01	-0.1782314E+01
2606	13	0.5759010E+01	0.2508978E+01	0.2204241E+01
2607	14	0.6907149E+01	0.4238153E+01	0.2074912E+01
2608	15	0.7031820E+01	0.8843143E+00	0.2105584E+01
2609	16	0.4552034E+01	0.2327003E+01	0.4613760E+01
2610	17	0.3662474E+01	0.3897292E+01	0.4937782E+01

2611

2612 Reading esp"s for MEP 29

2613 total number of atoms = 17

2614 total number of esp points = 840

2615

2616	Center	X	Y	Z
2617	1	0.7218638E+01	0.7890230E+00	0.2501100E+01
2618	2	0.6168396E+01	-0.7174137E+00	0.2497503E+01
2619	3	0.6598109E+01	0.2089525E+01	0.2451636E+00
2620	4	0.7300837E+01	0.1079326E+01	-0.1434884E+01
2621	5	0.7539066E+01	0.3930908E+01	0.3254429E+00
2622	6	0.3756970E+01	0.2453446E+01	0.0000000E+00
2623	7	0.3284125E+01	0.3474250E+01	-0.1755125E+01
2624	8	0.3039316E+01	0.3559607E+01	0.1612254E+01
2625	9	0.2668463E+01	0.0000000E+00	0.0000000E+00
2626	10	0.0000000E+00	0.0000000E+00	0.0000000E+00
2627	11	-0.7233852E+00	0.9762684E+00	-0.1700736E+01
2628	12	-0.7403002E+00	0.1032308E+01	0.1655750E+01
2629	13	-0.9643612E+00	-0.2709848E+01	0.6500657E-01
2630	14	-0.3030523E+01	-0.2658631E+01	0.3410029E+00
2631	15	-0.1391462E+00	-0.3685653E+01	0.1691305E+01
2632	16	-0.2802123E+00	-0.4162908E+01	-0.2077294E+01

B.3. PEG WITH HYDROXYETHYL TERMINAL, MULTIPLE CONFORMATIONS

2633 17 -0.9913937E+00 -0.3350934E+01 -0.3558923E+01
2634

2635 Reading esp"s for MEP 30

2636 total number of atoms = 17

2637 total number of esp points = 835

2638

Center	X	Y	Z	
2640	1	0.1175561E+00	-0.3839222E+01	-0.2501100E+01
2641	2	0.1920472E+01	-0.3490146E+01	-0.2497503E+01
2642	3	-0.8195496E+00	-0.2744604E+01	-0.2451636E+00
2643	4	-0.1811378E+00	-0.3796630E+01	0.1434884E+01
2644	5	-0.2884313E+01	-0.2857950E+01	-0.3254429E+00
2645	6	0.0000000E+00	0.0000000E+00	0.0000000E+00
2646	7	-0.7413319E+00	0.8461947E+00	0.1755125E+01
2647	8	-0.7200763E+00	0.1104586E+01	-0.1612254E+01
2648	9	0.2684072E+01	0.0000000E+00	0.0000000E+00
2649	10	0.3766249E+01	0.2439179E+01	0.0000000E+00
2650	11	0.3167228E+01	0.3496328E+01	0.1700736E+01
2651	12	0.3122863E+01	0.3534513E+01	-0.1655750E+01
2652	13	0.6634346E+01	0.2221721E+01	-0.6500657E-01
2653	14	0.7425446E+01	0.4131120E+01	-0.3410029E+00
2654	15	0.7191645E+01	0.1071681E+01	-0.1691305E+01
2655	16	0.7685100E+01	0.1007078E+01	0.2077294E+01
2656	17	0.7231309E+01	0.1986442E+01	0.3558923E+01

2657

2658 Reading esp"s for MEP 31

2659 total number of atoms = 17

2660 total number of esp points = 838

2661

Center	X	Y	Z	
2663	1	0.7181499E+01	0.8565334E+00	0.2647765E+01
2664	2	0.6101241E+01	-0.6273493E+00	0.2689758E+01
2665	3	0.6625364E+01	0.2083272E+01	0.3343360E+00
2666	4	0.7370646E+01	0.1017729E+01	-0.1293684E+01
2667	5	0.7572716E+01	0.3922223E+01	0.3781512E+00
2668	6	0.3795462E+01	0.2452014E+01	0.0000000E+00
2669	7	0.3369897E+01	0.3448561E+01	-0.1778557E+01
2670	8	0.3036931E+01	0.3572468E+01	0.1580225E+01
2671	9	0.2689777E+01	0.0000000E+00	0.0000000E+00
2672	10	0.0000000E+00	0.0000000E+00	0.0000000E+00
2673	11	-0.7095959E+00	0.1152153E+01	-0.1580164E+01
2674	12	-0.7335255E+00	0.7975022E+00	0.1778595E+01
2675	13	-0.8271387E+00	-0.2731310E+01	-0.3344947E+00
2676	14	-0.2892961E+01	-0.2838986E+01	-0.3783099E+00
2677	15	-0.1621366E+00	-0.3848816E+01	0.1293455E+01

B.3. PEG WITH HYDROXYETHYL TERMINAL, MULTIPLE CONFORMATIONS

2678 16 0.6254804E-01 -0.3742425E+01 -0.2647986E+01
2679 17 0.1859322E+01 -0.3367611E+01 -0.2689964E+01

2680

2681 Reading esp"s for MEP 32

2682 total number of atoms = 17

2683 total number of esp points = 838

2684

2685	Center	X	Y	Z
2686	1	0.6255182E-01	-0.3742578E+01	-0.2647765E+01
2687	2	0.1859326E+01	-0.3367788E+01	-0.2689758E+01
2688	3	-0.8271387E+00	-0.2731329E+01	-0.3343360E+00
2689	4	-0.1621461E+00	-0.3848741E+01	0.1293684E+01
2690	5	-0.2892959E+01	-0.2839003E+01	-0.3781512E+00
2691	6	0.0000000E+00	0.0000000E+00	0.0000000E+00
2692	7	-0.7335198E+00	0.7975967E+00	0.1778557E+01
2693	8	-0.7096016E+00	0.1152064E+01	-0.1580225E+01
2694	9	0.2689779E+01	0.0000000E+00	0.0000000E+00
2695	10	0.3795464E+01	0.2452014E+01	0.0000000E+00
2696	11	0.3036848E+01	0.3572499E+01	0.1580164E+01
2697	12	0.3369986E+01	0.3448527E+01	-0.1778595E+01
2698	13	0.6625347E+01	0.2083279E+01	0.3344947E+00
2699	14	0.7572701E+01	0.3922230E+01	0.3783099E+00
2700	15	0.7370710E+01	0.1017689E+01	-0.1293455E+01
2701	16	0.7181361E+01	0.8565996E+00	0.2647986E+01
2702	17	0.6101082E+01	-0.6272719E+00	0.2689964E+01

2703

2704 Reading esp"s for MEP 33

2705 total number of atoms = 17

2706 total number of esp points = 827

2707

2708	Center	X	Y	Z
2709	1	0.7407913E+01	0.9460138E+00	0.2367834E+01
2710	2	0.6446606E+01	-0.6127153E+00	0.2462479E+01
2711	3	0.6620644E+01	0.2155376E+01	0.1110573E+00
2712	4	0.7258851E+01	0.1113553E+01	-0.1575387E+01
2713	5	0.7519755E+01	0.4018693E+01	0.8754156E-01
2714	6	0.3766579E+01	0.2462880E+01	0.0000000E+00
2715	7	0.3208311E+01	0.3497630E+01	-0.1720185E+01
2716	8	0.3100995E+01	0.3536429E+01	0.1653865E+01
2717	9	0.2688481E+01	0.0000000E+00	0.0000000E+00
2718	10	0.0000000E+00	0.0000000E+00	0.0000000E+00
2719	11	-0.7240598E+00	0.9262794E+00	-0.1720223E+01
2720	12	-0.7165765E+00	0.1040288E+01	0.1653816E+01
2721	13	-0.8628205E+00	-0.2737845E+01	0.1111726E+00
2722	14	-0.1643022E+00	-0.3740363E+01	-0.1575190E+01

B.3. PEG WITH HYDROXYETHYL TERMINAL, MULTIPLE CONFORMATIONS

2723 15 -0.2930305E+01 -0.2814297E+01 0.8760581E-01
2724 16 -0.7073244E-01 -0.3943894E+01 0.2368048E+01
2725 17 0.1742700E+01 -0.3688518E+01 0.2462625E+01

2726

2727 Reading esp"s for MEP 34

2728 total number of atoms = 17

2729 total number of esp points = 827

2730

2731	Center	X	Y	Z
2732	1	-0.7061528E-01	-0.3944009E+01	-0.2367834E+01
2733	2	0.1742787E+01	-0.3688431E+01	-0.2462479E+01
2734	3	-0.8627884E+00	-0.2737854E+01	-0.1110573E+00
2735	4	-0.1643192E+00	-0.3740274E+01	0.1575387E+01
2736	5	-0.2930275E+01	-0.2814314E+01	-0.8754156E-01
2737	6	0.0000000E+00	0.0000000E+00	0.0000000E+00
2738	7	-0.7240447E+00	0.9263531E+00	0.1720185E+01
2739	8	-0.7165520E+00	0.1040222E+01	-0.1653865E+01
2740	9	0.2688508E+01	0.0000000E+00	0.0000000E+00
2741	10	0.3766594E+01	0.2462857E+01	0.0000000E+00
2742	11	0.3208400E+01	0.3497592E+01	0.1720223E+01
2743	12	0.3100959E+01	0.3536454E+01	-0.1653816E+01
2744	13	0.6620664E+01	0.2155387E+01	-0.1111726E+00
2745	14	0.7258942E+01	0.1113478E+01	0.1575190E+01
2746	15	0.7519768E+01	0.4018705E+01	-0.8760581E-01
2747	16	0.7407870E+01	0.9461423E+00	-0.2368048E+01
2748	17	0.6446736E+01	-0.6126945E+00	-0.2462625E+01

2749

2750 Reading esp"s for MEP 35

2751 total number of atoms = 17

2752 total number of esp points = 762

2753

2754	Center	X	Y	Z
2755	1	0.3191796E+01	0.3130546E+01	0.4488982E+01
2756	2	0.2383649E+01	0.1476269E+01	0.4645417E+01
2757	3	0.5069003E+01	0.2912782E+01	0.2599176E+01
2758	4	0.6446298E+01	0.1419007E+01	0.3056868E+01
2759	5	0.6094313E+01	0.4714042E+01	0.2543828E+01
2760	6	0.3943388E+01	0.2378299E+01	0.0000000E+00
2761	7	0.5445293E+01	0.2291565E+01	-0.1431082E+01
2762	8	0.2636510E+01	0.3903361E+01	-0.5275189E+00
2763	9	0.2674527E+01	0.0000000E+00	0.0000000E+00
2764	10	0.0000000E+00	0.0000000E+00	0.0000000E+00
2765	11	-0.6995237E+00	-0.7193110E+00	-0.1826080E+01
2766	12	-0.7514854E+00	0.1924032E+01	0.2387215E+00
2767	13	-0.9977678E+00	-0.1704393E+01	0.2098444E+01

B.3. PEG WITH HYDROXYETHYL TERMINAL, MULTIPLE CONFORMATIONS

```
2768 14 -0.2995783E-01 -0.3527943E+01 0.2012902E+01
2769 15 -0.3030414E+01 -0.2039774E+01 0.1813092E+01
2770 16 -0.5295182E+00 -0.7491233E+00 0.4582914E+01
2771 17 -0.1594451E+01 0.7247364E+00 0.4831232E+01
```

2772

2773 Reading esp"s for MEP 36

2774 total number of atoms = 17

2775 total number of esp points = 772

2776

2777	Center	X	Y	Z
2778	1	-0.3099113E+00	0.1017213E+01	-0.4488982E+01
2779	2	0.1530039E+01	0.9515375E+00	-0.4645417E+01
2780	3	-0.1001409E+01	-0.7415247E+00	-0.2599176E+01
2781	4	-0.3317849E+00	-0.2659835E+01	-0.3056868E+01
2782	5	-0.3073265E+01	-0.7982637E+00	-0.2543828E+01
2783	6	0.0000000E+00	0.0000000E+00	0.0000000E+00
2784	7	-0.6304428E+00	-0.1365935E+01	0.1431082E+01
2785	8	-0.7303753E+00	0.1870910E+01	0.5275189E+00
2786	9	0.2695611E+01	0.0000000E+00	0.0000000E+00
2787	10	0.3954548E+01	0.2359697E+01	0.0000000E+00
2788	11	0.4918460E+01	0.2638288E+01	0.1826080E+01
2789	12	0.2610736E+01	0.3928391E+01	-0.2387215E+00
2790	13	0.5927974E+01	0.2437731E+01	-0.2098444E+01
2791	14	0.7081302E+01	0.7254753E+00	-0.2012902E+01
2792	15	0.7180670E+01	0.4073238E+01	-0.1813092E+01
2793	16	0.4864740E+01	0.2474260E+01	-0.4582914E+01
2794	17	0.4065653E+01	0.4107601E+01	-0.4831232E+01

2795

2796 Reading esp"s for MEP 37

2797 total number of atoms = 17

2798 total number of esp points = 827

2799

2800	Center	X	Y	Z
2801	1	0.7407902E+01	0.9461253E+00	0.2367976E+01
2802	2	0.6446730E+01	-0.6126888E+00	0.2462598E+01
2803	3	0.6620655E+01	0.2155363E+01	0.1111197E+00
2804	4	0.7258885E+01	0.1113447E+01	-0.1575259E+01
2805	5	0.7519762E+01	0.4018678E+01	0.8752455E-01
2806	6	0.3766585E+01	0.2462853E+01	0.0000000E+00
2807	7	0.3208373E+01	0.3497599E+01	-0.1720212E+01
2808	8	0.3100976E+01	0.3536439E+01	0.1653835E+01
2809	9	0.2688485E+01	0.0000000E+00	0.0000000E+00
2810	10	0.0000000E+00	0.0000000E+00	0.0000000E+00
2811	11	-0.7240561E+00	0.9262889E+00	-0.1720220E+01
2812	12	-0.7165746E+00	0.1040279E+01	0.1653820E+01

B.3. PEG WITH HYDROXYETHYL TERMINAL, MULTIPLE CONFORMATIONS

```
2813 13 -0.8628092E+00 -0.2737848E+01 0.1111461E+00
2814 14 -0.1642739E+00 -0.3740344E+01 -0.1575227E+01
2815 15 -0.2930292E+01 -0.2814307E+01 0.8756234E-01
2816 16 -0.7073055E-01 -0.3943913E+01 0.2368012E+01
2817 17 0.1742700E+01 -0.3688530E+01 0.2462610E+01
```

2818

2819 Reading esp"s for MEP 38

2820 total number of atoms = 17

2821 total number of esp points = 827

2822

Center	X	Y	Z	
2824	1	-0.7075323E-01	-0.3943938E+01	-0.2367976E+01
2825	2	0.1742673E+01	-0.3688528E+01	-0.2462598E+01
2826	3	-0.8628149E+00	-0.2737848E+01	-0.1111197E+00
2827	4	-0.1642777E+00	-0.3740331E+01	0.1575259E+01
2828	5	-0.2930298E+01	-0.2814297E+01	-0.8752455E-01
2829	6	0.0000000E+00	0.0000000E+00	0.0000000E+00
2830	7	-0.7240580E+00	0.9263040E+00	0.1720212E+01
2831	8	-0.7165709E+00	0.1040262E+01	-0.1653835E+01
2832	9	0.2688485E+01	0.0000000E+00	0.0000000E+00
2833	10	0.3766585E+01	0.2462855E+01	0.0000000E+00
2834	11	0.3208384E+01	0.3497592E+01	0.1720220E+01
2835	12	0.3100961E+01	0.3536448E+01	-0.1653820E+01
2836	13	0.6620651E+01	0.2155359E+01	-0.1111461E+00
2837	14	0.7258895E+01	0.1113440E+01	0.1575227E+01
2838	15	0.7519768E+01	0.4018667E+01	-0.8756234E-01
2839	16	0.7407870E+01	0.9461140E+00	-0.2368012E+01
2840	17	0.6446721E+01	-0.6127134E+00	-0.2462610E+01

2841

2842 Reading esp"s for MEP 39

2843 total number of atoms = 17

2844 total number of esp points = 827

2845

Center	X	Y	Z	
2847	1	0.7407887E+01	0.9460649E+00	0.2367942E+01
2848	2	0.6446642E+01	-0.6127040E+00	0.2462574E+01
2849	3	0.6620655E+01	0.2155357E+01	0.1111083E+00
2850	4	0.7258876E+01	0.1113470E+01	-0.1575293E+01
2851	5	0.7519777E+01	0.4018665E+01	0.8754911E-01
2852	6	0.3766587E+01	0.2462861E+01	0.0000000E+00
2853	7	0.3208358E+01	0.3497607E+01	-0.1720204E+01
2854	8	0.3100986E+01	0.3536437E+01	0.1653841E+01
2855	9	0.2688489E+01	0.0000000E+00	0.0000000E+00
2856	10	0.0000000E+00	0.0000000E+00	0.0000000E+00
2857	11	-0.7240561E+00	0.9263361E+00	-0.1720197E+01

B.3. PEG WITH HYDROXYETHYL TERMINAL, MULTIPLE CONFORMATIONS

```
2858 12 -0.7165652E+00 0.1040243E+01 0.1653847E+01
2859 13 -0.8628149E+00 -0.2737848E+01 0.1110611E+00
2860 14 -0.1643230E+00 -0.3740282E+01 -0.1575368E+01
2861 15 -0.2930300E+01 -0.2814299E+01 0.8751132E-01
2862 16 -0.7070032E-01 -0.3944019E+01 0.2367857E+01
2863 17 0.1742722E+01 -0.3688592E+01 0.2462468E+01
```

2864

2865 Reading esp"s for MEP 40

2866 total number of atoms = 17

2867 total number of esp points = 827

2868

2869	Center	X	Y	Z
2870	1	-0.7067953E-01	-0.3943949E+01	-0.2367942E+01
2871	2	0.1742735E+01	-0.3688450E+01	-0.2462574E+01
2872	3	-0.8627979E+00	-0.2737854E+01	-0.1111083E+00
2873	4	-0.1642795E+00	-0.3740314E+01	0.1575293E+01
2874	5	-0.2930281E+01	-0.2814322E+01	-0.8754911E-01
2875	6	0.0000000E+00	0.0000000E+00	0.0000000E+00
2876	7	-0.7240523E+00	0.9263191E+00	0.1720204E+01
2877	8	-0.7165671E+00	0.1040251E+01	-0.1653841E+01
2878	9	0.2688490E+01	0.0000000E+00	0.0000000E+00
2879	10	0.3766589E+01	0.2462859E+01	0.0000000E+00
2880	11	0.3208345E+01	0.3497615E+01	0.1720197E+01
2881	12	0.3100995E+01	0.3536429E+01	-0.1653847E+01
2882	13	0.6620659E+01	0.2155372E+01	-0.1110611E+00
2883	14	0.7258865E+01	0.1113519E+01	0.1575368E+01
2884	15	0.7519766E+01	0.4018688E+01	-0.8751132E-01
2885	16	0.7407960E+01	0.9460535E+00	-0.2367857E+01
2886	17	0.6446777E+01	-0.6127512E+00	-0.2462468E+01

2887

2888 Reading esp"s for MEP 41

2889 total number of atoms = 17

2890 total number of esp points = 827

2891

2892	Center	X	Y	Z
2893	1	0.7407830E+01	0.9461234E+00	0.2368086E+01
2894	2	0.6446621E+01	-0.6126700E+00	0.2462700E+01
2895	3	0.6620655E+01	0.2155370E+01	0.1112141E+00
2896	4	0.7258942E+01	0.1113464E+01	-0.1575149E+01
2897	5	0.7519756E+01	0.4018688E+01	0.8765683E-01
2898	6	0.3766589E+01	0.2462855E+01	0.0000000E+00
2899	7	0.3208433E+01	0.3497575E+01	-0.1720244E+01
2900	8	0.3100917E+01	0.3536465E+01	0.1653794E+01
2901	9	0.2688490E+01	0.0000000E+00	0.0000000E+00
2902	10	0.0000000E+00	0.0000000E+00	0.0000000E+00

B.3. PEG WITH HYDROXYETHYL TERMINAL, MULTIPLE CONFORMATIONS

```
2903 11 -0.7240523E+00 0.9261982E+00 -0.1720269E+01
2904 12 -0.7165652E+00 0.1040379E+01 0.1653763E+01
2905 13 -0.8628168E+00 -0.2737837E+01 0.1112992E+00
2906 14 -0.1643136E+00 -0.3740427E+01 -0.1575030E+01
2907 15 -0.2930302E+01 -0.2814282E+01 0.8774376E-01
2908 16 -0.7071544E-01 -0.3943788E+01 0.2368214E+01
2909 17 0.1742696E+01 -0.3688278E+01 0.2462840E+01
```

2910

2911 Reading esp"s for MEP 42

2912 total number of atoms = 17

2913 total number of esp points = 827

2914

2915	Center	X	Y	Z
2916	1	-0.7071733E-01	-0.3943871E+01	-0.2368086E+01
2917	2	0.1742705E+01	-0.3688414E+01	-0.2462700E+01
2918	3	-0.8628187E+00	-0.2737845E+01	-0.1112141E+00
2919	4	-0.1643098E+00	-0.3740372E+01	0.1575149E+01
2920	5	-0.2930302E+01	-0.2814288E+01	-0.8765683E-01
2921	6	0.0000000E+00	0.0000000E+00	0.0000000E+00
2922	7	-0.7240580E+00	0.9262416E+00	0.1720244E+01
2923	8	-0.7165709E+00	0.1040328E+01	-0.1653794E+01
2924	9	0.2688485E+01	0.0000000E+00	0.0000000E+00
2925	10	0.3766587E+01	0.2462859E+01	0.0000000E+00
2926	11	0.3208467E+01	0.3497558E+01	0.1720269E+01
2927	12	0.3100868E+01	0.3536484E+01	-0.1653763E+01
2928	13	0.6620646E+01	0.2155376E+01	-0.1112992E+00
2929	14	0.7258991E+01	0.1113451E+01	0.1575030E+01
2930	15	0.7519749E+01	0.4018693E+01	-0.8774376E-01
2931	16	0.7407752E+01	0.9461575E+00	-0.2368214E+01
2932	17	0.6446496E+01	-0.6126019E+00	-0.2462840E+01

2933

2934 Reading esp"s for MEP 43

2935 total number of atoms = 17

2936 total number of esp points = 827

2937

2938	Center	X	Y	Z
2939	1	0.7407856E+01	0.9461045E+00	0.2368019E+01
2940	2	0.6446649E+01	-0.6126870E+00	0.2462625E+01
2941	3	0.6620647E+01	0.2155376E+01	0.1111631E+00
2942	4	0.7258921E+01	0.1113491E+01	-0.1575217E+01
2943	5	0.7519747E+01	0.4018693E+01	0.8761714E-01
2944	6	0.3766583E+01	0.2462857E+01	0.0000000E+00
2945	7	0.3208390E+01	0.3497592E+01	-0.1720223E+01
2946	8	0.3100944E+01	0.3536448E+01	0.1653816E+01
2947	9	0.2688487E+01	0.0000000E+00	0.0000000E+00

B.3. PEG WITH HYDROXYETHYL TERMINAL, MULTIPLE CONFORMATIONS

```
2948 10 0.0000000E+00 0.0000000E+00 0.0000000E+00
2949 11 -0.7240561E+00 0.9262832E+00 -0.1720221E+01
2950 12 -0.7165671E+00 0.1040281E+01 0.1653822E+01
2951 13 -0.8628016E+00 -0.2737854E+01 0.1111423E+00
2952 14 -0.1643192E+00 -0.3740321E+01 -0.1575270E+01
2953 15 -0.2930289E+01 -0.2814308E+01 0.8761526E-01
2954 16 -0.7065686E-01 -0.3943949E+01 0.2367957E+01
2955 17 0.1742764E+01 -0.3688505E+01 0.2462544E+01
```

2956

2957 Reading esp"s for MEP 44

2958 total number of atoms = 17

2959 total number of esp points = 827

2960

2961	Center	X	Y	Z
2962	1	-0.7070599E-01	-0.3943909E+01	-0.2368019E+01
2963	2	0.1742715E+01	-0.3688452E+01	-0.2462625E+01
2964	3	-0.8628149E+00	-0.2737843E+01	-0.1111631E+00
2965	4	-0.1643211E+00	-0.3740350E+01	0.1575217E+01
2966	5	-0.2930300E+01	-0.2814288E+01	-0.8761714E-01
2967	6	0.0000000E+00	0.0000000E+00	0.0000000E+00
2968	7	-0.7240580E+00	0.9262794E+00	0.1720223E+01
2969	8	-0.7165671E+00	0.1040290E+01	-0.1653816E+01
2970	9	0.2688487E+01	0.0000000E+00	0.0000000E+00
2971	10	0.3766581E+01	0.2462859E+01	0.0000000E+00
2972	11	0.3208386E+01	0.3497594E+01	0.1720221E+01
2973	12	0.3100951E+01	0.3536446E+01	-0.1653822E+01
2974	13	0.6620653E+01	0.2155359E+01	-0.1111423E+00
2975	14	0.7258893E+01	0.1113502E+01	0.1575270E+01
2976	15	0.7519762E+01	0.4018674E+01	-0.8761526E-01
2977	16	0.7407873E+01	0.9460441E+00	-0.2367957E+01
2978	17	0.6446677E+01	-0.6127550E+00	-0.2462544E+01

2979

2980 Reading esp"s for MEP 45

2981 total number of atoms = 17

2982 total number of esp points = 827

2983

2984	Center	X	Y	Z
2985	1	0.7407887E+01	0.9460460E+00	0.2367942E+01
2986	2	0.6446657E+01	-0.6127304E+00	0.2462551E+01
2987	3	0.6620653E+01	0.2155359E+01	0.1111216E+00
2988	4	0.7258893E+01	0.1113496E+01	-0.1575287E+01
2989	5	0.7519762E+01	0.4018672E+01	0.8758502E-01
2990	6	0.3766585E+01	0.2462855E+01	0.0000000E+00
2991	7	0.3208373E+01	0.3497599E+01	-0.1720212E+01
2992	8	0.3100969E+01	0.3536441E+01	0.1653831E+01

B.3. PEG WITH HYDROXYETHYL TERMINAL, MULTIPLE CONFORMATIONS

```
2993      9      0.2688483E+01  0.0000000E+00  0.0000000E+00
2994     10      0.0000000E+00  0.0000000E+00  0.0000000E+00
2995     11     -0.7240580E+00  0.9262757E+00 -0.1720225E+01
2996     12     -0.7165728E+00  0.1040294E+01  0.1653814E+01
2997     13     -0.8628187E+00 -0.2737846E+01  0.1111631E+00
2998     14     -0.1643173E+00 -0.3740344E+01 -0.1575221E+01
2999     15     -0.2930304E+01 -0.2814290E+01  0.8760770E-01
3000     16     -0.7071355E-01 -0.3943915E+01  0.2368012E+01
3001     17      0.1742711E+01 -0.3688481E+01  0.2462621E+01
```

3002

3003 Reading esp"s for MEP 46

3004 total number of atoms = 17

3005 total number of esp points = 827

3006

```
3007 Center      X              Y              Z
3008      1     -0.7067764E-01 -0.3943956E+01 -0.2367942E+01
3009      2      0.1742739E+01 -0.3688479E+01 -0.2462551E+01
3010      3     -0.8628130E+00 -0.2737848E+01 -0.1111216E+00
3011      4     -0.1643268E+00 -0.3740318E+01  0.1575287E+01
3012      5     -0.2930296E+01 -0.2814299E+01 -0.8758502E-01
3013      6      0.0000000E+00  0.0000000E+00  0.0000000E+00
3014      7     -0.7240561E+00  0.9263021E+00  0.1720212E+01
3015      8     -0.7165690E+00  0.1040270E+01 -0.1653831E+01
3016      9      0.2688487E+01  0.0000000E+00  0.0000000E+00
3017     10      0.3766587E+01  0.2462852E+01  0.0000000E+00
3018     11      0.3208401E+01  0.3497586E+01  0.1720225E+01
3019     12      0.3100951E+01  0.3536450E+01 -0.1653814E+01
3020     13      0.6620657E+01  0.2155361E+01 -0.1111631E+00
3021     14      0.7258916E+01  0.1113474E+01  0.1575221E+01
3022     15      0.7519760E+01  0.4018678E+01 -0.8760770E-01
3023     16      0.7407866E+01  0.9460913E+00 -0.2368012E+01
3024     17      0.6446672E+01 -0.6127096E+00 -0.2462621E+01
```

3025 Initial ssvpot = 9.136

3026

3027

3028 Number of unique UNfrozen centers= 8

3029

3030 Non-linear optimization requested.

3031 qchnge = 0.1082214511E-01

3032 qchnge = 0.3505139925E-03

3033 qchnge = 0.1954413601E-04

3034 qchnge = 0.1271240293E-05

3035 qchnge = 0.8533682420E-07

3036

3037 Convergence in 4 iterations

B.3. PEG WITH HYDROXYETHYL TERMINAL, MULTIPLE CONFORMATIONS

3038
3039 1 PEG2 nconf=1 norient=1 nmep=1/46
3040 2 PEG2 nconf=1 norient=2 nmep=2/46
3041 3 PEG2 nconf=2 norient=1 nmep=3/46
3042 4 PEG2 nconf=2 norient=2 nmep=4/46
3043 5 PEG2 nconf=3 norient=1 nmep=5/46
3044 6 PEG2 nconf=3 norient=2 nmep=6/46
3045 7 PEG2 nconf=4 norient=1 nmep=7/46
3046 8 PEG2 nconf=4 norient=2 nmep=8/46
3047 9 PEG2 nconf=5 norient=1 nmep=9/46
3048 10 PEG2 nconf=5 norient=2 nmep=10/46
3049 11 PEG2 nconf=6 norient=1 nmep=11/46
3050 12 PEG2 nconf=6 norient=2 nmep=12/46
3051 13 PEG2 nconf=7 norient=1 nmep=13/46
3052 14 PEG2 nconf=7 norient=2 nmep=14/46
3053 15 PEG2 nconf=8 norient=1 nmep=15/46
3054 16 PEG2 nconf=8 norient=2 nmep=16/46
3055 17 PEG2 nconf=9 norient=1 nmep=17/46
3056 18 PEG2 nconf=9 norient=2 nmep=18/46
3057 19 PEG2 nconf=10 norient=1 nmep=19/46
3058 20 PEG2 nconf=10 norient=2 nmep=20/46
3059 21 PEG2 nconf=11 norient=1 nmep=21/46
3060 22 PEG2 nconf=11 norient=2 nmep=22/46
3061 23 PEG2 nconf=12 norient=1 nmep=23/46
3062 24 PEG2 nconf=12 norient=2 nmep=24/46
3063 25 PEG2 nconf=13 norient=1 nmep=25/46
3064 26 PEG2 nconf=13 norient=2 nmep=26/46
3065 27 PEG2 nconf=14 norient=1 nmep=27/46
3066 28 PEG2 nconf=14 norient=2 nmep=28/46
3067 29 PEG2 nconf=15 norient=1 nmep=29/46
3068 30 PEG2 nconf=15 norient=2 nmep=30/46
3069 31 PEG2 nconf=16 norient=1 nmep=31/46
3070 32 PEG2 nconf=16 norient=2 nmep=32/46
3071 33 PEG2 nconf=17 norient=1 nmep=33/46
3072 34 PEG2 nconf=17 norient=2 nmep=34/46
3073 35 PEG2 nconf=18 norient=1 nmep=35/46
3074 36 PEG2 nconf=18 norient=2 nmep=36/46
3075 37 PEG2 nconf=19 norient=1 nmep=37/46
3076 38 PEG2 nconf=19 norient=2 nmep=38/46
3077 39 PEG2 nconf=20 norient=1 nmep=39/46
3078 40 PEG2 nconf=20 norient=2 nmep=40/46
3079 41 PEG2 nconf=21 norient=1 nmep=41/46
3080 42 PEG2 nconf=21 norient=2 nmep=42/46
3081 43 PEG2 nconf=22 norient=1 nmep=43/46
3082 44 PEG2 nconf=22 norient=2 nmep=44/46

B.3. PEG WITH HYDROXYETHYL TERMINAL, MULTIPLE CONFORMATIONS

3083 45 PEG2 nconf=23 norient=1 nmep=45/46
 3084 46 PEG2 nconf=23 norient=2 nmep=46/46

3085

3086 Point Charges Before & After Optimization

3087

3088	no.	At.no.	q(init)	q(opt)	ivary	d(rstr)/dq
3089	1	8	-0.576790	-0.576790	-1	0.001708
3090	2	1	0.360115	0.360115	-1	0.000000
3091	3	6	0.256038	0.335117	0	0.002859
3092	4	1	-0.000496	0.004532	0	0.000000
3093	5	1	0.057037	0.004532	4	0.000000
3094	6	6	-0.346939	-0.459651	0	0.002126
3095	7	1	0.118234	0.175573	0	0.000000
3096	8	1	0.151800	0.175573	7	0.000000
3097	9	8	-0.141500	-0.141500	-1	0.005771
3098	10	6	0.030353	0.040572	0	0.009266
3099	11	1	0.092801	0.086505	0	0.000000
3100	12	1	0.096057	0.086505	11	0.000000
3101	13	6	-0.507366	-0.496118	0	0.001976
3102	14	1	0.203097	0.212018	0	0.000000
3103	15	1	0.226558	0.212018	14	0.000000
3104	16	8	-0.376457	-0.376457	-1	0.002567
3105	17	1	0.357457	0.357457	-1	0.000000
3106						
3107	18	8	-0.576790	-0.576790	-1	0.001708
3108	19	1	0.360115	0.360115	-1	0.000000
3109	20	6	0.256038	0.335117	3	0.002859
3110	21	1	-0.000496	0.004532	4	0.000000
3111	22	1	0.057037	0.004532	4	0.000000
3112	23	6	-0.346939	-0.459651	6	0.002126
3113	24	1	0.118234	0.175573	7	0.000000
3114	25	1	0.151800	0.175573	7	0.000000
3115	26	8	-0.141500	-0.141500	-1	0.005771
3116	27	6	0.030353	0.040572	10	0.009266
3117	28	1	0.092801	0.086505	11	0.000000
3118	29	1	0.096057	0.086505	11	0.000000
3119	30	6	-0.507366	-0.496118	13	0.001976
3120	31	1	0.203097	0.212018	14	0.000000
3121	32	1	0.226558	0.212018	14	0.000000
3122	33	8	-0.376457	-0.376457	-1	0.002567
3123	34	1	0.357457	0.357457	-1	0.000000
3124						
3125	35	8	-0.576790	-0.576790	-1	0.001708
3126	36	1	0.360115	0.360115	-1	0.000000
3127	37	6	0.256038	0.335117	3	0.002859

B.3. PEG WITH HYDROXYETHYL TERMINAL, MULTIPLE CONFORMATIONS

3128	38	1	-0.000496	0.004532	4	0.000000
3129	39	1	0.057037	0.004532	4	0.000000
3130	40	6	-0.346939	-0.459651	6	0.002126
3131	41	1	0.118234	0.175573	7	0.000000
3132	42	1	0.151800	0.175573	7	0.000000
3133	43	8	-0.141500	-0.141500	-1	0.005771
3134	44	6	0.030353	0.040572	10	0.009266
3135	45	1	0.092801	0.086505	11	0.000000
3136	46	1	0.096057	0.086505	11	0.000000
3137	47	6	-0.507366	-0.496118	13	0.001976
3138	48	1	0.203097	0.212018	14	0.000000
3139	49	1	0.226558	0.212018	14	0.000000
3140	50	8	-0.376457	-0.376457	-1	0.002567
3141	51	1	0.357457	0.357457	-1	0.000000
3142						
3143	52	8	-0.576790	-0.576790	-1	0.001708
3144	53	1	0.360115	0.360115	-1	0.000000
3145	54	6	0.256038	0.335117	3	0.002859
3146	55	1	-0.000496	0.004532	4	0.000000
3147	56	1	0.057037	0.004532	4	0.000000
3148	57	6	-0.346939	-0.459651	6	0.002126
3149	58	1	0.118234	0.175573	7	0.000000
3150	59	1	0.151800	0.175573	7	0.000000
3151	60	8	-0.141500	-0.141500	-1	0.005771
3152	61	6	0.030353	0.040572	10	0.009266
3153	62	1	0.092801	0.086505	11	0.000000
3154	63	1	0.096057	0.086505	11	0.000000
3155	64	6	-0.507366	-0.496118	13	0.001976
3156	65	1	0.203097	0.212018	14	0.000000
3157	66	1	0.226558	0.212018	14	0.000000
3158	67	8	-0.376457	-0.376457	-1	0.002567
3159	68	1	0.357457	0.357457	-1	0.000000
3160						
3161	69	8	-0.576790	-0.576790	-1	0.001708
3162	70	1	0.360115	0.360115	-1	0.000000
3163	71	6	0.256038	0.335117	3	0.002859
3164	72	1	-0.000496	0.004532	4	0.000000
3165	73	1	0.057037	0.004532	4	0.000000
3166	74	6	-0.346939	-0.459651	6	0.002126
3167	75	1	0.118234	0.175573	7	0.000000
3168	76	1	0.151800	0.175573	7	0.000000
3169	77	8	-0.141500	-0.141500	-1	0.005771
3170	78	6	0.030353	0.040572	10	0.009266
3171	79	1	0.092801	0.086505	11	0.000000
3172	80	1	0.096057	0.086505	11	0.000000

B.3. PEG WITH HYDROXYETHYL TERMINAL, MULTIPLE CONFORMATIONS

3173	81	6	-0.507366	-0.496118	13	0.001976
3174	82	1	0.203097	0.212018	14	0.000000
3175	83	1	0.226558	0.212018	14	0.000000
3176	84	8	-0.376457	-0.376457	-1	0.002567
3177	85	1	0.357457	0.357457	-1	0.000000
3178						
3179	86	8	-0.576790	-0.576790	-1	0.001708
3180	87	1	0.360115	0.360115	-1	0.000000
3181	88	6	0.256038	0.335117	3	0.002859
3182	89	1	-0.000496	0.004532	4	0.000000
3183	90	1	0.057037	0.004532	4	0.000000
3184	91	6	-0.346939	-0.459651	6	0.002126
3185	92	1	0.118234	0.175573	7	0.000000
3186	93	1	0.151800	0.175573	7	0.000000
3187	94	8	-0.141500	-0.141500	-1	0.005771
3188	95	6	0.030353	0.040572	10	0.009266
3189	96	1	0.092801	0.086505	11	0.000000
3190	97	1	0.096057	0.086505	11	0.000000
3191	98	6	-0.507366	-0.496118	13	0.001976
3192	99	1	0.203097	0.212018	14	0.000000
3193	100	1	0.226558	0.212018	14	0.000000
3194	101	8	-0.376457	-0.376457	-1	0.002567
3195	102	1	0.357457	0.357457	-1	0.000000
3196						
3197	103	8	-0.576790	-0.576790	-1	0.001708
3198	104	1	0.360115	0.360115	-1	0.000000
3199	105	6	0.256038	0.335117	3	0.002859
3200	106	1	-0.000496	0.004532	4	0.000000
3201	107	1	0.057037	0.004532	4	0.000000
3202	108	6	-0.346939	-0.459651	6	0.002126
3203	109	1	0.118234	0.175573	7	0.000000
3204	110	1	0.151800	0.175573	7	0.000000
3205	111	8	-0.141500	-0.141500	-1	0.005771
3206	112	6	0.030353	0.040572	10	0.009266
3207	113	1	0.092801	0.086505	11	0.000000
3208	114	1	0.096057	0.086505	11	0.000000
3209	115	6	-0.507366	-0.496118	13	0.001976
3210	116	1	0.203097	0.212018	14	0.000000
3211	117	1	0.226558	0.212018	14	0.000000
3212	118	8	-0.376457	-0.376457	-1	0.002567
3213	119	1	0.357457	0.357457	-1	0.000000
3214						
3215	120	8	-0.576790	-0.576790	-1	0.001708
3216	121	1	0.360115	0.360115	-1	0.000000
3217	122	6	0.256038	0.335117	3	0.002859

B.3. PEG WITH HYDROXYETHYL TERMINAL, MULTIPLE CONFORMATIONS

3218	123	1	-0.000496	0.004532	4	0.000000
3219	124	1	0.057037	0.004532	4	0.000000
3220	125	6	-0.346939	-0.459651	6	0.002126
3221	126	1	0.118234	0.175573	7	0.000000
3222	127	1	0.151800	0.175573	7	0.000000
3223	128	8	-0.141500	-0.141500	-1	0.005771
3224	129	6	0.030353	0.040572	10	0.009266
3225	130	1	0.092801	0.086505	11	0.000000
3226	131	1	0.096057	0.086505	11	0.000000
3227	132	6	-0.507366	-0.496118	13	0.001976
3228	133	1	0.203097	0.212018	14	0.000000
3229	134	1	0.226558	0.212018	14	0.000000
3230	135	8	-0.376457	-0.376457	-1	0.002567
3231	136	1	0.357457	0.357457	-1	0.000000
3232						
3233	137	8	-0.576790	-0.576790	-1	0.001708
3234	138	1	0.360115	0.360115	-1	0.000000
3235	139	6	0.256038	0.335117	3	0.002859
3236	140	1	-0.000496	0.004532	4	0.000000
3237	141	1	0.057037	0.004532	4	0.000000
3238	142	6	-0.346939	-0.459651	6	0.002126
3239	143	1	0.118234	0.175573	7	0.000000
3240	144	1	0.151800	0.175573	7	0.000000
3241	145	8	-0.141500	-0.141500	-1	0.005771
3242	146	6	0.030353	0.040572	10	0.009266
3243	147	1	0.092801	0.086505	11	0.000000
3244	148	1	0.096057	0.086505	11	0.000000
3245	149	6	-0.507366	-0.496118	13	0.001976
3246	150	1	0.203097	0.212018	14	0.000000
3247	151	1	0.226558	0.212018	14	0.000000
3248	152	8	-0.376457	-0.376457	-1	0.002567
3249	153	1	0.357457	0.357457	-1	0.000000
3250						
3251	154	8	-0.576790	-0.576790	-1	0.001708
3252	155	1	0.360115	0.360115	-1	0.000000
3253	156	6	0.256038	0.335117	3	0.002859
3254	157	1	-0.000496	0.004532	4	0.000000
3255	158	1	0.057037	0.004532	4	0.000000
3256	159	6	-0.346939	-0.459651	6	0.002126
3257	160	1	0.118234	0.175573	7	0.000000
3258	161	1	0.151800	0.175573	7	0.000000
3259	162	8	-0.141500	-0.141500	-1	0.005771
3260	163	6	0.030353	0.040572	10	0.009266
3261	164	1	0.092801	0.086505	11	0.000000
3262	165	1	0.096057	0.086505	11	0.000000

B.3. PEG WITH HYDROXYETHYL TERMINAL, MULTIPLE CONFORMATIONS

3263	166	6	-0.507366	-0.496118	13	0.001976
3264	167	1	0.203097	0.212018	14	0.000000
3265	168	1	0.226558	0.212018	14	0.000000
3266	169	8	-0.376457	-0.376457	-1	0.002567
3267	170	1	0.357457	0.357457	-1	0.000000
3268						
3269	171	8	-0.576790	-0.576790	-1	0.001708
3270	172	1	0.360115	0.360115	-1	0.000000
3271	173	6	0.256038	0.335117	3	0.002859
3272	174	1	-0.000496	0.004532	4	0.000000
3273	175	1	0.057037	0.004532	4	0.000000
3274	176	6	-0.346939	-0.459651	6	0.002126
3275	177	1	0.118234	0.175573	7	0.000000
3276	178	1	0.151800	0.175573	7	0.000000
3277	179	8	-0.141500	-0.141500	-1	0.005771
3278	180	6	0.030353	0.040572	10	0.009266
3279	181	1	0.092801	0.086505	11	0.000000
3280	182	1	0.096057	0.086505	11	0.000000
3281	183	6	-0.507366	-0.496118	13	0.001976
3282	184	1	0.203097	0.212018	14	0.000000
3283	185	1	0.226558	0.212018	14	0.000000
3284	186	8	-0.376457	-0.376457	-1	0.002567
3285	187	1	0.357457	0.357457	-1	0.000000
3286						
3287	188	8	-0.576790	-0.576790	-1	0.001708
3288	189	1	0.360115	0.360115	-1	0.000000
3289	190	6	0.256038	0.335117	3	0.002859
3290	191	1	-0.000496	0.004532	4	0.000000
3291	192	1	0.057037	0.004532	4	0.000000
3292	193	6	-0.346939	-0.459651	6	0.002126
3293	194	1	0.118234	0.175573	7	0.000000
3294	195	1	0.151800	0.175573	7	0.000000
3295	196	8	-0.141500	-0.141500	-1	0.005771
3296	197	6	0.030353	0.040572	10	0.009266
3297	198	1	0.092801	0.086505	11	0.000000
3298	199	1	0.096057	0.086505	11	0.000000
3299	200	6	-0.507366	-0.496118	13	0.001976
3300	201	1	0.203097	0.212018	14	0.000000
3301	202	1	0.226558	0.212018	14	0.000000
3302	203	8	-0.376457	-0.376457	-1	0.002567
3303	204	1	0.357457	0.357457	-1	0.000000
3304						
3305	205	8	-0.576790	-0.576790	-1	0.001708
3306	206	1	0.360115	0.360115	-1	0.000000
3307	207	6	0.256038	0.335117	3	0.002859

B.3. PEG WITH HYDROXYETHYL TERMINAL, MULTIPLE CONFORMATIONS

3308	208	1	-0.000496	0.004532	4	0.000000
3309	209	1	0.057037	0.004532	4	0.000000
3310	210	6	-0.346939	-0.459651	6	0.002126
3311	211	1	0.118234	0.175573	7	0.000000
3312	212	1	0.151800	0.175573	7	0.000000
3313	213	8	-0.141500	-0.141500	-1	0.005771
3314	214	6	0.030353	0.040572	10	0.009266
3315	215	1	0.092801	0.086505	11	0.000000
3316	216	1	0.096057	0.086505	11	0.000000
3317	217	6	-0.507366	-0.496118	13	0.001976
3318	218	1	0.203097	0.212018	14	0.000000
3319	219	1	0.226558	0.212018	14	0.000000
3320	220	8	-0.376457	-0.376457	-1	0.002567
3321	221	1	0.357457	0.357457	-1	0.000000
3322						
3323	222	8	-0.576790	-0.576790	-1	0.001708
3324	223	1	0.360115	0.360115	-1	0.000000
3325	224	6	0.256038	0.335117	3	0.002859
3326	225	1	-0.000496	0.004532	4	0.000000
3327	226	1	0.057037	0.004532	4	0.000000
3328	227	6	-0.346939	-0.459651	6	0.002126
3329	228	1	0.118234	0.175573	7	0.000000
3330	229	1	0.151800	0.175573	7	0.000000
3331	230	8	-0.141500	-0.141500	-1	0.005771
3332	231	6	0.030353	0.040572	10	0.009266
3333	232	1	0.092801	0.086505	11	0.000000
3334	233	1	0.096057	0.086505	11	0.000000
3335	234	6	-0.507366	-0.496118	13	0.001976
3336	235	1	0.203097	0.212018	14	0.000000
3337	236	1	0.226558	0.212018	14	0.000000
3338	237	8	-0.376457	-0.376457	-1	0.002567
3339	238	1	0.357457	0.357457	-1	0.000000
3340						
3341	239	8	-0.576790	-0.576790	-1	0.001708
3342	240	1	0.360115	0.360115	-1	0.000000
3343	241	6	0.256038	0.335117	3	0.002859
3344	242	1	-0.000496	0.004532	4	0.000000
3345	243	1	0.057037	0.004532	4	0.000000
3346	244	6	-0.346939	-0.459651	6	0.002126
3347	245	1	0.118234	0.175573	7	0.000000
3348	246	1	0.151800	0.175573	7	0.000000
3349	247	8	-0.141500	-0.141500	-1	0.005771
3350	248	6	0.030353	0.040572	10	0.009266
3351	249	1	0.092801	0.086505	11	0.000000
3352	250	1	0.096057	0.086505	11	0.000000

B.3. PEG WITH HYDROXYETHYL TERMINAL, MULTIPLE CONFORMATIONS

3353	251	6	-0.507366	-0.496118	13	0.001976
3354	252	1	0.203097	0.212018	14	0.000000
3355	253	1	0.226558	0.212018	14	0.000000
3356	254	8	-0.376457	-0.376457	-1	0.002567
3357	255	1	0.357457	0.357457	-1	0.000000
3358						
3359	256	8	-0.576790	-0.576790	-1	0.001708
3360	257	1	0.360115	0.360115	-1	0.000000
3361	258	6	0.256038	0.335117	3	0.002859
3362	259	1	-0.000496	0.004532	4	0.000000
3363	260	1	0.057037	0.004532	4	0.000000
3364	261	6	-0.346939	-0.459651	6	0.002126
3365	262	1	0.118234	0.175573	7	0.000000
3366	263	1	0.151800	0.175573	7	0.000000
3367	264	8	-0.141500	-0.141500	-1	0.005771
3368	265	6	0.030353	0.040572	10	0.009266
3369	266	1	0.092801	0.086505	11	0.000000
3370	267	1	0.096057	0.086505	11	0.000000
3371	268	6	-0.507366	-0.496118	13	0.001976
3372	269	1	0.203097	0.212018	14	0.000000
3373	270	1	0.226558	0.212018	14	0.000000
3374	271	8	-0.376457	-0.376457	-1	0.002567
3375	272	1	0.357457	0.357457	-1	0.000000
3376						
3377	273	8	-0.576790	-0.576790	-1	0.001708
3378	274	1	0.360115	0.360115	-1	0.000000
3379	275	6	0.256038	0.335117	3	0.002859
3380	276	1	-0.000496	0.004532	4	0.000000
3381	277	1	0.057037	0.004532	4	0.000000
3382	278	6	-0.346939	-0.459651	6	0.002126
3383	279	1	0.118234	0.175573	7	0.000000
3384	280	1	0.151800	0.175573	7	0.000000
3385	281	8	-0.141500	-0.141500	-1	0.005771
3386	282	6	0.030353	0.040572	10	0.009266
3387	283	1	0.092801	0.086505	11	0.000000
3388	284	1	0.096057	0.086505	11	0.000000
3389	285	6	-0.507366	-0.496118	13	0.001976
3390	286	1	0.203097	0.212018	14	0.000000
3391	287	1	0.226558	0.212018	14	0.000000
3392	288	8	-0.376457	-0.376457	-1	0.002567
3393	289	1	0.357457	0.357457	-1	0.000000
3394						
3395	290	8	-0.576790	-0.576790	-1	0.001708
3396	291	1	0.360115	0.360115	-1	0.000000
3397	292	6	0.256038	0.335117	3	0.002859

B.3. PEG WITH HYDROXYETHYL TERMINAL, MULTIPLE CONFORMATIONS

3398	293	1	-0.000496	0.004532	4	0.000000
3399	294	1	0.057037	0.004532	4	0.000000
3400	295	6	-0.346939	-0.459651	6	0.002126
3401	296	1	0.118234	0.175573	7	0.000000
3402	297	1	0.151800	0.175573	7	0.000000
3403	298	8	-0.141500	-0.141500	-1	0.005771
3404	299	6	0.030353	0.040572	10	0.009266
3405	300	1	0.092801	0.086505	11	0.000000
3406	301	1	0.096057	0.086505	11	0.000000
3407	302	6	-0.507366	-0.496118	13	0.001976
3408	303	1	0.203097	0.212018	14	0.000000
3409	304	1	0.226558	0.212018	14	0.000000
3410	305	8	-0.376457	-0.376457	-1	0.002567
3411	306	1	0.357457	0.357457	-1	0.000000
3412						
3413	307	8	-0.576790	-0.576790	-1	0.001708
3414	308	1	0.360115	0.360115	-1	0.000000
3415	309	6	0.256038	0.335117	3	0.002859
3416	310	1	-0.000496	0.004532	4	0.000000
3417	311	1	0.057037	0.004532	4	0.000000
3418	312	6	-0.346939	-0.459651	6	0.002126
3419	313	1	0.118234	0.175573	7	0.000000
3420	314	1	0.151800	0.175573	7	0.000000
3421	315	8	-0.141500	-0.141500	-1	0.005771
3422	316	6	0.030353	0.040572	10	0.009266
3423	317	1	0.092801	0.086505	11	0.000000
3424	318	1	0.096057	0.086505	11	0.000000
3425	319	6	-0.507366	-0.496118	13	0.001976
3426	320	1	0.203097	0.212018	14	0.000000
3427	321	1	0.226558	0.212018	14	0.000000
3428	322	8	-0.376457	-0.376457	-1	0.002567
3429	323	1	0.357457	0.357457	-1	0.000000
3430						
3431	324	8	-0.576790	-0.576790	-1	0.001708
3432	325	1	0.360115	0.360115	-1	0.000000
3433	326	6	0.256038	0.335117	3	0.002859
3434	327	1	-0.000496	0.004532	4	0.000000
3435	328	1	0.057037	0.004532	4	0.000000
3436	329	6	-0.346939	-0.459651	6	0.002126
3437	330	1	0.118234	0.175573	7	0.000000
3438	331	1	0.151800	0.175573	7	0.000000
3439	332	8	-0.141500	-0.141500	-1	0.005771
3440	333	6	0.030353	0.040572	10	0.009266
3441	334	1	0.092801	0.086505	11	0.000000
3442	335	1	0.096057	0.086505	11	0.000000

B.3. PEG WITH HYDROXYETHYL TERMINAL, MULTIPLE CONFORMATIONS

3443	336	6	-0.507366	-0.496118	13	0.001976
3444	337	1	0.203097	0.212018	14	0.000000
3445	338	1	0.226558	0.212018	14	0.000000
3446	339	8	-0.376457	-0.376457	-1	0.002567
3447	340	1	0.357457	0.357457	-1	0.000000
3448						
3449	341	8	-0.576790	-0.576790	-1	0.001708
3450	342	1	0.360115	0.360115	-1	0.000000
3451	343	6	0.256038	0.335117	3	0.002859
3452	344	1	-0.000496	0.004532	4	0.000000
3453	345	1	0.057037	0.004532	4	0.000000
3454	346	6	-0.346939	-0.459651	6	0.002126
3455	347	1	0.118234	0.175573	7	0.000000
3456	348	1	0.151800	0.175573	7	0.000000
3457	349	8	-0.141500	-0.141500	-1	0.005771
3458	350	6	0.030353	0.040572	10	0.009266
3459	351	1	0.092801	0.086505	11	0.000000
3460	352	1	0.096057	0.086505	11	0.000000
3461	353	6	-0.507366	-0.496118	13	0.001976
3462	354	1	0.203097	0.212018	14	0.000000
3463	355	1	0.226558	0.212018	14	0.000000
3464	356	8	-0.376457	-0.376457	-1	0.002567
3465	357	1	0.357457	0.357457	-1	0.000000
3466						
3467	358	8	-0.576790	-0.576790	-1	0.001708
3468	359	1	0.360115	0.360115	-1	0.000000
3469	360	6	0.256038	0.335117	3	0.002859
3470	361	1	-0.000496	0.004532	4	0.000000
3471	362	1	0.057037	0.004532	4	0.000000
3472	363	6	-0.346939	-0.459651	6	0.002126
3473	364	1	0.118234	0.175573	7	0.000000
3474	365	1	0.151800	0.175573	7	0.000000
3475	366	8	-0.141500	-0.141500	-1	0.005771
3476	367	6	0.030353	0.040572	10	0.009266
3477	368	1	0.092801	0.086505	11	0.000000
3478	369	1	0.096057	0.086505	11	0.000000
3479	370	6	-0.507366	-0.496118	13	0.001976
3480	371	1	0.203097	0.212018	14	0.000000
3481	372	1	0.226558	0.212018	14	0.000000
3482	373	8	-0.376457	-0.376457	-1	0.002567
3483	374	1	0.357457	0.357457	-1	0.000000
3484						
3485	375	8	-0.576790	-0.576790	-1	0.001708
3486	376	1	0.360115	0.360115	-1	0.000000
3487	377	6	0.256038	0.335117	3	0.002859

B.3. PEG WITH HYDROXYETHYL TERMINAL, MULTIPLE CONFORMATIONS

3488	378	1	-0.000496	0.004532	4	0.000000
3489	379	1	0.057037	0.004532	4	0.000000
3490	380	6	-0.346939	-0.459651	6	0.002126
3491	381	1	0.118234	0.175573	7	0.000000
3492	382	1	0.151800	0.175573	7	0.000000
3493	383	8	-0.141500	-0.141500	-1	0.005771
3494	384	6	0.030353	0.040572	10	0.009266
3495	385	1	0.092801	0.086505	11	0.000000
3496	386	1	0.096057	0.086505	11	0.000000
3497	387	6	-0.507366	-0.496118	13	0.001976
3498	388	1	0.203097	0.212018	14	0.000000
3499	389	1	0.226558	0.212018	14	0.000000
3500	390	8	-0.376457	-0.376457	-1	0.002567
3501	391	1	0.357457	0.357457	-1	0.000000
3502						
3503	392	8	-0.576790	-0.576790	-1	0.001708
3504	393	1	0.360115	0.360115	-1	0.000000
3505	394	6	0.256038	0.335117	3	0.002859
3506	395	1	-0.000496	0.004532	4	0.000000
3507	396	1	0.057037	0.004532	4	0.000000
3508	397	6	-0.346939	-0.459651	6	0.002126
3509	398	1	0.118234	0.175573	7	0.000000
3510	399	1	0.151800	0.175573	7	0.000000
3511	400	8	-0.141500	-0.141500	-1	0.005771
3512	401	6	0.030353	0.040572	10	0.009266
3513	402	1	0.092801	0.086505	11	0.000000
3514	403	1	0.096057	0.086505	11	0.000000
3515	404	6	-0.507366	-0.496118	13	0.001976
3516	405	1	0.203097	0.212018	14	0.000000
3517	406	1	0.226558	0.212018	14	0.000000
3518	407	8	-0.376457	-0.376457	-1	0.002567
3519	408	1	0.357457	0.357457	-1	0.000000
3520						
3521	409	8	-0.576790	-0.576790	-1	0.001708
3522	410	1	0.360115	0.360115	-1	0.000000
3523	411	6	0.256038	0.335117	3	0.002859
3524	412	1	-0.000496	0.004532	4	0.000000
3525	413	1	0.057037	0.004532	4	0.000000
3526	414	6	-0.346939	-0.459651	6	0.002126
3527	415	1	0.118234	0.175573	7	0.000000
3528	416	1	0.151800	0.175573	7	0.000000
3529	417	8	-0.141500	-0.141500	-1	0.005771
3530	418	6	0.030353	0.040572	10	0.009266
3531	419	1	0.092801	0.086505	11	0.000000
3532	420	1	0.096057	0.086505	11	0.000000

B.3. PEG WITH HYDROXYETHYL TERMINAL, MULTIPLE CONFORMATIONS

3533	421	6	-0.507366	-0.496118	13	0.001976
3534	422	1	0.203097	0.212018	14	0.000000
3535	423	1	0.226558	0.212018	14	0.000000
3536	424	8	-0.376457	-0.376457	-1	0.002567
3537	425	1	0.357457	0.357457	-1	0.000000
3538						
3539	426	8	-0.576790	-0.576790	-1	0.001708
3540	427	1	0.360115	0.360115	-1	0.000000
3541	428	6	0.256038	0.335117	3	0.002859
3542	429	1	-0.000496	0.004532	4	0.000000
3543	430	1	0.057037	0.004532	4	0.000000
3544	431	6	-0.346939	-0.459651	6	0.002126
3545	432	1	0.118234	0.175573	7	0.000000
3546	433	1	0.151800	0.175573	7	0.000000
3547	434	8	-0.141500	-0.141500	-1	0.005771
3548	435	6	0.030353	0.040572	10	0.009266
3549	436	1	0.092801	0.086505	11	0.000000
3550	437	1	0.096057	0.086505	11	0.000000
3551	438	6	-0.507366	-0.496118	13	0.001976
3552	439	1	0.203097	0.212018	14	0.000000
3553	440	1	0.226558	0.212018	14	0.000000
3554	441	8	-0.376457	-0.376457	-1	0.002567
3555	442	1	0.357457	0.357457	-1	0.000000
3556						
3557	443	8	-0.576790	-0.576790	-1	0.001708
3558	444	1	0.360115	0.360115	-1	0.000000
3559	445	6	0.256038	0.335117	3	0.002859
3560	446	1	-0.000496	0.004532	4	0.000000
3561	447	1	0.057037	0.004532	4	0.000000
3562	448	6	-0.346939	-0.459651	6	0.002126
3563	449	1	0.118234	0.175573	7	0.000000
3564	450	1	0.151800	0.175573	7	0.000000
3565	451	8	-0.141500	-0.141500	-1	0.005771
3566	452	6	0.030353	0.040572	10	0.009266
3567	453	1	0.092801	0.086505	11	0.000000
3568	454	1	0.096057	0.086505	11	0.000000
3569	455	6	-0.507366	-0.496118	13	0.001976
3570	456	1	0.203097	0.212018	14	0.000000
3571	457	1	0.226558	0.212018	14	0.000000
3572	458	8	-0.376457	-0.376457	-1	0.002567
3573	459	1	0.357457	0.357457	-1	0.000000
3574						
3575	460	8	-0.576790	-0.576790	-1	0.001708
3576	461	1	0.360115	0.360115	-1	0.000000
3577	462	6	0.256038	0.335117	3	0.002859

B.3. PEG WITH HYDROXYETHYL TERMINAL, MULTIPLE CONFORMATIONS

3578	463	1	-0.000496	0.004532	4	0.000000
3579	464	1	0.057037	0.004532	4	0.000000
3580	465	6	-0.346939	-0.459651	6	0.002126
3581	466	1	0.118234	0.175573	7	0.000000
3582	467	1	0.151800	0.175573	7	0.000000
3583	468	8	-0.141500	-0.141500	-1	0.005771
3584	469	6	0.030353	0.040572	10	0.009266
3585	470	1	0.092801	0.086505	11	0.000000
3586	471	1	0.096057	0.086505	11	0.000000
3587	472	6	-0.507366	-0.496118	13	0.001976
3588	473	1	0.203097	0.212018	14	0.000000
3589	474	1	0.226558	0.212018	14	0.000000
3590	475	8	-0.376457	-0.376457	-1	0.002567
3591	476	1	0.357457	0.357457	-1	0.000000
3592						
3593	477	8	-0.576790	-0.576790	-1	0.001708
3594	478	1	0.360115	0.360115	-1	0.000000
3595	479	6	0.256038	0.335117	3	0.002859
3596	480	1	-0.000496	0.004532	4	0.000000
3597	481	1	0.057037	0.004532	4	0.000000
3598	482	6	-0.346939	-0.459651	6	0.002126
3599	483	1	0.118234	0.175573	7	0.000000
3600	484	1	0.151800	0.175573	7	0.000000
3601	485	8	-0.141500	-0.141500	-1	0.005771
3602	486	6	0.030353	0.040572	10	0.009266
3603	487	1	0.092801	0.086505	11	0.000000
3604	488	1	0.096057	0.086505	11	0.000000
3605	489	6	-0.507366	-0.496118	13	0.001976
3606	490	1	0.203097	0.212018	14	0.000000
3607	491	1	0.226558	0.212018	14	0.000000
3608	492	8	-0.376457	-0.376457	-1	0.002567
3609	493	1	0.357457	0.357457	-1	0.000000
3610						
3611	494	8	-0.576790	-0.576790	-1	0.001708
3612	495	1	0.360115	0.360115	-1	0.000000
3613	496	6	0.256038	0.335117	3	0.002859
3614	497	1	-0.000496	0.004532	4	0.000000
3615	498	1	0.057037	0.004532	4	0.000000
3616	499	6	-0.346939	-0.459651	6	0.002126
3617	500	1	0.118234	0.175573	7	0.000000
3618	501	1	0.151800	0.175573	7	0.000000
3619	502	8	-0.141500	-0.141500	-1	0.005771
3620	503	6	0.030353	0.040572	10	0.009266
3621	504	1	0.092801	0.086505	11	0.000000
3622	505	1	0.096057	0.086505	11	0.000000

B.3. PEG WITH HYDROXYETHYL TERMINAL, MULTIPLE CONFORMATIONS

3623	506	6	-0.507366	-0.496118	13	0.001976
3624	507	1	0.203097	0.212018	14	0.000000
3625	508	1	0.226558	0.212018	14	0.000000
3626	509	8	-0.376457	-0.376457	-1	0.002567
3627	510	1	0.357457	0.357457	-1	0.000000
3628						
3629	511	8	-0.576790	-0.576790	-1	0.001708
3630	512	1	0.360115	0.360115	-1	0.000000
3631	513	6	0.256038	0.335117	3	0.002859
3632	514	1	-0.000496	0.004532	4	0.000000
3633	515	1	0.057037	0.004532	4	0.000000
3634	516	6	-0.346939	-0.459651	6	0.002126
3635	517	1	0.118234	0.175573	7	0.000000
3636	518	1	0.151800	0.175573	7	0.000000
3637	519	8	-0.141500	-0.141500	-1	0.005771
3638	520	6	0.030353	0.040572	10	0.009266
3639	521	1	0.092801	0.086505	11	0.000000
3640	522	1	0.096057	0.086505	11	0.000000
3641	523	6	-0.507366	-0.496118	13	0.001976
3642	524	1	0.203097	0.212018	14	0.000000
3643	525	1	0.226558	0.212018	14	0.000000
3644	526	8	-0.376457	-0.376457	-1	0.002567
3645	527	1	0.357457	0.357457	-1	0.000000
3646						
3647	528	8	-0.576790	-0.576790	-1	0.001708
3648	529	1	0.360115	0.360115	-1	0.000000
3649	530	6	0.256038	0.335117	3	0.002859
3650	531	1	-0.000496	0.004532	4	0.000000
3651	532	1	0.057037	0.004532	4	0.000000
3652	533	6	-0.346939	-0.459651	6	0.002126
3653	534	1	0.118234	0.175573	7	0.000000
3654	535	1	0.151800	0.175573	7	0.000000
3655	536	8	-0.141500	-0.141500	-1	0.005771
3656	537	6	0.030353	0.040572	10	0.009266
3657	538	1	0.092801	0.086505	11	0.000000
3658	539	1	0.096057	0.086505	11	0.000000
3659	540	6	-0.507366	-0.496118	13	0.001976
3660	541	1	0.203097	0.212018	14	0.000000
3661	542	1	0.226558	0.212018	14	0.000000
3662	543	8	-0.376457	-0.376457	-1	0.002567
3663	544	1	0.357457	0.357457	-1	0.000000
3664						
3665	545	8	-0.576790	-0.576790	-1	0.001708
3666	546	1	0.360115	0.360115	-1	0.000000
3667	547	6	0.256038	0.335117	3	0.002859

B.3. PEG WITH HYDROXYETHYL TERMINAL, MULTIPLE CONFORMATIONS

3668	548	1	-0.000496	0.004532	4	0.000000
3669	549	1	0.057037	0.004532	4	0.000000
3670	550	6	-0.346939	-0.459651	6	0.002126
3671	551	1	0.118234	0.175573	7	0.000000
3672	552	1	0.151800	0.175573	7	0.000000
3673	553	8	-0.141500	-0.141500	-1	0.005771
3674	554	6	0.030353	0.040572	10	0.009266
3675	555	1	0.092801	0.086505	11	0.000000
3676	556	1	0.096057	0.086505	11	0.000000
3677	557	6	-0.507366	-0.496118	13	0.001976
3678	558	1	0.203097	0.212018	14	0.000000
3679	559	1	0.226558	0.212018	14	0.000000
3680	560	8	-0.376457	-0.376457	-1	0.002567
3681	561	1	0.357457	0.357457	-1	0.000000
3682						
3683	562	8	-0.576790	-0.576790	-1	0.001708
3684	563	1	0.360115	0.360115	-1	0.000000
3685	564	6	0.256038	0.335117	3	0.002859
3686	565	1	-0.000496	0.004532	4	0.000000
3687	566	1	0.057037	0.004532	4	0.000000
3688	567	6	-0.346939	-0.459651	6	0.002126
3689	568	1	0.118234	0.175573	7	0.000000
3690	569	1	0.151800	0.175573	7	0.000000
3691	570	8	-0.141500	-0.141500	-1	0.005771
3692	571	6	0.030353	0.040572	10	0.009266
3693	572	1	0.092801	0.086505	11	0.000000
3694	573	1	0.096057	0.086505	11	0.000000
3695	574	6	-0.507366	-0.496118	13	0.001976
3696	575	1	0.203097	0.212018	14	0.000000
3697	576	1	0.226558	0.212018	14	0.000000
3698	577	8	-0.376457	-0.376457	-1	0.002567
3699	578	1	0.357457	0.357457	-1	0.000000
3700						
3701	579	8	-0.576790	-0.576790	-1	0.001708
3702	580	1	0.360115	0.360115	-1	0.000000
3703	581	6	0.256038	0.335117	3	0.002859
3704	582	1	-0.000496	0.004532	4	0.000000
3705	583	1	0.057037	0.004532	4	0.000000
3706	584	6	-0.346939	-0.459651	6	0.002126
3707	585	1	0.118234	0.175573	7	0.000000
3708	586	1	0.151800	0.175573	7	0.000000
3709	587	8	-0.141500	-0.141500	-1	0.005771
3710	588	6	0.030353	0.040572	10	0.009266
3711	589	1	0.092801	0.086505	11	0.000000
3712	590	1	0.096057	0.086505	11	0.000000

B.3. PEG WITH HYDROXYETHYL TERMINAL, MULTIPLE CONFORMATIONS

3713	591	6	-0.507366	-0.496118	13	0.001976
3714	592	1	0.203097	0.212018	14	0.000000
3715	593	1	0.226558	0.212018	14	0.000000
3716	594	8	-0.376457	-0.376457	-1	0.002567
3717	595	1	0.357457	0.357457	-1	0.000000
3718						
3719	596	8	-0.576790	-0.576790	-1	0.001708
3720	597	1	0.360115	0.360115	-1	0.000000
3721	598	6	0.256038	0.335117	3	0.002859
3722	599	1	-0.000496	0.004532	4	0.000000
3723	600	1	0.057037	0.004532	4	0.000000
3724	601	6	-0.346939	-0.459651	6	0.002126
3725	602	1	0.118234	0.175573	7	0.000000
3726	603	1	0.151800	0.175573	7	0.000000
3727	604	8	-0.141500	-0.141500	-1	0.005771
3728	605	6	0.030353	0.040572	10	0.009266
3729	606	1	0.092801	0.086505	11	0.000000
3730	607	1	0.096057	0.086505	11	0.000000
3731	608	6	-0.507366	-0.496118	13	0.001976
3732	609	1	0.203097	0.212018	14	0.000000
3733	610	1	0.226558	0.212018	14	0.000000
3734	611	8	-0.376457	-0.376457	-1	0.002567
3735	612	1	0.357457	0.357457	-1	0.000000
3736						
3737	613	8	-0.576790	-0.576790	-1	0.001708
3738	614	1	0.360115	0.360115	-1	0.000000
3739	615	6	0.256038	0.335117	3	0.002859
3740	616	1	-0.000496	0.004532	4	0.000000
3741	617	1	0.057037	0.004532	4	0.000000
3742	618	6	-0.346939	-0.459651	6	0.002126
3743	619	1	0.118234	0.175573	7	0.000000
3744	620	1	0.151800	0.175573	7	0.000000
3745	621	8	-0.141500	-0.141500	-1	0.005771
3746	622	6	0.030353	0.040572	10	0.009266
3747	623	1	0.092801	0.086505	11	0.000000
3748	624	1	0.096057	0.086505	11	0.000000
3749	625	6	-0.507366	-0.496118	13	0.001976
3750	626	1	0.203097	0.212018	14	0.000000
3751	627	1	0.226558	0.212018	14	0.000000
3752	628	8	-0.376457	-0.376457	-1	0.002567
3753	629	1	0.357457	0.357457	-1	0.000000
3754						
3755	630	8	-0.576790	-0.576790	-1	0.001708
3756	631	1	0.360115	0.360115	-1	0.000000
3757	632	6	0.256038	0.335117	3	0.002859

B.3. PEG WITH HYDROXYETHYL TERMINAL, MULTIPLE CONFORMATIONS

3758	633	1	-0.000496	0.004532	4	0.000000
3759	634	1	0.057037	0.004532	4	0.000000
3760	635	6	-0.346939	-0.459651	6	0.002126
3761	636	1	0.118234	0.175573	7	0.000000
3762	637	1	0.151800	0.175573	7	0.000000
3763	638	8	-0.141500	-0.141500	-1	0.005771
3764	639	6	0.030353	0.040572	10	0.009266
3765	640	1	0.092801	0.086505	11	0.000000
3766	641	1	0.096057	0.086505	11	0.000000
3767	642	6	-0.507366	-0.496118	13	0.001976
3768	643	1	0.203097	0.212018	14	0.000000
3769	644	1	0.226558	0.212018	14	0.000000
3770	645	8	-0.376457	-0.376457	-1	0.002567
3771	646	1	0.357457	0.357457	-1	0.000000
3772						
3773	647	8	-0.576790	-0.576790	-1	0.001708
3774	648	1	0.360115	0.360115	-1	0.000000
3775	649	6	0.256038	0.335117	3	0.002859
3776	650	1	-0.000496	0.004532	4	0.000000
3777	651	1	0.057037	0.004532	4	0.000000
3778	652	6	-0.346939	-0.459651	6	0.002126
3779	653	1	0.118234	0.175573	7	0.000000
3780	654	1	0.151800	0.175573	7	0.000000
3781	655	8	-0.141500	-0.141500	-1	0.005771
3782	656	6	0.030353	0.040572	10	0.009266
3783	657	1	0.092801	0.086505	11	0.000000
3784	658	1	0.096057	0.086505	11	0.000000
3785	659	6	-0.507366	-0.496118	13	0.001976
3786	660	1	0.203097	0.212018	14	0.000000
3787	661	1	0.226558	0.212018	14	0.000000
3788	662	8	-0.376457	-0.376457	-1	0.002567
3789	663	1	0.357457	0.357457	-1	0.000000
3790						
3791	664	8	-0.576790	-0.576790	-1	0.001708
3792	665	1	0.360115	0.360115	-1	0.000000
3793	666	6	0.256038	0.335117	3	0.002859
3794	667	1	-0.000496	0.004532	4	0.000000
3795	668	1	0.057037	0.004532	4	0.000000
3796	669	6	-0.346939	-0.459651	6	0.002126
3797	670	1	0.118234	0.175573	7	0.000000
3798	671	1	0.151800	0.175573	7	0.000000
3799	672	8	-0.141500	-0.141500	-1	0.005771
3800	673	6	0.030353	0.040572	10	0.009266
3801	674	1	0.092801	0.086505	11	0.000000
3802	675	1	0.096057	0.086505	11	0.000000

B.3. PEG WITH HYDROXYETHYL TERMINAL, MULTIPLE CONFORMATIONS

3803	676	6	-0.507366	-0.496118	13	0.001976
3804	677	1	0.203097	0.212018	14	0.000000
3805	678	1	0.226558	0.212018	14	0.000000
3806	679	8	-0.376457	-0.376457	-1	0.002567
3807	680	1	0.357457	0.357457	-1	0.000000
3808						
3809	681	8	-0.576790	-0.576790	-1	0.001708
3810	682	1	0.360115	0.360115	-1	0.000000
3811	683	6	0.256038	0.335117	3	0.002859
3812	684	1	-0.000496	0.004532	4	0.000000
3813	685	1	0.057037	0.004532	4	0.000000
3814	686	6	-0.346939	-0.459651	6	0.002126
3815	687	1	0.118234	0.175573	7	0.000000
3816	688	1	0.151800	0.175573	7	0.000000
3817	689	8	-0.141500	-0.141500	-1	0.005771
3818	690	6	0.030353	0.040572	10	0.009266
3819	691	1	0.092801	0.086505	11	0.000000
3820	692	1	0.096057	0.086505	11	0.000000
3821	693	6	-0.507366	-0.496118	13	0.001976
3822	694	1	0.203097	0.212018	14	0.000000
3823	695	1	0.226558	0.212018	14	0.000000
3824	696	8	-0.376457	-0.376457	-1	0.002567
3825	697	1	0.357457	0.357457	-1	0.000000
3826						
3827	698	8	-0.576790	-0.576790	-1	0.001708
3828	699	1	0.360115	0.360115	-1	0.000000
3829	700	6	0.256038	0.335117	3	0.002859
3830	701	1	-0.000496	0.004532	4	0.000000
3831	702	1	0.057037	0.004532	4	0.000000
3832	703	6	-0.346939	-0.459651	6	0.002126
3833	704	1	0.118234	0.175573	7	0.000000
3834	705	1	0.151800	0.175573	7	0.000000
3835	706	8	-0.141500	-0.141500	-1	0.005771
3836	707	6	0.030353	0.040572	10	0.009266
3837	708	1	0.092801	0.086505	11	0.000000
3838	709	1	0.096057	0.086505	11	0.000000
3839	710	6	-0.507366	-0.496118	13	0.001976
3840	711	1	0.203097	0.212018	14	0.000000
3841	712	1	0.226558	0.212018	14	0.000000
3842	713	8	-0.376457	-0.376457	-1	0.002567
3843	714	1	0.357457	0.357457	-1	0.000000
3844						
3845	715	8	-0.576790	-0.576790	-1	0.001708
3846	716	1	0.360115	0.360115	-1	0.000000
3847	717	6	0.256038	0.335117	3	0.002859

B.3. PEG WITH HYDROXYETHYL TERMINAL, MULTIPLE CONFORMATIONS

3848	718	1	-0.000496	0.004532	4	0.000000
3849	719	1	0.057037	0.004532	4	0.000000
3850	720	6	-0.346939	-0.459651	6	0.002126
3851	721	1	0.118234	0.175573	7	0.000000
3852	722	1	0.151800	0.175573	7	0.000000
3853	723	8	-0.141500	-0.141500	-1	0.005771
3854	724	6	0.030353	0.040572	10	0.009266
3855	725	1	0.092801	0.086505	11	0.000000
3856	726	1	0.096057	0.086505	11	0.000000
3857	727	6	-0.507366	-0.496118	13	0.001976
3858	728	1	0.203097	0.212018	14	0.000000
3859	729	1	0.226558	0.212018	14	0.000000
3860	730	8	-0.376457	-0.376457	-1	0.002567
3861	731	1	0.357457	0.357457	-1	0.000000
3862						
3863	732	8	-0.576790	-0.576790	-1	0.001708
3864	733	1	0.360115	0.360115	-1	0.000000
3865	734	6	0.256038	0.335117	3	0.002859
3866	735	1	-0.000496	0.004532	4	0.000000
3867	736	1	0.057037	0.004532	4	0.000000
3868	737	6	-0.346939	-0.459651	6	0.002126
3869	738	1	0.118234	0.175573	7	0.000000
3870	739	1	0.151800	0.175573	7	0.000000
3871	740	8	-0.141500	-0.141500	-1	0.005771
3872	741	6	0.030353	0.040572	10	0.009266
3873	742	1	0.092801	0.086505	11	0.000000
3874	743	1	0.096057	0.086505	11	0.000000
3875	744	6	-0.507366	-0.496118	13	0.001976
3876	745	1	0.203097	0.212018	14	0.000000
3877	746	1	0.226558	0.212018	14	0.000000
3878	747	8	-0.376457	-0.376457	-1	0.002567
3879	748	1	0.357457	0.357457	-1	0.000000
3880						
3881	749	8	-0.576790	-0.576790	-1	0.001708
3882	750	1	0.360115	0.360115	-1	0.000000
3883	751	6	0.256038	0.335117	3	0.002859
3884	752	1	-0.000496	0.004532	4	0.000000
3885	753	1	0.057037	0.004532	4	0.000000
3886	754	6	-0.346939	-0.459651	6	0.002126
3887	755	1	0.118234	0.175573	7	0.000000
3888	756	1	0.151800	0.175573	7	0.000000
3889	757	8	-0.141500	-0.141500	-1	0.005771
3890	758	6	0.030353	0.040572	10	0.009266
3891	759	1	0.092801	0.086505	11	0.000000
3892	760	1	0.096057	0.086505	11	0.000000

B.3. PEG WITH HYDROXYETHYL TERMINAL, MULTIPLE CONFORMATIONS

3893	761	6	-0.507366	-0.496118	13	0.001976
3894	762	1	0.203097	0.212018	14	0.000000
3895	763	1	0.226558	0.212018	14	0.000000
3896	764	8	-0.376457	-0.376457	-1	0.002567
3897	765	1	0.357457	0.357457	-1	0.000000
3898						
3899	766	8	-0.576790	-0.576790	-1	0.001708
3900	767	1	0.360115	0.360115	-1	0.000000
3901	768	6	0.256038	0.335117	3	0.002859
3902	769	1	-0.000496	0.004532	4	0.000000
3903	770	1	0.057037	0.004532	4	0.000000
3904	771	6	-0.346939	-0.459651	6	0.002126
3905	772	1	0.118234	0.175573	7	0.000000
3906	773	1	0.151800	0.175573	7	0.000000
3907	774	8	-0.141500	-0.141500	-1	0.005771
3908	775	6	0.030353	0.040572	10	0.009266
3909	776	1	0.092801	0.086505	11	0.000000
3910	777	1	0.096057	0.086505	11	0.000000
3911	778	6	-0.507366	-0.496118	13	0.001976
3912	779	1	0.203097	0.212018	14	0.000000
3913	780	1	0.226558	0.212018	14	0.000000
3914	781	8	-0.376457	-0.376457	-1	0.002567
3915	782	1	0.357457	0.357457	-1	0.000000

3916

3917 Sum over the calculated charges: -0.000

3918

3919 Statistics of the fitting:

3920 The initial **sum** of squares (ssvpot) 9.136

3921 The residual **sum** of squares (chipot) 0.492

3922 The std err of estimate (sqrt(chipot/N)) 0.00364

3923 ESP relative RMS (SQRT(chipot/ssvpot)) 0.23212

3924 The Pearson correlation coefficient (r2) 0.94698

3925

3926 Center of Mass (a.u.):

3927	#MEP	X	Y	Z
3928	1	2.10084	0.36011	-0.47027
3929	2	2.60441	0.68375	0.47027
3930	3	2.19529	0.16307	-0.52164
3931	4	2.76843	0.52490	0.52164
3932	5	2.19524	0.16306	-0.52170
3933	6	2.76845	0.52493	0.52170
3934	7	2.19529	0.16305	-0.52168
3935	8	2.76845	0.52489	0.52168
3936	9	2.19529	0.16308	-0.52163
3937	10	2.76842	0.52490	0.52163

B.3. PEG WITH HYDROXYETHYL TERMINAL, MULTIPLE CONFORMATIONS

3938	11	2.03978	0.19351	-0.50206		
3939	12	2.79012	0.66614	0.50206		
3940	13	1.60287	0.25389	-0.97223		
3941	14	2.92374	1.08732	0.97223		
3942	15	1.61049	0.26767	-0.98910		
3943	16	2.90235	1.08853	0.98910		
3944	17	1.61048	0.26767	-0.98909		
3945	18	2.90235	1.08854	0.98909		
3946	19	1.61502	0.25239	-0.99994		
3947	20	2.91807	1.07559	0.99994		
3948	21	1.88907	0.91761	-2.06707		
3949	22	2.23132	1.11840	2.06707		
3950	23	1.88906	0.91762	-2.06706		
3951	24	2.23131	1.11842	2.06706		
3952	25	1.88906	0.91764	-2.06707		
3953	26	2.23130	1.11843	2.06707		
3954	27	1.88906	0.91760	-2.06706		
3955	28	2.23134	1.11840	2.06706		
3956	29	2.71741	-0.26663	0.09590		
3957	30	2.90794	-0.15287	-0.09590		
3958	31	2.81917	-0.20027	-0.00006		
3959	32	2.81915	-0.20028	0.00006		
3960	33	2.82451	-0.20803	0.75642		
3961	34	2.82453	-0.20803	-0.75642		
3962	35	1.87223	0.86154	2.04528		
3963	36	2.31314	1.11340	-2.04528		
3964	37	2.82451	-0.20802	0.75644		
3965	38	2.82450	-0.20803	-0.75644		
3966	39	2.82451	-0.20805	0.75640		
3967	40	2.82453	-0.20804	-0.75640		
3968	41	2.82450	-0.20800	0.75653		
3969	42	2.82449	-0.20801	-0.75653		
3970	43	2.82452	-0.20803	0.75645		
3971	44	2.82451	-0.20803	-0.75645		
3972	45	2.82451	-0.20804	0.75644		
3973	46	2.82451	-0.20804	-0.75644		
3974						
3975		Dipole moments (Debye) computed:				
3976		-with respect to the origin of coordinates (ooc)				
3977		-with respect to the center of mass (com)				
3978	#MEP	D	Dx	Dy	Dz	
3979	1 ooc	3.63096	-0.54983	3.23319	-1.55823	
3980	1 com	3.63096	-0.54983	3.23319	-1.55823	
3981						
3982	2 ooc	3.63096	-2.68088	1.88909	1.55823	

B.3. PEG WITH HYDROXYETHYL TERMINAL, MULTIPLE CONFORMATIONS

3983	2 com	3.63096	-2.68088	1.88909	1.55823
3984					
3985	3 ooc	1.47967	-1.00381	1.07715	0.14674
3986	3 com	1.47967	-1.00381	1.07715	0.14674
3987					
3988	4 ooc	1.47967	-0.54401	1.36819	-0.14674
3989	4 com	1.47967	-0.54401	1.36819	-0.14674
3990					
3991	5 ooc	1.47967	-1.00374	1.07720	0.14687
3992	5 com	1.47967	-1.00374	1.07720	0.14687
3993					
3994	6 ooc	1.47966	-0.54408	1.36814	-0.14687
3995	6 com	1.47966	-0.54408	1.36814	-0.14687
3996					
3997	7 ooc	1.47974	-1.00378	1.07726	0.14684
3998	7 com	1.47974	-1.00378	1.07726	0.14684
3999					
4000	8 ooc	1.47974	-0.54412	1.36821	-0.14684
4001	8 com	1.47974	-0.54412	1.36821	-0.14684
4002					
4003	9 ooc	1.47966	-1.00381	1.07714	0.14673
4004	9 com	1.47966	-1.00381	1.07714	0.14673
4005					
4006	10 ooc	1.47966	-0.54400	1.36818	-0.14673
4007	10 com	1.47966	-0.54400	1.36818	-0.14673
4008					
4009	11 ooc	2.80224	-2.63312	-0.91482	0.28695
4010	11 com	2.80224	-2.63312	-0.91482	0.28695
4011					
4012	12 ooc	2.80224	1.93686	2.00469	-0.28695
4013	12 com	2.80224	1.93686	2.00469	-0.28695
4014					
4015	13 ooc	1.66045	-1.44530	0.79406	-0.19409
4016	13 com	1.66045	-1.44530	0.79406	-0.19409
4017					
4018	14 ooc	1.66045	-0.11201	1.64526	0.19409
4019	14 com	1.66045	-0.11201	1.64526	0.19409
4020					
4021	15 ooc	2.27407	-1.42606	-1.18162	1.31967
4022	15 com	2.27407	-1.42606	-1.18162	1.31967
4023					
4024	16 ooc	2.27407	1.66824	0.80426	-1.31967
4025	16 com	2.27407	1.66824	0.80426	-1.31967
4026					
4027	17 ooc	2.27418	-1.42606	-1.18162	1.31985

B.3. PEG WITH HYDROXYETHYL TERMINAL, MULTIPLE CONFORMATIONS

4028	17	com	2.27418	-1.42606	-1.18162	1.31985
4029						
4030	18	ooc	2.27418	1.66824	0.80427	-1.31985
4031	18	com	2.27418	1.66824	0.80427	-1.31985
4032						
4033	19	ooc	3.16779	-1.47898	0.88059	2.65934
4034	19	com	3.16779	-1.47898	0.88059	2.65934
4035						
4036	20	ooc	3.16779	-0.17936	1.71191	-2.65934
4037	20	com	3.16779	-0.17936	1.71191	-2.65934
4038						
4039	21	ooc	4.12947	-3.43812	1.20286	1.94552
4040	21	com	4.12947	-3.43812	1.20286	1.94552
4041						
4042	22	ooc	4.12947	0.48752	3.60968	-1.94552
4043	22	com	4.12947	0.48752	3.60968	-1.94552
4044						
4045	23	ooc	4.12941	-3.43803	1.20280	1.94557
4046	23	com	4.12941	-3.43803	1.20280	1.94557
4047						
4048	24	ooc	4.12941	0.48752	3.60959	-1.94557
4049	24	com	4.12941	0.48752	3.60959	-1.94557
4050						
4051	25	ooc	4.12943	-3.43804	1.20282	1.94558
4052	25	com	4.12943	-3.43804	1.20282	1.94558
4053						
4054	26	ooc	4.12943	0.48753	3.60960	-1.94558
4055	26	com	4.12943	0.48753	3.60960	-1.94558
4056						
4057	27	ooc	4.12941	-3.43805	1.20280	1.94553
4058	27	com	4.12941	-3.43805	1.20280	1.94553
4059						
4060	28	ooc	4.12941	0.48753	3.60960	-1.94553
4061	28	com	4.12941	0.48753	3.60960	-1.94553
4062						
4063	29	ooc	3.84194	-3.11944	1.67530	-1.49095
4064	29	com	3.84194	-3.11944	1.67530	-1.49095
4065						
4066	30	ooc	3.84194	-0.26629	3.53081	1.49095
4067	30	com	3.84194	-0.26629	3.53081	1.49095
4068						
4069	31	ooc	1.44359	-0.96215	1.06007	-0.18571
4070	31	com	1.44359	-0.96215	1.06007	-0.18571
4071						
4072	32	ooc	1.44360	-0.57085	1.31286	0.18571

B.3. PEG WITH HYDROXYETHYL TERMINAL, MULTIPLE CONFORMATIONS

4073	32	com	1.44360	-0.57085	1.31286	0.18571
4074						
4075	33	ooc	2.55094	-0.94737	0.98395	-2.15444
4076	33	com	2.55094	-0.94737	0.98395	-2.15444
4077						
4078	34	ooc	2.55094	-0.52148	1.26243	2.15444
4079	34	com	2.55094	-0.52148	1.26243	2.15444
4080						
4081	35	ooc	2.48321	-1.64991	0.08836	-1.85373
4082	35	com	2.48321	-1.64991	0.08836	-1.85373
4083						
4084	36	ooc	2.48321	0.69867	1.49729	1.85373
4085	36	com	2.48321	0.69867	1.49729	1.85373
4086						
4087	37	ooc	2.55088	-0.94721	0.98384	-2.15450
4088	37	com	2.55088	-0.94721	0.98384	-2.15450
4089						
4090	38	ooc	2.55088	-0.52143	1.26224	2.15450
4091	38	com	2.55088	-0.52143	1.26224	2.15450
4092						
4093	39	ooc	2.55093	-0.94731	0.98399	-2.15444
4094	39	com	2.55093	-0.94731	0.98399	-2.15444
4095						
4096	40	ooc	2.55093	-0.52153	1.26239	2.15444
4097	40	com	2.55093	-0.52153	1.26239	2.15444
4098						
4099	41	ooc	2.55094	-0.94724	0.98393	-2.15451
4100	41	com	2.55094	-0.94724	0.98393	-2.15451
4101						
4102	42	ooc	2.55094	-0.52151	1.26231	2.15451
4103	42	com	2.55094	-0.52151	1.26231	2.15451
4104						
4105	43	ooc	2.55096	-0.94727	0.98395	-2.15451
4106	43	com	2.55096	-0.94727	0.98395	-2.15451
4107						
4108	44	ooc	2.55096	-0.52152	1.26234	2.15451
4109	44	com	2.55096	-0.52152	1.26234	2.15451
4110						
4111	45	ooc	2.55094	-0.94729	0.98397	-2.15448
4112	45	com	2.55094	-0.94729	0.98397	-2.15448
4113						
4114	46	ooc	2.55094	-0.52152	1.26236	2.15448
4115	46	com	2.55094	-0.52152	1.26236	2.15448
4116						
4117	Traceless Quadrupole moments (Buckingham) computed:					

B.3. PEG WITH HYDROXYETHYL TERMINAL, MULTIPLE CONFORMATIONS

```
4118 -with respect to the origin of coordinates (ooc)
4119 -with respect to the center of mass (com)
4120 #MEP      X      Y      Z
4121 1 ooc X -11.62614
4122      Y  8.50438  9.64021
4123      Z  8.51000 -5.12714  1.98593
4124 1 com X -7.17330
4125      Y -1.96444  6.72874
4126      Z 13.29644 -1.82251  0.44457
4127
4128 2 ooc X -14.30067
4129      Y -1.73954  6.28249
4130      Z  8.52475 15.88618  8.01818
4131 2 com X  2.62103
4132      Y -6.64013 -3.06559
4133      Z  4.08359 12.78442  0.44456
4134
4135 3 ooc X -4.12737
4136      Y -8.50421 12.10238
4137      Z 24.34793 16.11497 -7.97501
4138 3 com X  0.64203
4139      Y -11.99832  9.31730
4140      Z 23.00525 16.96899 -9.95933
4141
4142 4 ooc X -5.41898
4143      Y -5.39973 14.70646
4144      Z 24.08569 14.54217 -9.28748
4145 4 com X -1.55203
4146      Y -10.95955 11.51136
4147      Z 25.18112 13.53143 -9.95933
4148
4149 5 ooc X -4.12590
4150      Y -8.50450 12.10122
4151      Z 24.34767 16.11539 -7.97531
4152 5 com X  0.64295
4153      Y -11.99874  9.31630
4154      Z 23.00452 16.96953 -9.95925
4155
4156 6 ooc X -5.42037
4157      Y -5.39949 14.70773
4158      Z 24.08523 14.54122 -9.28735
4159 6 com X -1.55305
4160      Y -10.95906 11.51230
4161      Z 25.18134 13.53049 -9.95925
4162
```

B.3. PEG WITH HYDROXYETHYL TERMINAL, MULTIPLE CONFORMATIONS

4163	7 ooc X	-4.12670		
4164	Y	-8.50411	12.10149	
4165	Z	24.34781	16.11492	-7.97480
4166	7 com X	0.64250		
4167	Y	-11.99864	9.31644	
4168	Z	23.00473	16.96908	-9.95894
4169				
4170	8 ooc X	-5.42038		
4171	Y	-5.39939	14.70727	
4172	Z	24.08496	14.54174	-9.28689
4173	8 com X	-1.55282		
4174	Y	-10.95927	11.51177	
4175	Z	25.18096	13.53096	-9.95896
4176				
4177	9 ooc X	-4.12750		
4178	Y	-8.50416	12.10262	
4179	Z	24.34805	16.11490	-7.97513
4180	9 com X	0.64191		
4181	Y	-11.99823	9.31755	
4182	Z	23.00542	16.96889	-9.95946
4183				
4184	10 ooc X	-5.41862		
4185	Y	-5.39984	14.70627	
4186	Z	24.08573	14.54233	-9.28764
4187	10 com X	-1.55175		
4188	Y	-10.95964	11.51123	
4189	Z	25.18110	13.53161	-9.95947
4190				
4191	11 ooc X	-15.15616		
4192	Y	2.22416	30.59315	
4193	Z	16.80122	5.59949	-15.43699
4194	11 com X	-4.12716		
4195	Y	5.99544	25.13096	
4196	Z	13.77331	4.78220	-21.00381
4197				
4198	12 ooc X	34.71299		
4199	Y	3.64586	-6.27147	
4200	Z	10.40127	11.78177	-28.44152
4201	12 com X	24.53499		
4202	Y	-7.28201	-3.53118	
4203	Z	10.12856	10.48742	-21.00381
4204				
4205	13 ooc X	-12.55244		
4206	Y	-8.18650	14.71941	
4207	Z	27.53640	13.97995	-2.16698

B.3. PEG WITH HYDROXYETHYL TERMINAL, MULTIPLE CONFORMATIONS

4208	13 com X	-7.23576		
4209	Y	-9.62452	12.04059	
4210	Z	25.79955	15.28376	-4.80484
4211				
4212	14 ooc X	-1.50920		
4213	Y	-6.13106	7.46132	
4214	Z	25.45063	19.84501	-5.95212
4215	14 com X	1.27700		
4216	Y	-13.57422	3.52783	
4217	Z	24.72263	16.97062	-4.80483
4218				
4219	15 ooc X	-19.50725		
4220	Y	4.24424	29.95831	
4221	Z	17.14541	7.37192	-10.45105
4222	15 com X	-16.36211		
4223	Y	7.87128	26.81565	
4224	Z	11.53216	4.95573	-10.45354
4225				
4226	16 ooc X	35.98919		
4227	Y	-4.62232	-16.72180	
4228	Z	5.84798	7.40221	-19.26738
4229	16 com X	25.28553		
4230	Y	-11.21087	-14.83198	
4231	Z	9.30895	8.41983	-10.45354
4232				
4233	17 ooc X	-19.50753		
4234	Y	4.24399	29.95833	
4235	Z	17.14439	7.37070	-10.45080
4236	17 com X	-16.36256		
4237	Y	7.87101	26.81553	
4238	Z	11.53073	4.95445	-10.45297
4239				
4240	18 ooc X	35.98901		
4241	Y	-4.62238	-16.72185	
4242	Z	5.84536	7.40114	-19.26716
4243	18 com X	25.28522		
4244	Y	-11.21100	-14.83224	
4245	Z	9.30716	8.41908	-10.45298
4246				
4247	19 ooc X	-13.71825		
4248	Y	-9.10954	14.02563	
4249	Z	7.86369	2.73034	-0.30738
4250	19 com X	-11.24147		
4251	Y	-10.77468	8.21287	
4252	Z	-1.30235	3.06268	3.02860

B.3. PEG WITH HYDROXYETHYL TERMINAL, MULTIPLE CONFORMATIONS

4253					
4254	20 ooc X	-3.65189			
4255	Y	-6.76741	7.64685		
4256	Z	-10.36973	-4.28980	-3.99496	
4257	20 com X	-3.40964			
4258	Y	-14.39163	0.38105		
4259	Z	2.23445	-2.46646	3.02859	
4260					
4261	21 ooc X	-6.97311			
4262	Y	-1.74677	16.22822		
4263	Z	25.36111	1.41443	-9.25511	
4264	21 com X	3.68652			
4265	Y	-0.34566	2.76185		
4266	Z	8.24427	2.52753	-6.44838	
4267					
4268	22 ooc X	4.95877			
4269	Y	13.82251	15.42597		
4270	Z	0.70033	14.59190	-20.38474	
4271	22 com X	2.67264			
4272	Y	0.17038	3.77574		
4273	Z	5.99212	6.20087	-6.44838	
4274					
4275	23 ooc X	-6.97206			
4276	Y	-1.74708	16.22752		
4277	Z	25.36073	1.41509	-9.25545	
4278	23 com X	3.68701			
4279	Y	-0.34582	2.76136		
4280	Z	8.24410	2.52789	-6.44836	
4281					
4282	24 ooc X	4.95850			
4283	Y	13.82245	15.42636		
4284	Z	0.70042	14.59112	-20.38486	
4285	24 com X	2.67223			
4286	Y	0.17068	3.77614		
4287	Z	5.99235	6.20059	-6.44837	
4288					
4289	25 ooc X	-6.97248			
4290	Y	-1.74732	16.22803		
4291	Z	25.36066	1.41493	-9.25555	
4292	25 com X	3.68664			
4293	Y	-0.34603	2.76173		
4294	Z	8.24394	2.52774	-6.44837	
4295					
4296	26 ooc X	4.95852			
4297	Y	13.82205	15.42646		

B.3. PEG WITH HYDROXYETHYL TERMINAL, MULTIPLE CONFORMATIONS

4298		Z	0.70024	14.59107	-20.38498
4299	26	com X	2.67226		
4300		Y	0.17026	3.77611	
4301		Z	5.99217	6.20049	-6.44837
4302					
4303	27	ooc X	-6.97218		
4304		Y	-1.74690	16.22719	
4305		Z	25.36090	1.41503	-9.25501
4306	27	com X	3.68709		
4307		Y	-0.34576	2.76113	
4308		Z	8.24431	2.52794	-6.44822
4309					
4310	28	ooc X	4.95839		
4311		Y	13.82279	15.42610	
4312		Z	0.70062	14.59143	-20.38450
4313	28	com X	2.67209		
4314		Y	0.17083	3.77612	
4315		Z	5.99247	6.20074	-6.44821
4316					
4317	29	ooc X	-15.74834		
4318		Y	2.90112	3.14715	
4319		Z	-14.95925	-8.43647	12.60119
4320	29	com X	1.57053		
4321		Y	-5.64649	-5.03016	
4322		Z	-8.05239	-9.32261	3.45963
4323					
4324	30	ooc X	-9.04736		
4325		Y	15.02207	4.49959	
4326		Z	-4.86372	-4.47917	4.54777
4327	30	com X	-8.13088		
4328		Y	-1.34234	4.67125	
4329		Z	-11.78716	-3.57978	3.45963
4330					
4331	31	ooc X	-10.84824		
4332		Y	-8.00340	10.55866	
4333		Z	-25.20539	-14.42824	0.28958
4334	31	com X	-5.33141		
4335		Y	-13.05366	8.13729	
4336		Z	-24.37432	-14.48719	-2.80587
4337					
4338	32	ooc X	-7.05005		
4339		Y	-7.63203	7.87440	
4340		Z	-22.39501	-16.32342	-0.82435
4341	32	com X	-3.92187		
4342		Y	-13.68924	6.72775	

B.3. PEG WITH HYDROXYETHYL TERMINAL, MULTIPLE CONFORMATIONS

4343		Z	-23.22611	-16.26449	-2.80588
4344					
4345	33	ooc X	-13.16672		
4346		Y	-10.87771	10.36918	
4347		Z	-10.57682	-0.65833	2.79754
4348	33	com X	-9.44411		
4349		Y	-15.60263	6.24568	
4350		Z	0.22133	-2.55143	3.19843
4351					
4352	34	ooc X	-8.85553		
4353		Y	-10.51534	7.26981	
4354		Z	8.03825	-1.00163	1.58571
4355	34	com X	-7.74048		
4356		Y	-16.34836	4.54206	
4357		Z	-2.24855	1.22588	3.19842
4358					
4359	35	ooc X	14.80345		
4360		Y	0.62816	-2.33807	
4361		Z	-12.90494	-7.18294	-12.46539
4362	35	com X	17.40991		
4363		Y	2.62215	-9.78111	
4364		Z	-2.03807	-4.93446	-7.62880
4365					
4366	36	ooc X	4.09080		
4367		Y	19.48596	15.03808	
4368		Z	-0.77427	-1.06049	-19.12887
4369	36	com X	-1.57838		
4370		Y	12.75270	9.20717	
4371		Z	-5.31295	0.52457	-7.62879
4372					
4373	37	ooc X	-13.16433		
4374		Y	-10.87942	10.36786	
4375		Z	-10.57732	-0.65924	2.79646
4376	37	com X	-9.44272		
4377		Y	-15.60377	6.24467	
4378		Z	0.22094	-2.55223	3.19805
4379					
4380	38	ooc X	-8.85683		
4381		Y	-10.51612	7.27185	
4382		Z	8.03749	-1.00147	1.58498
4383	38	com X	-7.74212		
4384		Y	-16.34821	4.54407	
4385		Z	-2.24943	1.22586	3.19806
4386					
4387	39	ooc X	-13.16500		

B.3. PEG WITH HYDROXYETHYL TERMINAL, MULTIPLE CONFORMATIONS

4388		Y	-10.87851	10.36743	
4389		Z	-10.57758	-0.65890	2.79757
4390	39	com X	-9.44274		
4391		Y	-15.60360	6.24421	
4392		Z	0.22048	-2.55206	3.19852
4393					
4394	40	ooc X	-8.85776		
4395		Y	-10.51510	7.27168	
4396		Z	8.03738	-1.00206	1.58608
4397	40	com X	-7.74235		
4398		Y	-16.34794	4.54382	
4399		Z	-2.24947	1.22537	3.19853
4400					
4401	41	ooc X	-13.16357		
4402		Y	-10.87807	10.36761	
4403		Z	-10.57728	-0.65894	2.79596
4404	41	com X	-9.44198		
4405		Y	-15.60279	6.24413	
4406		Z	0.22118	-2.55209	3.19786
4407					
4408	42	ooc X	-8.85663		
4409		Y	-10.51468	7.27205	
4410		Z	8.03787	-1.00150	1.58457
4411	42	com X	-7.74170		
4412		Y	-16.34706	4.54384	
4413		Z	-2.24921	1.22601	3.19786
4414					
4415	43	ooc X	-13.16385		
4416		Y	-10.87849	10.36737	
4417		Z	-10.57786	-0.65896	2.79648
4418	43	com X	-9.44191		
4419		Y	-15.60339	6.24404	
4420		Z	0.22055	-2.55211	3.19788
4421					
4422	44	ooc X	-8.85735		
4423		Y	-10.51489	7.27230	
4424		Z	8.03761	-1.00203	1.58505
4425	44	com X	-7.74219		
4426		Y	-16.34747	4.54430	
4427		Z	-2.24949	1.22545	3.19789
4428					
4429	45	ooc X	-13.16484		
4430		Y	-10.87816	10.36796	
4431		Z	-10.57736	-0.65874	2.79687
4432	45	com X	-9.44281		

B.3. PEG WITH HYDROXYETHYL TERMINAL, MULTIPLE CONFORMATIONS

```
4433      Y -15.60313  6.24466
4434      Z   0.22088 -2.55190  3.19815
4435
4436  46 ooc X -8.85693
4437      Y -10.51509  7.27151
4438      Z   8.03781 -1.00181  1.58542
4439  46 com X -7.74170
4440      Y -16.34778  4.54355
4441      Z  -2.24916  1.22568  3.19815
4442
4443 Traceless Quadrupole moments (Buckingham) in principal axes computed:
4444 -with respect to the origin of coordinates (ooc)
4445 -with respect to the center of mass (com)
4446 #MEP      X      Y      Z
4447  1 ooc X  13.14990
4448      Y   0.00000  5.96955
4449      Z  -0.00000  0.00000 -19.11945
4450  1 com X  11.83230
4451      Y  -0.00000  5.37271
4452      Z  -0.00000 -0.00000 -17.20501
4453
4454  2 ooc X  23.74384
4455      Y  -0.00000 -4.16636
4456      Z   0.00000 -0.00000 -19.57748
4457  2 com X  11.83230
4458      Y  -0.00000  5.37271
4459      Z  -0.00000 -0.00000 -17.20502
4460
4461  3 ooc X  22.84154
4462      Y   0.00000  14.01710
4463      Z  -0.00000  0.00000 -36.85864
4464  3 com X  19.83475
4465      Y   0.00000  17.63786
4466      Z  -0.00000  0.00000 -37.47261
4467
4468  4 ooc X  23.57767
4469      Y   0.00000  12.08110
4470      Z  -0.00000  0.00000 -35.65877
4471  4 com X  19.83475
4472      Y  -0.00000  17.63787
4473      Z   0.00000  0.00000 -37.47261
4474
4475  5 ooc X  22.84119
4476      Y   0.00000  14.01728
4477      Z  -0.00000  0.00000 -36.85847
```

B.3. PEG WITH HYDROXYETHYL TERMINAL, MULTIPLE CONFORMATIONS

4478	5 com X	19.83440		
4479	Y	0.00000	17.63797	
4480	Z	0.00000	0.00000	-37.47237
4481				
4482	6 ooc X	23.57737		
4483	Y	0.00000	12.08090	
4484	Z	-0.00000	-0.00000	-35.65826
4485	6 com X	19.83440		
4486	Y	0.00000	17.63798	
4487	Z	0.00000	0.00000	-37.47238
4488				
4489	7 ooc X	22.84127		
4490	Y	0.00000	14.01694	
4491	Z	-0.00000	0.00000	-36.85820
4492	7 com X	19.83432		
4493	Y	0.00000	17.63786	
4494	Z	-0.00000	0.00000	-37.47218
4495				
4496	8 ooc X	23.57766		
4497	Y	0.00000	12.08032	
4498	Z	-0.00000	0.00000	-35.65799
4499	8 com X	19.83433		
4500	Y	0.00000	17.63785	
4501	Z	0.00000	0.00000	-37.47219
4502				
4503	9 ooc X	22.84160		
4504	Y	0.00000	14.01716	
4505	Z	-0.00000	0.00000	-36.85877
4506	9 com X	19.83482		
4507	Y	0.00000	17.63789	
4508	Z	0.00000	0.00000	-37.47271
4509				
4510	10 ooc X	23.57765		
4511	Y	0.00000	12.08121	
4512	Z	-0.00000	0.00000	-35.65886
4513	10 com X	19.83482		
4514	Y	-0.00000	17.63789	
4515	Z	0.00000	0.00000	-37.47271
4516				
4517	11 ooc X	31.69429		
4518	Y	0.00000	0.49794	
4519	Z	-0.00000	0.00000	-32.19223
4520	11 com X	27.54854		
4521	Y	0.00000	1.19927	
4522	Z	-0.00000	-0.00000	-28.74780

B.3. PEG WITH HYDROXYETHYL TERMINAL, MULTIPLE CONFORMATIONS

4523				
4524	12 ooc X	37.10102		
4525	Y	0.00000	-2.59602	
4526	Z	-0.00000	0.00000	-34.50500
4527	12 com X	27.54854		
4528	Y	-0.00000	1.19927	
4529	Z	0.00000	0.00000	-28.74781
4530				
4531	13 ooc X	25.24040		
4532	Y	-0.00000	14.44200	
4533	Z	0.00000	-0.00000	-39.68240
4534	13 com X	23.25755		
4535	Y	-0.00000	14.75997	
4536	Z	0.00000	-0.00000	-38.01752
4537				
4538	14 ooc X	27.51976		
4539	Y	0.00000	9.85864	
4540	Z	-0.00000	-0.00000	-37.37840
4541	14 com X	23.25755		
4542	Y	0.00000	14.75997	
4543	Z	-0.00000	0.00000	-38.01752
4544				
4545	15 ooc X	32.37722		
4546	Y	0.00000	0.35645	
4547	Z	0.00000	0.00000	-32.73367
4548	15 com X	29.46726		
4549	Y	-0.00000	-3.94917	
4550	Z	0.00000	0.00000	-25.51809
4551				
4552	16 ooc X	36.88013		
4553	Y	-0.00000	-10.48485	
4554	Z	0.00000	0.00000	-26.39529
4555	16 com X	29.46727		
4556	Y	-0.00000	-3.94917	
4557	Z	0.00000	-0.00000	-25.51810
4558				
4559	17 ooc X	32.37657		
4560	Y	0.00000	0.35616	
4561	Z	0.00000	0.00000	-32.73274
4562	17 com X	29.46649		
4563	Y	-0.00000	-3.94960	
4564	Z	0.00000	0.00000	-25.51688
4565				
4566	18 ooc X	36.87949		
4567	Y	-0.00000	-10.48582	

B.3. PEG WITH HYDROXYETHYL TERMINAL, MULTIPLE CONFORMATIONS

4568		Z	-0.00000	0.00000	-26.39367
4569	18	com X	29.46649		
4570		Y	-0.00000	-3.94962	
4571		Z	0.00000	0.00000	-25.51687
4572					
4573	19	ooc X	16.75811		
4574		Y	0.00000	3.20334	
4575		Z	0.00000	0.00000	-19.96145
4576	19	com X	14.00998		
4577		Y	-0.00000	2.02038	
4578		Z	-0.00000	-0.00000	-16.03036
4579					
4580	20	ooc X	10.84649		
4581		Y	0.00000	5.86312	
4582		Z	0.00000	0.00000	-16.70961
4583	20	com X	14.00998		
4584		Y	0.00000	2.02037	
4585		Z	-0.00000	0.00000	-16.03035
4586					
4587	21	ooc X	17.35193		
4588		Y	-0.00000	16.24870	
4589		Z	-0.00000	0.00000	-33.60063
4590	21	com X	8.45683		
4591		Y	0.00000	2.99913	
4592		Z	-0.00000	0.00000	-11.45596
4593					
4594	22	ooc X	28.25830		
4595		Y	-0.00000	-2.10331	
4596		Z	-0.00000	-0.00000	-26.15499
4597	22	com X	8.45683		
4598		Y	0.00000	2.99912	
4599		Z	-0.00000	-0.00000	-11.45595
4600					
4601	23	ooc X	17.35177		
4602		Y	0.00000	16.24821	
4603		Z	-0.00000	0.00000	-33.59999
4604	23	com X	8.45704		
4605		Y	0.00000	2.99880	
4606		Z	-0.00000	0.00000	-11.45584
4607					
4608	24	ooc X	28.25813		
4609		Y	-0.00000	-2.10364	
4610		Z	-0.00000	-0.00000	-26.15449
4611	24	com X	8.45704		
4612		Y	0.00000	2.99881	

B.3. PEG WITH HYDROXYETHYL TERMINAL, MULTIPLE CONFORMATIONS

4613		Z	-0.00000	-0.00000	-11.45585
4614					
4615	25	ooc X	17.35165		
4616		Y	-0.00000	16.24852	
4617		Z	-0.00000	0.00000	-33.60017
4618	25	com X	8.45656		
4619		Y	0.00000	2.99921	
4620		Z	-0.00000	0.00000	-11.45577
4621					
4622	26	ooc X	28.25780		
4623		Y	-0.00000	-2.10325	
4624		Z	-0.00000	0.00000	-26.15455
4625	26	com X	8.45657		
4626		Y	0.00000	2.99921	
4627		Z	-0.00000	0.00000	-11.45578
4628					
4629	27	ooc X	17.35200		
4630		Y	-0.00000	16.24797	
4631		Z	-0.00000	0.00000	-33.59997
4632	27	com X	8.45733		
4633		Y	0.00000	2.99857	
4634		Z	-0.00000	0.00000	-11.45590
4635					
4636	28	ooc X	28.25842		
4637		Y	-0.00000	-2.10401	
4638		Z	-0.00000	-0.00000	-26.15442
4639	28	com X	8.45732		
4640		Y	0.00000	2.99856	
4641		Z	-0.00000	0.00000	-11.45588
4642					
4643	29	ooc X	23.01939		
4644		Y	-0.00000	-0.81843	
4645		Z	-0.00000	-0.00000	-22.20095
4646	29	com X	11.62003		
4647		Y	0.00000	4.30112	
4648		Z	-0.00000	-0.00000	-15.92115
4649					
4650	30	ooc X	17.40973		
4651		Y	0.00000	1.46611	
4652		Z	-0.00000	-0.00000	-18.87584
4653	30	com X	11.62003		
4654		Y	-0.00000	4.30114	
4655		Z	0.00000	-0.00000	-15.92117
4656					
4657	31	ooc X	24.51839		

B.3. PEG WITH HYDROXYETHYL TERMINAL, MULTIPLE CONFORMATIONS

4658		Y	-0.00000	11.64275	
4659		Z	-0.00000	-0.00000	-36.16115
4660	31	com X	20.79956		
4661		Y	0.00000	16.07991	
4662		Z	-0.00000	0.00000	-36.87947
4663					
4664	32	ooc X	23.75533		
4665		Y	-0.00000	9.55120	
4666		Z	-0.00000	0.00000	-33.30653
4667	32	com X	20.79956		
4668		Y	-0.00000	16.07990	
4669		Z	0.00000	-0.00000	-36.87945
4670					
4671	33	ooc X	15.69613		
4672		Y	-0.00000	5.94343	
4673		Z	0.00000	0.00000	-21.63956
4674	33	com X	16.26634		
4675		Y	0.00000	2.85638	
4676		Z	-0.00000	-0.00000	-19.12272
4677					
4678	34	ooc X	14.25364		
4679		Y	0.00000	2.39720	
4680		Z	-0.00000	-0.00000	-16.65084
4681	34	com X	16.26633		
4682		Y	-0.00000	2.85637	
4683		Z	-0.00000	-0.00000	-19.12270
4684					
4685	35	ooc X	20.42690		
4686		Y	0.00000	-0.43694	
4687		Z	-0.00000	-0.00000	-19.98997
4688	35	com X	17.91268		
4689		Y	0.00000	-4.13794	
4690		Z	-0.00000	0.00000	-13.77475
4691					
4692	36	ooc X	29.83978		
4693		Y	0.00000	-10.67564	
4694		Z	0.00000	-0.00000	-19.16414
4695	36	com X	17.91267		
4696		Y	-0.00000	-4.13792	
4697		Z	0.00000	0.00000	-13.77474
4698					
4699	37	ooc X	15.69642		
4700		Y	0.00000	5.94305	
4701		Z	0.00000	0.00000	-21.63947
4702	37	com X	16.26713		

B.3. PEG WITH HYDROXYETHYL TERMINAL, MULTIPLE CONFORMATIONS

4703		Y	0.00000	2.85597	
4704		Z	-0.00000	-0.00000	-19.12310
4705					
4706	38	ooc X	14.25473		
4707		Y	0.00000	2.39696	
4708		Z	-0.00000	-0.00000	-16.65168
4709	38	com X	16.26713		
4710		Y	-0.00000	2.85598	
4711		Z	-0.00000	-0.00000	-19.12311
4712					
4713	39	ooc X	15.69568		
4714		Y	0.00000	5.94379	
4715		Z	0.00000	0.00000	-21.63947
4716	39	com X	16.26654		
4717		Y	0.00000	2.85658	
4718		Z	-0.00000	-0.00000	-19.12312
4719					
4720	40	ooc X	14.25407		
4721		Y	0.00000	2.39732	
4722		Z	-0.00000	-0.00000	-16.65140
4723	40	com X	16.26654		
4724		Y	-0.00000	2.85659	
4725		Z	-0.00000	-0.00000	-19.12313
4726					
4727	41	ooc X	15.69550		
4728		Y	-0.00000	5.94268	
4729		Z	0.00000	0.00000	-21.63818
4730	41	com X	16.26609		
4731		Y	0.00000	2.85573	
4732		Z	-0.00000	-0.00000	-19.12182
4733					
4734	42	ooc X	14.25389		
4735		Y	0.00000	2.39700	
4736		Z	0.00000	-0.00000	-16.65089
4737	42	com X	16.26607		
4738		Y	-0.00000	2.85573	
4739		Z	-0.00000	0.00000	-19.12180
4740					
4741	43	ooc X	15.69578		
4742		Y	0.00000	5.94317	
4743		Z	0.00000	0.00000	-21.63895
4744	43	com X	16.26646		
4745		Y	0.00000	2.85593	
4746		Z	-0.00000	-0.00000	-19.12239
4747					

B.3. PEG WITH HYDROXYETHYL TERMINAL, MULTIPLE CONFORMATIONS

```
4748 44 ooc X 14.25431
4749      Y 0.00000 2.39685
4750      Z 0.00000 -0.00000 -16.65116
4751 44 com X 16.26648
4752      Y -0.00000 2.85595
4753      Z -0.00000 0.00000 -19.12243
4754
4755 45 ooc X 15.69580
4756      Y -0.00000 5.94323
4757      Z 0.00000 0.00000 -21.63903
4758 45 com X 16.26644
4759      Y 0.00000 2.85614
4760      Z -0.00000 -0.00000 -19.12258
4761
4762 46 ooc X 14.25407
4763      Y 0.00000 2.39714
4764      Z -0.00000 -0.00000 -16.65121
4765 46 com X 16.26644
4766      Y -0.00000 2.85614
4767      Z -0.00000 0.00000 -19.12258
```

B.3.7 Amber Leap script for PEG-H(m)

```
1 #
2 # Generated by PyRED version SEP-2015
3 # http://q4md-forcefieldtools.org
4 #
5 logfile q4md-forcefieldtools.log
6 source /home/sajid/amber14/dat/leap/cmd/oldff/leaprc.ff99SB
7 # Web site: http://ambermd.org/doc6/html/AMBER-sh-5.9.html#sh-5.9.8
8 alias q quit
9 alias e edit
10 alias c charge
11
12 # Web site: http://ambermd.org/doc6/html/AMBER-sh-5.9.html#sh-5.9.73
13 verbosity 2
14
15 # Web site: http://ambermd.org/doc6/html/AMBER-sh-5.9.html#sh-5.9.2
16 addAtomTypes {
17     { "CT" "C" "sp3" }
18     { "H1" "H" "sp3" }
19     { "HO" "H" "sp3" }
20     { "OH" "O" "sp3" }
21     { "OS" "O" "sp3" }
22 }
```

B.3. PEG WITH HYDROXYETHYL TERMINAL, MULTIPLE CONFORMATIONS

```
23
24 # To force the correspondance between residue names
25 # PDB file versus force field libraries:
26 # Web site: http://ambermd.org/doc6/html/AMBER-sh-5.9.html#sh-5.9.7
27 # addPdbResMap {
28 #     { 0 ALA NALA } { 1 ALA CALA }
29 #     { ADE DADE }
30 # }
31
32 # Web site: http://ambermd.org/doc6/html/AMBER-sh-5.9.html#sh-5.9.41
33 frcmod1 = loadAmberParams ./frcmod.known
34 frcmod2 = loadAmberParams ./frcmod.correspondence
35 frcmod3 = loadAmberParams ./frcmod.unknown
36
37 # Web site: http://q4md-forcefieldtools.org/Tutorial/leap-mol3.php
38 # Web site: http://q4md-forcefieldtools.org/Tutorial/leap-mol2.php
39 F00 = loadmol3 ../Mol_m1/Mol-ial_m1-c1.mol2
40 F01 = loadmol3 ../Mol_m1/Mol-ia2_m1-c1.mol2
41 F02 = loadmol3 ../Mol_m1/Mol-ia3_m1-c1.mol2
42 U01 = loadmol3 ../Mol_m1/Mol-sm_m1-c1.mol2
43 # F00_8 = loadmol3 ../Mol_m1/Mol-ial_m1-c10.mol2
44 # F00_9 = loadmol3 ../Mol_m1/Mol-ial_m1-c11.mol2
45 # F00_10 = loadmol3 ../Mol_m1/Mol-ial_m1-c12.mol2
46 # F00_11 = loadmol3 ../Mol_m1/Mol-ial_m1-c13.mol2
47 # F00_12 = loadmol3 ../Mol_m1/Mol-ial_m1-c14.mol2
48 # F00_13 = loadmol3 ../Mol_m1/Mol-ial_m1-c15.mol2
49 # F00_14 = loadmol3 ../Mol_m1/Mol-ial_m1-c16.mol2
50 # F00_15 = loadmol3 ../Mol_m1/Mol-ial_m1-c17.mol2
51 # F00_16 = loadmol3 ../Mol_m1/Mol-ial_m1-c18.mol2
52 # F00_17 = loadmol3 ../Mol_m1/Mol-ial_m1-c19.mol2
53 # F00_0 = loadmol3 ../Mol_m1/Mol-ial_m1-c2.mol2
54 # F00_18 = loadmol3 ../Mol_m1/Mol-ial_m1-c20.mol2
55 # F00_19 = loadmol3 ../Mol_m1/Mol-ial_m1-c21.mol2
56 # F00_20 = loadmol3 ../Mol_m1/Mol-ial_m1-c22.mol2
57 # F00_21 = loadmol3 ../Mol_m1/Mol-ial_m1-c23.mol2
58 # F00_1 = loadmol3 ../Mol_m1/Mol-ial_m1-c3.mol2
59 # F00_2 = loadmol3 ../Mol_m1/Mol-ial_m1-c4.mol2
60 # F00_3 = loadmol3 ../Mol_m1/Mol-ial_m1-c5.mol2
61 # F00_4 = loadmol3 ../Mol_m1/Mol-ial_m1-c6.mol2
62 # F00_5 = loadmol3 ../Mol_m1/Mol-ial_m1-c7.mol2
63 # F00_6 = loadmol3 ../Mol_m1/Mol-ial_m1-c8.mol2
64 # F00_7 = loadmol3 ../Mol_m1/Mol-ial_m1-c9.mol2
65 # F01_8 = loadmol3 ../Mol_m1/Mol-ia2_m1-c10.mol2
66 # F01_9 = loadmol3 ../Mol_m1/Mol-ia2_m1-c11.mol2
67 # F01_10 = loadmol3 ../Mol_m1/Mol-ia2_m1-c12.mol2
```

B.3. PEG WITH HYDROXYETHYL TERMINAL, MULTIPLE CONFORMATIONS

```
68 # F01_11 = loadmol3 ../Mol_m1/Mol-ia2_m1-c13.mol2
69 # F01_12 = loadmol3 ../Mol_m1/Mol-ia2_m1-c14.mol2
70 # F01_13 = loadmol3 ../Mol_m1/Mol-ia2_m1-c15.mol2
71 # F01_14 = loadmol3 ../Mol_m1/Mol-ia2_m1-c16.mol2
72 # F01_15 = loadmol3 ../Mol_m1/Mol-ia2_m1-c17.mol2
73 # F01_16 = loadmol3 ../Mol_m1/Mol-ia2_m1-c18.mol2
74 # F01_17 = loadmol3 ../Mol_m1/Mol-ia2_m1-c19.mol2
75 # F01_0 = loadmol3 ../Mol_m1/Mol-ia2_m1-c2.mol2
76 # F01_18 = loadmol3 ../Mol_m1/Mol-ia2_m1-c20.mol2
77 # F01_19 = loadmol3 ../Mol_m1/Mol-ia2_m1-c21.mol2
78 # F01_20 = loadmol3 ../Mol_m1/Mol-ia2_m1-c22.mol2
79 # F01_21 = loadmol3 ../Mol_m1/Mol-ia2_m1-c23.mol2
80 # F01_1 = loadmol3 ../Mol_m1/Mol-ia2_m1-c3.mol2
81 # F01_2 = loadmol3 ../Mol_m1/Mol-ia2_m1-c4.mol2
82 # F01_3 = loadmol3 ../Mol_m1/Mol-ia2_m1-c5.mol2
83 # F01_4 = loadmol3 ../Mol_m1/Mol-ia2_m1-c6.mol2
84 # F01_5 = loadmol3 ../Mol_m1/Mol-ia2_m1-c7.mol2
85 # F01_6 = loadmol3 ../Mol_m1/Mol-ia2_m1-c8.mol2
86 # F01_7 = loadmol3 ../Mol_m1/Mol-ia2_m1-c9.mol2
87 # F02_8 = loadmol3 ../Mol_m1/Mol-ia3_m1-c10.mol2
88 # F02_9 = loadmol3 ../Mol_m1/Mol-ia3_m1-c11.mol2
89 # F02_10 = loadmol3 ../Mol_m1/Mol-ia3_m1-c12.mol2
90 # F02_11 = loadmol3 ../Mol_m1/Mol-ia3_m1-c13.mol2
91 # F02_12 = loadmol3 ../Mol_m1/Mol-ia3_m1-c14.mol2
92 # F02_13 = loadmol3 ../Mol_m1/Mol-ia3_m1-c15.mol2
93 # F02_14 = loadmol3 ../Mol_m1/Mol-ia3_m1-c16.mol2
94 # F02_15 = loadmol3 ../Mol_m1/Mol-ia3_m1-c17.mol2
95 # F02_16 = loadmol3 ../Mol_m1/Mol-ia3_m1-c18.mol2
96 # F02_17 = loadmol3 ../Mol_m1/Mol-ia3_m1-c19.mol2
97 # F02_0 = loadmol3 ../Mol_m1/Mol-ia3_m1-c2.mol2
98 # F02_18 = loadmol3 ../Mol_m1/Mol-ia3_m1-c20.mol2
99 # F02_19 = loadmol3 ../Mol_m1/Mol-ia3_m1-c21.mol2
100 # F02_20 = loadmol3 ../Mol_m1/Mol-ia3_m1-c22.mol2
101 # F02_21 = loadmol3 ../Mol_m1/Mol-ia3_m1-c23.mol2
102 # F02_1 = loadmol3 ../Mol_m1/Mol-ia3_m1-c3.mol2
103 # F02_2 = loadmol3 ../Mol_m1/Mol-ia3_m1-c4.mol2
104 # F02_3 = loadmol3 ../Mol_m1/Mol-ia3_m1-c5.mol2
105 # F02_4 = loadmol3 ../Mol_m1/Mol-ia3_m1-c6.mol2
106 # F02_5 = loadmol3 ../Mol_m1/Mol-ia3_m1-c7.mol2
107 # F02_6 = loadmol3 ../Mol_m1/Mol-ia3_m1-c8.mol2
108 # F02_7 = loadmol3 ../Mol_m1/Mol-ia3_m1-c9.mol2
109 # U01 = loadmol3 ../Mol_m1/Mol-sm_m1-c10.mol2
110 # U01 = loadmol3 ../Mol_m1/Mol-sm_m1-c11.mol2
111 # U01 = loadmol3 ../Mol_m1/Mol-sm_m1-c12.mol2
112 # U01 = loadmol3 ../Mol_m1/Mol-sm_m1-c13.mol2
```

B.3. PEG WITH HYDROXYETHYL TERMINAL, MULTIPLE CONFORMATIONS

```
113 # U01 = loadmol3 ../Mol_m1/Mol-sm_m1-c14.mol2
114 # U01 = loadmol3 ../Mol_m1/Mol-sm_m1-c15.mol2
115 # U01 = loadmol3 ../Mol_m1/Mol-sm_m1-c16.mol2
116 # U01 = loadmol3 ../Mol_m1/Mol-sm_m1-c17.mol2
117 # U01 = loadmol3 ../Mol_m1/Mol-sm_m1-c18.mol2
118 # U01 = loadmol3 ../Mol_m1/Mol-sm_m1-c19.mol2
119 # U01 = loadmol3 ../Mol_m1/Mol-sm_m1-c2.mol2
120 # U01 = loadmol3 ../Mol_m1/Mol-sm_m1-c20.mol2
121 # U01 = loadmol3 ../Mol_m1/Mol-sm_m1-c21.mol2
122 # U01 = loadmol3 ../Mol_m1/Mol-sm_m1-c22.mol2
123 # U01 = loadmol3 ../Mol_m1/Mol-sm_m1-c23.mol2
124 # U01 = loadmol3 ../Mol_m1/Mol-sm_m1-c3.mol2
125 # U01 = loadmol3 ../Mol_m1/Mol-sm_m1-c4.mol2
126 # U01 = loadmol3 ../Mol_m1/Mol-sm_m1-c5.mol2
127 # U01 = loadmol3 ../Mol_m1/Mol-sm_m1-c6.mol2
128 # U01 = loadmol3 ../Mol_m1/Mol-sm_m1-c7.mol2
129 # U01 = loadmol3 ../Mol_m1/Mol-sm_m1-c8.mol2
130 # U01 = loadmol3 ../Mol_m1/Mol-sm_m1-c9.mol2
131
132 # To match the residue names found in the PDB file
133 # Web site: http://ambermd.org/doc6/html/AMBER-sh-5.9.html#sh-5.9.19
134 # ZZZ = copy F00
135
136 # If a copy is done, define the molecule and residue
137 # Web site: http://ambermd.org/doc6/html/AMBER-sh-5.9.html#sh-5.9.63
138 # set ZZZ name "ZZZ"
139 # set ZZZ.1 name "ZZZ"
140
141 # Let's load the PDB file
142 # Web site: http://ambermd.org/doc6/html/AMBER-sh-5.9.html#sh-5.9.44
143 # VAR = loadPdb Your-PDB-file.ent
144
145 # Let's save the prmtop and prmcrd file with specific file extensions
146 # (to be automatically recognized by VMD http://www.ks.uiuc.edu/
    Research/vmd/)
147 # Web site: http://ambermd.org/doc6/html/AMBER-sh-5.9.html#sh-5.9.54
148 # saveAmberParm F00 F00.parm7 F00.rst7
149
150 # q
151
152 saveoff F00 F00pghlgauss.off
153 saveoff F01 F01pghlgauss.off
154 saveoff F02 F02pghlgauss.off
155
156
```

B.3. PEG WITH HYDROXYETHYL TERMINAL, MULTIPLE CONFORMATIONS

```
157 HPG8000 = sequence { F01 F02 F02 F02 F02 F02 F02 F02 F02 F02 F02 F02 F02
    F02 F02 F02 F02 F02 F02 F02 F02 F02 F02 F02 F02 F02 F02 F02 F02 F02
    F02 F02 F02 F02 F02 F02 F02 F02 F02 F02 F02 F02 F02 F02 F02 F02 F02
    F02 F02 F02 F02 F02 F02 F02 F02 F02 F02 F02 F02 F02 F02 F02 F02 F02
    F02 F02 F02 F02 F02 F02 F02 F02 F02 F02 F02 F02 F02 F02 F02 F02 F02
    F02 F02 F02 F02 F02 F02 F02 F02 F02 F02 F02 F02 F02 F02 F02 F02 F02
    F02 F02 F02 F02 F02 F02 F02 F02 F02 F02 F02 F02 F02 F02 F02 F02 F02
    F02 F02 F02 F02 F02 F02 F02 F02 F02 F02 F02 F02 F02 F02 F02 F02 F02
    F02 F02 F02 F02 F02 F02 F02 F02 F02 F02 F02 F02 F02 F02 F02 F02 F02
    F02 F02 F02 F00 }
```

```
158 # etc...
159
160 charge HPG8000
161 loadoff pghlgauss.off
162
163 saveamberparm HPG8000 pghlgauss.prmtop pghlgauss.inpcrd
164
165
166 quit
```

B.3.8 Multiple mini-PEG conformations

```

1  """
2  Generate multiple miniPEG conformations for FF development
3
4  Input Files: one miniPEG molecule
5
6  output: Txt file containing radgyr and pdb files
7  """
8  #####
9  # Import Libraries as listed in Sire sampling input file
10 #####
11 from MyFunctions import *
12
13 #####
14 #         Main program
15 #####
16 #Load initial system
17 inpcrd = "pyred.inpcrd"
18 prmtop = "pyred.prmtop"
19 dimensions = 'box101.dat'
20 save_sys_name = "pyredsampling.s3"
21 input_system = "restart_pyred.s3"
22
23 # Assign flexibility parameters necessary to evaluate internal MC moves
24 import os.path
25 check = os.path.isfile(input_system)
26 check = str(check)
27 if check == 'True':
28     print("Minimized or system with flexibility is available and load
29           it")
30     new_groups = load(input_system)
31     new_group = collect_mc_molecs(new_groups)
32     (system1,ljcp)=create_single_System(new_group,new_groups.property(
33         'space'))
34 else:
35     print("Making system with flexibility and defining rigid and
36           internal moves...")
37     (new_group,space)=load_files_to_prepare_system_for_flexibility(
38         inpcrd,prmtop,dimensions,save_sys_name)
39     (system1,ljcp)=create_single_System(new_group,space)
40
41     print("system is done!")
42 ## Define input simulation parameters
43

```

```
40 # Initiate random generator
41 rangen = RanGenerator()
42 ## Set the temperature
43 temperature = 298.15 * kelvin
44 ## Specify the maximum amount to move the
45 ## bonds, angles and dihedrals
46 max_delta_bond = 0.00 * angstrom
47 max_delta_angle = 3.5 * degrees
48 max_delta_dihedral = 10 * degrees
49 ## specify the maximum number of bonds,
50 ## angles and dihedrals to move per move
51 max_num_move = 250
52 # set the maximum delta parameters
53 params = {}
54 params["bond flex"] = max_delta_bond
55 params["angle flex"] = max_delta_angle
56 params["dihedral flex"] = max_delta_dihedral
57 params["h dihedral flex"] = max_delta_dihedral
58 params["maxvar"] = max_num_move
59 Parameter.push(params)
60
61 # Perform Rigid body and Internal MC simulations
62 #(system1,ljcp)=create_single_System(new_group,space)
63 (system_mc,wt_moves)=NVT_ensemble_moves(system1)
64 MGName = system_mc.groupNames()[-1]
65 internalmove = InternalMove(system_mc[MGName])
66 Sire.Stream.save( system_mc, "flex_system_peg1.s3" )
67 start_time = time.clock()
68 t = QTime()
69 t.start()
70 file = open('equi_pyred.log','w')
71 print("Perform MC simulations")
72 # perform 5000 blocks of 2*5000 moves
73 for i in range(1,2):
74     print("performing step %s"%i)
75     print("system_mc start energy %s"%system_mc.energy())
76     system_mc = simulation_moves_simple(system_mc,wt_moves,0)
77     print("system energy after RIGID BODY mc % s " % system_mc.energy
78           ())
79     internalmove.move(system_mc, 0)
80     print("Energy %s, nAccepted = %s, nRejected = %s" % \
81           (system_mc.energy(), internalmove.nAccepted(),
82           internalmove.nRejected() ) )
82     print("system final energy after internal Moves %s"%system_mc.
83           energy())
```

```
83 file.write(str(system_mc.energy())+'\n')
84 print("
      *****
      ")
85 if i % 1 == 0:
86     PDB().write(system_mc.molecules(), "output/Mol_red%00d.pdb" % i)
87     Sire.Stream.save( system_mc, "output/Mol_red%00d.s3" % i )
88 file.close()
89 elapsed = (time.clock() - start_time)
90 print("time taken %d"%elapsed)
```

B.3.9 FF effect on the PEG folding

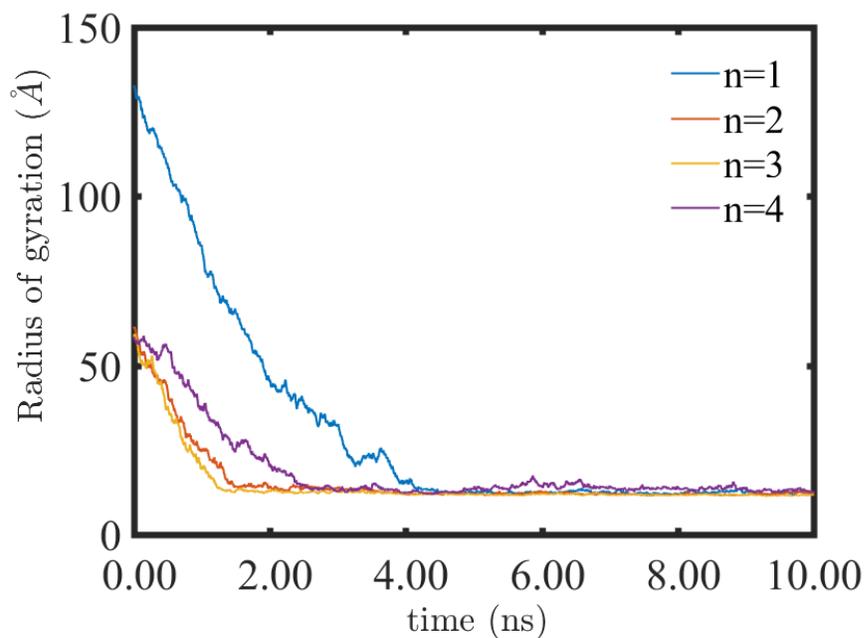


Figure B.1: Effect of length of central fragments on the radii of gyration of the 8 kDa PEG structures with hydroxyethyl terminals in the 10 ns long MD conformational sampling simulations performed with an NPT ensemble in an implicit solvent at 300 K using HFF parameters.

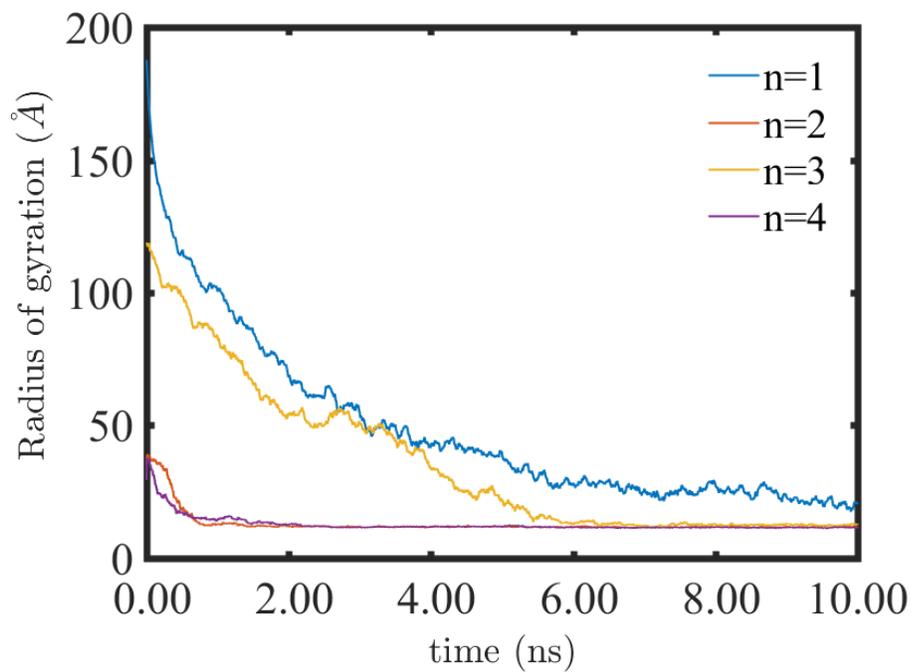


Figure B.2: Effect of length of central fragments on the radii of gyration of the 8 kDa PEG structures with methyl terminals in the 10 ns long MD conformational sampling simulations performed with an NPT ensemble in an implicit solvent at 300 K using MFF parameters.

B.4 MCCCS Towhee plots

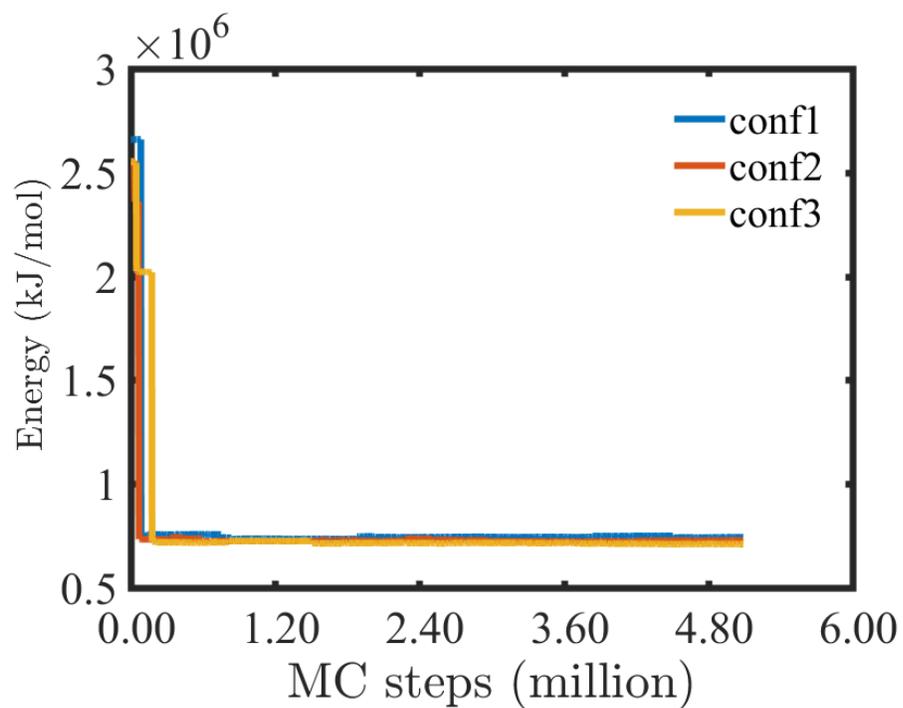


Figure B.3: Total energy variations in MCCCS Towhee simulations conducted at 300 K for three different starting conformations using the NPT ensemble and ‘RANLUX’ random number generator.

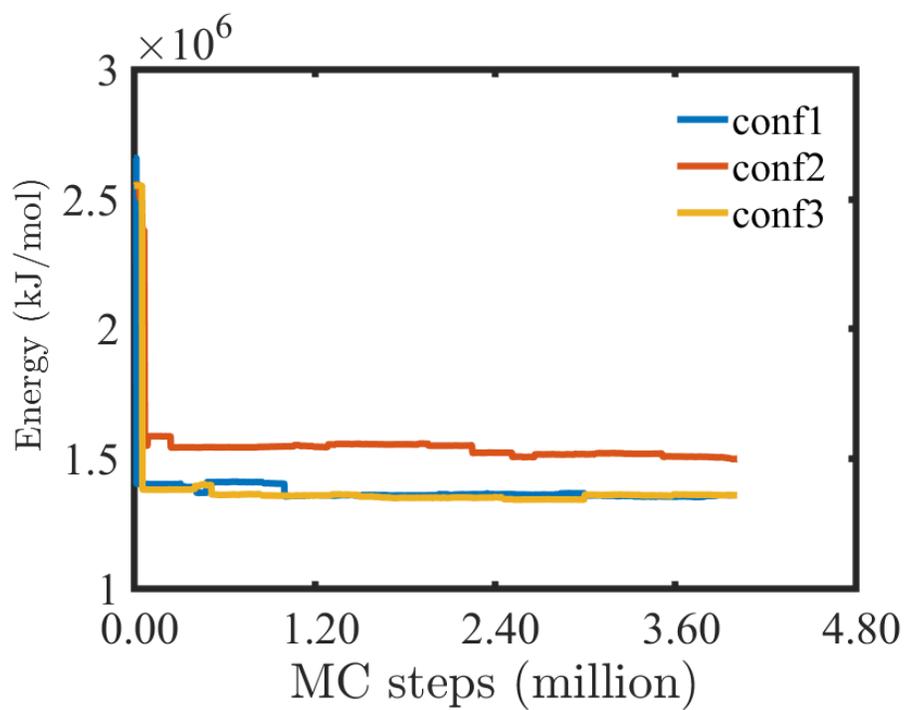


Figure B.4: Total energy variations in MCCC'S Towhee simulations conducted at 600 K for three different starting conformations using the NPT ensemble and 'RANLUX' random number generator.

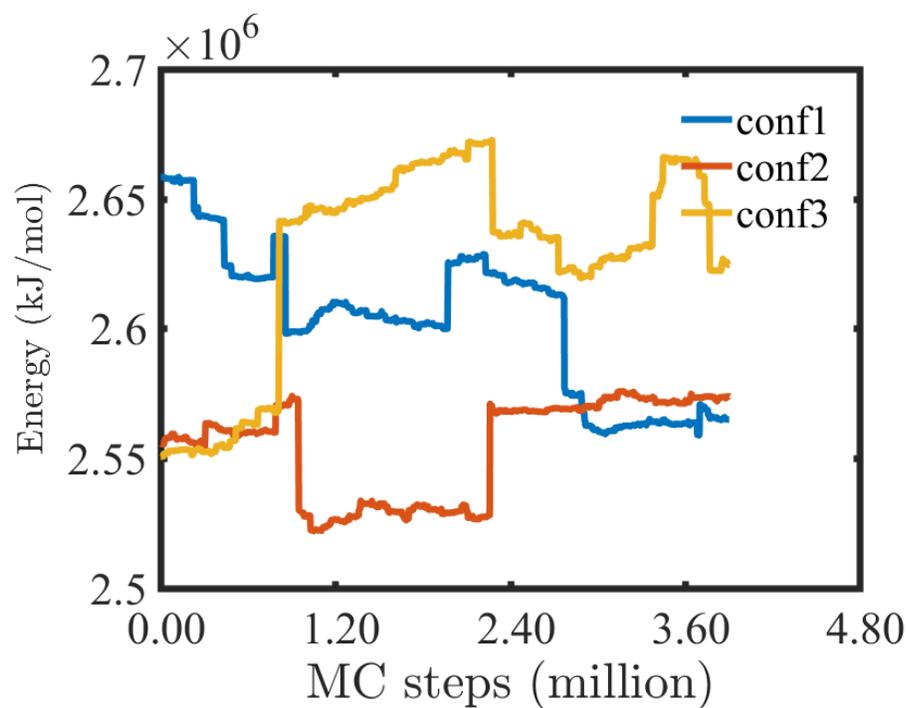


Figure B.5: Total energy variations in MCCCS Towhee simulations conducted at 1200 K for three different starting conformations using the NPT ensemble and 'RANLUX' random number generator.

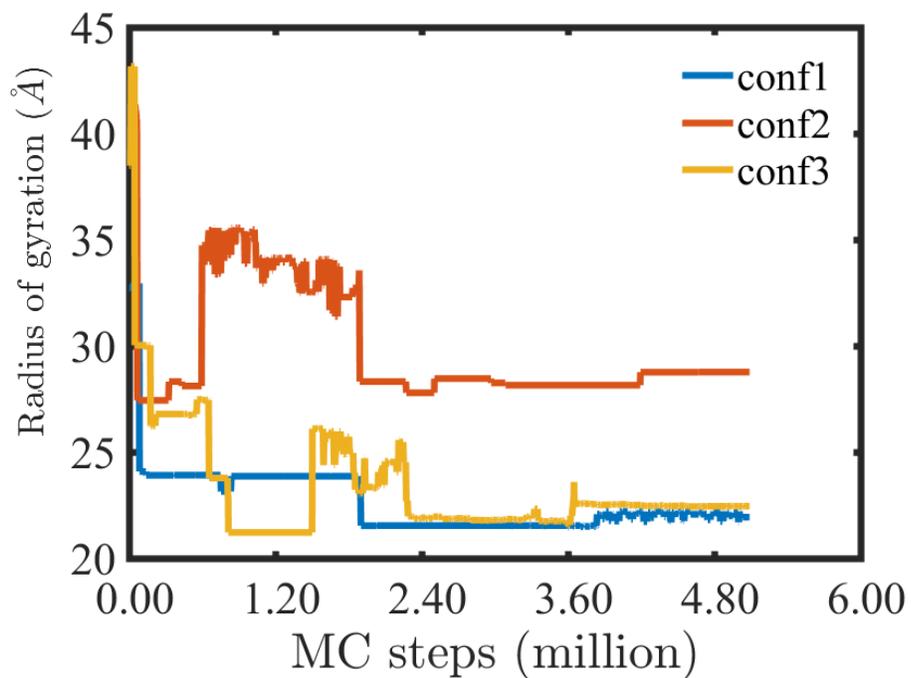


Figure B.6: Radii of gyration variations in MCCC'S Towhee simulations conducted at 300 K for three different starting conformations using the NPT ensemble and 'RANLUX' random number generator.

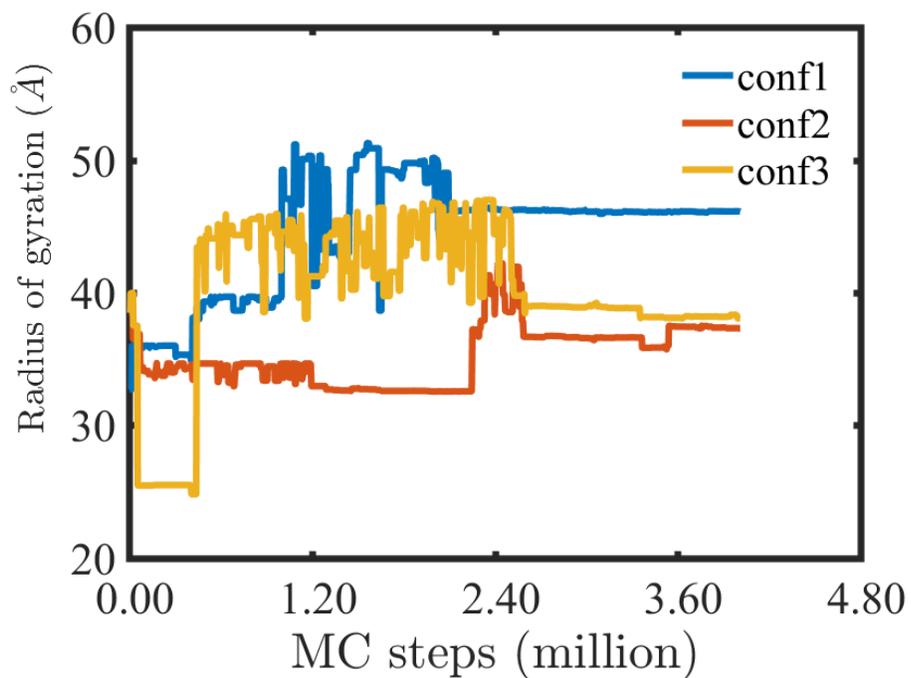


Figure B.7: Radii of gyration variations in MCCC'S Towhee simulations conducted at 600 K for three different starting conformations using the NPT ensemble and 'RANLUX' random number generator.

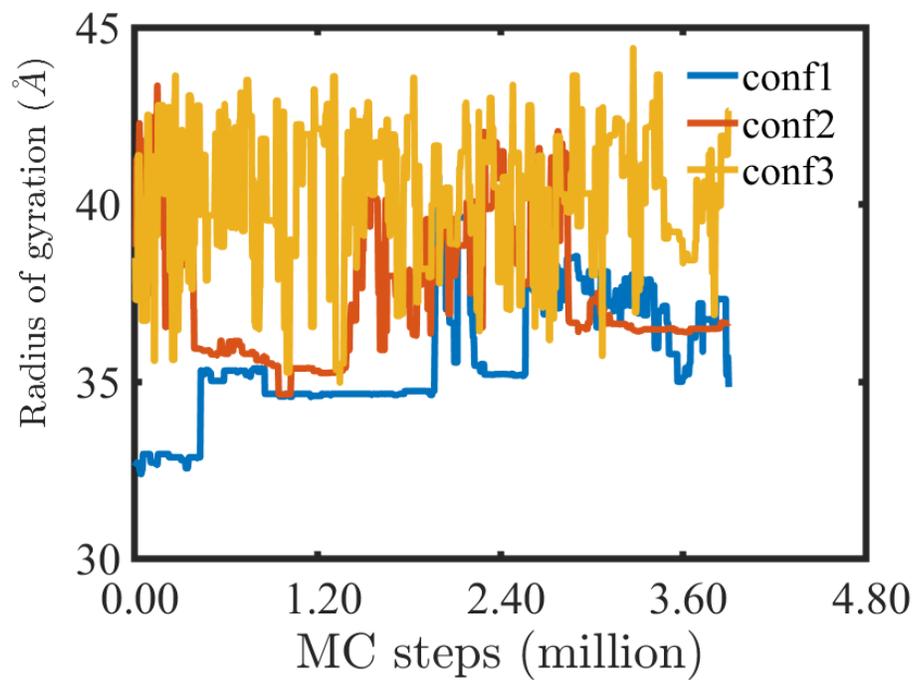


Figure B.8: Radii of gyration variations in MCCCS Towhee simulations conducted at 1200 K for three different starting conformations using the NPT ensemble and ‘RANLUX’ random number generator.

B.5 Sire plots

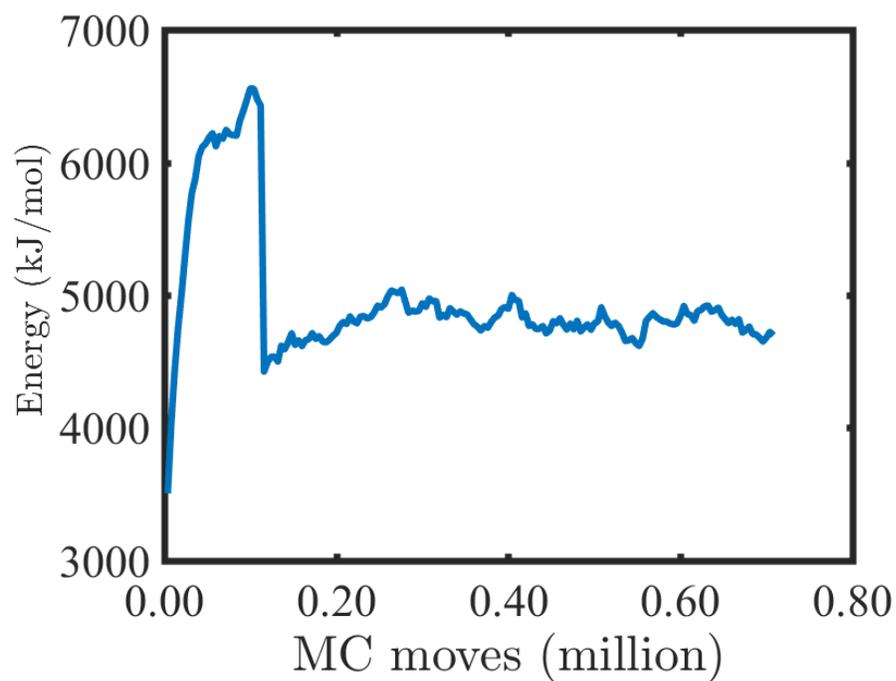


Figure B.9: Energy fluctuations in the NPT ensemble MC conformational sampling simulations conducted at 1200 K. These simulations were started with a linear PEG structure with a hydroxyethyl terminal and used HFF parameters.

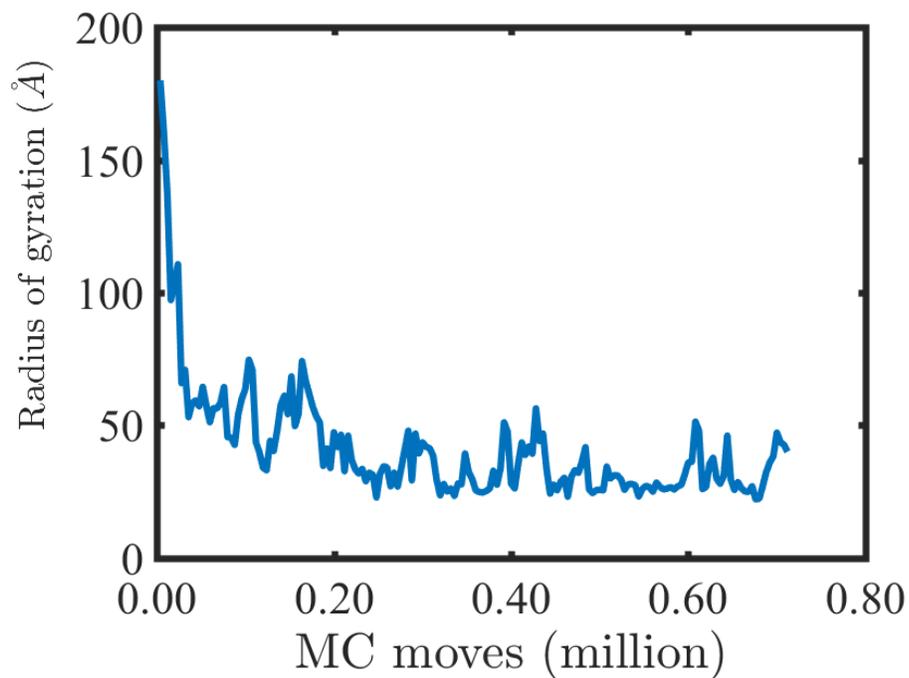


Figure B.10: Change in the radius of gyration in MC conformational sampling conducted at 1200 K, starting with a linear PEG structure. The structure reached an equilibrium state after completing less than 0.05 million steps.

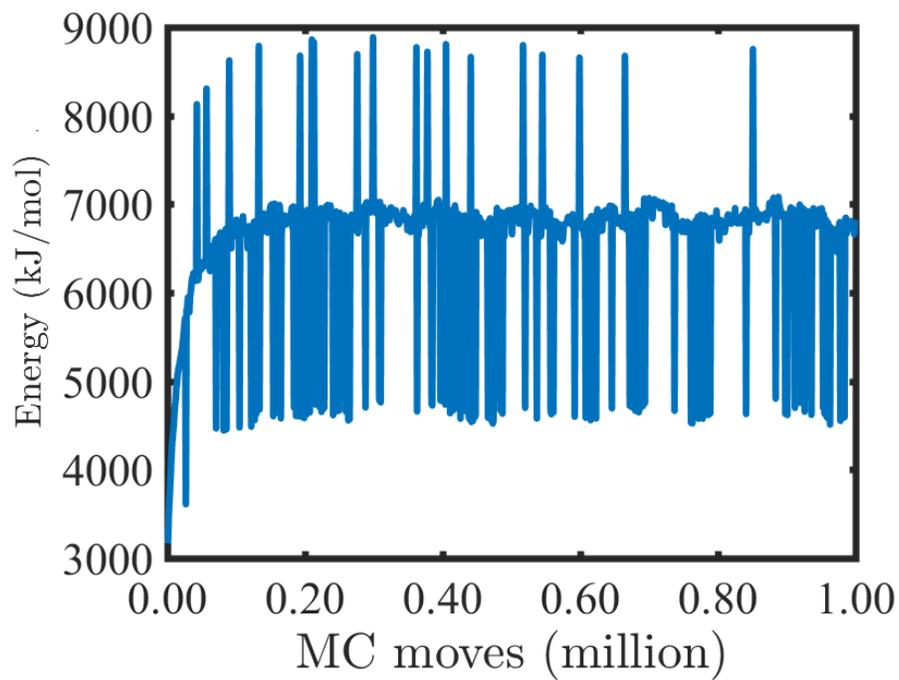


Figure B.11: Energy change during MC conformational sampling at 300 K, using a temperature quenching approach between 300-1200 K. These simulations used a linear 8 kDa PEG with a methyl terminal group and MFF parameters.

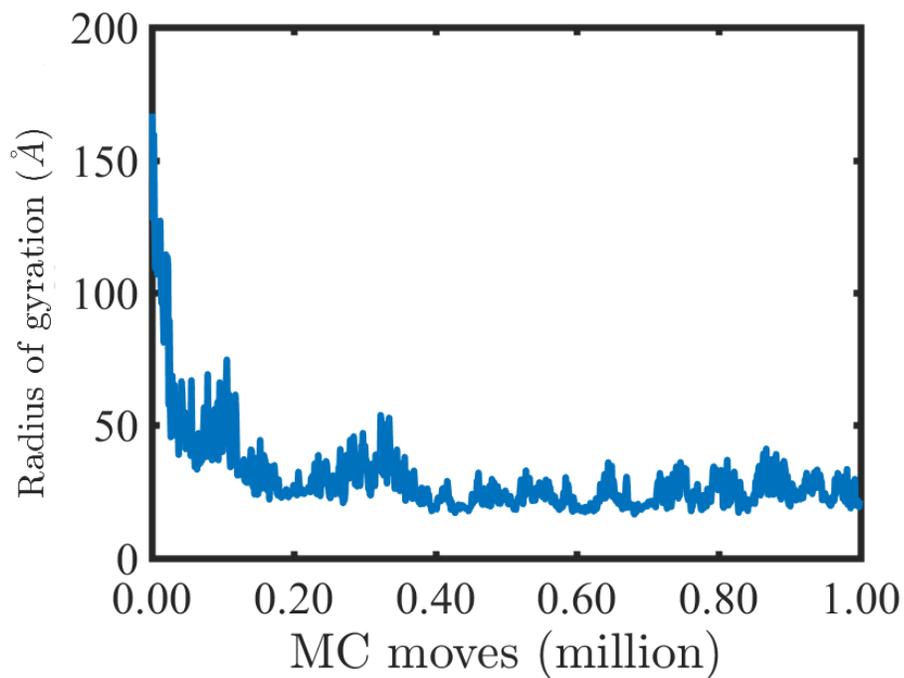


Figure B.12: Change in the radius of gyration in MC conformational sampling at 300 K, performed with a temperature quenching method. The quenched PEG structures are optimized by performing an additional 1000 internal moves. These simulations started with a linear 8 kDa PEG with methyl terminal group and MFF parameters.

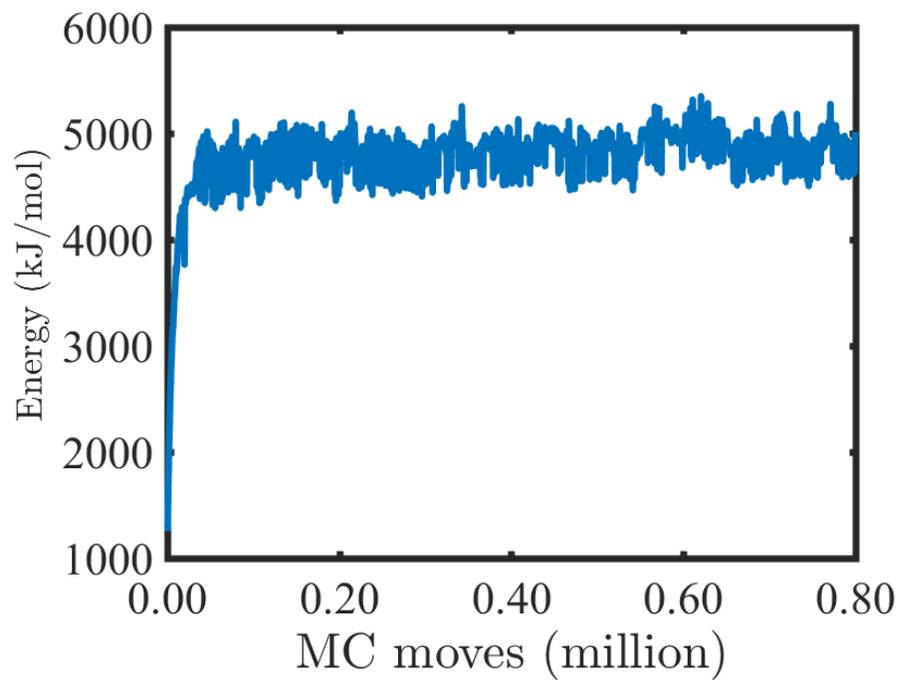


Figure B.13: Energy change during MC conformational sampling at 300 K, using a temperature quenching approach between 300-1200 K. These simulations used a linear 8 kDa PEG with a methyl terminal group and HFF parameters.

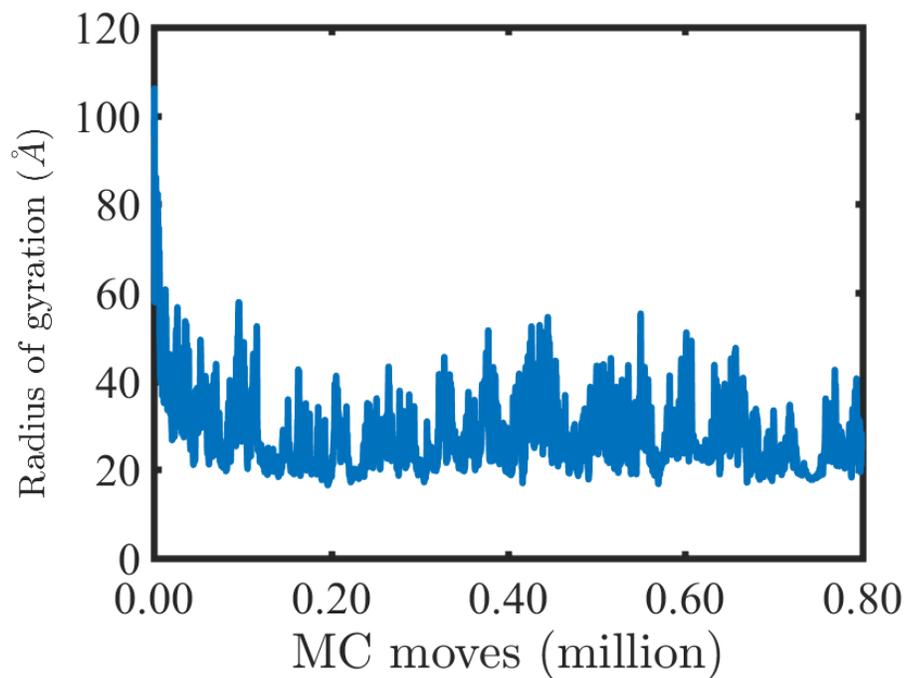


Figure B.14: Change in the radius of gyration in MC conformational sampling at 300 K, performed with a temperature quenching method. The quenched PEG structures are optimized by performing an additional 1000 internal moves. These simulations started with a linear 8 kDa PEG with methyl terminal group and HFF parameters.

Appendix C

Conformational equilibrium in crowded media appendix

C.1 Extract clusters

```
1
2 """
3 Program to extract clusters
4 this algorithm pick first molecule randomly and check whether if forms
   cluster with any other molecules around via checking distance
   threshold. It stores all the molecules in a list around the first
   molecule. In the second step, it selects a molecule from the list
   one by one and detects the additional molecules as a part of
   aggregate. This cycle continue till there is no more molecules
   participating in an aggregate. It saves the cluster as a pdb with
   total number of molecules in it and then output the remaining list
   of molecules. The 'newList' will go through the loop again. in any
   case the algorithm did not find any cluster then it will save the
   single molecule as a pdb and result in newList with number of
   molecules n-1. For example: if cluster is composed of 3 molecules
   then new list will be n-3 molecules.
5
6 INPUT: .inp/crd files
7
8 OUTPUT: The script saves the output files as a pdb files as '
   peg_box1_3_36.pdb', inwhich 'box1' represents the number of system,
   '3' is number of molecules participating in aggregate, and '36'
   remaining number of molecules in the system.
9 """
10 #####
11 # Import Libraries as listed in Sire sampling input file
12 #####
13 from MyFunctions import *
14
15 #####
```

```
16 #           Main program
17 #####
18 # define tolerance
19 clstr_tolrce = 10
20
21 # determine number of input systems
22 directory = os.path.abspath(os.getcwd())
23 list_of_files = []
24 extension = '.inpcrd'
25
26 for file_name in os.listdir(directory):
27     if file_name.endswith(extension):
28         list_of_files.append(file_name)
29
30 num_systems = len(list_of_files)
31
32 print('Total available systems %d'%num_systems)
33
34 # Loop to extract cluster based on the tolerance criteria
35 for i in range (1,num_systems+1):
36     inpcrd = 'box10'+str(i)+'.inpcrd'
37     prmtop = 'box10'+str(i)+'.prmtop'
38     box = 'box'+str(i)+'_'
39     print('Running system %d'%i)
40     (mols,space) = Amber().readCrdTop(inpcrd,prmtop)
41     mol_list = gen_list(mols)
42     #print('-----Total molecules -----')
43     mol_grp = MoleculeGroup()
44     presnt_mols = []
45     mol = mol_list[0]
46     presnt_mols.append(mol)
47     mol_grp.add(mol)
48     remList = mol_list[0:0:]+mol_list[0+1::]
49     count = 0
50     while mol_grp.nMolecules() > 0:
51         count = count +1
52         indx = cluster_search(presnt_mols,remList,clstr_tolrce)
53         #print(indx)
54         indx = remove_lists(indx)
55         (presnt_mols, remList, mol_grp) = acc_molecules(presnt_mols,
56                 remList,indx,mol_grp,box)
56     print('System %d is complete'% i)
57     print('-----')
58 print('All clustering is complete')
59
```

```
60
61 # now make all molecules in a cluster as a single molecule by removing
    'ter' and connect words
62 print('Now finalizing PDB files')
63 directory = os.path.abspath(os.getcwd())
64 list_of_files = []
65 extension = '.pdb'
66
67 for file_name in os.listdir(directory):
68     if file_name.endswith(extension):
69         list_of_files.append(file_name)
70 for fl in list_of_files:
71     gl = open(fl, 'r')
72     lines = gl.readlines()
73     gl.close()
74     nf = open(fl, 'w')
75     for line in lines:
76         if 'CONNECT' in line or 'TER' in line:
77             del line
78         else:
79             nf.writelines(line)
80     nf.close()
81 print('All complete')
```

C.2 Sensitivity coefficient calculations

C.2.1 Main program (Sensitivity coefficients) file

```

1 %% Sensitivity of SPT plots
2
3 % script to make plot of size distribution vs chemical potential at
4 % constant concentration.
5
6 clc
7 clear
8
9 % Input parameters
10
11 % Cube size and concentration
12 side_length = 0.0000000301; % units: meters
13 cell_volume = side_length^3;
14 conc = 0.1; % concentration in the simulation box units: g/ml
15 probe = '2K96.pdb';
16 [R,S,V] = geom_parameters(probe);
17 crowder = 'pegmd2.pdb';
18 [Rc,Sc,Vc] = geom_parameters(crowder);
19 probeParm = [R,S,V];
20 crowderParm = [Rc,Sc,Vc];
21 rangee = 0:(0.6/(6-1)):0.6; % define the concentration range for axis
    on plots
22
23
24 increment_percent = 10;
25 % compute the sensitivity coeff. by changing the geometrical parameters
    by
26 % small increments in percentage.
27 % third integer input in sensitivityCoefficient(probeParm, crowderParm
    ,1,side_length) function represent the 1 percent increment in all
    the geometrical parameters of crowder.
28 [ccr, ccs, ccv] = sensitivityCoefficient(probeParm, crowderParm,
    increment_percent,side_length);
29
30 %% OUTPUT FIGURES BY SOLVING ACTIVITY COEFFICIENT
31 h = figure;
32 plot(ccr,'LineWidth',3)
33 hold on
34 set(gca,'LineWidth',3,'FontSize',15,'FontName','Times');
35 ylabel('$C_{R}^{avail. vol.}$','interpreter','latex');
36 xlabel('Concentration (g/ml)','interpreter','latex');
37 set(gca,'XTickLabel',num2str(rangee.','%.2f'));

```

```
38 set(gca,'box','on')
39 filename = strcat('sensivityCCR',int2str(increment_percent));
40 print(h, '-dpng',filename)
41
42 h = figure;
43 plot(ccs,'LineWidth',3)
44 hold on
45 set(gca,'LineWidth',3,'FontSize',15,'FontName','Times');
46 ylabel('$C_{S}^{avail. vol.}$','interpreter','latex');
47 xlabel('Concentration (g/ml)','interpreter','latex');
48 set(gca,'XTickLabel',num2str(rangee.','%.2f'));
49 set(gca,'box','on')
50 filename = strcat('sensivityCCS',int2str(increment_percent));
51 print(h, '-dpng',filename)
52
53
54 h = figure;
55 plot(ccv,'LineWidth',3)
56 hold on
57 set(gca,'LineWidth',3,'FontSize',15,'FontName','Times');
58 ylabel('$C_{V}^{avail. vol.}$','interpreter','latex');
59 xlabel('Concentration (g/ml)','interpreter','latex');
60 set(gca,'XTickLabel',num2str(rangee.','%.2f'));
61 set(gca,'box','on')
62 filename = strcat('sensivityCCV',int2str(increment_percent));
63 print(h, '-dpng',filename)
64
65 STOP
66
67 %% MEASUREMENT OF EFFECT OF GEOMETRICAL PARAMETERS OF 1000
    CONFORMATIONS OF PEG ON THE CHEMICAL POTENTIAL
68
69 % Extract geometrical parameters and write the results in text files
70
71 % for i=1:999;
72 %
73 %     filename = sprintf('peg%d.pdb',i);
74 %     [curvrad,Area,vi] = geom_parameters(filename);
75 %     curvradl = curvrad;
76 %     if (curvrad > 6.0000e-09)
77 %     else
78 %
79 %     [i,curvradl,curvrad]
80 %     number = number_of_molecs(cell_volume,vi,conc);
```

```
81 % [Y,mu] = findactivity2(curvrad,curvrad,Area,Area,vi,vi,  
cell_volume,number);  
82 % Muex(i)= mu;  
83 % size(i) = curvrad*10^10;  
84 % rad(i) = curvrad;  
85 % vol(i) = vi;  
86 % area(i) = Area;  
87 % fileID1 = fopen('raDius.txt','w');  
88 % fileID2 = fopen('areA.txt','w');  
89 % fileID3 = fopen('volUme.txt','w');  
90 % fprintf(fileID1,'%d\n',rad);  
91 % fprintf(fileID2,'%d\n',area);  
92 % fprintf(fileID3,'%d\n',vol);  
93 % fclose(fileID1);  
94 % fclose(fileID2);  
95 % fclose(fileID3);  
96 % end  
97 % end  
98  
99 % Upload resultant files from the above loop. No need to run the  
expensive  
100 % loop again and again  
101 radiusfile = importdata('raDius.txt');  
102 areafile = importdata('areA.txt');  
103 volfile = importdata('volUme.txt');  
104 range = length(radiusfile);  
105  
106 % Compute the chemical potentials by the extended SPT model  
107 radiusrange = [radiusfile(593),radiusfile(399),radiusfile(444),  
radiusfile(683),radiusfile(408),radiusfile(36),radiusfile(635),  
radiusfile(784),radiusfile(64),radiusfile(758),radiusfile(668),  
radiusfile(612),radiusfile(9)];  
108 arearange = [areafile(593),areafile(399),areafile(444),areafile(683),  
areafile(408),areafile(36),areafile(635),areafile(784),areafile(64)  
,areafile(758),areafile(668),areafile(612),areafile(9)];  
109 volrange = [volfile(593),volfile(399),volfile(444),volfile(683),volfile  
(408),volfile(36),volfile(635),volfile(784),volfile(64),volfile  
(758),volfile(668),volfile(612),volfile(9)];  
110 areadifference = min(arearange)*10^20, max(arearange)*10^20  
111 voldifference = min(volrange)*10^30, max(volrange)*10^30  
112  
113 for i = 1:range;  
114 number = number_of_molecs(cell_volume,volfile(i),conc);  
115 [Y,mu] = findactivity2(radiusfile(i),radiusfile(i),areafile(i),  
areafile(i),volfile(i),volfile(i),cell_volume,number);
```

```

116     Muex(i) = mu;
117     size(i) = radiusfile(i)*10^10;
118     rad(i) = radiusfile(i);
119     vol(i) = volfile(i);
120     size2(i) = volfile(i)*10^30;
121     area(i) = areafile(i);
122     size3(i) = areafile(i)*10^20;
123 end
124
125 % Figures: Change of chemical potentials with respect of geometrical
126 % parameters of 1000 conformations
127
128 h=figure;
129 scatter(size,Muex,'LineWidth',3)
130 set(gca,'LineWidth',3,'FontSize',15,'FontName','Times');
131 ylabel('$$\mu^{NI}/kT$$','interpreter','latex');
132 xlabel('Radius of curvature $$AA$$','interpreter','latex');
133 set(gca,'box','on')
134 print(h, '-dpng','senstivity1')
135
136 h=figure;
137 scatter(size2,Muex,'LineWidth',3)
138 set(gca,'LineWidth',3,'FontSize',15,'FontName','Times');
139 ylabel('$$\mu^{NI}/kT$$','interpreter','latex');
140 xlabel('Volume $$AA^3$$','interpreter','latex');
141 set(gca,'box','on')
142 print(h, '-dpng','senstivity2')
143
144 h=figure;
145 scatter(size3,Muex,'LineWidth',3)
146 set(gca,'LineWidth',3,'FontSize',15,'FontName','Times');
147 ylabel('$$\mu^{NI}/kT$$','interpreter','latex');
148 xlabel('Surface area $$AA^2$$','interpreter','latex');
149 set(gca,'box','on')
150 print(h, '-dpng','senstivity3')
151
152 %% CHEMICAL POTENTIAL WITH MINIMUM, AVERAGE, AND MAXIMUM GEOMETRICAL
    PARAMETERS
153
154 % Avg. values
155 mean_rad = mean(rad);
156 mean_vol = mean(vol);
157 mean_area = mean(area);
158
159 % Max values

```

```

160 max_rad = max(rad);
161 max_vol = max(vol);
162 max_area = max(area);
163
164 % Min values
165 min_rad = min(rad);
166 min_vol = min(vol);
167 min_area = min(area);
168
169 % Compute chemical potentials
170 for i = 1:150;
171
172     [Y,mu0] = findactivity2(R,Rc,S,Sc,V,Vc,cell_volume,i);
173     [Y,mu1] = findactivity2(R,max_rad,S,Sc,V,Vc,cell_volume,i);
174     [Y,mu2] = findactivity2(R,Rc,S,Sc,V,max_vol,cell_volume,i);
175     [Y,mu3] = findactivity2(R,Rc,S,max_area,V,Vc,cell_volume,i);
176     mur0(i)= mu0;
177     mur(i)= mu1;
178     muv(i)= mu2;
179     mus(i)= mu3;
180
181 end
182
183 rangee = 0:(0.6/(4-1)):0.6;
184
185 h = figure;
186 plot(mur0,'LineWidth',3)
187 hold on
188 plot(mur,'LineWidth',3)
189 plot(muv,'LineWidth',3)
190 plot(mus,'LineWidth',3)
191 set(gca,'LineWidth',3,'FontSize',15,'FontName','Times');
192 ylabel('$$\mu^{NI}/kT$$','interpreter','latex');
193 xlabel('Concentration (g/ml)','interpreter','latex');
194 set(gca,'XTickLabel',num2str(rangee.','%.2f'));
195 legend('PEG2','Avg. R','Avg. V','Avg. S','Location','northwest');
196 set(gca,'box','on')
197 legend('boxoff')
198 print(h, '-dpng','sensitivityMAX')
199
200
201
202 % small increments in radius, volume, and surface area from minimum to
    maximum at
203 % constant concentration

```

```

204
205 stepR = (mean_rad - min_rad)/162;
206 radii = [min_rad:stepR:mean_rad];
207 range2 = length(radii);
208 stepsize = radii(2)*10^10-radii(1)*10^10;
209 maxvalueR = radii(end)*10^10;
210 rangee = 0:(maxvalueR/(5-1)):maxvalueR;
211
212 for i = 1:range2
213     number = number_of_molecs(cell_volume,Vc,conc);
214     [Y,mu0] = findactivity2(R,radii(i),S,Sc,V,Vc,cell_volume,number);
215     mur0(i)= mu0;
216 end
217 chemcontR = mur0(end)-mur0(end-1)
218
219 h = figure;
220 plot(mur0,'LineWidth',3)
221 set(gca,'LineWidth',3,'FontSize',15,'FontName','Times');
222 ylabel('$$\mu^{\{NI\}}/kT$$','interpreter','latex');
223 xlabel('Radius of Curvature ($$AA$$)','interpreter','latex');
224 set(gca,'XTickLabel',num2str(rangee.','%.2f'));
225 set(gca,'box','on')
226 print(h, '-dpng','senstivityRad')
227
228 stepV = (mean_vol - min_vol)/373000;
229 vols = [min_vol:stepV:mean_vol];
230 range3 = length(vols);
231 stepsize3 = vols(2)*10^30-vols(1)*10^30;
232 maxvalueV = vols(end)*10^30;
233 rangee = 0:(maxvalueV/(5-1)):maxvalueV;
234
235 for i = 1:range3
236     number = number_of_molecs(cell_volume,Vc,conc);
237     [Y,mu3] = findactivity2(R,Rc,S,Sc,V,vols(i),cell_volume,number);
238     mur3(i)= mu3;
239 end
240 chemcontV = mur3(end)-mur3(end-1)
241
242 h = figure;
243 plot(mur3,'LineWidth',3)
244 set(gca,'LineWidth',3,'FontSize',15,'FontName','Times');
245 ylabel('$$\mu^{\{NI\}}/kT$$','interpreter','latex');
246 xlabel('Volume ($$AA^3$$)','interpreter','latex');
247 set(gca,'XTickLabel',num2str(rangee.','%.2f'));
248 set(gca,'box','on')

```

```

249 print(h, '-dpng', 'sensitivityVol')
250
251 stepS = (mean_area - min_area)/45500;
252 areas = [min_area:stepS:mean_area];
253 range4 = length(areas);
254 stepsize4 = areas(2)*10^20-areas(1)*10^20;
255 maxvalueS = areas(end)*10^20;
256 rangee = 0:(maxvalueS/(6-1)):maxvalueS;
257
258 for i = 1:range4
259     number = number_of_molecs(cell_volume,Vc,conc);
260     [Y,mu4] = findactivity2(R,Rc,S,areas(i),V,Vc,cell_volume,number);
261     mur4(i)= mu4;
262 end
263 chemcontS = mur4(end)-mur4(end-1)
264
265 h = figure;
266 plot(mur4,'LineWidth',3)
267 set(gca,'LineWidth',3,'FontSize',15,'FontName','Times');
268 ylabel('$$\mu^{NI}/kT$$','interpreter','latex');
269 xlabel('Surface area ($$AA^2$$)','interpreter','latex');
270 set(gca,'XTickLabel',num2str(rangee.','%.2f'));
271 legend('before','after','Location','northwest');
272 set(gca,'box','on')
273 legend('boxoff')
274 print(h, '-dpng', 'sensitivityArea')

```

C.2.2 Sensitivity coefficients function

```

1 function [ccr, ccs, ccv] = sensitivityCoefficient(probe, crowder,incr,
    side_length);
2
3 % Function to estimate the sensitivity coefficient as follows
4
5 % Method1:  $c = [\ln(v)2 - \ln(v)1]/[\ln(gem)2-\ln(gem)1]$ 
6
7
8 % Cube size and concentration
9 cell_volume = side_length^3; % cubic meters
10
11 % compute percent increment
12 convertIncr1 = (crowder(1,1))*incr/100;
13 convertIncr2 = (crowder(1,2))*incr/100;
14 convertIncr3 = (crowder(1,3))*incr/100;
15 %rator = (crowder(1,1)+convertIncr1)/crowder(1,1)

```

```
16 %ratios = (crowder(1,2)+convertIncr2)/crowder(1,2)
17 %ratiov = (crowder(1,3)+convertIncr3)/crowder(1,3)
18 for i = 1:6
19   %conc = 0.1;
20   %number = number_of_molecs(cell_volume,crowder(1,3),i)
21
22   % These calculations are used to compute the chemical potentials using
      the
23   % extended SPT and then these mu values are converted to the fractional
      available
24   % volumes that are used in the sensitivity analysis.
25
26   number = 25*i; % concentration of the box in terms of number of PEG
27
28   % calculations of mu
29   [y,mu1] = findactivity2(probe(1,1),crowder(1,1),probe(1,2),crowder(1,2)
      ,probe(1,3),crowder(1,3),cell_volume,number);
30   [y,mu2] = findactivity2(probe(1,1),crowder(1,1)+convertIncr1,probe(1,2)
      ,crowder(1,2),probe(1,3),crowder(1,3),cell_volume,number);
31   [y,mu3] = findactivity2(probe(1,1),crowder(1,1),probe(1,2),crowder(1,2)
      +convertIncr2,probe(1,3),crowder(1,3),cell_volume,number);
32   [y,mu4] = findactivity2(probe(1,1),crowder(1,1),probe(1,2),crowder(1,2)
      ,probe(1,3),crowder(1,3)+convertIncr3,cell_volume,number);
33   mu = [mu1 mu2 mu3 mu4];
34   availvol = chem_to_vol(mu);
35
36   % sensitivity coeff. calculations
37   cr = (log(availvol(1,2))-log(availvol(1,1)))/(log(crowder(1,1)+
      convertIncr1)-log(crowder(1,1)));
38   cs = (log(availvol(1,3))-log(availvol(1,1)))/(log(crowder(1,2)+
      convertIncr2)-log(crowder(1,2)));
39   cv = (log(availvol(1,4))-log(availvol(1,1)))/(log(crowder(1,3)+
      convertIncr3)-log(crowder(1,3)));
40
41   % collect sensitivity coeff. in vectors
42   ccr(i) = cr;
43   ccs(i) = cs;
44   ccv(i) = cv;
45 end
46 end
```

C.3 Fractional available volume plots

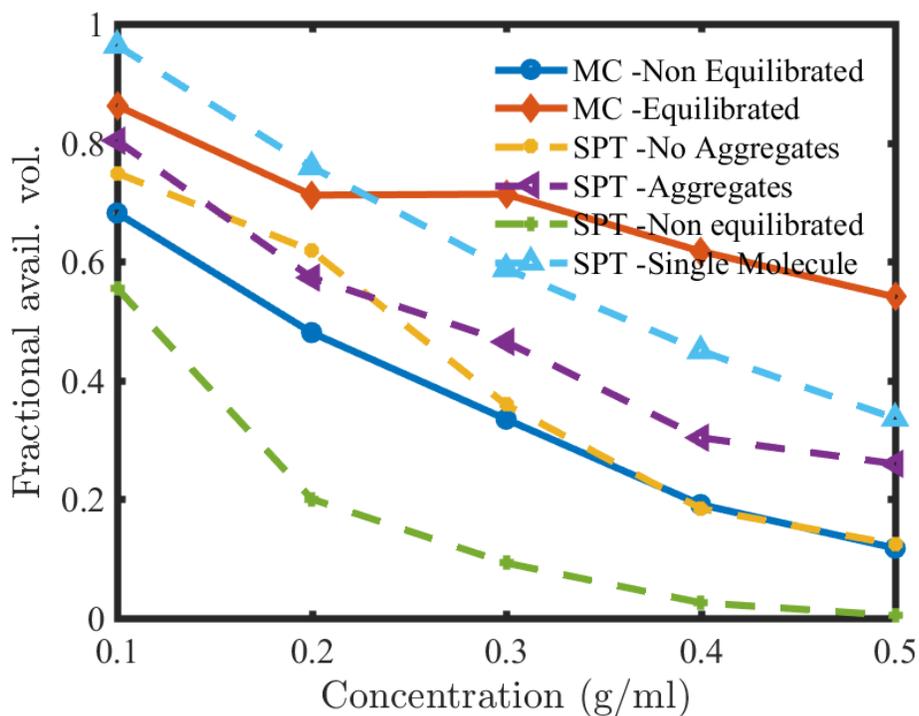


Figure C.1: Comparisons of fractional available volumes for an open conformation of adenylate kinase enzyme (1AKE) measured in the crowded boxes filled with 8 kDa PEG by using the MC (solid lines) and extended SPT models (dashed lines). Only two types of crowded systems, i.e. non-equilibrated and equilibrated systems, were used to determine the chemical potentials using an MC method. The SPT approach used equilibrated systems only with and without aggregates, whereas ‘SPT Single Molecule’ represents the equilibrated single PEG conformation (PEG2) used to compute the fractional available volumes.

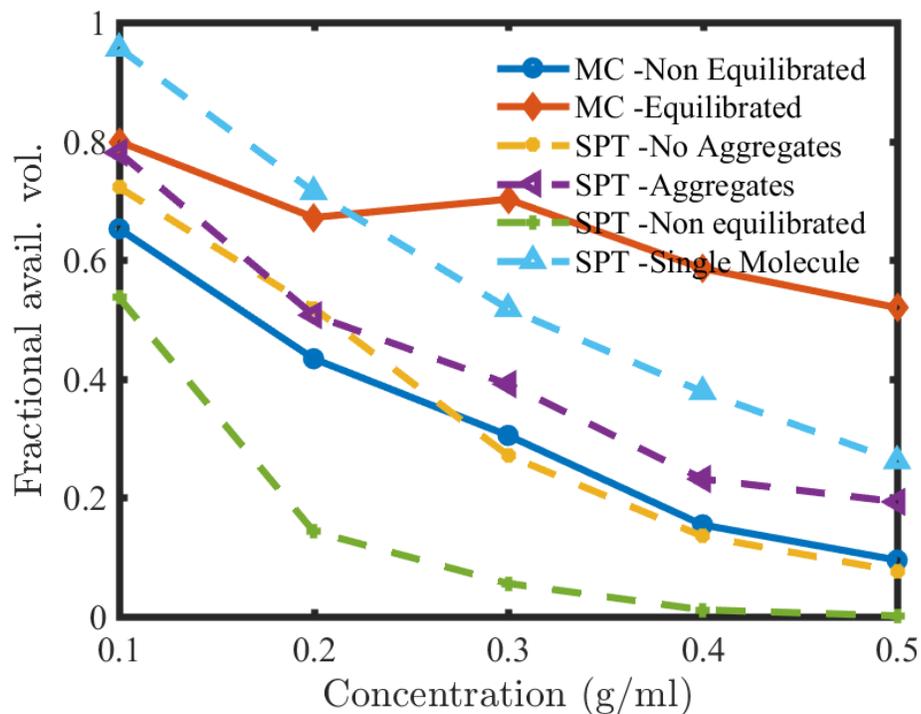


Figure C.2: Comparisons of fractional available volumes for closed conformation of adenylylate kinase enzyme (4AKE) measured in the crowded boxes filled with 8 kDa PEG by using the MC (solid lines) and extended SPT models (dashed lines). Only two types of crowded systems, i.e. non-equilibrated and equilibrated systems, were used to determine the chemical potentials using an MC method. The SPT approach used equilibrated systems only with and without aggregates, whereas ‘SPT Single Molecule’ represents the equilibrated single PEG conformation (PEG2) used to compute the fractional available volumes.

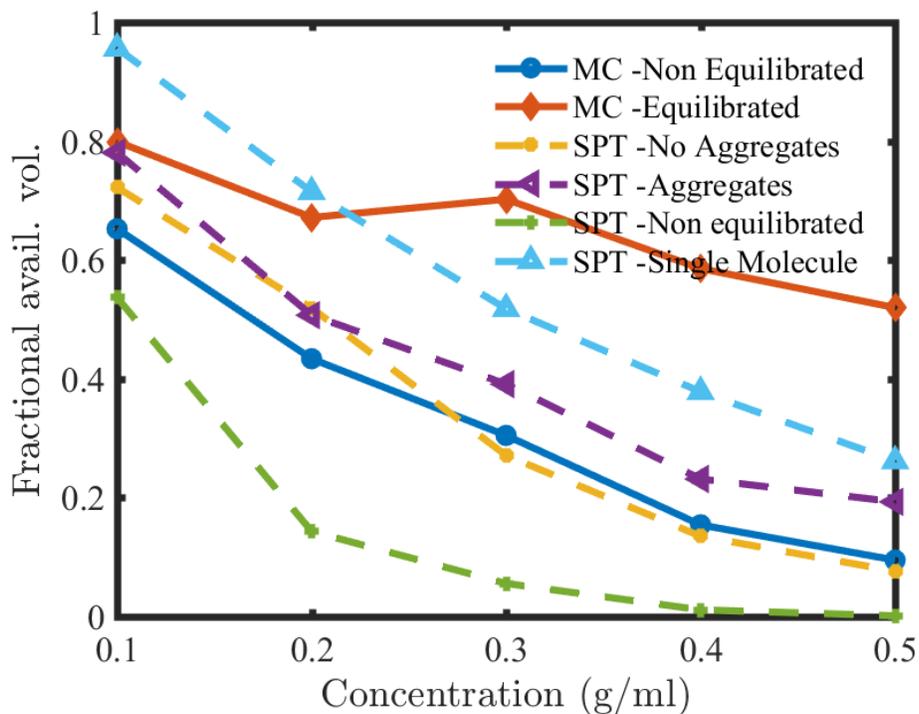


Figure C.3: Comparisons of fractional available volumes for closed conformation of adenylylate kinase enzyme (4AKE) measured in the crowded boxes filled with 8 kDa PEG by using the MC (solid lines) and extended SPT models (dashed lines). Only two types of crowded systems, i.e. non-equilibrated and equilibrated systems, were used to determine the chemical potentials using an MC method. The SPT approach used equilibrated systems only with and without aggregates, whereas ‘SPT Single Molecule’ represents the equilibrated single PEG conformation (PEG2) used to compute the fractional available volumes.

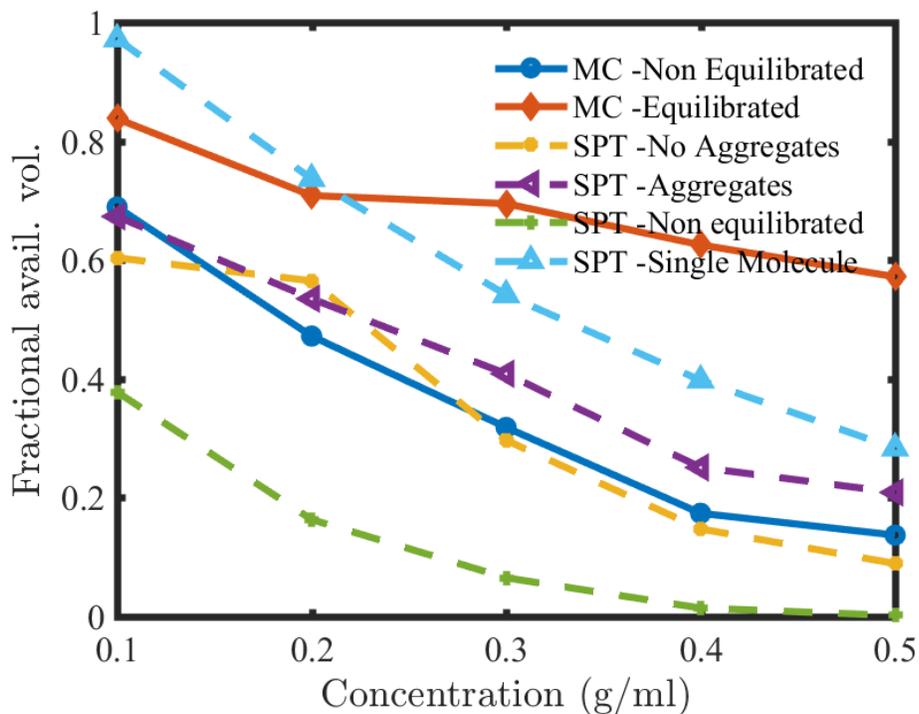


Figure C.4: Comparisons of fractional available volumes for closed conformation of *lac* repressor (2P9H) measured in the crowded boxes filled with 8 kDa PEG by using the MC (solid lines) and extended SPT models (dashed lines). Only two types of crowded systems, i.e. non-equilibrated and equilibrated systems, were used to determine the chemical potentials using an MC method. The SPT approach used equilibrated systems only with and without aggregates, whereas ‘SPT Single Molecule’ represents the equilibrated single PEG conformation (PEG2) used to compute the fractional available volumes.

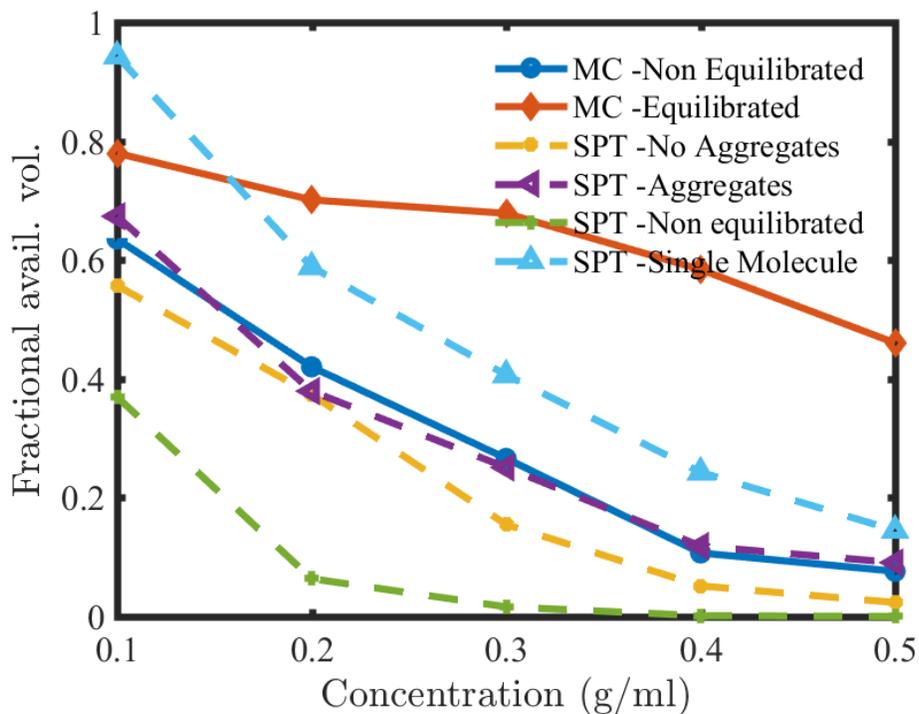


Figure C.5: Comparisons of fractional available volumes for open conformation of *lac* repressor (2PE5) measured in the crowded boxes filled with 8 kDa PEG by using the MC (solid lines) and extended SPT models (dashed lines). Only two types of crowded systems, i.e. non-equilibrated and equilibrated systems, were used to determine the chemical potentials using an MC method. The SPT approach used equilibrated systems only with and without aggregates, whereas ‘SPT Single Molecule’ represents the equilibrated single PEG conformation (PEG2) used to compute the fractional available volumes.

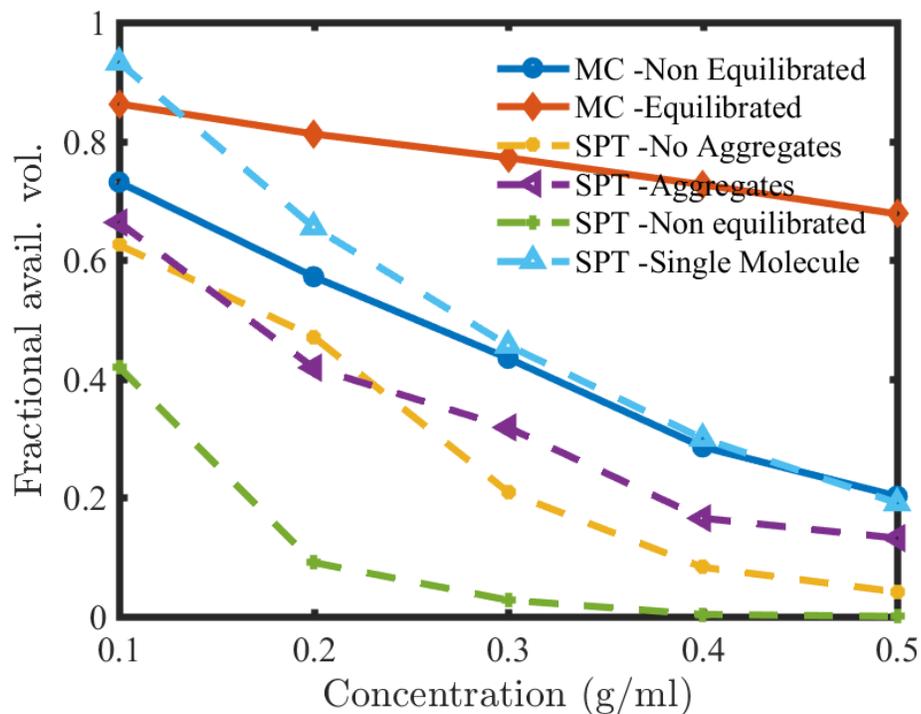


Figure C.6: Comparisons of fractional available volumes for a pseudoknot RNA (2K96) measured in the crowded boxes filled with 8 kDa PEG by using the MC (solid lines) and extended SPT models (dashed lines). Only two types of crowded systems, i.e. non-equilibrated and equilibrated systems, were used to determine the chemical potentials using an MC method. The SPT approach used equilibrated systems only with and without aggregates, whereas ‘SPT Single Molecule’ represents the equilibrated single PEG conformation (PEG2) used to compute the chemical potential.

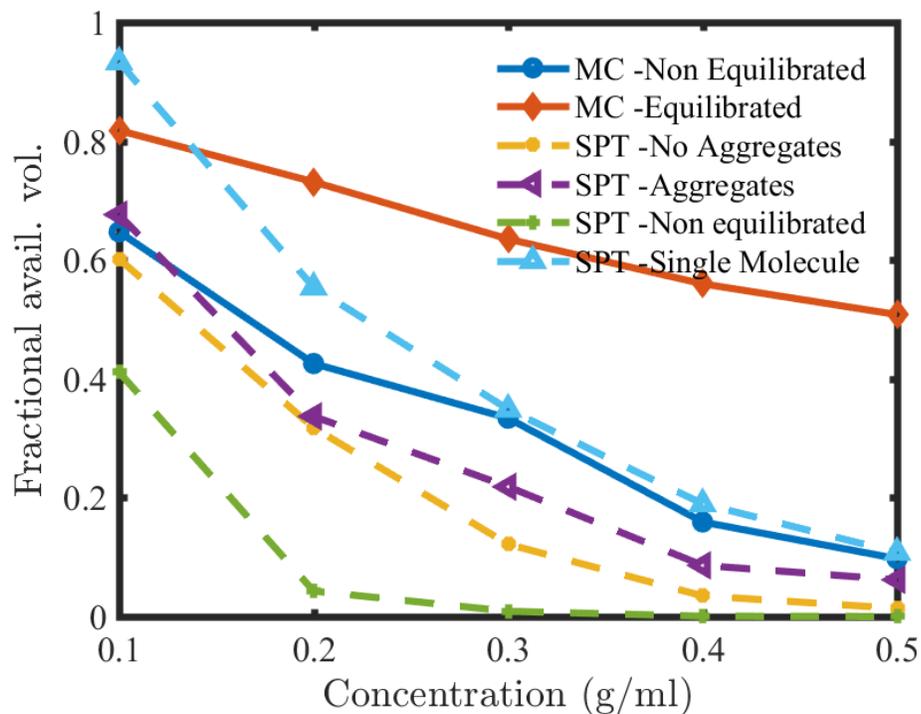


Figure C.7: Comparisons of fractional available volumes for hairpin RNA (1NA2) measured in the crowded boxes filled with 8 kDa PEG by using the MC (solid lines) and extended SPT models (dashed lines). Only two types of crowded systems, i.e. non-equilibrated and equilibrated systems, were used to determine the chemical potentials using an MC method. The SPT approach used equilibrated systems only with and without aggregates, whereas ‘SPT Single Molecule’ represents the equilibrated single PEG conformation (PEG2) used to compute the chemical potential.

C.4 Nonideal chemical potential plots

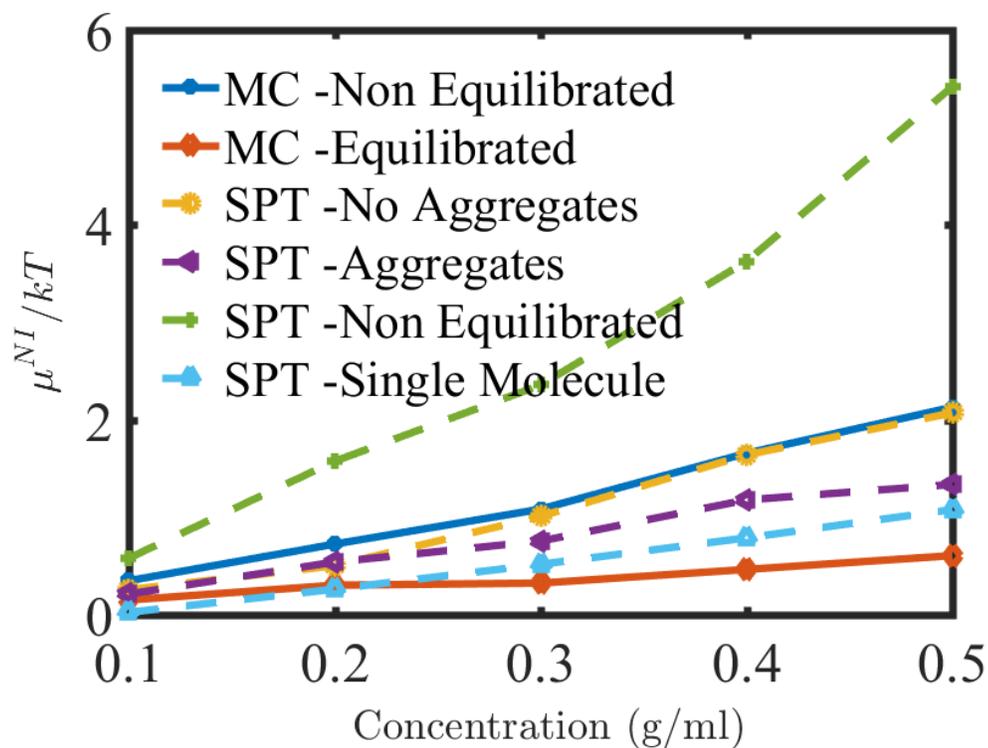


Figure C.8: Comparisons of nonideal chemical potential contributions for an open conformation of adenylate kinase enzyme (1AKE) measured in the crowded boxes filled with 8 kDa PEG by using the MC (solid lines) and extended SPT models (dashed lines). Only two types of crowded systems, i.e. non-equilibrated and equilibrated systems, were used to determine the chemical potentials using an MC method. The SPT approach used equilibrated systems only with and without aggregates, whereas ‘SPT Single Molecule’ represents the equilibrated single PEG conformation (PEG2) used to compute the chemical potential.

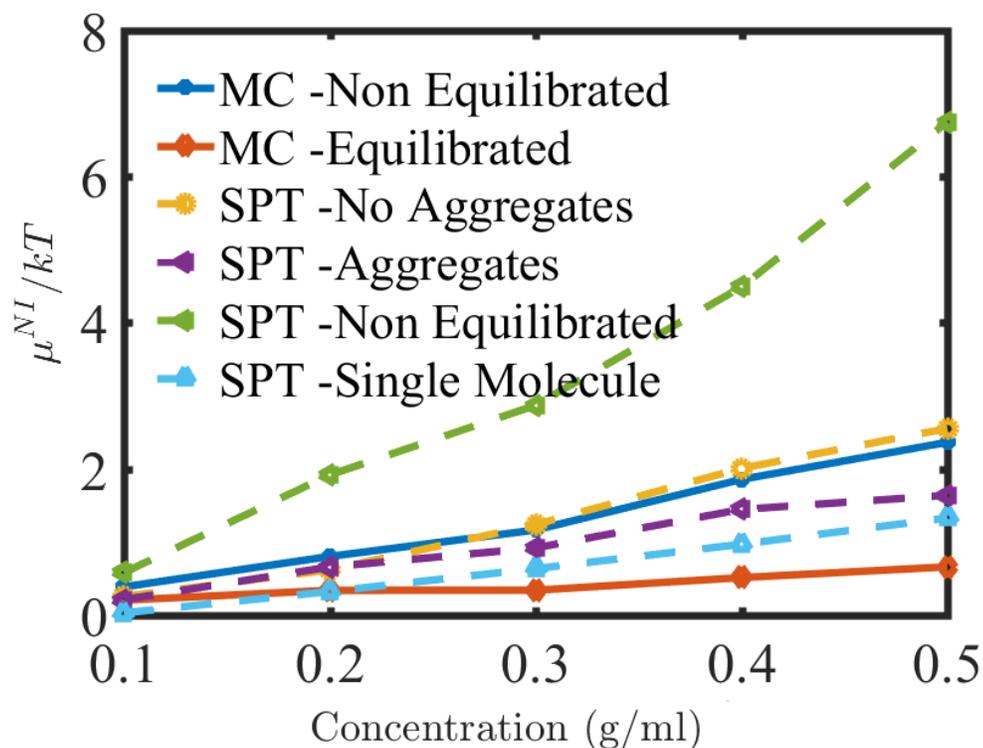


Figure C.9: Comparisons of nonideal chemical potential contributions for closed conformation of adenylate kinase enzyme (4AKE) measured in the crowded boxes filled with 8 kDa PEG by using the MC (solid lines) and extended SPT models (dashed lines). Only two types of crowded systems, i.e. non-equilibrated and equilibrated systems, were used to determine the chemical potentials using an MC method. The SPT approach used equilibrated systems only with and without aggregates, whereas ‘SPT Single Molecule’ represents the equilibrated single PEG conformation (PEG2) used to compute the chemical potential.

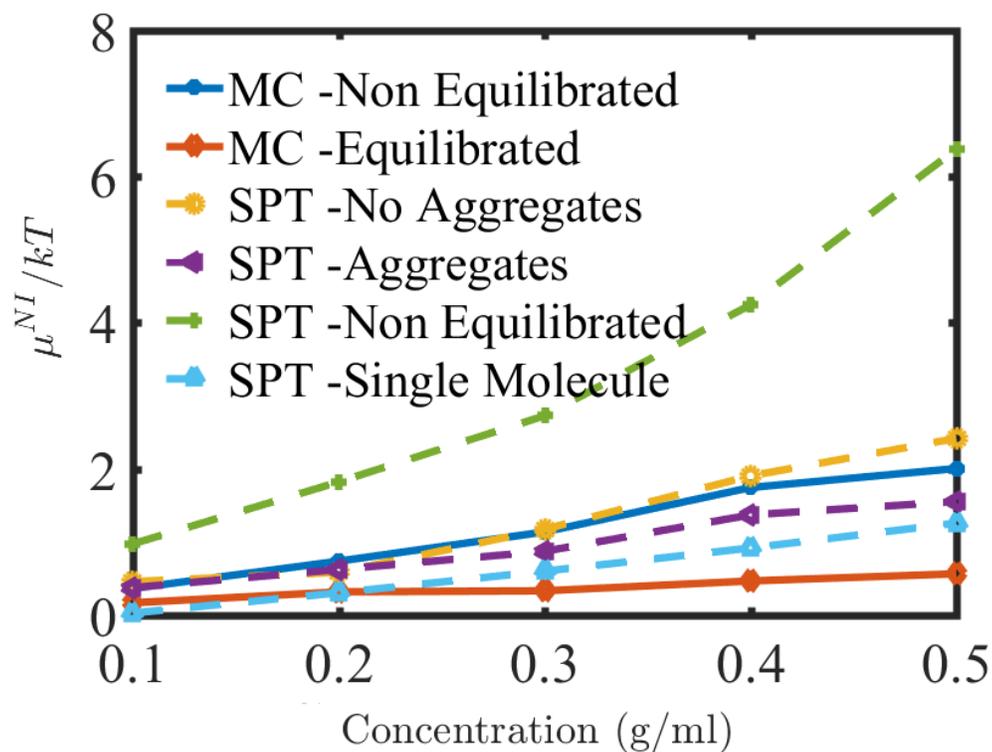


Figure C.10: Comparisons of nonideal chemical potential contributions for closed conformation of *lac* repressor (2P9H) measured in the crowded boxes filled with 8 kDa PEG by using the MC (solid lines) and extended SPT models (dashed lines). Only two types of crowded systems, i.e. non-equilibrated and equilibrated systems, were used to determine the chemical potentials using an MC method. The SPT approach used equilibrated systems only with and without aggregates, whereas ‘SPT Single Molecule’ represents the equilibrated single PEG conformation (PEG2) used to compute the chemical potential.

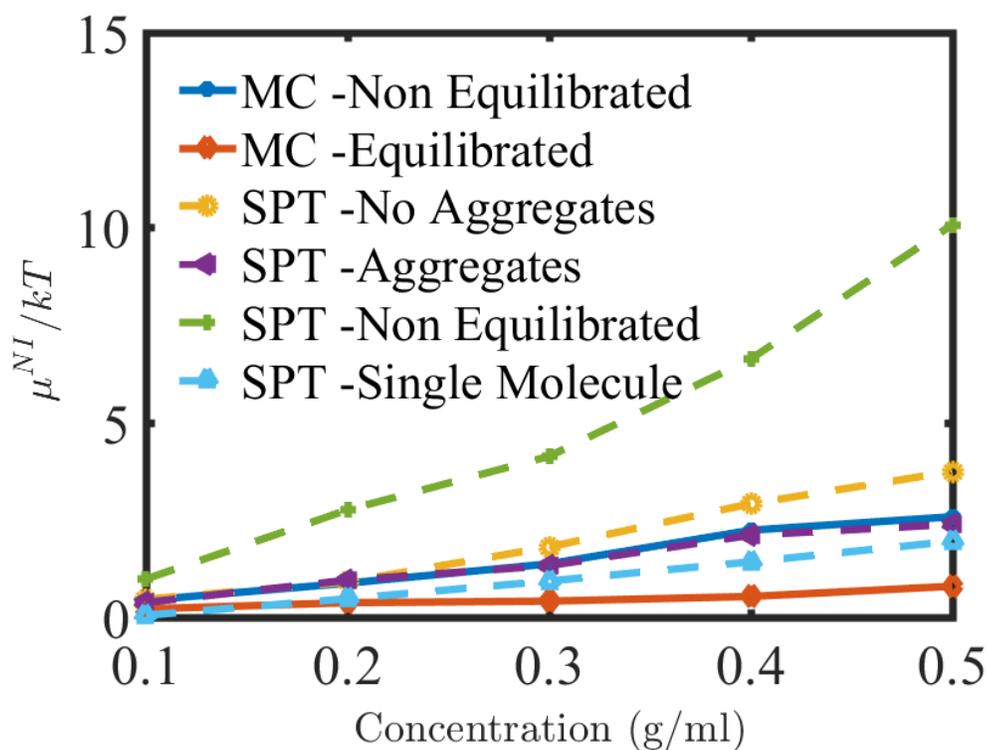


Figure C.11: Comparisons of nonideal chemical potential contributions for open conformation of *lac* repressor (2PE5) measured in the crowded boxes filled with 8 kDa PEG by using the MC (solid lines) and extended SPT models (dashed lines). Only two types of crowded systems, i.e. non-equilibrated and equilibrated systems, were used to determine the chemical potentials using an MC method. The SPT approach used equilibrated systems only with and without aggregates, whereas ‘SPT Single Molecule’ represents the equilibrated single PEG conformation (PEG2) used to compute the chemical potential.

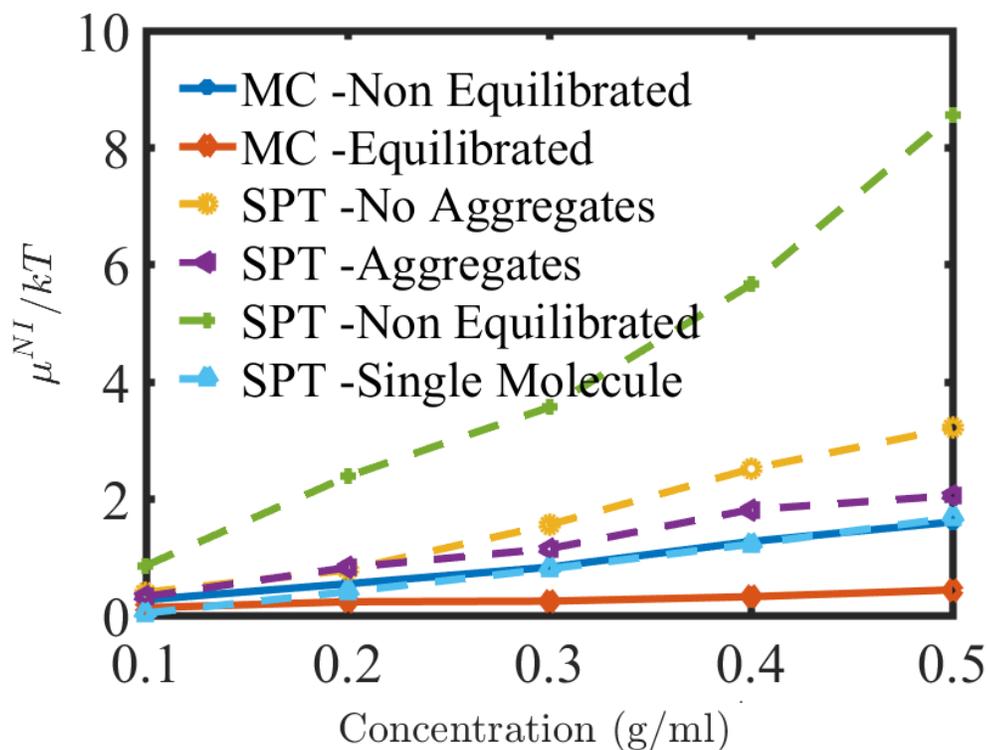


Figure C.12: Comparisons of nonideal chemical potential contributions for pseudoknot RNA (2K96) measured in the crowded boxes filled with 8 kDa PEG by using the MC (solid lines) and extended SPT models (dashed lines). Only two types of crowded systems, i.e. non-equilibrated and equilibrated systems, were used to determine the chemical potentials using an MC method. The SPT approach used equilibrated systems only with and without aggregates, whereas ‘SPT Single Molecule’ represents the equilibrated single PEG conformation (PEG2) used to compute the chemical potential.

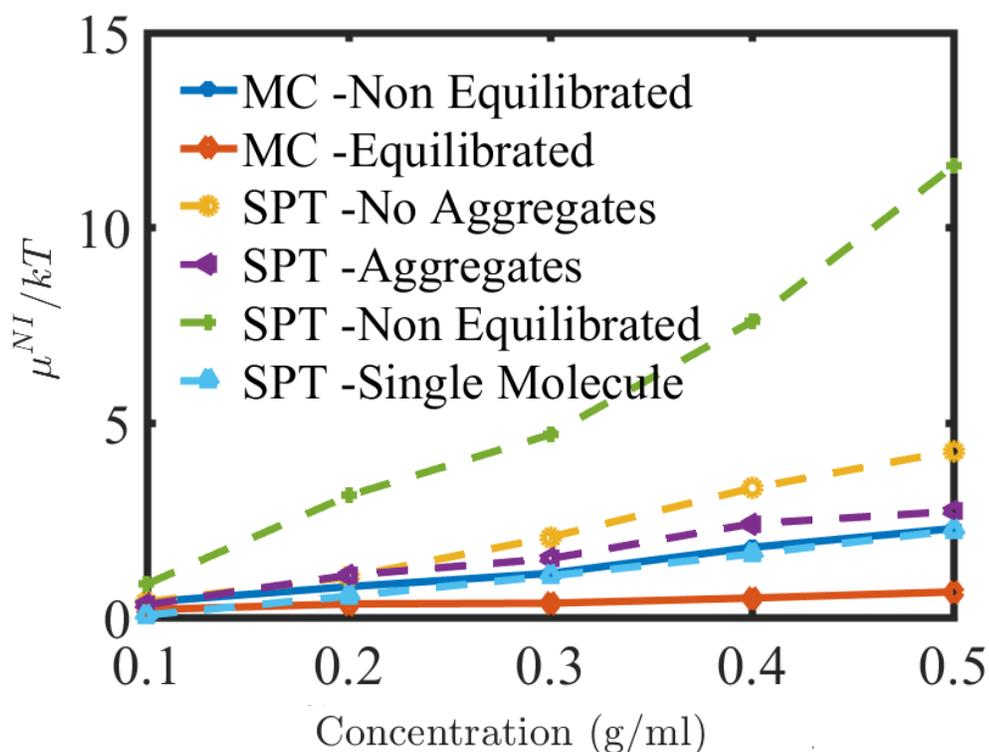


Figure C.13: Comparisons of nonideal chemical potential contributions for hairpin RNA (1NA2) measured in the crowded boxes filled with 8 kDa PEG by using the MC (solid lines) and extended SPT models (dashed lines). Only two types of crowded systems, i.e. non-equilibrated and equilibrated systems, were used to determine the chemical potentials using an MC method. The SPT approach used equilibrated systems only with and without aggregates, whereas ‘SPT Single Molecule’ represents the equilibrated single PEG conformation (PEG2) used to compute the chemical potential.

C.5 Standard free energy change plots

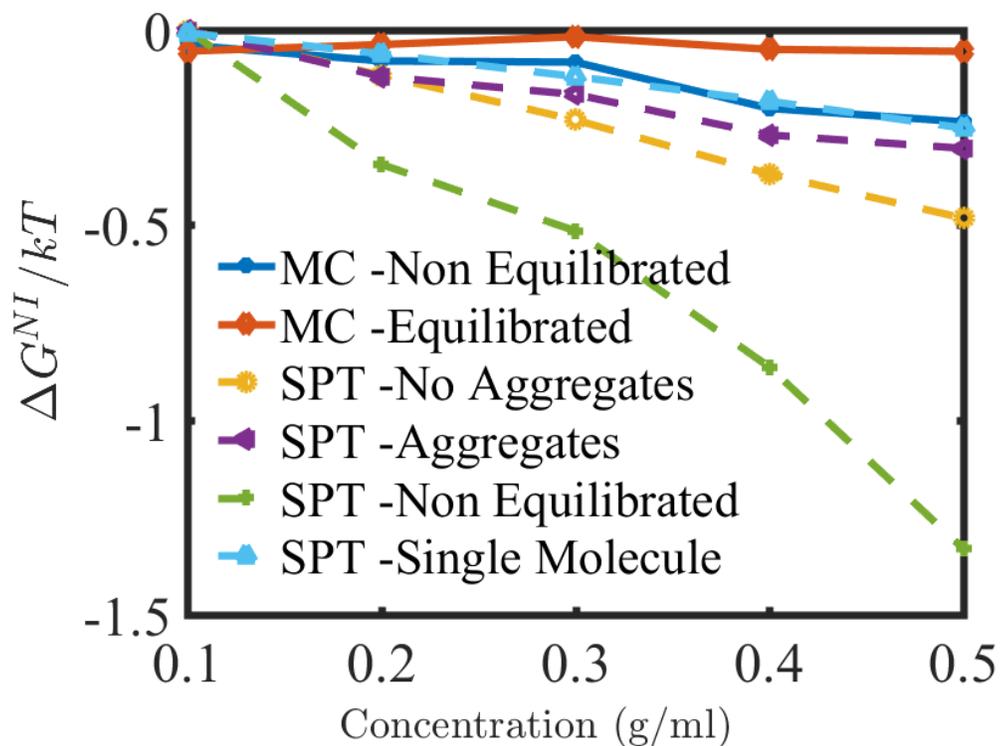


Figure C.14: Nonideal contribution to the standard state free energy change of conformational equilibrium between open and closed conformers in the crowded medium ($4AKE \rightleftharpoons 1AKE$). The macromolecular crowding favors the formation of compact conformation of the kinase enzyme.

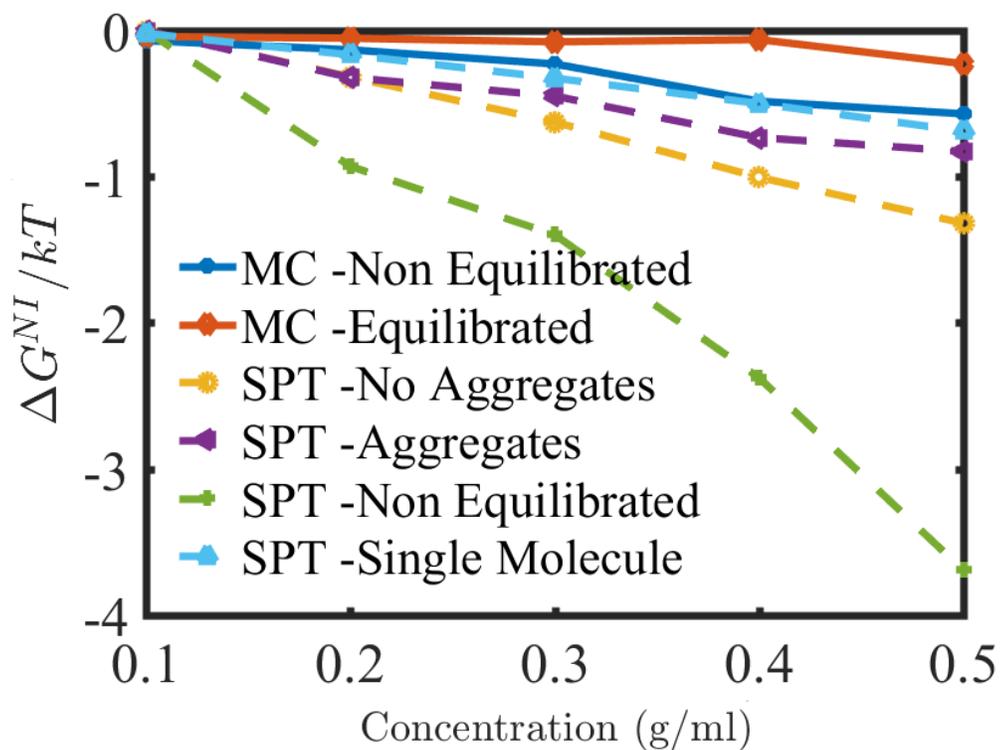


Figure C.15: Nonideal contribution to the standard state free energy change of conformational equilibrium between open and closed conformers in the crowded medium ($2PE5 \rightleftharpoons 2P9H$). The macromolecular crowding favors the formation of compact conformation of the lac repressor.